

# The hidden-charm pentaquark and tetraquark states

Hua-Xing Chen<sup>1a,b</sup>, Wei Chen<sup>1c</sup>, Xiang Liu<sup>d,e,\*</sup>, Shi-Lin Zhu<sup>a,f,g,\*\*</sup>

<sup>a</sup>*School of Physics and State Key Laboratory of Nuclear Physics and Technology, Peking University, Beijing 100871, China*

<sup>b</sup>*School of Physics and Nuclear Energy Engineering, Beihang University, Beijing 100191, China*

<sup>c</sup>*Department of Physics and Engineering Physics, University of Saskatchewan, Saskatoon, Saskatchewan S7N 5E2, Canada*

<sup>d</sup>*School of Physical Science and Technology, Lanzhou University, Lanzhou 730000, China*

<sup>e</sup>*Research Center for Hadron and CSR Physics, Lanzhou University and Institute of Modern Physics of CAS, Lanzhou 730000, China*

<sup>f</sup>*Collaborative Innovation Center of Quantum Matter, Beijing 100871, China*

<sup>g</sup>*Center of High Energy Physics, Peking University, Beijing 100871, China*

---

## Abstract

In the past decade many charmonium-like states were observed experimentally. Especially those charged charmonium-like  $Z_c$  states and bottomonium-like  $Z_b$  states can not be accommodated within the naive quark model. These charged  $Z_c$  states are good candidates of either the hidden-charm tetraquark states or molecules composed of a pair of charmed mesons. Recently, the LHCb Collaboration discovered two hidden-charm pentaquark states, which are also beyond the quark model. In this work, we review the current experimental progress and investigate various theoretical interpretations of these candidates of the multi-quark states. We list the puzzles and theoretical challenges of these models when confronted with the experimental data. We also discuss possible future measurements which may distinguish the theoretical schemes on the underlying structures of the hidden-charm multi-quark states.

*Keywords:* Hidden-charm pentaquark, Hidden-charm tetraquark, Charmonium-like state, Charmonium, Exotic state, Phenomenological models

*PACS:* 21.10.-k, 21.10.Pc, 21.60.Jz, 11.30.Pb, 03.65.Pm

---

## Contents

<b>1</b>	<b>Introduction</b>	<b>3</b>
1.1	Quark model and the multi-quark states . . . . .	3
1.1.1	Quark model . . . . .	4
1.1.2	Exotic states and multi-quark states . . . . .	5
1.1.3	Comparison of QED and QCD and their spectrum . . . . .	6
1.2	General status of hadron spectroscopy . . . . .	6
<b>2</b>	<b>Experimental progress on the hidden-charm multi-quark states</b>	<b>7</b>
2.1	The Charmonium-like XYZ states . . . . .	7
2.1.1	XYZ states produced through $B$ meson decays . . . . .	8
2.1.2	$Y$ states produced through the $e^+e^-$ annihilation . . . . .	24
2.1.3	$X$ states produced through double charmonium production . . . . .	29
2.1.4	The XYZ states from $\gamma\gamma$ fusion processes . . . . .	30
2.1.5	Charged charmonium-like $Z_c$ states . . . . .	33
2.2	The hidden-charm pentaquark states observed by LHCb . . . . .	38
2.3	Charged bottomonium-like states $Z_b(10610)$ and $Z_b(10650)$ . . . . .	39

---

<sup>1</sup>These authors equally contribute to this work.

\*Corresponding author

\*\*Corresponding author

*Email addresses:* hxchen@buaa.edu.cn (Hua-Xing Chen), wec053@mail.usask.ca (Wei Chen), xiangliu@lzu.edu.cn (Xiang Liu), zhusl@pku.edu.cn (Shi-Lin Zhu)

<b>3</b>	<b>Theoretical interpretations of the hidden-charm pentaquark states</b>	<b>41</b>
3.1	The molecular scheme . . . . .	42
3.1.1	The deuteron as a hadronic molecule . . . . .	43
3.1.2	The meson exchange model . . . . .	43
3.1.3	Predictions for the hidden-charm pentaquarks before LHCb's discovery . . . . .	45
3.1.4	Molecular assignments after LHCb's discovery . . . . .	45
3.1.5	Configuration mixing . . . . .	48
3.1.6	Orbital excitations and the $P_c$ parity . . . . .	48
3.2	Dynamically generated resonance . . . . .	49
3.3	QCD sum rules . . . . .	52
3.3.1	A short introduction to the method of QCD sum rule . . . . .	52
3.3.2	Pentaquark currents . . . . .	53
3.3.3	Operator Product Expansion . . . . .	55
3.3.4	Parity of Pentaquarks . . . . .	55
3.3.5	Numerical results and discussions . . . . .	56
3.4	Tightly bound pentaquark state in the quark model . . . . .	57
3.4.1	Chiral quark model . . . . .	57
3.4.2	The diquark/triquark model . . . . .	59
3.5	Kinematical effect . . . . .	60
3.6	Other theoretical schemes . . . . .	61
3.7	Production and decay patterns . . . . .	62
3.7.1	Production of the $P_c$ via weak decays . . . . .	62
3.7.2	Photo-production of the $P_c$ . . . . .	63
3.7.3	Strong decay patterns of the $P_c$ states . . . . .	63
3.8	The hidden-bottom and doubly heavy pentaquark states . . . . .	63
3.9	Theoretical and experimental challenges . . . . .	65
<b>4</b>	<b>Theoretical interpretations of the XYZ states</b>	<b>67</b>
4.1	$Z_b(10610)$ and $Z_b(10650)$ . . . . .	67
4.1.1	Molecular scheme . . . . .	67
4.1.2	The tetraquark assignment . . . . .	70
4.1.3	Kinematical effect . . . . .	72
4.1.4	Production and decay patterns . . . . .	72
4.1.5	A short summary . . . . .	74
4.2	$Z_c(3900)$ , $Z_c(4020)$ and $Z_c(4025)$ . . . . .	74
4.2.1	Molecular scheme . . . . .	74
4.2.2	Tetraquark state assignment . . . . .	78
4.2.3	Kinematical effect . . . . .	80
4.2.4	Production and decay patterns . . . . .	81
4.2.5	A short summary . . . . .	81
4.3	$Z^+(4430)$ . . . . .	81
4.3.1	Molecular state scheme . . . . .	81
4.3.2	The tetraquark assignment . . . . .	83
4.3.3	Cusp effect . . . . .	83
4.3.4	Production, decay patterns, and other theoretical schemes . . . . .	84
4.3.5	A short summary . . . . .	84
4.4	Other charged states: $Z^+(4051)$ , $Z^+(4248)$ and $Z^+(4200)$ . . . . .	84
4.4.1	Molecular state scheme . . . . .	84
4.4.2	Tetraquark state assignment . . . . .	85
4.4.3	Production and decay patterns . . . . .	85
4.4.4	A short summary . . . . .	85
4.5	$X(3872)$ . . . . .	85

4.5.1	Molecular scheme . . . . .	85
4.5.2	The axial vector tetraquark state . . . . .	90
4.5.3	Radial excitation of the axial vector charmonium . . . . .	93
4.5.4	Lattice QCD . . . . .	94
4.5.5	Other theoretical schemes, production and decay patterns . . . . .	95
4.5.6	A short summary . . . . .	98
4.6	$Y(4260)$ . . . . .	98
4.6.1	Is $Y(4260)$ a higher charmonium? . . . . .	99
4.6.2	The hybrid charmonium . . . . .	99
4.6.3	The vector tetraquark state . . . . .	102
4.6.4	The molecular state . . . . .	103
4.6.5	Non-resonant explanations . . . . .	104
4.6.6	Other theoretical schemes, production and decay patterns . . . . .	104
4.6.7	A short summary . . . . .	106
4.7	$Y(3940)$ , $Y(4140)$ and $Y(4274)$ . . . . .	106
4.7.1	Molecular state scheme . . . . .	106
4.7.2	Other theoretical schemes, production and decay patterns . . . . .	108
4.7.3	A short summary . . . . .	109
4.8	Other charmonium-like states . . . . .	109
4.8.1	$Y(4008)$ and $Y(4360)$ . . . . .	109
4.8.2	$Y(4660)$ and $Y(4630)$ . . . . .	110
4.8.3	$X(3915)$ , $X(4350)$ and $Z(3930)$ . . . . .	112
4.8.4	$X(3940)$ and $X(4160)$ . . . . .	113
4.8.5	Narrow enhancement structures around 4.2 GeV in the hidden-charm channels . . . . .	114
4.8.6	$X(3823)$ . . . . .	116
4.8.7	A short summary . . . . .	117
<b>5</b>	<b>Outlook and summary</b> . . . . .	<b>117</b>
5.1	Current status and future confirmation of the hidden-charm multiquark states . . . . .	117
5.2	Non-resonant schemes . . . . .	119
5.3	Partner states . . . . .	119
5.4	Connections between different XYZ states . . . . .	120
5.5	Open-charm, pionic and radiative decays . . . . .	121
5.6	Hidden-charm baryonium or dibaryons with two charm quarks . . . . .	122
5.7	Future facilities . . . . .	122
5.8	Outlook . . . . .	122

## 1. Introduction

### 1.1. Quark model and the multiquark states

Quantum Chromodynamics (QCD) is the underlying theory of strong interaction. According to QCD, quarks and anti-quarks are in the fundamental representation of the non-Abelian SU(3) color gauge group while gluons belong to the adjoint representation. The QCD Lagrangian reads

$$\mathcal{L} = \bar{\psi}_i (i\gamma^\mu (D_\mu)_{ij} - m\delta_{ij}) \psi_j - \frac{1}{4} G_{\mu\nu}^a G_a^{\mu\nu}, \quad (1)$$

where the covariant derivative is defined as

$$(D_\mu)_{ij} = \partial_\mu \delta_{ij} - igA_\mu^a T_{ij}^a. \quad (2)$$

In Eq. (1),  $\psi_i(x)$  is the quark field, and  $A_\mu^a$  is the gluon field, both of which carry the color charge.  $\gamma_\mu$  is the Dirac matrix and  $T_{ij}^a = \lambda_{ij}^a/2$  is the generator of the SU(3) gauge group.

QCD has three important properties: asymptotic freedom, confinement, approximate chiral symmetry and its spontaneous breaking. Quarks and gluons are confined within the mesons and baryons. Their color interactions increase as the involved energy scale decreases. At the hadronic scale, QCD is highly non-perturbative due to the complicated infrared behavior of the non-Abelian SU(3) gauge group.

At present it's still impossible for us to derive the hadron spectrum analytically from the QCD Lagrangian. Lattice QCD was invented to solve QCD numerically through simulations on the lattice, which has proven very powerful in the calculation of the hadron spectrum and hadronic matrix elements. Besides lattice QCD, many phenomenological models with some kind of QCD spirit were proposed. Among them, the quark model may be the most successful one, which categorizes hadrons into two families: mesons and baryons. The former are made of one quark and one antiquark, and the latter are made of three quarks.

With the experimental progress in the past decade, dozens of charmonium-like  $XYZ$  states have been reported [1]. They provide good opportunities to identify tetraquark states, which are made of two quarks and two antiquarks. Moreover, the LHCb Collaboration recently observed two hidden-charm pentaquark resonances,  $P_c(4380)$  and  $P_c(4450)$ , in the  $J/\psi p$  invariant mass spectrum [2]. They are good candidates of pentaquark states, which are made of four quarks and one antiquark. We shall briefly review the experimental progress on these charmonium-like states and hidden-charm pentaquark resonances in Sec. 2.

To study these tetraquark and pentaquark candidates, the traditional quark model as well as its updated version seems to be incapable any more. Various theoretical frameworks were proposed to interpret these new multi-quark systems, such as the one-boson-exchange (OBE) model, the one-pion-exchange (OPE) model, the chiral unitary model, the QCD sum rule, the chiral quark model, the diquark-antidiquark model etc. We shall briefly introduce these models and review their applications on the hidden-charm pentaquark resonances in Sec. 3, and review the applications of more theoretical frameworks on the charmonium-like states in Sec. 4. An outlook and a brief summary will be given in Sec. 5.

### 1.1.1. Quark model

According to the traditional quark model, a meson is composed of a pair of quark and antiquark and a baryon is composed of three quarks. Both mesons and baryons are color singlets. The quark in the quark model is sometimes denoted as the constituent quark, which is different from the current quark in the QCD Lagrangian. For example, the constituent up/down quark mass is about one third of the nucleon mass or one half of the  $\rho$  meson mass. At the energy scale around 2 GeV, the up/down current quark mass is around several MeV.

Within the quark model, each quark carries the energy  $\sqrt{m^2 + \mathbf{p}^2}$ , where  $m$  is the constituent quark mass and  $\mathbf{p}$  denotes its momentum. In the non-relativistic limit, the energy term is expanded as the sum of the mass and kinetic energy. The inter-quark interactions include the linear confinement force and the one gluon exchange force. There also exist various hyperfine interactions such as the spin-spin interaction, the color-magnetic interaction, the spin-orbit interaction, and the tensor force etc. Up to now, nearly all the mesons and baryons can be classified within such a simple quark model picture.

The discovery of  $J/\psi$  [3, 4] in 1974 inspired theorists to propose potential models [5, 6]. The mass spectrum of the charmonium family was obtained by solving the Schrödinger equation. The hadron spectroscopy was reconsidered in the framework of quark model [7, 8, 9, 10, 11, 12, 13, 14, 15, 16, 17]. In the following, we take the well-known Godfrey-Isgur (GI) quark model as an example and introduce it briefly [17].

In the GI model [17], the interaction between the quark and antiquark is described by the Hamiltonian

$$\mathcal{H} = \sqrt{m_1^2 + \mathbf{p}^2} + \sqrt{m_2^2 + \mathbf{p}^2} + V_{\text{eff}}(\mathbf{p}, \mathbf{r}), \quad (3)$$

where the subscripts 1 and 2 denote the quark and the antiquark, respectively.  $V_{\text{eff}}(\mathbf{p}, \mathbf{r})$  is the effective potential of the  $q\bar{q}$  system, and contains the short-distance one-gluon-exchange interaction and the long-distance linear confining interaction. The latter was at first employed by the Cornell group and later confirmed by the lattice QCD simulations.

$V_{\text{eff}}(\mathbf{p}, \mathbf{r})$  is obtained from the on-shell  $q\bar{q}$  scattering amplitudes in the center-of-mass (CM) frame [17]. In the non-relativistic limit,  $V_{\text{eff}}(\mathbf{p}, \mathbf{r})$  is transformed into the standard non-relativistic potential  $V_{\text{eff}}(r)$ :

$$V_{\text{eff}}(r) = H^{\text{conf}} + H^{\text{hyp}} + H^{\text{SO}}. \quad (4)$$

The first term  $H^{\text{conf}}$  includes the spin-independent linear confinement and Coulomb-type interactions

$$H^{\text{conf}} = -\left[\frac{3}{4}c + \frac{3}{4}br - \frac{\alpha_s(r)}{r}\right] \mathbf{F}_1 \cdot \mathbf{F}_2, \quad (5)$$

the second term  $H^{\text{hyp}}$  is the color-hyperfine interaction

$$H^{\text{hyp}} = -\frac{\alpha_s(r)}{m_1 m_2} \left[ \frac{8\pi}{3} \mathbf{S}_1 \cdot \mathbf{S}_2 \delta^3(\mathbf{r}) + \frac{1}{r^3} \left( \frac{3\mathbf{S}_1 \cdot \mathbf{r} \mathbf{S}_2 \cdot \mathbf{r}}{r^2} - \mathbf{S}_1 \cdot \mathbf{S}_2 \right) \right] \mathbf{F}_1 \cdot \mathbf{F}_2, \quad (6)$$

and the third term  $H^{\text{SO}}$  is the spin-orbit interaction

$$H^{\text{SO}} = H^{\text{SO(cm)}} + H^{\text{SO(tp)}}, \quad (7)$$

where  $H^{\text{SO(cm)}}$  is the color-magnetic term and  $H^{\text{SO(tp)}}$  is the Thomas-precession term, i.e.,

$$H^{\text{SO(cm)}} = -\frac{\alpha_s(r)}{r^3} \left( \frac{1}{m_1} + \frac{1}{m_2} \right) \left( \frac{\mathbf{S}_1}{m_1} + \frac{\mathbf{S}_2}{m_2} \right) \cdot \mathbf{L} \mathbf{F}_1 \cdot \mathbf{F}_2, \quad (8)$$

$$H^{\text{SO(tp)}} = \frac{-1}{2r} \frac{\partial H^{\text{conf}}}{\partial r} \left( \frac{\mathbf{S}_1}{m_1^2} + \frac{\mathbf{S}_2}{m_2^2} \right) \cdot \mathbf{L}. \quad (9)$$

In the above expressions,  $\mathbf{S}_1/\mathbf{S}_2$  denotes the spin of the quark/antiquark and  $\mathbf{L}$  is the orbital momentum between the quark and the antiquark.  $\mathbf{F}$  is related to the Gell-Mann matrix,  $\mathbf{F}_1 = \lambda_1/2$  and  $\mathbf{F}_2 = -\lambda_2^*/2$ . Especially, we have  $\langle \mathbf{F}_1 \cdot \mathbf{F}_2 \rangle = -4/3$  for the mesons.

The relativistic effects were also taken into account in the GI model. More details of the GI model can be found in Appendices of Ref. [17]. The GI quark model was very successful in the description of the spectrum and static properties of the mesons and baryons.

### 1.1.2. Exotic states and multiquark states

According to the quark model, the parity  $P = (-)^{L+1}$  and  $C$ -parity  $C = (-)^{L+S}$  for a neutral meson, where  $L$  and  $S$  are the orbital and spin angular momentum, respectively. The allowed  $J^{PC}$  reads:  $0^{-+}, 0^{++}, 1^{--}, 1^{+-}, 1^{++}, \dots$ . In contrast, a conventional  $q\bar{q}$  meson in the quark model can not carry the following quantum numbers:  $0^{--}, 0^{+-}, 1^{-+}, 2^{+-}, \dots$ . States with these  $J^{PC}$  quantum numbers are beyond the naive quark model, which are sometimes denoted as the exotic or non-conventional states. Different from the meson case, the  $qqq$  baryon in the quark model can exhaust all the  $J^P$  quantum numbers, i.e.,  $J^P = \frac{1}{2}^{\pm}, \frac{3}{2}^{\pm}, \frac{5}{2}^{\pm}, \dots$ .

However, the constituent quark model can not be derived rigorously from QCD. The quark model spectrum is not necessarily the same as the QCD hadron spectrum. QCD may allow much richer hadron spectrum.

In fact, at the birth of the quark model [18, 19], Gell-Mann and Zweig proposed not only the existence of the  $q\bar{q}$  mesons and  $qqq$  baryons but also the possible existence of the  $qq\bar{q}\bar{q}$  tetraquarks and  $qqqq\bar{q}$  pentaquarks. The concept of the multiquarks was proposed even before the advent of quantum chromodynamics (QCD)!

In Ref. [18], M. Gell-Mann wrote: “Baryons can now be constructed from quarks by using the combinations ( $qqq$ ), ( $qqq\bar{q}$ ), etc., while mesons are made out of ( $q\bar{q}$ ), ( $qq\bar{q}\bar{q}$ ), etc.”

In Ref. [19], G. Zweig also wrote: “In general, we would expect that baryons are built not only from the product of these aces, AAA, but also from  $\bar{A}AAAA$ ,  $\bar{A}\bar{A}AAAA$ , etc., where  $\bar{A}$  denotes an anti-ace. Similarly, mesons could be formed from  $\bar{A}A$ ,  $\bar{A}\bar{A}AA$ , etc.”

The multiquarks can be further classified into tetraquarks ( $qq\bar{q}\bar{q}$ ), pentaquarks ( $qqqq\bar{q}$ ), dibaryon ( $qqqqqq$ ) and baryonium ( $qqq\bar{q}\bar{q}\bar{q}$ ) etc. Jaffe studied the tetraquark states within the framework of the MIT bag model in 1976 [20, 21]. Strotmann investigated the pentaquarks ( $qqqq\bar{q}$ ) composed of light quarks in 1979 [22]. The name “pentaquark” was first proposed by Lipkin in 1987 [23]. Two groups studied possible pentaquarks containing one charm quark in 1987 [24, 23].

In 2003, the LEPS Collaboration announced the observation of the  $\Theta$  pentaquark which is composed of  $uudd\bar{s}$  [25]. However, this state was not confirmed by the subsequent more advanced experiments [26].

Jaffe also discussed the H-dibaryon, where six light quarks  $uuddss$  are confined within one MIT bag [21]. In nature there exists the deuteron which is also composed of six light quarks. The difference between the dibaryon and deuteron lies in their color configurations. Within the deuteron, there are two quark clusters, both of which are color singlets. For the dibaryon, one expects six quarks within one cluster.

In QCD, the gluons not only mediate the strong interaction between quarks but also interact among themselves since they carry color charges. Two or more gluons may form the color singlet, which is called the glueball. One or more gluons may interact with a pair of quark and antiquark to form the hybrid meson. The hybrid mesons or tetraquark states or the glueballs can carry all the so-called exotic  $J^{PC}$  quantum numbers in the quark model. Strictly speaking, there does not exist any exotic quantum number from the viewpoint of QCD. One can construct color-singlet local operators to verify that these quantum numbers are allowed in QCD. We shall illustrate this point in the following sections. Throughout this review, either the word “exotic” or “non-conventional” should be understood within the context of the quark model.

### 1.1.3. Comparison of QED and QCD and their spectrum

Quantum Electrodynamics (QED) is very different from QCD. The gauge group of QED is U(1). The photon mediates the electromagnetic interactions between charges. However, the photon is neutral and does not carry charge. There does not exist the photon self-interaction. We do not have the analogue of the glueball and hybrid meson in QED. Instead there are free electrons and photons while all quarks and gluons are confined within the hadrons.

Except the above big difference, it’s intriguing to notice the similarity between QED and QCD. In the following, we compare the well-known bound states in QED and possible hadrons in QCD. In QED we have the bound states composed of  $e^+e^-$ ,  $\mu^+\mu^-$ ,  $\mu^+e^-$ . In QCD we have the light mesons composed of  $q\bar{q}$ ,  $s\bar{s}$ ,  $s\bar{q}$ , where  $q = u, d$  is the up/down quark, and  $s$  is the strange quark. For the hydrogen atom in QED, the electron circles around the proton. For the heavy-flavored meson/baryon in QCD, the light quarks circle around the heavy charm or bottom quark.

In QED there exist the bound states composed of  $e^+e^-e^+e^-$  and  $e^+e^-\mu^+\mu^-$  [27, 28]. In QCD some of the scalar mesons below 1 GeV may have the flavor configurations  $q\bar{q}q\bar{q}$  and  $q\bar{q}s\bar{s}$ . In QED we have the hydrogen molecule where two electrons are shared by the two protons and the valence bond binds this system tightly. In QCD we may expect the  $q\bar{Q}q\bar{Q}$  and  $\bar{q}Qq\bar{Q}$  tetraquark states within one MIT bag, where the two light quarks are shared by the two heavy quarks.

In QED there exist many molecules which are loosely bound by the van der Waals force. The van der Waals force is nothing but the residual electromagnetic force arising from the two-photon exchange process in QED. In QCD we have the deuteron which is the hadronic molecular state bound by the meson exchange force. At the quark-gluon level, the meson exchange force is the residual strong interaction force arising from the gluon and quark exchange process. In QCD we may also expect other loosely bound deuteron-like molecular states composed of two heavy flavored hadrons.

### 1.2. General status of hadron spectroscopy

Although most of the observed hadrons can be classified as the ordinary  $q\bar{q}$  mesons and  $qqq$  baryons, there have been huge theoretical and experimental efforts to search for the candidates of the exotic hadrons. These exotic states encode important information of QCD. For example, the identification of the glueballs and hybrid mesons will establish the direct evidence of the dynamical role of the gluons in the low energy sector.

The exotic  $J^{PC}$  quantum numbers provide a convenient handle in the search of the nonconventional states. If a resonance decays into the final state with  $J^{PC} = 1^{-+}$ , the parent resonance is a good candidate of the hybrid meson.

On the other hand, the exotic flavor quantum number is also a valuable asset in the experimental search of the exotic states. If the resonance carries the isospin  $I = 2$  or a meson has an isospin  $I = 3/2$ , it may be a multiquark candidate. For the  $\Theta$  resonance, its baryon number is 1 and strangeness  $S = +1$ . Hence, it must be a candidate of pentaquarks.

Some hadrons do not have exotic  $J^{PC}$  or flavor quantum numbers. But they may have exotic color or flavor or spatial configurations. These states can be searched for through the overpopulation of the quark model spectrum. Sometimes the deviation from the quark model predictions of their masses, decay widths, various reactions, production and decay behaviors may also provide insightful clues in the search of the exotic states.

Let’s take the  $J^{PC} = 0^{++}$  scalar isoscalar mesons as an example. Below 2 GeV, we have  $\sigma$ ,  $f_0(980)$ ,  $f_0(1370)$ ,  $f_0(1500)$ ,  $f_0(1710)$ ,  $f_0(1790)$ ,  $f_0(1810)$  [1]. Within the quark model, there are only four scalar isoscalar mesons

within this mass range even if we consider the radial excitations. Clearly there is serious overpopulation of the scalar spectrum. The quark content of some of the above states can not be  $q\bar{q}$ . Overpopulation of the spectrum provides another useful window in the experimental search of the non-conventional states.

Let's move on to the nine scalar mesons below 1 GeV, which play a fundamental role in the spontaneous breaking of the chiral symmetry in QCD. The scalar meson carries one orbital excitation. Hence, its mass is expected to be several hundred MeV higher than the  $\rho$  meson mass in the quark model. Either lattice QCD simulation or other theoretical approaches indicates the  $L = 1$   $q\bar{q}$  state lies around 1.2 GeV. Within the quark model, the  $f_0(980)$  meson with the quark content  $s\bar{s}$  should be 200 ~ 300 MeV heavier than the  $a_0(980)$  with the quark content  $q\bar{q}$ . However, they are almost degenerate in reality. The unusual low mass of the scalar nonet and the abnormal mass ordering of the  $f_0(980)$  and  $a_0(980)$  are two puzzles in the quark model. In contrast, both puzzles can be solved very naturally if the scalar mesons belong to the tetraquark nonet [21, 29].

Since 2003, many charmonium-like states have been observed through  $B$  meson decays, the initial state radiation (ISR), double charmonium production, two photon fusion, and excited charmonium or bottomonium decays. Some of them do not fit into the quark model spectrum easily and are proposed as the candidates of the hidden-charm exotic mesons, including the di-meson molecular states, tetraquarks, hybrid charmonium states and conventional charmonium states distorted by the coupled-channel effects, etc. Molecular states are loosely bound states composed of a pair of heavy mesons. They are probably bound by the long-range color-singlet pion exchange. Tetraquarks are bound states of two quarks and two antiquarks, which are bound by the colored force between quarks and antiquarks. There are many states within the same tetraquark multiplet. Some members are charged or even carry strangeness. Hybrid charmonia are bound states composed of a charm quark-antiquark pair and one excited gluon.

In this review, we focus on the recent experimental and theoretical progress on the hidden-charm multi-quark systems such as hybrid charmonia, hidden-charm tetraquarks, hidden-charm pentaquarks, and hadronic molecules composed of a pair of heavy-flavored hadrons. Interested readers may also consult reviews in Refs. [30, 31, 32, 33, 34, 35, 36, 37, 38, 39, 40, 41, 42, 43, 44, 45, 46, 47, 48].

## 2. Experimental progress on the hidden-charm multi-quark states

### 2.1. The Charmonium-like XYZ states

With the experimental progress, the family of the charmonium-like states has become more and more abundant. To date, dozens of charmonium-like states have been observed by several major particle physics experimental collaborations such as CLEO-c, BaBar, Belle, BESIII, CDF, DØ, LHCb, CMS and so on. Since 2003, these collaborations have been continuing to surprise us with novel discoveries, which have inspired theorists' extensive interests in exploring the underlying mechanism behind those exotic phenomena. As one of the most important issues in hadron physics, the study of the charmonium-like states provides us a good chance to deepen our understanding of the complicated non-perturbative behavior of QCD in the low energy regime. Especially, investigations of the underlying structures of the charmonium-like states may help us to understand the mechanism of the confinement and chiral symmetry breaking better.

All the above major particle physics experimental collaborations have contributed to the observations of the charmonium-like states. Before reviewing the experimental status of the charmonium-like states, we would like to introduce the collaborations briefly:

1. **CLEO-c**: CLEO-c was the experiment at the Cornell Electron Storage Ring (CESR) located at Wilson Laboratory of Cornell University. As the upgrade of CLEO, the CLEO-c experiment ran at lower energies and carried out the study of charmonia and charmed mesons due to the competition from two  $B$  factories BaBar and Belle. The CLEO-c experiment confirmed the observation of the  $Y(4260)$  [49]. Although CLEO-c finished data-collecting on 3 March 2008, the accumulated CLEO-c data was applied to confirm the observation of the charged charmonium-like structure  $Z_c(3900)$  [50].
2. **BaBar**: As one of the two  $B$  factories, the BaBar experiment was designed to study CP violation in the  $B$  meson system. Its detector was located at SLAC National Accelerator Laboratory, which ceased operation on 7 April 2008. However, its data analysis is still ongoing. Due to the development of the Initial State Radiation (ISR) technique, the BaBar experiment also focused on the study of charmonia and charmonium-like states. In the

past decade, BaBar has played a crucial role in the discoveries of many charmonium-like states. For example, BaBar first observed the famous  $Y(4260)$  in the  $e^+e^- \rightarrow J/\psi\pi^+\pi^-$  process [51].

3. **Belle:** As the other  $B$  factory, the Belle experiment was located at the High Energy Accelerator Research Organization (KEK), which was also set up to study CP violation in the  $B$  meson system. As a byproduct, the Belle Collaboration discovered many charmonium-like states. For example, Belle reported the observation of the  $X(3872)$  in 2003 [52], which is the first member in the family of the charmonium-like states. Although Belle finished its data-taking on 30 June 2010, its data analysis is going on.
4. **BESIII:** BESIII is the experiment at Beijing Electron-Positron Collider II (BEPC II), located at Institute of High Energy Physics (IHEP). Since its center of mass energy can go up to 4.6 GeV, the BESIII experiment has become an ideal platform to explore the charmonium-like states. In 2013, BESIII announced the observation of the charged charmonium-like structure  $Z_c(3900)$  [53].
5. **CDF and DØ:** CDF and DØ were the two particle experiments located at the Tevatron at Fermilab. They discovered the top quark in 1995 [54, 55]. The CDF and DØ experiments both confirmed the  $X(3872)$  [56, 57]. The CDF Collaboration also reported the charmonium-like state  $Y(4140)$  [58].
6. **LHCb:** As one of seven particle physics experiments at the Large Hadron Collider (LHC) at CERN, the LHCb experiment focuses on  $B$ -physics. LHCb also studies the productions of the charmonium-like states through the direct  $pp$  collisions and the  $B$  meson decays. For example, the LHCb Collaboration measured the spin-parity quantum number of the  $X(3872)$  [59].
7. **CMS:** CMS is another important experiment at LHC at CERN. The CMS and ATLAS collaborations discovered the Higgs Boson in July 2012 [60, 61]. In recent years, CMS also contributed to the search of the charmonium-like states such as the  $X(3872)$  [62] and the  $Y(4140)$  [63].



Figure 1: (Color online) The logos of the experimental collaborations which contributed to the observation of the charmonium-like states.

In Fig. 1, we collect Logos of these experimental collaborations which have contributed to the observations of the charmonium-like states.

According to the different production mechanisms, all the observed charmonium-like states can be categorized into five groups as shown in Fig. 2. The states collected in the first, second, third, and fourth columns are produced via the  $B$  meson decays, initial state radiation technique (ISR) in the  $e^+e^-$  annihilation, the double charmonium production processes, and two photon fusion processes, respectively. The  $Z_c(3900)/Z_c(4025)/Z_c(3885)/Z_c(4200)$  listed in the fifth column are produced from the hadronic decays of the  $Y(4260)$ .

### 2.1.1. XYZ states produced through $B$ meson decays

2.1.1.1.  $X(3872)$ . The  $X(3872)$  resonance was first observed by the Belle Collaboration in 2003 [52]. Since its discovery, its existence was confirmed by many subsequent experiments [64, 65, 66, 67, 68, 69, 56, 70, 71, 72, 57, 73, 74, 75, 76, 77, 78, 79, 80, 59, 81, 62, 82] as shown in Fig. 3. Despite the huge experimental efforts, we still do not fully understand its nature.

The mass and width of the  $X(3872)$  from different experiments are summarized in Table 1. A fit to these parameters yields an average mass  $(3871.69 \pm 0.17)$  MeV [1] and a width  $< 1.2$  MeV at 90% C.L. [69]. Its mass is extremely

<p><math>X(3872)</math></p> <p><math>Y(3940)</math></p> <p><math>Z^+(4430)</math></p> <p><math>Z^+(4051)</math></p> <p><math>Z^+(4248)</math></p> <p><math>Y(4140)</math></p> <p><math>Y(4274)</math></p> <p><math>Z_c^+(4200)</math></p> <p><math>Z^+(4240)</math></p> <p><math>X(3823)</math></p>	<p><math>Y(4260)</math></p> <p><math>Y(4008)</math></p> <p><math>Y(4360)</math></p> <p><math>Y(4630)</math></p> <p><math>Y(4660)</math></p>	<p><math>X(3940)</math></p> <p><math>X(4160)</math></p>	<p><math>X(3915)</math></p> <p><math>X(4350)</math></p> <p><math>Z(3930)</math></p>	<p><math>Z_c(3900)</math></p> <p><math>Z_c(4025)</math></p> <p><math>Z_c(4020)</math></p> <p><math>Z_c(3885)</math></p>

Figure 2: (Color online) Five groups of the charmonium-like states corresponding to five production mechanisms.

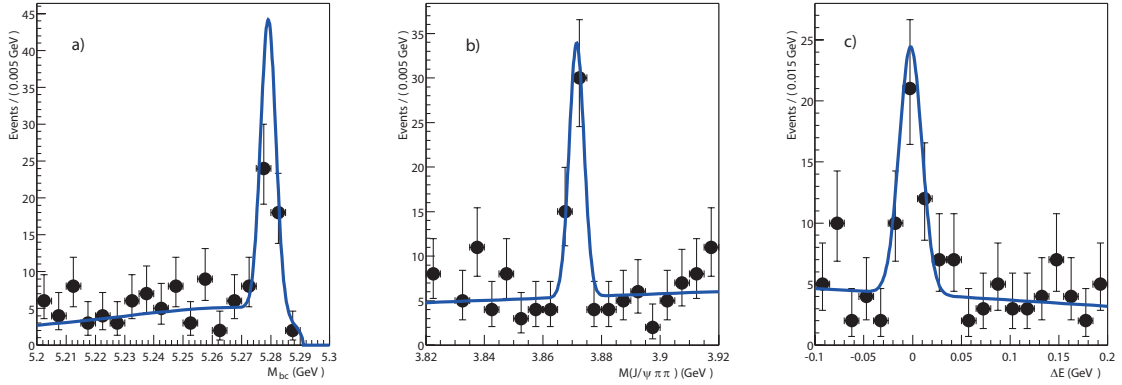


Figure 3: (Color online) The beam-energy constrained mass  $M_{bc} = \sqrt{(E_{\text{beam}}^{\text{CM}})^2 - (p_B^{\text{CM}})^2}$  (left), the  $\pi^+ \pi^- J/\psi$  invariant mass (middle), and the energy difference  $\Delta E = E_B^{\text{CM}} - E_{\text{beam}}^{\text{CM}}$  (right) for the  $X(3872) \rightarrow \pi^+ \pi^- J/\psi$  signal region, from Belle [52].

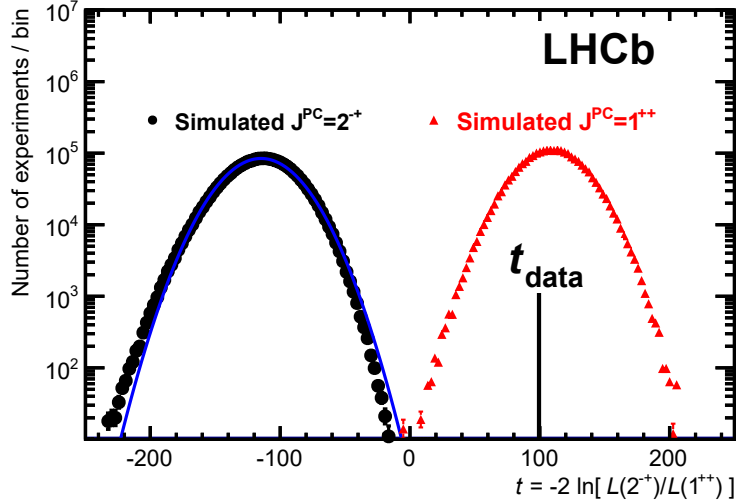


Figure 4: (Color online) Distribution of the test statistic  $t$  for the simulated experiments with  $J^{PC} = 2^{-+}$  and  $1^{++}$ , from LHCb [59], with  $t_{\text{data}}$  the value of the test statistic for the data.

close to the  $D^0 \bar{D}^{*0}$  mass threshold,  $(3871.81 \pm 0.09)$  MeV. We also collect its productions and decay modes in Table 1. The  $X(3872)$  was mostly observed in the  $B$  meson decay process  $B^{\pm,0} \rightarrow K_{(S)}^{\pm,0} X(3872)$  with the  $X(3872)$  decaying into  $\pi^+ \pi^- J/\psi$ . The  $X(3872)$  was also produced in  $p\bar{p}$  annihilations,  $pp$  collisions, and  $e^+e^-$  annihilations (possibly through the  $Y(4260)$ , see Sec. 2.1.2.1) and decays into  $D^{*0} \bar{D}^0$ ,  $D^0 \bar{D}^0 \pi^0$ ,  $\gamma J/\psi$ ,  $\gamma \psi(3686)$ , and  $\omega J/\psi$  with  $\omega$  decaying into  $\pi^+ \pi^- \pi^0$ . Its quantum numbers have been studied by Belle, BaBar and CDF, and determined to be  $I^G J^{PC} = 0^+ 1^{++}$  by the recent LHCb experiment [59], as shown in Fig. 4.

Besides the resonance parameters listed in Table 1, these experiments provided many branching fractions. They are also useful experimental information, and we summarize some of them in Table 2. Particularly, we list the following isospin-violating branching fractions

$$\frac{\Gamma(X \rightarrow \pi^+ \pi^- \pi^0 J/\psi)}{\Gamma(X \rightarrow \pi^+ \pi^- J/\psi)} = 1.0 \pm 0.4 \pm 0.3, \quad (10)$$

$$\frac{\Gamma(X \rightarrow \omega J/\psi)}{\Gamma(X \rightarrow \pi^+ \pi^- J/\psi)} = \begin{cases} 0.7 \pm 0.3 & \text{for } B^+ \text{ events} \\ 1.7 \pm 1.3 & \text{for } B^0 \text{ events} \end{cases}, \quad (11)$$

which were observed by Belle [64] and BaBar [79], respectively.

The difference between  $B^0 \rightarrow K^0 X$  and  $B^\pm \rightarrow K^\pm X$  also attracted much experimental interest. The Belle Collaboration measured the ratio of branching fractions  $\Gamma(B^0 \rightarrow K^0 X)/\Gamma(B^+ \rightarrow K^+ X)$  to be  $(0.82 \pm 0.22 \pm 0.05)$  [66],  $(1.26 \pm 0.65 \pm 0.06)$  [67] and  $(0.50 \pm 0.14 \pm 0.04)$  [69], and the mass difference between the  $X(3872)$  states produced in  $B^+$  and  $B^0$  decay to be  $\delta M = M_{(B^+ \rightarrow K^+ X)} - M_{(B^0 \rightarrow K^0 X)} = (0.18 \pm 0.89 \pm 0.26)$  MeV [66] and  $(-0.69 \pm 0.97 \pm 0.19)$  MeV [69], while the BaBar Collaboration measured this ratio to be  $(0.50 \pm 0.30 \pm 0.05)$  [74], and  $(0.41 \pm 0.24 \pm 0.05)$  [77], and this mass difference to be  $(2.7 \pm 1.3 \pm 0.2)$  MeV [74] and  $(2.7 \pm 1.6 \pm 0.4)$  MeV [77], where we have assumed experimental results from  $B^+$  and  $B^-$  are the same.

Besides the above observations, the  $X(3872)$  resonance was not seen (all values are given at 90% confidence level (C.L.)):

1. in the  $\gamma \chi_{c1}$  decay mode in Belle [52], and the upper limit was measured to be

$$\frac{\Gamma(X(3872) \rightarrow \gamma \chi_{c1})}{\Gamma(X(3872) \rightarrow \pi^+ \pi^- J/\psi)} < 0.89. \quad (12)$$

Table 1: The resonance parameters of the  $X(3872)$  and its observed productions and decay channels. Here the  $X(3872)$  is abbreviated as  $X$ .

Experiment	Mass [MeV]	Width [MeV]	Productions and Decay Modes	$J^{PC}$
Belle [52]	$3872 \pm 0.6 \pm 0.5$	$< 2.3$	$B \rightarrow KX(\rightarrow \pi^+\pi^- J/\psi)$	
Belle [64]	–	–	$B \rightarrow KX(\rightarrow \gamma J/\psi, \omega J/\psi \rightarrow \pi^+\pi^-\pi^0 J/\psi)$	$C = +1$
Belle [65]	$3875.4 \pm 0.7^{+0.4}_{-1.7} \pm 0.9$	–	$B \rightarrow KX(\rightarrow D^0\bar{D}^0\pi^0)$	$1^{++}/2^{++}$
Belle [66]	$3871.46 \pm 0.37 \pm 0.07$	–	$B \rightarrow KX(\rightarrow \pi^+\pi^- J/\psi)$	
Belle [67]	$3872.9^{+0.6+0.4}_{-0.4-0.5}$	$3.9^{+2.8+0.2}_{-1.4-1.1}$	$B \rightarrow KX(\rightarrow D^{*0}\bar{D}^0)$	
Belle [68]	–	–	$B \rightarrow KX(\rightarrow \gamma J/\psi)$	
Belle [69]	$3871.84 \pm 0.27 \pm 0.19$	$< 1.2$	$B \rightarrow KX(\rightarrow \pi^+\pi^- J/\psi)$	
CDF [56]	$3871.3 \pm 0.7 \pm 0.4$	–	$p\bar{p} \rightarrow \text{anything} + X(\rightarrow \pi^+\pi^- J/\psi)$	
CDF [70]	–	–	$p\bar{p} \rightarrow \text{anything} + X(\rightarrow \pi^+\pi^- J/\psi)$	$C = +1$
CDF [71]	–	–	$p\bar{p} \rightarrow \text{anything} + X(\rightarrow \pi^+\pi^- J/\psi)$	$1^{++}/2^{--}$
CDF [72]	$3871.61 \pm 0.16 \pm 0.19$	–	$p\bar{p} \rightarrow \text{anything} + X(\rightarrow \pi^+\pi^- J/\psi)$	
DØ [57]	$3871.8 \pm 3.1 \pm 3.0$	–	$p\bar{p} \rightarrow \text{anything} + X(\rightarrow \pi^+\pi^- J/\psi)$	
BaBar [73]	$3873.4 \pm 1.4$	–	$B^- \rightarrow K^- X(\rightarrow \pi^+\pi^- J/\psi)$	
BaBar [74]	$3871.3 \pm 0.6 \pm 0.1$	$< 4.1$	$B^- \rightarrow K^- X(\rightarrow \pi^+\pi^- J/\psi)$	
	$3868.6 \pm 1.2 \pm 0.2$	–	$B^0 \rightarrow K^0 X(\rightarrow \pi^+\pi^- J/\psi)$	
BaBar [75]	–	–	$B \rightarrow KX(\rightarrow \gamma J/\psi)$	$C = +1$
BaBar [76]	$3875.1^{+0.7}_{-0.5} \pm 0.5$	$3.0^{+1.9}_{-1.4} \pm 0.9$	$B \rightarrow KX(\rightarrow \bar{D}^{*0}D^0)$	
BaBar [77]	$3871.4 \pm 0.6 \pm 0.1$	$< 3.3$	$B^+ \rightarrow K^+ X(\rightarrow \pi^+\pi^- J/\psi)$	
	$3868.7 \pm 1.5 \pm 0.4$	–	$B^0 \rightarrow K^0 X(\rightarrow \pi^+\pi^- J/\psi)$	
BaBar [78]	–	–	$B \rightarrow KX(\rightarrow \gamma J/\psi, \rightarrow \gamma\psi(3686))$	
BaBar [79]	$3873.0^{+1.8}_{-1.6} \pm 1.3$	–	$B \rightarrow KX(\rightarrow \omega J/\psi \rightarrow \pi^+\pi^-\pi^0 J/\psi)$	$2^-$
LHCb [80]	$3871.95 \pm 0.48 \pm 0.12$	–	$pp \rightarrow \text{anything} + X(\rightarrow \pi^+\pi^- J/\psi)$	
LHCb [59]	–	–	$pp \rightarrow \text{anything} + X(\rightarrow \pi^+\pi^- J/\psi)$	$1^{++}$
LHCb [81]	–	–	$pp \rightarrow \text{anything} + X(\rightarrow \gamma J/\psi, \rightarrow \gamma\psi(3686))$	
CMS [62]	–	–	$pp \rightarrow \text{anything} + X(\rightarrow \pi^+\pi^- J/\psi)$	
BESIII [82]	$3871.9 \pm 0.7 \pm 0.2$	$< 2.4$	$e^+e^-[\rightarrow Y(4260)] \rightarrow \gamma X(\rightarrow \pi^+\pi^- J/\psi)$	

Table 2: Some product branching fractions of the  $X(3872)$  resonance. Here, the  $X(3872)$  is abbreviated as  $X$ .

Experiment	Product Branching Fractions
Belle [52]	$\frac{\mathcal{B}(B^+ \rightarrow K^+ X) \times \mathcal{B}(X \rightarrow \pi^+ \pi^- J/\psi)}{\mathcal{B}(B^+ \rightarrow K^+ \psi(3686)) \times \mathcal{B}(\psi(3686) \rightarrow \pi^+ \pi^- J/\psi)} = 0.063 \pm 0.012 \pm 0.007$
Belle [64]	$\mathcal{B}(B \rightarrow KX) \times \mathcal{B}(X \rightarrow \gamma J/\psi) = (1.8 \pm 0.6 \pm 0.1) \times 10^{-6}$
Belle [65]	$\mathcal{B}(B \rightarrow KD^0 \bar{D}^0 \pi^0) = (1.27 \pm 0.31^{+0.22}_{-0.39}) \times 10^{-4}$ , near $X$ threshold
Belle [67]	$\mathcal{B}(B \rightarrow KX) \times \mathcal{B}(X \rightarrow D^{*0} \bar{D}^0) = (0.80 \pm 0.20 \pm 0.10) \times 10^{-4}$
Belle [68]	$\mathcal{B}(B^+ \rightarrow K^+ X) \times \mathcal{B}(X \rightarrow \gamma J/\psi) = (1.78^{+0.48}_{-0.44} \pm 0.12) \times 10^{-6}$
Belle [69]	$\mathcal{B}(B^+ \rightarrow K^+ X) \times \mathcal{B}(X \rightarrow \pi^+ \pi^- J/\psi) = (8.61 \pm 0.82 \pm 0.52) \times 10^{-6}$
BaBar [73]	$\mathcal{B}(B^- \rightarrow K^- X) \times \mathcal{B}(X \rightarrow \pi^+ \pi^- J/\psi) = (1.28 \pm 0.41) \times 10^{-5}$
BaBar [74]	$\mathcal{B}(B^0 \rightarrow K^0 X) \times \mathcal{B}(X \rightarrow \pi^+ \pi^- J/\psi) = (5.1 \pm 2.8 \pm 0.7) \times 10^{-6}$ $\mathcal{B}(B^- \rightarrow K^- X) \times \mathcal{B}(X \rightarrow \pi^+ \pi^- J/\psi) = (10.1 \pm 2.5 \pm 1.0) \times 10^{-6}$
BaBar [75]	$\mathcal{B}(B^+ \rightarrow K^+ X) \times \mathcal{B}(X \rightarrow \gamma J/\psi) = (3.3 \pm 1.0 \pm 0.3) \times 10^{-6}$
BaBar [77]	$\mathcal{B}(B^+ \rightarrow K^+ X) \times \mathcal{B}(X \rightarrow \pi^+ \pi^- J/\psi) = (8.4 \pm 1.5 \pm 0.7) \times 10^{-6}$ $\mathcal{B}(B^0 \rightarrow K^0 X) \times \mathcal{B}(X \rightarrow \pi^+ \pi^- J/\psi) = (3.5 \pm 1.9 \pm 0.4) \times 10^{-6}$
BaBar [78]	$\mathcal{B}(B^\pm \rightarrow K^\pm X) \times \mathcal{B}(X \rightarrow \gamma J/\psi) = (2.8 \pm 0.8 \pm 0.1) \times 10^{-6}$ $\mathcal{B}(B^\pm \rightarrow K^\pm X) \times \mathcal{B}(X \rightarrow \gamma \psi(3686)) = (9.5 \pm 2.7 \pm 0.6) \times 10^{-6}$
BaBar [79]	$\mathcal{B}(B^+ \rightarrow K^+ X) \times \mathcal{B}(X \rightarrow \omega J/\psi) = (0.6 \pm 0.2 \pm 0.1) \times 10^{-5}$ $\mathcal{B}(B^0 \rightarrow K^0 X) \times \mathcal{B}(X \rightarrow \omega J/\psi) = (0.6 \pm 0.3 \pm 0.1) \times 10^{-5}$
LHCb [80]	$\sigma(pp \rightarrow \text{anything} + X) \times \mathcal{B}(X \rightarrow \pi^+ \pi^- J/\psi) = (5.4 \pm 1.3 \pm 0.8)$ nb, for $5 < p_T < 20$ GeV
CMS [62]	$\sigma(pp \rightarrow \text{anything} + X) \times \mathcal{B}(X \rightarrow \pi^+ \pi^- J/\psi) = (1.06 \pm 0.11 \pm 0.15)$ nb, for $10 < p_T < 30$ GeV
BESIII [82]	$\sigma^B(e^+ e^- \rightarrow \gamma X) \times \mathcal{B}(X \rightarrow \pi^+ \pi^- J/\psi) = (0.33 \pm 0.12 \pm 0.02)$ nb, at $\sqrt{s} = 4.260$ GeV

2. in the  $\eta J/\psi$  decay mode in BaBar [83], and the upper limit was measured to be

$$\mathcal{B}(B^\pm \rightarrow K^\pm X(3872)) \times \mathcal{B}(X(3872) \rightarrow \eta J/\psi) < 7.7 \times 10^{-6}. \quad (13)$$

3. in the  $\gamma\psi(3686)$  decay mode in Belle [68], and the upper limit was measured to be

$$\frac{\Gamma(X(3872) \rightarrow \gamma\psi(3686))}{\Gamma(X(3872) \rightarrow \gamma J/\psi)} < 2.1. \quad (14)$$

However, both the BaBar and LHCb experiments observed this decay mode, and this branching fraction was measured to be  $(3.4 \pm 1.4)$  [78] and  $(2.46 \pm 0.64 \pm 0.29)$  [81], respectively.

Another useful upper limit is

$$\mathcal{B}(B^\pm \rightarrow K^\pm X(3872)) < 3.2 \times 10^{-4}, \quad (15)$$

which was given by the BaBar Collaboration at 90% C.L. [84].

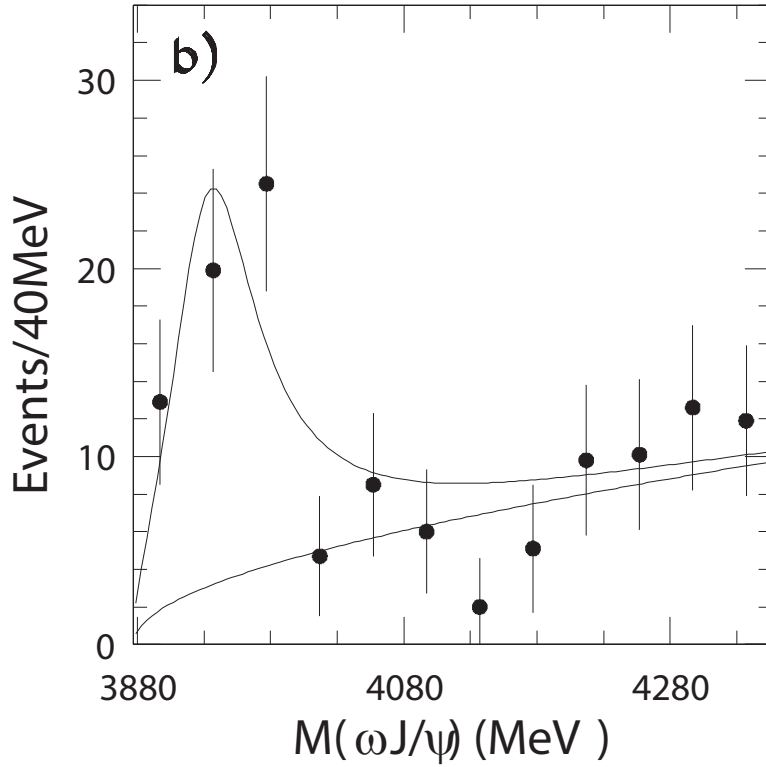


Figure 5: The  $\omega J/\psi$  invariant mass spectrum of  $B \rightarrow K\omega J/\psi$  from Belle [85].

2.1.1.2.  $Y(3940)$ . The charmonium-like state  $Y(3940)$  was firstly reported by the Belle Collaboration in the  $\omega J/\psi$  invariant mass distribution in the exclusive  $B \rightarrow K\omega J/\psi$  decay in 2004 [85], as shown in Fig. 5. Its statistical significance was estimated to be greater than  $8\sigma$ , and its mass and width were measured to be  $M = (3943 \pm 11 \pm 13)$  MeV and  $\Gamma = (87 \pm 22 \pm 26)$  MeV, respectively. This mass value is very close to that of the  $X(3940)$  resonance, which was observed in the double charmonium production and will be discussed in Sec. 2.1.3.1. The Belle Collaboration also measured the product of branching fractions, i.e.,

$$\mathcal{B}(B \rightarrow KY(3940)) \times \mathcal{B}(Y(3940) \rightarrow \omega J/\psi) = (7.1 \pm 1.3 \pm 3.1) \times 10^{-5}. \quad (16)$$

Later, the BaBar Collaboration confirmed this observation in the same process with a lower mass. In 2007, its mass and width were measured to be  $M = (3914.6_{-3.4}^{+3.8} \pm 2.0)$  MeV and  $\Gamma = (34_{-8}^{+12} \pm 5)$  MeV, respectively [86]. In the subsequent experiment in 2010 [79] its mass and width were measured to be  $M = (3919.1_{-3.5}^{+3.8} \pm 2.0)$  MeV and  $\Gamma = (31_{-8}^{+10} \pm 5)$  MeV, respectively.

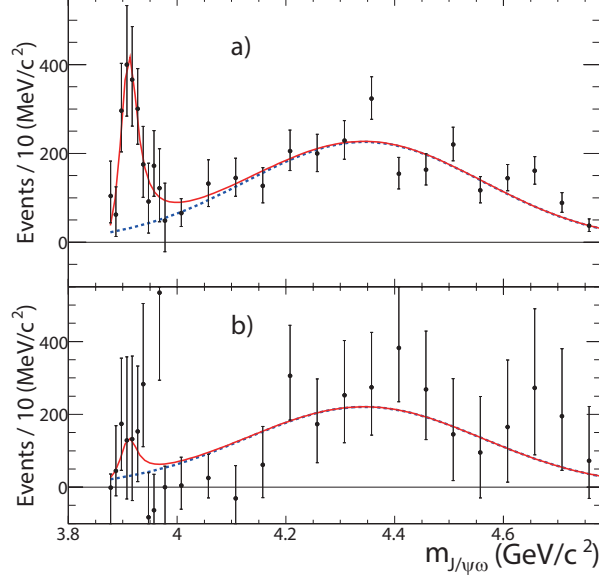


Figure 6: (Color online) The  $\omega J/\psi$  invariant mass spectrum of  $B \rightarrow K\omega J/\psi$  from BaBar [86]. Here,  $B^+$  and  $B^0$  decays are shown in the upper and lower panels, respectively.

Since these two BaBar experiments studied both the  $B^0 \rightarrow K^0\omega J/\psi$  and  $B^+ \rightarrow K^+\omega J/\psi$  processes, it allows them to evaluate the two parameters,  $R_Y$  and  $R_{NR}$ , defined as the ratios between the number of  $B^0$  and  $B^+$  events for the  $Y(3940)$  signal and for the nonresonant contribution, respectively. The results are shown in Fig. 6. The former experiment [86] obtained

$$\begin{aligned} \mathcal{B}(B^+ \rightarrow Y(3940)K^+) \times \mathcal{B}(Y(3940) \rightarrow J/\psi\omega) &= (4.9_{-0.9}^{+1.0} \pm 0.5) \times 10^{-5}, \\ \mathcal{B}(B^0 \rightarrow Y(3940)K^0) \times \mathcal{B}(Y(3940) \rightarrow J/\psi\omega) &= (1.3_{-1.1}^{+1.3} \pm 0.2) \times 10^{-5}, \end{aligned} \quad (17)$$

and  $R_Y = 0.27_{-0.23-0.01}^{+0.28+0.04}$  and  $R_{NR} = 0.97_{-0.22-0.02}^{+0.23+0.03}$ .  $R_Y$  is three standard deviations below the isospin expectation, but agrees with that of  $X(3872)$  [77], while  $R_{NR}$  agrees with the isospin expectation. The latter experiment [79] got

$$\begin{aligned} \mathcal{B}(B^+ \rightarrow Y(3940)K^+) \times \mathcal{B}(Y(3940) \rightarrow J/\psi\omega) &= (3.0_{-0.6-0.3}^{+0.7+0.5}) \times 10^{-5}, \\ \mathcal{B}(B^0 \rightarrow Y(3940)K^0) \times \mathcal{B}(Y(3940) \rightarrow J/\psi\omega) &= (2.1 \pm 0.9 \pm 0.3) \times 10^{-5}, \end{aligned} \quad (18)$$

and  $R_Y = 0.7_{-0.3}^{+0.4} \pm 0.1$  and  $R_{NY} = 0.7 \pm 0.1 \pm 0.1$ , which are both consistent with the previous results [86], and at the same time (almost) agree with the isospin expectation.

To date, the only observed decay mode of the  $Y(3940)$  is  $\omega J/\psi$ . The Belle Collaboration searched for its open charm decay mode  $D^{*0}\bar{D}^0$  and set an upper limit [67]

$$\mathcal{B}(B \rightarrow Y(3940)K) \times \mathcal{B}(Y(3940) \rightarrow D^{*0}\bar{D}^0) < 0.67 \times 10^{-4}. \quad (19)$$

at 90% C.L.. They further used this value, together with the results from Refs. [85, 86, 87], to indicate that the  $X(3940)$  and  $Y(3940)$  are different states.

Besides the  $Y(3940)$  and  $X(3940)$  states, two other resonances  $X(3915)$  and  $Z(3930)$  were observed in the  $\gamma\gamma$  fusion and will be discussed in Sec. 2.1.4. These four neutral states were all discovered in the 3.90-3.95 GeV mass

region, and need to be carefully studied and classified. We note that the two charmonium-like states,  $Y(3940)$  and  $X(3915)$ , were identified as the same state  $\chi_{c0}(2P)$  in Particle Data Group (PDG) [1]. In this review we will discuss them in Sec. 2.1.4.2.

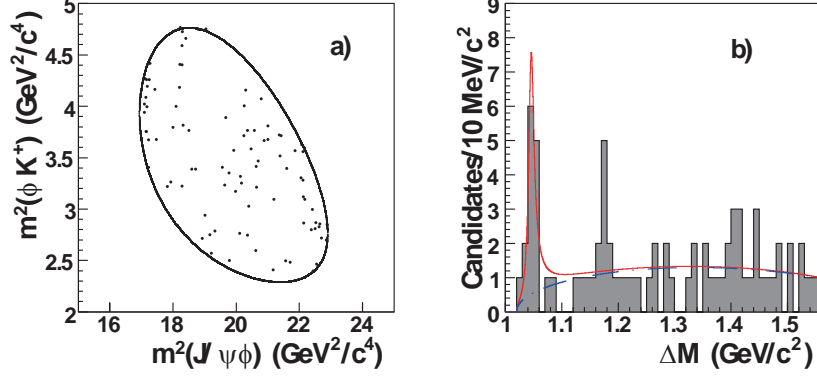


Figure 7: (Color online) The mass difference,  $\Delta M$ , between  $\mu^+\mu^-K^+K^-$  and  $\mu^+\mu^-$ , in the  $B^+$  mass window from CDF [58].

2.1.1.3.  $Y(4140)$  and  $Y(4274)$ . In 2009, the  $Y(4140)$  state was first announced by the CDF Collaboration [58], where they reported evidence for a narrow structure near the  $J/\psi\phi$  threshold in the exclusive  $B \rightarrow KJ/\psi\phi$  decay in  $\bar{p}p$  collisions at  $\sqrt{s} = 1.96 \text{ TeV}$ , with an integrated luminosity of  $2.7 \text{ fb}^{-1}$  and a statistical significance of  $3.8\sigma$ . The results are shown in Fig. 7. The mass and width of the  $Y(4140)$  were measured to be  $M = (4143.0 \pm 2.9 \pm 1.2) \text{ MeV}$  and  $\Gamma = (11.7^{+8.3}_{-5.0} \pm 3.7) \text{ MeV}$ , respectively.

However, this structure was not seen in the following Belle experiment, which measured the  $J/\psi\phi$  invariant mass in the process  $\gamma\gamma \rightarrow \phi J/\psi$  with the  $J/\psi$  decaying into lepton pairs and  $\phi$  decaying into  $K^+K^-$  pairs [88]. They gave the following upper limits on the branching fraction of  $Y(4140) \rightarrow \phi J/\psi$ :

$$\Gamma(Y(4140) \rightarrow \gamma\gamma) \times \mathcal{B}(Y(4140) \rightarrow \phi J/\psi) < \begin{cases} 41 \text{ eV}, & \text{for } J^P = 0^+, \\ 6.0 \text{ eV}, & \text{for } J^P = 2^+, \end{cases} \quad (20)$$

at 90% C.L.. Instead, the Belle Collaboration observed another resonance, the  $X(4350)$ , which will be discussed in Sec. 2.1.4.3.

Later in 2011, the CDF Collaboration reported a further study based on the increased  $B^+ \rightarrow J/\psi\phi K^+$  sample, and confirmed the  $Y(4140)$  structure, with an integrated luminosity of  $6.0 \text{ fb}^{-1}$  and a significance greater than  $5\sigma$  [89]. The mass and width of the  $Y(4140)$  were measured slightly more precisely, to be  $M = (4143.4^{+2.9}_{-3.0} \pm 0.6) \text{ MeV}$  and  $\Gamma = (15.3^{+10.4}_{-6.1} \pm 2.5) \text{ MeV}$ . They also extracted the relative branching fraction  $\mathcal{B}_{rel}$  to be

$$\mathcal{B}_{rel} = \frac{\mathcal{B}(B^+ \rightarrow Y(4140)K^+) \times \mathcal{B}(Y(4140) \rightarrow J/\psi\phi)}{\mathcal{B}(B^+ \rightarrow J/\psi\phi K^+)} = 0.149 \pm 0.039 \pm 0.024. \quad (21)$$

Besides the  $Y(4140)$ , the CDF Collaboration reported another structure, named as  $Y(4274)$ , in the  $J/\psi\phi$  invariant mass spectrum, with a significance of  $3.1\sigma$  [89]. Its mass and width were measured to be  $M = (4274.4^{+8.4}_{-6.7} \pm 1.9) \text{ MeV}$  and  $\Gamma = (32.3^{+21.9}_{-15.3} \pm 7.6) \text{ MeV}$ .

One year later, the LHCb Collaboration searched for the  $Y(4140)$  decaying to  $J/\psi\phi$  using  $B \rightarrow KJ/\psi\phi$  decay events with an integrated luminosity of  $0.37 \text{ fb}^{-1}$  in  $pp$  collisions and at significantly larger energy  $\sqrt{s} = 7 \text{ TeV}$  [90]. They did not observe these two states, and set two upper limits on the relative branching fractions:

$$\mathcal{B}_{rel} = \frac{\mathcal{B}(B^+ \rightarrow Y(4140)K^+) \times \mathcal{B}(Y(4140) \rightarrow J/\psi\phi)}{\mathcal{B}(B^+ \rightarrow J/\psi\phi K^+)} < 0.07, \quad (22)$$

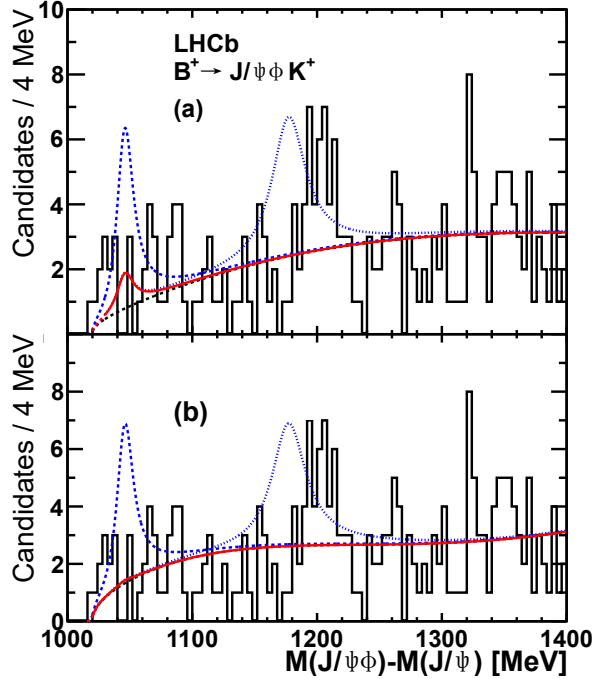


Figure 8: (Color online) Distribution of the mass difference  $M(J/\psi\phi) - M(J/\psi)$  for the  $B^+ \rightarrow J/\psi\omega K^+$  from LHCb [90].

at 90% C.L., and

$$\frac{\mathcal{B}(B^+ \rightarrow Y(4274)K^+) \times \mathcal{B}(Y(4274) \rightarrow J/\psi\phi)}{\mathcal{B}(B^+ \rightarrow J/\psi\phi K^+)} < 0.08, \quad (23)$$

at 90% C.L..

The situation changed in 2013. Both the DØ and CMS collaborations confirmed the observation of the  $Y(4140)$  [91, 63]. The DØ experiment investigated the decay process  $B^+ \rightarrow J/\psi\phi K^+$  produced in  $\bar{p}p$  collisions at  $\sqrt{s} = 1.96$  TeV, as shown in the left panel of Fig. 9. Their results supported the existence of the  $Y(4140)$ , with an integrated luminosity of  $10.4 \text{ fb}^{-1}$  and a statistical significance of  $3.1\sigma$ . The relative branching fraction was extracted to be

$$\frac{\mathcal{B}(B^+ \rightarrow Y(4140)K^+)}{\mathcal{B}(B^+ \rightarrow J/\psi\phi K^+)} = (21 \pm 8 \pm 4)\%, \text{ for } M(J/\psi\phi) < 4.59 \text{ GeV}. \quad (24)$$

Their data also indicated the possible existence of a structure around 4300 MeV, but they did not obtain a stable fit with an unconstrained width.

The CMS experiment studied the  $J/\psi\phi$  mass spectrum in the same decay process  $B^\pm \rightarrow J/\psi\phi K^\pm$  produced in  $pp$  collisions at  $\sqrt{s} = 7$  TeV, and confirmed the existence of the  $Y(4140)$  resonance, with an integrated luminosity of  $5.2 \text{ fb}^{-1}$  and a significance greater than  $5\sigma$  [63]. Their results are shown in the right panel of Fig. 9. The relative branching fraction  $\mathcal{B}_{rel}$  was extracted to be about 0.10 with a statistical uncertainty of about 30%, which is consistent with Eq. (21), the value measured by CDF, and Eq. (22), the upper limit given by LHCb. The CMS Collaboration also confirmed the existence of the second structure,  $Y(4274)$ .

We summarize the information of the  $Y(4140)$  and  $Y(4274)$  resonance parameters from different experiments in Table 3. Since these two resonances were both observed in the  $J/\psi\phi$  decay mode, their  $C$ -parity and  $G$ -parity should be even.

**2.1.1.4.  $Z^+(4430)$ .** The charged charmonium-like state  $Z^+(4430)$  was first observed by the Belle Collaboration in the  $\pi^\pm\psi(3686)$  invariant mass distribution in  $B \rightarrow K\pi^\pm\psi(3686)$  decays in 2007 [92], with a statistical significance of  $6.5\sigma$ .

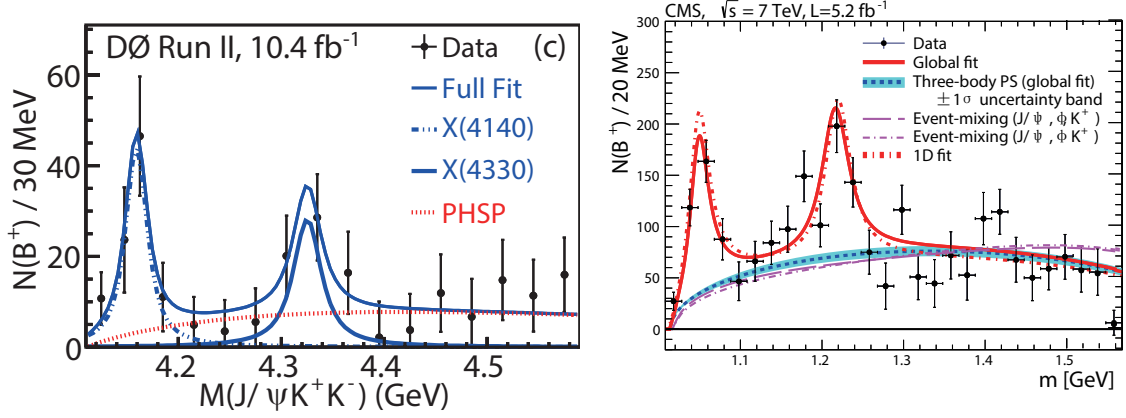


Figure 9: (Color online) Left: The  $J/\psi K^+ K^-$  invariant mass spectrum of  $B^+ \rightarrow J/\psi \phi K^+$  from DØ [91]. Right: The number of  $B^+ \rightarrow J/\psi \phi K^+$  candidates as a function of  $\Delta m = m(\mu^+ \mu^- K^+ K^-) - m(\mu^+ \mu^-)$  from CMS [63].

Table 3: The resonance parameters of the  $Y(4140)$  and  $Y(4274)$ . Here, all results are in units of MeV.

Experiment	$Y(4140)$	$Y(4274)$
CDF [58]	$M = 4143.0 \pm 2.9 \pm 1.2, \Gamma = 11.7^{+8.3}_{-5.0} \pm 3.7$	—
CDF [89]	$M = 4143.4^{+2.9}_{-3.0} \pm 0.6, \Gamma = 15.3^{+10.4}_{-6.1} \pm 2.5$	$M = 4274.4^{+8.4}_{-6.7} \pm 1.9, \Gamma = 32.3^{+21.9}_{-15.3} \pm 7.6$
DØ [91]	$M = 4159.0 \pm 4.3 \pm 6.6, \Gamma = 19.9 \pm 12.6^{+1.0}_{-8.0}$	—
CMS [63]	$M = 4148.0 \pm 2.4 \pm 6.3, \Gamma = 28^{+15}_{-11} \pm 19$	$M = 4313.8 \pm 5.3 \pm 7.3, \Gamma = 38^{+30}_{-15} \pm 16$

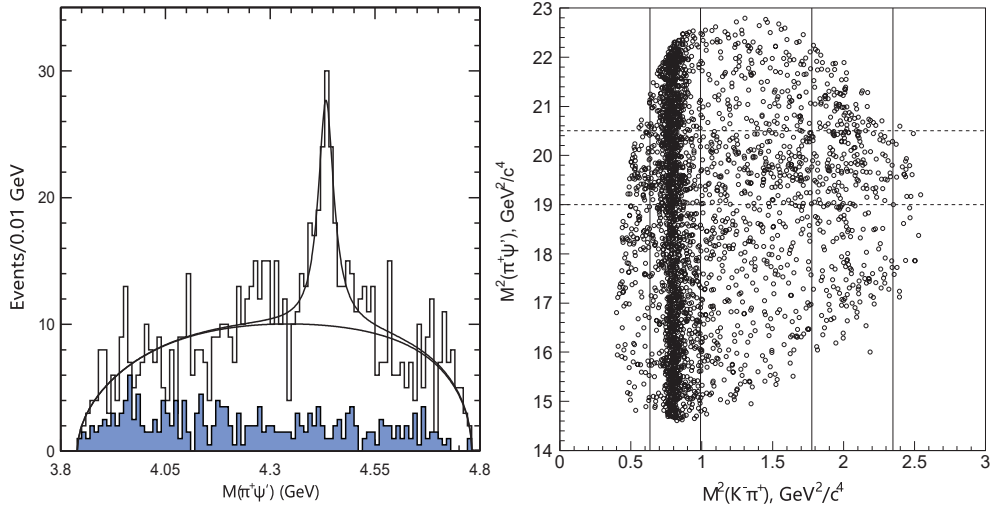


Figure 10: (Color online) The  $\pi^+ \psi(3686)$  invariant mass spectrum of  $\bar{B}^0 \rightarrow K^- \pi^+ \psi(3686)$  (left) from Belle [92], and its Dalitz plot (right) from Belle [93].

The results are shown in the left panel of Fig. 10. Its mass and width were measured to be  $M = (4433 \pm 4 \pm 2)$  MeV and  $\Gamma = (45^{+18+30}_{-13-13})$  MeV, respectively. They also extracted the product of branching fractions as

$$\mathcal{B}(\bar{B}^0 \rightarrow K^- Z^+(4430)) \times \mathcal{B}(Z^+(4430) \rightarrow \pi^+ \psi(3686)) = (4.1 \pm 1.0 \pm 1.4) \times 10^{-5}. \quad (25)$$

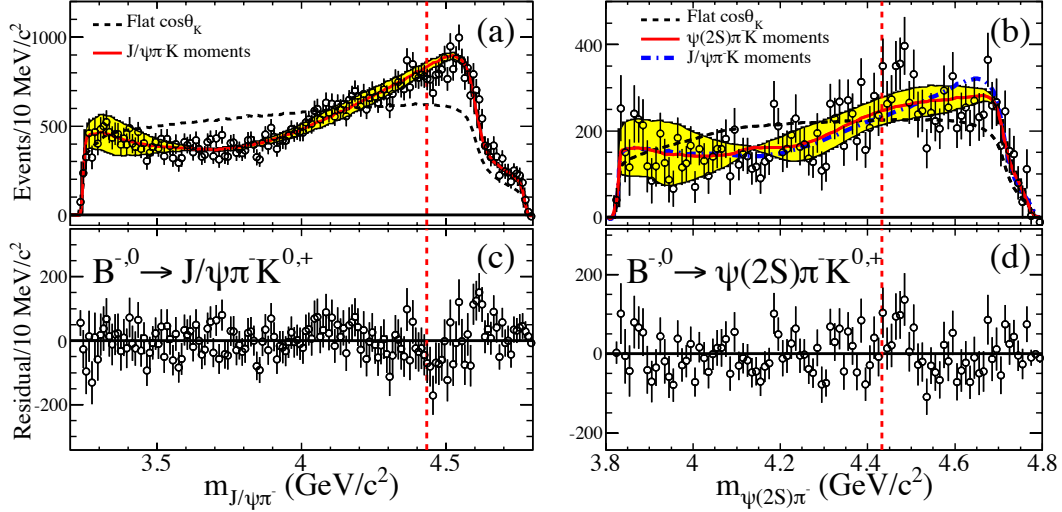


Figure 11: (Color online) The  $\pi^- J/\psi$  and  $\pi^- \psi(3686)$  mass distributions from BaBar [94] for the combined decay modes (a)  $B^{0,-} \rightarrow K^{+,0}\pi^- J/\psi$  and (b)  $B^{0,-} \rightarrow K^{+,0}\pi^- \psi(3686)$ . (c) and (d) are the residuals (data-solid curve) for (a) and (b), respectively.

However, this signal was not seen in the following BaBar experiment, which analyzed both  $\pi^- J/\psi$  and  $\pi^- \psi(3686)$  invariant masses in  $B^{0,-} \rightarrow K^{+,0}\pi^- J/\psi$  and  $B^{0,-} \rightarrow K^{+,0}\pi^- \psi(3686)$  decays [94], respectively. The results are shown in Fig. 11. They found no evidence for  $Z^-(4430)$  in the  $\pi^- J/\psi$  mass distributions in  $B^{0,-} \rightarrow K^{+,0}\pi^- J/\psi$  decays, and no clear evidence for  $Z^-(4430)$  in the  $\pi^- \psi(3686)$  mass distributions in  $B^{0,-} \rightarrow K^{+,0}\pi^- \psi(3686)$  decays. More precisely, they fit the  $\pi^- \psi(3686)$  invariant mass distribution and obtained a 2.7 standard deviation signal. This signal has a fitted width consistent with the value obtained by Belle [92], but its central mass value was 43 MeV higher than that reported by Belle [92], with a difference of  $+4.7\sigma$ . They set two upper limits on the branching fractions

$$\begin{aligned} \mathcal{B}(B^0 \rightarrow K^+ Z^-(4430)) \times \mathcal{B}(Z^-(4430) \rightarrow \pi^- \psi(3686)) &< 3.1 \times 10^{-5}, \\ \mathcal{B}(B^- \rightarrow \bar{K}^0 Z^-(4430)) \times \mathcal{B}(Z^-(4430) \rightarrow \pi^- \psi(3686)) &< 4.7 \times 10^{-5}, \end{aligned} \quad (26)$$

at 95% C.L..

In the following years, the Belle Collaboration continued their studies on the  $Z^+(4430)$  [93, 95, 96]. We summarize the information of the resonance parameters from all these Belle experiments in Table 4.

In Ref. [93] the Belle Collaboration performed a Dalitz plot analysis of  $B \rightarrow K\pi^+ \psi(3686)$ , and observed a signal for  $Z^+(4430) \rightarrow \pi^+ \psi(3686)$  with a significance of  $6.4\sigma$ . The results are shown in the right panel of Fig. 10. They measured the product of branching fractions, i.e.,

$$\mathcal{B}(\bar{B}^0 \rightarrow K^- Z^+(4430)) \times \mathcal{B}(Z^+(4430) \rightarrow \pi^+ \psi(3686)) = (3.2^{+1.8+5.3}_{-0.9-1.6}) \times 10^{-5}. \quad (27)$$

They also determined the branching fraction

$$\mathcal{B}(B^0 \rightarrow K^{*0}(892)\psi(3686)) = (5.52^{+0.35+0.53}_{-0.32-0.58}) \times 10^{-4}, \quad (28)$$

and the fraction of the  $K^*(892)$  meson that was longitudinally polarized to be  $f_L = (44.8^{+4.0+4.0}_{-2.7-5.3})\%$ .

In Ref. [95] the Belle Collaboration performed a full amplitude analysis of  $B^0 \rightarrow K^+ \pi^- \psi(3686)$  decays to determine the spin and parity of the  $Z^+(4430)$ . Their results show that the  $Z^+(4430)$  has quantum numbers  $J^P = 1^+$ , which

hypothesis is favored over the  $0^-$ ,  $1^-$ ,  $2^-$  and  $2^+$  hypotheses at the levels of  $3.4\sigma$ ,  $3.7\sigma$ ,  $4.7\sigma$  and  $5.1\sigma$ , respectively. They also calculated the following branching fractions

$$\begin{aligned}\mathcal{B}(B^0 \rightarrow K^+\pi^-\psi(3686)) &= (5.80 \pm 0.39) \times 10^{-4}, \\ \mathcal{B}(B^0 \rightarrow K^{*0}(892)\psi(3686)) &= (5.55^{+0.22+0.41}_{-0.23-0.84}) \times 10^{-4}, \\ \mathcal{B}(B^0 \rightarrow K^+Z^-(4430)) \times \mathcal{B}(Z^-(4430) \rightarrow \pi^-\psi(3686)) &= (6.0^{+1.7+2.5}_{-2.0-1.4}) \times 10^{-5},\end{aligned}\quad (29)$$

together with  $f_L = (45.5^{+3.1+1.4}_{-2.9-4.9})\%$ .

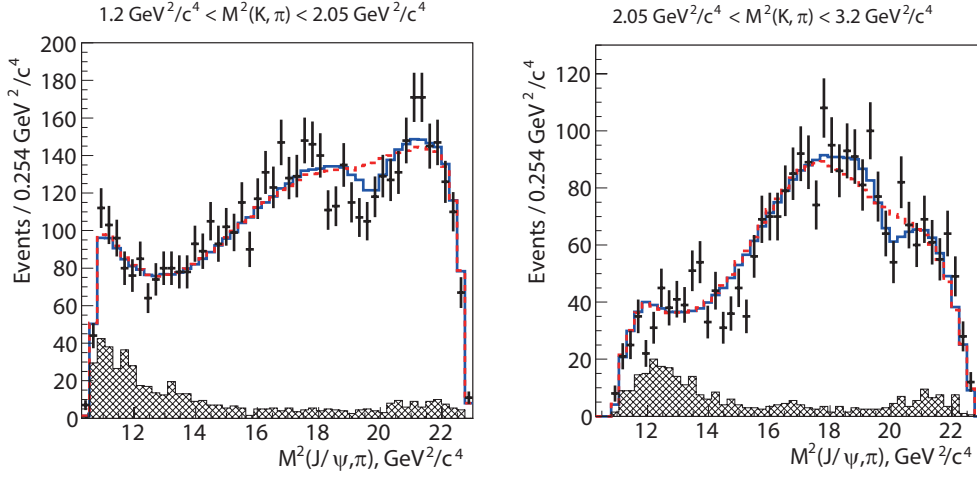


Figure 12: (Color online) The fit results with (solid line) and without (dashed line) the  $Z^+(4430)$  from Belle [96], where the  $Z_c(4200)$  contribution has been included.

In Ref. [96] the Belle Collaboration found evidence for  $Z^+(4430) \rightarrow \pi^+ J/\psi$  in  $\bar{B}^0 \rightarrow K^-\pi^+ J/\psi$  decays, as shown in Fig. 12. They also measured its branching fraction

$$\mathcal{B}(\bar{B}^0 \rightarrow K^-Z^+(4430)) \times \mathcal{B}(Z^+(4430) \rightarrow \pi^+ J/\psi) = (5.4^{+4.0+1.1}_{-1.0-0.9}) \times 10^{-6}. \quad (30)$$

Besides these Belle experiments, the LHCb Collaboration also confirmed the existence of the  $Z^+(4430)$ , by performing a four-dimensional fit in the analysis of the  $\pi^-\psi(3686)$  invariant mass distribution in the  $B^0 \rightarrow K^+\pi^-\psi(3686)$  decay [97], as shown in Fig. 13. They measured its mass and width, as listed also in Table 4, and established its spin-parity to be  $J^P = 1^+$ , both with very high significance. Moreover, they ruled out the  $0^-$ ,  $1^-$ ,  $2^+$  and  $2^-$  hypotheses for its spin-parity by at least  $9.7\sigma$ ,  $15.8\sigma$ ,  $16.1\sigma$  and  $14.6\sigma$ , respectively. Its amplitude fraction was determined to be  $f_{Z^+(4430)} = (5.9 \pm 0.9^{+1.5}_{-3.3})\%$ , whose definition is  $f_R \equiv \int S_R(\Phi)d\Phi / \int S(\Phi)d\Phi$ , for the component  $R$ , where in  $S_R(\Phi)$  all except the  $R$  amplitude terms are set to zero.

**2.1.1.5.  $Z^+(4051)$  and  $Z^+(4248)$ .** The two charged charmonium-like states,  $Z^+(4051)$  and  $Z^+(4248)$ , were first observed by the Belle Collaboration in 2008 [98], one year after they reported the observation of the  $Z^+(4430)$  [92]. They studied the  $\pi^+\chi_{c1}$  invariant mass distribution in the exclusive  $\bar{B}^0 \rightarrow K^-\pi^+\chi_{c1}$  decay, as shown in Fig. 14. After performing a Dalitz plot analysis, they reported two resonance-like structures,  $Z^+(4051)$  and  $Z^+(4248)$ . The masses and widths of the  $Z^+(4051)$  and  $Z^+(4248)$  were determined to be  $M = (4051 \pm 14^{+20}_{-41})$  MeV,  $\Gamma = (82^{+21+47}_{-17-22})$  MeV and  $M = (4248^{+44+180}_{-29-35})$  MeV,  $\Gamma = (177^{+54+316}_{-39-61})$  MeV, respectively. They also provided the following branching fractions

$$\mathcal{B}(\bar{B}^0 \rightarrow K^-Z^+(4051)) \times \mathcal{B}(Z^+(4051) \rightarrow \pi^+ J/\psi) = (3.0^{+1.5+3.7}_{-0.8-1.6}) \times 10^{-5}, \quad (31)$$

$$\mathcal{B}(\bar{B}^0 \rightarrow K^-Z^+(4248)) \times \mathcal{B}(Z^+(4248) \rightarrow \pi^+ J/\psi) = (4.0^{+2.3+19.7}_{-0.9-0.5}) \times 10^{-5}. \quad (32)$$

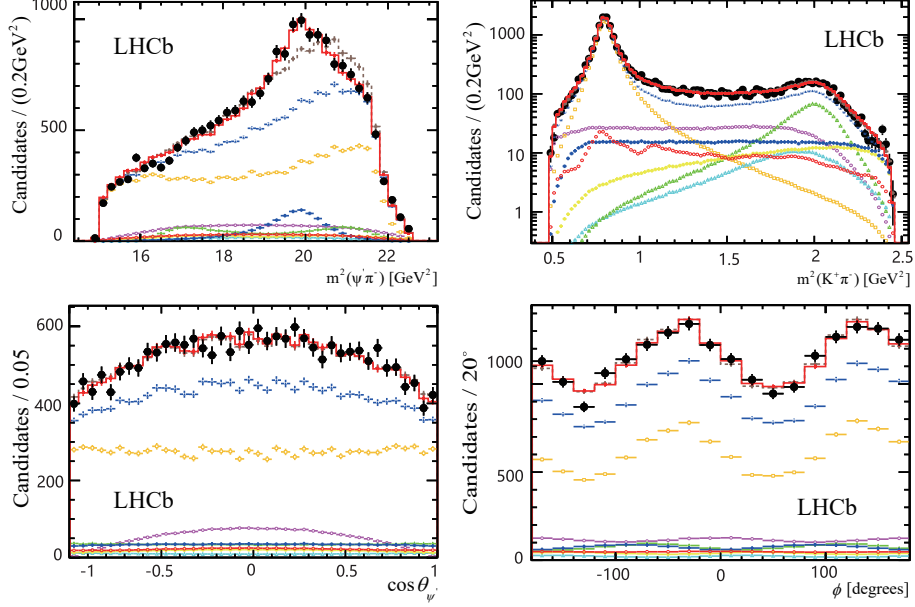


Figure 13: (Color online) The four-dimensional fit to study the  $B^0 \rightarrow K^+ \pi^- \psi(3686)$  decays, performed by LHCb [97]. The red solid and brown dashed histograms represent the total amplitude with and without the  $Z^+(4430)$ , respectively.

Table 4: The resonance parameters for the  $Z^+(4430)$  and the observed decay channels.

Experiment	Mass [MeV]	Width [MeV]	Decay Mode
Belle <sup>1</sup> [92]	$4433 \pm 4 \pm 2$	$45^{+18+30}_{-13-13}$	$Z^+(4430) \rightarrow \pi^+ \psi(3686)$
Belle <sup>2</sup> [93]	$4443^{+15+19}_{-12-13}$	$107^{+86+74}_{-43-56}$	$Z^+(4430) \rightarrow \pi^+ \psi(3686)$
Belle <sup>3</sup> [95]	$4485 \pm 22^{+28}_{-11}$	$200^{+41+26}_{-46-35}$	$Z^-(4430) \rightarrow \pi^- \psi(3686)$
Belle <sup>4</sup> [96]	—	—	evidence for $Z^+(4430) \rightarrow \pi^+ J/\psi$
LHCb [97]	$4475 \pm 7^{+15}_{-25}$	$172 \pm 13^{+37}_{-34}$	$Z^-(4430) \rightarrow \pi^- \psi(3686)$

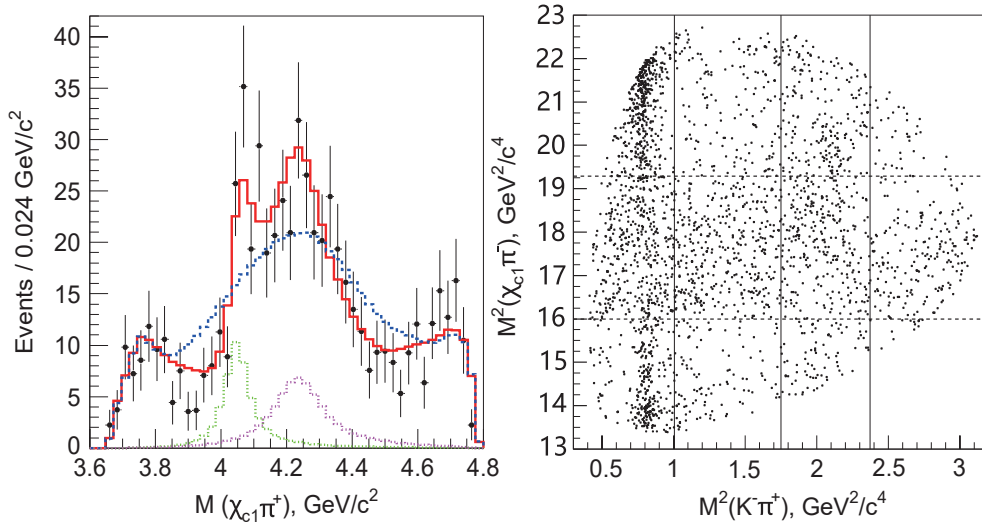


Figure 14: (Color online) The  $\pi^+\chi_{c1}$  invariant mass spectrum of  $\bar{B}^0 \rightarrow K^-\pi^+\chi_{c1}$  (left), and its Dalitz plot (right) from Belle [98].

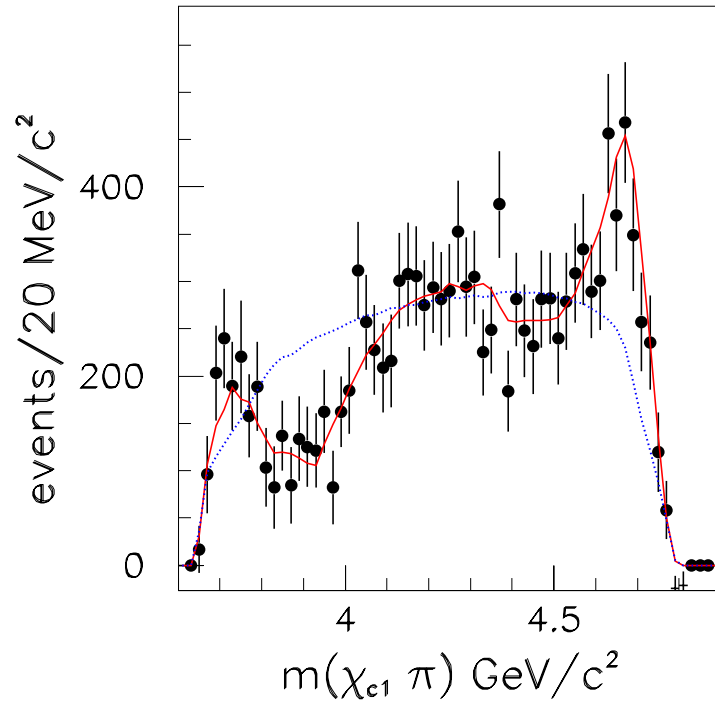


Figure 15: (Color online) The  $\pi^+\chi_{c1}$  invariant mass spectrum of  $\bar{B} \rightarrow K\pi^+\chi_{c1}$  from BaBar [99], with background subtracted and efficiency corrected.

Neither of these two observations was seen in the following BaBar experiment, which studied the  $\pi^+\chi_{c1}$  invariant mass in  $\bar{B}^0 \rightarrow K^-\pi^+\chi_{c1}$  and  $B^+ \rightarrow K_S^0\pi^+\chi_{c1}$  decays [99]. The results are shown in Fig. 15. They found no significant resonant structure in both the  $\pi\chi_{c1}$  and  $\pi J/\psi$  mass distributions in  $B \rightarrow K\pi\chi_{c1}$  decays. They set two upper limits on the branching fractions at 90% C.L.

$$\mathcal{B}(\bar{B}^0 \rightarrow K^-Z^+(4051)) \times \mathcal{B}(Z^+(4051) \rightarrow \pi^+J/\psi) < 1.8 \times 10^{-5}, \quad (33)$$

$$\mathcal{B}(\bar{B}^0 \rightarrow K^-Z^+(4248)) \times \mathcal{B}(Z^+(4248) \rightarrow \pi^+J/\psi) < 4.0 \times 10^{-5}, \quad (34)$$

which are consistent with the Belle results listed in Eqs. (31) and (32).

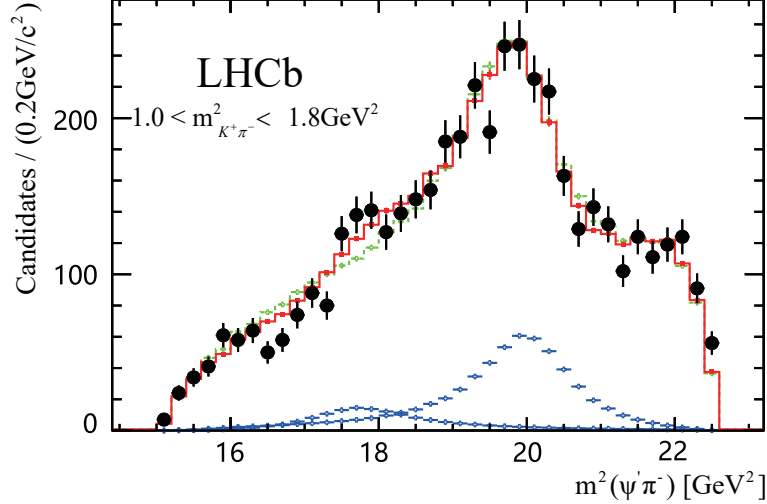


Figure 16: (Color online) The square of the  $\pi^-\psi(3686)$  invariant mass spectrum of  $B^0 \rightarrow K^+\pi^-\psi(3686)$  from LHCb [97]. The solid-line red and dashed-line green histograms represent the fit with two  $Z^+$ 's ( $Z^+(4430)$  and  $Z^+(4240)$ ) and the fit with only one  $Z^+$  ( $Z^+(4430)$ ), respectively.

2.1.1.6.  $Z_c^+(4200)$  and  $Z^+(4240)$ . Besides finding the evidence of  $Z^+(4430) \rightarrow \pi^+J/\psi$  in the  $\bar{B}^0 \rightarrow K^-\pi^+J/\psi$  decay, Belle observed a new charged charmonium-like structure  $Z_c^+(4200)$  [96], which decays into  $J/\psi\pi^+$  with a significance of  $6.2\sigma$ . The measured mass and width of the  $Z_c^+(4200)$  are  $(4196^{+31+17}_{-29-13})$  MeV and  $(370^{+70+70}_{-70-132})$  MeV, respectively. It is obvious that the  $Z_c^+(4200)$  is a very broad structure [96]. The spin-parity quantum number of the  $Z_c^+(4200)$  favors  $J^P = 1^+$  according to the analysis of Belle [96]. Additionally, the branching fraction relevant to the  $Z_c^+(4200)$  [96] was measured, i.e.,

$$\mathcal{B}(\bar{B}^0 \rightarrow Z_c^+(4200)K^-) \times \mathcal{B}(Z_c^+(4200) \rightarrow J/\psi\pi^+) = (2.2^{+0.7+1.1}_{-0.5-0.6}) \times 10^{-5}. \quad (35)$$

In Ref. [97], LHCb not only confirmed the existence of the  $Z^+(4430)$ , but also found a new structure the  $Z^+(4240)$  in the  $\pi^-\psi(3686)$  invariant mass distribution of  $B^0 \rightarrow K^+\pi^-\psi(3686)$  decay with a statistical significance of  $6\sigma$ , as shown in Fig. 16. Its mass and width were measured to be  $M = (4239 \pm 18^{+45}_{-10})$  MeV and  $\Gamma = (220 \pm 47^{+108}_{-74})$  MeV, respectively. Its spin-parity quantum number  $J^P = 0^-$  was preferred over  $1^-$ ,  $2^-$  and  $2^+$  by  $8\sigma$ . But  $J^P = 0^-$  was preferred over  $1^+$  only by  $1\sigma$ . In other words, the  $J^P = 1^+$  assignment is not fully excluded for the  $Z^+(4240)$ . In addition, its amplitude fraction was determined to be  $f_{Z^+(4240)} = (1.6 \pm 0.5^{+1.9}_{-0.4})\%$ .

To date, three charged charmonium-like structures around 4.2 GeV were observed in  $B$  meson decays, the  $Z^+(4248)$  which is discussed in Sec. 2.1.1.5, and the  $Z_c^+(4200)$  and  $Z^+(4240)$ . We note that the  $Z^+(4248)$  and  $Z^+(4240)$  are denoted as  $X(4250)^\pm$  and  $X(4240)^\pm$  in PDG [1], respectively.

We need to mention an opinion from Belle. In Ref. [96], Belle indicated that the resonance parameters of the  $Z^+(4240)$  reported by LHCb were close to those of the  $Z_c^+(4200)$  while  $J^P = 1^+$  is not excluded for the  $Z^+(4240)$ . Thus, the  $Z_c^+(4200)$  and  $Z^+(4240)$  may be the same state.

In order to further clarify the above three charged charmonium-like structures, more precise experimental studies are needed, especially the measurement of their spin-parity quantum numbers.

2.1.1.7.  $X(3823)$ . In 1994, the E705 Collaboration reported a  $2.8\sigma$  structure at 3.836 GeV in the  $J/\psi\pi^+\pi^-$  channel [100]. If this structure was a resonance, the  ${}^3D_2(2^{--})$  assignment was favored by the experimental data. However, there were only  $58 \pm 21$  events in the E705 data [100].

In 2013, the Belle Collaboration observed a new narrow resonance decaying to  $\chi_{c1}\gamma$  in the  $B \rightarrow \chi_{c1}\gamma K$  process with a statistical significance of  $3.8\sigma$  [101]. This state has a mass of  $(3823.1 \pm 1.8 \pm 0.7)$  MeV. The invariant mass of the  $\chi_{c1}\gamma$  distribution is shown in Fig. 17. Belle measured the branching fraction product  $\mathcal{B}(B^\pm \rightarrow X(3823)K^\pm) \times \mathcal{B}(X(3823) \rightarrow \chi_{c1}\gamma) = (9.7 \pm 2.8 \pm 1.1) \times 10^{-6}$ . They found no evidence for  $X(3823) \rightarrow \chi_{c2}\gamma$  decay and set an upper limit of the ratio  $R_B \equiv \frac{\mathcal{B}(X(3823) \rightarrow \chi_{c2}\gamma)}{\mathcal{B}(X(3823) \rightarrow \chi_{c1}\gamma)} < 0.41$  at 90% C.L. They suggested this new resonance  $X(3823)$  as the  $1^3D_2$  charmonium state with  $J^{PC} = 2^{--}$ . The mass and radiative decay behavior agree with the theoretical predictions for the  $1^3D_2$  state [102, 103, 104, 17, 105, 106].

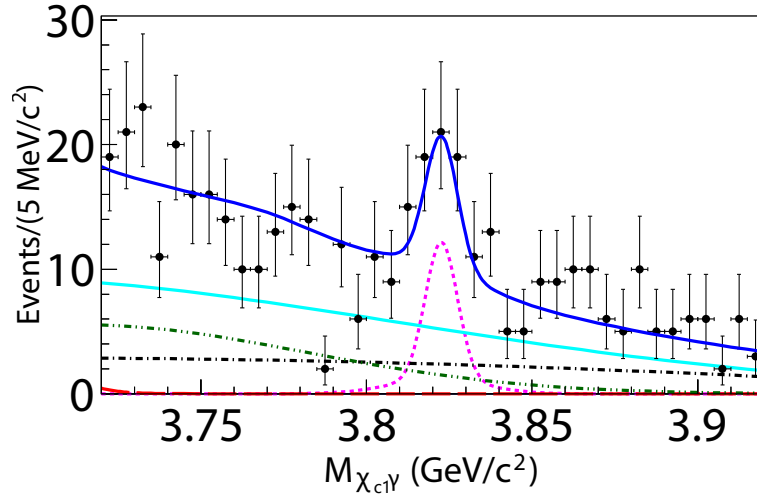


Figure 17: (Color online) The invariant mass distribution  $M_{\chi_{c1}\gamma}$  in the  $B \rightarrow \chi_{c1}\gamma K$  process for  $M_{bc} > 5.27$  GeV/ $c^2$ , from Belle [101].

Recently, the BESIII Collaboration confirmed the  $X(3823)$  resonance in the process of  $e^+e^- \rightarrow \pi^+\pi^-X(3823) \rightarrow \pi^+\pi^-\gamma\chi_{c1}$  at  $6.2\sigma$ , with a mass  $(3821.7 \pm 1.3 \pm 0.7)$  MeV and width less than 16 MeV at the 90% C.L. [107]. This observation is consistent with the measurement by Belle [101]. The simultaneous fit to the  $M_{\text{recoil}}(\pi^+\pi^-)$  distribution of  $\gamma\chi_{c1}$  is shown in Fig. 18. BESIII also provided the production cross sections of  $\sigma^B(e^+e^- \rightarrow \pi^+\pi^-X(3823)) \cdot \mathcal{B}_1(X(3823) \rightarrow \gamma\chi_{c1})$  at  $\sqrt{s} = 4.230, 4.260, 4.360, 4.420,$  and  $4.600$  GeV, as shown in Table 5.

Table 5: The production cross sections of  $\sigma^B(e^+e^- \rightarrow \pi^+\pi^-X(3823)) \cdot \mathcal{B}_1(X(3823) \rightarrow \gamma\chi_{c1})$  ( $\sigma_X^B \cdot \mathcal{B}_1$ ) and  $\mathcal{B}_2(X(3823) \rightarrow \gamma\chi_{c2})$  ( $\sigma_X^B \cdot \mathcal{B}_2$ ), and the Born cross section  $\sigma^B(e^+e^- \rightarrow \pi^+\pi^-\psi')$  ( $\sigma_{\psi'}^B$ ) at different energies from BESIII [107]. The relative ratio  $\mathcal{R}_{\psi'}$  corresponds to  $\frac{\sigma^B[e^+e^- \rightarrow \pi^+\pi^-X(3823)]\mathcal{B}(X(3823) \rightarrow \gamma\chi_{c1})}{\sigma^B[e^+e^- \rightarrow \pi^+\pi^-\psi']\mathcal{B}(\psi' \rightarrow \gamma\chi_{c1})}$ .

$\sqrt{s}$ (GeV)	$\sigma_X^B \cdot \mathcal{B}_1$ (pb)	$\sigma_X^B \cdot \mathcal{B}_2$ (pb)	$\sigma_{\psi'}^B$ (pb)	$\mathcal{R}_{\psi'}$
4.230	$0.12^{+0.24}_{-0.12} \pm 0.02$ ( $< 0.64$ )	-	$34.1 \pm 8.1 \pm 4.7$	-
4.260	$0.23^{+0.38}_{-0.24} \pm 0.04$ ( $< 0.98$ )	-	$25.9 \pm 8.1 \pm 3.6$	-
4.360	$1.10^{+0.64}_{-0.47} \pm 0.15$ ( $< 2.27$ )	( $< 1.92$ )	$58.6 \pm 14.2 \pm 8.1$	$0.20^{+0.13}_{-0.10}$
4.420	$1.23^{+0.59}_{-0.46} \pm 0.17$ ( $< 2.19$ )	( $< 0.54$ )	$33.4 \pm 7.8 \pm 4.6$	$0.39^{+0.21}_{-0.17}$
4.600	$0.47^{+0.44}_{-0.27} \pm 0.07$ ( $< 1.32$ )	-	$10.4^{+6.4}_{-4.7} \pm 1.5$	-

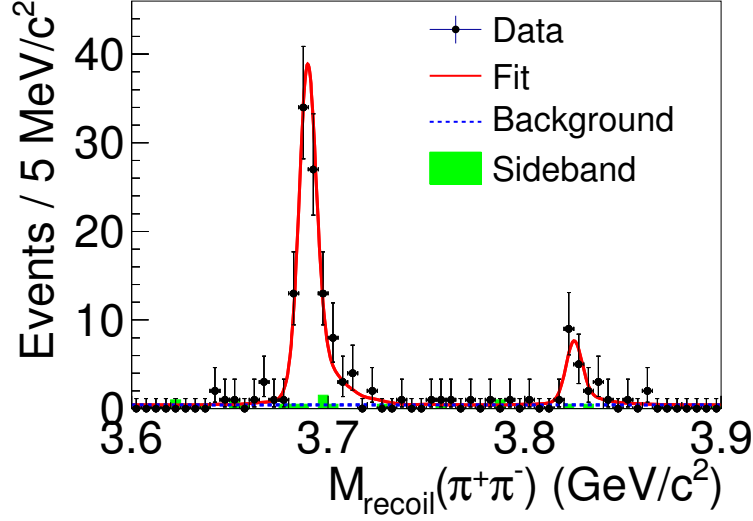


Figure 18: (Color online) Simultaneous fit to the  $M_{\text{recoil}}(\pi^+\pi^-)$  distribution of the  $\gamma\chi_{c1}$  events, from BESIII [107].

### 2.1.2. $Y$ states produced through the $e^+e^-$ annihilation

So far, five charmonium-like states, the  $Y(4260)$ ,  $Y(4008)$ ,  $Y(4360)$ ,  $Y(4660)$  and  $Y(4630)$ , have been reported in the  $e^+e^-$  annihilation processes, which are due to the development of the initial-state radiation (ISR) technique. As the first  $Y$  state in the charmonium-like state family, the  $Y(4260)$  has attracted great attentions from both experimentalists and theorists. To some extent, the  $X(3872)$  and  $Y(4260)$  are the two superstars among all the observed charmonium-like states. Those charmonium-like states observed in the  $e^+e^-$  annihilation follow the same naming convention as that of the  $Y(4260)$ .

Before giving the experimental details of these  $Y$  states, we briefly list their discovery modes:

$$\begin{aligned}
 Y(4260) \text{ and } Y(4008) & : e^+e^- \rightarrow \gamma_{\text{ISR}}\pi^+\pi^-J/\psi, \\
 Y(4360) \text{ and } Y(4660) & : e^+e^- \rightarrow \gamma_{\text{ISR}}\pi^+\pi^-\psi(3686), \\
 Y(4630) & : e^+e^- \rightarrow \gamma_{\text{ISR}}\Lambda_c\bar{\Lambda}_c.
 \end{aligned}$$

**2.1.2.1.  $Y(4260)$  and  $Y(4008)$ .** The observation of the  $Y(4260)$  was first announced by the BaBar Collaboration in 2005 [51], where they used the ISR technique to study the process  $e^+e^- \rightarrow \gamma_{\text{ISR}}\pi^+\pi^-J/\psi$  at  $\sqrt{s} = 10.58$  GeV, as shown in Fig. 19. Later, the  $Y(4260)$  was confirmed by both the CLEO [49] and Belle [108] collaborations in the same process. Besides the above experimental measurement of the  $Y(4260)$ , CLEO analyzed the data at the CESR  $e^+e^-$  collisions at  $\sqrt{s} = 3.97 - 4.26$  GeV [109]. They confirmed the  $Y(4260) \rightarrow \pi^+\pi^-J/\psi$  decay channel at  $11\sigma$  significance and observed a new decay mode  $Y(4260) \rightarrow \pi^0\pi^0J/\psi$  at  $5.1\sigma$  significance. CLEO also found the evidence of  $Y(4260) \rightarrow K^+K^-J/\psi$  [109]. The Belle Collaboration set the following upper limits at 90% C.L. [110, 111]:

$$\begin{aligned}
 \Gamma(Y \rightarrow e^+e^-) \times \mathcal{B}(Y \rightarrow K^+K^-J/\psi) & < 1.2 \text{ eV [110]}, \\
 \Gamma(Y \rightarrow e^+e^-) \times \mathcal{B}(Y \rightarrow K^+K^-J/\psi) & < 1.7 \text{ eV [111]}, \\
 \Gamma(Y \rightarrow e^+e^-) \times \mathcal{B}(Y \rightarrow K_S^0K_S^0J/\psi) & < 0.85 \text{ eV [111]}.
 \end{aligned} \tag{36}$$

The BaBar Collaboration searched for the signal of the  $Y(4260)$  via  $B^- \rightarrow J/\psi\pi^+\pi^-K^-$  [74], and set an upper limit  $\mathcal{B}(B^- \rightarrow Y(4260)K^-, Y(4260) \rightarrow J/\psi\pi^+\pi^-) < 2.9 \times 10^{-5}$  [74]. Thus, there does not exist direct evidence for the  $Y(4260)$  in the  $B$  meson decay at present.

A fit to the  $Y(4260)$  resonance yielded a mass  $(4251 \pm 9)$  MeV and a decay width  $(120 \pm 12)$  MeV [1]. We also summarize its resonance parameters from different experiments in Table 6. Since the  $Y(4260)$  was directly produced from the  $e^+e^-$  annihilation, its quantum number is  $J^{PC} = 1^{--}$ .

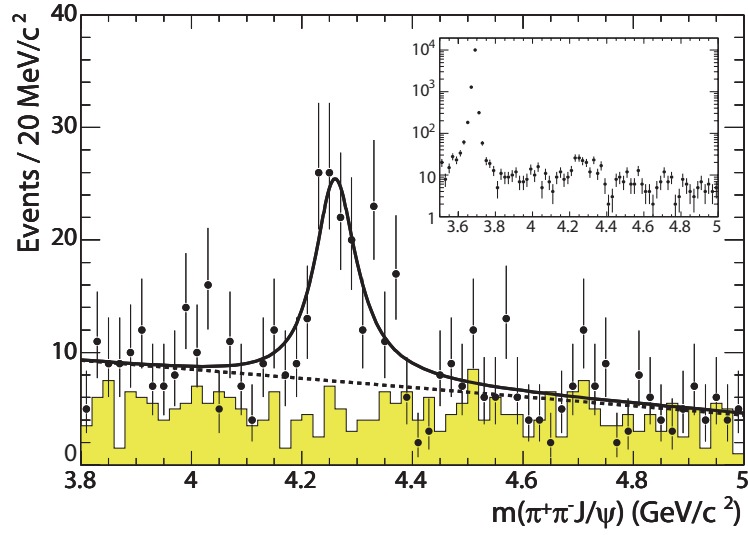


Figure 19: (Color online) The  $\pi^+\pi^-J/\psi$  invariant mass spectrum of  $e^+e^- \rightarrow \gamma_{\text{ISR}}\pi^+\pi^-J/\psi$  at  $\sqrt{s} = 3.8 - 5.0 \text{ GeV}/c^2$  and the  $Y(4260)$  structure (black solid curve), from BaBar [51].

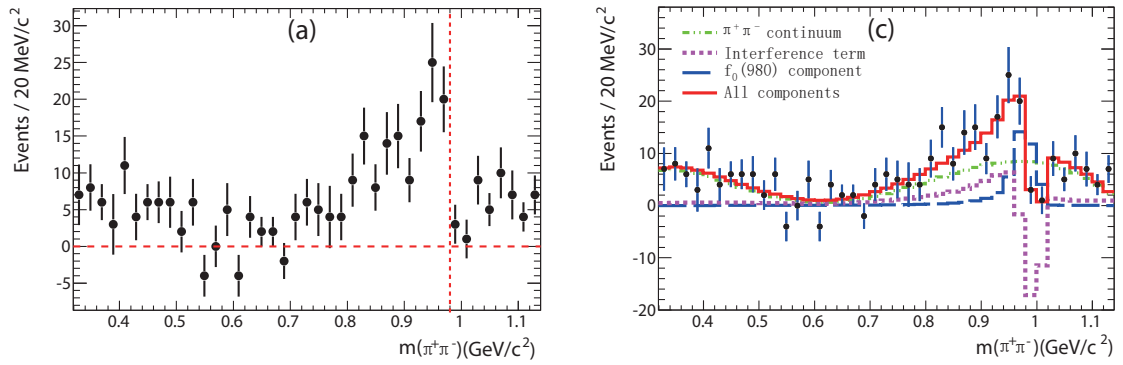


Figure 20: (Color online) The dipion invariant mass spectrum (left) of  $e^+e^- \rightarrow \gamma_{\text{ISR}}\pi^+\pi^-J/\psi$  and the corresponding experimental analysis (right), from BaBar [112].

The observed decay modes of the  $Y(4260)$  include  $J/\psi\pi^+\pi^-$  [51, 49, 108],  $J/\psi\pi^0\pi^0$  [109], and possibly  $J/\psi K^+K^-$  [109]. Additionally, the dipion mass distribution of  $Y(4260) \rightarrow \pi^+\pi^- J/\psi$  was measured [51, 49, 108, 112], and there exists an enhancement around 980 MeV, which may arise from the scalar meson  $f_0(980)$ . Especially, BaBar further carried out the analysis of the dipion mass distribution of  $Y(4260) \rightarrow \pi^+\pi^- J/\psi$  (see Fig. 20) and obtained the branching ratio  $\mathcal{B}(Y(4260) \rightarrow J/\psi f_0(980), f_0(980) \rightarrow \pi^+\pi^-)/\mathcal{B}(Y(4260) \rightarrow J/\psi\pi^+\pi^-) = (0.17 \pm 0.13)$  [112]. Thus, the intermediate  $f_0(980)$  contribution to  $Y(4260) \rightarrow \pi^+\pi^- J/\psi$  is not dominant [112]. Besides  $Y(4260) \rightarrow J/\psi f_0(980) \rightarrow J/\psi\pi^+\pi^-$ , the  $Y(4260) \rightarrow Z_c(3900)^\pm\pi^\mp \rightarrow J/\psi\pi^+\pi^-$  mode was also seen [53, 113], where the charged charmonium-like structure  $Z_c(3900)$  was observed in the corresponding  $J/\psi\pi^\pm$  invariant mass spectrum, which we will discuss in detail later.

The product branching fractions of the  $Y(4260)$  in the  $e^+e^-$  annihilations were measured by several experiments [51, 49, 112]:

$$\begin{aligned}\Gamma(Y(4260) \rightarrow e^+e^-) \times \mathcal{B}(Y(4260) \rightarrow \pi^+\pi^- J/\psi) &= (5.5 \pm 1.0_{-0.7}^{+0.8}) \text{ eV [51]}, \\ \Gamma(Y(4260) \rightarrow e^+e^-) \times \mathcal{B}(Y(4260) \rightarrow \pi^+\pi^- J/\psi) &= (8.9_{-3.1}^{+3.9} \pm 1.8) \text{ eV [49]}, \\ \Gamma(Y(4260) \rightarrow e^+e^-) \times \mathcal{B}(Y(4260) \rightarrow \pi^+\pi^- J/\psi) &= (9.2 \pm 0.8 \pm 0.7) \text{ eV [112]}.\end{aligned}\quad (37)$$

Its open charm decay modes  $D\bar{D}$ ,  $D^*\bar{D}$ ,  $D^*\bar{D}^*$ ,  $D_s^+D_s^-$ ,  $D_s^{*+}D_s^-$ ,  $D_s^{*+}D_s^{*-}$ ,  $D^0D^{*-}\pi^+$ ,  $D^*\bar{D}\pi$ ,  $D^*\bar{D}^*\pi$  were not seen [114, 115, 116, 117, 118, 119, 120] with the following upper limits:

$$\begin{aligned}\mathcal{B}(Y(4260) \rightarrow D\bar{D})/\mathcal{B}(Y(4260) \rightarrow \pi^+\pi^- J/\psi) &< 7.6 [114], \\ \mathcal{B}(Y(4260) \rightarrow D_s^+D_s^-)/\mathcal{B}(Y(4260) \rightarrow \pi^+\pi^- J/\psi) &< 0.7 [120], \\ \mathcal{B}(Y(4260) \rightarrow D_s^{*+}D_s^-)/\mathcal{B}(Y(4260) \rightarrow \pi^+\pi^- J/\psi) &< 44 [120], \\ \mathcal{B}(Y(4260) \rightarrow D_s^{*+}D_s^{*-})/\mathcal{B}(Y(4260) \rightarrow \pi^+\pi^- J/\psi) &< 30 [120],\end{aligned}\quad (38)$$

at 95% C.L., and

$$\begin{aligned}\mathcal{B}(Y(4260) \rightarrow D^0D^{*-}\pi^+)/\mathcal{B}(Y(4260) \rightarrow \pi^+\pi^- J/\psi) &< 9 [117], \\ \sigma(Y(4260) \rightarrow D\bar{D})/\sigma(Y(4260) \rightarrow \pi^+\pi^- J/\psi) &< 4.0 [118], \\ \sigma(Y(4260) \rightarrow D^*\bar{D})/\sigma(Y(4260) \rightarrow \pi^+\pi^- J/\psi) &< 45 [118], \\ \sigma(Y(4260) \rightarrow D^*\bar{D}^*)/\sigma(Y(4260) \rightarrow \pi^+\pi^- J/\psi) &< 11 [118], \\ \sigma(Y(4260) \rightarrow D_s^+D_s^-)/\sigma(Y(4260) \rightarrow \pi^+\pi^- J/\psi) &< 1.3 [118], \\ \sigma(Y(4260) \rightarrow D_s^{*+}D_s^-)/\sigma(Y(4260) \rightarrow \pi^+\pi^- J/\psi) &< 0.8 [118], \\ \sigma(Y(4260) \rightarrow D_s^{*+}D_s^{*-})/\sigma(Y(4260) \rightarrow \pi^+\pi^- J/\psi) &< 9.5 [118], \\ \sigma(Y(4260) \rightarrow D^*\bar{D}\pi)/\sigma(Y(4260) \rightarrow \pi^+\pi^- J/\psi) &< 15 [118], \\ \sigma(Y(4260) \rightarrow D^*\bar{D}^*\pi)/\sigma(Y(4260) \rightarrow \pi^+\pi^- J/\psi) &< 8.2 [118], \\ \mathcal{B}(Y(4260) \rightarrow D^*\bar{D})/\mathcal{B}(Y(4260) \rightarrow \pi^+\pi^- J/\psi) &< 34 [119], \\ \mathcal{B}(Y(4260) \rightarrow D^*\bar{D}^*)/\mathcal{B}(Y(4260) \rightarrow \pi^+\pi^- J/\psi) &< 40 [119],\end{aligned}\quad (39)$$

at 90% C.L.. Its hidden charm decay modes  $J/\psi\eta$ ,  $J/\psi K_s^0 K_s^0$  [121, 122, 111], and charmless decay modes  $\pi^+\pi^-\phi$ ,  $K^+K^-\pi^0$ ,  $K_s^0 K^\pm\pi^\mp$ ,  $p\bar{p}$  [123, 124, 125] were not seen in experiments, neither, and the following upper limits were given:

$$\begin{aligned}\Gamma(Y(4260) \rightarrow e^+e^-) \times \mathcal{B}(Y(4260) \rightarrow \eta J/\psi) &< 14.2 \text{ eV [122]}, \\ \Gamma(Y(4260) \rightarrow e^+e^-) \times \mathcal{B}(Y(4260) \rightarrow \pi^+\pi^-\phi) &< 0.4 \text{ eV [123]}, \\ \Gamma(Y(4260) \rightarrow e^+e^-) \times \mathcal{B}(Y(4260) \rightarrow K^+K^-\pi^0) &< 0.6 \text{ eV [124]}, \\ \Gamma(Y(4260) \rightarrow e^+e^-) \times \mathcal{B}(Y(4260) \rightarrow K_s^0 K^\pm\pi^\mp) &< 0.5 \text{ eV [124]}, \\ \mathcal{B}(Y(4260) \rightarrow p\bar{p})/\mathcal{B}(Y(4260) \rightarrow \pi^+\pi^-\phi) &< 13\% [125],\end{aligned}\quad (40)$$

at 90% C.L.. A puzzling phenomenon of the  $Y(4260)$  is that it is absent in the  $R$  value scan [126, 127, 128, 129, 118, 130], which is the challenge to the traditional vector charmonium interpretation of the  $Y(4260)$ .

In Ref. [82], the BESIII Collaboration studied the  $e^+e^- \rightarrow \gamma X(3872)$  process and measured the product of the cross section  $\sigma(e^+e^- \rightarrow \gamma X(3872))$  and the branching ratio  $\mathcal{B}(X(3872) \rightarrow \pi^+\pi^- J/\psi)$  at center-of-mass energies 4.009, 4.229, 4.26 and 4.360 GeV, which hinted the existence of the  $Y(4260) \rightarrow \gamma X(3872)$  radiative decay. More experiment information is needed to confirm the  $Y(4260) \rightarrow \gamma X(3872)$  mode. The experimental observation of the new decay mode of the  $Y(4260)$  is important to reveal its underlying structure.

Table 6: The resonance parameters for the  $Y(4260)$  and the observed decay channels.

Experiment	Mass (MeV)	Width (MeV)	Decay Mode
BaBar [51]	$4259 \pm 8_{-6}^{+2}$	$88 \pm 23_{-4}^{+6}$	$J/\psi\pi^+\pi^-$
CLEO [49]	$4284_{-16}^{+17} \pm 4$	$73_{-25}^{+39} \pm 5$	$J/\psi\pi^+\pi^-$
Belle [131]	$4295 \pm 10_{-3}^{+10}$	$133 \pm 26_{-6}^{+13}$	$J/\psi\pi^+\pi^-$
Belle [108]	$4247 \pm 12_{-32}^{+17}$	$108 \pm 19 \pm 10$	$J/\psi\pi^+\pi^-$
BaBar [132]	$4252 \pm 6_{-3}^{+2}$	$105 \pm 18_{-6}^{+4}$	$J/\psi\pi^+\pi^-$
BaBar [112]	$4244 \pm 5 \pm 4$	$114_{-15}^{+16} \pm 7$	$J/\psi f_0(980) (\rightarrow \pi^+\pi^-)$ ,
Belle [113]	$4258.6 \pm 8.3 \pm 12.1$	$134.1 \pm 16.4 \pm 5.5$	$\pi^\mp Z_c(3900)^\pm (\rightarrow J/\psi\pi^\pm)$

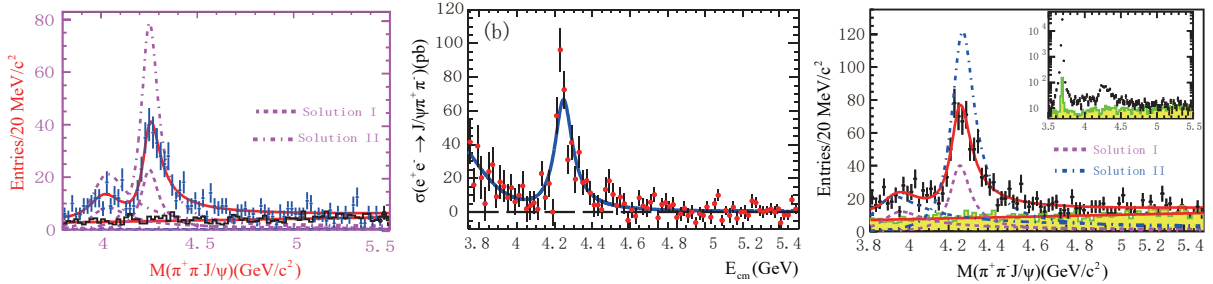


Figure 21: (Color online) The  $\pi^+\pi^- J/\psi$  invariant mass spectrum of  $e^+e^- \rightarrow \gamma_{\text{ISR}}\pi^+\pi^- J/\psi$  from Belle [108] (left), BaBar [112] (middle) and Belle [113] (right).

Besides the  $Y(4260)$ , the Belle Collaboration indicated that there may exist another very broad structure  $Y(4008)$  around 4.05 GeV in the measured  $\pi^+\pi^- J/\psi$  mass spectrum [108]. By adopting two interfering Breit-Wigner formalism to fit the experimental data, a broad structure with the mass  $(4008 \pm 40_{-28}^{+114})$  MeV and width  $(226 \pm 44 \pm 87)$  MeV was extracted, which was named as  $Y(4008)$ . However, BaBar did not find the  $Y(4008)$  signal in the same process  $e^+e^- \rightarrow \pi^+\pi^- J/\psi$  [112]. Later, based on the new measurement of  $e^+e^- \rightarrow \pi^+\pi^- J/\psi$  with a  $967 \text{ fb}^{-1}$  data sample, Belle confirmed that there exists an event cluster around 4.08 GeV [113]. The inconsistency between BaBar [112] and Belle [108, 113] results of the  $Y(4008)$  should be clarified in future experiments. In Fig. 21, we list the Belle and BaBar experimental data of the  $\pi^+\pi^- J/\psi$  mass spectrum of  $e^+e^- \rightarrow \pi^+\pi^- J/\psi$  for comparison.

2.1.2.2.  $Y(4360)$  and  $Y(4660)$ . After the observation of the  $Y(4260)$  in  $e^+e^- \rightarrow \gamma_{\text{ISR}}\pi^+\pi^- J/\psi$ , the BaBar Collaboration analyzed a similar process  $e^+e^- \rightarrow \gamma_{\text{ISR}}\pi^+\pi^-\psi(3686)$ , where a resonant structure  $Y(4360)$  was observed [133]. Later, the Belle Collaboration confirmed the existence of the  $Y(4360)$  in the same process.

Besides the  $Y(4360)$ , Belle further indicated that there was another enhancement structure  $Y(4660)$  [134] associated with the  $Y(4360)$  in the  $\pi^+\pi^-\psi(3686)$  invariant mass spectrum of  $e^+e^- \rightarrow \gamma_{\text{ISR}}\pi^+\pi^-\psi(3686)$ . Belle's observation

of the  $Y(4660)$  [134] was not confirmed by BaBar [133], which resulted in a long-term debate whether there is a  $Y(4660)$  structure in  $e^+e^- \rightarrow \gamma_{\text{ISR}}\pi^+\pi^-\psi(3686)$ . Finally in 2012, BaBar confirmed the existence of the  $Y(4660)$  with new data on the  $e^+e^- \rightarrow \gamma_{\text{ISR}}\pi^+\pi^-\psi(3686)$  process [135]. In Fig. 22, the  $\pi^+\pi^-\psi(3686)$  invariant mass spectrum of  $e^+e^- \rightarrow \gamma_{\text{ISR}}\pi^+\pi^-\psi(3686)$  is presented.

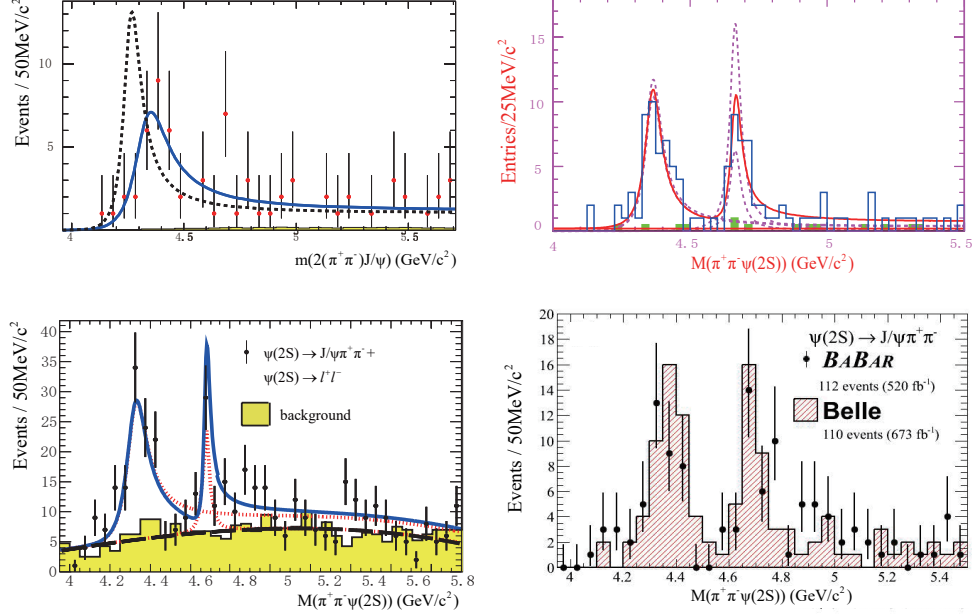


Figure 22: (Color online) The measured  $\pi^+\pi^-\psi(2S)$  invariant mass spectrum of  $e^+e^- \rightarrow \gamma_{\text{ISR}}\pi^+\pi^-\psi(2S)$  from BaBar and Belle. Here, the upper left and lower left panels are taken from BaBar [133, 135], and the upper right panel is taken from Belle [134]. The lower right panel is a comparison of the Belle (dots with errors) and BaBar (hatched histogram) data from BaBar [135].

A fit to the  $Y(4360)$  structure yielded a mass  $(4354 \pm 10)$  MeV and a width  $(78 \pm 16)$  MeV while a fit to the  $Y(4660)$  yielded a mass  $(4665 \pm 10)$  MeV and a width  $(53 \pm 16)$  MeV, where these resonance parameters of the  $Y(4360)$  and  $Y(4660)$  are the averaged values listed in PDG [1]. We summarize their resonance parameters from different experiments in Table 7. Since they are produced from the  $e^+e^-$  annihilation, the quantum numbers of the  $Y(4360)$  and  $Y(4660)$  are  $J^{PC} = 1^{--}$ .

Table 7: The resonance parameters for the  $Y(4360)$  and  $Y(4660)$  and the observed decay channels. The results shown in the last row were obtained by Liu, Qin and Yuan by performing a combined fit to BaBar and Belle data of  $e^+e^- \rightarrow \psi(3686)\pi^+\pi^-$ . Here, the mass and width are in units of MeV.

Experiment	$Y(4360)$	$Y(4660)$	Decay Mode
BaBar [133]	$M = 4324 \pm 24, \Gamma = 172 \pm 33$	–	$\psi(2S)\pi^+\pi^-$
Belle [134]	$M = 4361 \pm 9 \pm 9, \Gamma = 74 \pm 15 \pm 10$	$M = 4664 \pm 11 \pm 5, \Gamma = 48 \pm 15 \pm 3$	$\psi(2S)\pi^+\pi^-$
BaBar [135]	$M = 4340 \pm 16 \pm 9, \Gamma = 94 \pm 32 \pm 13$	$M = 4669 \pm 21 \pm 3, \Gamma = 104 \pm 48 \pm 10$	$\psi(2S)\pi^+\pi^-$
LQY [121]	$M = 4355^{+9}_{-10} \pm 9, \Gamma = 103^{+17}_{-15} \pm 11$	$M = 4661^{+9}_{-8} \pm 6, \Gamma = 42^{+17}_{-12} \pm 6$	$\psi(2S)\pi^+\pi^-$

For the  $Y(4360)$  and  $Y(4660)$ , only the  $\psi(3686)\pi^+\pi^-$  decay mode was observed [133, 134, 135]. Their open charm decay modes such as  $Y(4360)/Y(4660) \rightarrow D^0 D^{*-} \pi^+$  are still missing [117]. Belle [122] also indicated that there was

no evidence for the  $Y(4360)$  and  $Y(4660)$  in the  $J/\psi\eta$  final state from the  $e^+e^-$  annihilations.

2.1.2.3.  $Y(4630)$ . In 2008, the Belle Collaboration measured the exclusive  $e^+e^- \rightarrow \Lambda_c\bar{\Lambda}_c$  cross section, and observed an enhancement  $Y(4630)$  with a significance of  $8.2\sigma$ , which was close to the  $\Lambda_c\bar{\Lambda}_c$  threshold [136], as shown in Fig. 23. Its mass and width were determined to be  $M = (4634^{+8+5}_{-7-8})$  MeV and  $\Gamma = (92^{+40+10}_{-24-21})$  MeV, respectively, which are consistent within errors with the mass and width of the  $Y(4660)$  resonance [136]. Further experiments are needed to determine whether the  $Y(4630)$  and  $Y(4660)$  are the same structure.

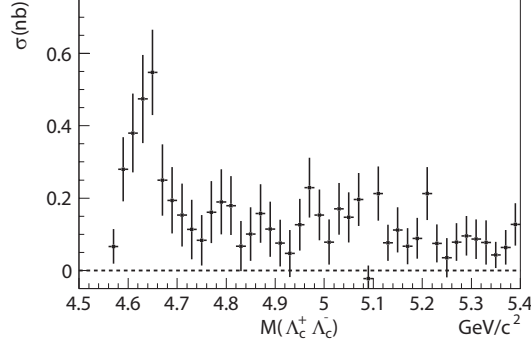


Figure 23: The cross section of the  $e^+e^- \rightarrow \Lambda_c\bar{\Lambda}_c$  process [136], where an enhancement structure  $Y(4630)$  appears in the  $\Lambda_c\bar{\Lambda}_c$  invariant mass spectrum.

### 2.1.3. $X$ states produced through double charmonium production

Two charmonium-like states  $X(3940)$  and  $X(4160)$  were observed through the double charmonium production. If one compares the Feynman diagrams shown in the second and third columns of Fig. 2, one would notice the similarity between the double charm production and the  $e^+e^-$  annihilation. However, there still exists difference, i.e., the final states of the double charmonium production process include a charmonium-like state plus a  $J/\psi$ . In contrast, those  $Y$  states discussed in Sec. 2.1.2 were directly produced via the  $e^+e^-$  annihilation. The two  $X$  states,  $X(3940)$  and  $X(4160)$ , were produced from the following processes:

$$\begin{aligned} X(3940) & : e^+e^- \rightarrow J/\psi\bar{D}D^*, \\ X(4160) & : e^+e^- \rightarrow J/\psi D^{*+}D^{*-}. \end{aligned}$$

2.1.3.1.  $X(3940)$ . The charmonium-like state  $X(3940)$  was first observed by the Belle Collaboration in the process  $e^+e^- \rightarrow J/\psi X(3940)$  with a significance of  $5.0\sigma$  [87], as shown in Fig. 24. Besides the  $X(3940)$ , three conventional charmonia  $\eta_c$ ,  $\chi_{c0}$ , and  $\eta_c(2S)$  were seen very clearly [87]. The mass of the  $X(3940)$  was measured to be  $(3943 \pm 6 \pm 6)$  MeV.

By performing a fit to the  $M_{\text{recoil}}(J/\psi)$  distributions for events tagged and constrained as  $e^+e^- \rightarrow J/\psi D\bar{D}$  and  $e^+e^- \rightarrow J/\psi D^*\bar{D}$  [87] (see Fig. 24), Belle found that there was no evidence of the  $X(3940) \rightarrow D\bar{D}$  decay mode, while the  $X(3940) \rightarrow D^*\bar{D}$  mode was observed. From this analysis, the width of the  $X(3940)$  was determined to be  $\Gamma = (15.4 \pm 10.1)$  MeV, and the upper limit of the branching ratio of the  $X(3940) \rightarrow D\bar{D}$  was set, i.e.,

$$\mathcal{B}(X(3940) \rightarrow D\bar{D}) < 41\%, \quad (41)$$

at 90% C.L.. In addition, Belle also set the upper limit for the hidden-charm decay  $X(3940) \rightarrow J/\psi\omega$ , i.e.,

$$\mathcal{B}(X(3940) \rightarrow J/\psi\omega) < 26\%, \quad (42)$$

at 90% C.L..

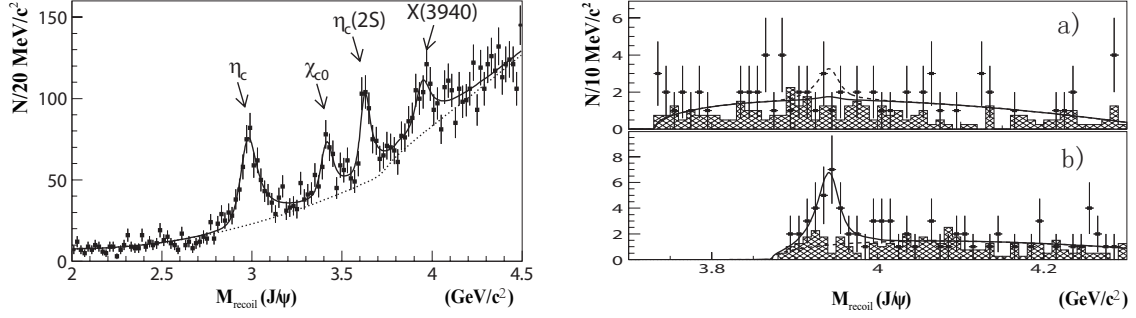


Figure 24: The distribution of masses recoiling against the reconstructed  $J/\psi$  in inclusive  $e^+e^- \rightarrow J/\psi X$  events (left). (a) and (b) are  $M_{\text{recoil}}(J/\psi)$  distributions for events tagged and constrained as  $e^+e^- \rightarrow J/\psi D\bar{D}$  and  $e^+e^- \rightarrow J/\psi D^*\bar{D}$ , respectively. Both taken from Belle [87].

Later, Belle confirmed the  $X(3940)$  in the process  $e^+e^- \rightarrow J/\psi D^*\bar{D}$  with a significance of  $5.7\sigma$  [137], where the resonance parameters of the  $X(3940)$  were measured to be  $M = (3942^{+7}_{-6} \pm 6)$  MeV and  $\Gamma = (37^{+26}_{-15} \pm 8)$  MeV [137].

At present, the only observed decay mode of the  $X(3940)$  was  $D^*\bar{D}$ . All the other decay modes like  $D\bar{D}$  and  $J/\psi\omega$  were not seen [87]. If  $e^+e^- \rightarrow J/\psi X(3940)$  is dominated by  $e^+e^- \rightarrow \gamma^* \rightarrow J/\psi X(3940)$ , the  $C$  parity of the  $X(3940)$  should be even, i.e.,  $C = +$ .

**2.1.3.2.  $X(4160)$ .** Using a data sample with an integrated luminosity of  $693 \text{ fb}^{-1}$  near the  $\Upsilon(4S)$  resonance, the Belle Collaboration also analyzed the  $e^+e^- \rightarrow J/\psi D^{*+}D^{*-}$  process and found a new charmonium-like state  $X(4160)$  with a significance of  $5.1\sigma$  [137]. The  $D^{*+}D^{*-}$  invariant mass spectrum is shown in Fig. 25. The mass and width of the  $X(4160)$  were measured to be  $M = (4156^{+25}_{-20} \pm 15)$  MeV and  $\Gamma = (139^{+111}_{-61} \pm 21)$  MeV [137], respectively. The  $C$  parity of the  $X(4160)$  is also even.

Besides the above observations, the analysis of Belle [137] showed that there may exist a broad structure in the  $M_{D\bar{D}}$  distribution (see Fig. 25 (a)), which can not be described by the non-resonant  $e^+e^- \rightarrow J/\psi D\bar{D}$  events. This structure was quite puzzling. Unfortunately the present data sample was not large enough to analyze this possible resonant structure [137].

Although both the  $X(3940)$  and  $X(4160)$  have a statistical significance larger than  $5\sigma$ , they were only observed by the Belle experiments, and still need to be confirmed by other experiments.

#### 2.1.4. The XYZ states from $\gamma\gamma$ fusion processes

The  $\gamma\gamma$  fusion process  $\gamma\gamma \rightarrow X$  produces  $C$ -even charmonium states in  $B$  factories. According to the Landau-Yang selection rule [138, 139], two photons do not couple to any  $J = 1$  state. Therefore,  $\gamma\gamma$  fusion process can only produce charmonium-like states with quantum numbers  $I^G J^{PC} = 0^+0^{++}$  and  $0^+2^{++}$ . To date, three new charmonium-like states were reported in the  $\gamma\gamma$  fusion processes. They are the  $Z(3930)$  in the  $\gamma\gamma \rightarrow D\bar{D}$  process [140], the  $X(3915)$  in the  $\gamma\gamma \rightarrow \omega J/\psi$  process [141], and the  $X(4350)$  in the  $\gamma\gamma \rightarrow \phi J/\psi$  process [88].

$$\begin{aligned} Z(3930) &: \quad \gamma\gamma \rightarrow D\bar{D}, \\ X(3915) &: \quad \gamma\gamma \rightarrow J/\psi\omega, \\ X(4350) &: \quad \gamma\gamma \rightarrow J/\psi\phi. \end{aligned}$$

The possible quantum numbers of the  $Z(3930)$ ,  $X(3915)$  and  $X(4350)$  states are either  $I^G J^{PC} = 0^+0^{++}$  or  $0^+2^{++}$ .

**2.1.4.1.  $Z(3930)$ .** The  $Z(3930)$  is one of the four charmonium-like states around 3940 MeV reported by the Belle Collaboration in 2005 [140]. The others are the  $Y(3940)$ ,  $X(3940)$ , and  $X(3915)$ , which are discussed in Sec. 2.1.1.2, 2.1.3.1 and 2.1.4.2, respectively. The  $Z(3930)$  was observed in the  $D\bar{D}$  invariant mass spectrum of the process of  $\gamma\gamma \rightarrow D\bar{D}$  (see Fig. 26), with the mass  $M = (3929 \pm 5 \pm 2)$  MeV, width  $\Gamma = (29 \pm 10 \pm 2)$  MeV, and its two-photon

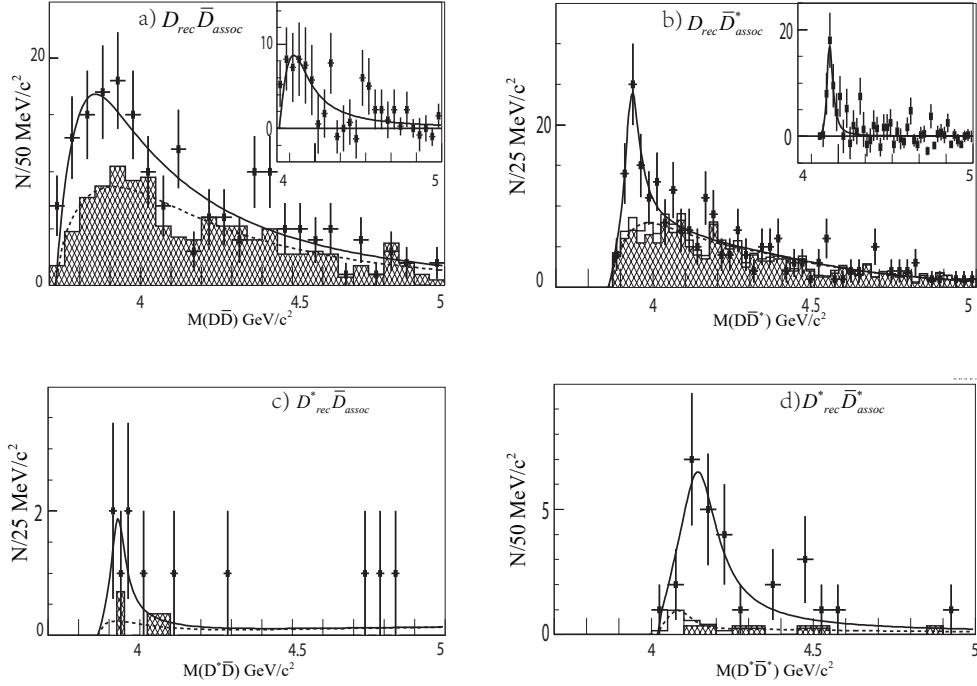


Figure 25: The  $M(D_{\text{rec}}^{(*)}\bar{D}_{\text{assoc}}^{(*)})$  spectra for events tagged and constrained as (a)  $e^+e^- \rightarrow J/\psi D\bar{D}$ , (b)  $e^+e^- \rightarrow J/\psi D\bar{D}^*$ , (c)  $e^+e^- \rightarrow J/\psi D^*\bar{D}$ , and (d)  $e^+e^- \rightarrow J/\psi D^*\bar{D}^*$ , from Belle [137].

decay width times the branching fraction  $\Gamma(Z(3930) \rightarrow \gamma\gamma) \times \mathcal{B}(Z(3930) \rightarrow D\bar{D}) = (0.18 \pm 0.05 \pm 0.03) \text{ keV}$  (for  $J = 2$ ) [140].

In Ref. [140], Belle also measured the  $\cos\theta^*$  distributions in the  $3.91 < M(D\bar{D}) < 3.95 \text{ GeV}$  region, where  $\theta^*$  denotes the angle of a  $D$  meson relative to the beam axis in the  $\gamma\gamma$  center of mass frame [140] (see the left panel in Fig. 27). The experimental analysis indicated that the  $J = 2$  assignment was favored significantly. In addition, Belle measured the ratio of the branching fractions for the  $D^0\bar{D}^0$  and  $D^+D^-$  modes to be  $\mathcal{B}(Z(3930) \rightarrow D^+D^-)/\mathcal{B}(Z(3930) \rightarrow D^0\bar{D}^0) = (0.74 \pm 0.43 \pm 0.16)$ , suggesting isospin invariance as expected for the conventional  $c\bar{c}$  states. As indicated in Ref. [140], the measured mass, decay width, decay angular distribution and  $\Gamma(Z(3930) \rightarrow \gamma\gamma) \times \mathcal{B}(Z(3930) \rightarrow D\bar{D})$  of the  $Z(3930)$  state supported the  $Z(3930)$  as the candidate of the missing  $2^3P_2$  charmonium state  $\chi'_{c2}(2P)$ , which was predicted in Refs. [140, 17, 106, 142].

The BaBar Collaboration confirmed the  $Z(3930)$  state in the  $D\bar{D}$  invariant mass distribution of  $\gamma\gamma \rightarrow D\bar{D}$  process, with the mass  $M = (3926.7 \pm 2.7 \pm 1.1) \text{ MeV}$  and width  $\Gamma = (21.3 \pm 6.8 \pm 3.6) \text{ MeV}$ , respectively [143]. They identified the  $Z(3930)$  as a tensor state with  $J^{PC} = 2^{++}$  as shown in the right panel of Fig. 27.

The open charm decay mode  $Z(3930) \rightarrow D\bar{D}^*$  is also expected since the  $Z(3930)$  lies above the  $D\bar{D}^*$  threshold, which will test the assignment of the  $Z(3930)$  as the  $\chi'_{c2}(2P)$  charmonium state. In PDG [1], the  $Z(3930)$  state was assigned as the radially excited charmonium  $\chi'_{c2}(2P)$  with  $J^{PC} = 2^{++}$ .

**2.1.4.2.  $X(3915)$ .** The  $X(3915)$  ( $\chi'_{c0}(2P)$  in PDG [1]) state was first reported by the Belle Collaboration in  $\gamma\gamma \rightarrow \omega J/\psi$  process [141] (see the left panel in Fig. 28). The measured mass and decay width were  $M = (3915 \pm 3 \pm 2) \text{ MeV}$  and  $\Gamma = (17 \pm 10 \pm 3) \text{ MeV}$ , respectively. Since the quantum numbers of both the  $J/\psi$  and  $\omega$  are  $I^C J^{PC} = 0^- 1^{--}$ , the  $X(3915)$  carries positive  $C$ -parity and  $G$ -parity. As discussed above for the  $\gamma\gamma$  fusion process, the possible spin-parity for the  $X(3915)$  is  $J^P = 0^+$  or  $2^+$ . For these two assignments, Belle gave the products of the two-photon decay width

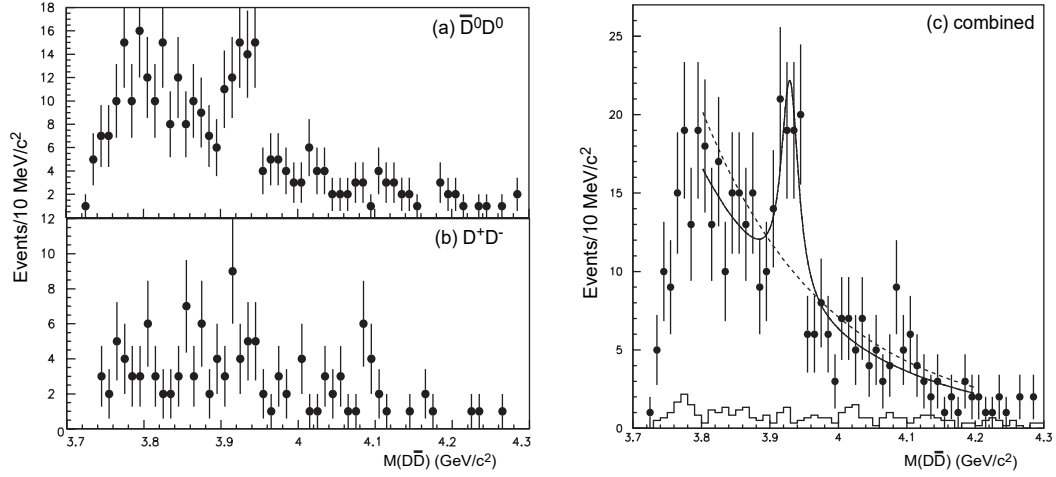


Figure 26: The  $D\bar{D}$  invariant mass distribution from Belle [140], in which (a) is the  $D^0\bar{D}^0$ , (b) the  $D^+D^-$  mode and (c) the combined distribution.

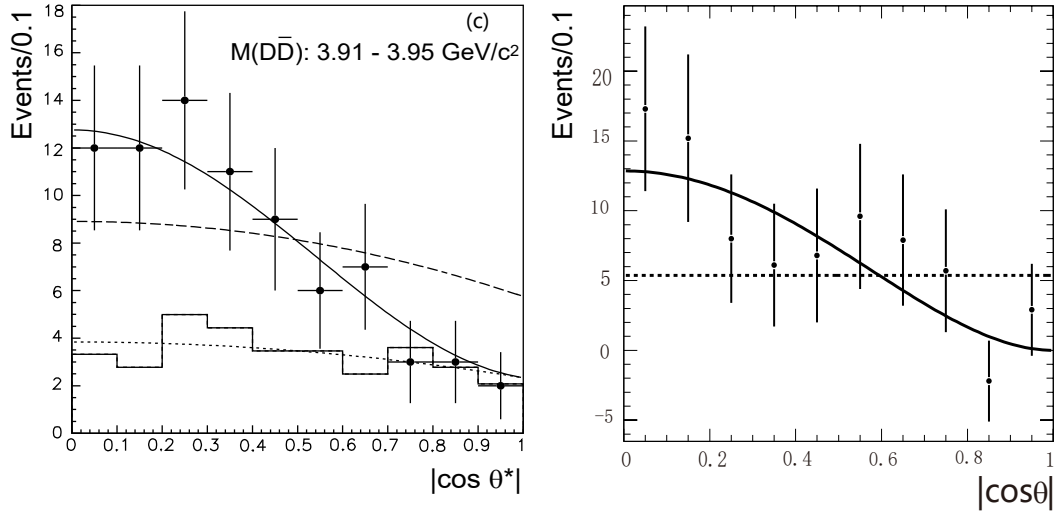


Figure 27: The  $|\cos \theta^*|$  and  $|\cos \theta|$  distributions from Belle [140] and BaBar [143], respectively.

and the branching fraction to  $\omega J/\psi$  as [141]

$$\Gamma(X(3915) \rightarrow \gamma\gamma) \times \mathcal{B}(X(3915) \rightarrow \omega J/\psi) = \begin{cases} (61 \pm 17 \pm 8) \text{ eV} & \text{for } J^P = 0^+, \\ (18 \pm 5 \pm 2) \text{ eV} & \text{for } J^P = 2^+, \text{ helicity-2.} \end{cases} \quad (43)$$

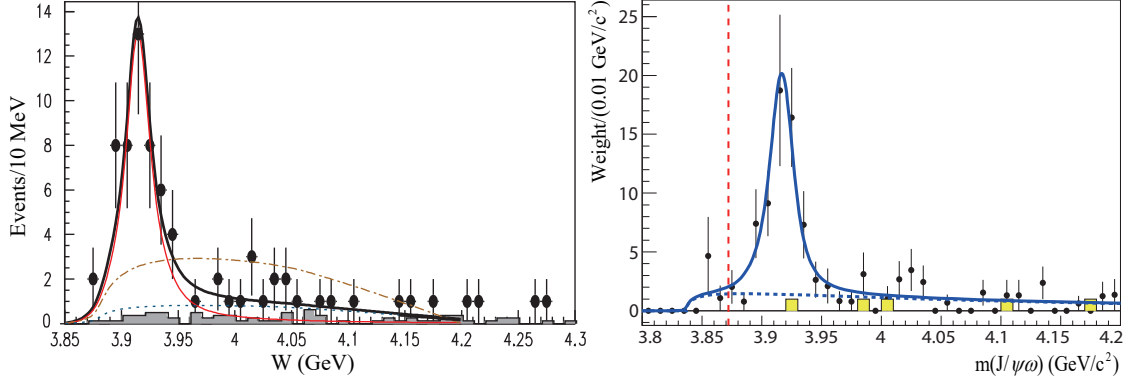


Figure 28: (Color online) The  $X(3915) \rightarrow \omega J/\psi$  signals in the  $\gamma\gamma \rightarrow \omega J/\psi$  process from Belle [141] (left) and BaBar [144] (right).

The BaBar Collaboration confirmed the existence of the  $X(3915)$  decaying into  $\omega J/\psi$  in  $\gamma\gamma \rightarrow \omega J/\psi$  process (see the right panel in Fig. 28), with the mass  $(3919.4 \pm 2.2 \pm 1.6)$  MeV and width  $(13 \pm 6 \pm 3)$  MeV [144]. Their analysis favored the  $J^P = 0^+$  assignment. BaBar also measured  $\Gamma(X(3915) \rightarrow \gamma\gamma) \times \mathcal{B}(X(3915) \rightarrow \omega J/\psi) = (52 \pm 10 \pm 3)$  eV, which was consistent with Belle's measurement for the  $J^P = 0^+$  assignment [141].

According to the BaBar's measurement, PDG assigned the  $X(3915)$  as the charmonium radial excitation  $\chi'_{c0}(2P)$  [1]. The open-charm decay mode  $X(3915) \rightarrow D^{(*)}\bar{D}^{(*)}$  was expected for the conventional  $\chi'_{c0}(2P)$  state. However, there were no signs of the  $D^{(*)}\bar{D}^{(*)}$  peak around 3915 MeV in both Belle [145] and BaBar's [76] analyses of the  $B \rightarrow KD^{(*)}\bar{D}^{(*)}$  process. This puzzling phenomenon should be clarified in future experiments.

Belle also studied the radiative decay of  $\Upsilon(2S)$  to search for the  $X(3915)$ . They found no significant signals and set an upper limit  $\mathcal{B}(\Upsilon(2S) \rightarrow \gamma X(3915)) \times \mathcal{B}(X(3915) \rightarrow \omega J/\psi) < 2.8 \times 10^{-6}$  at 90% C.L. [146, 147].

**2.1.4.3.  $X(4350)$ .** In Sec. 2.1.1.3, we introduced the discovery of the  $Y(4140)$  by the CDF Collaboration [58]. The Belle Collaboration studied the  $\gamma\gamma \rightarrow \phi J/\psi$  process to search for the  $Y(4140)$  state [88]. However, they did not see the  $Y(4140)$  signal in the  $\gamma\gamma$  fusion process. Unexpectedly, they observed another new narrow structure around 4.35 GeV in the  $\phi J/\psi$  invariant mass distribution (see Fig. 29), which was named as  $X(4350)$ . The mass and width of this charmonium-like state was measured to be  $(4350.6_{-5.1}^{+4.6} \pm 0.7)$  MeV and  $(13_{-9}^{+18} \pm 4)$  MeV, respectively. Similar to the  $Y(4140)$  and  $X(3915)$ , the possible quantum number of the  $X(4350)$  is either  $I^G J^{PC} = 0^+0^{++}$  or  $0^+2^{++}$ . Belle also measured the product of the two-photon decay width of the  $X(4350)$  and its branching fraction to  $\phi J/\psi$  [88], i.e.,

$$\Gamma(X(4350) \rightarrow \gamma\gamma) \times \mathcal{B}(X(4350) \rightarrow \phi J/\psi) = \begin{cases} (6.7_{-2.4}^{+3.2} \pm 1.1) \text{ eV} & \text{for } J^P = 0^+, \\ (1.5_{-20.6}^{+0.7} \pm 0.3) \text{ eV} & \text{for } J^P = 2^+. \end{cases} \quad (44)$$

Later, Belle also tried to search for the  $X(4350)$  via the radiative decay of  $\Upsilon(2S)$ , and only obtained the upper limit  $\mathcal{B}(\Upsilon(2S) \rightarrow \gamma X(4350)) \times \mathcal{B}(X(4350) \rightarrow \phi J/\psi) < 1.3 \times 10^{-6}$  at 90% C.L. [146, 147].

### 2.1.5. Charged charmonium-like $Z_c$ states

Until now, there have accumulated abundant experimental observations of the charged charmonium-like states. In Sec. 2.1.1, we have introduced the charged charmonium-like states observed in the  $B$  meson decays. In this section, we focus on the charged charmonium-like states from the hadronic decays of the  $Y(4260)$  and higher charmonia. We

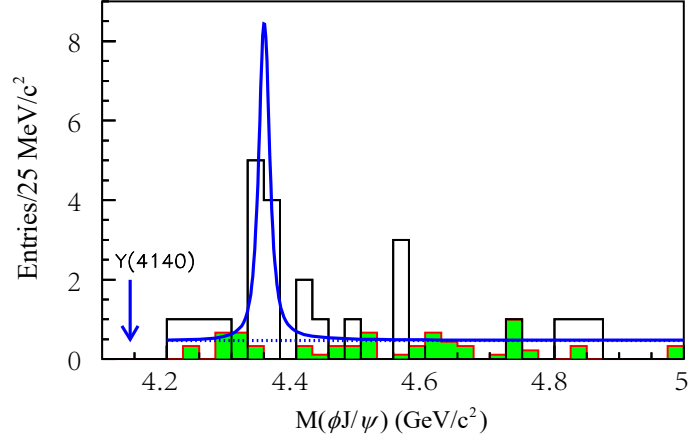


Figure 29: (Color online) The  $\omega J/\psi$  invariant mass distribution of  $\gamma\gamma \rightarrow \omega J/\psi$  from Belle [88].

collect the productions and decay modes of the four charged charmonium-like states  $Z_c(3900)$ ,  $Z_c(3885)$ ,  $Z_c(4025)$  and  $Z_c(4020)$  below,

$$e^+e^- \rightarrow \begin{cases} Z_c(3900)\pi^\mp \rightarrow J/\psi\pi^\pm\pi^\mp, \\ Z_c(4025)\pi^\mp \rightarrow (D^*\bar{D}^*)^\pm\pi^\mp, \\ Z_c(4020)\pi^\mp \rightarrow h_c\pi^\pm\pi^\mp, \\ Z_c(3885)\pi^+ \rightarrow (D\bar{D}^*)^-\pi^+. \end{cases}$$

2.1.5.1.  $Z_c(3900)$  and  $Z_c(3885)$ . Since 2013, the BESIII Collaboration announced several charged charmonium-like states  $Z_c(3900)$  [53],  $Z_c(3885)$  [148],  $Z_c(4020)$  [149] and  $Z_c(4025)$  [150] at  $\sqrt{s} = 4.26$  GeV. All these structures were observed in the process  $Y(4260) \rightarrow \pi^- Z_c^+$  (as shown in Table 8). The  $Z_c(3900)$  state was also observed by Belle [113] and confirmed later using data of CLEO-c [50]. Before we discuss these charged charmonium-like states, we collect the experimental information of these states in Table 8, including their masses, widths, production processes from different experiments.

Table 8: Experimental information of the charged charmonium-like states  $Z_c(3900)$ ,  $Z_c(3885)$ ,  $Z_c(4020)$  and  $Z_c(4025)$ , including their masses, widths and production processes.

State	$M$ (MeV)	$\Gamma$ (MeV)	Process (decay mode)	Experiment
$Z_c(3900)$	$3899.0 \pm 3.6 \pm 4.9$	$46 \pm 10 \pm 20$	$e^+e^- \rightarrow Y(4260) \rightarrow \pi^- + (J/\psi\pi^+)$	BESIII [53]
	$3894.5 \pm 6.6 \pm 4.5$	$63 \pm 24 \pm 26$	$e^+e^- \rightarrow Y(4260) \rightarrow \pi^- + (J/\psi\pi^+)$	Belle [113]
	$3886 \pm 4 \pm 2$	$37 \pm 4 \pm 8$	$e^+e^- \rightarrow \psi(4160) \rightarrow \pi^- + (J/\psi\pi^+)$	Xiao <i>et al.</i> [50]
$Z_c(3885)$	$3883.9 \pm 1.5 \pm 4.2$	$24.8 \pm 3.3 \pm 11.0$	$e^+e^- \rightarrow Y(4260) \rightarrow \pi^- + (D\bar{D}^*)^+$	BESIII [148]
$Z_c(4020)$	$4022.9 \pm 0.8 \pm 2.7$	$7.9 \pm 2.7 \pm 2.6$	$e^+e^- \rightarrow Y(4260) \rightarrow \pi^- + (h_c\pi^+)$	BESIII [149]
$Z_c(4025)$	$4026.3 \pm 2.6 \pm 3.7$	$24.8 \pm 5.6 \pm 7.7$	$e^+e^- \rightarrow Y(4260) \rightarrow \pi^- + (D^*\bar{D}^*)^+$	BESIII [150]

The  $Z_c(3900)$  was observed in the  $J/\psi\pi^\pm$  invariant mass distribution of the  $e^+e^- \rightarrow J/\psi\pi^+\pi^-$  process by the BESIII Collaboration [53]. As shown in Fig. 30, the mass peak of the  $Z_c(3900)$  in this channel lies about 23 MeV above the open-charm threshold  $D^+\bar{D}^{*0}$  (or  $D^{*+}\bar{D}^0$ ). In the same production channel, Belle also reported the  $Z_c(3900)$  structure [113]. Meanwhile, Xiao *et al.* analyzed the decay  $\psi(4160) \rightarrow J/\psi\pi^+\pi^-$  and observed the charged  $Z_c(3900)$  [50]. As shown in Table 8, the mass and decay width of the charged  $Z_c(3900)$  from different experiments are consistent with each other. From these three experiments, the quantum number of the  $Z_c(3900)$  was argued to be  $I^G J^P = 1^+ 1^+$  assuming the orbital angular momentum between the  $J/\psi$  and  $\pi$  is zero.

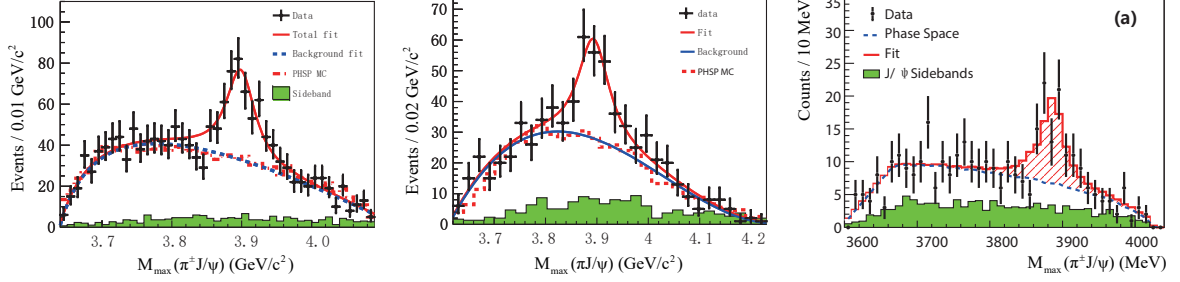


Figure 30: (Color online) The  $Z_c(3900)$  enhancements in the  $J/\psi\pi^\pm$  mass spectrum from BESIII [53] (left), Belle [113] (middle) and Xiao *et al.* [50] (right) respectively.

BESIII also studied the open-charm decay  $e^+e^- \rightarrow Y(4260) \rightarrow (D\bar{D}^*)^\pm\pi^\mp$  [148] and found a charged structure in the  $(D\bar{D}^*)^\pm$  mass spectrum, as shown in Fig. 31. BESIII named this structure as the  $Z_c(3885)$  since its measured mass (see Table 8) was slightly lower than that of the  $Z_c(3900)$  measured in the  $J/\psi\pi$  channel by BESIII [53] and Belle [113]. However, the measured mass and width of the  $Z_c(3885)$  [148] were consistent with those of the  $Z_c(3900)$  state obtained by Xiao *et al.* [50]. If we consider the  $Z_c(3900)$  and  $Z_c(3885)$  as the same state, the  $Z_c(3900)/Z_c(3885)$  was observed in both the hidden-charm  $J/\psi\pi$  and open-charm  $D\bar{D}^*$  decay channels.

BESIII also performed the analysis on the angular distribution of the  $\pi Z_c(3885)$  system [148]. As shown in Fig. 31, the data supported the  $J^P = 1^+$  assignment and ruled out the  $J^P = 0^-, 1^-$  possibilities. With the same spin-parity and similar mass and width, the  $Z_c(3900)$  and  $Z_c(3885)$  were probably the same state. Under this assumption, the ratio of the partial decay width of these two decay modes was measured as [148]

$$\frac{\Gamma(Z_c(3885) \rightarrow D\bar{D}^*)}{\Gamma(Z_c(3900) \rightarrow J/\psi\pi)} = (6.2 \pm 1.1 \pm 2.7). \quad (45)$$

In other words,  $D\bar{D}^*$  was the dominant decay mode of the  $Z_c(3900)/Z_c(3885)$ . However, this ratio is still much smaller than those of the established conventional charmonium states above the open-charm threshold, such as the  $\psi(3770)$  and  $\psi(4040)$ :

$$\begin{aligned} \frac{\Gamma(\psi(3770) \rightarrow D\bar{D})}{\Gamma(\psi(3770) \rightarrow \pi\pi J/\psi)} &= (482 \pm 84) [1], \\ \frac{\Gamma(\psi(4040) \rightarrow D^{(*)}\bar{D}^{(*)})}{\Gamma(\psi(4040) \rightarrow \eta J/\psi)} &= (192 \pm 27) [151]. \end{aligned} \quad (46)$$

The neutral partners of the charged  $Z_c(3900)^\pm$  and  $Z_c(3885)^\pm$  states were also reported. In Ref. [50], Xiao *et al.* provided evidence of the neutral state  $Z_c(3900)^0$  decaying into  $\pi^0 J/\psi$  at a  $3.5\sigma$  significance level, as shown in Fig. 32. The mass and decay width of the  $Z_c(3900)^0$  were obtained as  $(3904 \pm 9 \pm 5)$  MeV and 37 MeV [50], respectively. Recently, the  $Z_c(3900)^0$  was discovered by BESIII in the  $e^+e^- \rightarrow \pi^0 Z_c(3900)^0 \rightarrow \pi^0\pi^0 J/\psi$  process with a significance of  $10.4\sigma$  [152] (see Fig. 32). The measured mass  $(3894.8 \pm 2.3 \pm 3.2)$  MeV and width  $(29.6 \pm 8.2 \pm 8.2)$  MeV were consistent with the results obtained in Ref. [50]. BESIII also reported a neutral state  $Z_c(3885)^0$  in the  $e^+e^- \rightarrow (D\bar{D}^*)^0\pi^0$  process with the mass  $M = (3885.7^{+4.3}_{-5.7} \pm 8.4)$  MeV and width  $\Gamma = (35^{+11}_{-12} \pm 15)$  MeV [153].

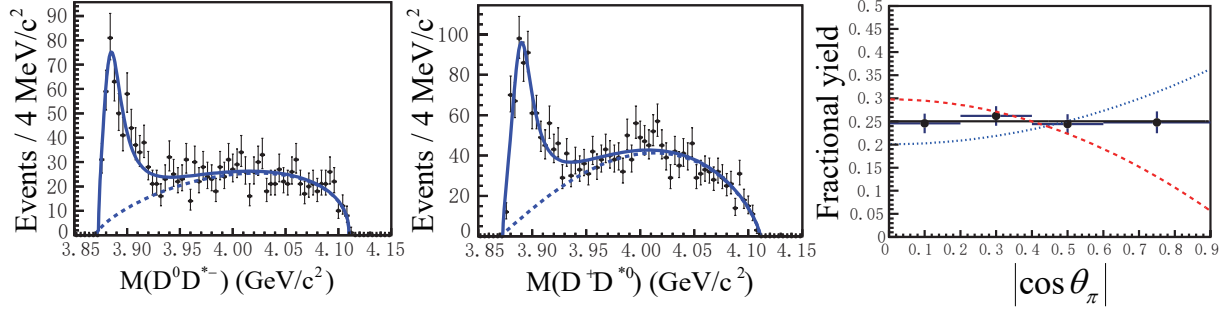


Figure 31: (Color online) The  $Z_c(3900)$  structure in the  $(D\bar{D}^*)^\pm$  final states from BESIII [148].

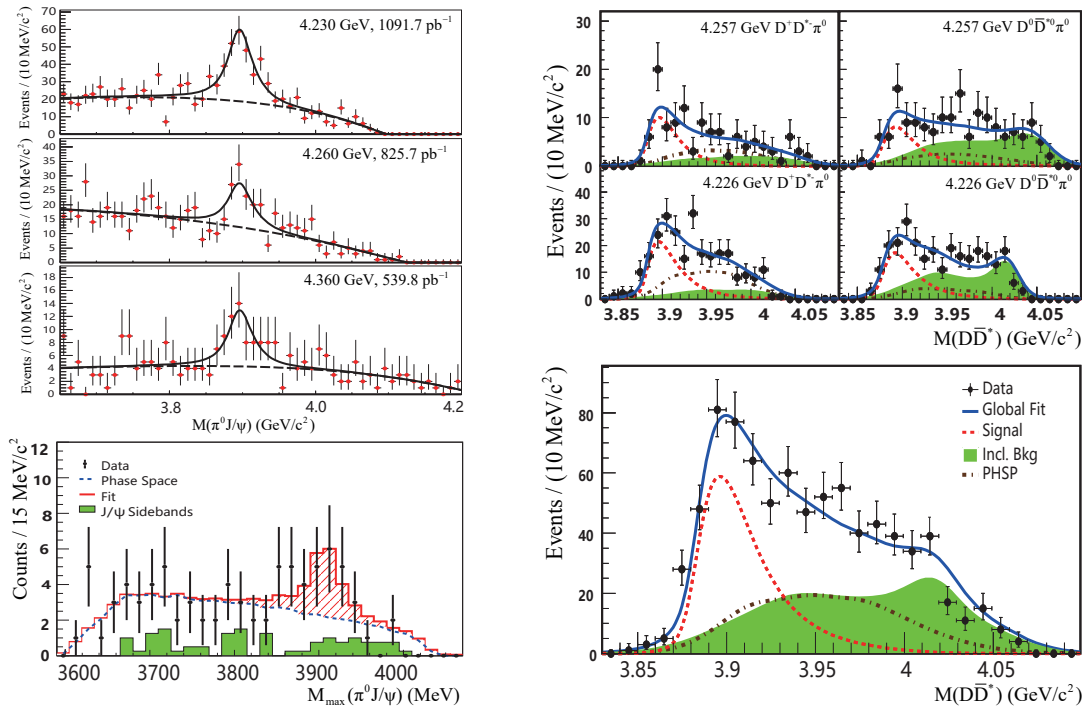


Figure 32: (Color online) The neutral  $Z_c(3900)^0$  state in  $\pi^0 J/\psi$  mass spectrum from BESIII [152] and Xiao *et al.* [50] and  $(D\bar{D}^*)^0$  final states from BESIII [153].

Besides, a search for the  $Z_c(3900)^\pm$  state in the exclusive production process by virtual photons was performed in the channel  $Z_c(3900)^\pm \rightarrow J/\psi\pi^\pm$  at COMPASS [154]. There was no signal of the exclusive photoproduction of the  $Z_c(3900)^\pm$  state and its decay into  $J/\psi\pi^\pm$ . The upper limit of the ratio  $\mathcal{B}(Z_c(3900)^\pm \rightarrow J/\psi\pi^\pm) \times \sigma_{\gamma N \rightarrow Z_c(3900)^\pm N} / \sigma_{\gamma N \rightarrow J/\psi N}$  was determined to be  $3.7 \times 10^{-3}$ , which suggested that the hidden-charm decay mode  $Z_c(3900)^\pm \rightarrow J/\psi\pi^\pm$  was not its dominant decay mode.

BESIII studied the  $Z_c(3900)^\pm \rightarrow \omega\pi^\pm$  decay and found no significant  $Z_c(3900)^\pm$  signals [155]. In Ref. [156], the isospin violating decay  $Y(4260) \rightarrow J/\psi\eta\pi^0$  was also studied by BESIII. No signal was observed and the upper limit of the branching fraction ratio  $\mathcal{B}(Z_c^0 \rightarrow J/\psi\eta) / \mathcal{B}(Z_c^0 \rightarrow J/\psi\pi^0)$  was measured to be 0.15 at  $\sqrt{s} = 4.226$  GeV and 0.65 at  $\sqrt{s} = 4.257$  GeV.

**2.1.5.2.  $Z_c(4025)$  and  $Z_c(4020)$ .** The  $Z_c(4025)$  state was first observed in the  $(D^*\bar{D}^*)^\pm$  mass spectrum in the  $e^+e^- \rightarrow Y(4260) \rightarrow (D^*\bar{D}^*)^\pm\pi^\mp$  process by BESIII [150]. Almost at the same time, BESIII reported another charged charmonium-like structure  $Z_c(4020)$  in the  $\pi^\pm h_c$  invariant mass distribution in the process of  $e^+e^- \rightarrow Y(4260) \rightarrow \pi^\pm\pi^\mp h_c$  [149]. The masses and widths of the  $Z_c(4025)$  and  $Z_c(4020)$  resonances are collected in Table 8. As shown in Fig. 33, the mass of the  $Z_c(4025)$  state is very close to that of the  $Z_c(4020)$  while the  $Z_c(4025)$  is much broader than the  $Z_c(4020)$ . In general, the resonance parameters of the  $Z_c(4020)$  agree with those of the  $Z_c(4025)$  state within  $1.5\sigma$  [149]. If the  $Z_c(4025)$  and  $Z_c(4020)$  are the same state, its quantum number was probably  $I^G J^P = 1^+ 1^+$  [157].

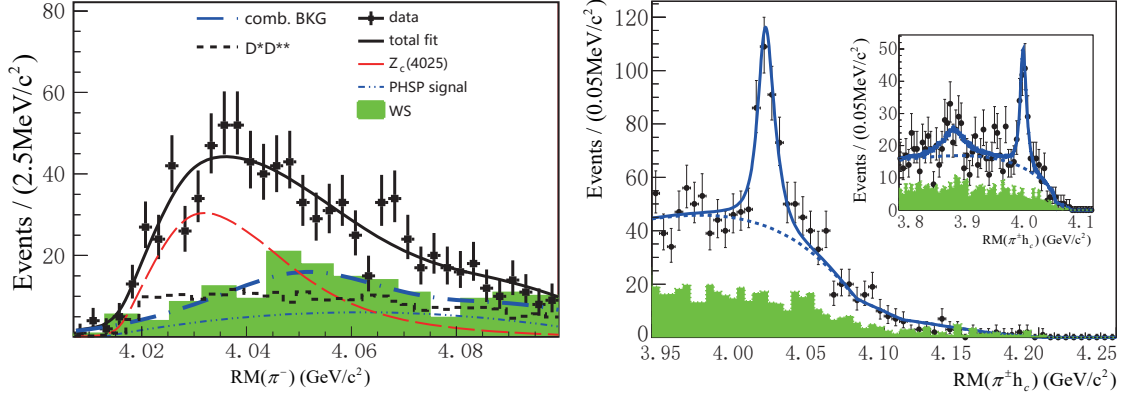


Figure 33: (Color online) The mass peaks of the  $Z_c(4025)$  [150] and  $Z_c(4020)$  [149] resonances in  $(D^*\bar{D}^*)^\pm$  (left) and  $\pi^\pm h_c$  (right) invariant mass distributions, respectively. The inset in the right panel shows the result of distributions including both the  $Z_c(4020)$  and  $Z_c(3900)$  decaying into  $\pi^\pm h_c$ .

The  $Z_c(3900)^\pm \rightarrow h_c\pi^\pm$  process was also included in the fit, which was shown as the inset in the right panel in Fig. 33 [149]. There was a weak signal of the  $Z_c(3900)$  with a statistical significance of  $2.1\sigma$  in this situation. The production cross section of  $Z_c(3900)^\pm \rightarrow \pi^\pm h_c$  was found to be smaller than 11 pb at  $\sqrt{s} = 4.26$  GeV at 90% C.L. [149]. This upper limit was lower than the production cross section of  $Z_c(3900)^\pm \rightarrow \pi^\pm J/\psi$  obtained in Ref. [53], which is about 14 pb.

Recently, the neutral partners of the  $Z_c(4025)$  and  $Z_c(4020)$  states were also observed by BESIII. In Ref. [158], a neutral state  $Z_c(4020)^0$  was reported in the  $e^+e^- \rightarrow \pi^0\pi^0 h_c$  process. Its production cross section was half of that in the  $e^+e^- \rightarrow \pi^+\pi^- h_c$  process within less than  $2\sigma$ . The mass of the  $Z_c(4020)^0$  was  $(4023.9 \pm 2.2 \pm 3.8)$  MeV, which was consistent with that of the charged  $Z_c^\pm(4020)$  state. Later, BESIII observed another neutral state  $Z_c(4025)^0$  in the  $(D^*\bar{D}^*)^0$  invariant mass distribution of  $e^+e^- \rightarrow \pi^0(D^*\bar{D}^*)^0$  process at  $\sqrt{s} = 4.23$  GeV and 4.26 GeV [159]. The measured mass and decay width were  $(4025.5^{+2.0}_{-4.7} \pm 3.1)$  MeV and  $(23.0 \pm 6.0 \pm 1.0)$  MeV, respectively. The production cross section  $\sigma(e^+e^- \rightarrow Z_c(4025)^0\pi^0 \rightarrow \pi^0(D^*\bar{D}^*)^0)$  was measured to be  $(43.4 \pm 8.0 \pm 5.4)$  pb at  $\sqrt{s} = 4.26$  GeV. Thus, the ratio  $\frac{\sigma(e^+e^- \rightarrow Z_c(4025)^0\pi^0 \rightarrow \pi^0(D^*\bar{D}^*)^0)}{\sigma(e^+e^- \rightarrow Z_c^\pm(4025)\pi^\mp \rightarrow \pi^\mp(D^*\bar{D}^*)^\pm)} \sim 1$  at  $\sqrt{s} = 4.26$  GeV [159]. This result is consistent with the expectation of isospin symmetry. The mass peaks of the neutral states  $Z_c(4020)^0$  and  $Z_c(4025)^0$  in the  $\pi^0 h_c$  and  $(D^*\bar{D}^*)^0$  invariant mass distributions are shown in Fig. 34.

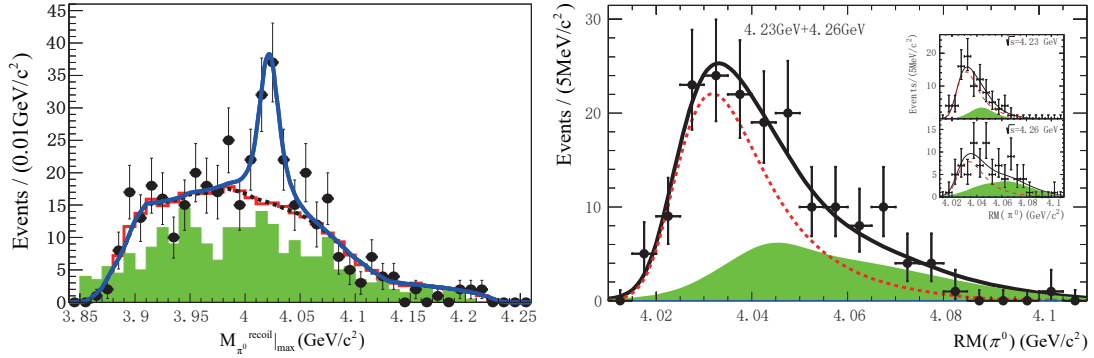


Figure 34: (Color online) The neutral states  $Z_c(4020)^0$  and  $Z_c(4025)^0$  in the  $\pi^0 h_c$  [158] and  $(D^* \bar{D}^*)^0$  [159] invariant mass distributions. For the  $(D^* \bar{D}^*)^0$  distribution, the main fit is for the combination of all data while the inset plots are for the two collision energy.

## 2.2. The hidden-charm pentaquark states observed by LHCb

Recently, the LHCb Collaboration reported the observation of two exotic structures, denoted as the  $P_c(4380)^+$  and  $P_c(4450)^+$ , in the  $J/\psi p$  invariant mass spectrum of the  $\Lambda_b^0 \rightarrow J/\psi K^- p$  decay [2]. They used the data of  $pp$  collisions corresponding to  $1 \text{ fb}^{-1}$  of integrated luminosity at 7 TeV, and  $2 \text{ fb}^{-1}$  at 8 TeV. The significances of the lower mass and higher mass states are  $9\sigma$  and  $12\sigma$ , respectively. Both resonances decay into the  $J/\psi p$  final states. They must have minimal quark contents  $c\bar{c}uud$ , and thus are good candidates of exotic hidden-charm pentaquarks. Further experimental research should be pursued to confirm these pentaquark states.

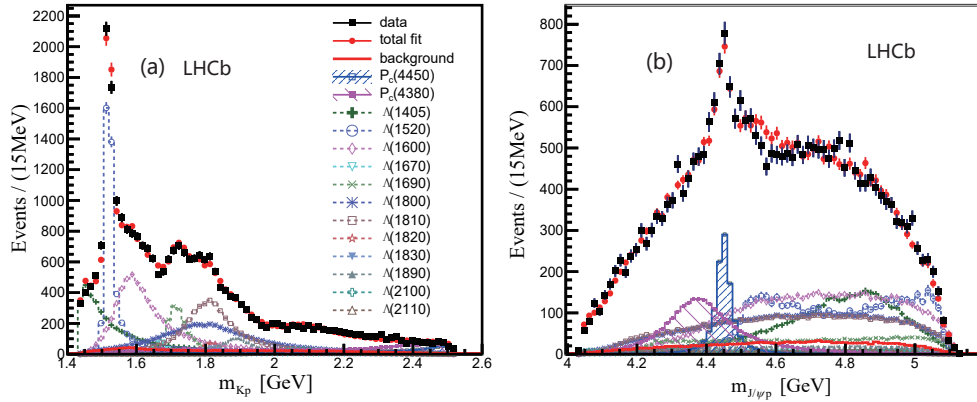


Figure 35: (Color online) The  $K^- p$  (left) and  $J/\psi p$  (right) invariant mass spectrum of  $\Lambda_b^0 \rightarrow J/\psi K^- p$  from LHCb [2], where the background has been subtracted. Fit projections for the reduced  $\Lambda^*$  model with two  $P_c^+$  states are also shown.

The LHCb Collaboration used an amplitude analysis of the three-body final-state, and extracted the masses and widths of the  $P_c(4380)^+$  and  $P_c(4450)^+$  to be

$$\begin{aligned}
 M_{P_c(4380)^+} &= (4380 \pm 8 \pm 29) \text{ MeV}, \\
 \Gamma_{P_c(4380)^+} &= (205 \pm 18 \pm 86) \text{ MeV}, \\
 M_{P_c(4450)^+} &= (4449.8 \pm 1.7 \pm 2.5) \text{ MeV}, \\
 \Gamma_{P_c(4450)^+} &= (39 \pm 5 \pm 19) \text{ MeV}.
 \end{aligned} \tag{47}$$

The  $P_c(4380)^+$  and  $P_c(4450)^+$  states preferred the  $J^P$  assignments  $(3/2^-, 5/2^+)$ . However, the  $-2 \ln \mathcal{L}$  values were

only 1 unit better than those of the parity reversed combination  $(3/2^+, 5/2^-)$ , and  $2.3^2$  units better than those of the  $(5/2^+, 3/2^-)$  assignment. All the other combinations from  $1/2^\pm$  through  $7/2^\pm$  were tested and ruled out.

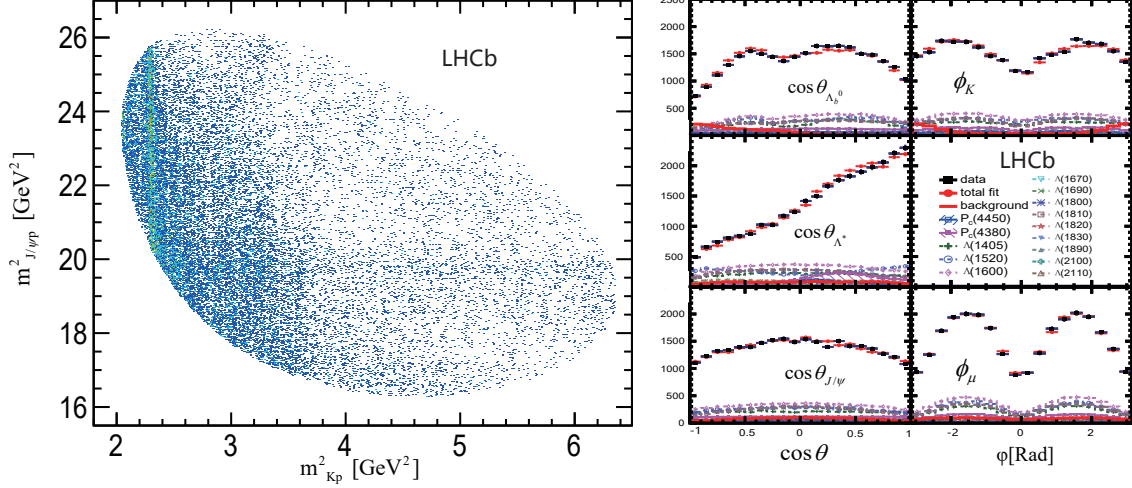


Figure 36: (Color online) Left: the Dalitz plot using the  $K^- p$  and  $J/\psi p$  invariant masses-squared from LHCb [2]. Right: various decay angular distributions for the best fit with the two  $P_c^+$  states.

Their best fit projections with these two  $P_c^+$  states are shown in Fig. 35, where the fractions of the total sample due to the  $P_c(4380)^+$  and  $P_c(4450)^+$  are  $(8.4 \pm 0.7 \pm 4.2)\%$  and  $(4.1 \pm 0.5 \pm 1.1)\%$ , respectively. For comparison, the fractions of the  $\Lambda(1405)$  and  $\Lambda(1520)$  are  $(15 \pm 1 \pm 6)\%$  and  $(19 \pm 1 \pm 4)\%$ , respectively. The Dalitz plot and the decay angular distributions for this best fit are shown in Fig. 36.

The LHCb Collaboration reported the branching fraction of the  $\Lambda_b^0 \rightarrow J/\psi K^- p$  decay recently [160]:

$$\mathcal{B}(\Lambda_b^0 \rightarrow J/\psi K^- p) = (3.04 \pm 0.04 \pm 0.06 \pm 0.33_{-0.27}^{+0.43}) \times 10^{-4}. \quad (48)$$

Hence, the product branching ratios of the  $P_c(4380)^+$  and  $P_c(4450)^+$  were determined to be

$$\mathcal{B}(\Lambda_b^0 \rightarrow K^- P_c(4380)^+) \times \mathcal{B}(P_c(4380)^+ \rightarrow J/\psi p) = (2.56 \pm 0.22 \pm 1.28_{-0.36}^{+0.46}) \times 10^{-5}, \quad (49)$$

$$\mathcal{B}(\Lambda_b^0 \rightarrow K^- P_c(4450)^+) \times \mathcal{B}(P_c(4450)^+ \rightarrow J/\psi p) = (1.25 \pm 0.15 \pm 0.33_{-0.18}^{+0.22}) \times 10^{-5}, \quad (50)$$

### 2.3. Charged bottomonium-like states $Z_b(10610)$ and $Z_b(10650)$

In 2011, the Belle Collaboration reported two narrow structures in the invariant mass distributions of the  $\pi^\pm \Upsilon(nS)$  ( $n = 1, 2, 3$ ) and  $\pi^\pm h_b(mP)$  ( $m = 1, 2$ ) final states in the processes  $\Upsilon(5S) \rightarrow \Upsilon(nS) \pi^\pm \pi^\mp$  ( $n = 1, 2, 3$ ) and  $\Upsilon(5S) \rightarrow h_b(mP) \pi^\pm \pi^\mp$  ( $m = 1, 2$ ) [161] (see Fig. 37). We collect the observed channels, masses and widths of these two bottomonium-like states in Table 9. The averaged masses and widths over the five final states are  $M_1 = (10607.2 \pm 2.0)$  MeV,  $\Gamma_1 = (18.4 \pm 2.4)$  MeV for  $Z_b(10610)$  and  $M_2 = (10652.2 \pm 1.5)$  MeV,  $\Gamma_2 = (11.5 \pm 2.2)$  MeV for  $Z_b(10650)$ , which are also listed in the Table. The observed  $Z_b(10610)$  and  $Z_b(10650)$  states lie slightly above the  $B\bar{B}^*$  and  $B^* \bar{B}^*$  thresholds, respectively.

Belle also performed the charged pion angular distribution analysis in Ref. [162], which favored the  $J^P = 1^+$  spin-parity assignment for both the  $Z_b(10610)$  and  $Z_b(10650)$ . Since the initial state  $\Upsilon(5S)$  has  $I^G = 1^-$ , the isospin and  $G$ -parity of the  $Z_b$  states should be  $I^G = 1^+$  due to the pion emission [162]. The recent amplitude analysis of the three-body  $\Upsilon(nS) \pi^+ \pi^-$  final states confirmed the  $I^G J^P = 1^+ 1^+$  assignment for both the  $Z_b(10610)$  and  $Z_b(10650)$  states [163].

The neutral  $Z_b^0(10610)$  state was also observed soon in a Dalitz analysis of  $\Upsilon(10860) \rightarrow \Upsilon(nS) \pi^0 \pi^0$ , ( $n = 1, 2, 3$ ) decays by the Belle Collaboration [164, 165]. The observed mass of the  $Z_b(10610)^0$  was  $(10609 \pm 4 \pm 4)$  MeV, which was consistent with that of the charged  $Z_b(10610)^\pm$  state. There was no significant signal for the  $Z_b(10610)^0$  in the

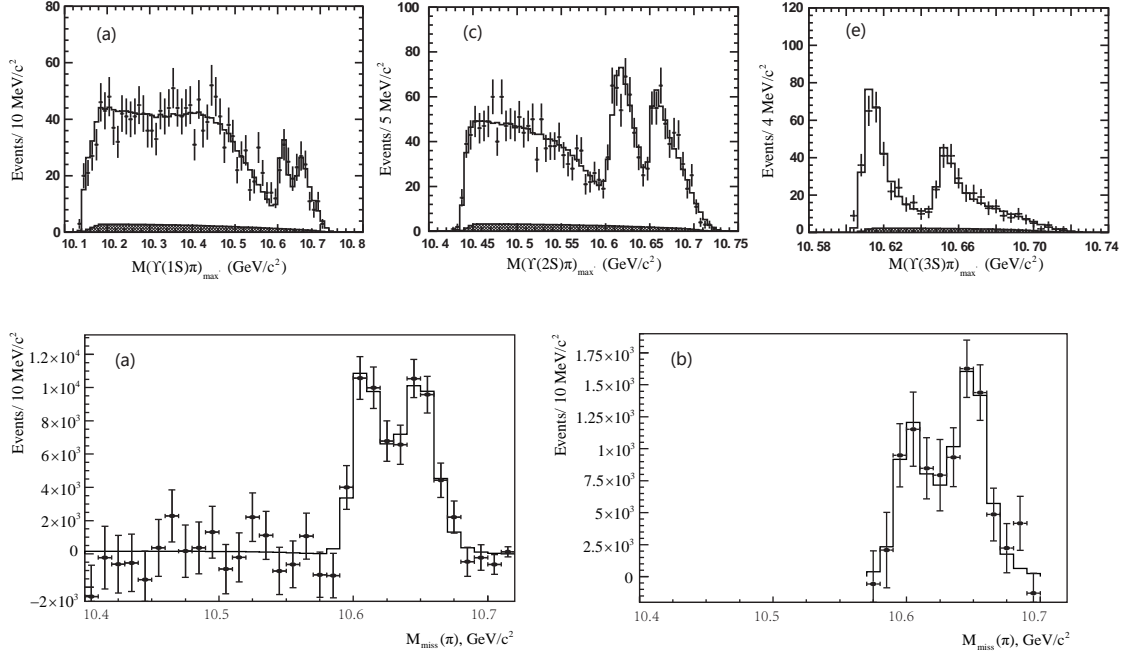


Figure 37: Signals for the  $Z_b(10610)$  and  $Z_b(10650)$  structures in  $\Upsilon(1S)\pi$ ,  $\Upsilon(2S)\pi$ ,  $\Upsilon(3S)\pi$ ,  $h_b(1P)\pi$  and (e)  $h_b(2P)\pi$  from Belle [161].

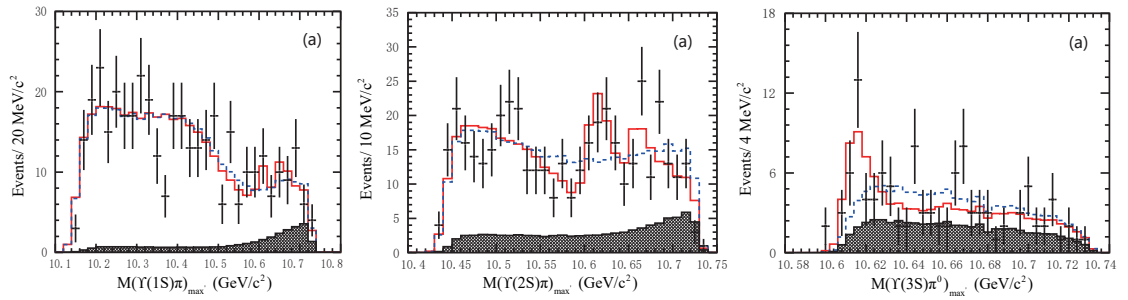


Figure 38: (Color online) The neutral partner the  $Z_b(10610)^0$  in the  $\Upsilon(nS)\pi^0$  ( $n = 1, 2, 3$ ) final states from Belle [165].

Table 9: The resonance parameters for the  $Z_b(10610)$  and  $Z_b(10650)$  from the  $\pi^\pm \Upsilon(nS)$  ( $n = 1, 2, 3$ ) and  $\pi^\pm h_b(mP)$  ( $m = 1, 2$ ) decay channels [161].

Channels	$Z_b(10610)$		$Z_b(10650)$	
	Mass (MeV)	Width (MeV)	Mass (MeV)	Width (MeV)
$\pi^\pm \Upsilon(1S)$	$10611 \pm 4 \pm 3$	$22.3 \pm 7.7^{+3.0}_{-4.0}$	$10657 \pm 6 \pm 3$	$16.3 \pm 9.8^{+6.0}_{-2.0}$
$\pi^\pm \Upsilon(2S)$	$10609 \pm 2 \pm 3$	$24.2 \pm 3.1^{+2.0}_{-3.0}$	$10651 \pm 2 \pm 3$	$13.3 \pm 3.3^{+4.0}_{-3.0}$
$\pi^\pm \Upsilon(3S)$	$10608 \pm 2 \pm 3$	$17.6 \pm 3.0 \pm 3.0$	$10652 \pm 1 \pm 2$	$8.4 \pm 2.0 \pm 2.0$
$\pi^\pm h_b(1P)$	$10605 \pm 2^{+3}_{-1}$	$11.4^{+4.5+2.1}_{-3.9-1.2}$	$10654 \pm 3^{+1}_{-2}$	$20.9^{+5.4+2.1}_{-4.7-5.7}$
$\pi^\pm h_b(2P)$	$10599^{+6+5}_{-3-4}$	$13^{+10+9}_{-8-7}$	$10651^{+2+3}_{-3-2}$	$19 \pm 7^{+11}_{-7}$
Averaged	$10607.2 \pm 2.0$	$18.4 \pm 2.4$	$10652.2 \pm 1.5$	$11.5 \pm 2.2$

$\Upsilon(1S)\pi^0$  final states, as shown in Fig. 38. However, the present data are insufficient to observe the neutral partner of the  $Z_b(10650)$  in the  $\Upsilon(nS)\pi^0\pi^0$  ( $n = 1, 2, 3$ ) channels [164, 165].

In Ref. [166], Belle observed the open-bottom decay modes of the  $Z_b(10610)$  and  $Z_b(10650)$  states via  $\Upsilon(10860) \rightarrow Z_b(10610)^\pm \pi^\mp \rightarrow [B\bar{B}^* + \text{c.c.}]^\pm \pi^\mp$  and  $\Upsilon(10860) \rightarrow Z_b(10650)^\pm \pi^\mp \rightarrow [B^*\bar{B}^*]^\pm \pi^\mp$  processes. Meanwhile, they also studied the  $\Upsilon(10860) \rightarrow \Upsilon(nS)\pi^+\pi^-$  ( $n = 1, 2, 3$ ) and  $\Upsilon(10860) \rightarrow h_b(mP)\pi^+\pi^-$  ( $m = 1, 2$ ) decays. They measured the ratios of the branching fractions [166]:

$$\frac{\mathcal{B}(Z_b(10610) \rightarrow B\bar{B}^*)}{\sum_{n=1,2,3} \mathcal{B}(Z_b(10610) \rightarrow \Upsilon(nS)\pi) + \sum_{m=1,2} \mathcal{B}(Z_b(10610) \rightarrow h_b(mP)\pi)} = 6.2 \pm 0.7 \pm 1.3^{+0.0}_{-1.8}, \quad (51)$$

and

$$\frac{\mathcal{B}(Z_b(10650) \rightarrow B^*\bar{B}^*)}{\sum_{n=1,2,3} \mathcal{B}(Z_b(10650) \rightarrow \Upsilon(nS)\pi) + \sum_{m=1,2} \mathcal{B}(Z_b(10650) \rightarrow h_b(mP)\pi)} = 2.8 \pm 0.4 \pm 0.6^{+0.0}_{-0.4}, \quad (52)$$

which indicated that the open-bottom decays  $Z_b(10610) \rightarrow B\bar{B}^*$  and  $Z_b(10610) \rightarrow B^*\bar{B}^*$  were the dominant decay modes for the  $Z_b(10610)$  and  $Z_b(10650)$  respectively.

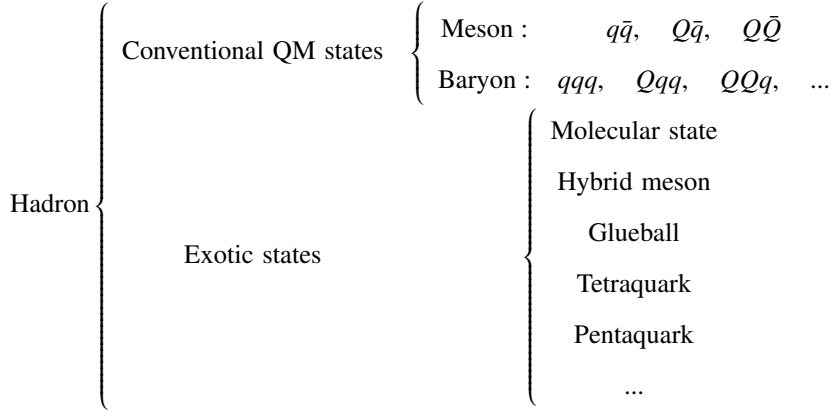
Recently, the Belle Collaboration studied the  $\Upsilon(11020) \rightarrow h_b(nP)\pi^+\pi^-$  ( $n = 1, 2$ ) transitions and found evidence for the  $\Upsilon(11020)$  decays into the charged bottomonium-like  $Z_b(10610)$  and/or  $Z_b(10650)$  states [167].

There were some other efforts to search for the new bottomonium-like states. In Ref. [168], Belle studied the  $X_b \rightarrow \omega\Upsilon(1S)$  process and found no significant bottomonium-like signal decaying into  $\omega\Upsilon(1S)$  with a mass between 10.55 GeV and 10.65 GeV. The ATLAS Collaboration tried to search for the bottomonium-like states in the  $X_b \rightarrow \Upsilon(1S)\pi^+\pi^-$  channel near  $\sqrt{s} = 8$  TeV at LHC [169]. However, they found no evidence for new structure in the mass ranges 10.05 – 10.31 GeV and 10.40 – 11.00 GeV.

### 3. Theoretical interpretations of the hidden-charm pentaquark states

At the birth of the quark model (QM), the multiquark states with configurations like  $(qq\bar{q}\bar{q})$  and  $(qqqq\bar{q})$  were proposed together with the conventional mesons and baryons [18, 170]. In general, the possible hadron configurations

include



where  $q$  and  $Q$  denote the light ( $u, d, s$ ) and heavy ( $c, b$ ) quarks, respectively. Among the above configurations, the molecular states, hybrid mesons, glueballs, tetraquarks and pentaquarks etc are exotic states within the context of the quark model as emphasized in the introduction. Exploration of these exotic states has been one of the central topics of hadron physics in the past several decades.

### 3.1. The molecular scheme

Among these exotic states, the molecular states have received extensive attentions, which are composed of two color-singlet hadrons. The deuteron is a very typical example of the molecular state, which is a loosely bound state of a proton and a neutron with a binding energy around 2.225 MeV only. Sometimes the molecular states are also denoted as the multi-quark states in literatures. However, they are loosely bound by the color-singlet meson exchange force with the binding energy around several MeV to several tens MeV only. In contrast, the “genuine” multi-quark states are confined within one MIT bag via the color force. In some phenomenological models, their building blocks are colored objects such as quarks, diquarks and triquarks etc.

Forty years ago, Voloshin and Okun investigated the interaction of a pair of charmed mesons and the possible molecular states [171]. de Rujula, Georgi, and Glashow studied the possibility of the  $\psi(4040)$  as a  $D^*\bar{D}^*$  molecular charmonium [172]. With the quark-pion interaction model, Törnqvist calculated the possible  $D\bar{D}^*$  and  $D^*\bar{D}$  molecular states in Refs. [173, 174]. Later, Dubynskiy and Voloshin also indicated the existence of a possible resonance around the  $D\bar{D}^*$  threshold [175, 176].

Lipkin discussed the molecular anticharmed strange pentaquark  $P_{\bar{c}s}$  composed of a nucleon and  $\bar{D}_s$  meson with a simplified version of the color-spin hyperfine interaction model [23]. In the light quark sector, Weinstein and Isgur proposed the  $f_0(980)$  and  $a_0(980)$  as the  $K\bar{K}$  molecular states in Refs. [177, 178, 179]. However, their partner states  $\sigma$  and  $\kappa$  within the nonet can not be explained within the molecular scheme.

Unfortunately, the early-stage theoretical efforts on the hidden-charm molecular states were not supported by the subsequent experimental progress. Before 2003, all the experimental observed charmonium states could be accommodated within the quark model easily. In fact, there was no need to introduce the molecular picture into the charmonium spectroscopy at that time.

The story of the molecular states changed dramatically in 2003, which is the renaissance year of the hadron spectroscopy. Since 2003, more and more new light hadron states and charmonium-like states were reported experimentally. Some of them lie close to the threshold of two mesons and are considered as good candidates of the molecular states. In the following, we list several typical examples:

- In 2003, the  $X(1835)$  was observed by the BESII Collaboration in the  $p\bar{p}$  mass spectrum of the  $J/\psi \rightarrow \gamma p\bar{p}$  radiative decay [180], with mass  $M = (1859_{-10}^{+3} \text{ }_{-25}^{+5})$  MeV and width  $\Gamma < 30$  MeV. Since this enhancement structure is close to the  $p\bar{p}$  threshold, the  $X(1835)$  was suggested to be a baryonium state in Refs. [181, 182, 183].

- In 2003, the charmonium-like state  $X(3872)$  was announced by the Belle Collaboration [52] (see Sec. 2.1.1.1 for its experimental information). The  $X(3872)$  sits on the  $D\bar{D}^*$  threshold, which inspired the  $D\bar{D}^*$  molecular explanation [184]. Over the past 13 years, there have been heated discussions on this issue. In Sec. 4.5, we will introduce the current status of the  $X(3872)$  in detail.
- BaBar observed a narrow state  $D_{s0}(2317)$  in the  $D_s^+\pi^0$  invariant mass spectrum from the  $e^+e^-$  annihilation [185]. The observation of the  $D_{s0}(2317)$  also stimulated discussions of the  $D\bar{K}$  molecular state [186].
- The  $Y(3930)$  and  $Y(4140)$  were reported by the Belle [85] and CDF [58] collaborations (see Sec. 2.1.1.2 and Sec. 2.1.1.3 for more details), respectively. Due to their similarity and proximity to the two-meson thresholds, the  $Y(3930)$  and  $Y(4140)$  were proposed as the  $D\bar{D}^*$  and  $D_s\bar{D}_s^*$  molecular states in Ref. [187], respectively.
- As the first observed charged charmonium-like state, the  $Z^+(4430)$  was once suggested to be the  $D_1(D'_1)\bar{D}^*$  molecule in Ref. [188] and was reexamined in Refs. [189, 190] by a dynamical calculation. Later, more charged states  $Z_b(10610)$ ,  $Z_b(10650)$  and  $Z_c(3900)$  were reported. Lying very close to the  $B\bar{B}^*$  and  $B^*\bar{B}^*$  thresholds, the  $Z_b(10610)$  and  $Z_b(10650)$  were proposed as the  $B\bar{B}^*$  and  $B^*\bar{B}^*$  molecular states in Ref. [191], respectively. Their hidden-charm partners were also predicted, which can be related to the  $Z_c(3900)$  [192].

### 3.1.1. The deuteron as a hadronic molecule

To date, the deuteron is the only well-established hadronic molecular state. As a loosely bound state composed of a proton and a neutron, the deuteron is the only bound state of the  $NN$  system with  $J^P = 1^+$  and a binding energy  $E = 2.225$  MeV. The deuteron is a very typical molecular system, where the internal motion of nucleons is governed by the non-relativistic nuclear force. By solving the Schrödinger equation, one can get useful information of the deuteron.

Yukawa first proposed that the nucleon-nucleon interaction is mediated through the exchange of the  $\pi$  meson, which contributes to the long-range part of the nuclear force. The effective  $\pi NN$  interaction Lagrangian reads

$$\mathcal{L} = g_{NN\pi}\bar{\psi}i\gamma_5\boldsymbol{\tau}\psi \cdot \boldsymbol{\pi}, \quad (53)$$

with  $\psi = (p, n)$ ,  $\boldsymbol{\pi} = (\pi_1, \pi_2, \pi_3)$  in the isospin space, and  $g_{NN\pi}$  the coupling constant. With Eq. (53), the non-relativistic nucleon-nucleon potential via  $\pi$  meson exchange can be obtained as

$$V_\pi = \frac{g_{NN\pi}^2}{4\pi} \frac{m_\pi^2}{12m_N^2} (\boldsymbol{\tau}_1 \cdot \boldsymbol{\tau}_2) \left\{ \boldsymbol{\sigma}_1 \cdot \boldsymbol{\sigma}_2 + \left[ \frac{3(\boldsymbol{\sigma}_1 \cdot \mathbf{r})(\boldsymbol{\sigma}_2 \cdot \mathbf{r})}{r^2} - \boldsymbol{\sigma}_1 \cdot \boldsymbol{\sigma}_2 \right] \left[ 1 + \frac{3}{m_\pi r} + \frac{3}{m_\pi^2 r^2} \right] \right\} \frac{e^{-m_\pi r}}{r}, \quad (54)$$

where  $m_N$  and  $m_\pi$  denote the masses of nucleon and  $\pi$  meson, respectively.

There exists strong attraction between two nucleons in the medium range. Such attraction can be reproduced well through the scalar meson  $\sigma$  exchange with a mass around 600 MeV, which mimics the correlated two-pion exchange in the modern version of the nuclear force based on the chiral perturbation theory. The short-range nuclear force is strongly repulsive. The repulsion is described by the exchange of the vector mesons  $\rho$  and  $\omega$ , which play the same role as the multiple pion exchange and the low-energy-constant contributions in the chiral perturbation theory. The meson exchange model is the basis of the Nijmegen potential and Bonn potential.

The deuteron is a very shallow bound state with a large spatial distribution. Its radial wave function extends to 2 fm. In fact, a small binding energy and a large radius are key features of the hadronic molecular states. The long-range attraction through the pion exchange, the S-wave and D-wave channel coupling, the tensor force and short-range repulsion work together to form the extremely loosely bound deuteron. This is an important lesson we learn from the deuteron, which should guide us in the exploration of the hidden-charm hadronic molecules.

### 3.1.2. The meson exchange model

Since 2003, many enhancement structures near the two-hadron thresholds have been reported as shown in Table 10. The proximity of their masses to the thresholds inspired molecular explanations of these structures [183, 196, 197, 189, 198, 199, 200, 201, 202, 203, 204, 205, 206, 190, 207, 187, 208, 209, 210, 211, 212, 213, 214, 215, 216, 217, 218, 219, 220]. With the refinement of the meson exchange model, many subtle aspects of this framework

Table 10: Some new hadron states which are close to the two-hadron thresholds.

Observation	Threshold	Observation	Threshold
$X(1860)$ [180]	$p\bar{p}$	$D_{s0}(2317)$ [185]	$DK$
$D_{s1}(2460)$ [193]	$D^*K$	$X(3872)$ [52]	$D^*D$
$Y(3940)$ [85]	$D^*D^*$	$Y(4140)$ [58]	$D_s^*D_s^*$
$Y(4274)$ [89]	$D_{s0}(2317)D$	$Y(4630)$ [136]	$\Lambda_c\Lambda_c$
$Z^+(4430)$	$D_1D^*/D_1'D^*$	$Z^+(4250)$ [98]	$D_1D/D_0D^*$
$\Lambda_c(2940)$ [194]	$D^*N$	$\Sigma_c(2800)$ [195]	$DN$

were investigated, such as the S-D wave mixing effect [173, 184], coupled-channel effect [221, 222, 223], and recoil correction [224, 225].

In the deduction of the effective potential of the molecular system, one first derives the relativistic scattering amplitude at the tree level

$$\langle f|S|i\rangle = \delta_{fi} + i\langle f|T|i\rangle = \delta_{fi} + i(2\pi)^4\delta^4(p_f - p_i)\mathcal{M}_{fi}, \quad (55)$$

where  $T$  is the interaction part of the  $S$  matrix and  $\mathcal{M}$  denotes the invariant matrix element. After applying the Bonn approximation to the Lippmann-Schwinger equation, the  $S$  matrix reads

$$\langle f|S|i\rangle = \delta_{fi} - i2\pi\delta(E_f - E_i)V_{fi}, \quad (56)$$

where  $V_{fi}$  is the effective potential in the momentum space. Considering the different normalization conventions adopted for the scattering amplitude  $\mathcal{M}_{fi}$  and the  $T$ -matrix  $T_{fi}$  and  $V_{fi}$ , the scattering amplitude  $\mathcal{M}_{fi}$  can be related to the corresponding effective potential in the momentum space  $V(\mathbf{q})$  [226]

$$V_{fi}(\mathbf{q}) = -\frac{\mathcal{M}_{fi}}{\sqrt{\Pi_f 2p_f^0 \Pi_i 2p_i^0}} \approx -\frac{\mathcal{M}_{fi}}{\sqrt{\Pi_f 2m_f^0 \Pi_i 2m_i^0}}, \quad (57)$$

where  $p_{f(i)}$  and  $m_{f(i)}$  denote the four-momentum and mass of the final (initial) state, respectively.

Generally, one also needs to introduce the form factor in each interaction vertex, which reflects the off-shell effect of the exchanged meson and the structure effect, because the components of the molecular state and exchanged mesons are not elemental particles. Although various form factors were adopted in dealing with different systems [174, 203, 227, 228], we take the simple monopole form factor as an example

$$F(q) = \frac{\Lambda^2 - m_E^2}{\Lambda^2 - q^2}, \quad (58)$$

where  $m_E$  and  $q$  denote the mass and four-momentum of the exchanged meson, respectively, and  $\Lambda$  is a cutoff.

As  $q^2 \rightarrow 0$  and  $\Lambda \gg m$ , the form factor approaches to the unity. As  $q^2 \rightarrow \infty$ , the form factor approaches to zero. Within the framework of the meson exchange model, a constituent hadron is treated as a whole. Its inner structure should not be explored by the exchanged meson. The large momentum contribution from the meson exchange should be suppressed. Otherwise, such a formalism is not self-consistent. In other words, the form factor is introduced to cut off the ultraviolet contribution [190].

By performing the Fourier transformation to  $V_{fi}(\mathbf{q})$ , one obtains the effective potential  $V_{fi}(\mathbf{r})$  in the coordinate space, which can be applied to search for the bound state solution by solving the Schrödinger equation.

### 3.1.3. Predictions for the hidden-charm pentaquarks before LHCb's discovery

Before LHCb's discovery of the  $P_c(4380)$  and  $P_c(4450)$  [2], the possible hidden-charm molecular baryons composed of an S-wave anti-charmed meson and an S-wave charmed baryon were studied extensively in the framework of one boson exchange (OBE) model in 2011 [229].

As shown in Fig. 39, the S-wave charmed baryons belong to either the symmetric  $6_F$  or antisymmetric  $\bar{3}_F$  flavor representation with  $J^P = 1/2^+$  or  $3/2^+$  for  $6_F$  and  $J^P = 1/2^+$  for  $\bar{3}_F$ . Additionally, the pseudoscalar and vector anti-charmed mesons form an S-wave anti-charmed meson family. In Ref. [229], the authors mainly focused on the hidden-charm molecular states composed of the charmed baryons and anti-charmed mesons in the green range of Fig. 39.

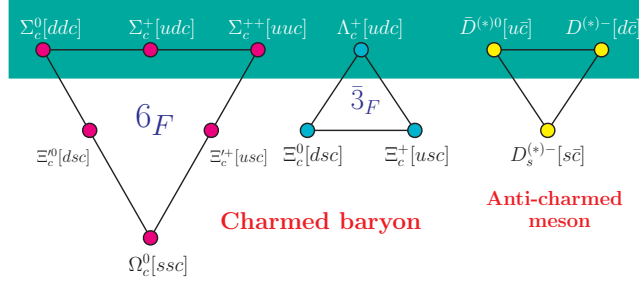


Figure 39: (Color online) The S-wave charmed baryons with  $J^P = 1/2^+$  and the S-wave anti-charmed pseudoscalar/vector mesons contributing to the hidden-charm molecular baryons. Taken from Ref. [229].

The effective meson exchange potentials of the hidden-charm systems  $\Lambda_c \bar{D}$  with  $I(J^P) = \frac{1}{2}(\frac{1}{2}^-)$ ,  $\Lambda_c \bar{D}^*$  with  $\frac{1}{2}(\frac{1}{2}^-)$ ,  $\frac{1}{2}(\frac{3}{2}^-)$ ,  $\Sigma_c \bar{D}$  with  $\frac{1}{2}(\frac{1}{2}^-)$ ,  $\frac{3}{2}(\frac{1}{2}^-)$ ,  $\Sigma_c \bar{D}^*$  with  $\frac{1}{2}(\frac{1}{2}^-)$ ,  $\frac{3}{2}(\frac{3}{2}^-)$ ,  $\frac{1}{2}(\frac{1}{2}^-)$ ,  $\frac{3}{2}(\frac{3}{2}^-)$  were extracted in the OBE model. After solving the coupled-channel Schrödinger equation, the numerical results indicated that there do not exist the  $\Lambda_c \bar{D}$  and  $\Lambda_c \bar{D}^*$  molecular states.

There do exist molecular bound state solutions for five channels: the  $\Sigma_c \bar{D}^*$  system with  $I(J^P) = \frac{1}{2}(\frac{1}{2}^-)$ ,  $\frac{1}{2}(\frac{3}{2}^-)$ ,  $\frac{3}{2}(\frac{1}{2}^-)$ ,  $\frac{3}{2}(\frac{3}{2}^-)$  and the  $\Sigma_c \bar{D}$  system with  $\frac{3}{2}(\frac{1}{2}^-)$  [229]. Especially, the predicted  $\Sigma_c \bar{D}^*$  molecular state with  $I(J^P) = \frac{1}{2}(\frac{3}{2}^-)$  [229] seems to match one of the two pentaquark states observed by the LHCb Collaboration in 2015 [2].

The LHCb Collaboration reported two enhancement structures  $P_c(4380)$  and  $P_c(4450)$  in the  $J/\psi p K$  [2]. The experimental information was reviewed in Sec. 2.2. Since their final states are  $J/\psi p$ , each of these  $P_c$  states with isospin  $I = 1/2$  contains a pair of  $c\bar{c}$ .

The  $P_c(4380)$  lies near the  $\Sigma_c(2455)\bar{D}^*(2010)$  and  $\Sigma_c^*(2520)\bar{D}(1870)$  thresholds while the  $P_c(4450)$  is very close to the  $\Sigma_c(2520)\bar{D}^*$  and  $\Sigma_c^*(2520)\bar{D}^*$  thresholds. It is interesting to note that the mass gap between the  $P_c(4450)$  and  $P_c(4380)$  is almost the same as the mass difference between the  $\Sigma_c^*(2520)$  and  $\Sigma_c(2455)$ .

### 3.1.4. Molecular assignments after LHCb's discovery

After LHCb's discovery, several groups explored the molecular assignment of these two  $P_c$  states [230, 231]. In Ref. [230], the assignments of the  $P_c(4380)$  and  $P_c(4450)$  as the hidden-charm  $\Sigma_c(2455)\bar{D}^*$  and  $\Sigma_c^*(2520)\bar{D}^*$  molecular pentaquarks and their partner states were investigated carefully with the one pion exchange (OPE) model. Their flavor wave functions  $|I, I_3\rangle$  were constructed as

$$\left\{ \begin{array}{l} \left| \frac{1}{2}, \frac{1}{2} \right\rangle = \sqrt{\frac{2}{3}} |\Sigma_c^{(*)++} D^{*-}\rangle - \frac{1}{\sqrt{3}} |\Sigma_c^{(*)+} \bar{D}^{*0}\rangle \\ \left| \frac{1}{2}, -\frac{1}{2} \right\rangle = \frac{1}{\sqrt{3}} |\Sigma_c^{(*)+} D^{*-}\rangle - \sqrt{\frac{2}{3}} |\Sigma_c^{(*)0} \bar{D}^{*0}\rangle \end{array} \right\}, \quad \left\{ \begin{array}{l} \left| \frac{3}{2}, \frac{3}{2} \right\rangle = |\Sigma_c^{(*)++} \bar{D}^{*0}\rangle \\ \left| \frac{3}{2}, \frac{1}{2} \right\rangle = \frac{1}{\sqrt{3}} |\Sigma_c^{(*)++} D^{*-}\rangle + \sqrt{\frac{2}{3}} |\Sigma_c^{(*)+} \bar{D}^{*0}\rangle \\ \left| \frac{3}{2}, -\frac{1}{2} \right\rangle = \sqrt{\frac{2}{3}} |\Sigma_c^{(*)+} D^{*-}\rangle + \frac{1}{\sqrt{3}} |\Sigma_c^{(*)0} \bar{D}^{*0}\rangle \\ \left| \frac{3}{2}, -\frac{3}{2} \right\rangle = |\Sigma_c^{(*)0} D^{*-}\rangle \end{array} \right\}.$$

The effective Lagrangians, which were constructed with the heavy quark symmetry and chiral symmetry [232, 233, 234, 235, 236, 237], were adopted to obtain the OPE effective potentials of the  $\Sigma_c(2455)\bar{D}^*$  and  $\Sigma_c^*(2520)\bar{D}^*$

systems,

$$\mathcal{L} = ig\text{Tr}\left[\bar{H}_a^{(\bar{Q})}\gamma^\mu A_{ab}^\mu\gamma_5 H_b^{(\bar{Q})}\right], \quad (59)$$

$$\mathcal{L} = -\frac{3}{2}g_1\varepsilon^{\mu\nu\lambda\kappa}v_\kappa\text{Tr}\left[\bar{\mathcal{S}}_\mu A_\nu\mathcal{S}_\lambda\right]. \quad (60)$$

The multiplet field composed of the pseudoscalar  $P$  and vector  $P^{*(\bar{Q})}$  with  $P^{*(\bar{Q})} = (\bar{D}^{*0}, D^{*-})^T$  is defined as  $H_a^{(\bar{Q})} = [P_a^{*(\bar{Q})\mu}\gamma_\mu - P_a^{(\bar{Q})}\gamma_5]\frac{1-\not{v}}{2}$  with  $v = (1, \vec{0})$ . The superfield  $\mathcal{S}_\mu$  is composed of spinor operators as  $\mathcal{S}_\mu = -\sqrt{\frac{1}{3}}(\gamma_\mu + v_\mu)\gamma^5\mathcal{B}_6 + \mathcal{B}_{6\mu}^*$ , where  $\mathcal{B}_6$  and  $\mathcal{B}_6^*$  are the multiplets corresponding to  $J^P = 1/2^+$  and  $J^P = 3/2^+$  in the  $6_F$  flavor representation, respectively. The axial current  $A_\mu = \frac{1}{2}(\xi^\dagger\partial_\mu\xi - \xi\partial_\mu\xi^\dagger)$  with  $\xi = \exp(i\mathbb{P}/f_\pi)$  and  $f_\pi = 132$  MeV. The expressions of  $\mathbb{P}$ ,  $\mathcal{B}_6$ , and  $\mathcal{B}_6^*$  are

$$\mathbb{P} = \begin{pmatrix} \frac{\pi^0}{\sqrt{2}} & \pi^+ \\ \pi^- & -\frac{\pi^0}{\sqrt{2}} \end{pmatrix}, \quad \mathcal{B}_6 = \begin{pmatrix} \Sigma_c^{++} & \frac{\Sigma_c^+}{\sqrt{2}} \\ \frac{\Sigma_c^+}{\sqrt{2}} & \Sigma_c^0 \end{pmatrix}, \quad \mathcal{B}_6^* = \begin{pmatrix} \Sigma_c^{*++} & \frac{\Sigma_c^{*+}}{\sqrt{2}} \\ \frac{\Sigma_c^{*+}}{\sqrt{2}} & \Sigma_c^{*0} \end{pmatrix}. \quad (61)$$

Eqs. (59) and (60) can be further expanded as

$$\mathcal{L}_{\bar{D}^*\bar{D}^*\mathbb{P}} = i\frac{2g}{f_\pi}v^\alpha\varepsilon_{\alpha\mu\nu\lambda}\bar{D}_a^{*\mu\dagger}\bar{D}_b^{*\lambda}\partial^\nu\mathbb{P}_{ab}, \quad (62)$$

$$\mathcal{L}_{\mathcal{B}_6\mathcal{B}_6\mathbb{P}} = i\frac{g_1}{2f_\pi}\varepsilon^{\mu\nu\lambda\kappa}v_\kappa\text{Tr}\left[\bar{\mathcal{B}}_6\gamma_\mu\gamma_\lambda\partial_\nu\mathbb{P}\mathcal{B}_6\right], \quad (63)$$

$$\mathcal{L}_{\mathcal{B}_6^*\mathcal{B}_6^*\mathbb{P}} = -i\frac{3g_1}{2f_\pi}\varepsilon^{\mu\nu\lambda\kappa}v_\kappa\text{Tr}\left[\bar{\mathcal{B}}_{6\mu}^*\partial_\nu\mathbb{P}\mathcal{B}_{6\nu}^*\right], \quad (64)$$

where the coupling constant  $g = 0.59 \pm 0.07 \pm 0.01$  was extracted from the  $D^*$  decay width [238] and  $g_1 = 0.94$  fixed in Refs. [237, 229].

With the standard procedure of the meson exchange model, one gets the general expressions of the effective potentials for the  $\Sigma_c\bar{D}^*$  and  $\Sigma_c^*\bar{D}^*$  systems,

$$V_{\Sigma_c\bar{D}^*}(r) = \frac{1}{3}\frac{gg_1}{f_\pi^2}\nabla^2 Y(\Lambda, m_\pi, r)\mathcal{J}_0\mathcal{G}_0, \quad (65)$$

$$V_{\Sigma_c^*\bar{D}^*}(r) = \frac{1}{2}\frac{gg_1}{f_\pi^2}\nabla^2 Y(\Lambda, m_\pi, r)\mathcal{J}_1\mathcal{G}_1, \quad (66)$$

where the  $Y(\Lambda, m, r)$  function reads

$$Y(\Lambda, m, r) = \frac{1}{4\pi r}\left(e^{-mr} - e^{-\Lambda r}\right) - \frac{\Lambda^2 - m^2}{8\pi\Lambda}e^{-\Lambda r}. \quad (67)$$

In Eqs. (65) and (66), the coefficients  $\mathcal{J}_i$  and  $\mathcal{G}_i$  ( $i = 0, 1$ ) for different isospin and  $^{2S+1}L_J$  quantum numbers are collected in Table 11.

We summarize some interesting observations in Ref. [230]:

- Under the molecular scheme, the masses of the  $P_c(4380)$  and  $P_c(4450)$  are reproduced very well as shown in Figs. 40 (a) and 40 (b). Moreover their spatial extension is quite large, around 1-2 fm, which is a characteristic feature of a hadronic molecule.
- If the  $P_c$  states are S-wave molecular states, both of them carry negative parity. They can transit into  $J/\psi p$  via the exchange of an S-wave charmed meson. The  $\Sigma_c\bar{D}^*$  state with  $(I = 1/2, J = 3/2)$  decays into  $J/\psi p$  via S-wave while the  $\Sigma_c^*\bar{D}^*$  state with  $(I = 1/2, J = 5/2)$  decays into  $J/\psi p$  via D-wave. The D-wave decay is strongly suppressed by small phase space. In other words, the  $P_c(4450)$  is quite narrow while the  $P_c(4380)$  is broad [2]. These two  $P_c$  states also decay into  $\eta_c p$ .

Table 11: The values of the  $\mathcal{J}_i$  and  $\mathcal{G}_i$  coefficients for the S-wave  $\Sigma_c(2455)\bar{D}^*$  and  $\Sigma_c^*(2520)\bar{D}^*$  systems. Here,  $S$ ,  $L$ , and  $J$  denote the spin, orbital, and total angular quantum numbers, respectively. Taken from Ref. [230].

$I$	$\mathcal{G}_0$	$\mathcal{G}_1$	$ ^{2S+1}L_J\rangle$	$\mathcal{J}_0$	$\mathcal{J}_1$
1/2	1	-1	$ ^2\mathcal{G}_{\frac{1}{2}}\rangle$	-2	5/3
3/2	-1/2	1/2	$ ^4\mathcal{G}_{\frac{3}{2}}\rangle$	1	2/3
...	...	...	$ ^6\mathcal{G}_{\frac{5}{2}}\rangle$	...	-1

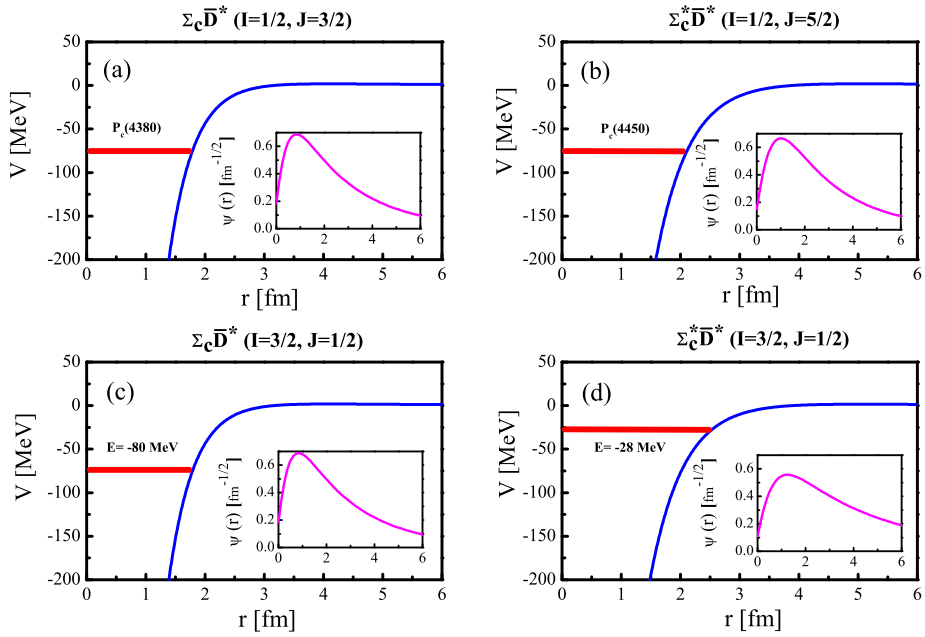


Figure 40: (Color online) The variation of the OPE potential and the radial wave function with  $r$  for the  $\Sigma_c^{(*)}\bar{D}^*$  systems.  $\Lambda = 2.35$  GeV and  $\Lambda = 1.77$  GeV for the  $\Sigma_c\bar{D}^*$  and  $\Sigma_c^*\bar{D}^*$  systems, respectively. The blue curve is the effective potentials, and the red line is the energy level. Taken from Ref. [230].

- There exist several isospin partners of the  $P_c$  states as shown in Fig. 40 (c) and (d). With the same set of parameters, the binding energy of the  $\Sigma_c \bar{D}^*$  system with  $(I = 3/2, J = 1/2)$  is the same as that of the  $\Sigma_c \bar{D}^*$  system with  $(I = 1/2, J = 3/2)$ . With the same set of parameters, the binding energy of the  $\Sigma_c^* \bar{D}^*$  system with  $(I = 3/2, J = 1/2)$  is 28 MeV, which is smaller than that of the  $\Sigma_c^* \bar{D}^*$  system with  $(I = 1/2, J = 5/2)$ . The allowed decay modes of these two  $I = 3/2$  states include  $\Delta(1232)J/\psi$  and  $\Delta(1232)\eta_c$ .

### 3.1.5. Configuration mixing

Besides the assignment of the  $P_c(4380)$  and  $P_c(4450)$  as the hidden-charm  $\Sigma_c(2455)\bar{D}^*$  and  $\Sigma_c^*(2520)\bar{D}^*$  molecular pentaquarks in Ref. [230], He also studied the molecular baryons [231]. He derived the OBE effective potentials and solved the Bethe-Salpeter equation with a spectator quasipotential approximation, where the  $P_c(4380)$  and  $P_c(4450)$  were explained as the  $\bar{D}\Sigma_c^*$  molecular state with  $J^P = 3/2^-$  and the  $\bar{D}^*\Sigma_c$  molecular state with  $J^P = 5/2^+$ , respectively.

In the heavy quark symmetry limit, the  $(D, D^*)$  pair forms a degenerate doublet. The  $(\Sigma_c, \Sigma_c^*)$  pair is also degenerate. Except for the isospin and spin factors, the interactions between the  $(D, D^*)$  and  $(\Sigma_c, \Sigma_c^*)$  pairs are essentially the same and governed by the same coupling constants. For example, the  $\bar{D}\Sigma_c^*$  molecular state with  $J^P = 3/2^-$  discussed in Ref. [231] is essentially the same as the  $\Sigma_c(2455)\bar{D}^*$  molecular state with  $J^P = 3/2^-$  in Ref. [230] in the heavy quark symmetry limit.

Generally speaking, several degenerate flavor configurations contribute to the same hidden-charm molecular baryons with fixed  $I(J^P)$  in the heavy quark symmetry limit. There exists strong configuration mixing. In the real world, the charm mass is around 1.5 GeV. The mass degeneracy of the heavy hadron pair is removed by the  $1/M_c$  correction with a mass splitting around 100 MeV. The mass gap between different mass thresholds is around several tens MeV, which is comparable with (or even larger than) the binding energy for the hidden-charm molecular baryons. The couple-channel effects due to the flavor configuration mixing may turn out to be important. Such an investigation is still missing at present.

### 3.1.6. Orbital excitations and the $P_c$ parity

If both the  $P_c(4380)$  and  $P_c(4450)$  are the S-wave hidden-charm molecular states, their parities are negative which seems in conflict with LHCb's measurement that the  $P_c(4380)$  and  $P_c(4450)$  have opposite parities [2]. However, the same parities are not completely excluded by LHCb [2].

Recall that the D-wave contribution is only a few percent in the case of the deuteron, where the binding energy is around 2 MeV. However, the D-wave component contributes significantly to the formation of the shallow bound state through the tensor force and S-D wave mixing. The lesson is that the orbital excitation is important!

In the case of the hidden-charm molecular baryons, the P-wave, D-wave or even higher orbital excitations may accompany the lowest S-wave state if the binding energy of the hadronic molecule ground state reaches several MeV to several tens MeV. Especially, the P-wave state may lie very close to the S-wave ground state with an excitation energy around several to tens MeV. These two levels are almost degenerate but carry opposite parities. They may completely overlap with each other.

For the P-wave orbitally excited molecular baryons, they decay into the  $J/\psi P, \eta_c P$  modes via P-wave while their S-wave decay modes  $\chi_{cJ} P$  are either kinematically forbidden or strongly suppressed by phase space.

Compared with the S-wave decay, the P-wave decay width is suppressed by the factor  $(k/M)^2$  because of the centrifugal barrier, where  $k$  is decay momentum and  $M$  is the pentaquark mass. For the  $J/\psi P$  mode of the  $P_c(4450)$  state, the suppression factor is around 30. In other words, the P-wave hidden-charm molecular pentaquarks are expected to be quite narrow.

As pointed out in Ref. [239], there may exist two or more resonant signals around 4380 MeV which are close to each other but may carry different parity. If the P-wave or higher excitation is very broad with a width around 500 MeV, such a state may easily be mistaken as the background. On the other hand, if an excitation lies several MeV within 4380 MeV but with a width as narrow as several MeV, then it may probably be buried by the  $P_c(4380)$  resonance with a width around 205 MeV! The same situation may also occur around 4450 MeV.

The above speculation may partly explain why the different assignments of the spins and parities for these two  $P_c$  states yielded roughly the same good fit [2]. The identification of the nearly degenerate resonances with different parities and widths may require huge amount experimental data.

We want to emphasize that the possible existence of the P-wave excitation together with the S-wave ground state is the first intrinsic property of the hadronic molecular scheme.

The second intrinsic feature of the hidden-charm molecular states is that the open-charm decay modes should dominate the hidden-charm decay modes. This observation is supported by the current experimental measurements of the decay modes of the charged  $Z_c$  (or  $Z_b$ ) states, where the open-charm decay width is much larger than the  $J/\psi\pi$  partial width.

In other words, the  $J/\psi p$  is not necessarily the dominant decay mode of the  $P_c(4380)$  state although it was observed in the very clean  $J/\psi p$  final state. Instead, the broad Breit-Wigner distribution of the  $P_c(4380)$  ensures that it could decay into the open-charm modes such as  $\bar{D}\Sigma_c^*$ ,  $\Sigma_c\bar{D}^*$ ,  $\bar{D}\Sigma_c\pi$ ,  $\bar{D}\Lambda_c^*$ ,  $\bar{D}^*\Lambda_c$  etc.

### 3.2. Dynamically generated resonance

In Refs. [240, 241], Wu, Molina, Oset and Zou studied the interaction between various charmed mesons and charmed baryons within the framework of the coupled channel unitary approach with the local hidden gauge formalism. The hidden-charm baryons are generated dynamically [240, 241]. The same/similar method was also used to study the hidden-charm baryons in a series of papers [242, 243, 244, 245, 246, 247, 248], all of which are done before the LHCb's discovery of the  $P_c(4380)$  and  $P_c(4450)$  [2]. The same/similar approach was applied to study hidden-bottom baryons [249, 250] and their productions [251, 252, 253, 254], some of which will be discussed in Sec. 3.7 and Sec. 3.8, respectively. In this review we introduce this method and review their results briefly. However, we shall not discuss its application for open-charm baryons [255, 256, 257, 258, 259].

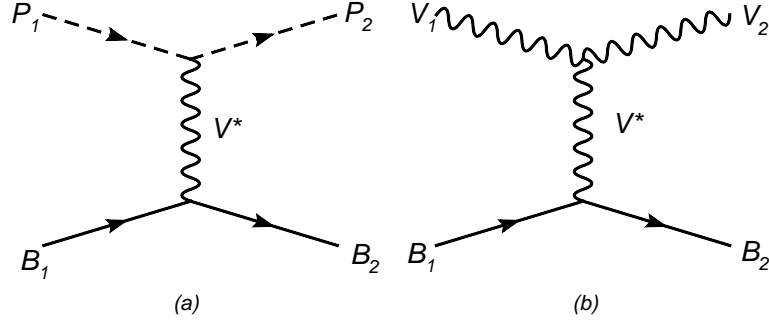


Figure 41: Feynman diagrams for the pseudoscalar-baryon (a) and vector-baryon (b) interactions via the exchange of a vector meson. Taken from Ref. [241].

In Refs. [240, 241], Wu *et al.* considered the  $PB \rightarrow PB$  and  $VB \rightarrow VB$  interactions by exchanging a vector meson  $V^*$ , where  $P$  denotes the pseudoscalar charmed mesons  $D$  and  $D_s$ ,  $V$  denotes the vector charmed mesons  $D^*$  and  $D_s^*$ , and  $B$  denotes the charmed baryons  $\Sigma_c$ ,  $\Lambda_c$ ,  $\Xi_c$ ,  $\Xi'_c$  and  $\Omega_c$ . The corresponding Feynman diagrams are shown in Fig. 41, where the exchanged vector meson  $V^*$  can be the  $\rho$ ,  $\omega$ ,  $K^*$  and  $\phi$ . The vertices for exchanging vector mesons come from the following three Lagrangians

$$\begin{aligned}\mathcal{L}_{VVV} &= ig\langle V^\mu[V^\nu, \partial_\mu V_\nu]\rangle, \\ \mathcal{L}_{PPV} &= -ig\langle V^\mu[P, \partial_\mu P]\rangle, \\ \mathcal{L}_{BBV} &= g(\langle \bar{B}\gamma_\mu[V^\mu, B]\rangle + \langle \bar{B}\gamma_\mu B\rangle\langle V^\mu\rangle).\end{aligned}\quad (68)$$

Here, the first Lagrangian was constructed based on the hidden gauge interaction for vector mesons [260, 261, 262, 263]; the third Lagrangian was introduced in Refs. [264, 265, 266, 267, 268] for the case of three flavors, and was extended to the case of four flavors in Refs. [240, 241], where

$$P = \begin{pmatrix} \frac{\pi^0}{\sqrt{2}} + \frac{\eta_8}{\sqrt{6}} + \frac{\tilde{\eta}_c}{\sqrt{12}} + \frac{\tilde{\eta}'_c}{\sqrt{4}} & \pi^+ & K^+ & \bar{D}^0 \\ \pi^- & -\frac{\pi^0}{\sqrt{2}} + \frac{\eta_8}{\sqrt{6}} + \frac{\tilde{\eta}_c}{\sqrt{12}} + \frac{\tilde{\eta}'_c}{\sqrt{4}} & K^0 & D^- \\ K^- & \bar{K}^0 & \frac{-2\eta_8}{\sqrt{6}} + \frac{\tilde{\eta}_c}{\sqrt{12}} + \frac{\tilde{\eta}'_c}{\sqrt{4}} & D_s^- \\ D^0 & D^+ & D_s^+ & -\frac{3\tilde{\eta}_c}{\sqrt{12}} + \frac{\tilde{\eta}'_c}{\sqrt{4}} \end{pmatrix}, \quad (69)$$

$$V_\mu = \begin{pmatrix} \frac{\rho^0}{\sqrt{2}} + \frac{\omega_8}{\sqrt{6}} + \frac{\tilde{\omega}_c}{\sqrt{12}} + \frac{\tilde{\omega}'_c}{\sqrt{4}} & \rho^+ & K^{*+} & \bar{D}^{*0} \\ \rho^- & -\frac{\rho^0}{\sqrt{2}} + \frac{\omega_8}{\sqrt{6}} + \frac{\tilde{\omega}_c}{\sqrt{12}} + \frac{\tilde{\omega}'_c}{\sqrt{4}} & K^{*0} & D^{*-} \\ K^{*-} & \bar{K}^{*0} & \frac{-2\omega_8}{\sqrt{6}} + \frac{\tilde{\omega}_c}{\sqrt{12}} + \frac{\tilde{\omega}'_c}{\sqrt{4}} & D_s^{*-} \\ D^{*0} & D^{*+} & D_s^{*+} & -\frac{3\tilde{\omega}_c}{\sqrt{12}} + \frac{\tilde{\omega}'_c}{\sqrt{4}} \end{pmatrix}_\mu. \quad (70)$$

However, the  $BBV$  vertex in the case of four flavors does not have a simple representation as in the case of three flavors. Wu *et al.* evaluated the matrix elements using  $SU(4)$  symmetry in terms of the Clebsch-Gordan coefficients and reduced matrix elements.

Recall that the  $SU(3)$  flavor symmetry is broken at the level of 20% ~ 30%. In general, the flavor  $SU(4)$  symmetry is badly broken. One should be very cautious about the uncertainty of the  $J/\psi DD$  and  $J/\psi BB$  couplings derived from the equations under the  $SU(4)$  symmetry.

The transition potential corresponding to the diagrams of Fig. 41 was given by [240, 241]

$$V_{ab(P_1 B_1 \rightarrow P_2 B_2)} = \frac{C_{ab}}{4f^2} (q_1^0 + q_2^0), \quad (71)$$

$$V_{ab(V_1 B_1 \rightarrow V_2 B_2)} = \frac{C_{ab}}{4f^2} (q_1^0 + q_2^0) \vec{\epsilon}_1 \cdot \vec{\epsilon}_2, \quad (72)$$

where  $q_1^0$  and  $q_2^0$  are the energies of the initial and final mesons, respectively. The  $C_{ab}$  coefficients can be found in Refs. [240, 241] for six cases with different isospin and strangeness  $(I, S) = (3/2, 0), (1/2, 0), (1/2, -2), (1, -1), (0, -1), (0, -3)$ .

In the derivation of the above transition potential, the authors assumed that the three-momentum were much smaller than its mass and kept  $\gamma^0$  and the time component only. In this way they derived the contact interaction for the charmed meson and baryon. Such an approximation may not work very well when a light vector meson is exchanged.

The scattering matrix  $T$  was evaluated by solving the coupled channels Bethe-Salpeter equation in the on-shell factorization approach [269, 270, 271]

$$T = [1 - VG]^{-1} V, \quad (73)$$

where  $G$  is the loop function of a meson and a baryon, and was evaluated in the dimensional regularization as [269]

$$\begin{aligned} G(s) &= i \int \frac{d^4 q}{(2\pi)^4} \frac{2M_B}{(P-q)^2 - M_B^2 + i\epsilon} \frac{1}{q^2 - M_P^2 + i\epsilon}, \\ &= \frac{2M_B}{16\pi^2} \left\{ a_\mu + \ln \frac{M_B^2}{\mu^2} + \frac{M_P^2 - M_B^2 + s}{2s} \ln \frac{M_P^2}{M_B^2} \right. \\ &\quad \left. + \frac{q_{cm}}{\sqrt{s}} [\ln(s - (M_B^2 - M_P^2) + 2q_{cm} \sqrt{s}) + \ln(s + (M_B^2 - M_P^2) + 2q_{cm} \sqrt{s}) \right. \\ &\quad \left. - \ln(-s - (M_B^2 - M_P^2) + 2q_{cm} \sqrt{s}) - \ln(-s + (M_B^2 - M_P^2) + 2q_{cm} \sqrt{s}) \right\}, \end{aligned} \quad (74)$$

where the regularization scale  $\mu = 1$  GeV and the parameter  $a_\mu$  is fixed around  $-2.3$ .

Wu *et al.* also took into account some decay mechanisms by considering the decay of the states to a light baryon plus either a light meson or a charmonium through heavy charmed meson exchanges [272, 273].

Their results of the pole positions and coupling constants are listed in Tables 12 and 13, where two  $N_{c\bar{c}}^*$  states and four  $\Lambda_{c\bar{c}}^*$  states were found in the  $PB$  and  $VB$  scattering channels [240, 241]. All these states have masses larger than 4200 MeV due to their  $c\bar{c}$  components. Their decay properties were discussed and cross sections for their production were estimated, suggesting that the  $\eta_c N$  and  $\eta_c \Lambda$  are possible decay modes for the  $PB$  channels, and the  $J/\psi N$  and  $J/\psi \Lambda$  are possible modes for the  $VB$  channels. These results were used by Molina, Xiao, and Oset to study the interaction of the  $J/\psi$  with nuclei in Ref. [243]. They evaluated the total inelastic cross section of the  $J/\psi N$  and found a maximum around  $\sqrt{s} = 4415$  MeV, where the  $J/\psi N$  couples to a resonance predicted in Refs. [240, 241] (see 4412 MeV in Table 13).

Later, Wu, Lee, and Zou considered several coupled-channel models derived from relativistic quantum field theory [242]. They used both a unitary transformation method [274, 275], and the three-dimensional reductions of the

Table 12: Mass ( $M$ ), total width ( $\Gamma$ ), and the partial decay width ( $\Gamma_i$ ) for the states from  $PB \rightarrow PB$ , with units in MeV, taken from Refs. [240, 241].

$(I, S)$	$M$	$\Gamma$	$\Gamma_i$					
$(1/2, 0)$			$\pi N$	$\eta N$	$\eta' N$	$K\Sigma$	$\eta_c N$	
	4261	56.9	3.8	8.1	3.9	17.0	23.4	
$(0, -1)$			$\bar{K}N$	$\pi\Sigma$	$\eta\Lambda$	$\eta'\Lambda$	$K\Xi$	$\eta_c\Lambda$
	4209	32.4	15.8	2.9	3.2	1.7	2.4	5.8
	4394	43.3	0	10.6	7.1	3.3	5.8	16.3

Table 13: Mass ( $M$ ), total width ( $\Gamma$ ), and the partial decay width ( $\Gamma_i$ ) for the states from  $VB \rightarrow VB$  with units in MeV, taken from Refs. [240, 241].

$(I, S)$	$M$	$\Gamma$	$\Gamma_i$					
$(1/2, 0)$			$\rho N$	$\omega N$	$K^*\Sigma$	$J/\psi N$		
	4412	47.3	3.2	10.4	13.7	19.2		
$(0, -1)$			$\bar{K}^*N$	$\rho\Sigma$	$\omega\Lambda$	$\phi\Lambda$	$K^*\Xi$	$J/\psi\Lambda$
	4368	28.0	13.9	3.1	0.3	4.0	1.8	5.4
	4544	36.6	0	8.8	9.1	0	5.0	13.8

Bethe-Salpeter Equation [276], and found that all models gave very narrow molecular-like nucleon resonances with hidden-charm in the mass range 4.3 – 4.5 GeV. Their results are consistent with the previous predictions [240, 241].

In Ref. [245], Xiao, Nieves, and Oset improved these results by including the leading order constraints of heavy quark spin symmetry [277, 278, 279], and developed a series of relationships for the transition potentials between the different meson-baryon channels in different combinations of spin and isospin. They found seven states with different energies or different spin-isospin quantum numbers, all of which have  $I = 1/2$ :

the  $J = 1/2$  sector : (4261.87 +  $i$ 17.84) MeV , (4410.13 +  $i$ 29.44) MeV , (4481.35 +  $i$ 28.91) MeV ,

the  $J = 3/2$  sector : (4334.45 +  $i$ 19.41) MeV , (4417.04 +  $i$ 4.11) MeV , (4481.04 +  $i$ 17.38) MeV ,

the  $J = 5/2$  sector : (4487.10 +  $i$ 0) MeV .

These poles can be easily classified as four basic states: a) the first pole (4261.87 +  $i$ 17.84) MeV, corresponding to a  $\bar{D}\Sigma_c$  state; b) the fourth pole (4334.45 +  $i$ 19.41) MeV, corresponding to a  $\bar{D}\Sigma_c^*$  state; c) the second pole (4410.13 +  $i$ 29.44) MeV and the fifth pole (4417.04 +  $i$ 4.11) MeV, both corresponding to a  $\bar{D}^*\Sigma_c$  state; d) the third pole (4481.35 +  $i$ 28.91) MeV, the sixth pole (4481.04 +  $i$ 17.38) MeV, and the seventh pole (4487.10 +  $i$ 0) MeV, all corresponding to a  $\bar{D}^*\Sigma_c^*$  state. All these states are bound with about 50 MeV with respect to the corresponding  $\bar{D}B$  thresholds.

In 2013, Garcia-Recio, Nieves, Romanets, Salcedo and Tolos studied the hidden charm  $N$  and  $\Delta$  resonances using a similar method constrained by the extended SU(8) spin-flavour symmetry, but their obtained masses were substantially smaller than these values [244]. For the  $J^P = 1/2^-, 3/2^-,$  and  $5/2^-$  hidden-charm resonances, their masses were predicted to be 3918 ~ 3974 MeV, 3946 ~ 4006 MeV, 4027 MeV, respectively. The total decay widths of the above three resonances were less than 10 MeV.

The results of Refs. [240, 241] were used by Xiao and Meissner to investigate the elastic and inelastic cross sections of the  $J/\psi N$ ,  $\eta_c N$ ,  $\Upsilon N$  and  $\eta_b N$  channels, where the predicted neutral partners  $P_c^0$  of the  $P_c^+$  states may be

found in Ref. [248].

In a recent work [246], Uchino, Liang, and Oset once more improved their results by considering two types of additional interactions as a box diagram correction. They found six states whose masses, widths, dominant components, and main decay channel are collected in Table VIII of Ref. [246].

In short summary, there exist extensive theoretical investigations of the hidden-charm baryons within the coupled channel unitary approach before and after the LHCb's discovery of the  $P_c(4380)$  and  $P_c(4450)$  [2]. We summarize several general features of the unitary approach.

- Only the hidden-charm baryons with negative parity are generated dynamically through the S-wave charmed meson and baryon scattering.
- Nearly all the model calculations indicated that the total width of the hidden-charm baryons were less than 60 MeV. In other words, these resonances are very narrow.
- The  $J/\psi N$  (or  $\eta_c N$ ) is one of the dominant decay modes of the non-strange hidden-charm baryons.
- The charm-less decay modes contribute significantly to the total decay width of the non-strange hidden-charm baryons.
- In general, several hidden-charm baryons are generated dynamically for one set of  $J^P$ .
- Within the same unitary approach, slightly different models led to diverse predictions for the mass of the hidden-charm baryon [240, 241, 242, 244, 245, 246], which indicated inherent uncertainties of this framework [246].

Sometimes spurious resonances are dynamically generated within the same approach, which are excluded experimentally. A recent investigation indicated that the inclusion of the higher order corrections changes the mass prediction significantly [258].

### 3.3. QCD sum rules

In the previous two subsections, we reviewed the meson exchange model and the chiral unitary approach. These two methods used the interactions between the charmed mesons and charmed baryons at the hadronic level to interpret the hidden-charm pentaquarks discovered by the LHCb Collaboration [2]. It is also interesting to study the internal structures of these pentaquarks at the quark gluon level. There have been several investigations of the hidden-charm pentaquarks with the method of QCD sum rule.

#### 3.3.1. A short introduction to the method of QCD sum rule

QCD sum rule techniques have proven to be a powerful and successful non-perturbative method over the past few decades. Various aspects of this formalism has been reviewed in Refs. [280, 281, 282, 283, 38]. It can also be applied in the framework of heavy quark effective theory [284, 285, 286] to study heavy mesons [287, 288, 289, 290, 291, 292, 293, 294, 295, 296, 297, 298] and heavy baryons [299, 300, 301, 302, 303, 304, 305, 306, 307, 308, 309, 310].

In addition to the operator product expansion (OPE), a key idea of the QCD sum rule is the quark-hadron duality, i.e., the equivalence of the (integrated) correlation functions at both the hadronic level and the quark-gluon level. One considers the correlation function

$$\Pi(q^2) = i \int d^4x e^{iqx} \langle 0 | T J(x) J^\dagger(0) | 0 \rangle, \quad (75)$$

where  $J(x)$  is an interpolating current which has the same quantum numbers as the hadron  $H$  we want to study. The strength of  $J(x)$  coupling to  $H$  is defined as  $f_H$ :

$$\langle 0 | J(0) | H \rangle \equiv f_H. \quad (76)$$

At the hadronic level, one expresses the correlation function in the form of the dispersion relation:

$$\Pi(q^2) = \frac{1}{\pi} \int_{s_\zeta}^{\infty} \frac{\text{Im}\Pi(s)}{s - q^2 - i\epsilon} ds, \quad (77)$$

where the integration starts from the physical threshold. The imaginary part of the two-point correlation function is the spectral density

$$\rho_{\text{phen}}(s) \equiv \frac{1}{\pi} \text{Im}\Pi(s) = \sum_n \delta(s - M_n^2) \langle 0 | J | n \rangle \langle n | J^\dagger | 0 \rangle. \quad (78)$$

One usually adopts a parametrization of one pole dominance for the ground state  $H$  and a continuum contribution:

$$\rho_{\text{phen}}(s) = f_H^2 \delta(s - M_H^2) + \text{higher states}. \quad (79)$$

At the quark-gluonic level, one computes  $\Pi(q^2)$  in the operator product expansion and evaluates  $\rho(s) = \rho_{\text{OPE}}(s)$  up to certain order in the expansion. The sum rule analysis is then performed by using the Borel transformation

$$\Pi^{(all)}(M_B^2) \equiv \mathcal{B}_{M_B^2} \Pi(p^2) = \int_{s_c}^{\infty} e^{-s/M_B^2} \rho(s) ds. \quad (80)$$

Assuming the contribution from the continuum states can be approximated well by the OPE spectral density above a threshold value  $s_0$ , one arrives at the sum rule relation

$$f_H^2 e^{-M_H^2/M_B^2} = \int_0^{s_0} e^{-s/M_B^2} \rho(s) ds. \quad (81)$$

Differentiating Log[Eq. (81)] with respect to  $1/M_B^2$ , finally one obtains

$$M_H^2 = \frac{\int_0^{s_0} e^{-s/M_B^2} s \rho(s) ds}{\int_0^{s_0} e^{-s/M_B^2} \rho(s) ds}. \quad (82)$$

### 3.3.2. Pentaquark currents

The hidden-charm local pentaquark interpolating currents of spins  $J = \frac{1}{2}/\frac{3}{2}/\frac{5}{2}$  were systematically constructed in Refs. [311, 312] based on the results of Refs. [313, 314, 315, 316, 317, 318, 319, 320, 321, 322, 29, 323, 324, 325, 326] which studied light baryon, tetraquark and dibaryon currents. We pick out two of them and discuss their internal color and flavor structure:

$$\eta_{1\mu}^{c\bar{c}uud}(x) = [\bar{c}_d(x) \gamma_\mu c_d(x)] [\epsilon_{abc} (u_a^T(x) \mathbb{C} d_b(x)) \gamma_5 u_c(x)], \quad (83)$$

$$J_\mu^{\bar{D}^* \Sigma_c}(x) = [\bar{c}_d(x) \gamma_\mu d_d(x)] [\epsilon_{abc} (u_a^T(x) \mathbb{C} \gamma_\nu u_b(x)) \gamma^\nu \gamma_5 c_c(x)]. \quad (84)$$

Here, the sum over repeated indices ( $\mu, \nu, \dots$  for Dirac spinor indices, and  $a, b, \dots$  for color indices) is taken; the superscript  $T$  represents the transpose of the Dirac indices only;  $\mathbb{C}$  is the charge-conjugation operator;  $u(x), d(x), c(x)$ , and  $\bar{c}(x)$  are the *up*, *down*, *charm*, and *anti-charm* quark fields at location  $x$ , respectively.

These two currents contain the same quark content  $c\bar{c}uud$  and have the same quantum number  $J^P = 3/2^-$ . However, their internal structures are totally different. The first one  $\eta_{1\mu}^{c\bar{c}uud}$  consists of two color-singlet components:  $\bar{c}_d \gamma_\mu c_d$  and  $\epsilon_{abc} (u_a^T \mathbb{C} d_b) \gamma_5 u_c$ , which have quantum numbers  $J^P = 1^-$  and  $1/2^+$ , and couple to the  $J/\psi$  and proton, respectively. The second one  $J_\mu^{\bar{D}^* \Sigma_c}$  consists of two color-singlet components:  $\bar{c}_d \gamma_\mu d_d$  and  $\epsilon_{abc} (u_a^T \mathbb{C} \gamma_\nu u_b) \gamma^\nu \gamma_5 c_c$ , which also have quantum numbers  $J^P = 1^-$  and  $1/2^+$ , but couple to the  $\bar{D}^*$  and  $\Sigma_c$ , respectively. Hence, the  $\eta_{1\mu}^{c\bar{c}uud}$  couples well to the combination of the  $J/\psi$  and  $p$ , and the  $J_\mu^{\bar{D}^* \Sigma_c}$  couples well to the combination of  $\bar{D}^*$  and  $\Sigma_c$ .

These different internal structures suggest that the choice of currents could be important when applying the method of QCD sum rule to study multiquark states, in which cases there always exist many currents of different color, flavor, orbit and spin structures [312]. For example, if one wants to study a physical pentaquark state of the molecular type, it would be best to choose an interpolating current also of the molecular type to ensure a large overlap with that state. Moreover, if one obtains a good sum rule result by using such a current, the relevant state might be a molecular state. But we note that even in this case it is difficult to fully distinguish between a tightly-bound pentaquark structure and a weakly-bound molecular structure, because all the quark and anti-quark fields inside the current are at the same space-time point.

Furthermore, the  $\eta_{\mu}^{\bar{c}iud}$  and  $J_{\mu}^{\bar{D}^* \Sigma_c}$  still have some overlap and can be partly related to each other through the color rearrangement and the Fierz transformation (see the example given in Ref. [312]), despite of their different internal structures. The color rearrangement for pentaquarks was given in Ref. [311]

$$\delta^{de} \epsilon^{abc} = \delta^{da} \epsilon^{ebc} + \delta^{db} \epsilon^{aec} + \delta^{dc} \epsilon^{abe}, \quad (85)$$

which can be used to relate the two color configurations,  $[\bar{c}_d c_d][\epsilon^{abc} q_a q_b q_c]$  and  $[\bar{c}_d q_d][\epsilon^{abc} c_a q_b q_c]$ . Two similar ones for tetraquarks are given in Ref. [321]

$$\begin{aligned} \delta^{ad} \delta^{bc} &= \frac{1}{3} \delta^{ab} \delta^{cd} + \frac{1}{2} \lambda_n^{ab} \lambda_n^{cd}, \\ \lambda_n^{ad} \lambda_n^{bc} &= \frac{16}{9} \delta^{ab} \delta^{cd} - \frac{1}{3} \lambda_n^{ab} \lambda_n^{cd}. \end{aligned} \quad (86)$$

Based on these formulae, the color structure used in Ref. [327, 328] can be simplified to

$$\epsilon^{abf} \epsilon^{ceg} \epsilon^{dfg} = -\delta^{da} \epsilon^{ebc} - \delta^{db} \epsilon^{aec}. \quad (87)$$

There are several formulae related to the Fierz transformation, which were given and discussed in Ref. [321, 313, 312]:

1. Products of two Dirac matrices without Lorentz indices:

$$\begin{pmatrix} \mathbf{1} \otimes \gamma_5 \\ \gamma_{\mu} \otimes \gamma^{\mu} \gamma_5 \\ \sigma_{\mu\nu} \otimes \sigma^{\mu\nu} \gamma_5 \\ \gamma_{\mu} \gamma_5 \otimes \gamma^{\mu} \\ \gamma_5 \otimes \mathbf{1} \end{pmatrix}_{ab,cd} = \begin{pmatrix} \frac{1}{4} & -\frac{1}{4} & \frac{1}{8} & \frac{1}{4} & \frac{1}{4} \\ -1 & -\frac{1}{2} & 0 & -\frac{1}{2} & 1 \\ 3 & 0 & -\frac{1}{2} & 0 & 3 \\ 1 & -\frac{1}{2} & 0 & -\frac{1}{2} & -1 \\ \frac{1}{4} & \frac{1}{4} & \frac{1}{8} & -\frac{1}{4} & \frac{1}{4} \end{pmatrix} \begin{pmatrix} \mathbf{1} \otimes \gamma_5 \\ \gamma_{\mu} \otimes \gamma^{\mu} \gamma_5 \\ \sigma_{\mu\nu} \otimes \sigma^{\mu\nu} \gamma_5 \\ \gamma_{\mu} \gamma_5 \otimes \gamma^{\mu} \\ \gamma_5 \otimes \mathbf{1} \end{pmatrix}_{ad,bc}. \quad (88)$$

2. Products of two Dirac matrices with one Lorentz index:

$$\begin{pmatrix} \mathbf{1} \otimes \gamma^{\mu} \\ \gamma^{\mu} \otimes \mathbf{1} \\ \gamma_5 \otimes \gamma_{\mu} \gamma_5 \\ \gamma_{\mu} \gamma_5 \otimes \gamma_5 \\ \gamma^{\nu} \otimes \sigma_{\mu\nu} \\ \sigma_{\mu\nu} \otimes \gamma^{\nu} \\ \gamma^{\nu} \gamma_5 \otimes \sigma_{\mu\nu} \gamma_5 \\ \sigma_{\mu\nu} \gamma_5 \otimes \gamma^{\nu} \gamma_5 \end{pmatrix}_{ab,cd} = \begin{pmatrix} \frac{1}{4} & \frac{1}{4} & \frac{1}{4} & -\frac{1}{4} & -\frac{i}{4} & \frac{i}{4} & \frac{i}{4} & \frac{i}{4} \\ \frac{1}{4} & \frac{1}{4} & -\frac{1}{4} & \frac{1}{4} & \frac{i}{4} & -\frac{i}{4} & \frac{i}{4} & \frac{i}{4} \\ \frac{1}{4} & -\frac{1}{4} & \frac{1}{4} & \frac{1}{4} & \frac{i}{4} & \frac{i}{4} & -\frac{i}{4} & \frac{i}{4} \\ -\frac{1}{4} & \frac{1}{4} & \frac{1}{4} & \frac{1}{4} & \frac{i}{4} & \frac{i}{4} & \frac{i}{4} & -\frac{i}{4} \\ \frac{3i}{4} & -\frac{3i}{4} & -\frac{3i}{4} & -\frac{3i}{4} & -\frac{1}{4} & -\frac{1}{4} & -\frac{1}{4} & \frac{1}{4} \\ -\frac{3i}{4} & \frac{3i}{4} & -\frac{3i}{4} & -\frac{3i}{4} & -\frac{1}{4} & -\frac{1}{4} & -\frac{1}{4} & -\frac{1}{4} \\ -\frac{3i}{4} & -\frac{3i}{4} & \frac{3i}{4} & -\frac{3i}{4} & -\frac{1}{4} & \frac{1}{4} & -\frac{1}{4} & -\frac{1}{4} \\ -\frac{3i}{4} & -\frac{3i}{4} & -\frac{3i}{4} & \frac{3i}{4} & \frac{1}{4} & -\frac{1}{4} & -\frac{1}{4} & -\frac{1}{4} \end{pmatrix} \begin{pmatrix} \mathbf{1} \otimes \gamma^{\mu} \\ \gamma^{\mu} \otimes \mathbf{1} \\ \gamma_5 \otimes \gamma_{\mu} \gamma_5 \\ \gamma_{\mu} \gamma_5 \otimes \gamma_5 \\ \gamma^{\nu} \otimes \sigma_{\mu\nu} \\ \sigma_{\mu\nu} \otimes \gamma^{\nu} \\ \gamma^{\nu} \gamma_5 \otimes \sigma_{\mu\nu} \gamma_5 \\ \sigma_{\mu\nu} \gamma_5 \otimes \gamma^{\nu} \gamma_5 \end{pmatrix}_{ad,bc}. \quad (89)$$

3. Products of two Dirac matrices with two anti-symmetric Lorentz indices:

$$\begin{pmatrix} \mathbf{1} \otimes \sigma_{\mu\nu} \gamma_5 \\ \gamma_5 \otimes \sigma_{\mu\nu} \\ \sigma_{\mu\nu} \otimes \gamma_5 \\ \sigma_{\mu\nu} \gamma_5 \otimes \mathbf{1} \\ \epsilon_{\mu\nu\rho\sigma} \sigma_{\rho\lambda} \otimes \sigma_{\sigma\lambda} \\ \gamma_{\mu} \otimes \gamma_{\nu} \gamma_5 - (\mu \leftrightarrow \nu) \\ \gamma_{\mu} \gamma_5 \otimes \gamma_{\nu} - (\mu \leftrightarrow \nu) \\ \epsilon_{\mu\nu\rho\sigma} \gamma_{\rho} \otimes \gamma_{\sigma} \\ \epsilon_{\mu\nu\rho\sigma} \gamma_{\rho} \gamma_5 \otimes \gamma_{\sigma} \gamma_5 \end{pmatrix}_{ab,cd} = \begin{pmatrix} \frac{1}{4} & \frac{1}{4} & \frac{1}{4} & \frac{1}{4} & \frac{1}{4} & \frac{i}{4} & -\frac{i}{4} & \frac{1}{4} & -\frac{1}{4} \\ \frac{1}{4} & \frac{1}{4} & \frac{1}{4} & \frac{1}{4} & \frac{1}{4} & -\frac{i}{4} & \frac{i}{4} & -\frac{1}{4} & \frac{1}{4} \\ \frac{1}{4} & \frac{1}{4} & \frac{1}{4} & \frac{1}{4} & -\frac{1}{4} & -\frac{i}{4} & \frac{i}{4} & \frac{1}{4} & -\frac{1}{4} \\ \frac{1}{4} & \frac{1}{4} & \frac{1}{4} & \frac{1}{4} & -\frac{1}{4} & \frac{i}{4} & -\frac{i}{4} & \frac{1}{4} & -\frac{1}{4} \\ 1 & 1 & -1 & -1 & 0 & 0 & 0 & 0 & 0 \\ -\frac{i}{2} & \frac{i}{2} & \frac{i}{2} & -\frac{i}{2} & 0 & 0 & 0 & \frac{i}{2} & \frac{i}{2} \\ \frac{i}{2} & -\frac{i}{2} & -\frac{i}{2} & \frac{i}{2} & 0 & 0 & 0 & \frac{i}{2} & \frac{i}{2} \\ \frac{1}{2} & -\frac{1}{2} & \frac{1}{2} & -\frac{1}{2} & 0 & -\frac{i}{2} & -\frac{i}{2} & 0 & 0 \\ -\frac{1}{2} & \frac{1}{2} & -\frac{1}{2} & \frac{1}{2} & 0 & -\frac{i}{2} & \frac{i}{2} & 0 & 0 \end{pmatrix} \begin{pmatrix} \mathbf{1} \otimes \sigma_{\mu\nu} \gamma_5 \\ \gamma_5 \otimes \sigma_{\mu\nu} \\ \sigma_{\mu\nu} \otimes \gamma_5 \\ \sigma_{\mu\nu} \gamma_5 \otimes \mathbf{1} \\ \epsilon_{\mu\nu\rho\sigma} \sigma_{\rho\lambda} \otimes \sigma_{\sigma\lambda} \\ \gamma_{\mu} \otimes \gamma_{\nu} \gamma_5 - (\mu \leftrightarrow \nu) \\ \gamma_{\mu} \gamma_5 \otimes \gamma_{\nu} - (\mu \leftrightarrow \nu) \\ \epsilon_{\mu\nu\rho\sigma} \gamma_{\rho} \otimes \gamma_{\sigma} \\ \epsilon_{\mu\nu\rho\sigma} \gamma_{\rho} \gamma_5 \otimes \gamma_{\sigma} \gamma_5 \end{pmatrix}_{ad,bc}. \quad (90)$$

4. Products of two Dirac matrices with two symmetric Lorentz indices:

$$\begin{pmatrix} g_{\mu\nu} \mathbf{1} \otimes \mathbf{1} \\ g_{\mu\nu} \gamma_{\rho} \otimes \gamma^{\rho} \\ g_{\mu\nu} \sigma_{\rho\sigma} \otimes \sigma^{\rho\sigma} \\ g_{\mu\nu} \gamma_{\rho} \gamma_5 \otimes \gamma^{\rho} \gamma_5 \\ g_{\mu\nu} \gamma_5 \otimes \gamma_5 \\ \gamma_{\mu} \otimes \gamma_{\nu} + (\mu \leftrightarrow \nu) \\ \gamma_{\mu} \gamma_5 \otimes \gamma_{\nu} \gamma_5 + (\mu \leftrightarrow \nu) \\ \sigma_{\mu\rho} \otimes \sigma_{\nu\rho} + (\mu \leftrightarrow \nu) \end{pmatrix}_{ab,cd} = \begin{pmatrix} \frac{1}{4} & \frac{1}{4} & \frac{1}{8} & -\frac{1}{4} & \frac{1}{4} & 0 & 0 & 0 & 0 \\ 1 & -\frac{1}{2} & 0 & -\frac{1}{2} & -1 & 0 & 0 & 0 & 0 \\ 3 & 0 & -\frac{1}{2} & 0 & 3 & 0 & 0 & 0 & 0 \\ -1 & -\frac{1}{2} & 0 & -\frac{1}{2} & 1 & 0 & 0 & 0 & 0 \\ \frac{1}{4} & -\frac{1}{4} & \frac{1}{8} & \frac{1}{4} & \frac{1}{4} & 0 & 0 & 0 & 0 \\ \frac{1}{2} & -\frac{1}{2} & \frac{1}{4} & -\frac{1}{2} & -\frac{1}{2} & \frac{1}{2} & \frac{1}{2} & -\frac{1}{2} & -\frac{1}{2} \\ -\frac{1}{2} & -\frac{1}{2} & -\frac{1}{4} & -\frac{1}{2} & -\frac{1}{2} & \frac{1}{2} & \frac{1}{2} & \frac{1}{2} & \frac{1}{2} \\ \frac{3}{2} & \frac{1}{2} & -\frac{1}{4} & -\frac{1}{2} & \frac{3}{2} & -1 & 1 & 0 & 0 \end{pmatrix} \begin{pmatrix} g_{\mu\nu} \mathbf{1} \otimes \mathbf{1} \\ g_{\mu\nu} \gamma_{\rho} \otimes \gamma^{\rho} \\ g_{\mu\nu} \sigma_{\rho\sigma} \otimes \sigma^{\rho\sigma} \\ g_{\mu\nu} \gamma_{\rho} \gamma_5 \otimes \gamma^{\rho} \gamma_5 \\ g_{\mu\nu} \gamma_5 \otimes \gamma_5 \\ \gamma_{\mu} \otimes \gamma_{\nu} + (\mu \leftrightarrow \nu) \\ \gamma_{\mu} \gamma_5 \otimes \gamma_{\nu} \gamma_5 + (\mu \leftrightarrow \nu) \\ \sigma_{\mu\rho} \otimes \sigma_{\nu\rho} + (\mu \leftrightarrow \nu) \end{pmatrix}_{ad,bc}. \quad (91)$$

We note that these equations only change the Lorentz structures, and the minus sign due to the exchange of quark fields is not included yet.

### 3.3.3. Operator Product Expansion

After the current is fixed, one can calculate the correlation function, Eq. (75). For example

$$\begin{aligned}\Pi_{\mu\nu}^{\bar{D}^*\Sigma_c}(q^2) &= i \int d^4x e^{iqx} \langle 0 | T J_\mu^{\bar{D}^*\Sigma_c}(x) \bar{J}_\nu^{\bar{D}^*\Sigma_c}(0) | 0 \rangle \\ &= 2\epsilon_{a_1 b_1 c_1} \epsilon_{a_2 b_2 c_2} \times \text{Tr}[S_d^{d_1 d_2}(x) \gamma_\nu S_c^{d_2 d_1}(-x) \gamma_\mu] \times \text{Tr}[S_u^{b_1 b_2}(x) \gamma_{\rho_2} \mathbb{C} S_u^{a_1 a_2}(x) \mathbb{C} \gamma_{\rho_1}] \times \gamma^{\rho_1} \gamma_5 S_c^{c_1 c_2}(x) \gamma^{\rho_2} \gamma_5.\end{aligned}\quad (92)$$

Then the light quark propagator can be expanded in the OPE expansion in the fixed-point gauge as

$$\begin{aligned}S_q^{ab}(x) &\equiv \langle 0 | T [q^a(x) \bar{q}^b(0)] | 0 \rangle \\ &= \frac{i\delta^{ab}}{2\pi^2 x^4} \not{x} + \frac{i}{32\pi^2} \frac{\lambda_{ab}^n}{2} g_c G_{\mu\nu}^n \frac{1}{x^2} (\sigma^{\mu\nu} \not{x} + \not{x} \sigma^{\mu\nu}) - \frac{\delta^{ab}}{12} \langle \bar{q}q \rangle + \frac{\delta^{ab} x^2}{192} \langle g_s \bar{q} \sigma G q \rangle \\ &\quad - \frac{\delta^{ab} m_q}{4\pi^2 x^2} + \frac{i\delta^{ab} m_q}{48} \langle \bar{q}q \rangle \not{x} + \frac{i\delta^{ab} m_q^2}{8\pi^2 x^2} \not{x},\end{aligned}\quad (93)$$

and the heavy quark propagator can be expanded as

$$\begin{aligned}S_c^{ab}(p) &\equiv \int d^4x e^{ipx} S_c^{ab}(x) = \int d^4x e^{ipx} \langle 0 | T [c^a(x) \bar{c}^b(0)] | 0 \rangle \\ &= i \frac{\not{p} + m_c}{p^2 - m_c^2} \delta^{ab} + \frac{i}{4} \frac{\lambda_{ab}^n}{2} g_c G_{\mu\nu}^n \frac{\sigma^{\mu\nu} (\not{p} + m_c) + (\not{p} + m_c) \sigma^{\mu\nu}}{(p^2 - m_c^2)^2} + \frac{i\delta^{ab} m_c}{12} \langle g_s^2 G^2 \rangle \frac{p^2 + m_c \not{p}}{(p^2 - m_c^2)^4}.\end{aligned}\quad (94)$$

After inserting these two equations into Eq. (93) and performing the Borel transformation

$$\mathcal{B}_{M_B^2}[\Pi(q^2)] = \lim_{\substack{-q^2, n \rightarrow \infty \\ -q^2/n = M_B^2}} \frac{(-q^2)^{n+1}}{n} \left( \frac{d}{dq^2} \right)^n \Pi(q^2), \quad (95)$$

we can obtain the spectral density  $\rho(s)$ . In Ref. [311],  $\rho(s)$  was evaluated up to dimension eight, including the perturbative term, the quark condensate  $\langle \bar{q}q \rangle$ , the gluon condensate  $\langle g_s^2 GG \rangle$ , the quark-gluon mixed condensate  $\langle g_s \bar{q} \sigma G q \rangle$ , and their combinations  $\langle \bar{q}q \rangle^2$  and  $\langle \bar{q}q \rangle \langle g_s \bar{q} \sigma G q \rangle$ . For example, when the pentaquark current  $J_\mu^{\bar{D}^*\Sigma_c}(x)$  is used, one can obtain

$$\begin{aligned}\rho_{\mu\nu}^{\bar{D}^*\Sigma_c}(s) &= \mathbf{1} \times g_{\mu\nu} \times m_c \times \left( \rho_1^{\text{pert}}(s) + \rho_1^{\langle \bar{q}q \rangle}(s) + \rho_1^{\langle GG \rangle}(s) + \rho_1^{\langle \bar{q}q \rangle^2}(s) + \rho_1^{\langle \bar{q}Gq \rangle}(s) + \rho_1^{\langle \bar{q}q \rangle \langle \bar{q}Gq \rangle}(s) \right) \\ &\quad + \not{q} \times g_{\mu\nu} \times \left( \rho_2^{\text{pert}}(s) + \rho_2^{\langle \bar{q}q \rangle}(s) + \rho_2^{\langle GG \rangle}(s) + \rho_2^{\langle \bar{q}q \rangle^2}(s) + \rho_2^{\langle \bar{q}Gq \rangle}(s) + \rho_2^{\langle \bar{q}q \rangle \langle \bar{q}Gq \rangle}(s) \right) + \dots,\end{aligned}\quad (96)$$

where  $\dots$  denotes other Lorentz structures, such as  $\mathbf{1} \times \sigma_{\mu\nu}$ , etc.. The expressions of the spectral densities can be found in Ref. [311].

### 3.3.4. Parity of Pentaquarks

In the previous section, two sum rules are obtained when one pentaquark current  $J_\mu^{\bar{D}^*\Sigma_c}(x)$  is used. One is proportional to  $\mathbf{1} \times g_{\mu\nu}$ , and the other is proportional to  $\not{q} \times g_{\mu\nu}$ . They can be used to calculate the mass of the pentaquark and determine its parity at the same time. This technique was used in Ref. [311], and can be applied for other baryons and pentaquarks.

Although a pentaquark current has definite parity, it can couple to states of both positive and negative parities via (see discussions in Refs. [329, 330, 331, 332]):

$$\langle 0 | J | H \rangle = f_H u(p), \quad (97)$$

$$\langle 0 | J | H' \rangle = f_{H'} \gamma_5 u'(p), \quad (98)$$

where  $|H\rangle$  has the same parity as  $J$ , and  $|H'\rangle$  has the opposite parity. Oppositely, the current  $J$  and its partner  $\gamma_5 J$  can also couple to the same state  $H$ .

In Ref. [311], the non- $\gamma_5$  coupling in Eq. (97) was used,

$$\langle 0 | J_\mu^{\bar{D}^* \Sigma_c} | [\bar{D}^* \Sigma_c] \rangle = f_{\bar{D}^* \Sigma_c} u_\mu(p). \quad (99)$$

Then the two-point correlation functions can be written as:

$$\begin{aligned} \Pi_{\mu\nu}^{\bar{D}^* \Sigma_c}(q^2) &= i \int d^4x e^{iq \cdot x} \langle 0 | T [J_\mu^{\bar{D}^* \Sigma_c}(x) \bar{J}_\nu^{\bar{D}^* \Sigma_c}(0)] | 0 \rangle \\ &= \left( \frac{q_\mu q_\nu}{q^2} - g_{\mu\nu} \right) (\not{q} + M_H) \Pi^{\bar{D}^* \Sigma_c}(q^2) + \dots, \end{aligned} \quad (100)$$

where the spin 1/2 components are all contained in  $\dots$ , such as  $q_\mu q_\nu (\not{q} + m) \Pi_{1/2}^{\bar{D}^* \Sigma_c}(q^2)$ , etc.

One can also use the  $\gamma_5$  couplings in Eq. (98). The resulting two-point correlation function is similar to Eq. (100), but with  $(\not{q} + M_H)$  replaced by  $(-\not{q} + M_H)$ . This difference would tell us the parity of  $H$ . If the two sum rules from these two tensor structures lead to almost the same numerical results, the current  $J_\mu^{\bar{D}^* \Sigma_c}(x)$  couples to a state having the same parity, that is  $P = -$ . We note that the result does not change when using  $\gamma_5 J_\mu^{\bar{D}^* \Sigma_c}$  having the opposite parity.

### 3.3.5. Numerical results and discussions

Several currents were used in Ref. [311] to perform QCD sum rule analyses. The current

$$J_\mu^{\bar{D}^* \Sigma_c} = [\bar{c}_d \gamma_\mu d_d] [\epsilon_{abc} (u_a^T C \gamma_\nu u_b) \gamma^\nu \gamma_5 c_c], \quad (101)$$

was used to obtain:

$$M_{[\bar{D}^* \Sigma_c], 3/2^-} = 4.37_{-0.12}^{+0.19} \text{ GeV}. \quad (102)$$

The results are shown in Fig. 42. Both the mass value and the spin-parity are consistent with the experimental results of the  $P_c(4380)$  [2], supporting it to be a  $[\bar{D}^* \Sigma_c]$  hidden-charm pentaquark with the quantum numbers  $J^P = 3/2^-$ . This  $[\bar{D}^* \Sigma_c]$  structure may be interpreted as a tightly-bound pentaquark structure or a  $[\bar{D}^* \Sigma_c]$  molecular state. But in both cases, it can easily decay into  $\bar{D}^* \Sigma_c$  final states if its mass is above the  $\bar{D}^* \Sigma_c$  threshold. Moreover, the current  $J_\mu^{\bar{D}^* \Sigma_c}$  has some overlap with  $\eta_{1\mu}^{c\bar{c}uud}(x)$ , suggesting that it can also decay into S-wave  $J/\psi p$  final states.

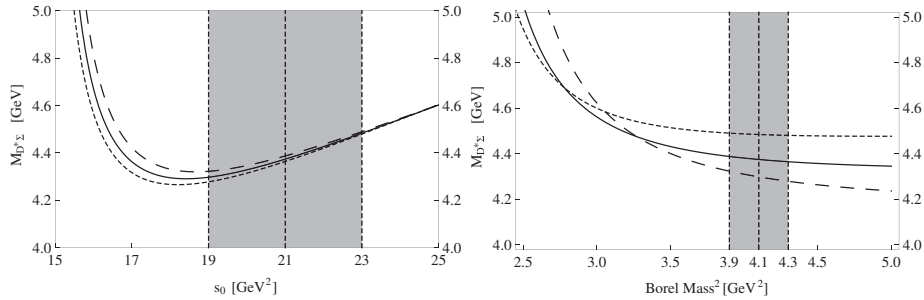


Figure 42: The variation of  $M_{[\bar{D}^* \Sigma_c]}$  with respect to the threshold value  $s_0$  (left) and the Borel mass  $M_B$  (right), taken from Ref. [311].

A mixed current consisting of  $J_{\{\mu\nu\}}^{\bar{D}^* \Sigma_c^*}$  and  $J_{\{\mu\nu\}}^{\bar{D}^* \Lambda_c}$  was used in Ref. [311]:

$$J_{\{\mu\nu\}}^{\bar{D}^* \Sigma_c^* \& \bar{D}^* \Lambda_c} = \sin \theta \times J_{\{\mu\nu\}}^{\bar{D}^* \Sigma_c^*} + \cos \theta \times J_{\{\mu\nu\}}^{\bar{D}^* \Lambda_c}, \quad (103)$$

where

$$J_{\{\mu\nu\}}^{\bar{D}^* \Sigma_c^*} = [\bar{c}_d \gamma_\mu \gamma_5 d_d] [\epsilon_{abc} (u_a^T C \gamma_\nu u_b) c_c] + \{\mu \leftrightarrow \nu\}, \quad (104)$$

$$J_{\{\mu\nu\}}^{\bar{D}^* \Lambda_c} = [\bar{c}_d \gamma_\mu u_d] [\epsilon_{abc} (u_a^T C \gamma_\nu \gamma_5 d_b) c_c] + \{\mu \leftrightarrow \nu\}. \quad (105)$$

The mixing angle  $\theta$  was fine-tuned to be  $-51 \pm 5^\circ$ , and the hadron mass was extracted as

$$M_{[\bar{D}\Sigma_c^* \& \bar{D}^* \Lambda_c], 5/2^+} = 4.47_{-0.13}^{+0.20} \text{ GeV}. \quad (106)$$

The results are shown in Fig. 43. Both the mass value and the spin-parity are consistent with the experimental results of the  $P_c(4450)$  [2], supporting it to be an admixture of  $[\bar{D}^* \Lambda_c]$  and  $[\bar{D}\Sigma_c^*]$  with quantum numbers  $J^P = 5/2^+$ . According to its internal structure described by  $J^{\bar{D}\Sigma_c^* \& \bar{D}^* \Lambda_c}$ , its main decay modes include the P-wave  $\bar{D}^* \Lambda_c$  and  $\bar{D}\Sigma_c^*$ . Moreover, the P-wave  $J/\psi p$  decay mode is also possible.

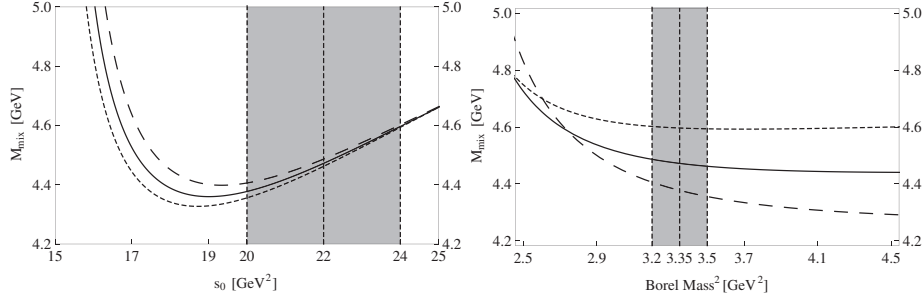


Figure 43: The variation of  $M_{[\bar{D}\Sigma_c^* \& \bar{D}^* \Lambda_c]}$  with respect to the threshold value  $s_0$  (left) and the Borel mass  $M_B$  (right).

According to Ref. [311], there may also exist a  $[\bar{D}\Sigma_c^*]$  hidden-charm pentaquark and a  $[\bar{D}^* \Sigma_c^*]$  one, having masses around 4.5 GeV, and two hidden-bottom pentaquarks as partners of the  $P_c(4380)$  and  $P_c(4450)$ , having masses around 11.6 GeV. Their possible decay modes were also discussed. The same approach was used to systematically study hidden-charm pentaquarks of spins  $J = \frac{1}{2}/\frac{3}{2}/\frac{5}{2}$  [312], where a full classification of the local hidden-charm pentaquark interpolating currents is given.

Besides Refs. [311, 312], Wang applied the method of QCD sum rule to study the hidden-charm pentaquarks  $P_c(4380)$  and  $P_c(4450)$ , but used the diquark-diquark-antiquark type interpolating currents [327, 328]

$$\epsilon^{ila} \bar{c}_a [\epsilon^{ijk} u_j d_k] [\epsilon^{lmn} u_m c_n]. \quad (107)$$

His results also favor assigning the  $P_c(4380)$  and  $P_c(4450)$  to be the  $3/2^-$  and  $5/2^+$  pentaquark states, respectively.

### 3.4. Tightly bound pentaquark state in the quark model

In the previous subsection we reviewed the application of the QCD sum rule to the hidden-charm pentaquarks. There are many hidden-charm pentaquark interpolating currents, suggesting the internal color-flavor structures of hidden-charm pentaquarks can be extraordinarily complicated. Among these various internal structures, the tightly bound pentaquark state is very interesting where the five quarks are confined within one MIT bag. In this subsection we review those models which are based on this interpretation. Even for the tightly bound pentaquark picture, there exist many variations, such as the antiquark-diquark-diquark picture and the diquark-triquark picture etc.

Recall that the mass gap between  $\Lambda_c$  and  $\Sigma_c$  is around 170 MeV, which indicates that the attraction between the up and down quarks is strong when the  $[ud]$  pair stays in the scalar isoscalar color anti-triplet configuration. The diquark or triquark is sometimes used to denote the spin, isospin and color correlation between the quarks. From the very beginning, we want to emphasize that there do not exist point-like or extremely compact colored building blocks such as diquarks or triquarks. Within the nucleons, the scalar and axial vector diquarks transform into each other freely. Moreover, all the tetraquark or pentaquark color configurations can be rigorously decomposed into the sum of a series of product of two color-singlet hadrons, as shown in the previous subsection.

#### 3.4.1. Chiral quark model

The constituent quark model is very successful in the description of the static properties of hadrons. On the other hand, chiral symmetry of QCD and its spontaneous breaking play a pivotal role in the low energy sector. The chiral

quark model includes the interaction between the constituent quark and chiral fields ( $\pi, K, \eta$ ) besides the quark gluon interaction. Replacing the nucleon fields in the linear  $\sigma$  model [333] with quarks, one gets the SU(2)  $\sigma$  model at the quark level [334]. The interaction term reads

$$\mathcal{L}_I = -g\bar{\psi}(\sigma + i\gamma_5\boldsymbol{\tau}\cdot\boldsymbol{\pi})\psi, \quad (108)$$

where  $\boldsymbol{\tau}$  denotes the Pauli matrix and the coupling constant  $g$  can be related to the nucleon-nucleon-pion coupling constant  $g_{NN\pi}$ . Zhang *et al.* extended this model to the three flavor case and named it as the chiral SU(3) quark model [335, 336]

$$\begin{pmatrix} u \\ d \end{pmatrix} \rightarrow \begin{pmatrix} u \\ d \\ s \end{pmatrix}, \quad (109)$$

$$(\sigma + i\gamma_5\boldsymbol{\tau}\cdot\boldsymbol{\pi}) \rightarrow \left( \sum_{a=0}^8 \lambda_a \sigma_a + i \sum_{a=0}^8 \lambda_a \pi_a \right), \quad (110)$$

where  $\lambda_0$  is the unit matrix and  $\lambda_i (i = 1, \dots, 8)$  are Gell-Mann matrices.

To figure out whether the one gluon exchange (OGE) or vector meson exchange is a right mechanism for the short range strong interaction, they further extended the model to the case involving vector mesons, which was called the extended chiral SU(3) quark model [337]. This version of the chiral quark model contains the one-boson-exchange potential, one-gluon-exchange potential, and confinement potential. For the hadron-hadron interactions, the short-range quark exchange effects between two hadrons were also taken into account.

Both of the three-flavor chiral quark models can reasonably describe the spectrum of the ground state baryons, the binding energy of the deuteron, the baryon-baryon scattering data, and the kaon-nucleon scattering phase shifts etc. Within this framework, various di-hadron bound states were investigated such as  $\Delta\Delta$  [338],  $\Omega\Omega$  [339],  $N\bar{\Omega}$  [340],  $\Delta K$  [341, 342],  $N\phi$  [343],  $\Sigma K$  [344],  $\Omega\pi$  [345], and  $\Omega\omega$  [346].

The chiral SU(3) quark model and its extended version were also employed to study the heavy quark systems [213, 212]. In Ref. [347], the authors studied the  $\Sigma_c\bar{D}$  and  $\Lambda_c\bar{D}$  systems by solving a resonating group method (RGM) equation, which is a well-established method for studying interactions between composite particles or quark clusters [348]. The extension to the heavy quark case introduces additional parameters: the charm quark mass, a coupling constant of OGE, and confinement strengths involving the charm quark. Except the charm quark mass, these parameters can be fixed with the masses of heavy quark hadrons  $\Sigma_c, \Lambda_c, D, D^*, J/\psi$ , and  $\eta_c$ . The heavy quark mass is treated as an adjustable parameter.

Before LHCb's discovery of the  $P_c(4380)$  and  $P_c(4450)$  resonances, there were some explorations of the hidden-charm pentaquarks in chiral constituent quark model [347]. In Ref. [347], the authors performed a dynamical investigation of the  $\Sigma_c\bar{D}$  and  $\Lambda_c\bar{D}$  systems with spin  $S = 1/2$  and isospin  $I = 1/2$  by solving a resonating group method equation. They calculated the effective Hamiltonian of the  $\Sigma_c\bar{D}$  and  $\Lambda_c\bar{D}$  systems in three different models (according to the different coupling between the vector meson field and the quark field). They found that the interaction between  $\Sigma_c$  and  $\bar{D}$  is attractive and a  $\Sigma_c\bar{D}$  bound state can be formed by considering either the linear confinement potential or the quadratic one. The energy of the  $\Sigma_c\bar{D}$  bound state was predicted as 4.279 – 4.312 GeV in the linear confinement potential. They found no  $\Lambda_c\bar{D}$  bound state due to the repulsive interaction between  $\Lambda_c$  and  $\bar{D}$ . In a coupled-channel calculation, they found that the coupled-channel effect of the  $\Sigma_c\bar{D}$  and  $\Lambda_c\bar{D}$  can be negligible due to the large mass difference between the  $\Sigma_c\bar{D}$  and  $\Lambda_c\bar{D}$  thresholds and the small off-diagonal matrix elements of the  $\Sigma_c\bar{D}$  and  $\Lambda_c\bar{D}$ . Thus, there was no  $\Sigma_c\bar{D}$ - $\Lambda_c\bar{D}$  resonance as a result. These predicted  $\Sigma_c\bar{D}$  bound states are potential candidates of hidden-charm pentaquarks, although they have lower spin than the observed  $P_c(4380)$  and  $P_c(4450)$  resonances.

Inspired by the discovery of the  $P_c(4380)$  and  $P_c(4450)$  states in LHCb [2], further investigation of the hidden-charm pentaquarks in the chiral quark model was performed in Ref. [349] by considering the quark delocalization color screening effect to solve the RGM equation.

It is known that electron delocalization contributes to the formation of chemical bonds in molecular physics. Noticing the similarity between the force of hadrons and that of atoms, quarks confined in one nucleon are speculated to delocalize into another nucleon [350], which leads to the screened confinement potential between quarks belonging

to different nucleons. Along this line, there were many investigations on the various aspects of hadron properties [351, 352, 353, 354, 355]. It was shown that the modified confinement potential gives an equivalent description for the contribution from the hidden-color channels [356].

The modified chiral quark model used in Ref. [349] contains the  $\pi$ -exchange potential, OGE potential, and a quark delocalization color screening confinement potential, which also describes well the  $NN$  and  $YN$  interactions. For the heavy quark systems, one has to determine the heavy quark mass and a color screening parameter. The former is fixed from heavy hadron masses while the latter is treated as an adjustable parameter. All the other parameters are determined in the studies of the light quark systems [357, 358, 359, 360].

The authors of Ref. [349] introduced a phenomenological color screening confinement potential in the model Hamiltonian with the color screening parameter as an adjustable parameter. They investigated the possible hidden-charm molecular pentaquarks composed of the  $D/D^*$  and  $\Sigma_c/\Sigma_c^*/\Lambda_c$  with quantum numbers  $Y = 1, I = \frac{1}{2}, \frac{3}{2}$  and  $J^P = \frac{1}{2}^-, \frac{3}{2}^-, \frac{5}{2}^-$ . For the  $IJ^P = \frac{1}{2}\frac{1}{2}^-, \frac{1}{2}\frac{3}{2}^-$  systems. They found that the potentials are all attractive for the channels  $\Sigma_c\bar{D}, \Sigma_c^*\bar{D}$  and  $\Sigma_c^*\bar{D}^*$  but repulsive for the channels  $\Lambda_c\bar{D}$  and  $\Lambda_c\bar{D}^*$ . For the  $IJ^P = \frac{1}{2}\frac{5}{2}^-$  systems, only the  $\Sigma_c^*\bar{D}^*$  channel has an attractive potential. For the isospin  $I = \frac{3}{2}$  systems, all channels are repulsive except the  $\Sigma_c^*\bar{D}$  and  $\Sigma_c^*\bar{D}^*$  which have a very weak attractive potential. The binding energies of the attractive channels were calculated by solving the RGM equation and the masses were obtained. They also considered the channel coupling effects in the evaluations. They concluded that the  $P_c(4380)$  was a mixed structure of the  $\Lambda_c\bar{D}^*, \Sigma_c^*\bar{D}, \Sigma_c^*\bar{D}$  and  $\Sigma_c^*\bar{D}^*$  with  $IJ^P = \frac{1}{2}\frac{3}{2}^-$  and the main channel was the  $\Sigma_c^*\bar{D}$ , while the  $P_c(4450)$  state was a  $\Sigma_c^*\bar{D}^*$  resonance with  $IJ^P = \frac{1}{2}\frac{5}{2}^-$ . They also predicted another pentaquark state  $\Sigma_c\bar{D}$  with  $IJ^P = \frac{1}{2}\frac{1}{2}^-$ . The corresponding hidden-bottom pentaquark partners were also discussed.

In Ref. [361], the authors performed a dynamical calculation of five-quark systems with quantum numbers  $I = \frac{1}{2}$  and  $J^P = \frac{1}{2}^\pm, \frac{3}{2}^\pm, \frac{5}{2}^\pm$  in the framework of the chiral quark model with the gaussian expansion method. The authors pointed out that the negative parity states could be bound states while all the positive parity states are the scattering states. The  $P_c(4380)$  and  $P_c(4450)$  were treated as the bound states of the  $\Sigma_c^*\bar{D}$  and  $\Sigma_c\bar{D}^*$  respectively. For the first time, the authors calculated the average distance between each quark, some of which may reach 2 fm! The authors concluded that the distances between quarks confirm the molecular nature of the  $P_c$  states.

### 3.4.2. The diquark/triquark model

In Ref. [362], Maiani, Polosa, and Riquer discussed the hidden-charm pentaquarks discovered by the LHCb Collaboration [2], and pointed out that they can be a natural expectation of an extended picture of hadrons where quarks and diquarks are fundamental units [363]. The diquark  $[qq]$  here is a color anti-triplet member, similar to an anti-quark  $\bar{q}$  [20, 364, 365]. They used the combinations of one antiquark  $[\bar{c}]$ , one heavy diquark  $[cq]$ , and one light diquark  $[qq]$ :

$$P_c(4380, 3/2^-) = \bar{c}[cq]_{s=1}[qq]_{s=1}, L = 0, \quad (111)$$

$$P_c(4450, 5/2^+) = \bar{c}[cq]_{s=1}[qq]_{s=0}, L = 1, \quad (112)$$

to explain the newly observed  $P_c(4380)$  and  $P_c(4450)$ . The  $S$ -wave state  $P_c(4380)$  has negative parity, and the  $P$ -wave state  $P_c(4450)$  has positive parity. The mass difference between the  $P_c(4380)$  and  $P_c(4450)$  is about 70 MeV, a) partly due to the orbital excitation, which is of order 280 MeV, estimated for  $XYZ$  mesons [366], and b) partly due to the mass difference between diquarks with spin  $s = 1$  and  $s = 0$ , which is of order 200 MeV, estimated from charm and beauty baryons spectra [367]. They also studied the flavor structures of the pentaquarks, and proposed several flavor partners of the  $P_c(4380)$  and  $P_c(4450)$  to be observed in the  $\Xi_b$  and  $\Omega_b$  decays. The idea was extended by the same authors for charmed dibaryons in Ref. [368] where they proposed several possible channels to search for them in the  $\Lambda_b(5620)$  decays.

The same antiquark-diquark-diquark system was applied to study the hidden-charm pentaquarks in later studies [369, 370, 371, 372]. In Ref. [369, 370], Anisovich *et al.* gave the spin and isospin structure of these states and estimated their masses, based on their previous study of the tetraquark states [373]. Their results suggested that the  $P_c(4450)$  is an antiquark-diquark-diquark state with spin-parity  $5/2^-$ , while the  $P_c(4380)$  is the result of rescatterings in the  $pJ/\psi$  spectrum, and can be related with possible resonances of the  $K^-J/\psi$  channel located in the mass region 4000-4500 MeV.

In Ref. [372], Ghosh, Bhattacharya, and Chakrabarti used the quasi particle diquark model, where diquarks are supposed to behave like a quasi particle in an analogy with an electron in the crystal lattice which behaves as a quasi particle. They estimated the masses of the  $P_c(4380)$  in both  $[ud]_0[uc]_1\bar{c}$  and  $[ud]_1[uc]_0\bar{c}$  configurations to be 4403 MeV and 4345 MeV, respectively, and the mass of the  $P_c(4450)$  in the  $[ud]_1[uc]_1\bar{c}$  configuration to be 4443 MeV, both of which are consistent with the LHCb experiment [2].

A similar combination of diquark  $[cq]$  and triquark  $[\bar{c}(ud)]$  was proposed by Lebed to study the hidden-charm pentaquarks in Ref. [374], which was based upon a mechanism proposed to study tetraquark states [375]. The  $P_c(4380)$  and  $P_c(4450)$  were described in terms of a confined but rapidly separating color-antitriplet diquark  $[cu]$  and color-triplet antitriquark  $[\bar{c}(ud)]$ . The separations between diquark and antitriquark were estimated to be 0.64 fm for the  $P_c(4380)$  and 0.70 fm for the  $P_c(4450)$ . These distances were achieved before the hadronization, providing a qualitative explanation for the suppression of the measured widths of the  $P_c(4380)$  and  $P_c(4450)$ . Later in Ref. [376], Lebed applied the same method to investigate the hidden-strangeness pentaquarks  $P_s$ , and proposed to observe it in the  $\Lambda_c \rightarrow P_s^+ \pi^0 \rightarrow \phi p \pi^0$  decay.

This diquark-triquark system was also used by Zhu and Qiao in Ref. [377], where both diquark and triquark are not compact objects, and have nonzero sizes. They analyzed the color attractive configuration for the triquark and defined the nonlocal wave functions for the pentaquark state, which are later used to construct an effective diquark-triquark Hamiltonian based on spin-orbital interaction. The pentaquark spectrum were obtained using this Hamiltonian, where the pentaquark state with mass 4.349 GeV can explain the  $P_c(4380)$ , and the pentaquark state with mass 4.453 GeV can explain the  $P_c(4450)$ . Their mass splitting near 100 MeV is also consistent with the LHCb experiment [2]. They further suggested to analyze the  $J/\psi \Sigma^+$  and  $J/\psi \Lambda$  mass spectrum near 4.682 GeV in  $\Xi_b^0 \rightarrow J/\psi \Sigma^+ K^-$  and  $\Xi_b^- \rightarrow J/\psi \Lambda K^-$  decays, to look for the charged and neutral hidden charm pentaquarks with  $J^P = 5/2^+$  and strange number  $S = -1$ .

### 3.5. Kinematical effect

There also exist the non-resonant explanations to the LHCb's observation [2]. In Refs. [378, 379, 380], these authors proposed various rescattering mechanisms to show that the narrow  $P_c(4450)$  state might arise from the kinematical effect.

Guo *et al.* [378] studied the possibility of the  $P_c^+(4450)$  as the kinematical effect since it is around the  $\chi_{c1}P$  threshold. The  $J^P$  quantum number of the P-wave  $\chi_{c1}P$  system matches the quantum number of the  $P_c^+(4450)$  [2]. Two typical decay mechanisms for the  $\Lambda_b \rightarrow K^- J/\psi p$  were introduced, i.e., (a)  $\Lambda_b \rightarrow K^- p \chi_{c1} \rightarrow K^- p J/\psi$  via  $p \chi_{c1} \rightarrow p J/\psi$  rescattering, (b)  $\Lambda_b \rightarrow \Lambda^* \chi_{c1} \rightarrow K^- p J/\psi$  via exchanging a proton. In the above two processes, the  $p \chi_{c1} \rightarrow p J/\psi$  rescattering occurs via exchanging soft gluons. When dealing with the first process, they adopted a similar method to that in Ref. [381] to get a loop function. With a phenomenological amplitude which includes a constant background contribution, the Argand diagram given by LHCb [2] can be reproduced [378].

Guo *et al.* further considered the second mechanism and discussed whether that the  $P_c(4450)$  signal can arise from the triangle singularity. By solving the Landau equation, the leading Landau singularities for the triangle diagram were extracted. Through investigating the motion of the solutions in the complex  $\sqrt{s}$  plane, they noticed that the  $\Lambda^*$  as the intermediate state introduced in this decay mechanism can only correspond to the  $\Lambda(1890)$ . The corresponding triangle singularity is close to the  $\chi_{c1}P$  threshold, which can produce a threshold enhancement. Thus, they concluded that the  $P_c^+(4450)$  can also be the kinematical effects around the  $\chi_{c1}P$  threshold [378].

Later, Liu *et al.* also investigated the possibility of the  $P_c(4450)$  as kinematical effects [380] and considered three typical decay mechanisms which include (a)  $\Lambda_b \rightarrow \Lambda^* \chi_{cJ} \rightarrow K^- p J/\psi$  via exchanging a proton which is the same as one of the mechanisms proposed in Ref. [378], (b)  $\Lambda_b \rightarrow D_s^* \Lambda_c^* \rightarrow K^- p J/\psi$  through exchanging  $\bar{D}^{(*)}$ , (c)  $\Lambda_b \rightarrow K \bar{D}^{(*)} \Sigma_c^* \rightarrow K J/\psi p$  via  $\bar{D}^{(*)} \Sigma_c^* \rightarrow J/\psi p$  rescattering. To deal with the triangle loop diagrams, the same approach as in Ref. [382] was adopted, where the possible  $\chi_{cJ}P$  and  $\Lambda_c^* \bar{D}^{(*)}$  threshold enhancements due to the triangle singularities were considered.

Although both Guo *et al.* [378] and Liu *et al.* [380] studied similar issues of  $\Lambda_b \rightarrow \Lambda^* \chi_{cJ} \rightarrow K^- p J/\psi$ , there exist some difference. In Ref. [380], Liu *et al.* indicated that the mass thresholds for the  $p \chi_{cJ}$  ( $J = 0, 1, 2$ ) are all close to the peak masses for the  $P_c^+(4450)$ . Including these thresholds in their calculation, they found that the corresponding mass of the  $\Lambda^*$  is larger than 2 GeV, which is in contrast with  $m(\Lambda^*) = 1.89 \sim 2.11$  GeV in Ref. [378].

In Ref. [378], the authors pointed out that the charmonium was produced by the weak current  $[\bar{c} \gamma^\mu (1 - \gamma_5) c]$  at the leading order. This current has no projection onto the  $\chi_{c0}$  or  $\chi_{c2}$ , although the rescattering interaction strength for

$\chi_{c0,2p} \rightarrow J/\psi p$  is of the similar size to that for the  $\chi_{c1p} \rightarrow J/\psi p$  scattering due to heavy quark spin symmetry. So the production of these two charmonium states  $\chi_{c0,2}$  in the  $b$  decays can only come from higher-order QCD corrections which are suppressed. According to the above qualitative analysis, there do not exist enhancements around the  $\chi_{c0p}$  and  $\chi_{c2p}$  thresholds in the  $J/\psi p$  invariant mass distribution of the  $\Lambda_b \rightarrow K^- J/\psi p$  decay. Thus, Guo *et al.* only presented the  $\chi_{c1p}$  peak structure in the mass distribution of the  $J/\psi p$ , while Liu *et al.* gave two peak structures around the  $\chi_{c1p}$  and  $\chi_{c2p}$  thresholds.

Liu *et al.* further analyzed the second mechanism [380], and pointed out that there also exist the conditions required by the triangle singularity. When the  $\Lambda_c^{(*)} \bar{D}_{sJ}^{(*)}$  threshold is close to the  $\Lambda_b$  mass, a sizeable enhancement at the  $\Lambda_c^{(*)} \bar{D}^{(*)}$  thresholds is allowed, where the  $\Lambda_c(2595) \bar{D}$  threshold results in an enhancement around 4.45 GeV. If the  $\Lambda_c(2595) \bar{D}$  is in S-wave, the quantum number of the obtained enhancement around 4.45 GeV in Ref. [380] must be  $J^P = 1/2^+$ , which does match the experimental measurement of the  $P_c(4450)$  quantum number. Under this situation, the  $P_c(4450)$  cannot be explained as the enhancement due to the S-wave  $\Lambda_c(2595) \bar{D}$  threshold. They also argued that there still exists the possible enhancement near 4.45 GeV when the  $\Lambda_c(2595) \bar{D}$  is in P-wave, which is suppressed compared with the S-wave case [380]. At present, a quantitative study of this point is still absent.

Besides discussing  $\Lambda_b \rightarrow \Lambda^* \chi_{cJ} \rightarrow K^- p J/\psi$  via exchanging a proton and  $\Lambda_b \rightarrow D_s^{*+} \Lambda_c^* \rightarrow K^- p J/\psi$  through exchanging the  $\bar{D}^{(*)}$ , Liu *et al.* also studied the mechanism  $\Lambda_b \rightarrow K \bar{D}^{(*)} \Sigma_c^* \rightarrow K J/\psi p$  via the  $\bar{D}^{(*)} \Sigma_c^* \rightarrow J/\psi p$  rescattering, which generated the cusp structure around 4.45 GeV in the  $J/\psi p$  mass distribution. As indicated in Ref. [380], the cusp structure can be ignored comparing with the enhancement from the triangle singularity.

Mikhasenko studied the triangle diagram  $\Lambda_b \rightarrow D_s^{*+} \Sigma_c^+ \rightarrow K^- J/\psi p$  via a  $D^{*0}$  exchange, where there exists the  $\Sigma_c^+ D^{*0} \rightarrow J/\psi p$  interaction [379]. To some extent, this triangle diagram is similar to the third decay mechanism proposed in Ref. [380] since this triangle diagram in Ref. [379] can be abbreviated to the third decay mechanism in Ref. [380] when this  $D_s^*$  exchange is absorbed into the vertex. Mikhasenko used the  $D_s^{*-}$ ,  $\Sigma_c^+$  and  $D^{*0}$  as building blocks of the triangle loop and found an enhancement near the  $\Sigma_c^+ D^{*0}$  threshold from the triangle singularity, which may correspond to the observed  $P_c^+(4450)$  structure [379].

### 3.6. Other theoretical schemes

Besides the theoretical works introduced in previous subsections, there are other theoretical schemes to explain the nature of the hidden-charm pentaquarks  $P_c(4380)$  and  $P_c(4450)$ , such as the topological soliton model [383], the two-channel framework [384], doublet-exotic molecule structure [385] and so on.

Based on the existence of a  $C = -1$  ( $C$  is charm quantum number) meson bound state [386, 387], Scoccola, Riska and Rho employed the soliton- $\bar{D}D$  system to study hidden-charm pentaquark states in the topological soliton model in Ref. [383]. They discussed both the Naive Skyrme Model (NSM) and its incorporation with heavy quark symmetry (HQS), named the SMHQS model. Using the single meson spectra obtained from the NSM and SMHQS formulations, they first estimated the masses of the pentaquark candidates with quantum numbers  $J^P = 3/2^-, 5/2^+$  and isospin  $I = 1/2$  without the contributions of the non-adiabatic corrections. Then they considered the first order perturbation theory of the rotational corrections to find the mass of a system composed of a soliton and two bound mesons (one  $C = -1$  and the other with  $C = +1$ ) in the NSM model. They did not give predictions in the SMHQS scheme because of the absence of the hyperfine splittings, which were needed in the calculation of the rotational corrections. Their results suggested the existence of a soliton- $\bar{D}D$  pentaquark-type state with  $(I, J^P) = (1/2, 3/2^-)$  and mass consistent with the  $P_c(4380)$  resonance. In the case of the  $5/2^+$  channel, the predicted mass was in the range of 4.57 – 4.71 GeV, which was too high as compared with the mass of the  $P_c(4450)$ . Besides, they also predicted two  $1/2^+$  and one  $3/2^+$  pentaquarks.

In Ref. [384], Meissner and Oller analyzed the composite nature of the  $P_c(4450)$  in a two-channel scenario: the lower mass channel  $J/\psi p$  and the heavier one  $\chi_{c1p}$ . Using a probabilistic interpretation of the compositeness relation, they calculated the couplings and partial decay widths of the  $P_c(4450)$  resonance to the two-body channels  $J/\psi p$  and  $\chi_{c1p}$ . Their result showed that the coupling to the heavier mass channel  $\chi_{c1p}$  is much larger than that to the lower one  $J/\psi p$ , which results in a larger partial decay width of the former decay channel. This is very similar to the scalar meson  $f_0(980)$ , where the higher  $K\bar{K}$  channel has a strong coupling while the coupling to the lower  $\pi\pi$  channel is suppressed although the second one has a larger phase space. They concluded that the  $P_c(4450)$  is almost entirely a  $\chi_{c1p}$  resonance.

The authors of Ref. [385] discussed the possibility of the two pentaquarks  $P_c(4380)$  and  $P_c(4450)$  composed of two colored constituents with configuration  $[q_1\bar{q}_2]_{\mathbf{8}_c}[q_3q_4q_5]_{\mathbf{8}_c}$ , where the subscript  $\mathbf{8}_c$  denotes the color structure. Such a configuration results in a doublet of pentaquark states.

In Ref. [388], Burns studied the model-independent phenomenology of the  $P_c(4380)$  and  $P_c(4450)$  pentaquark states based on the meson-baryon molecular configuration. He analyzed possible spin-parity assignments for these two states and speculated various decay patterns and production processes. The author argued that these two  $P_c$  states were mixtures of isospins  $1/2$  and  $3/2$  among several possible meson-baryon pairs. In the same configuration, the neutral partners of the  $P_c(4380)$  and  $P_c(4450)$  states and other possible states with different quantum numbers were predicted.

In Ref. [389], the authors interpreted the  $P_c(4450)$  as a bound state of the charmonium  $\psi(2S)$  and the nucleon. The binding potential arises from the charmonium-nucleon interaction in the form of the product of the charmonium chromoelectric polarizability and the nucleon energy-momentum distribution. The authors estimated the quarkonium polarizability and calculated the nucleon properties in the framework of the mean-field picture of light baryons in the large  $N_c$  limit. They arrived at two almost degenerate states  $J^P = (1/2)^-$  and  $J^P = (3/2)^-$  around 4450 MeV with a narrow width.

Motivated by the surface potential in the Hasenfratz-Kuti model, the authors of Ref. [390] assumed that there exists a surface potential between the proton and the  $J/\psi$  in the form,  $V_S(l) = V_s x^{\alpha-1}(1-x)^{\beta-1}$ , where  $x = r/r_0$ ,  $\alpha = 9$ ,  $\beta = 5$ ,  $r_0 = 0.85$  fm and  $l$  is the orbital angular momentum. Both the  $P_c(4450)$  and  $P_c(4380)$  were interpreted as the molecular resonances of the proton and  $J/\psi$ . They adjusted the well depth  $V_s = 2350$  MeV to obtain the resonance at the observed excitation energy. They identified the  $l = 4$  state as the  $P_c(4450)$ , fixed its excitation energy at  $E = 410$  MeV and derived its width to be around 50 MeV. The  $l = 3$  resonance is identified with the  $P_c(4380)$ , which has a width around 142 MeV and excitation energy around 340 MeV if the well depth  $V_s = 1410$  MeV.

### 3.7. Production and decay patterns

#### 3.7.1. Production of the $P_c$ via weak decays

Considering the LHCb's measurement of the  $K^-p$  and  $J/\psi p$  invariant mass distributions [2], Roca, Nieves and Oset studied the  $\Lambda_b \rightarrow K^- J/\psi p$  process. They introduced three mechanisms, i.e., (a) a quark-level basic process to produce the  $J/\psi K^- p$  final state through the weak decay of  $\Lambda_b$ , (b) a hadronic level description of  $\Lambda_b \rightarrow K^- J/\psi p \rightarrow K^- J/\psi p$  with the  $K^- p \rightarrow K^- p$  final state interaction in coupled channels, (c) a hadronic level description of  $\Lambda_b \rightarrow K^- J/\psi p \rightarrow K^- J/\psi p$  with the  $J/\psi p \rightarrow J/\psi p$  final state interaction in coupled channels [251]. The first two mechanisms reflect the contribution from the  $\Lambda(1405)$ , while the third mechanism contains the  $J/\psi N$  final state interaction in coupled channels including the  $\bar{D}^* \Lambda_c$ ,  $\bar{D}^* \Sigma_c$ ,  $\bar{D} \Sigma_c^*$ ,  $\bar{D}^* \Sigma_c^*$ , which may produce poles at  $4334 \pm 19i$ ,  $4417 + 4i$  and  $4481 + 17i$  MeV [245]. Since these poles couple with the  $J/\psi p$ , the corresponding resonance shape appears in the  $J/\psi p$  invariant mass spectrum. After comparing the invariant mass spectra of the  $J/\psi p$  and  $K^- p$  with the experimental data, the authors of Ref. [251] noticed that the shape and relative strength of the  $K^- p$  invariant mass spectrum near the threshold and the structure  $P_c(4450)$  in the  $J/\psi p$  invariant mass distribution can be reproduced simultaneously, which supports the  $P_c(4450)$  as a  $J^P = 3/2^-$  hidden-charm molecular state composed of the  $\bar{D}^* \Sigma_c$  and  $\bar{D}^* \Sigma_c^*$  [251]. Wang *et al.* considered the  $\Lambda_b \rightarrow \pi^- J/\psi p$  reaction in analogy to the  $\Lambda_b \rightarrow K^- J/\psi p$  process and studied the possible manifestation of the hidden-charm pentaquarks in the sharp structure of the  $J/\psi p$  mass distribution around 4450 MeV [391]. While, Lu *et al.* studied the  $\Lambda_b \rightarrow J/\psi K^0 \Lambda$  reaction by taking into account a hidden-charm state with strangeness that couples to  $J/\psi \Lambda$  [392].

The authors of Refs. [371, 393] carried out the analysis of the production of hidden-charm pentaquarks via weak decays of bottom baryons based on SU(3) flavor symmetry, which were extensively applied to study the  $B$  decay and  $CP$  violation. Under the assumption of the  $P_c(4380)$  and  $P_c(4450)$  with configurations  $\{\bar{c}[cq]_{s=1}[q'q']_{s=1}, L=0\}$  and  $\{\bar{c}[cq]_{s=1}[q'q']_{s=0}, L=1\}$  respectively as suggested in Ref. [362], Li *et al.* [371] derived the amplitude relations under SU(3) flavor symmetry. There exist  $\mathbf{3} \otimes \mathbf{3} = \mathbf{1} \oplus \mathbf{8}$  and  $\mathbf{3} \otimes \mathbf{6} = \mathbf{8} \oplus \mathbf{10}$  multiplets for pentaquarks. The invariant weak decay amplitude of bottom baryons into an octet or a decuplet pentaquark plus a light pseudoscalar octet meson was decomposed into several terms. For the hidden-charm pentaquarks with the same  $J^P$  quantum number, there exist amplitude relations which can be tested experimentally [371].

Cheng and Chua studied the weak decays of the bottom baryons in the  $\bar{\mathbf{3}}$  representation and  $\Omega_b^-$  in the  $\mathbf{6}$  representation into a pseudoscalar meson and an octet (a decuplet) hidden-charm pentaquark [393]. The decay amplitudes

of  $(\Lambda_b^0, \Xi_b^0, \Xi_b^-) \rightarrow P_8 + M$ ,  $(\Lambda_b^0, \Xi_b^0, \Xi_b^-) \rightarrow P_{10} + M$ ,  $\Omega_b^- \rightarrow P_8 + M$ ,  $\Omega_b^- \rightarrow P_{10} + M$  were calculated, where  $P_8$  and  $P_{10}$  stand for the hidden-charm pentaquarks in octet and decuplet, respectively. The authors suggested that the channel  $\Xi_b^0 \rightarrow P_{\Sigma^+} K^-$ ,  $\Xi_b^- \rightarrow P_{\Sigma^-} \bar{K}^0$ ,  $\Omega_b^- \rightarrow P_{\Xi^-} \bar{K}^0$ , and  $\Omega_b^- \rightarrow P_{\Xi^0} K^-$  may have contributions comparable with that of  $\Lambda_b^0 \rightarrow P_p^+ K^-$ .

Hsiao *et al.* [394] assumed that  $\Lambda_b \rightarrow J/\psi p K^-$  occurs via  $b \rightarrow c\bar{c}s$  and ignored those contributions via the non-resonant  $\Lambda_b \rightarrow p K^-$  and resonant  $\Lambda_b \rightarrow \Lambda^* \rightarrow p K^-$ . Thus, the  $P_c(4380)$  and  $P_c(4450)$  would be produced mainly by the charmless  $\Lambda_b$  decays with  $b \rightarrow u\bar{u}s$ . The two observed  $P_c$  pentaquarks are produced from the intrinsic charms within  $\Lambda_b$ . According to this mechanism, the ratio of branching ratios was obtained,  $\mathcal{B}(\Lambda_b \rightarrow \pi^-(P_c(4380)/P_c(4450))) \rightarrow \pi^- J/\psi p / \mathcal{B}(\Lambda_b \rightarrow K^-(P_c(4380)/P_c(4450))) \rightarrow K^- J/\psi p = 0.58 \pm 0.05$ . Additionally, the direct CP violating asymmetries were also predicted as  $\mathcal{A}_{CP}(\Lambda_b \rightarrow \pi^-(P_c(4380)/P_c(4450))) \rightarrow \pi^- J/\psi p = (-7.4 \pm 0.9)\%$  and  $\mathcal{A}_{CP}(\Lambda_b \rightarrow K^-(P_c(4380)/P_c(4450))) \rightarrow K^- J/\psi p = (+6.3 \pm 0.2)\%$  [394].

### 3.7.2. Photo-production of the $P_c$

The authors of Ref. [395] studied the photo-production of the two hidden-charm pentaquark states  $P_c(4380)$  and  $P_c(4450)$  via  $\gamma p \rightarrow J/\psi p$ . The estimated total and differential cross sections of  $\gamma p \rightarrow J/\psi p$  depend on the unknown coupling of the  $P_c(4380)/P_c(4450)$  with  $J/\psi p$ . Under the assignment of the  $P_c(4450)$  as the  $\Sigma_c \bar{D}^*$  molecular state, Karliner and Rosner [396] made an estimate of the  $P_c(4450)$  production cross section through the vector dominance. They pointed out that the events of the  $P_c(4450)$  produced at CLAS12 and forthcoming GlueX are considerable. Voloshin also studied the  $\gamma p \rightarrow P_c(4380)/P_c(4450) \rightarrow J/\psi + p$  process and estimated the cross section [397]. These investigations indicate that there exists good potential to search for the two  $P_c$  states through the photo-production.

In Ref. [398], the authors proposed to search for the production of the neutral hidden-charm pentaquarks  $P_c(4380)^0$  and  $P_c(4450)^0$  via the  $\pi^- p \rightarrow J/\psi n$  reaction. Their calculation shows that there exist clear signals corresponding to the  $P_c(4380)^0$  and  $P_c(4450)^0$  with the cross section around  $1 \mu\text{b}$ , which suggests that the  $\pi^- p \rightarrow J/\psi n$  reaction is suitable to produce the two neutral  $P_c$  states [398]. In Ref. [399], the authors discussed the production of the hidden-charm baryon  $N_{cc}^*(4261)$  with  $J^P = \frac{1}{2}^-$  in the above reaction process.

### 3.7.3. Strong decay patterns of the $P_c$ states

Assuming the  $P_c(4380)$  and  $P_c(4450)$  to be molecular states composed of  $\bar{D}^{(*)}$  and  $\Sigma_c^{(*)}$ , their strong decay patterns were studied with the spin rearrangement scheme in Ref. [239]. Several typical ratios of the partial decay widths of the hidden-charm pentaquarks were obtained. Especially, for the three S-wave ( $\bar{D}\Sigma_c^*$ ), ( $\bar{D}^*\Sigma_c$ ) and ( $\bar{D}^*\Sigma_c^*$ ) molecular pentaquarks with  $J^P = 3/2^-$ , the obtained ratio of their  $J/\psi N$  decay widths is  $\Gamma[(\bar{D}\Sigma_c^*)] : \Gamma[(\bar{D}^*\Sigma_c)] : \Gamma[(\bar{D}^*\Sigma_c^*)] = 2.7 : 1.0 : 5.4$ . These ratios are model independent.

### 3.8. The hidden-bottom and doubly heavy pentaquark states

If there exist the hidden-charm pentaquarks, their hidden-bottom partners should also exist. The hidden-bottom and doubly heavy pentaquark states were predicted with different theoretical models. In the following, we brief review these states.

The hidden-bottom molecular pentaquarks composed of a bottom meson and a bottom baryon were studied extensively within the OBE model [229]. There exist hidden-bottom molecular pentaquarks, which include the  $\Sigma_b B$  with  $\frac{3}{2}(\frac{1}{2}^-)$ ,  $\Sigma_b^* B^*$  with  $\frac{1}{2}(\frac{1}{2}^-)$ ,  $\frac{1}{2}(\frac{3}{2}^-)$ ,  $\frac{3}{2}(\frac{1}{2}^-)$ ,  $\frac{3}{2}(\frac{3}{2}^-)$ , while the  $\Lambda_b B$  with  $\frac{1}{2}(\frac{1}{2}^-)$ ,  $\Lambda_b B^*$  with  $\frac{1}{2}(\frac{1}{2}^-)$ ,  $\frac{1}{2}(\frac{3}{2}^-)$  do not exist.

In a subsequent work, Chen *et al.* studied the hidden-bottom molecular pentaquarks and  $B_c$ -like pentaquarks with the OPE model, which is an important extension of the hidden-charm molecular pentaquark states reviewed in Sec. 4.1.1. The results are collected in Table 14, which indicate that the  $\Sigma_b B^*$ ,  $\Sigma_c B^*$ ,  $\Sigma_b \bar{D}^*$  bound states with either  $(I = 1/2, J = 3/2)$  or  $(I = 3/2, J = 1/2)$  may exist. The decay modes of the  $\Sigma_b B^*$ ,  $\Sigma_c B^*$ , and  $\Sigma_b \bar{D}^*$  states with  $(I = 1/2, J = 3/2)$  include the  $\Upsilon(1S)N/\Upsilon(2S)N$ ,  $B_c(1^-)N$ , and  $\bar{B}_c(1^-)N$ , respectively. The  $\Sigma_b B^*$ ,  $\Sigma_c B^*$ , and  $\Sigma_b \bar{D}^*$  states with  $(I = 3/2, J = 1/2)$  can decay into the  $\Upsilon(1S)\Delta(1232)$ ,  $B_c(1^-)\Delta(1232)$ , and  $\bar{B}_c(1^-)\Delta(1232)$ , respectively [230].

For the  $\Sigma_b^* B^*$ ,  $\Sigma_c^* B^*$ ,  $\Sigma_b^* \bar{D}^*$  S-wave systems with  $(I = 1/2, J = 3/2)$  and  $(I = 3/2, J = 1/2)$ , there also exist the bound state solutions. The  $\Sigma_b^* B^*$  state can also carry  $(I = 3/2, J = 3/2)$ . The  $\Upsilon(1S)N/\Upsilon(2S)N$ ,  $B_c(1^-)N$ , and  $\bar{B}_c(1^-)N$  are the main decay modes of the  $\Sigma_b^* B^*$ ,  $\Sigma_c^* B^*$ ,  $\Sigma_b^* \bar{D}^*$  with  $(I = 1/2, J = 3/2)$ , respectively, while the main

Table 14: The typical values of the obtained bound state solutions  $[E(\text{MeV}), \Lambda(\text{GeV})]$  for the hidden-bottom  $\Sigma_b^{(*)} B^*$  and  $B_c$ -like  $\Sigma_c^{(*)} B^*$  and  $\Sigma_b^{(*)} \bar{D}^*$  systems. Based on the experience of the S-wave  $\Sigma_c^{(*)} \bar{D}^*$  systems, the bound state solution is searched for in the range of  $\Lambda < 2.35$  GeV for  $\Sigma_b B^*$  and the range of  $\Lambda < 1.77$  GeV for  $\Sigma_b^* B^*$ . Taken from Ref. [230].

$(I, J)$	$\Sigma_c B^*$	$\Sigma_b \bar{D}^*$	$\Sigma_b B^*$	$\Sigma_c^* B^*$	$\Sigma_b^* \bar{D}^*$	$\Sigma_b^* B^*$
(1/2,1/2)	×	×	×	×	×	×
(1/2,3/2)	[-0.27, 1.22]	[-0.26, 1.34]	[-0.27, 0.84]	×	×	×
	[-2.58, 1.32]	[-2.62, 1.44]	[-2.36, 0.94]	×	×	×
	[-7.48, 1.42]	[-7.63, 1.54]	[-6.88, 1.04]	×	×	×
(1/2,5/2)	×	×	×	[-0.28, 0.88]	[-0.14, 0.96]	[-0.30, 0.64]
	×	×	×	[-3.18, 0.98]	[-2.78, 1.06]	[-3.11, 0.74]
	×	×	×	[-9.67, 1.08]	[-8.97, 1.16]	[-9.51, 0.84]
(3/2,1/2)	[-0.27, 1.22]	[-0.26, 1.34]	[-0.27, 0.84]	[-0.42, 1.02]	[-0.30, 1.12]	[-0.28, 0.72]
	[-2.58, 1.32]	[-2.62, 1.44]	[-2.36, 0.94]	[-3.33, 1.12]	[-3.03, 1.22]	[-2.74, 0.82]
	[-7.48, 1.42]	[-7.63, 1.54]	[-6.88, 1.04]	[-9.37, 1.22]	[-8.91, 1.32]	[-8.19, 0.92]
(3/2,3/2)	×	×	×	×	×	[-0.28, 1.44]
	×	×	×	×	×	[-3.28, 1.60]
	×	×	×	×	×	[-9.13, 1.74]
(3/2,5/2)	×	×	×	×	×	

decay channels of the  $\Sigma_b^* B^*$ ,  $\Sigma_c^* B^*$ ,  $\Sigma_b^* \bar{D}^*$  states with  $(I = 3/2, J = 1/2)$  are the  $\Upsilon(1S)\Delta(1232)$ ,  $B_c(1^-)\Delta(1232)$ , and  $\bar{B}_c(1^-)\Delta(1232)$ , respectively. The  $\Sigma_b^* B^*$  state with  $(I = 3/2, J = 3/2)$  mainly decays into the  $\Upsilon(1S)\Delta(1232)$  [230].

In Ref. [400], Karliner and Rosner also suggested the existence of doubly heavy molecular pentaquarks. The above hidden-bottom and doubly heavy pentaquark states from the OBE and OPE models may be accessible at future experiments. In a recent reference [401], Karliner and Rosner considered the  $\eta$  exchange, which can be important for hadrons without  $u$  and  $d$  light quark, such as the  $D_s$ . They suggested to observe the  $\Lambda_c \bar{D}_s^*$  resonance in the process  $\Lambda_b \rightarrow J/\psi \Lambda(\pi^+ \pi^- \text{ or } \eta)$ .

The coupled channel unitary approach with the local hidden gauge formalism, reviewed in Sec. 3.2, was also applied to study the hidden bottom pentaquarks in Refs. [249, 250]. In Ref. [249] Wu, Zhao, and Zou predicted two  $N_{bb}^*$  states with mass and width  $(M, \Gamma) = (11052, 1.38)$  MeV and  $(11100, 1.33)$  MeV and four  $\Lambda_{bb}^*$  states with  $(M, \Gamma) = (11021, 2.21)$  MeV,  $(11191, 1.24)$  MeV,  $(11070, 2.17)$  MeV, and  $(11239, 1.19)$  MeV. In Ref. [250], Xiao and Oset found seven hidden bottom pentaquark states, all of which have  $I = 1/2$ :

$$\begin{aligned} \text{the } J = 1/2 \text{ sector : } & (10963.04 + i8.59) \text{ MeV , } (11002.81 + i19.97) \text{ MeV , } (11023.55 + i22.75) \text{ MeV ,} \\ \text{the } J = 3/2 \text{ sector : } & (10984.43 + i9.19) \text{ MeV , } (11007.28 + i3.00) \text{ MeV , } (11019.00 + i14.80) \text{ MeV ,} \\ \text{the } J = 5/2 \text{ sector : } & (11026.10 + i0) \text{ MeV .} \end{aligned}$$

These poles were classified as four basic states: a) the first pole  $(10963.04 + i8.59)$  MeV, corresponding to a  $B\Sigma_b$  state; b) the fourth pole  $(10984.43 + i9.19)$  MeV, corresponding to a  $B\Sigma_b^*$  state; c) the second pole  $(11002.81 + i19.97)$  MeV and the fifth pole  $(11007.28 + i3.00)$  MeV, both corresponding to a  $B^*\Sigma_b$  state; d) the third pole  $(11023.55 + i22.75)$  MeV, the sixth pole  $(11019.00 + i14.80)$  MeV, and the seventh pole  $(11026.10 + i0)$  MeV, all corresponding to a  $B^*\Sigma_b^*$  state. All these states are bound with about 50-130 MeV with respect to the corresponding  $B^{(*)}\Sigma_b^{(*)}$  thresholds.

Two hidden-bottom pentaquarks were predicted in Ref. [311] using the method of QCD sum rule as partners of the  $P_c(4380)$  and  $P_c(4450)$ . Their masses were extracted as  $11.55^{+0.23}_{-0.14}$  MeV and  $11.66^{+0.28}_{-0.27}$  MeV, and spin-parity quantum numbers  $J^P = 3/2^-$  and  $5/2^+$ , respectively.

Zhu and Qiao used the constituent diquark-triquark model to study hidden bottom pentaquarks [377], where they have used the diquark mass  $m_\delta = m_{[bq]} = 5.249$  GeV and the triquark mass  $m_\theta = m_{[u\bar{d}\bar{b}]} = 5.618$  GeV.

### 3.9. Theoretical and experimental challenges

The presence of the heavy quarks (or charmed/bottomed hadrons) lowers the kinetic energy of the system, which favors the formation of either the ‘‘genuine’’ pentaquark states or the molecular baryons. For the molecular scheme, the light quarks are also essential since the meson exchange force between the light quarks, especially the long-range pionic interaction binds the hadronic system.

The discovery of the  $P_c(4350)$  and  $P_c(4450)$  opens a new era in the exploration of the multi-quark states. There remain many theoretical and experimental challenges, some of which are highlighted below:

- At present, the  $P_c(4380)$  and  $P_c(4450)$  were only reported by the LHCb Collaboration [2]. These states should be confirmed in other processes and analyses.
- BelleII, CLAS12, GlueX and JPARC may have the potential to search for the hidden-charm  $P_c$  states through the  $e^+e^-$  annihilation, photoproduction, or  $\pi^- p \rightarrow J/\psi n$  reaction.
- Since it is very close to the  $\chi_{c1} p$  threshold, could the  $P_c(4450)$  arise from kinematical effects through various rescattering mechanisms such as the triangle singularity?
- Various theoretical approaches predict many isospin and spin partner states of the  $P_c(4380)$  and  $P_c(4450)$ . Where and how can these states be observed?
- The experimental identification of the parity for each  $P_c$  state is crucial for the discrimination of various models. For example, the S-wave molecular pentaquark has negative parity while its nearby P-wave excitation carries positive parity in the framework of the molecular scheme. In contrast, only the pentaquarks with negative parity are dynamically generated through S-wave rescattering within the unitary approach.

- The identification of the dominant decay modes of the two  $P_c$  states is important. Although they were observed in the clean  $J/\psi p$  final state, the  $J/\psi p$  mode is not necessarily their main decay mode. Recall the similar situations in the case of the charged hidden-charm/bottom tetraquark states. The  $Z_c(3900)$  was first observed in the hidden-charm mode. Later its open-charm decay width was measured to be much larger. As molecular baryons, the open-charm decay modes of the  $P_c$  states would be dominant. As a compact “genuine” pentaquark state confined within one MIT bag, the  $J/\psi p$  mode may be the dominant mode of the  $P_c$  state.
- For a dynamically generated hidden-charm baryon, its total width was quite small and less than 60 MeV according to most of the model calculations within the unitary approach. However, the sum of the partial decay widths of the charm-less decay modes are larger than the decay width of their main hidden-charm modes. This feature is characteristic of the dynamically generated resonance and the unitary approach. The observation of significant charm-less decay modes will support the  $P_c$  states as the dynamically generated resonance within the unitary framework.
- Is it possible to produce the hidden-bottom pentaquark states experimentally?
- Is it feasible to simulate the scattering of the charmed baryon and anticharmed meson on the lattice? Can the molecular bound states be isolated from the scattering states? Or can the “genuine” pentaquark resonances be observed directly on the lattice?
- Besides hidden-charm pentaquarks, the hidden-charm (or hidden-bottom) systems with six quarks may also exist [219, 221, 402, 396]. There may exist some potential to observe the molecular systems composed of a pair of charmed baryons and a pair of charmed and anti-charmed baryons at LHCb [219, 221].
- Through the decay products  $\Sigma_c^{(*)}$  and  $\Lambda_c^{(*)}$  of the  $\Lambda_b$  weak decay, one may explore the production mechanism of the  $P_c$  states within the molecular scheme. There exist three types of Feynman diagrams which contribute to the  $\Lambda_b \rightarrow J/\psi p K$  decay, as shown in Fig. 44.

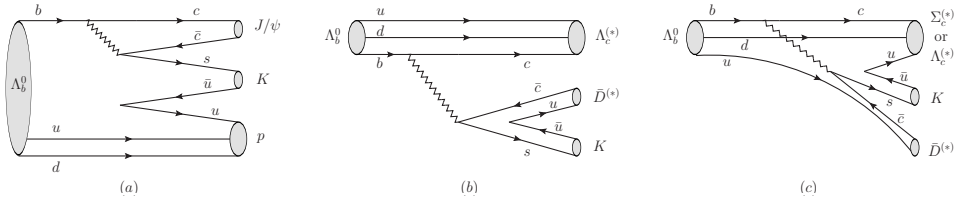


Figure 44: The types of production mechanisms of the  $P_c$  states via the  $\Lambda_b$  weak decay.

- (a) The  $b$  quark decays weakly via  $b \rightarrow c\bar{c}s$  and the  $c\bar{c}$  pair transforms into the  $J/\psi$  while the scalar isoscalar  $[ud]$  diquark within the  $\Lambda_b$  is not pulled apart and acts as the spectator throughout the whole process. This mechanism contributes to the non-resonant  $J/\psi p$  production and explains naturally why only  $\Lambda^*$  and no  $\Sigma^*$  intermediate states were observed by the LHCb Collaboration.
- (b) The  $b$  quark decays weakly via  $b \rightarrow c\bar{c}s$ . The  $c$  quark combines with the scalar isoscalar  $[ud]$  diquark to form the  $\Lambda_c^{(*)}$ . At the same time, a pair of light quarks  $q\bar{q}$  is produced from the vacuum. The  $\bar{c}$  quark picks up the quark  $q$  and becomes a  $\bar{D}^{(*)}$  meson while the remaining  $s\bar{q}$  forms the kaon. Some of the  $\Lambda_c^{(*)}\bar{D}^{(*)}$  rescatter into the  $J/\psi p$  final states. However, the interaction between the  $\Lambda_c^{(*)}$  and  $\bar{D}^{(*)}$  is rather weak. Therefore, most of the  $\Lambda_c^{(*)}\bar{D}^{(*)}$  events are non-resonant. In other words, one would expect many  $\Lambda_c^{(*)}$  in the final states.
- (c) The  $b$  quark decays weakly via  $b \rightarrow c\bar{c}s$ . A pair of light quarks  $q\bar{q}$  are produced from the vacuum while the scalar isoscalar  $[ud]$  diquark within  $\Lambda_b$  is pulled apart into  $q_1$  and  $q_2$  by non-perturbative QCD interaction. The  $\bar{c}$  quark picks up the quark  $q_1$  from the original diquark and becomes a  $\bar{D}^{(*)}$  meson. The  $s\bar{q}$  forms the kaon. The charm quark and remaining  $q_2q$  transforms into a charmed baryon. Since the total

isospin of the  $q_2q$  pair is either 0 or 1, the charmed baryon could be  $\Lambda_c^{(*)}$  or  $\Sigma_c^{(*)}$ , the probability of which is 50% respectively. According to the molecular scheme, the hidden-charm pentaquark states are produced through the rescattering process  $\Sigma_c^{(*)}\bar{D}^{(*)} \rightarrow P_c \rightarrow J/\psi p$ . Besides this resonant process, there exist many  $\Sigma_c^{(*)}\bar{D}^{(*)}$  and  $\Lambda_c^{(*)}\bar{D}^{(*)}$  events. One would expect many  $\Sigma_c^{(*)}$  and more  $\Lambda_c^{(*)}$  in the final states.

## 4. Theoretical interpretations of the XYZ states

### 4.1. $Z_b(10610)$ and $Z_b(10650)$

#### 4.1.1. Molecular scheme

4.1.1.1. *Meson exchange model.* In 2008, the authors of Ref. [201] discussed the possible S-wave molecular states composed of  $D\bar{D}^*$  and  $B\bar{B}^*$  and pointed out that “*there probably exists a loosely bound S-wave  $B\bar{B}^*$  molecular state*”. Within the meson exchange model, the possible attraction between the heavy mesons arises from the exchange of the light mesons. Especially the chiral interaction between the light quarks and pions plays a central role in the formation of the shallow heavy meson bound states, which does not depend on the heavy quark mass. As the heavy quark mass increases, the heavy meson mass increases and the kinetic energy of the dimeson system decreases, while the potential between the heavy meson pair remains roughly the same. The formation of the bound states relies on the competition between the kinetic energy and attractive potential of the system. In other words, the  $B\bar{B}^*$  meson pairs are easier and more likely to form a loosely bound molecular state than the  $D\bar{D}^*$  [201].

In 2011, the charged bottomonium-like states  $Z_b(10610)$  and  $Z_b(10650)$  were reported by the Belle Collaboration in five hidden-bottom dipion decays of  $\Upsilon(5S)$  [161]. Their experimental information was summarized in Sec. 2.3. The discovery of these states stimulated further theoretical studies of the  $Z_b(10610)$  and  $Z_b(10650)$  as the  $B\bar{B}^*$  and  $B^*\bar{B}^*$  molecular states [191], respectively. Their flavor wave functions read [191]

$$|Z_b(10610)^\pm\rangle = \frac{1}{\sqrt{2}}(|B^{*\pm}\bar{B}^0\rangle + |B^\pm\bar{B}^{*0}\rangle), \quad (113)$$

$$|Z_b(10610)^0\rangle = \frac{1}{2}\left[ (|B^{*+}B^-\rangle - |B^{*0}\bar{B}^0\rangle) + (|B^+B^{*-}\rangle - |B^0\bar{B}^{*0}\rangle) \right], \quad (114)$$

$$|Z_b(10650)^\pm\rangle = |B^{*\pm}\bar{B}^{*0}\rangle, \quad (115)$$

$$|Z_b(10650)^0\rangle = \frac{1}{\sqrt{2}}(|B^{*+}B^{*-}\rangle - |B^{*0}\bar{B}^{*0}\rangle). \quad (116)$$

The total effective potential of the  $Z_b(10610)$  system is

$$\mathcal{V}^{Z_b(10610)} = V_\sigma^{\text{Direct}} - \frac{1}{2}V_\rho^{\text{Direct}} + \frac{1}{2}V_\omega^{\text{Direct}} + \frac{1}{4}\left(-2V_\pi^{\text{Cross}} + \frac{2}{3}V_\eta^{\text{Cross}} - 2V_\rho^{\text{Corss}} + 2V_\omega^{\text{Cross}}\right) \quad (117)$$

with these subpotentials from the  $\pi$ ,  $\eta$ ,  $\sigma$ ,  $\rho$  and  $\omega$  meson exchanges, i.e.,

$$\begin{aligned} V_\pi^{\text{Cross}} &= -\frac{g^2}{f_\pi^2}\left[\frac{1}{3}(\boldsymbol{\epsilon}_2 \cdot \boldsymbol{\epsilon}_3^\dagger)Z(\Lambda_2, m_2, r) + \frac{1}{3}S(\hat{\boldsymbol{r}}, \boldsymbol{\epsilon}_2, \boldsymbol{\epsilon}_3^\dagger)T(\Lambda_2, m_2, r)\right], \\ V_\eta^{\text{Cross}} &= -\frac{g^2}{f_\pi^2}\left[\frac{1}{3}(\boldsymbol{\epsilon}_2 \cdot \boldsymbol{\epsilon}_3^\dagger)Z(\Lambda_3, m_3, r) + \frac{1}{3}S(\hat{\boldsymbol{r}}, \boldsymbol{\epsilon}_2, \boldsymbol{\epsilon}_3^\dagger)T(\Lambda_3, m_3, r)\right], \\ V_\sigma^{\text{Direct}} &= -g_s^2(\boldsymbol{\epsilon}_2 \cdot \boldsymbol{\epsilon}_4^\dagger)Y(\Lambda, m_\sigma, r), \\ V_\rho^{\text{Direct}} &= -\frac{1}{2}\beta^2 g_V^2(\boldsymbol{\epsilon}_2 \cdot \boldsymbol{\epsilon}_4^\dagger)Y(\Lambda, m_\rho, r), \\ V_\rho^{\text{Cross}} &= 2\lambda^2 g_V^2\left[\frac{2}{3}(\boldsymbol{\epsilon}_2 \cdot \boldsymbol{\epsilon}_3^\dagger)Z(\Lambda_0, m_0, r) - \frac{1}{3}S(\hat{\boldsymbol{r}}, \boldsymbol{\epsilon}_2, \boldsymbol{\epsilon}_3^\dagger)T(\Lambda_0, m_0, r)\right], \\ V_\omega^{\text{Direct}} &= -\frac{1}{2}\beta^2 g_V^2(\boldsymbol{\epsilon}_2 \cdot \boldsymbol{\epsilon}_4^\dagger)Y(\Lambda, m_\omega, r), \\ V_\omega^{\text{Cross}} &= 2\lambda^2 g_V^2\left[\frac{2}{3}(\boldsymbol{\epsilon}_2 \cdot \boldsymbol{\epsilon}_3^\dagger)Z(\Lambda_1, m_1, r) - \frac{1}{3}S(\hat{\boldsymbol{r}}, \boldsymbol{\epsilon}_2, \boldsymbol{\epsilon}_3^\dagger)T(\Lambda_1, m_1, r)\right], \end{aligned} \quad (118)$$

where  $\Lambda_{0,1,2,3}^2 = \Lambda^2 - (m_{B^*} - m_B)^2$ ,  $m_{0,1,2,3}^2 = m_{\rho,\omega,\pi,\eta}^2 - (m_{B^*} - m_B)^2$  and  $S(\hat{\mathbf{r}}, \mathbf{a}, \mathbf{b}) = 3(\hat{\mathbf{r}} \cdot \mathbf{a})(\hat{\mathbf{r}} \cdot \mathbf{b}) - \mathbf{a} \cdot \mathbf{b}$ . The functions  $Y(\Lambda, m, r)$ ,  $Z(\Lambda, m, r)$  and  $T(\Lambda, m, r)$  are defined as:

$$\begin{aligned} Y(\Lambda, m_E, r) &= \frac{1}{4\pi r}(e^{-m_E r} - e^{-\Lambda r}) - \frac{\Lambda^2 - m_E^2}{8\pi\Lambda}e^{-\Lambda r}, \\ Z(\Lambda, m_E, r) &= \nabla^2 Y(\Lambda, m_E, r) = \frac{1}{r^2} \frac{\partial}{\partial r} r^2 \frac{\partial}{\partial r} Y(\Lambda, m_E, r), \\ T(\Lambda, m_E, r) &= r \frac{\partial}{\partial r} \frac{1}{r} \frac{\partial}{\partial r} Y(\Lambda, m_E, r). \end{aligned} \quad (119)$$

One notes that  $m_2$  is much smaller than  $m_\pi$ , which implies the OPE potential decreases very slowly. In Ref. [191], both the S-wave and D-wave interactions between the  $B$  and  $\bar{B}^*$  mesons were considered. In the derivation of the final effective potential in the form of the  $2 \times 2$  matrix, one makes the following replacement in the subpotentials,

$$\left. \begin{array}{l} (\boldsymbol{\epsilon}_2 \cdot \boldsymbol{\epsilon}_3^\dagger) \\ (\boldsymbol{\epsilon}_2 \cdot \boldsymbol{\epsilon}_4^\dagger) \end{array} \right\} \mapsto \begin{pmatrix} 1 & 0 \\ 0 & 1 \end{pmatrix}, \quad S(\hat{\mathbf{r}}, \boldsymbol{\epsilon}_2, \boldsymbol{\epsilon}_3^\dagger) \mapsto \begin{pmatrix} 0 & -\sqrt{2} \\ -\sqrt{2} & 1 \end{pmatrix}. \quad (120)$$

Similarly, the total effective potential of the  $Z_b(10650)$  system is

$$\mathcal{V}^{Z_b(10650)} = W_\sigma - \frac{1}{2}W_\rho + \frac{1}{2}W_\omega - \frac{1}{2}W_\pi + \frac{1}{6}W_\eta, \quad (121)$$

where the corresponding subpotentials from the  $\pi$ ,  $\eta$ ,  $\sigma$ ,  $\rho$  and  $\omega$  meson exchanges are

$$\begin{aligned} W_\pi &= -\frac{g^2}{f_\pi^2} \left[ \frac{1}{3} (\boldsymbol{\epsilon}_1 \times \boldsymbol{\epsilon}_3^\dagger) \cdot (\boldsymbol{\epsilon}_2 \times \boldsymbol{\epsilon}_4^\dagger) Z(\Lambda, m_\pi, r) + \frac{1}{3} S(\hat{\mathbf{r}}, \boldsymbol{\epsilon}_1 \times \boldsymbol{\epsilon}_3^\dagger, \boldsymbol{\epsilon}_2 \times \boldsymbol{\epsilon}_4^\dagger) T(\Lambda, m_\pi, r) \right], \\ W_\eta &= -\frac{g^2}{f_\pi^2} \left[ \frac{1}{3} (\boldsymbol{\epsilon}_1 \times \boldsymbol{\epsilon}_3^\dagger) \cdot (\boldsymbol{\epsilon}_2 \times \boldsymbol{\epsilon}_4^\dagger) Z(\Lambda, m_\eta, r) + \frac{1}{3} S(\hat{\mathbf{r}}, \boldsymbol{\epsilon}_1 \times \boldsymbol{\epsilon}_3^\dagger, \boldsymbol{\epsilon}_2 \times \boldsymbol{\epsilon}_4^\dagger) T(\Lambda, m_\eta, r) \right], \\ W_\sigma &= -g_s^2 (\boldsymbol{\epsilon}_1 \cdot \boldsymbol{\epsilon}_3^\dagger) (\boldsymbol{\epsilon}_2 \cdot \boldsymbol{\epsilon}_4^\dagger) Y(\Lambda, m_\sigma, r), \\ W_\rho &= -\frac{1}{4} \left\{ 2\beta^2 g_V^2 (\boldsymbol{\epsilon}_1 \cdot \boldsymbol{\epsilon}_3^\dagger) (\boldsymbol{\epsilon}_2 \cdot \boldsymbol{\epsilon}_4^\dagger) Y(\Lambda, m_\rho, r) - 8\lambda^2 g_V^2 \left[ \frac{2}{3} (\boldsymbol{\epsilon}_1 \times \boldsymbol{\epsilon}_3^\dagger) \cdot (\boldsymbol{\epsilon}_2 \times \boldsymbol{\epsilon}_4^\dagger) Z(\Lambda, m_\rho, r) \right. \right. \\ &\quad \left. \left. - \frac{1}{3} S(\hat{\mathbf{r}}, \boldsymbol{\epsilon}_1 \times \boldsymbol{\epsilon}_3^\dagger, \boldsymbol{\epsilon}_2 \times \boldsymbol{\epsilon}_4^\dagger) T(\Lambda, m_\rho, r) \right] \right\}, \\ W_\omega &= -\frac{1}{4} \left\{ 2\beta^2 g_V^2 (\boldsymbol{\epsilon}_1 \cdot \boldsymbol{\epsilon}_3^\dagger) (\boldsymbol{\epsilon}_2 \cdot \boldsymbol{\epsilon}_4^\dagger) Y(\Lambda, m_\omega, r) - 8\lambda^2 g_V^2 \left[ \frac{2}{3} (\boldsymbol{\epsilon}_1 \times \boldsymbol{\epsilon}_3^\dagger) \cdot (\boldsymbol{\epsilon}_2 \times \boldsymbol{\epsilon}_4^\dagger) Z(\Lambda, m_\omega, r) \right. \right. \\ &\quad \left. \left. - \frac{1}{3} S(\hat{\mathbf{r}}, \boldsymbol{\epsilon}_1 \times \boldsymbol{\epsilon}_3^\dagger, \boldsymbol{\epsilon}_2 \times \boldsymbol{\epsilon}_4^\dagger) T(\Lambda, m_\omega, r) \right] \right\}. \end{aligned} \quad (122)$$

There also exists the S-wave and D-wave mixing for the  $B^* \bar{B}^*$  system. The total effective potential of the  $Z_b(10650)$  with  $J = 1$  is a  $3 \times 3$  matrix, where the polarization related terms in the subpotentials should be replaced by the following expressions

$$(\boldsymbol{\epsilon}_1 \cdot \boldsymbol{\epsilon}_3^\dagger) (\boldsymbol{\epsilon}_2 \cdot \boldsymbol{\epsilon}_4^\dagger) \mapsto \begin{pmatrix} 1 & 0 & 0 \\ 0 & 1 & 0 \\ 0 & 0 & 1 \end{pmatrix}, \quad (\boldsymbol{\epsilon}_1 \times \boldsymbol{\epsilon}_3^\dagger) \cdot (\boldsymbol{\epsilon}_2 \times \boldsymbol{\epsilon}_4^\dagger) \mapsto \begin{pmatrix} 1 & 0 & 0 \\ 0 & 1 & 0 \\ 0 & 0 & -1 \end{pmatrix}, \quad S(\hat{\mathbf{r}}, \boldsymbol{\epsilon}_1 \times \boldsymbol{\epsilon}_3^\dagger, \boldsymbol{\epsilon}_2 \times \boldsymbol{\epsilon}_4^\dagger) \mapsto \begin{pmatrix} 0 & -\sqrt{2} & 0 \\ -\sqrt{2} & 1 & 0 \\ 0 & 0 & 1 \end{pmatrix}.$$

The bound state solutions for the  $Z_b(10610)$  and  $Z_b(10650)$  systems are listed in Table 15. Let's summarize [191]:

- The long-range one-pion-exchange (OPE) force alone is strong enough to form the loosely bound isovector molecular states composed of the  $B\bar{B}^*$  and  $B^*\bar{B}$ .
- The short-range vector meson exchange force provides some effective repulsion in these channels and prevents the heavy meson from moving very close to the anti-meson. As can be seen in the case of the  $Z_b(10650)$  with  $\Lambda = 2.2$  GeV, the binding energy from the OPE potential is 8 MeV and the root-mean-square radius is 0.68 fm. In contrast, the binding energy from the OBE potential is 0.81 MeV and its radius is 1.38 fm.

Table 15: The bound state solutions (binding energy  $E$  and root-mean-square radius  $r_{\text{RMS}}$ ) for the  $Z_b(10610)$  and  $Z_b(10650)$  systems. Here the results of Ref. [191] for two situations are listed, i.e., including all OBE contribution and only considering the OPE potential.

State	OBE			OPE		
	$\Lambda$	$E$ (MeV)	$r_{\text{RMS}}$ (fm)	$\Lambda$	$E$ (MeV)	$r_{\text{RMS}}$ (fm)
$Z_b(10610)$	2.1	-0.22	3.05	2.2	-8.69	0.62
	2.3	-1.64	1.31	2.4	-20.29	0.47
	2.5	-4.74	0.84	2.6	-38.54	0.36
$Z_b(10650)$	2.2	-0.81	1.38	2	-2.17	1.15
	2.4	-3.31	0.95	2.2	-8.01	0.68
	2.6	-7.80	0.68	2.4	-19.00	0.48
	2.8	-14.94	0.52	2.6	-36.36	0.38

- When the binding energies of the  $B\bar{B}^*$  and  $B^*\bar{B}^*$  systems are less than 1 MeV, their root-mean-square radius may reach 1.4-3 fm, which is characteristic of the molecular states.
- With the molecular scheme, the mass splittings  $M(Z_b(10650)) - M(Z_b(10610)) = M(B^*) - M(B)$  and  $M(Z_c(4020)) - M(Z_c(3900)) = M(D^*) - M(D)$  are governed by the spin-spin interaction and scale with the heavy quark masses as expected in QCD if  $Z_c(4020)$  and  $Z_c(3900)$  are molecular resonances (see also discussions in Sec. 4.2).

*4.1.1.2. Other models.* In Ref. [403], Yang, Ping, Deng, and Zong applied the chiral quark model to study the possible molecular states composed of a pair of heavy mesons,  $B\bar{B}$ ,  $B\bar{B}^*$ ,  $B^*\bar{B}^*$ , and  $B_s\bar{B}$ , in the  $S$ -wave sector. They found the  $B\bar{B}^*$  and  $B^*\bar{B}^*$  bound states with quantum numbers  $I(J^{PC}) = 1(1^{+-})$ , which are good candidates of the  $Z_b(10610)$  and  $Z_b(10650)$ , respectively. They also predicted three bound states:  $B\bar{B}^*$  with  $I(J^{PC}) = 0(1^{++})$ ,  $B^*\bar{B}^*$  with  $I(J^{PC}) = 1(0^{++})$  and  $0(2^{++})$ .

The coupled channel unitary approach with the local hidden gauge formalism, reviewed in Sec. 3.2, was also applied to study the  $B\bar{B}^*$  and  $B^*\bar{B}^*$  interactions. In Ref. [404], Ozpineci, Xiao, and Oset investigated the meson-meson interaction with hidden beauty in both  $I = 0$  and  $I = 1$  sectors. They found the interactions are too weak in the  $I = 1$  sector to create any bound state.

In Ref. [405], Dias, Aceti, and Oset used the local hidden gauge approach to study the  $B\bar{B}^*$  and  $B^*\bar{B}^*$  interactions in the  $I = 1$  sector. They considered the contributions due to the exchange of two pions and heavy vector mesons. They found a loosely bound state with mass in the range 10587-10601 MeV for the  $B\bar{B}^*$  interaction, very close to the experimental value of the  $Z_b(10610)$  and a cusp at 10650 MeV for the  $B^*\bar{B}^*$  interaction for  $J = 0, 1, 2$ .

The method of QCD sum rules was also used to study the two  $Z_b$  states [406, 407, 408, 409, 410, 411, 412, 413]. Using the  $B\bar{B}^*$  and  $B^*\bar{B}^*$  molecule-type interpolating currents with  $I^G J^P = 1^+ 1^+$ , their extracted masses were roughly consistent with the masses of the  $Z_b(10610)$  and  $Z_b(10650)$  mesons, respectively.

*4.1.1.3. Symmetry analysis.* Within the molecular picture, Bondarn *et al.* discussed the heavy quark spin structure and the  $Z_b$  states. Especially, they noticed that the  $b\bar{b}$  pair within the  $Z_b(10610)$  and  $Z_b(10650)$  resonances is a mixture of a spin-triplet and a spin-singlet of equal amplitude [414]. Voloshin investigated their isoscalar analogs and proposed to observe them in the  $I^G(J^P) = 0^-(1^+)$  channel [415]. He pointed out that the ratio of the yield for the pairs of the charged and neutral  $B^{(*)}$  mesons in the processes  $\Upsilon(5S) \rightarrow \pi^0 B\bar{B}^*$  and  $\Upsilon(5S) \rightarrow \pi^0 B^*\bar{B}^*$  is very sensitive to the interaction between the mesons due to significant isospin breaking by the Coulomb force.

The heavy quark flavor symmetry was applied to study the heavy meson hadronic molecules in Refs. [416, 417]. In Ref. [416], Nieves and Valderrama discussed the possible  $B\bar{B}^*$  bound states using the analogue to the weakly bound

$X(3872)$  state and under certain assumptions about the short range dynamics. In Ref. [417], Guo, Hidalgo-Duque, Nieves, and Valderrama investigated the consequences of the heavy quark flavor symmetry and predicted many new hadronic molecules.

In Ref. [418], Cleven, Guo, Hanhart, and Meissner used the measured invariant mass distributions for the transitions of the  $\Upsilon(5S)$  to the final states  $h_b\pi^+\pi^-$  and  $h_b(2P)\pi^+\pi^-$  to test the molecular picture. They made use of the power counting for the bottom meson loops in the framework of a nonrelativistic effective field theory. Their results showed the data [162] is consistent with the assumption that the main components of  $Z_b$  states are  $S$ -wave  $B\bar{B}^*$  and  $B^*\bar{B}^*$  bound states, although a small compact tetraquark component can not be excluded. Possible power counting schemes were also discussed in Ref. [419].

Assuming the binding mechanism between two heavy mesons is mostly molecular-like isospin-exchange attraction, Karliner and Rosner studied the bottomonium-like and charmonium-like multi-quark states in Ref. [400]. They also interpreted the  $Z_b(10610)$  and  $Z_b(10650)$  as the weakly bound molecular states composed of the  $\bar{B}B^*$  and  $\bar{B}^*B^*$ , respectively.

#### 4.1.2. The tetraquark assignment

4.1.2.1. *QCD sum rules.* The color configurations of the tetraquarks include  $(\bar{\mathbf{3}}_{[qQ]} \otimes \mathbf{3}_{[Q\bar{q}]})$ ,  $(\mathbf{6}_{[qQ]} \otimes \bar{\mathbf{6}}_{[Q\bar{q}]})$  and  $(\mathbf{8}_{[qQ]} \otimes \mathbf{8}_{[Q\bar{q}]})$ . The first two types correspond to the diquark configuration.

In 2011, Chen and Zhu had performed an extensive investigation of the hidden-bottom tetraquark systems with quantum numbers  $J^{PC} = 1^{+-}$  in QCD sum rules in Ref. [420]. They considered all six kinds of diquark fields  $q_a^T C Q_b$ ,  $q_a^T C \gamma_5 Q_b$ ,  $q_a^T C \gamma_\mu Q_b$ ,  $q_a^T C \gamma_\mu \gamma_5 Q_b$ ,  $q_a^T C \sigma_{\mu\nu} Q_b$ , and  $q_a^T C \sigma_{\mu\nu} \gamma_5 Q_b$  to construct the eight tetraquark interpolating currents

$$\begin{aligned}
J_{1\mu} &= q_a^T C Q_b (\bar{q}_a \gamma_\mu \gamma_5 C \bar{Q}_b^T + \bar{q}_b \gamma_\mu \gamma_5 C \bar{Q}_a^T) - q_a^T C \gamma_\mu \gamma_5 Q_b (\bar{q}_a C \bar{Q}_b^T + \bar{q}_b C \bar{Q}_a^T), \\
J_{2\mu} &= q_a^T C Q_b (\bar{q}_a \gamma_\mu \gamma_5 C \bar{Q}_b^T - \bar{q}_b \gamma_\mu \gamma_5 C \bar{Q}_a^T) - q_a^T C \gamma_\mu \gamma_5 Q_b (\bar{q}_a C \bar{Q}_b^T - \bar{q}_b C \bar{Q}_a^T), \\
J_{3\mu} &= q_a^T C \gamma_5 Q_b (\bar{q}_a \gamma_\mu C \bar{Q}_b^T + \bar{q}_b \gamma_\mu C \bar{Q}_a^T) - q_a^T C \gamma_\mu Q_b (\bar{q}_a \gamma_5 C \bar{Q}_b^T + \bar{q}_b \gamma_5 C \bar{Q}_a^T), \\
J_{4\mu} &= q_a^T C \gamma_5 Q_b (\bar{q}_a \gamma_\mu C \bar{Q}_b^T - \bar{q}_b \gamma_\mu C \bar{Q}_a^T) - q_a^T C \gamma_\mu Q_b (\bar{q}_a \gamma_5 C \bar{Q}_b^T - \bar{q}_b \gamma_5 C \bar{Q}_a^T), \\
J_{5\mu} &= q_a^T C \gamma^\nu Q_b (\bar{q}_a \sigma_{\mu\nu} \gamma_5 C \bar{Q}_b^T + \bar{q}_b \sigma_{\mu\nu} \gamma_5 C \bar{Q}_a^T) - q_a^T C \sigma_{\mu\nu} \gamma_5 Q_b (\bar{q}_a \gamma^\nu C \bar{Q}_b^T + \bar{q}_b \gamma^\nu C \bar{Q}_a^T), \\
J_{6\mu} &= q_a^T C \gamma^\nu Q_b (\bar{q}_a \sigma_{\mu\nu} \gamma_5 C \bar{Q}_b^T - \bar{q}_b \sigma_{\mu\nu} \gamma_5 C \bar{Q}_a^T) - q_a^T C \sigma_{\mu\nu} \gamma_5 Q_b (\bar{q}_a \gamma^\nu C \bar{Q}_b^T - \bar{q}_b \gamma^\nu C \bar{Q}_a^T), \\
J_{7\mu} &= q_a^T C \gamma^\nu \gamma_5 Q_b (\bar{q}_a \sigma_{\mu\nu} C \bar{Q}_b^T + \bar{q}_b \sigma_{\mu\nu} C \bar{Q}_a^T) - q_a^T C \sigma_{\mu\nu} Q_b (\bar{q}_a \gamma^\nu \gamma_5 C \bar{Q}_b^T + \bar{q}_b \gamma^\nu \gamma_5 C \bar{Q}_a^T), \\
J_{8\mu} &= q_a^T C \gamma^\nu \gamma_5 Q_b (\bar{q}_a \sigma_{\mu\nu} C \bar{Q}_b^T - \bar{q}_b \sigma_{\mu\nu} C \bar{Q}_a^T) - q_a^T C \sigma_{\mu\nu} Q_b (\bar{q}_a \gamma^\nu \gamma_5 C \bar{Q}_b^T - \bar{q}_b \gamma^\nu \gamma_5 C \bar{Q}_a^T),
\end{aligned} \tag{123}$$

where  $q$  represents the up or down quark and  $Q$  the bottom quark. The color structures are symmetric  $\mathbf{6} \otimes \bar{\mathbf{6}}$  for the currents  $J_1, J_3, J_5, J_7$ , and antisymmetric  $\bar{\mathbf{3}} \otimes \mathbf{3}$  for the currents  $J_2, J_4, J_6, J_8$ . All these tetraquark currents in Eq. (123) can couple to both isotriplet and isosinglet hadron states

$$J_\mu \sim q Q \bar{q} \bar{Q} \sim \begin{cases} Z^+ : d Q \bar{u} \bar{Q} \\ Z^0 : u Q \bar{u} \bar{Q} + d Q \bar{d} \bar{Q} \\ Z^- : u Q \bar{d} \bar{Q} \\ Z^0 : u Q \bar{u} \bar{Q} - d Q \bar{d} \bar{Q}, \end{cases} \text{ Isovector with } I = 1, \tag{124}$$

The extracted masses of the hidden-bottom tetraquarks are collected in Table 16.

Besides the diquark configuration, the color octet-octet  $(\mathbf{8}_{[qQ]} \otimes \mathbf{8}_{[Q\bar{q}]})$  types of interpolating currents were also considered for the hidden-bottom tetraquark systems in Refs. [410, 411]

$$\begin{aligned}
J_{1\mu}^{(\mathbf{8})} &= (\bar{q}_a \gamma_5 \lambda_{ab}^n Q_b) (\bar{Q}_c \gamma_\mu \lambda_{cd}^n q_d) + (\bar{q}_a \gamma_\mu \lambda_{ab}^n Q_b) (\bar{Q}_c \gamma_5 \lambda_{cd}^n q_d), \\
J_{2\mu}^{(\mathbf{8})} &= (\bar{q}_a \lambda_{ab}^n Q_b) (\bar{Q}_c \gamma_\mu \gamma_5 \lambda_{cd}^n q_d) - (\bar{q}_a \gamma_\mu \gamma_5 \lambda_{ab}^n Q_b) (\bar{Q}_c \lambda_{cd}^n q_d), \\
J_{3\mu}^{(\mathbf{8})} &= (\bar{q}_a \gamma^\alpha \lambda_{ab}^n Q_b) (\bar{Q}_c \sigma_{\alpha\mu} \gamma_5 \lambda_{cd}^n q_d) - (\bar{q}_a \sigma_{\alpha\mu} \gamma_5 \lambda_{ab}^n Q_b) (\bar{Q}_c \gamma^\alpha \lambda_{cd}^n q_d), \\
J_{4\mu}^{(\mathbf{8})} &= (\bar{q}_a \gamma^\alpha \gamma_5 \lambda_{ab}^n Q_b) (\bar{Q}_c \sigma_{\alpha\mu} \lambda_{cd}^n q_d) + (\bar{q}_a \sigma_{\alpha\mu} \lambda_{ab}^n Q_b) (\bar{Q}_c \gamma^\alpha \gamma_5 \lambda_{cd}^n q_d).
\end{aligned} \tag{125}$$

The extracted masses are collected in Table 17.

From Tables 17 and 16, the extracted masses of the tetraquark states using both the diquark-diquark and color octet-octet types of interpolating currents are roughly the same. The bottomonium-like  $qb\bar{q}\bar{b}$  and  $sb\bar{s}\bar{b}$  tetraquark states are nearly degenerate around 9.9 – 10.2 GeV. These values are much lower than the masses of the  $Z_b(10610)$  and  $Z_b(10650)$  states.

There exist colored forces between the  $[q\bar{b}]_8$  and  $[b\bar{q}]_8$  clusters or the diquark antidiquark pair. The tetraquarks may be more compact than the color singlet-singlet hadron molecules. In other words, the numerical results from the QCD sum rule approach do not support the tetraquark interpretation of these two charged  $Z_b$  mesons [420].

Table 16: Numerical results for the  $J^{PC} = 1^{+-}$  bottomonium-like tetraquark states using the diquark-diquark interpolating currents [420].

	Current	$s_0$ (GeV <sup>2</sup> )	Borel window (GeV <sup>2</sup> )	$m_x$ (GeV)	PC (%)
$qb\bar{q}\bar{b}$	$J_{3\mu}$	10.6 <sup>2</sup>	7.5 – 8.5	10.08 ± 0.10	45.9
	$J_{4\mu}$	10.6 <sup>2</sup>	7.5 – 8.5	10.07 ± 0.10	46.2
	$J_{5\mu}$	10.6 <sup>2</sup>	7.5 – 8.4	10.05 ± 0.10	45.3
	$J_{6\mu}$	10.7 <sup>2</sup>	7.5 – 8.7	10.15 ± 0.10	47.6
$sb\bar{s}\bar{b}$	$J_{3\mu}$	10.6 <sup>2</sup>	7.5 – 8.3	10.11 ± 0.10	43.8
	$J_{4\mu}$	10.6 <sup>2</sup>	7.5 – 8.4	10.10 ± 0.10	44.1
	$J_{5\mu}$	10.6 <sup>2</sup>	7.5 – 8.3	10.08 ± 0.10	43.7
	$J_{6\mu}$	10.7 <sup>2</sup>	7.5 – 8.5	10.18 ± 0.10	46.5

Table 17: Numerical results for the  $J^{PC} = 1^{+-}$  bottomonium-like tetraquark states using the color octet-octet interpolating currents [410, 411].

Current	$s_0$ (GeV <sup>2</sup> )	Borel window (GeV <sup>2</sup> )	$m_x$ (GeV)	$f_x$ (10 <sup>-2</sup> GeV <sup>5</sup> )
$J_{1\mu}^{(8)}(B\bar{B}^*)$	108	7.5 – 8.8	9.93 ± 0.15	1.02 ± 0.30
$J_{3\mu}^{(8)}(B^*\bar{B}^*)$	108	7.8 – 8.7	9.92 ± 0.15	2.17 ± 0.62

4.1.2.2. *Diquark model.* Motivated by the  $Y_b(10890)$  resonance observed by the Belle Collaboration [421], Ali *et al.* studied the spectroscopy and decays of the bottomonium-like tetraquarks in Ref. [422]. Assuming the existence of the tightly bound diquarks ( $bq$ ) and antidiquarks ( $\bar{b}\bar{q}$ ) [422, 423], they adopted the effective Hamiltonian

$$H = 2m_Q + H_{SS}^{(QQ)} + H_{SS}^{(Q\bar{Q})} + H_{SL} + H_{LL}, \quad (126)$$

which includes the constituent diquark mass  $m_Q$ , spin-spin interaction inside the single diquark  $H_{SS}^{(QQ)}$ , spin-spin interaction between quark and antiquark belonging to two diquarks  $H_{SS}^{(Q\bar{Q})}$ , spin-orbit term  $H_{SL}$ , and purely orbital term  $H_{LL}$ . One notes that there does not exist any confinement dynamics in the above Hamiltonian. The dominant contribution arises from the constituent diquark mass. Various hyperfine interactions have to be determined through fitting to data under the assumption that some observed states are tetraquark states. In contrast, the hyperfine interactions

in the quark model were derived rigorously with the help of the one gluon exchange potential and linear confinement potential.

Later in Ref. [424], Ali, Hambrock, and Wang reproduced the observed masses of the  $Z_b(10610)$  and  $Z_b(10650)$  in terms of the decay widths for the  $h_b(2P)\pi^\pm$ . They obtained a ratio for the relative decay amplitudes in the decays  $Z_b(10610)/Z_b(10650) \rightarrow h_b(mP)\pi^\pm$ , which agrees with the experimental data [161]. Under the tetraquark hypothesis, the  $Z_b(10610)$  and  $Z_b(10650)$  were further investigated with the non-relativistic QCD factorization scheme [425]. Ali *et al.* identified the  $Z_b(10610)$  and  $Z_b(10650)$  as the  $S$ -wave  $J^{PG} = 1^{++}$  states with the diquark spin distribution [426]:

$$Z_b(10610) = \frac{1}{\sqrt{2}} \left[ |1_{[bq]}, 0_{[\bar{b}\bar{q}]}\rangle - |0_{[bq]}, 1_{[\bar{b}\bar{q}]}\rangle \right], \quad (127)$$

$$Z_b(10650) = |1_{[bq]}, 1_{[\bar{b}\bar{q}]}\rangle_{J=1}, \quad (128)$$

where  $s_{[bq]}$  and  $s_{[\bar{b}\bar{q}]}$  are the diquark and antidiquark spins, respectively. Moreover, there also exists the partner of the  $X(3872)$  in the bottom sector  $X_b$  with  $J^{PC} = 1^{++}$

$$X_b = \frac{1}{\sqrt{2}} \left[ |1_{[bq]}, 0_{[\bar{b}\bar{q}]}\rangle + |0_{[bq]}, 1_{[\bar{b}\bar{q}]}\rangle \right]. \quad (129)$$

#### 4.1.3. Kinematical effect

Besides the above resonant interpretations of the  $Z_b(10610)$  and  $Z_b(10650)$ , Bugg proposed the  $Z_b(10610)$  and  $Z_b(10650)$  as the cusp effect around the  $\bar{B}B^*$  and  $\bar{B}^*B^*$  thresholds [427]. Szczepaniak analyzed the properties of the partial waves in the kinematic region of the direct channel which corresponds to the  $Z_b(10610)$ . He pointed out that the triangle singularities would also give considerable contributions to the  $Z_b(10610)$  peak [428].

Swanson also discussed the cusp hypothesis of the  $Z_b(10610)$ ,  $Z_b(10650)$ ,  $Z_c(3900)$  and  $Z_c(4025)$  [429]. The decay amplitude  $\Upsilon \rightarrow \pi\pi\Upsilon$  can be related to the scattering amplitude of  $\pi\Upsilon \rightarrow \pi\Upsilon$  in Fig. 45. He considered the angular momentum barrier factors and reproduced the experimental data of  $\Upsilon(5S) \rightarrow \Upsilon(mS)\pi\pi$  ( $m = 1, 2, 3$ ) and  $\Upsilon(5S) \rightarrow h_b(nP)\pi\pi$  ( $n = 1, 2$ ) (see Figures 3-5 of Ref. [429] for more details). He concluded that the  $Z_b(10610)$  and  $Z_b(10650)$  may arise from the kinematical effect [429].

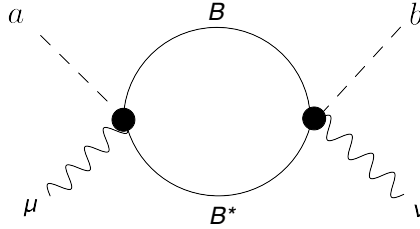


Figure 45: The  $\Upsilon\pi$  scattering by including the coupled-channel effect. Taken from Ref. [429].

In Ref. [430], Chen and Liu proposed the *initial single pion emission (ISPE)* mechanism in the hidden-bottom dipion decays of the  $\Upsilon(5S)$ . The direct emission of the single pion from the  $\Upsilon(5S)$  ensures that the intermediate  $B^{(*)}\bar{B}^{(*)}$  pairs carry low momenta. Then meson pairs interact with each other to transit into final states through the exchange of one  $B^{(*)}$  meson (see Fig. 46). There exist sharp structures around 10610 MeV and 10650 MeV in the line shapes of the  $d\Gamma(\Upsilon(5S) \rightarrow \Upsilon(nS)\pi^+\pi^-)/dm_{\Upsilon(nS)\pi^+}$  and  $d\Gamma(\Upsilon(5S) \rightarrow h_b(mP)\pi^+\pi^-)/dm_{h_b(mP)\pi^+}$  distributions in Fig. 47, which could correspond to the  $Z_b(10610)$  and  $Z_b(10650)$  structures.

#### 4.1.4. Production and decay patterns

Assuming the  $Z_b(10610)$  and  $Z_b(10650)$  to be hadronic molecules composed of the  $\bar{B}B^*$  and  $\bar{B}^*B^*$ , their radiative productions from the  $\Upsilon(5S)$  were studied in the heavy quark spin symmetry limit in Ref. [431]. Their two-body

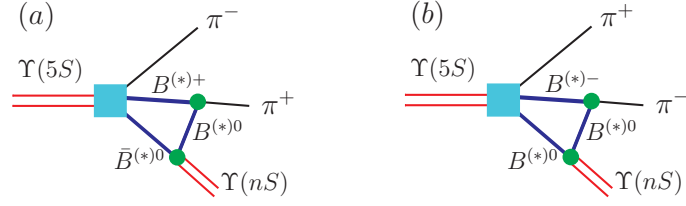


Figure 46: (Color online) The schematic diagrams describing the ISPE mechanism of the  $\Upsilon(5S)$ . Here, we use  $\Upsilon(5S) \rightarrow \Upsilon(nS)\pi^+\pi^-$  as an example. Taken from Ref. [430].

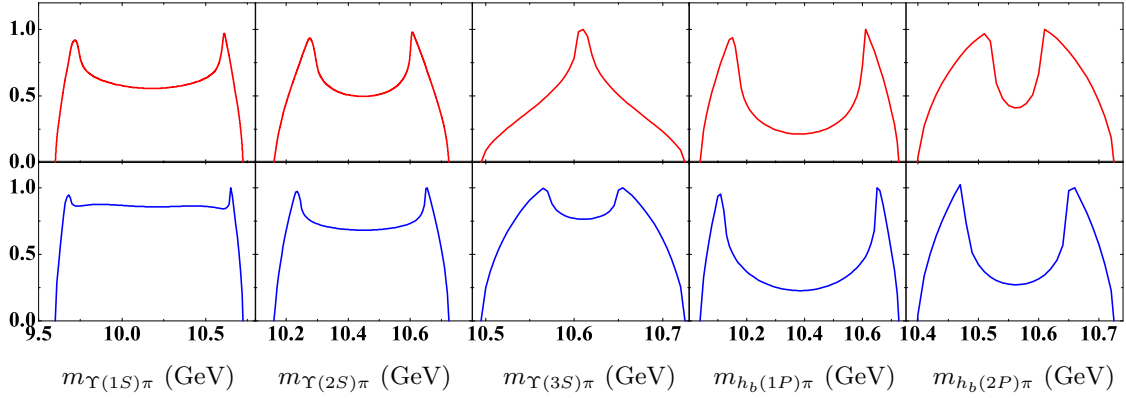


Figure 47: (Color online) The invariant mass spectra of the  $\Upsilon(nS)\pi^\pm$  ( $n = 1, 2, 3$ ) and  $h_b(mP)\pi^\pm$  ( $m = 1, 2$ ) in  $\Upsilon(5S) \rightarrow \Upsilon(nS)\pi^+\pi^-$  and  $\Upsilon(5S) \rightarrow h_b(mP)\pi^+\pi^-$  decays. Here, the maximum of the theoretical line shape is normalized to 1. Taken from Ref. [430].

strong decays  $Z_b^+(10610) \rightarrow \Upsilon(nS)\pi^+$  and  $Z_b^+(10650) \rightarrow \Upsilon(nS)\pi^+$  were evaluated in a phenomenological Lagrangian approach in Ref. [432]. Their transitions to the bottomonium with the emission of a pion were investigated with the application of the leading (dipole) term in the QCD multipole expansion in Ref. [433]. These transitions were also studied via the intermediate  $B\bar{B}$  meson loops in Ref. [434] and via the triangle diagrams in Ref. [435].

In Ref. [436], the authors adopted the spin rearrangement scheme in the heavy quark limit and extensively investigated three classes of the radiative decays:  $\mathfrak{M} \rightarrow (b\bar{b}) + \gamma$ ,  $(b\bar{b}) \rightarrow \mathfrak{M} + \gamma$ ,  $\mathfrak{M} \rightarrow \mathfrak{M}' + \gamma$ , corresponding to the electromagnetic transitions between one molecular state and bottomonium, one bottomonium and molecular state, and two molecular states respectively. Some model independent ratios were derived when the initial or final states belong to the same spin flavor multiplet.

With the spin rearrangement scheme in the heavy quark limit, the authors of Ref. [437] performed a comprehensive investigation of the decay pattern and production mechanism of the hidden bottom di-meson states, which are either composed of a P-wave bottom meson and an S-wave bottom meson or two S-wave bottom mesons. The model-independent ratios can be measured by future experiments like BESIII, Belle, LHCb and the forthcoming BelleII, which will provide important clues to the inner structures of the exotic states.

Line shapes in the vicinity of the  $B^{(*)}\bar{B}^{(*)}$  thresholds as well as two-body decay rates of the  $Z_b(10610)$  and  $Z_b(10650)$  were studied using the heavy quark symmetry in Ref. [438]. The mixing of the S-D partial waves for the heavy meson pairs in the decays  $\Upsilon(5S) \rightarrow B^*\bar{B}\pi$  and  $\Upsilon(5S) \rightarrow B^*\bar{B}^*\pi$  was studied in Ref. [439], where the  $Z_b(10610)$  and  $Z_b(10650)$  were taken into account. Decays and productions of the  $Z_b$  and other  $B\bar{B}$  molecules resonances via the bottomonium were studied under the heavy quark symmetry in Ref. [440]. The contribution of the  $Z_b$  resonances to  $\Upsilon(5S) \rightarrow \pi\pi\pi\chi_b$  was studied in Ref. [441].

The decays of the  $Z_b(10610)$  and  $Z_b(10650)$  to  $\Upsilon(nS)\pi$ ,  $h_b(mP)\pi$  and  $\chi_{bJ}(mP)\gamma$  ( $n = 1, 2, 3$ ,  $m = 1, 2$  and  $J = 0, 1, 2$ ) were investigated within a nonrelativistic effective field theory in Ref. [442]. The authors argued that the decays to  $\Upsilon(nS)\pi$  suffer from potentially large higher order corrections. However, the P-wave transitions of the  $Z_b$  states are dominated by a single one-loop diagram and therefore offer the best possibility to confirm the nature of the  $Z_b$  states as molecular states and to further study their properties. In Ref. [443], the contribution of the charged  $Z_b$

states to the  $\Upsilon(3S) \rightarrow \Upsilon(1S)\pi\pi$  decays was discussed.

#### 4.1.5. A short summary

- The  $Z_b(10610)$  and  $Z_b(10650)$  are charged hidden-bottom states with narrow widths, which are close to the thresholds of the  $B\bar{B}^*$  and  $B^*\bar{B}^*$ , respectively. The  $B\bar{B}^*$  branching ratio is  $(86.0 \pm 3.6)\%$  for the  $Z_b(10610)$ . For the  $Z_b(10650)$ , the  $B^{(*)}\bar{B}^*$  branching ratio is  $(73.4 \pm 7.0)\%$ . Both the  $Z_b(10610)$  and  $Z_b(10650)$  are very probably either the  $B^*\bar{B}^*$  or  $B\bar{B}^*$  molecular states respectively.
- There exists attraction in the isovector axial vector channel. In fact the one-pion-exchange force alone is strong enough to form the shallow bound states composed of the  $B\bar{B}^*$  and  $B^*\bar{B}^*$ . There also exist their isoscalar molecular partners.
- The  $\Upsilon(5S)$  [or  $\Upsilon(6S)$ ] is the ideal factory of the heavy molecular states, which shall be produced abundantly at BelleII in the near future! The masses of the  $B\bar{B}^*\pi$  and  $B^*\bar{B}^*\pi$  are 10.744 GeV and 10.790 GeV respectively, which are very close to the  $\Upsilon(5S)$  mass 10.860 GeV. Because of the tiny decay phase space, the relative motion between the  $B^{(*)}\bar{B}^*$  pair is very slow, which is favorable to the formation of the  $B^{(*)}\bar{B}^*$  molecular states.
- If the four quarks  $q\bar{q}b\bar{b}$  are confined within the MIT bag to form an isovector axial vector tetraquark state, such a system will decay into the  $\Upsilon(1S)\pi$  via S-wave easily and has a very large decay width around several hundred MeV. The  $\Upsilon(1S)\pi$  should be its dominant decay mode.
- To explain the narrow total width and the dominant open-bottom decay modes, the diquark within the tetraquark was assumed to be tightly bound and compact, which awaits future experimental confirmation.

## 4.2. $Z_c(3900)$ , $Z_c(4020)$ and $Z_c(4025)$

### 4.2.1. Molecular scheme

4.2.1.1. *Meson exchange model.* In 2008, the possible  $D^{(*)}\bar{D}^{(*)}$  molecular states within the OBE model were discussed in Ref. [207]. Later, Sun *et al.* considered the S-D wave mixing effect and performed an intensive study of the  $D\bar{D}^*$  and  $D^*\bar{D}^*$  molecular state systems in Ref. [192].

Except the one-pion-exchange potential, the effective potential of the  $D\bar{D}^*$  system is similar to that of the  $B\bar{B}^*$  system listed in Sec. 4.1.1.1. The mass gap between  $m_{D^*}$  and  $m_D$  is larger than the pion mass, which is different from the case of the  $B\bar{B}^*$  system. In the derivation of the OPE potential in the coordinate space, one generally keeps the principal value only when making the Fourier transformation to the scattering amplitude in the momentum space. The OPE potential of the  $D\bar{D}^*$  system not only oscillates but also decreases very slowly [201, 207], which is an inherent uncertainty of the OBE model when the mass gap of the final and initial states in the crossed diagram is larger than the exchanged meson mass. The potential from the  $\pi$  meson exchange is

$$V_\pi^{\text{Cross}} = -\frac{g^2}{f_\pi^2} \left[ \frac{1}{3} (\boldsymbol{\epsilon}_2 \cdot \boldsymbol{\epsilon}_3^\dagger) Z_\pi^{DD^*}(\Lambda_4, m_4, r) + \frac{1}{3} S(\hat{\mathbf{r}}, \boldsymbol{\epsilon}_2, \boldsymbol{\epsilon}_3^\dagger) T_\pi^{DD^*}(\Lambda_4, m_4, r) \right], \quad (130)$$

where

$$\begin{aligned} Y_\pi^{DD^*}(\Lambda_4, m_4, r) &= \frac{1}{4\pi r} \left( -e^{-\Lambda_4 r} - \frac{r(\Lambda_4^2 + m_4^2)}{2\Lambda_4} e^{-\Lambda_4 r} + \cos(m_4 r) \right), \\ Z_\pi^{DD^*}(\Lambda_4, m_4, r) &= \nabla^2 Y_\pi^{DD^*}(\Lambda_4, m_4, r) = \frac{1}{r^2} \frac{\partial}{\partial r} r^2 \frac{\partial}{\partial r} Y_\pi^{DD^*}(\Lambda_4, m_4, r), \\ T_\pi^{DD^*}(\Lambda_4, m_4, r) &= r \frac{\partial}{\partial r} \frac{1}{r} \frac{\partial}{\partial r} Y_\pi^{DD^*}(\Lambda_4, m_4, r). \end{aligned} \quad (131)$$

The parameters  $\Lambda_4$  and  $m_4$  are defined as  $\Lambda_4 = \sqrt{\Lambda^2 - (m_{D^*} - m_D)^2}$  and  $m_4 = \sqrt{(m_{D^*} - m_D)^2 - m_\pi^2}$ . The potentials of the  $D^*\bar{D}^*$  system and  $B^*\bar{B}^*$  system have the same form (see Sec. 4.1.1.1).

In Tables 18 and 19, the obtained bound state solutions for the  $D\bar{D}^*$  and  $D^*\bar{D}^*$  systems are correlated with the cutoff parameter  $\Lambda$  in the monopole form factor  $F(q) = (\Lambda^2 - m_E^2)/(\Lambda^2 - q^2)$ , which is introduced to suppress the

Table 18: The obtained bound state solutions (binding energy  $E$  and root-mean-square radius  $r_{\text{RMS}}$ ) for the  $D\bar{D}^*$  system. Taken from Ref. [192].

$I^G(J^{PC})$	State	OBE			OPE		
		$\Lambda$	$E$ (MeV)	$r_{\text{RMS}}$ (fm)	$\Lambda$	$E$ (MeV)	$r_{\text{RMS}}$ (fm)
$1^+(1^{+-})$	$\hat{\Phi}^*$	-	-	-	4.6	-0.85	1.46
		-	-	-	4.7	-3.42	1.17
		-	-	-	4.8	-7.18	0.93
		-	-	-	4.9	-12.40	0.75
$1^-(1^{++})$	$\Phi^*$	-	-	-	-	-	-
		1.3	-	-	3.4	-0.11	1.74
$0^-(1^{+-})$	$\hat{\Phi}_8^*$	1.4	-1.56	1.61	3.5	-2.03	1.50
		1.5	-12.95	0.98	3.6	-4.79	1.26
		1.6	-35.73	0.69	3.7	-9.62	1.06
		1.1	-0.61		1.7	-3.01	1.37
$0^+(1^{++})$	$\Phi_8^*$	1.2	-4.42	1.38	1.8	-7.41	1.06
		1.3	-11.78	1.05	1.9	-14.15	0.84
		1.4	-21.88	0.86	2	-23.82	0.68

Table 19: The obtained bound state solutions (binding energy  $E$  and root-mean-square radius  $r_{\text{RMS}}$ ) for the  $D^*\bar{D}^*$  system. Taken from Ref. [192].

$I^G(J^{PC})$	State	OBE			OPE		
		$\Lambda$	$E$ (MeV)	$r_{\text{RMS}}$ (fm)	$\Lambda$	$E$ (MeV)	$r_{\text{RMS}}$ (fm)
$1^+(0^+)$	$\Phi^{**}[J=0]$	3.6	-0.94	1.74	2.8	-2.03	1.47
		3.8	-6.16	1.00	2.9	-6.10	1.00
		4	-16.44	0.66	3	-12.51	0.74
		4.2	-33.23	0.49	3.1	-21.56	0.59
		1.4	-1.72	1.62	3	-5.70	1.24
$0^-(0^{+-})$	$\Phi_8^{**}[J=0]$	1.5	-17.98	0.88	3.1	-12.15	0.96
		1.6	-54.60	0.47	3.2	-21.83	0.78
					4.7	-6.96	0.94
$1^+(1^+)$	$\Phi^{**}[J=1]$	-	-	-	4.8	-12.29	0.73
					4.9	-19.36	0.60
					5	-28.31	0.51
		1.3	-	-	3.6	-9.91	1.01
$0^-(1^{+-})$	$\Phi_8^{**}[J=1]$	1.4	-3.44	1.44	3.7	-15.25	0.87
		1.5	-16.57	0.90	3.8	-22.07	0.76
		1.6	-41.25	0.66	3.9	-30.53	0.68
$1^+(2^+)$	$\Phi^{**}[J=2]$	-	-	-	-	-	-
		1.1	-0.61	1.72	1.6	-3.89	1.28
$0^-(2^{+-})$	$\Phi_8^{**}[J=2]$	1.2	-7.50	1.19	1.7	-9.64	0.98
		1.3	-19.22	0.89	1.8	-18.38	0.77
		1.4	-35.93	0.73	1.9	-30.71	0.64

contribution from the large momentum exchange. When  $\Lambda$  is very large,  $F(q) \approx 1$  for the soft momentum exchange. As we emphasized, the deuteron is the only well established di-hadron molecule. Various meson and nucleon coupling constants are known well. After fitting to the experimental data, the value of  $\Lambda$  turns out to be 1-2 GeV in the deuteron case. Such a value is regarded as “reasonable” and used in the discussion of the hidden-charm molecular states and other molecular systems. The readers should be cautious about the uncertainty of this criteria.

From the numerical results in Tables 18 and 19, we list some interesting observations from the OPE and OBE models below.

- There exists the long-range attraction due to the pion exchange in the  $I^G J^P = 1^+ 1^+ D\bar{D}^*$  and  $D^* \bar{D}^*$  systems.
- There exist loosely bound  $D\bar{D}^*$  and  $D^* \bar{D}^*$  molecular states in the isoscalar channel for a reasonable cutoff around 1-2 GeV, where the short-range vector meson exchange provides additional attraction.
- With a large cutoff around 4.7 GeV which corresponds to the form factor  $F(q) \approx 1$ , the one-pion-exchange force is strong enough to form the isovector  $D\bar{D}^*$  and  $D^* \bar{D}^*$  molecular bound states. However, the short-range interaction from the vector meson exchange in the OBE model tends to dissolve these loosely bound systems.
- Increasing the pionic coupling constant  $g$  is helpful to form the bound states [157].
- There do not exist the isovector  $D\bar{D}^*$  and  $D^* \bar{D}^*$  molecular bound states if one uses the value of the pionic coupling extracted from the  $D^*$  decay width and insists a cutoff around 1-2 GeV. However, the cutoff requirement arises from the experience with the deuteron only. One needs to keep this point in mind.
- The  $Z_c(3900)$  and  $Z_c(4020)$  may be the molecular resonances generated by the long-range one-pion-exchange force, although the OPE force might not be strong enough to form the molecular bound states below the threshold with a cutoff around 1-2 GeV.

4.2.1.2. *Other molecular models on the  $Z_c(3900)$  and  $Z_c(4025)$ .* The observation of the  $Z_c(3900)$  has triggered intensive discussions. In Ref. [224], Zhao, Ma, and Zhu considered the spin-orbit force and recoil corrections in the  $D\bar{D}^*$  interaction in the OBE model. They found two isoscalar  $D\bar{D}^*$  molecular states with  $J^{PC} = 1^{++}$  and  $1^{+-}$ , the first of which corresponds to the  $X(3872)$ . However, they found it not easy to accommodate the  $Z_c(3900)$  as the candidate of the isovector molecular bound state of the  $D\bar{D}^*$ . Later, He investigated the  $D\bar{D}^*$  systems in the framework of the Bethe-Salpeter approach with the quasipotential approximation [444], where both direct and cross diagrams in the one-boson-exchange potential were considered. His results indicated the existence of an isoscalar bound state  $D\bar{D}^*$  with  $J^{PC} = 1^{++}$ , which may be related to the  $X(3872)$ . But no bound state was produced from the  $D\bar{D}^*$  interaction in the isovector sector [444].

The authors of Refs. [192, 224, 444] noticed that it is not so easy to accommodate  $Z_c(3900)$  as an isovector  $D\bar{D}^*$  molecular bound state, which is supported by several Lattice studies [445, 446, 447, 448]. Prelovsek and Leskovec searched for the  $Z_c(3900)$  on the lattice in the channel with  $J^{PC} = 1^{+-}$  and  $I = 1$  without success [445]. Instead, they found discrete scattering states  $D\bar{D}^*$  and  $J/\psi\pi$  only. Later in Ref. [446], a search for the  $Z_c^+$  with mass below 4.2 GeV was performed for the  $\bar{c}c\bar{d}u$  channel with  $I^G(J^{PC}) = 1^+(1^{+-})$ . The authors of Ref. [446] were able to find all the expected signals. But again they found no convincing signal for an extra  $Z_c^+$  state. In Ref. [447], Chen *et al.* analyzed the low-energy scattering of the  $D\bar{D}^*$  meson system using Lattice QCD with  $N_f = 2$  twisted mass fermion configurations with three pion mass values. Their results indicated a weak repulsive interaction between the two mesons  $D$  and  $\bar{D}^*$ , and did not support a bound state in this channel corresponding to the  $Z_c(3900)$ . In Ref. [448], the low-energy scattering of the  $D^* \bar{D}^*$  meson system was studied by Chen *et al.* by Lattice QCD calculation. Their results indicated a weak repulsive interaction between the two vector charmed mesons, and did not support a bound state in this channel corresponding to the  $Z_c(4020)/Z_c(4025)$ .

In Ref. [449], Aceti *et al.* studied the  $D\bar{D}^*$  interaction in the isovector channel in the local hidden gauge approach with heavy quark spin symmetry. They found a state with a mass of 3869-3875 MeV and a width around 40 MeV with  $I = 1$  and positive  $G$ -parity, which is interpreted as the isospin partner of the  $X(3872)$ . They reanalyzed the  $e^+e^- \rightarrow \pi^\pm(D\bar{D}^*)^\mp$  reaction [148] and found a solution with a mass of 3875 MeV and a width around 30 MeV. But they did not firmly interpret it as the  $Z_c(3900)$ . In Ref. [450], Aceti *et al.* studied the isovector  $D^* \bar{D}^*$  interaction in the

local hidden gauge approach, and interpreted the  $Z_c(4020)/Z_c(4025)$  as a possible  $2^+$  bound state of the  $D^*\bar{D}^*$  with  $I = 1$ .

Besides the light meson exchange, He also considered the additional very short-range attraction from the  $J/\psi$  exchange in Ref. [451] and found that the  $Z_c(3900)$  can be interpreted as a resonance above the threshold from the  $D\bar{D}^*$  interaction. In Ref. [400], Karliner and Rosner interpreted the  $Z_c(3900)$ , together with the  $X(3872)$ , as weakly bound molecular states with the  $D\bar{D}^*$  component and the  $Z_c(4020)/Z_c(4025)$  as a  $D^*\bar{D}^*$  molecular state.

The molecular type of interpolating currents were employed to investigate the  $Z_c(3900)$  and  $Z_c(4020)$  states in QCD sum rules in Refs [410, 411, 452, 453, 408, 409, 454, 455]. The extracted mass agrees with the experimental values within errors. However, one should be cautious in the interpretation of the extracted resonances as the molecular states even if the color singlet-singlet ( $\mathbf{1}_{[q\bar{c}]} \otimes \mathbf{1}_{[c\bar{q}]}$ ) molecular type of interpolating currents were used. The four quarks in the currents have the same space-time position. Moreover, the interpolating current “sees” only the quantum numbers of the resonance. Different interpolating currents with the same quantum numbers can generally couple to the same physical state.

#### 4.2.2. Tetraquark state assignment

4.2.2.1. *QCD sum rules.* In 2010, Chen and Zhu studied the mass spectrum of the hidden-charm tetraquark states with  $J^{PC} = 1^{+-}$  in QCD sum rules in Ref. [420]. They used the interpolating currents listed in Eq. (123). The numerical results are collected in Table 20. Later in Refs. [410, 411], the interpolating currents listed in Eq. (125) with the color octet-octet ( $\mathbf{8}_{[q\bar{c}]} \otimes \mathbf{8}_{[c\bar{q}]}$ ) configuration were also used. The results are collected in Table 21. The extracted masses of the  $J^{PC} = 1^{+-}$  hidden-charm tetraquark states are roughly consistent with the masses of the  $Z_c(3900)$  and  $Z_c(4020)/Z_c(4025)$ . There were some other QCD sum rule investigations of the charged  $Z_c$  mesons as charmonium-like tetraquarks in Refs [456, 457, 458].

Table 20: Numerical results for the  $J^{PC} = 1^{+-}$  hidden-charm tetraquark states with the diquark-antidiquark interpolating currents [420].

	Current	$s_0(\text{GeV}^2)$	Borel window ( $\text{GeV}^2$ )	$m_X$ (GeV)	PC(%)
$qc\bar{q}\bar{c}$	$J_{3\mu}$	$4.6^2$	3.0 – 3.4	$4.16 \pm 0.10$	46.2
	$J_{4\mu}$	$4.5^2$	3.0 – 3.3	$4.02 \pm 0.09$	44.6
	$J_{5\mu}$	$4.5^2$	3.0 – 3.4	$4.00 \pm 0.11$	46.0
	$J_{6\mu}$	$4.6^2$	3.0 – 3.4	$4.14 \pm 0.09$	47.0
$sc\bar{s}\bar{c}$	$J_{3\mu}$	$4.7^2$	3.0 – 3.6	$4.24 \pm 0.10$	49.6
	$J_{4\mu}$	$4.6^2$	3.0 – 3.5	$4.12 \pm 0.11$	47.3
	$J_{5\mu}$	$4.5^2$	3.0 – 3.3	$4.03 \pm 0.11$	44.2
	$J_{6\mu}$	$4.6^2$	3.0 – 3.4	$4.16 \pm 0.11$	46.0

4.2.2.2. *Diquark model.* The  $Z_c(3900)$  and  $Z_c(4020)/Z_c(4025)$  were interpreted as tightly bound tetraquark states composed of diquarks. In Refs. [459, 460], Maiani *et al.* interpreted the  $Z_c(3900)$  as a diquark-antidiquark charmonium-like tetraquark state and investigated its decay modes. This idea was further developed in Ref. [366], where Maiani, Piccinini, Polosa and Riquer proposed a “type-II” diquark-antidiquark model. This is the extension of their “type-I” diquark-antidiquark model [363], which will be discussed in Sec. 4.5.2. In this model, the S-wave tetraquarks can be written in the spin basis as  $|s, \bar{s}\rangle_J$ , where  $s = s_{qc}$  and  $\bar{s} = s_{\bar{q}\bar{c}}$  are the diquark and antidiquark spins, respectively. The authors identified the  $X(3872)$  to be  $X_1 = \frac{1}{\sqrt{2}}(|1, 0\rangle_1 + |0, 1\rangle_1)$ , and the  $Z_c(3900)$  and  $Z_c(4020)$  to be the linear

Table 21: Numerical results for the  $J^{PC} = 1^{+-}$  hidden-charm tetraquark states with the color octet-octet interpolating currents [410, 411].

Current	$s_0(\text{GeV}^2)$	Borel window ( $\text{GeV}^2$ )	$m_X$ (GeV)	$f_X$ ( $10^{-2}\text{GeV}^5$ )
$J_{1\mu}^{(8)}(D\bar{D}^*)$	18	2.8 – 3.7	$3.90 \pm 0.12$	$0.69 \pm 0.21$
$J_{3\mu}^{(8)}(D^*\bar{D}^*)$	18	3.1 – 3.9	$3.85 \pm 0.11$	$1.51 \pm 0.46$
$J_{4\mu}^{(8)}(D_1\bar{D}_1)$	20	2.8 – 3.1	$4.03 \pm 0.18$	$0.59 \pm 0.23$

combinations of  $Z = \frac{1}{\sqrt{2}}(|1, 0\rangle_1 - |0, 1\rangle_1)$  and  $Z' = |1, 1\rangle_1$ . They further used the approximation that the dominant spin interactions are within each diquark:

$$H \approx 2\kappa_{qc} (s_q \cdot s_c + s_{\bar{q}} \cdot s_{\bar{c}}) = \kappa_{qc} [s(s+1) + \bar{s}(\bar{s}+1) - 3], \quad (132)$$

which leads to

$$X(3872) = X_1, Z(3900) \approx Z, Z(4020) \approx Z' \quad (133)$$

with the mass ordering

$$M(X_1) \approx M(Z), M(Z') - M(Z) \approx 2\kappa_{qc}. \quad (134)$$

The parameter  $\kappa_{qc}$  is fixed to be 67 MeV. There are three other  $S$ -wave tetraquarks:  $X_0 = |0, 0\rangle_0$ ,  $X'_0 = |1, 1\rangle_0$  and  $X_2 = |1, 1\rangle_2$ , with the masses  $M(X_0) \approx 3770$  MeV and  $M(X'_0) = M(X_2) \approx 4000$  MeV. The last two states,  $X'_0$  and  $X_2$ , are identified with the  $X(3940)$  and  $X(3916)$ , while the first one  $X_0$  has a smaller mass than that of the  $X(3872)$  and not yet identified. In this scheme, the authors identified the  $Z^+(4430)$  to be the first radial excitation of the  $Z(3900)$ , which will be reviewed in Sec. 4.3.2.

The same diquark-antidiquark picture is used in Ref. [461] to study the  $Z_c(3900)/Z_c(3885)$  and  $Z_c(4020)/Z_c(4025)$  states. In Ref. [461], Patel, Shah, and Vinodkumar used the non-relativistic interaction potential

$$V(r) = V_V + V_S = k_s \frac{\alpha_s}{r} + \sigma r, \quad (135)$$

which is just the Cornell potential consisting of the Coulomb potential and the linear confining potential. They assigned the  $Z_c(3900)$  and  $Z_c(4025)$  as  $Q\bar{Q} - \bar{Q}q$  molecular-like four quark states, and the  $Z_c(3885)$  as a diquark-antidiquark tetraquark state.

In Ref. [462], Deng, Ping, Huang, and Wang systematically investigated the charged tetraquark states  $[cu][\bar{c}\bar{d}]$  using the color flux-tube model with a four-body confinement potential. Their Hamiltonian was given as follows:

$$H_4 = \sum_{i=1}^4 \left( m_i + \frac{\mathbf{p}_i^2}{2m_i} \right) - T_C + \sum_{i>j}^4 V_{ij} + V_{min}^C + V_{min}^{C,SL}, \quad (136)$$

where  $T_C$  is the center-of-mass kinetic energy of the state, and  $V_{min}^C$  ( $V_{min}^C$  and  $V_{min}^{C,SL}$ ) is the quadratic confinement potential.  $V_{ij}$  contains the one-boson-exchange potential  $V_{ij}^B$ , the  $\sigma$ -meson exchange potential  $V_{ij}^\sigma$ , the one-gluon-exchange potential  $V_{ij}^G$ . They identified the  $Z_c(3900)/Z_c(3885)$  as the tetraquark state  $[cu][\bar{c}\bar{d}]$  with the quantum numbers  $1^3S_1$  and  $J^P = 1^+$ , and the  $Z_c(4020)/Z_c(4025)$  as the tetraquark state  $[cu][\bar{c}\bar{d}]$  with  $1^5S_2$  and  $J^P = 2^+$ . This is an extension of their previous study [463], where Deng, Ping, and Wang interpreted the  $Z_c(3900)$  and  $Z_c(4025)/Z_c(4020)$  as the  $S$ -wave tetraquark states  $[cu][\bar{c}\bar{d}]$  with quantum numbers  $I = 1$  and  $J = 1$  and 2, respectively.

Within the framework of the color-magnetic interaction, the mass spectra of the hidden-charm and hidden-bottom tetraquark states were studied systematically by Zhao, Deng and Zhu in Ref. [464]. They considered the chromomagnetic interaction which was derived from one gluon exchange

$$H_{CM} = - \sum_{i>j} v_{ij} \vec{\lambda}_i \cdot \vec{\lambda}_j \vec{\sigma}_i \cdot \vec{\sigma}_j, \quad (137)$$

where  $\vec{\lambda}_i$  is the quark color operator and  $\vec{\sigma}_i$  the spin operator. For the tetraquark system  $q_1q_2\bar{q}_3\bar{q}_4$  with four different flavors, the interaction matrix element between two  $SU(6)_{cs}$  eigenstates  $|k\rangle$  and  $|l\rangle$  is

$$V_{CM}(q_1q_2\bar{q}_3\bar{q}_4) = \langle k|H_{CM}|l\rangle = V_{12}(q_1q_2) + V_{13}(q_1\bar{q}_3) + V_{14}(q_1\bar{q}_4) + V_{23}(q_2\bar{q}_3) + V_{24}(q_2\bar{q}_4) + V_{34}(\bar{q}_3\bar{q}_4). \quad (138)$$

They considered the configurations  $qc\bar{q}\bar{c}$ ,  $qc\bar{s}\bar{c}$ ,  $sc\bar{s}\bar{c}$ ,  $qb\bar{q}\bar{b}$ ,  $qb\bar{s}\bar{b}$ ,  $sb\bar{s}\bar{b}$  with  $J^P = 1^+, 0^+, 2^+$ . They used two schemes and found that it was impossible to accommodate all the three charged states  $Z_c(3900)$ ,  $Z_c(4025)$  and  $Z_c(4200)$  as tightly bound tetraquark states, and at least one or two of these states is a molecular state or some other structures. Furthermore, they tended to conclude that both the  $Z_c(3900)$  and  $Z_c(4025)$  are good molecular candidates, while the  $Z_c(4200)$  is a very promising candidate of the lowest axial-vector hidden-charm tetraquark state.

The internal structure of the  $Z_c(3900)$  was discussed in Ref. [465] by Voloshin. To differentiate the molecular model as well as the hadro-charmonium and tetraquark schemes, he urged the measurements of the quantum numbers of the resonance and its decay rates into yet unseen channels  $\pi\psi'$ ,  $\pi h_c$ ,  $\rho\eta_c$  and into pairs of heavy mesons  $D^*\bar{D}$  and  $D\bar{D}^*$ .

### 4.2.3. Kinematical effect

**4.2.3.1. ISPE mechanism.** The ISPE mechanism was also used to study the hidden-charm dipion decays of higher charmonia [466]. The line shapes of  $d\Gamma/dm_{J/\psi\pi^+}$ ,  $d\Gamma/dm_{\psi(2S)\pi^+}$  and  $d\Gamma/dm_{h_c(1P)\pi^+}$  of the  $\psi(4040)$ ,  $\psi(4160)$ ,  $\psi(4415)$ ,  $Y(4260)$  decays into  $J/\psi\pi^+\pi^-$ ,  $\psi(2S)\pi^+\pi^-$ ,  $h_c(1P)\pi^+\pi^-$  showed the existence of the charged charmonium-like structures near the  $D\bar{D}^*$  and  $D^*\bar{D}$  thresholds [466]. The  $h_c\pi^\pm$  mass distribution of  $\psi(4160) \rightarrow h_c(1P)\pi^+\pi^-$  (red solid line) from the ISPE mechanism [466] agrees roughly with the measurement by CLEO-c [467] (see Fig. 48). The  $Z_c(3900)$  structure and its reflection observed by the BESIII and Belle collaborations in  $Y(4260) \rightarrow \pi^+\pi^-J/\psi$  [53, 113] can also be reproduced with the ISPE mechanism [468]. The results are shown in Fig. 49.

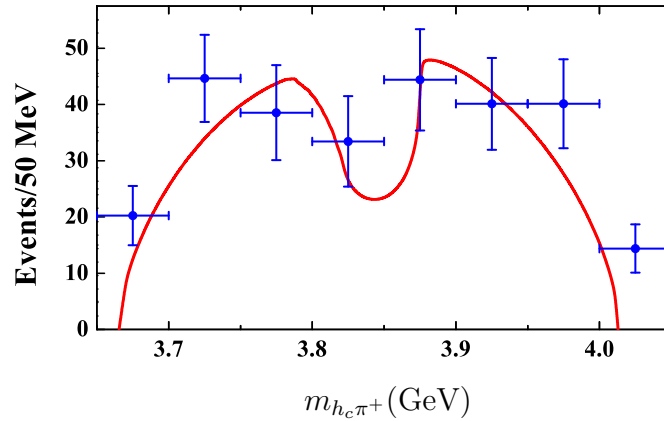


Figure 48: (Color online) A comparison of the  $h_c\pi^\pm$  mass distribution of  $\psi(4160) \rightarrow h_c(1P)\pi^+\pi^-$  (red solid line) from the ISPE mechanism and measurement by CLEO-c (blue points with errors) [467]. Taken from Ref. [466].

**4.2.3.2. Coupled channel cusp.** In Ref. [429], Swanson proposed the charged  $Z_c(3900)$  and  $Z_c(4025)$  states as the coupled channel cusp [429]. He pointed out that similar  $Z_c$  structures may exist in  $\bar{B}^0 \rightarrow J/\psi\pi^0\pi^0$  and  $B^\pm \rightarrow J/\psi\pi^\pm\pi^0$ . Neutral charmonium-like structures may exist near the  $D_s\bar{D}_s^*$  and  $D_s^*\bar{D}_s$  thresholds in  $\bar{B}_s \rightarrow J/\psi\phi\phi$  and  $\bar{B}^0 \rightarrow J/\psi\phi K$  decays, and near the  $D\bar{D}^*$ ,  $D^*\bar{D}$ ,  $D_s\bar{D}_s^*$  and  $D_s^*\bar{D}_s$  thresholds in  $\bar{B}_0 \rightarrow J/\psi\eta K$ . Later, Szczepaniak also indicated that triangle singularities would give considerable contributions to the  $Z_c(3900)$  [428]. However, Guo *et al.* insisted that these XYZ states cannot be purely kinematic effects, and the genuine S-matrix poles corresponding to states should be introduced [381]. In Ref. [469], Swanson used a causal and analytic model of final state rescattering to describe the current experimental data on the  $Z_c(3900)$  and  $Z_c(4025)$  without poles in the scattering matrix. In Ref. [470], the authors analyzed the  $Z_c^\pm(3900)/Z_c^\pm(3885)$  structure using both energy dependent and independent  $D\bar{D}^*$  S-wave interaction. The authors noticed that the  $Z_c$  peak is either due to a resonance with a mass around the  $D\bar{D}^*$  threshold or arises from a virtual state of the molecular nature. They concluded that a  $\bar{D}^*D$  bound state solution is not allowed.

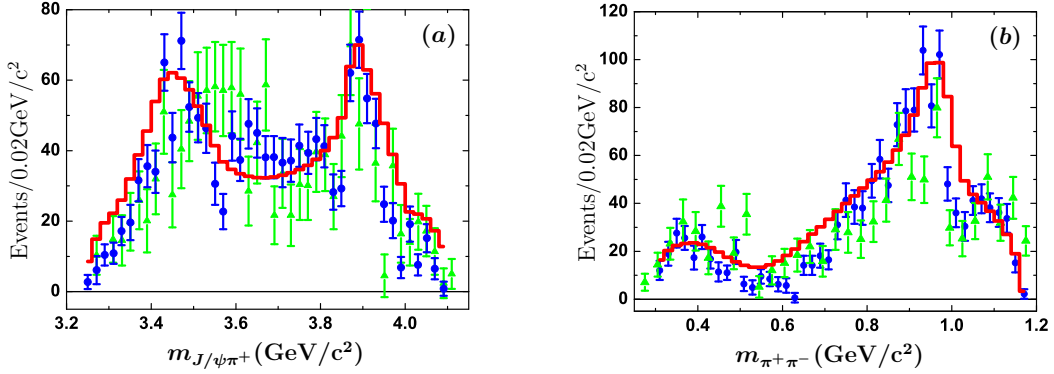


Figure 49: (Color online) The distributions of the  $J/\psi\pi^+$  and  $\pi^+\pi^-$  invariant mass spectra of  $Y(4260) \rightarrow \pi^+\pi^- J/\psi$ . The blue dots and green triangles with error bars are the experimental data given by BESIII [53] and Belle [113], respectively. The red histograms are our results considering contributions of the ISPE mechanism to the  $Y(4260) \rightarrow \pi^+\pi^- J/\psi$  decay. Taken from Ref. [468].

#### 4.2.4. Production and decay patterns

Under the  $D^*\bar{D}^*$  molecular state assumption, the pionic, dipionic, and radiative decays of the  $Z_c(3900)$  and  $Z_c(4025)$  and their productions via excited charmonia decays were studied extensively with the spin rearrangement scheme in Refs. [157, 436, 437]. The electromagnetic structure of the  $Z_c(3900)$  as an axial vector molecule was discussed using an effective theory with contact interactions in Ref. [471]. Hidden-charm decays of the  $Z_c(3900)$  and  $Z_c(4025)$  were investigated via the intermediate  $D^{(*)}\bar{D}^{(*)}$  meson loop in Ref. [472]. Strong decays of the  $Z_c(3900)$  were studied using a phenomenological Lagrangian approach by Dong *et al.* in Ref. [473]. The decay rates of the  $Z_c(3900)$  to  $J/\psi\pi$ ,  $\psi(2S)\pi$ ,  $\eta_c\rho$  and  $D^*\bar{D}^*$  were studied within the light front model in Ref. [474]. The  $Z_c(3900)/Z_c(4020) \rightarrow \eta_c\rho$  decays were studied within both tetraquark and molecular pictures in Ref. [475]. Radiative and dilepton decays of the  $Z_c(3900)$  were studied using a phenomenological Lagrangian approach in Ref. [476]. Radiative decays of the neutral  $Z_c(3900)$  were studied in a hadronic molecule scenario in Ref. [477].

The photoproduction of the  $Z_c(3900)$  in the  $\gamma p \rightarrow Z_c(3900)^+n$  process was proposed in Ref. [478]. The possible contribution of the  $Z_c(4025)$  resonance in the  $e^+e^- \rightarrow (D^*\bar{D}^*)^\pm\pi^\mp$  reaction was reanalyzed in Ref. [479].

#### 4.2.5. A short summary

- The  $Z_c(3900)$  and  $Z_c(4025)$  structures may arise from some kinematical effects, such as the ISPE mechanism, triangle singularities, and coupled channel cusp effects.
- There exists the long-range attraction due to the pion exchange in the isovector  $J^P = 1^+ D\bar{D}^*$  and  $D^*\bar{D}^*$  systems. However, the attraction may not be strong enough to form molecular bound states. The  $Z_c(3900)$  and  $Z_c(4025)$  states may be molecular resonances.
- In the diquark-antidiquark model, the  $Z_c(3900)$  and  $Z(4020)/Z_c(4025)$  were interpreted as the S-wave tetraquark states. To explain their narrow decay widths and the dominance of the open-charm decay modes, very special dynamics has to be introduced such as the existence of the tightly bound diquarks.

### 4.3. $Z^+(4430)$

#### 4.3.1. Molecular state scheme

4.3.1.1.  $\bar{D}_1 D^*$  molecule. After its discovery, the subsequent experimental progress on the  $Z^+(4430)$  was accompanied by surprises. There are valuable lessons for us to learn from the history of this interesting particle.

After the observation of the  $Z^+(4430)$  [92], Meng and Chao suggested the  $Z^+(4430)$  as the S-wave  $\bar{D}_1 D^*$  (or  $\bar{D}'_1 D^*$ ) molecular state in Ref. [188] since the  $Z^+(4430)$  is close to the  $D^*(2010)D_1(2420)$  and  $D^*(2010)D'_1(2430)$  thresholds. Under this assignment, the  $Z^+(4430)$  can be produced through the  $B^+$  decay. The branching ratio of the Cabibbo-Kobayashi-Maskawa (CKM) favored decay mode  $B^+ \rightarrow \bar{D}^{*0}(2010)D_s^{*+}$  is large, where the  $D_s^{*+}$  denotes the

ground or excited state, which can decay into  $D^+K^0$  and  $D^0K^+$  or  $D_1^+(2420)K^0$  and  $D_1^0(2420)K^+$ . The  $Z^+(4430)$  can be formed in the  $\bar{D}^{*0}D_1^+(2420)$  scattering process [188]. This scheme was also proposed by Rosner in Ref. [480].

To answer whether the  $\bar{D}_1(\bar{D}'_1)$  and  $D^*$  interaction is strong enough to form a bound state corresponding to the  $Z^+(4430)$ , the dynamical calculation of the S-wave  $\bar{D}_1D^*$  (or  $\bar{D}'_1D^*$ ) system with  $J^P = 0^-, 1^-, 2^-$  was carried out with the OPE model [189], where  $D'_1$  and  $D_1$  belong to  $(0^+, 1^+)$  and  $(1^+, 2^+)$  doublets, respectively. The potential from the crossed diagram is much larger than that from the diagonal scattering diagram. With various trial wave functions, the numerical results indicated that the attraction from the OPE potential alone is not strong enough to form a bound state with realistic pionic coupling constants deduced from the decay widths of  $D_1$  and  $D'_1$  [189].

Later, the authors of Ref. [190] reexamined this issue by considering both the pion and  $\sigma$  meson exchange potentials, where the form factor was introduced to take into account the structure effect of the interaction vertex. Different from the treatment in Ref. [189], the authors solved the Schrödinger equation with the obtained effective potentials [190]. They found the OPE potential from the crossed diagram plays a dominant role in the formation of the S-wave  $\bar{D}'_1D^*$  or  $\bar{D}_1D^*$  molecular system. There exists the bound state solution for the S-wave  $\bar{D}'_1D^*$  system with  $J^P = 0^-, 1^-, 2^-$ , where the contribution from the  $\sigma$  meson exchange is small. Whether the broad width of  $D'_1$  disfavors the formation of a molecular state should be carefully studied in the future [190]. The S-wave  $\bar{D}_1D^*$  molecular state with  $J^P = 0^-$  may exist if taking appropriate parameters as input. Different from the case of the S-wave  $\bar{D}'_1D^*$  system, the contribution from the  $\sigma$  meson exchange is significant for the S-wave  $\bar{D}_1D^*$  molecular state.

Ding *et al.* [216] also studied the  $D^*\bar{D}_1$  interaction in the quark model. The interaction between a quark and an antiquark includes the short distance one-gluon exchange potential and the long distance confinement interaction [216]. After solving the multichannel Schrödinger equation, they found that the  $Z^+(4430)$  can be explained as a loosely  $\bar{D}_1D^*$  molecular state with  $J^P = 0^-$  [216], which is consistent with the conclusion from the OPE model [190]. In Refs. [481, 482], the  $Z^+(4430)$  was proposed as a  $D^*\bar{D}_1$  molecule with  $J^P = 0^-$  using the molecular type of interpolating currents in QCD sum rules.

Liu and Zhang applied a chiral quark model to study the S-wave  $D_1\bar{D}^*$  ( $D'_1\bar{D}^*$ ) system by solving the resonating group method equation [214]. Their results disfavored the assignment of the  $Z^+(4430)$  as the S-wave  $D_1\bar{D}^*$  ( $D'_1\bar{D}^*$ ) molecular state [214]. Later in Ref. [483], Li *et al.* used the SU(3) chiral quark model to study the interaction potentials between one S-wave and one P-wave heavy mesons systematically. Their results also disfavored the assumption that the  $Z^+(4430)$  as an isovector  $D_1\bar{D}^*$  charged molecule.

The quenched lattice QCD using Lüscher formalism was adopted to study the interaction between the  $D^*$  and  $\bar{D}_1$  in Ref. [484]. The authors concluded that the interaction of  $D^*$  and  $\bar{D}_1$  is attractive in the  $J^P = 0^-$  channel but not strong enough to form a bound state [484]. Both the phenomenological models [189, 190, 216, 214] and the quenched lattice QCD calculation [484] indicated that the S-wave  $D_1\bar{D}^*$  interaction is attractive. The authors of Ref. [485] proposed that the  $Z^+(4430)$  is either a  $D^*\bar{D}_1$  state dominated by the long-range pion exchange, or a  $D\bar{D}^*(1S, 2S)$  state with important short-range components.

*4.3.1.2.  $Z^+(4430)$  as a  $J^P = 1^+$  molecule.* After Belle and LHCb established its spin-parity  $J^P = 1^+$ , it is obvious that the S-wave  $\bar{D}_1D^*$  (or  $\bar{D}'_1D^*$ ) molecular state assignment of the  $Z^+(4430)$  does not hold. The authors of Ref. [486] proposed three possible molecular configurations: (1) the  $Z^+(4430)$  as the P-wave excitation of the S-wave  $D_1\bar{D}^*$  or  $D_2\bar{D}^*$  molecule; (2) the  $Z^+(4430)$  as the S-wave molecule composed of a  $D$  or  $D^*$  meson and a D-wave vector  $D$  meson; (3) the  $Z^+(4430)$  as the cousin molecular state of the  $Z_c(3900)$  and  $Z_c(4020)$  composed of a  $D$  or  $D^*$  meson and their radial excitations. In the heavy quark symmetry, they further investigated the radiative and strong decay patterns of the  $Z^+(4430)$ , and found [486]

- If the charm quark mass goes to infinity and heavy quark symmetry is exact, the S-wave molecule composed of a  $D$  or  $D^*$  meson and a D-wave vector  $D$  meson does not decay into the  $\psi'\pi$  final states, which is the discovery mode of the  $Z^+(4430)$ . Unfortunately, the charm quark is only 1.5 GeV.
- The  $Z^+(4430)$  could be the P-wave excitation of the  $D_1\bar{D}^*$  or  $D_2\bar{D}^*$  molecule, their radiative and strong decay patterns can be investigated with the spin rearrangement scheme in the heavy quark symmetry limit, together with their S-wave molecular ground states. Their radiative decays are presented in Ref. [436]. Within this scheme, the non-observation of the  $Z^+(4430)$  in the  $J/\psi\pi$  mode is always a serious challenge. There exists no manifest symmetry forbidding this mode. The same challenge holds for the tetraquark interpretation. Moreover, if the  $Z^+(4430)$  is the P-wave molecule, where is the ground state?

- If the  $Z^+(4430)$  happens to be the molecular cousin of the  $Z_c(3900)$  and  $Z_c(4020)$  composed of a  $D$  or  $D^*$  meson and their radial excitations, it would decay into the  $J/\psi\pi$  and  $\psi'\pi$  easily. However, it would not decay into the  $\psi(1^3D_1)\pi$  in the heavy quark symmetry limit. The neutral component will also decay into the  $\chi_{cJ}$  through the  $M1$  transition. The resulting decay width ratio is 1:3:5. Since the  $Z^+(4430)$  contains one radial excitation as its molecular component, one may expect that the  $Z^+(4430)$  may decay into the final state containing a radial excitation more easily.

#### 4.3.2. The tetraquark assignment

In Ref. [459], Maiani, Polosa and Riquer suggested the  $Z^+(4430)$  as the first radial excitation of the tetraquark basic supermultiplet to which the  $X(3872)$  belong. Later in their “type-II” diquark-antidiquark model [366], reviewed in Sec. 4.2.2, Maiani *et al.* identified the  $Z^+(4430)$  as the first radial excitation of the  $Z(3900)$ . The mass difference between the  $Z_c(4430)$  and  $Z_c(3900)$  is 593 MeV, which is very close to the mass difference between the  $\psi(2S)$  and  $\psi(1S)$  with 589 MeV.

A similar but relativistic diquark-antidiquark picture was proposed in Ref. [487], where Ebert, Faustov, and Galkin calculated the masses of the excited heavy tetraquarks with hidden-charm in the diquark-antidiquark picture. They used the dynamical approach based on the relativistic quark model, and took into account the diquark structure by calculating the diquark-gluon form factor. They used  $S$  and  $A$  to denote scalar and axial vector diquarks which are flavour antisymmetric and symmetric, respectively. Their studies suggested that the  $Z^+(4430)$  can be either the  $1^+ 2S [cu][\bar{c}\bar{d}]$  tetraquark state consisting of  $(S\bar{A} - \bar{S}A)/\sqrt{2}$ , or the  $0^+ 2S [cu][\bar{c}\bar{d}]$  consisting of  $A\bar{A}$ .

In Ref. [461], Patel, Shah, and Vinodkumar once more identified the  $Z^+(4430)$  as the first radial excitation of the  $Z_c(3885)$  using a non-relativistic quark model. Later in Ref. [488], Hadizadeh and Khaledi-Nasab studied heavy tetraquarks with hidden-charm and hidden-bottom by solving the homogeneous Lippmann-Schwinger integral equation in momentum space. The  $Z^+(4430)$  was again explained as the  $2S c\bar{q}\bar{c}\bar{q}$  tetraquark state consisting of  $A\bar{A}$ , with  $A$  the axial vector diquark. Its mass was evaluated to be 4535 MeV and 4469 MeV from nonrelativistic and relativistic Lippmann-Schwinger equations, respectively.

Hence, the idea that the  $Z^+(4430)$  is the first radial excitation of the tetraquark basic supermultiplet to which the  $X(3872)$  and  $Z_c(3900)$  belong is accepted in many models which interpreted the charged charmonium-like states as the tightly bound diquark-antidiquark states. However, in Ref. [462], Deng *et al.* systematically investigated the charged tetraquark states  $[cu][\bar{c}\bar{d}]$  using the color flux-tube model with a four-body confinement potential. They can not describe the  $Z^+(4430)$  as such a tetraquark state.

Especially, the Belle experiment measured the ratio  $\mathcal{B}(Z^+(4430) \rightarrow \psi(2S)\pi^+)/\mathcal{B}(Z^+(4430) \rightarrow J/\psi\pi^+)$  to be about 10 [489]. As discussed in Ref. [490], it would be extremely challenging to accommodate this ratio if the  $Z_c(4430)$  is an S-wave tetraquark ground state or its radial excitation. Hence, the tetraquark interpretations of the  $Z_c(3900)$  (as the ground state of the  $Z^+(4430)$ ) and its partner  $X(3872)$ , would be crucial for the diquark-antidiquark picture, which has been/will be reviewed in Sec. 4.2.2 and Sec. 4.5.2, respectively.

Assuming the  $Z^+(4430)$  to be a tetraquark bound state made up of  $(cu)(\bar{c}\bar{d})$ , its bottom partners were investigated in Ref. [491]. First, Cheung, Keung, and Yuan replaced one of the charm quarks by a bottom quark, and obtained the mass of  $Z_{bc}$  to be around 7.6 GeV. Then, they replaced both the charm quark and antiquark by the bottom quark and antiquark, and obtained the mass of  $Z_{bb}$  to be about 10.7 GeV. They also proposed two channels to observe them, i.e.,  $Z_{bc}^{++} \rightarrow B_c^+(2^3S_1)\pi^+$  and  $Z_{bb}^+ \rightarrow \Upsilon(2S)\pi^+$ .

To distinguish whether the tetraquarks are segregated into di-meson molecules, diquark-antidiquark pairs, or more democratically arranged four-quark states, Brodsky and Lebed proposed a number of experimentally straightforward and feasible tests in Ref. [492], which can be applied to tetraquark candidates such as the  $X(3872)$  and  $Z^+(4430)$ . A new dynamical picture was introduced in Ref. [493], where Lebed proposed that some subset of charmonium-like states are bound (not molecular) states of color  $\mathbf{3} - \bar{\mathbf{3}}$  compact diquarks, which have achieved substantial separation due to the large energy release of the process in which they are formed. This mechanism relies on the existence of compact diquarks and gives a qualitative picture of the strong preference of the  $Z^+(4430)$  to decay to the  $\psi(2S)$  rather than the  $J/\psi$ . However, a dynamical quantitative calculation is still missing.

#### 4.3.3. Cusp effect

Besides the above exotic assignments, the  $Z^+(4430)$  was proposed as the  $D^*(2010)\bar{D}_1(2420)$  threshold cusp effect in Ref. [494]. The author adopted the unitarized quark model [495] with the T-matrix method. The  $Z(4430)$  structure

in the Belle data could be reproduced by either a resonance or a bare cusp. For the later case, although there was no second or third-sheet pole in the vicinity of the cusp, the Argand diagram and the peak were all reproduced well.

#### 4.3.4. Production, decay patterns, and other theoretical schemes

The  $Z^+(4430)$  was also studied using various theoretical frameworks, including the utilization of the SU(3) flavor symmetry [496], the large N scalar QCD in two dimensions [497], the semirelativistic quark potential model [498], and the  $\pi\psi'$  interaction [499].

In Ref. [500], Liu, Zhao, and Close studied the photoproduction of the  $Z^+(4430)$  in the  $\gamma p \rightarrow Z^+(4430)n \rightarrow \psi'\pi^+n$  process. This process was further studied in Ref. [501], where Galata presented a model for high energy and forward angle  $Z^+(4430)$  photoproduction in an effective Lagrangian approach.

In Ref. [502], Ke and Liu studied the  $Z^+(4430)$  in the nucleon-antinucleon scattering, and discussed the production of the  $Z^+(4430)$  in the PANDA experiment. Productions of the neutral  $Z^0(4430)$  in  $p\bar{p} \rightarrow \psi'\pi^0$  reaction was discussed using an effective Lagrangian in Ref. [503]. The  $(D\bar{D}^*)^+ \rightarrow \psi(2S)\pi^+$  rescattering process in the decay chain  $B \rightarrow D_s(2S)^-D$ ,  $D_s(2S)^- \rightarrow \bar{D}^*K$  was investigated to explain the peak structure in the  $\psi(2S)\pi^+$  mass spectrum around 4.43 GeV in Refs. [504, 505].

The decay properties of the  $Z^+(4430)$  were generally discussed under the QCD-string based explanation in Ref. [506]. The hidden-charm and radiative decays of the  $Z^+(4430)$  were studied in Ref. [507], and its open-charm decays were studied in Ref. [508], assuming it as a  $D_1\bar{D}^*$  molecular state. Line shapes of the  $Z^+(4430)$  in the  $\psi'\pi^+$  decay channel and in  $D^*\bar{D}^*\pi$  decay channels were investigated in Ref. [509]. The typical radiative and hidden-charm and open-charm strong decay patterns of the  $Z^+(4430)$  were investigated with the help of the heavy quark symmetry in Ref. [486]. The phase motion in the  $Z^-(4430)$  amplitude in the  $B^0 \rightarrow \psi'\pi^-K^+$  decay was studied using the isobar-based amplitude difference method in Ref. [510].

#### 4.3.5. A short summary

- Some model calculations and one quenched lattice QCD calculation indicated that the S-wave  $D_1\bar{D}^*$  interaction is attractive. There may exist bound states in the S-wave and P-wave  $\bar{D}_1D^*$  system. The  $Z^+(4430)$  may be the P-wave  $D_1\bar{D}^*$  or  $D_2\bar{D}^*$  molecular state.
- The  $Z^+(4430)$  may be the molecular cousin of the  $Z_c(3900)$  and  $Z_c(4020)$  composed of a  $D$  or  $D^*$  meson and their radial excitations, which decays into the  $J/\psi\pi$  and  $\psi'\pi$  easily. However, it will not decay into the  $\psi(1^3D_1)\pi$  in the heavy quark symmetry limit.
- In many diquark-antidiquark models, the  $Z^+(4430)$  was described as the first radial excitation of the basic tetraquark supermultiplet containing the  $X(3872)$  and  $Z_c(3900)$ .
- The presence of one radial excitation within the  $Z^+(4430)$  may help to explain the measured ratio  $\mathcal{B}(Z^+(4430) \rightarrow \psi(2S)\pi^+)/\mathcal{B}(Z^+(4430) \rightarrow J/\psi\pi^+)$ .

### 4.4. Other charged states: $Z^+(4051)$ , $Z^+(4248)$ and $Z^+(4200)$

#### 4.4.1. Molecular state scheme

Like the  $Z^+(4430)$ , the  $Z^+(4051)$  and  $Z^+(4248)$  must contain at least four quarks if they are resonances, which also inspired discussions whether they can be hadronic molecular states.

The possible molecular states composed of S-wave charmed and anti-charm mesons were systematically studied in Ref. [207], which can be categorized into a flavor octet and a singlet. Through the OBE model, the effective potentials were obtained to check whether the corresponding bound state solution can be found. The total effective potentials of the  $D^*\bar{D}^*$  systems with  $J = 0, 1$  and  $J = 2$  are attractive and repulsive in the range  $r < 1$  fm respectively (see Fig. 5 of Ref. [207]). They found that there does not exist the  $D^*\bar{D}^*$  molecular bound state with a reasonable cutoff, so the  $Z^+(4051)$  is probably not a molecular bound state [207]. However, the possibility of interpreting it as the  $D^*\bar{D}^*$  molecular resonance was still not excluded.

In Ref. [212], the authors systematically studied the bound state problem of the S-wave heavy meson-antimeson systems in a chiral SU(3) quark model by solving the resonating group method equation. There does not exist the isovector (charm-anticharm) molecular state. The assignment of the  $Z^+(4051)$  as an S-wave  $D^*\bar{D}^*$  molecule was

disfavored [212]. Moreover, the  $Z^+(4248)$  can not be explained as the  $D^*\bar{D}_0^*$  molecule according to the analysis in the chiral quark model [483]. The  $Z^+(4248)$  was suggested as a  $D_1\bar{D}$  molecular state using QCD sum rule approach [511]. Ding applied the OBE model to study the interaction between the  $D_1$  and  $\bar{D}$ , and he concluded that the  $Z^+(4248)$  as a  $D_1\bar{D}$  molecular state was disfavored due to the large cutoff [217].

Various theoretical investigations do not support the molecular assignment of the  $Z^+(4051)$  and  $Z^+(4248)$  [207, 212, 217].

#### 4.4.2. Tetraquark state assignment

The  $Z^+(4051)$  and  $Z^+(4248)$  were discussed as the diquark-antidiquark states in Refs. [487, 461, 462]. In Ref. [487], Ebert, Faustov, and Galkin found no tetraquark candidates for the  $Z^+(4051)$  structure, but they found that the  $Z^+(4248)$  can be interpreted as the charged partner of the  $1^- 1P [cu][\bar{c}\bar{d}]$  tetraquark state consisting of  $S\bar{S}$ , or the  $0^- 1P [cu][\bar{c}\bar{d}]$  tetraquark state consisting of  $(S\bar{A} \pm \bar{S}A)/\sqrt{2}$ , where  $S$  and  $A$  are the scalar and axial vector diquarks respectively. In Ref. [461], Patel, Shah, and Vinodkumar assigned the  $Z^+(4051)$  as a  $Q\bar{q} - \bar{Q}q$  molecular-like tetraquark state. In Ref. [462], Deng, Ping, Huang, and Wang identified the  $Z^+(4051)$  as the tetraquark state  $[cu][\bar{c}\bar{d}]$  with the quantum numbers  $1^3P_1$  and  $1^-$ , the  $Z^+(4248)$  as the tetraquark state  $[cu][\bar{c}\bar{d}]$  with  $1^5D_1$  and  $1^+$ , and the  $Z^+(4200)$  as the tetraquark state  $[cu][\bar{c}\bar{d}]$  with  $1^3D_1$  and  $1^+$ .

#### 4.4.3. Production and decay patterns

As a tetraquark state, the hadronic decays  $Z_c(4200)^+ \rightarrow J/\psi\pi^+$ ,  $Z_c(4200)^+ \rightarrow \eta_c\rho^+$  and  $Z_c(4200)^+ \rightarrow D^+\bar{D}^{*0}$  were calculated with the three-point functions in the framework of the QCD sum rules in Ref. [512]. The decay widths of the dominant decay modes  $\eta_c\rho$  and  $J/\psi\pi$  are 253 MeV and 87 MeV, respectively. Because of the suppression of the phase space, the decay width of its open-charm mode is around several MeV. Including all these channels, the full decay width of the  $Z_c(4200)^+$  state is consistent with the experimental value reported by the Belle Collaboration, supporting the tetraquark interpretation of the  $Z^+(4200)$  [512].

The photoproduction of the  $Z^+(4200)$  was investigated using an effective Lagrangian approach and the Regge trajectories model in Ref. [513]. Productions of the neutral  $Z^0(4200)$  in  $p\bar{p} \rightarrow J/\psi\pi^0$  reaction was discussed in Ref. [514]. The rescattering effects in the  $e^+e^- \rightarrow D^{(*)}\bar{D}^{(*)}$  process were investigated to understand the  $Z^+(4051)$ ,  $X(3872)$  and the relevant bound state problem in a meson exchange model in Ref. [515].

#### 4.4.4. A short summary

- Further experimental confirmation of the charged states  $Z^+(4051)$ ,  $Z^+(4248)$  and  $Z^+(4200)$  will be helpful.
- Various theoretical investigations do not support molecular assignments of the  $Z^+(4051)$  and  $Z^+(4248)$ .
- The tetraquark assignments for the  $Z^+(4051)$ ,  $Z^+(4248)$  and  $Z_c(4200)$  were discussed using several theoretical models.

### 4.5. $X(3872)$

As the first observed state in the  $XYZ$  family, the  $X(3872)$  has attracted extensive attentions from both theoretical and experimental groups all over the world. As shown in Sec. 2.1.1.1, the experimental information of the  $X(3872)$  is the most abundant among all the observed  $XYZ$  states. However, we still do not fully understand its nature, although more than ten years passed since its observation in 2003. During these years, various pictures/interpretations have been proposed to explain the nature of the  $X(3872)$ . In the following, we mainly focus on several popular theoretical schemes of the  $X(3872)$ , i.e., the  $D\bar{D}^*$  molecular state, the axial vector tetraquark assignment, and the radial excitation of the axial vector charmonium state, etc.

#### 4.5.1. Molecular scheme

Before reviewing the theoretical progress on the molecular assignment of the  $X(3872)$ , we note that the mass of the  $\chi'_{c1}(2P)$  charmonium state was estimated to be 3.95 GeV [17], which is significantly higher (around 80 MeV) than the observed mass of the  $X(3872)$  [1].

4.5.1.1. *Swanson's model.* Swanson proposed to interpret the  $X(3872)$  as a  $J^{PC} = 1^{++} D^0 \bar{D}^{*0}$  hadronic resonance stabilized by the admixture of  $\omega J/\psi$  and  $\rho J/\psi$  [184], due to the proximity of this state to the  $D\bar{D}^*$  threshold. He analysed the  $X(3872)$  based on a microscopic model, which incorporates both the quark exchange induced effective interaction

$$\sum_{i<j} \frac{\lambda(i)}{2} \cdot \frac{\lambda(j)}{2} \left\{ \frac{\alpha_s}{r_{ij}} - \frac{3}{4} br_{ij} - \frac{8\pi\alpha_s}{3m_i m_j} \mathbf{S}_i \cdot \mathbf{S}_j \left( \frac{\sigma^3}{\pi^{3/2}} \right) e^{-\sigma^2 r_{ij}^2} \right\}, \quad (139)$$

as well as the pion exchange induced effective interaction [173, 174, 516]

$$V_\pi = -\gamma V_0 \left[ \begin{pmatrix} 1 & 0 \\ 0 & 1 \end{pmatrix} C(r) + \begin{pmatrix} 0 & -\sqrt{2} \\ -\sqrt{2} & 1 \end{pmatrix} T(r) \right]. \quad (140)$$

He found that the quark exchange effects can cause binding in the coupled  $D\bar{D}^*$ ,  $\omega J/\psi$  or  $\rho J/\psi$  systems, but the potential depth is not sufficient to form a resonance. On the other hand, the pion exchange effects can not bind the  $D\bar{D}^*$  system with canonical parameters. However, the combined pion and quark induced effective interactions are sufficient to cause binding, and he found there is only one binding  $D\bar{D}^*$  state of  $1^{++}$ , which can be used to explain the  $X(3872)$ . He found no other  $J^{PC}$ , no charged modes, and no  $D\bar{D}$  molecules exist in this model.

Under this molecule picture, Swanson calculated the ratio of  $\mathcal{B}(X(3872) \rightarrow \psi' \gamma)$  with respect to  $\mathcal{B}(X(3872) \rightarrow J/\psi \gamma)$  to be  $4 \times 10^{-3}$  [184, 200], which largely deviated from the experimental data  $3.4 \pm 1.4$  [78] and  $2.46 \pm 0.64 \pm 0.29$  [81]. He derived the ratio of  $\mathcal{B}(X(3872) \rightarrow \gamma J/\psi)$  with respect to  $\mathcal{B}(X(3872) \rightarrow J/\psi \pi^+ \pi^-)$  to be around  $10^{-2}$  [184, 200], while the experimental value is  $0.14 \pm 0.05$  [64] and  $0.33 \pm 0.12$  [78]. Within this model, the ratio of  $\mathcal{B}(X(3872) \rightarrow D^0 \bar{D}^0 \pi^0)$  with respect to  $\mathcal{B}(X(3872) \rightarrow J/\psi \pi^+ \pi^-)$  was inconsistent with experimental data.

4.5.1.2.  *$X(3872)$  as the  $D\bar{D}^*$  molecule.* Wong [517] applied a quark-based model to study the molecular states composed of two heavy mesons, in terms of a four-body non-relativistic Hamiltonian with pairwise effective interactions. The calculated masses of the  $D^0 \bar{D}^{*0}$  and  $D^+ D^{*-}$  molecular systems are 3863.67 MeV and 3871.77 MeV, respectively. He suggested that the molecular states  $D^0 \bar{D}^{*0}$ ,  $D^+ \bar{D}^{*-}$ , and  $D^- \bar{D}^{*+}$  are mixed to form components of  $I = 0$  and  $I = 1$  states, and the  $I = 0$  state can be interpreted as the  $X(3872)$ .

Such a molecule assignment was used in many theoretical studies to investigate the  $X(3872)$ . The authors of Ref. [518] used an effective Lagrangian to describe the  $X(3872)$ , which is consistent with the heavy-quark and chiral symmetries needed. They modified the Weinberg's approach to describe bound states [519, 520], and found that the  $X(3872)$  can be a molecular bound state of the  $D^{*0}$  and  $\bar{D}^0$  mesons. They also proposed the molecular bound state  $X_b$  of the  $B^{*0}$  and  $\bar{B}^0$  with the mass of 10604 MeV. Fleming *et al.* [521] also developed an effective field theory of non-relativistic pions and  $D$  mesons, and applied it to describe the  $X(3872)$  as a bound state of the  $D^0 \bar{D}^{*0}$  and  $\bar{D}^0 D^{*0}$ . They calculated the next-to-leading-order correction to the partial decay width  $X(3872) \rightarrow D^0 \bar{D}^0 \pi^0$ .

However, Suzuki pointed out that some of the observed properties of the  $X(3872)$  are incompatible with the molecule interpretation [522]. Especially, there is no long-range force to bind the  $D$  and  $\bar{D}^*$  into a deuteron-like state, and the observed production rates of the  $X(3872)$  in  $B$  decay and  $pp$  collision are too large for a very loosely bound state. Alternately, he interpreted the  $X(3872)$  as the excited  $^3P_1$  charmonium state mixing with  $D$  and  $\bar{D}^*$  mesons. Detailed reviews about this charmonium picture can be found in Sec. 4.5.3.

At the same time, many experiments were devoted to study the  $X(3872)$ , and more and more experimental information was available. Some of them are very interesting, see reviews in Sec. 2.1.1.1. More research groups joined the debate on whether the interaction between the  $D$  and  $\bar{D}^*$  mesons is large enough to form a bound state.

The one pion exchange potential alone does not bind the proton and neutron pair into the deuteron, and the strong attractive force in the intermediate range has to be introduced in order to form the deuteron, which is modeled as the sigma meson exchange potential. This is well-known in nuclear physics. Liu *et al.* [201] performed a dynamical calculation of the  $D^0 \bar{D}^{*0}$  system taking into account both the pion and sigma meson exchange potential. Their analysis disfavored the interpretation of the  $X(3872)$  as a loosely bound molecular state with the experimental  $D^* D \pi$  coupling constant  $g = 0.59$  and a reasonable cutoff around 1 GeV. In contrast, they proposed that there exists a loosely bound  $S$ -wave  $B\bar{B}^*$  molecular state.

In Ref. [523], Thomas and Close studied the pion exchange between charm and bottom mesons. They found that the  $X(3872)$  can be a bound state, but the results are very sensitive to a poorly constrained parameter, such as a cutoff

Table 22: The different channels for Cases I, II, III and IV of the  $X(3872)$  with  $J^{PC} = 1^{++}$ . “-” means the corresponding channel does not exist. Taken from Ref. [222].

Cases	Channels					
	1	2	3	4	5	6
I	$[D^0\bar{D}^{*0}] ^3S_1\rangle$	$[D^0\bar{D}^{*0}] ^3D_1\rangle$	-	-	-	-
II	$(D\bar{D}^*) ^3S_1\rangle$	$(D\bar{D}^*) ^3D_1\rangle$	-	-	-	-
III	$(D\bar{D}^*) ^3S_1\rangle$	$(D\bar{D}^*) ^3D_1\rangle$	-	-	$\{D^*\bar{D}^*\}^3S_1\rangle$	$\{D^*\bar{D}^*\}^3D_1\rangle$
IV(Phy)	$[D^0\bar{D}^{*0}] ^3S_1\rangle$	$[D^0\bar{D}^{*0}] ^3D_1\rangle$	$[D^+D^{*-}] ^3S_1\rangle$	$[D^+D^{*-}] ^3D_1\rangle$	$\{D^*\bar{D}^*\}^3S_1\rangle$	$\{D^*\bar{D}^*\}^3D_1\rangle$

around 1500 MeV and the relatively large  $L = 2$  components, etc. They confirmed the results obtained in Ref. [201], as well as confirmed that bound states in the  $B\bar{B}$  sector are possible.

Later in Ref. [207], Liu *et al.* further considered the vector meson exchange, besides the pseudoscalar and scalar meson exchanges [201]. They applied this OBE model to systematically study possible molecular states composed of S-wave charmed and anti-charm mesons, such as the  $D\bar{D}$ ,  $D\bar{D}^*$ , and  $D^*\bar{D}^*$ . They found that the vector meson exchange provides strong attraction in the  $D^*\bar{D}$  system together with the pion exchange, and the  $X(3872)$  may be accommodated as a molecular state.

Lee *et al.* [204] also discussed this issue in the framework of a potential model generated by the exchange of pseudoscalar, scalar and vector mesons. They considered both charged and neutral  $D\bar{D}^*$  components, and both S-wave and D-wave contributions. Additionally, the isospin symmetry breaking effects were fully taken into account. Their result showed that there exists a bound state in the  $D\bar{D}^*$  system with  $J^{PC} = 1^{++}$  for a reasonable value of the meson-exchange regularization parameter,  $\Lambda \sim 1.2$  GeV. They also suggested that the  $B\bar{B}^*$  bound states can be bounded in the isoscalar limit for  $J^{PC} = 1^{++}$  and  $1^{+-}$ .

After the observation of the two charged  $Z_b$  states [161], the authors of Ref. [192] performed an extensive study of the possible  $B^*\bar{B}$ ,  $B^*\bar{B}^*$ ,  $D^*\bar{D}$ ,  $D^*\bar{D}^*$  molecule states in the framework of the OBE model. They considered neutral and charged  $D\bar{D}^*$  modes and S-wave and D-wave mixing. Their results indicated that there exists a bound state solution in the  $D\bar{D}^*$  system. See Table 18 in Sec. 4.2.1, where  $\Phi_8^*$  corresponds to the  $X(3872)$ .

The unitarized heavy meson chiral perturbation theory was applied in Ref. [524] by Wang and Wang to study the  $D\bar{D}^*$  scattering with the pion exchange and a contact interaction. They found a loosely bound state  $X(3872)$ , with the pole position being  $3871.70 - i0.39$  MeV, which is not sensitive to the strength of the contact interaction. Hence, their calculation provides a theoretical confirmation of the existence of the  $1^{++}$  state  $X(3872)$ , and the light quark mass dependence of the pole position indicates that the  $X(3872)$  has a predominately  $D\bar{D}^*$  molecular nature. Their analysis is reexamined in Ref. [525] by Baru *et al.* However, assuming the  $X(3872)$  to be a  $D\bar{D}^*$  molecular state, they concluded that the pion mass dependence of its pole position is expected to depend strongly on the pion mass dependence of the  $D\bar{D}^*$  interaction at short range. They also argued that a more deeply bound  $X(3872)$  for an increased pion mass as found in Ref. [526] does not contradict its molecular nature.

**4.5.1.3. Isospin violation, S-D wave mixing and coupled channel effects.** The authors of [222] further investigated the  $X(3872)$  as a  $J^{PC} = 1^{++}$   $D\bar{D}^*$  molecular state in the OPE model and the OBE model. They not only took into account the S-D wave mixing effect, but also considered the isospin breaking and the coupled-channel effect. In order to find out the specific role of the charged  $D\bar{D}^*$  mode, the isospin breaking and the channel coupling of the  $X(3872)$  to the  $D^*\bar{D}^*$  in forming the shallow bound state, the authors first considered the neutral component  $D^0\bar{D}^{*0}$  only and included the S-D wave mixing, which corresponds to Case I. Then the charged  $D^+D^{*-}$  component was added to form the exact  $D\bar{D}^*$  isospin singlet with the S-D mixing, which is Case II. Since the  $1^{++}$   $D^*\bar{D}^*$  channel lies only 140 MeV above and couples strongly to the  $D\bar{D}^*$  channel, the authors further introduced the coupling of the  $D\bar{D}^*$  to  $D^*\bar{D}^*$  in Case III. Finally, they took into account the explicit mass splitting between the charged and neutral  $D(D^*)$  mesons, which is the physical Case IV. The authors considered six channels of these four cases in Table 22.

From Tables 23 and 24, one notes that the mass difference between the charged and neutral charmed mesons leads

to large isospin violation in the probability of the  $[D^0\bar{D}^{*0}]$  and  $[D^+D^{*-}]$  components in the flavor wave functions of the  $X(3872)$ . Moreover, the isospin breaking effect is amplified by the tiny binding energy. As an example, when the binding energy is 0.3 MeV, they found that the isovector component inside the  $X(3872)$  is 26%, and the ratio of the two hidden-charm decay modes  $\mathcal{B}(X(3872) \rightarrow \pi^+\pi^-\pi^0 J/\psi)/\mathcal{B}(X(3872) \rightarrow \pi^+\pi^- J/\psi)$  was estimated to be 0.42, consistent with the experimental value [64, 79].

Table 23: The molecular solutions of the  $X(3872)$  with the OPE potential. “×” means no binding solutions, and “–” denotes that the corresponding component does not exist. Taken from Ref. [222].

Cases	$\Lambda$ (GeV)	B.E. (MeV)	Mass (MeV)	$r_{rms}$ (fm)	$P_1$ (%)	$P_2$ (%)	$P_3$ (%)	$P_4$ (%)	$P_5$ (%)	$P_6$ (%)
I	0.80 ~ 2.0			×			–	–	–	–
							–	–	–	–
								–	–	–
	1.55	0.32	3871.49	4.97	98.81	1.19	–	–	–	–
	1.60	0.92	3870.89	3.51	98.39	1.61	–	–	–	–
II	1.65	1.90	3869.91	2.56	98.01	1.99	–	–	–	–
	1.70	3.31	3868.50	1.99	97.69	2.31	–	–	–	–
	1.80	7.70	3864.11	1.36	97.18	2.82	–	–	–	–
	1.10	0.76	3871.05	3.79	97.82	0.73	–	–	1.24	0.20
	1.15	2.72	3869.09	2.17	96.15	0.82	–	–	2.64	0.40
III	1.20	6.25	3865.56	1.49	94.26	0.77	–	–	4.37	0.60
	1.25	11.66	3860.15	1.13	92.20	0.67	–	–	6.32	0.81
	1.30	19.21	3852.60	0.91	90.05	0.55	–	–	8.38	1.02
	1.55	95.79	3776.02	0.47	80.68	0.16	–	–	17.37	1.80
	1.15	0.26	3871.55	4.79	85.68	0.22	12.29	0.24	0.36	0.21
	1.17	1.03	3870.78	2.99	76.37	0.30	20.27	0.33	2.39	0.35
IV(Phy)	1.20	2.93	3868.88	1.84	66.18	0.34	28.74	0.36	3.84	0.54
	1.25	7.99	3863.82	1.20	56.72	0.32	35.76	0.34	6.08	0.79
	1.30	15.36	3856.45	0.93	51.59	0.27	38.61	0.28	8.25	1.01

The authors emphasized that the existence of the shallow bound state  $X(3872)$  and very large isospin violation in its hidden-charm decay arise from the very delicate combined efforts of the several driving forces including the long-range one-pion exchange, the S-D wave mixing, the mass splitting between the charged and neutral  $D(D^*)$  mesons, and the coupled-channel effects [222].

In a recent work [224], Zhao, Ma, and Zhu further studied the  $D\bar{D}^*$  system in the framework of the OBE model. They examined the spin-orbit force correction up to  $\mathcal{O}(1/M)$  and the recoil correction up to  $\mathcal{O}(1/M^2)$ , and found that the former one is important for the very loosely bound state. Their result suggested that there exists an isoscalar molecular state in the  $D\bar{D}^*$  system with  $J^{PC} = 1^{++}$ . Their result also suggested that the recoil correction may be larger than the binding energy of the  $X(3872)$ , which may partly force the  $X(3872)$  to become a very shallow bound state [224].

In Fig. 50, we summarized the above investigations, which attempted to answer whether the  $X(3872)$  is a  $D\bar{D}^*$  molecular state or not. Until now, many theoretical studies suggested that the interaction in the  $D\bar{D}^*$  system with  $J^G(J^{PC}) = 0^+(1^{++})$  is attractive, which can result in a shallow bound state. However, further experimental and theoretical studies are needed to test this hadronic molecular state assignment to the  $X(3872)$ . Especially, studies on its

Table 24: The molecular solutions of the  $X(3872)$  with the OBE potential. “x” means no binding solutions, and “-” denotes that the corresponding component does not exist. Taken from Ref. [222].

Cases	$\Lambda$ (GeV)	B.E. (MeV)	Mass (MeV)	$r_{rms}$ (fm)	$P_1$ (%)	$P_2$ (%)	$P_3$ (%)	$P_4$ (%)	$P_5$ (%)	$P_6$ (%)
I	1.85	0.21	3871.60	5.36	99.54	0.46	-	-	-	-
	1.90	0.53	3871.28	4.32	99.27	0.63	-	-	-	-
	1.95	0.96	3870.85	3.48	99.18	0.82	-	-	-	-
	2.00	1.51	3870.30	2.88	98.99	1.01	-	-	-	-
II	1.10	0.61	3871.20	4.21	98.82	1.18	-	-	-	-
	1.15	2.15	3869.66	2.54	98.27	1.73	-	-	-	-
	1.20	4.58	3867.23	1.84	97.28	2.18	-	-	-	-
	1.25	7.84	3863.97	1.48	97.40	2.60	-	-	-	-
	1.30	11.87	3859.94	1.26	97.01	2.99	-	-	-	-
III	1.00	0.74	3871.07	3.92	98.38	0.79	-	-	0.66	0.18
	1.10	5.69	3866.12	1.66	96.39	1.07	-	-	1.91	0.62
	1.15	9.67	3862.14	1.34	95.51	1.12	-	-	2.46	0.92
	1.20	14.51	3857.30	1.15	94.65	1.15	-	-	2.94	1.26
	1.25	20.18	3851.63	1.02	93.82	1.17	-	-	3.35	1.67
	1.30	26.68	3845.13	0.92	92.98	1.18	-	-	3.71	2.14
IV(Phy)	1.05	0.30	3871.51	4.76	86.80	0.27	11.77	0.28	0.67	0.20
	1.06	0.60	3871.21	3.85	82.83	0.33	15.35	0.34	0.88	0.27
	1.08	1.43	3870.38	2.69	75.80	0.41	21.68	0.42	1.28	0.41
	1.10	2.53	3869.28	2.09	70.44	0.46	26.46	0.47	1.62	0.54
	1.12	3.84	3867.97	1.75	66.40	0.50	30.00	0.51	1.92	0.67
	1.15	6.16	3865.65	1.46	62.03	0.53	33.72	0.54	2.31	0.87
	1.20	10.83	3860.98	1.19	57.38	0.56	37.42	0.56	2.85	1.23

decay behaviors are important, which will be reviewed in Sec. 4.5.5.

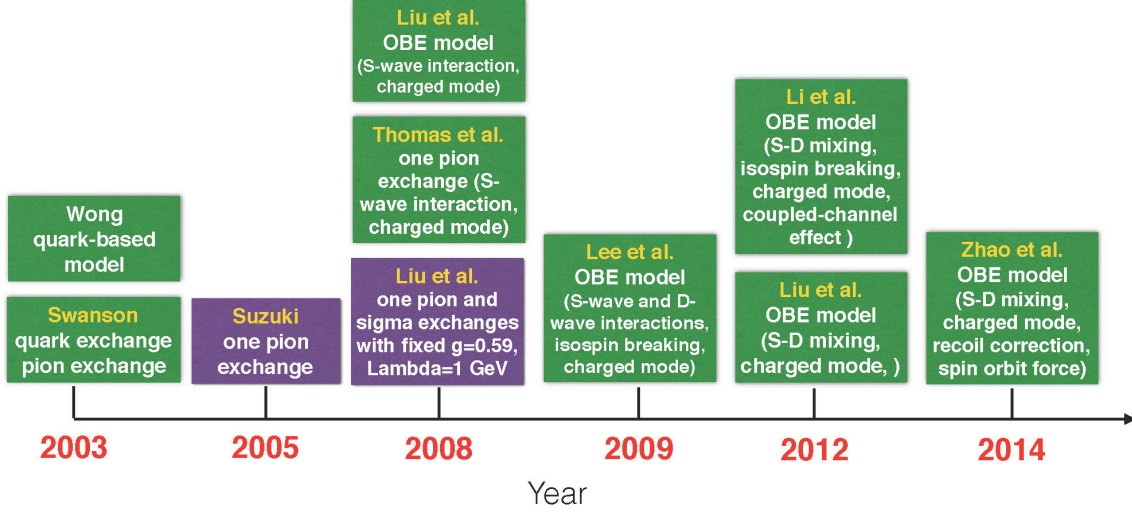


Figure 50: (Color online) A summary of the theoretical progresses on the dynamical studies of the  $D\bar{D}^*$  molecular state of the  $X(3872)$ . Here, these studies are marked by green and purple backgrounds when the corresponding conclusion of whether the  $X(3872)$  is a  $D\bar{D}^*$  molecular state is positive and negative, respectively.

**4.5.1.4. QCD sum rule.** In QCD sum rule, Lee, Nielsen and Wiedner studied a  $D^*\bar{D}_s$  molecule with  $J^P = 1^+$  in Ref. [527]. They proposed such molecule as a natural generalized state to the strangeness sector of the  $X(3872)$ . They calculated the two-point correlation function by keeping the  $m_s$  proportional term in the OPE series. As an extension, they studied the  $D^0\bar{D}^{*0} - D^{*0}\bar{D}^0$  molecule to assign the  $X(3872)$  meson by taking  $m_s = 0$ . They obtained  $m_{D^*\bar{D}} = (3.88 \pm 0.06)$  GeV, in agreement with the experimental value of the  $X(3872)$  meson [527]. This result was consistent with the calculations of the  $D^*\bar{D}$  state in Refs. [482, 408, 410]. In Ref. [528], Lee, Morita and Nielsen extended their discussion to include the total width by employing the Breit-Wigner function to the pole term, using the same molecular current with that in Ref. [527]. They found that introducing the width slightly modified the predicted mass and resulted in a better reproduction of the  $X(3872)$ .

However, the narrow decay width of the  $X(3872)$  can not be explained in QCD sum rule if it is a pure four-quark state [529]. To reproduce the small width of the  $X(3872)$ , it was considered as a mixture between charmonium and molecular state with  $J^{PC} = 1^{++}$  in Ref. [530]. They found a small mixing angle  $5^\circ \leq \theta \leq 13^\circ$  to reproduce the parameters  $m_X = (3.77 \pm 0.18)$  GeV and  $\Gamma(X \rightarrow J/\psi\pi^+\pi^-) = (9.3 \pm 6.9)$  MeV. They concluded that the  $X(3872)$  is approximately 97% a charmonium state with 3% molecule (admixture of 88%  $D^0\bar{D}^{*0}$  and 12%  $D^+\bar{D}^{*-}$ ). Later, this configuration was used to study the radiative decay of the  $X(3872)$  in Ref. [531]. The authors calculated the three-point functions for the vertex  $X(3872)J/\psi\gamma$  to study the partial decay width of  $X(3872) \rightarrow J/\psi\gamma$ . They obtained the branching ratio  $\Gamma(X(3872) \rightarrow J/\psi\gamma)/\Gamma(X(3872) \rightarrow J/\psi\pi^+\pi^-) = 0.19 \pm 0.13$ , which is consistent with the experiment result for the radiative decay of the  $X(3872)$  [64, 75].

Besides the above references, the  $X(3872)$  was also studied as a molecular state in Refs. [532, 533, 534, 535, 400, 536].

#### 4.5.2. The axial vector tetraquark state

**4.5.2.1. Diqurk model.** A diquark-antidiquark model was proposed in Ref. [363] by Maiani, Piccinini, Polosa, and Riquer to explain the  $X(3872)$ , based on their previous studies on the lightest scalar mesons [537]. We note that this is the “type-I” diquark-antidiquark model, and the “type-II” diquark-antidiquark model [366] has been reviewed in Sec. 4.2.2.

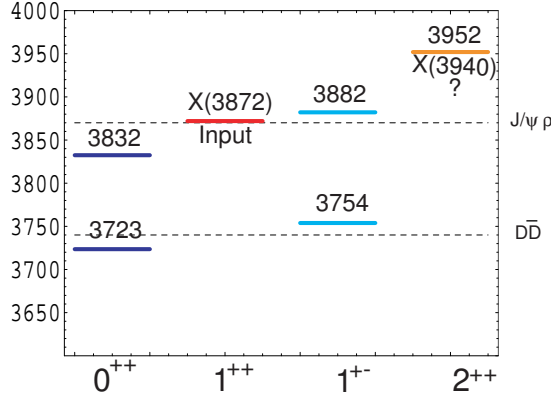


Figure 51: (Color online) The mass spectrum of the  $X$  particles. Taken from Ref. [363].

In this model the hadron masses depend on three ingredients: quark composition, constituent quark masses and spin-spin interactions. The Hamiltonian is

$$H = \sum_i m_i + \sum_{i<j} 2\kappa_{ij}(S_i \cdot S_j), \quad (141)$$

where the coefficients  $\kappa_{ij}$  depend on the flavor of the constituents  $i, j$  and the particular color state of the pair. All these parameters can be derived from the quark-antiquark mesons and three-quark baryons. Especially, they considered the “good” diquark having  $S = 0$  and the “bad” diquark having  $S = 1$ , whose masses are derived from the light scalar mesons as well as the  $X(3872)$ . Using these components, they constructed six  $[cq][\bar{c}\bar{q}']$  states, including two states with  $J^{PC} = 0^{++}$ , one state with  $J^P = 1^{++}$ , two states with  $J^P = 1^{+-}$ , and one state with  $J^{PC} = 2^{++}$ :

$$\begin{aligned} |0^{++}\rangle &= |0_{cq}, 0_{\bar{c}\bar{q}'}; J = 0\rangle, \\ |0^{++'}\rangle &= |1_{cq}, 1_{\bar{c}\bar{q}'}; J = 0\rangle, \\ |1^{++}\rangle &= \frac{1}{\sqrt{2}}(|0_{cq}, 1_{\bar{c}\bar{q}'}; J = 1\rangle + |1_{cq}, 0_{\bar{c}\bar{q}'}; J = 1\rangle), \\ |1^{+-}\rangle &= \frac{1}{\sqrt{2}}(|0_{cq}, 1_{\bar{c}\bar{q}'}; J = 1\rangle - |1_{cq}, 0_{\bar{c}\bar{q}'}; J = 1\rangle), \\ |1^{+-'}\rangle &= |1_{cq}, 1_{\bar{c}\bar{q}'}; J = 1\rangle, \\ |2^{+-'}\rangle &= |1_{cq}, 1_{\bar{c}\bar{q}'}; J = 2\rangle. \end{aligned} \quad (142)$$

The authors used the  $1^{++}$  state to fit the  $X(3872)$ , and calculated masses of the other five states as well as masses of the six  $[cq][\bar{s}\bar{q}']$  states, as shown in Fig. 51. They also studied the isospin breaking effects, and predicted that the  $X(3872)$  was made of two components with a mass difference related to  $m_u - m_d$  and discussed the production of the  $X(3872)$  and of its charged partner  $X^\pm$  in the weak decays of  $B^{+,0}$  [538]. This idea was further developed in Ref. [539] by Maiani, Polosa, and Riquer, where they proposed four states:  $X_u = [cu][\bar{c}\bar{u}]$ ,  $X_d = [cd][\bar{c}\bar{d}]$ ,  $X^+ = [cu][\bar{c}\bar{d}]$ , and  $X^- = [cd][\bar{c}\bar{u}]$ , and used  $X_u$  and  $X_d$  to explain the mass difference between the  $X(3872)$  state decaying into  $J/\psi\pi^+\pi^-$  [52, 79] and the one decaying into  $D^0\bar{D}^0\pi^0$  [57]. The quantum numbers of the  $X(3872)$ , both  $J^{PC} = 2^{-+}$  and  $1^{++}$ , were discussed by Burns, Piccinini, Polosa, and Sabelli in Ref. [540]. According to the prediction for the charged partner of the  $X(3872)$  in Ref. [539], BaBar carried out a careful search for them in the  $B \rightarrow X^-K$ ,  $X^- \rightarrow J/\psi\pi^-\pi^0$  [541]. However, the charged partners of the  $X(3872)$  have not been observed in experiment.

The diquark-antidiquark picture was later used to calculate the masses of heavy tetraquarks by Ebert, Faustov and Galkin in the relativistic quark model in Ref. [542]. They also found that the  $X(3872)$  can be the neutral charm

tetraquark state, and concluded that one more neutral and two charged tetraquark states must exist with close masses. Similar conclusions were obtained in Ref. [543] by Terasaki that the  $X(3872)$  consists of two iso-singlet tetra-quark mesons,  $X^\pm \sim [cn](\bar{c}\bar{n}) \pm (cn)[\bar{c}\bar{n}]_{I=0}$ , with opposite  $G$  parities. Here the parentheses and the square brackets denote symmetry and anti-symmetry, respectively, of the wave function under the exchange of flavors between them.

**4.5.2.2. QCD sum rule.** Using the diquark-antidiquark configuration, Chen and Zhu studied the hidden-charm tetraquark systems with  $J^{PC} = 1^{++}$  in the QCD sum rules in a systematical way [420]. The constructed all charmonium-like tetraquark interpolating currents with quantum numbers  $J^{PC} = 1^{++}$  without derivative operators

$$\begin{aligned}
J_{1\mu} &= q_a^T C Q_b (\bar{q}_a \gamma_\mu \gamma_5 C \bar{Q}_b^T + \bar{q}_b \gamma_\mu \gamma_5 C \bar{Q}_a^T) + q_a^T C \gamma_\mu \gamma_5 Q_b (\bar{q}_a C \bar{Q}_b^T + \bar{q}_b C \bar{Q}_a^T), \\
J_{2\mu} &= q_a^T C Q_b (\bar{q}_a \gamma_\mu \gamma_5 C \bar{Q}_b^T - \bar{q}_b \gamma_\mu \gamma_5 C \bar{Q}_a^T) + q_a^T C \gamma_\mu \gamma_5 Q_b (\bar{q}_a C \bar{Q}_b^T - \bar{q}_b C \bar{Q}_a^T), \\
J_{3\mu} &= q_a^T C \gamma_5 Q_b (\bar{q}_a \gamma_\mu C \bar{Q}_b^T + \bar{q}_b \gamma_\mu C \bar{Q}_a^T) + q_a^T C \gamma_\mu Q_b (\bar{q}_a \gamma_5 C \bar{Q}_b^T + \bar{q}_b \gamma_5 C \bar{Q}_a^T), \\
J_{4\mu} &= q_a^T C \gamma_5 Q_b (\bar{q}_a \gamma_\mu C \bar{Q}_b^T - \bar{q}_b \gamma_\mu C \bar{Q}_a^T) + q_a^T C \gamma_\mu Q_b (\bar{q}_a \gamma_5 C \bar{Q}_b^T - \bar{q}_b \gamma_5 C \bar{Q}_a^T), \\
J_{5\mu} &= q_a^T C \gamma^\nu Q_b (\bar{q}_a \sigma_{\mu\nu} \gamma_5 C \bar{Q}_b^T + \bar{q}_b \sigma_{\mu\nu} \gamma_5 C \bar{Q}_a^T) + q_a^T C \sigma_{\mu\nu} \gamma_5 Q_b (\bar{q}_a \gamma^\nu C \bar{Q}_b^T + \bar{q}_b \gamma^\nu C \bar{Q}_a^T), \\
J_{6\mu} &= q_a^T C \gamma^\nu Q_b (\bar{q}_a \sigma_{\mu\nu} \gamma_5 C \bar{Q}_b^T - \bar{q}_b \sigma_{\mu\nu} \gamma_5 C \bar{Q}_a^T) + q_a^T C \sigma_{\mu\nu} \gamma_5 Q_b (\bar{q}_a \gamma^\nu C \bar{Q}_b^T - \bar{q}_b \gamma^\nu C \bar{Q}_a^T), \\
J_{7\mu} &= q_a^T C \gamma^\nu \gamma_5 Q_b (\bar{q}_a \sigma_{\mu\nu} C \bar{Q}_b^T + \bar{q}_b \sigma_{\mu\nu} C \bar{Q}_a^T) + q_a^T C \sigma_{\mu\nu} Q_b (\bar{q}_a \gamma^\nu \gamma_5 C \bar{Q}_b^T + \bar{q}_b \gamma^\nu \gamma_5 C \bar{Q}_a^T), \\
J_{8\mu} &= q_a^T C \gamma^\nu \gamma_5 Q_b (\bar{q}_a \sigma_{\mu\nu} C \bar{Q}_b^T - \bar{q}_b \sigma_{\mu\nu} C \bar{Q}_a^T) + q_a^T C \sigma_{\mu\nu} Q_b (\bar{q}_a \gamma^\nu \gamma_5 C \bar{Q}_b^T - \bar{q}_b \gamma^\nu \gamma_5 C \bar{Q}_a^T),
\end{aligned} \tag{143}$$

where  $q$  the represents up or down quark and  $Q$  the charm quark. The color structures are symmetric  $\mathbf{6} \otimes \bar{\mathbf{6}}$  for the currents  $J_1, J_3, J_5, J_7$  and antisymmetric  $\bar{\mathbf{3}} \otimes \mathbf{3}$  for the currents  $J_2, J_4, J_6, J_8$ . As shown in Eq. (124), all these interpolating currents in Eq. (143) can couple to both isotriplet and isosinglet hadron states.

Using these interpolating currents, the authors obtained the mass spectra of the charmonium-like and bottomonium-like tetraquark states with  $J^{PC} = 1^{++}$  in Table 25. The hidden-strange tetraquark states were also studied. Using the current  $J_{4\mu}$  in Eq. (143), the mass of the  $qc\bar{q}\bar{c}$  tetraquark state was extracted as  $m_X = (4.03 \pm 0.11)$  GeV, slightly above the mass of the  $X(3872)$ . The interpolating current  $J_{4\mu}$  was also used to study the  $X(3872)$  as a tetraquark state in Refs. [544, 545], where the extracted hadron masses were consistent with the result in Table 25.

Table 25: Mass spectra for the  $J^{PC} = 1^{++}$  charmonium-like and bottomonium-like tetraquark states in diquark-antidiquark configuration [420].

	Current	$s_0$ (GeV <sup>2</sup> )	Borel window (GeV <sup>2</sup> )	$m_X$ (GeV)	PC (%)
$qc\bar{q}\bar{c}$	$J_{3\mu}$	4.6 <sup>2</sup>	3.0 – 3.4	4.19 ± 0.10	47.3
	$J_{4\mu}$	4.5 <sup>2</sup>	3.0 – 3.3	4.03 ± 0.11	46.8
$qb\bar{q}\bar{b}$	$J_{3\mu}$	10.9 <sup>2</sup>	8.5 – 9.5	10.32 ± 0.09	47.0
	$J_{4\mu}$	10.8 <sup>2</sup>	8.5 – 9.2	10.22 ± 0.11	44.6
	$J_{7\mu}$	10.7 <sup>2</sup>	7.8 – 8.4	10.14 ± 0.10	44.8
	$J_{8\mu}$	10.7 <sup>2</sup>	7.8 – 8.4	10.14 ± 0.09	44.8

**4.5.2.3. Chromomagnetic interaction.** The chromomagnetic interaction

$$H = \sum_i m_i + H_{CM} = \sum_i m_i - \sum_{i>j} v_{ij} \vec{\lambda}_i \cdot \vec{\lambda}_j \vec{\sigma}_i \cdot \vec{\sigma}_j, \tag{144}$$

was also applied to study the  $X(3872)$  in Refs. [546, 547, 548]. In Ref. [546], Hogaasen, Richard, and Sorba found that the chromomagnetic interaction, with proper account for flavour-symmetry breaking, can be used to explain the mass

and coupling properties of the  $X(3872)$  resonance as a  $J^{PC} = 1^{++}$  state consisting of a heavy quark-antiquark pair and a light one. This study was extended to study the S-wave configurations containing two quarks and two antiquarks in Ref. [548] by Buccella, Hogaasen, Richard, and Sorba, where they investigated light, charmed, charmed and strange, hidden-charm and double-charm mesons, as well as their analogues with bottom quarks. In Ref. [547], Cui, Chen, Deng, and Zhu performed a schematic study of the masses of possible heavy tetraquarks using the chromomagnetic interaction with the flavor symmetry breaking corrections, and they found that the chromomagnetic interaction is repulsive for the  $2^+$  heavy tetraquarks, while the  $0^+$   $qc\bar{q}\bar{c}$  states will also exist if the  $X(3872)$  is a  $1^+$  tetraquark.

4.5.2.4. *Constituent quark model.* However, in Ref. [549], Vijande, Weissman, Barnea, and Valcarce studied the four-quark system  $c\bar{c}q\bar{q}$  in the framework of the constituent quark model. They solved the four-body Schrödinger equation by means of the hyperspherical harmonic formalism using different types of quark-quark potentials, and ruled out the possibility that the  $X(3872)$  is a compact tetraquark system, unless additional correlations, either in the form of diquarks or at the level of the interacting potential, not considered in simple quark models do contribute.

#### 4.5.3. Radial excitation of the axial vector charmonium

4.5.3.1. *Quark model.* There are lots of discussions on the interpretation of the  $X(3872)$  as a P-wave charmonium state [550, 551, 552, 553, 554, 555, 556, 557, 558, 559, 560, 561, 562, 563, 564]. But there exist two major difficulties: (1) the mass of the  $X(3872)$  is significantly lower than the predictions of quark models, for example, see Fig. 52 obtained using the GI model [17]; (2) the large isospin violation in the  $X(3872) \rightarrow J/\psi\rho$  decay was observed in Refs. [64, 79], as shown in Eqs. (10) and (11) in Sec. 2.1.1.1. One natural speculation is that the  $X(3872)$  may not be a pure  $\chi'_{c1}(2P)$  charmonium state. Instead, the  $X(3872)$  may be a mixture of the bare  $c\bar{c}$  charmonium state and the  $D\bar{D}^*$  molecule component. In other words, the coupled channel effect may play a very important role in the case of the  $X(3872)$ .

Comparing the mass spectrum of charmonium states calculated by the GI model [17] with the current experimental data [1] (see Fig. 52), one quickly notices that the charmonium states below 3.9 GeV (or the thresholds of the charmed meson pair) can be produced reasonably well by the GI model. However, many XYZ states above 3.9 GeV can not be simply categorized into the charmonium family, especially when they are close to the thresholds of the charmed meson pair, where the coupled-channel effects become important.

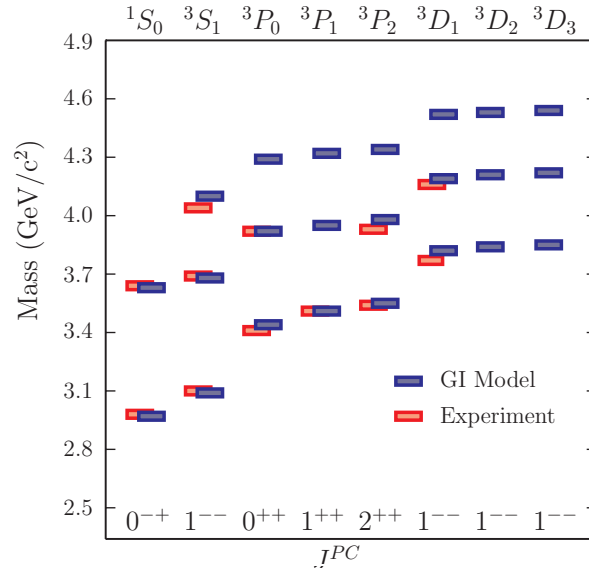


Figure 52: (Color online) The comparison between the result from the GI model [17] and the experimental data [1] for charmonium family.

4.5.3.2. *Coupled channel effects.* Kalashnikova employed the simplest version of the coupled-channel model to study the charmonium mass spectrum [565]. First he calculated the mass of the bare  $2^3P_1$  state to be 4180 MeV, using a simple potential model with Hamiltonian  $H_0 = p^2/m_c + V(r) + C$  with  $V(r) = \delta r - 4\alpha_s/(3r)$ . Then he considered the coupling of this state to the  $D\bar{D}^*$  channel. Together with the  $1^{++}$  resonance with the mass of 3990 MeV, a near-threshold virtual state with the width about 0.3 MeV was generated, and may be identified with the  $X(3872)$ .

In Ref. [566], Zhang, Meng, Zheng used the coupled-channel Flatté formula to perform an analysis of the Belle data on the  $X(3872)$  [67]. They found the co-existence of two poles: one is a sheet II (or sheet IV) pole very close to the  $D^{*0}\bar{D}^0$  threshold, and the other one is a sheet III pole below the  $D^{*0}\bar{D}^0$  threshold. They pointed out that the  $X(3872)$  can be a conventional  $2^3P_1$   $c\bar{c}$  state strongly polluted by coupled channel effects since there exist two poles around the  $D^0\bar{D}^{*0}$  threshold. They also analyzed the data from BaBar [76]. But as suggested in Ref. [567] by Kalashnikova and Nefediev, the description was not very satisfactory, reflecting incompatibility of the Belle and BaBar data.

In Ref. [567], Kalashnikova and Nefediev analyzed the same data from Belle [67] and BaBar [76]. They found that the BaBar data [76] is more compatible with the assumption of the  $X(3872)$  being a virtual state of a dynamical nature in the  $D\bar{D}^*$  system, and the charmonium admixture is small. In contrast, they found that the Belle data [67] clearly indicated a sizeable  $c\bar{c}$   $2^3P_1$  component in the  $X(3872)$  wave function, which conclusion is similar to that in Ref. [566]. The conclusion in Ref. [566] was partly supported by the coupled-channel analysis of the  $X(3872)$  in Ref. [568], where Danilkin and Simonov adopted a coupled-channel model developed in Ref. [569] to carry out a pole analysis and the calculation of the  $D\bar{D}^*$  production cross section. They obtained a sharp peak structure at the  $D^0\bar{D}^{*0}$  threshold, where the original position of 3954 MeV for the  $2^3P_1$   $c\bar{c}$  state was shifted by the coupled-channel effect from the  $D\bar{D}^*$  channel [568].

In Ref. [570], Li and Chao studied the higher charmonia with the screened potential. One notes that the screened potential and the coupled-channel model roughly play the same role in lowering the mass of the  $\chi'_{c1}(2P)$  charmonium state, which can reach 3901 MeV and is close to the mass of the  $X(3872)$  [571].

The nature of the  $X(3872)$  enhancement was analyzed in the framework of the resonance-spectrum expansion in Ref. [572] by Coito, Rupp, and Beveren. They studied the  $X(3872)$  as a regular  $J^{PC} = 1^{++}$  charmonium state, though strongly influenced and shifted by the open-charm decay channels, and found a very delicate interplay among the  $D^0\bar{D}^{*0}$ ,  $\rho^0 J/\psi$ , and  $\omega J/\psi$  channels. Their results suggested that the  $X(3872)$  is a very narrow axial-vector  $c\bar{c}$  resonance, with a pole at or slightly below the  $D^0\bar{D}^{*0}$  threshold. Later in Ref. [573], Coito, Rupp, and Beveren studied the  $X(3872)$  as a confined  $^3P_1$   $c\bar{c}$  state coupling to the almost unbound  $S$ -wave  $D^0\bar{D}^{*0}$  channel via the  $^3P_0$  mechanism. They calculated the two-component wave function for different values of the binding energy and the transition radius  $a$ , and found a significant  $c\bar{c}$  component. In the case of a small binding energy of 0.16 MeV and  $a$  between 2 and 3  $\text{GeV}^{-1}$ , the  $c\bar{c}$  probability can be strongly limited to be roughly around 7-11%. Then the  $X(3872)$  r.m.s. radius and the  $S$ -wave  $D^0\bar{D}^{*0}$  scattering length are 7.8 fm and 11.6 fm, respectively. Hence, they concluded that the  $X(3872)$  is not a genuine meson-meson molecule, nor actually any other mesonic system with non-exotic quantum numbers, due to the inevitable mixing with the corresponding quark-antiquark states.

#### 4.5.4. Lattice QCD

In Ref. [574], the TWQCD Collaboration used a molecular type operator composed of the  $D$  and  $\bar{D}^*$ ,  $(\bar{q}\gamma_i c)(\bar{c}\gamma_5 q) - (\bar{c}\gamma_i q)(\bar{q}\gamma_5 c)$ , and detected a  $1^{++}$  resonance with a mass around  $3890 \pm 30$  MeV in quenched lattice QCD simulation with exact chiral symmetry, which was identified as the  $X(3872)$ . They also used a diquark-antidiquark operator,  $(q^T C\gamma_i c)(\bar{q}C\gamma_5 \bar{c}^T) - (\bar{q}^T C\gamma_i \bar{c})(qC\gamma_5 c^T)$ , and detected the same resonance. Later in Ref. [575], this study was extended to the mass spectrum of the  $1^+$  exotic mesons with quark content  $(cs\bar{c}\bar{q})/(cq\bar{c}\bar{s})$ , and they detected a  $1^+$  resonance with mass around  $4010 \pm 50$  MeV.

The lattice QCD simulation was also applied to study the  $X(3872)$  as a charmonium state. In Ref. [576] the Hadron Spectrum Collaboration studied the highly excited charmonium mesons up to around 4.5 GeV using dynamical QCD configurations. They found that the  $D$ -wave  $2^{-+}$  charmonium state is around 30 MeV below the  $X(3872)$ , while the first radial excitation of the  $P$ -wave  $1^{++}$  state is around 110 MeV above the  $X(3872)$ . In Ref. [577] the CLQCD Collaboration also studied the  $2^{-+}$  charmonium in quenched lattice QCD, and its mass was determined to be  $3.80 \pm 0.03$  GeV, which is close to the mass of the  $D$ -wave charmonium  $\psi(3770)$  and in agreement with quark model predictions, but again significantly smaller than the mass of the  $X(3872)$ .

Many dynamical studies suggested that the  $D$  and  $D^*$  interaction is strongly attractive [184, 517, 522, 201, 523, 207, 204, 192, 222, 224]. Hence, a pure  $\chi'_{c1}(2P)$  with  $J^{PC} = 1^{++}$  can easily couple to the  $S$ -wave  $D\bar{D}^*$  scattering

state if their masses are similar. Moreover, their mixture can result in a small mass [522, 578], which value can be significantly lower than the mass of the pure  $\chi_{c1}(2P)$  state predicted in the GI model [17], but close to the mass of the  $X(3872)$ .

This picture was supported by the lattice QCD calculations [526, 579]. In Ref. [526], Prelovsek and Leskovec found a candidate for the  $X(3872)$  using dynamical  $N_f = 2$  lattice simulation with  $J^{PC} = 1^{++}$  and  $I = 0$ , in addition to the nearby  $D\bar{D}^*$  and  $J/\psi\omega$  discrete scattering states. In their simulation, they chose the interpolating fields that couple to  $\bar{c}c$  as well as the scattering states, i.e.,  $O^{\bar{c}c}$ ,  $O^{DD^*}$ ,  $O^{J/\psi\omega}$  (for  $I = 0$ ), and  $O^{J/\psi\rho}$  (for  $I = 1$ ). They extracted large and negative  $D\bar{D}^*$  scattering length,  $a_0^{DD^*} = -1.7 \pm 0.4$  fm, and the effective range,  $r_0^{DD^*} = 0.5 \pm 0.1$  fm. They did not find a candidate for the  $X(3872)$  in the  $I = 1$  channel, which may be due to the exact isospin symmetry in their simulation.

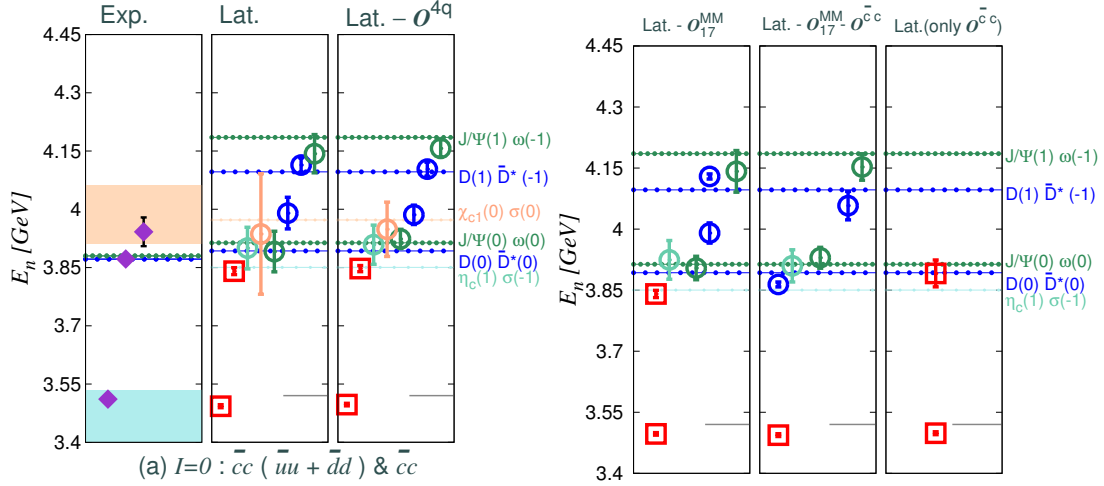


Figure 53: (Color online) The spectra of states with  $J^{PC} = 1^{++}$  for the cases with  $u/d$  valence quarks, taken from Ref. [579]. From the left to the right: a) physical thresholds and possible experimental candidates, including the  $\chi_{c1}$ ,  $X(3872)$ , and  $X(3940)$ ; b) the discrete spectrum determined from the optimized basis of Ref. [579], including the  $\bar{c}c$ , two-meson and diquark-antidiquark operators; c) the spectrum obtained from the optimized basis, without the two-meson operators; d) the spectrum obtained from the optimized basis, without one of the two-meson operators,  $O_{17}^{MM}$ ; e) the spectrum obtained from the optimized basis, without  $\bar{c}c$  and  $O_{17}^{MM}$  operators; f) the spectrum obtained with only  $\bar{c}c$  operators.

This study was extended in Ref. [579] by Padmanath, Lang, and Prelovsek, where a large basis of interpolating fields was utilized, including  $\bar{c}c$ , two-meson and diquark-antidiquark ones. The obtained discrete spectrum are shown in Fig. 53. Again they found a lattice candidate for the  $X(3872)$  with  $J^{PC} = 1^{++}$  and  $I = 0$ , but only if both  $\bar{c}c$  and  $D\bar{D}^*$  interpolators are included. However, this candidate can not be found if the diquark-antidiquark and  $D\bar{D}^*$  are used in the absence of  $\bar{c}c$ . Moreover, no candidate for the neutral or charged  $X(3872)$ , or any other exotic candidates are found in the  $I = 1$  channel, and no signatures of the exotic  $\bar{c}c\bar{s}s$  candidates are found below 4.2 GeV. In other words, the most recent dynamical lattice QCD simulation strongly disfavors either the diquark-antidiquark or various four-quark interpretations of the  $X(3872)$ .

This dynamical lattice QCD simulation was performed with  $N_f = 2$  and  $m_\pi = 266$  MeV. The pion mass on the lattice is still much larger than its physical mass 140 MeV. Within the molecular scheme, the long range one-pion-exchange force plays a dominant role in the formation of the loosely bound molecular state [222, 224], which decays exponentially as the pion mass increases. The present lattice simulation with the pion mass  $m_\pi = 266$  MeV is still unable to explore and judge whether the  $X(3872)$  is a molecular state or not.

#### 4.5.5. Other theoretical schemes, production and decay patterns

4.5.5.1. Other schemes. There exist some other theoretical schemes. The  $X(3872)$  was interpreted as a  $c\bar{c}g$  hybrid state [580], a vector glueball mixed with the neighboring vector charmonium [581], and a dynamically generated mixed state of a  $DD^*$  molecule and  $\chi_{c1}(2P)$  [582] etc. Whether the  $X(3872)$  is due to the cusp effect and threshold effect was discussed in Refs. [583, 584, 585, 494, 381, 586]. Since the  $X(3872)$  is very close to the  $D^{*0}\bar{D}^0$  threshold, the rescattering effects of the  $D$  and  $D^*$  mesons were studied in Refs. [587, 588, 589, 590, 591].

The chiral unitary approach in coupled channels was applied to study the  $X(3872)$  in Refs. [592, 593, 594, 595, 596]. The  $X(3872)$  was investigated using the AdS/QCD in Ref. [597]. An effective field theory, called XEFT, was proposed in Refs. [598, 599, 600, 601, 602] to study the  $X(3872)$  as a loosely-bound charm-meson molecule. A dynamical picture to explain the nature of the exotic  $XYZ$  states was proposed in Ref. [375] based on a diquark-antidiquark open-string configuration, while the three-body  $D\bar{D}\pi$  dynamics for the  $X(3872)$  was investigated in Refs. [603, 604].

Heavy quark spin selection rule and power counting schemes were investigated in Refs. [605, 419, 606]. Line shapes of the  $X(3872)$  were studied in Refs. [607, 608, 609, 610, 611]. The lattice QCD simulation and related studies can be found in Refs. [612, 613, 614, 615]. The analogous states of the  $X(3872)$ , such as  $X_b$  involving  $b$  quarks, were investigated in Refs. [616, 617, 618, 619, 620, 621, 622, 623, 624, 625].

**4.5.5.2. Decay.** Voloshin pointed out in Ref. [626] that the internal structure of the  $X(3872)$  can be studied by measuring the rate and the spectra in the decays  $X(3872) \rightarrow D^0\bar{D}^0\pi^0$  and  $X(3872) \rightarrow D^0\bar{D}^0\gamma$ . The hadronic transitions from the  $X(3872)$  to  $\chi_{cJ}$  were investigated in Refs. [627, 628, 629, 630], which can also be used to test different theoretical proposals related to the  $X(3872)$ . Later, various methods/models were applied to study the radiative transitions of the  $X(3872)$  such as  $\psi(4160) \rightarrow \gamma X(3872)$ ,  $X(3872) \rightarrow \gamma J/\psi(\psi')$ ,  $X(3872) \rightarrow D^0\bar{D}^0\gamma$  [631, 632, 633, 634, 635, 636, 637, 638, 639], which may play a fundamental role in the determination of the nature of the  $X(3872)$ .

The isospin-violating branching fraction observed by Belle [64] and BaBar [79] experiments (see Eqs. (10)-(11)) are very interesting. The related two-pion and three-pion decays,  $X(3872) \rightarrow J/\psi\rho(\rightarrow \pi^+\pi^-)$  and  $X(3872) \rightarrow J/\psi\omega(\rightarrow \pi^+\pi^-\pi^0)$ , were studied in Refs. [640, 641, 642, 643, 644, 645, 646]. The  $D^0\bar{D}^0\pi^0$  mode was studied in Refs. [647, 648, 649, 521]. The  $D\bar{D}^*$  molecular state assignment to the  $X(3872)$  not only answers why the  $X(3872)$  is close to the  $D^0\bar{D}^{*0}$  threshold, but also explains its isospin violating in the  $J/\psi\rho$  decay mode [184, 200, 222].

The ratio of  $\mathcal{B}(X(3872) \rightarrow \psi'\gamma)$  to  $\mathcal{B}(X(3872) \rightarrow J/\psi\gamma)$  was measured to be  $3.4 \pm 1.4$  [78] and  $2.46 \pm 0.64 \pm 0.29$  [81]. Under the molecule picture, several groups studied the above ratio [650, 651]. In Refs. [652, 650], Dong *et al.* studied the  $\gamma J/\psi$  and  $\gamma\psi'$  decay modes of the  $X(3872)$  using a phenomenological Lagrangian approach. They noticed that a nontrivial interplay between a possible charmonium and the molecular components in the  $X(3872)$  can explain the ratio of  $\mathcal{B}(X(3872) \rightarrow \psi'\gamma)$  with respect to  $\mathcal{B}(X(3872) \rightarrow J/\psi\gamma)$ . In Ref. [651], Guo *et al.* studied the radiative decays of the  $X(3872)$  into  $\gamma J/\psi$  and  $\gamma\psi'$  using an effective field theory. Their results also suggested that their experimental ratio [78, 81] is not in conflict with the hadronic molecular picture that the  $X(3872)$  is dominated by the  $D\bar{D}^*$  component.

The ratio of  $\mathcal{B}(X(3872) \rightarrow \gamma J/\psi)$  with respect to  $\mathcal{B}(X(3872) \rightarrow J/\psi\pi^+\pi^-)$  was measured to be  $0.14 \pm 0.05$  [64] and  $0.33 \pm 0.12$  [78]. This ratio also encodes important information on the underlying structure of the  $X(3872)$ , which was reexamined using a phenomenological Lagrangian approach in Refs. [652, 650]. This ratio was explained using the molecular components in the  $X(3872)$ . Moreover, the authors noticed that this ratio suggests that the  $c\bar{c}$  component plays a subleading role only [652, 650].

Li and Chao considered the  $X(3872)$  as a  $\chi'_{c1}(2P)$  charmonium with the mixture of the  $D\bar{D}^*$  channel [570]. The isospin violating decay process,  $X(3872) \rightarrow J/\psi\rho(\rightarrow \pi^+\pi^-)$ , can happen through final state interactions with the intermediate  $D\bar{D}^*$  loop [653]. With this mechanism, the ratio  $R_{\rho/\omega} \equiv \frac{\Gamma(X(3872) \rightarrow J/\psi\rho)}{\Gamma(X(3872) \rightarrow J/\psi\omega)} \simeq 1$  [654]. With the screening potential, the ratio of  $\mathcal{B}(X(3872) \rightarrow \psi'\gamma)$  to  $\mathcal{B}(X(3872) \rightarrow J/\psi\gamma)$  was  $1.3 - 6.0$  [570], which is consistent with the present experimental data [78, 81].

**4.5.5.3. Production.** The production of the  $X(3872)$  in  $B$  meson decays was also studied in Refs. [655, 656, 657, 658, 659]. Its production in the charmonia radiative decays was studied in Ref. [660]. Its production in  $e^+e^-$  annihilations was studied in Refs. [661, 662, 663]. Its production in high energy heavy ion collisions was studied in Ref. [664]. Its hadronic effects in heavy ion collisions were studied in Ref. [665]. Its production at PANDA was studied in Refs. [666, 667]. Its production at the Tevatron and LHC was studied in Refs. [668, 669]. Its production at CDF was studied in Ref. [670].

Braaten and Kusunoki [671] found that the branching ratio of  $B^0 \rightarrow X(3872)K^0$  is one order of magnitude smaller than that of  $B^+ \rightarrow X(3872)K^+$  assuming the  $X(3872)$  as a  $D\bar{D}^*$  molecular state. However, the ratio of  $\mathcal{B}(B^0 \rightarrow K^0 X(3872))$  to  $\mathcal{B}(B^+ \rightarrow K^+ X(3872))$  was measured to be  $0.82 \pm 0.22 \pm 0.05$  [66],  $1.26 \pm 0.65 \pm 0.06$  [67], and  $0.50 \pm 0.14 \pm 0.04$  [69]. This difference was reexamined in their later work [609], which investigated line shapes of the  $X(3872)$ . They pointed out that the prediction of Ref. [671] was based on the current-current approximation and heavy quark symmetry, and a conceptual error was identified as the implicit assumption that the scattering parameters  $\gamma_0$

and  $\gamma_1$  are small compared to  $\kappa_1(0)$ . Actually, they suggested that  $\gamma_0$  and  $\gamma_1$  could be determined phenomenologically from ratios of rates for  $B^0 \rightarrow K^0 X(3872)$  and  $B^+ \rightarrow K^+ X(3872)$ .

Table 26: Integrated cross sections for  $pp/\bar{p} \rightarrow X(3872)$ , in units of  $nb$ . The results of Ref. [620] were obtained using Herwig and Pythia, which are written outside and inside brackets, respectively.

$\sigma(pp/\bar{p} \rightarrow X(3872))$	Experiment	Ref. [669]	Ref. [668]	Ref. [620]	Ref. [620]
				with $\Lambda = 0.5$ GeV	with $\Lambda = 1$ GeV
Tevatron	37–115 [672, 620]	< 0.085	1.5–23	10(7)	47(33)
LHC with $\sqrt{s} = 7$ TeV	13–39 [62, 620]	–	45–100	16(7)	72(32)

In Ref. [620], Guo, Meissner, Wang, and Yang used the Monte Carlo event generator tools Pythia and Herwig to simulate the production of bottom/charm meson and antimeson pairs at hadron colliders in proton-proton/antiproton collisions, and then derived an order-of-magnitude estimate for the production cross sections of the  $X(3872)$  as a  $D\bar{D}^*$  molecular state at the LHC and Tevatron experiments. Their results are consistent with the experimental measurement by the CDF [672] and CMS [62] collaborations, which are shown in Table 26 together with the predictions of Refs. [669, 668]. They also simulated the production of the bottom analogues and the spin partner of the  $X(3872)$ , including  $X_b$  of  $1^{++}$ , and  $X_{b2}$  and  $X_{c2}$  of  $2^{++}$ . They found that the cross sections are at the  $nb$  level for the  $X_b$  and  $X_{b2}$ , which are two orders of magnitude larger than that for the  $X_{c2}$ . They also proposed a search for these states at the Tevatron and LHC.

In Ref. [578], Meng, Gao, and Chao treated charmonia as nonrelativistic bound states in QCD factorization and obtained  $\mathcal{B}(B^0 \rightarrow K^0 X(3872)) = \mathcal{B}(B^+ \rightarrow K^+ X(3872)) \approx 2 \times 10^{-4}$ , which might imply that the  $X(3872)$  contains a dominant  $J^{PC} = 1^{++}(2P) c\bar{c}$  component and a substantial  $D^0\bar{D}^{*0}$  continuum component.

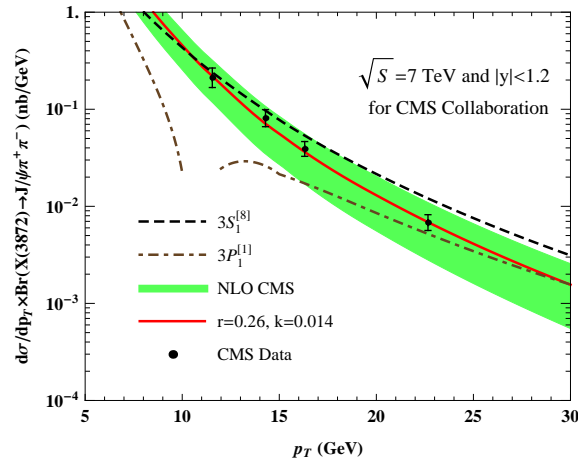


Figure 54: (Color online) The fit of the CMS  $p_T$  distribution data [62]. Taken from Ref. [673].

Especially, the production rate of the  $X(3872)$  is comparable to that of  $\psi'$  at hadron colliders [56, 669, 62], which may also imply a  $c\bar{c}$  core within the  $X(3872)$ . In Ref. [673], Meng, Han, and Chao assumed that the short distance production of the  $X(3872)$  proceeds dominantly through its  $\chi'_{c1}$  component, and evaluated its production cross sections at Tevatron and LHC at NLO in  $\alpha_s$  within the framework of NRQCD factorization. The results are shown in Fig. 54. They fit the CMS experimental data [62] and obtained the ratio  $r = m_c^2 \langle O_{c1}^2(3S_1^{[8]}) \rangle / \langle O_{c1}^2(3P_1^{[1]}) \rangle = 0.26 \pm 0.07$ ,

which is almost the same with that for  $\chi_{c1}$  [674]. With this input, the authors were able to account for the CDF data [56, 669]. The fit of the production cross section of the  $X(3872)$  at hadron colliders leads to the same value of  $k = Z_{c\bar{c}} \cdot \mathcal{B}(X(3872) \rightarrow J/\psi\pi^+\pi^-)$  constrained by the  $B$  meson decay data [1].

In Ref. [558], Butenschoen, He, and Kniehl studied the inclusive hadroproduction of the  $\chi_{c1}(2P)$  within the factorization formalism of nonrelativistic QCD at the next-to-leading order. They tested the hypothesis that the  $X(3872)$  is a pure  $\chi_{c1}(2P)$  charmonium state using the data from the CDF [56, 672], CMS [62], and LHCb [80] collaborations. The authors concluded that NLO NRQCD is inconsistent with the hypothesis  $X(3872) \equiv \chi_{c1}(2P)$ , because they either obtained an unacceptably high value of  $\chi^2$ , a value of  $|R'_{2p}(0)|$  incompatible with well-established potential models, or an intolerable violation of the NRQCD velocity rules.

#### 4.5.6. A short summary

The  $X(3872)$  is the first observed charmonium-like state in the  $XYZ$  family. It's very interesting to quote the prediction which Swanson wrote in 2003 [184]: “Thus the discovery of the  $X(3872)$  may be the entree into a new regime of hadronic physics which will offer important insight into the workings of strong QCD and should help clarify many open issues in light quark spectroscopy.”

- The dynamical lattice QCD simulation with hidden-charm tetraquark operators and  $m_\pi = 266$  MeV is unable to reproduce the  $X(3872)$  signal on the lattice [579]. Moreover, if it is a tetraquark state, the  $X(3872)$  will always be accompanied with several charged partners having similar masses, which have not been observed in the  $B$  meson decays and other experiments.
- The  $X(3872)$  is extremely close to the  $D^0D^{*0}$  threshold. Its  $J/\psi\rho$  decay mode is isospin violating. All these features can be naturally explained by the molecular assignment of the  $X(3872)$  as an S-wave  $D\bar{D}^*$  bound state. In fact, there exists enough attraction in the isoscalar  $D\bar{D}^*$  system to form a shallow bound state. Within the molecular scheme, both the decay and production behaviors can be accounted for naturally.
- The existence of the  $X(3872)$  as a shallow bound state is extremely sensitive to the one-pion-exchange force, which decreases exponentially as the pion mass increases. It will be very desirable to perform a dynamical lattice QCD simulation with (1) the  $D\bar{D}^*$  interpolators only, (2) explicit isospin violation and (3) the pion mass around 140 MeV.
- The assignment of the  $X(3872)$  as  $\chi'_{c1}$  is also feasible if there exist strong coupled channel effects between the bare  $c\bar{c}$  state in the quark model and the  $\bar{D}D^*$  scattering state, which helps to lower the mass of the bare  $c\bar{c}$  state and explain the isospin violating decay mode. In fact, a lattice candidate for the  $X(3872)$  with  $J^{PC} = 1^{++}$  and  $I = 0$  was found only if both  $\bar{c}c$  and  $D\bar{D}^*$  interpolators are included [579]. As a mixture of  $c\bar{c}$  and  $\bar{D}D^*$ , the large  $\psi'\gamma$  decay ratio of the  $X(3872)$  and its large production rate at hadron colliders can be understood easily.
- The extreme proximity of the  $X(3872)$  to the  $D\bar{D}^*$  threshold requires a large  $D\bar{D}^*$  component in its wave function. Otherwise, such proximity seems too accidental to be convincing.
- If the  $X(3872)$  turns out to be a mixture of the  $J^{PC} = 1^{++}(2P)$   $c\bar{c}$  component and a substantial  $D^0\bar{D}^{*0}$  continuum component, one may expect the existence of another  $X(3872)$ -like state. The flavor wave function of this state is orthogonal to that of the  $X(3872)$ . Its mass may be higher than 3872 MeV and has the same quantum numbers as the  $\chi'_{c1}$ . This state may be quite broad due to the existence of the open-charm decay modes. In other words, the  $X(3872)$  may be more molecule-like while the other state is more  $c\bar{c}$ -like.
- The experimental identification of the  $\chi'_{c1}$  state is extremely important, which shall shed light not only on the  $X(3872)$  but also on the  $c\bar{c}(2P)$  states.

#### 4.6. $Y(4260)$

The  $Y(4260)$ , which has been reviewed in Sec. 2.1.2.1, also attracted great attentions from both experimentalists and theorists. However, its nature is still controversial. In the following, we mainly focus on several major theoretical aspects of the  $Y(4260)$ , i.e., the hybrid charmonium, the vector tetraquark state, the molecular state and non-resonant explanation.

#### 4.6.1. Is $Y(4260)$ a higher charmonium?

Since the  $Y(4260)$  is directly produced from the  $e^+e^-$  annihilation process, its spin-parity quantum number must be  $J^{PC} = 1^{--}$ , which is consistent with that of a vector charmonium state. Thus, theorists tried to categorize it into the vector charmonium family. Different proposals were proposed, such as the  $3D$  ( $3^3D_1$ ) and the  $4S$  ( $4^3S_1$ ) charmonium states, and so on.

In Ref. [675], Llanes-Estrada endorsed the  $Y(4260)$  as the  $\psi(4260)$ , corresponding to the  $4S$  vector charmonium state, where the S-D wave interference was used to explain the lack of a signal in  $e^+e^-$  annihilations. They also suggested some avenues that can exclude exotic meson assignments. In Ref. [676], Zhang studied the charmonium spectrum by combining the linearity and parallelism of the Regge trajectories with a hyperfine splitting relation in multiplet, and interpreted the  $Y(4260)$  as the  $3^3D_1$  charmonium state. In Ref. [570], Li and Chao calculated the masses, electromagnetic decays, and E1 transitions of charmonium states in the screened potential model. In their model, the mass of the  $\psi(4S)$  was predicted to be 4273 MeV, which is roughly compatible with the observed masses of the  $Y(4260)$ . In Ref. [677], Shah, Parmar, and Vinodkumar studied the masses of the S-wave quarkonia based on the Martin-like potential. They also found that the  $Y(4260)$  can be interpreted as the  $4S$  charmonium state.

However, in Ref. [678], Eichten, Lane, and Quigg refined the Cornell coupled-channel model for the coupling of the  $c\bar{c}$  levels to two-meson states in light of new experimental information. Especially, they calculated the decay behavior of the  $2^3D_1$  charmonium state and excluded this assignment of the  $Y(4260)$ . In Ref. [679], Segovia, Yasser, Entem, and Fernandez studied the energy spectrum, electromagnetic, and strong decays of the  $J^{PC} = 1^{--}$  hidden charm resonances in a constituent quark model, in order to assert if they are  $c\bar{c}$  states or more complicated structures. They found that the new  $Y(4360)$  state can be identified as the  $4S$  state and the  $\psi(4415)$  as the  $3D$  state. However, they found that the  $Y(4260)$  cannot be categorized into the charmonium family.

In Ref. [680], Dai, Shi, Tang, and Zheng studied the property of the  $Y(4260)$  resonance by re-analyzing the experimental data till March 2015. They took into account the final state interactions of the  $\pi\pi$  and  $K\bar{K}$  couple channels, and found a sizable coupling between the  $Y(4260)$  and the  $\omega\chi_{c0}$ . They found two nearby poles in the  $Y(4260)$  propagator, indicating that the  $Y(4260)$  is most likely a confining state. They argued that the small value of  $\Gamma_{e^+e^-}$  is consistent with the hybrid scenario, and also consistent with the explanation that the  $Y(4260)$  is the  $3D$  charmonium state. However, the difficulty of the  $3D$  explanation comes from the role of the  $X(4160)$ , which is considered as a good candidate of the  $3D$  charmonium state in quark model.

The resonant parameters of the  $Y(4260)$  listed in Table 6 show that it has a large width. Under the higher charmonium assignment, the open-charm decays of the  $Y(4260)$  are probably dominant. However, the  $Y(4260)$  was only observed in its hidden-charm decay mode  $J/\psi\pi^+\pi^-$ , but missing in any open-charm decay mode (see Fig. 55). In fact, the non-observation of the  $Y(4260)$  in the open-charm modes is challenging for all theoretical interpretations.

In addition, the  $R$  value scan (the ratio of  $\sigma(e^+e^- \rightarrow \text{hadrons})$  and  $\sigma(e^+e^- \rightarrow \mu^+\mu^-)$ ) is applied to identify vector resonances like  $\rho$ ,  $\omega$ ,  $\phi$ , and  $J/\psi$ . However, one cannot find an enhancement structure corresponding to the  $Y(4260)$  from the  $R$  value scan (see Fig. 56).

#### 4.6.2. The hybrid charmonium

Among various assignments, the hybrid charmonium configuration is particularly interesting. After its observation in 2005, the author of Ref. [682] proposed the hybrid charmonium interpretation of the  $Y(4260)$ . He discussed several possible structures of the  $Y(4260)$  meson with  $J^{PC} = 1^{--}$  as a conventional  $c\bar{c}$  state, couple-channel effect, hadron molecule, tetraquark state, glueball and charmonium hybrid. The main points are summarized below [682]

- The  $Y(4260)$  does not look like a conventional  $c\bar{c}$  state with  $J^{PC} = 1^{--}$ . In PDG [1], the  $1^{--}$  radially excited S-wave states  $\psi(2S)$ ,  $\psi(3S)$ ,  $\psi(4S)$  and D-wave state  $\psi(2D)$  were established to be  $\psi'$ ,  $\psi(4040)$ ,  $\psi(4415)$  and  $\psi(4160)$  respectively. The  $\psi(3D)$  and  $\psi(5S)$  were predicted above 4.5 GeV in quark model. It is nearly impossible to accommodate  $Y(4260)$  as a conventional charmonium state.
- It is very difficult to shift the mass of the  $\psi(3D)$  from above 4.5 GeV down to 4.26 GeV by the couple-channel effects. As indicated in Ref. [106], the couple-channel effects of the open-charm thresholds can only cause around tens MeV mass shift of the  $c\bar{c}$  state, which is too small compared with the mass difference between the  $\psi(3D)$  and the  $Y(4260)$  meson.

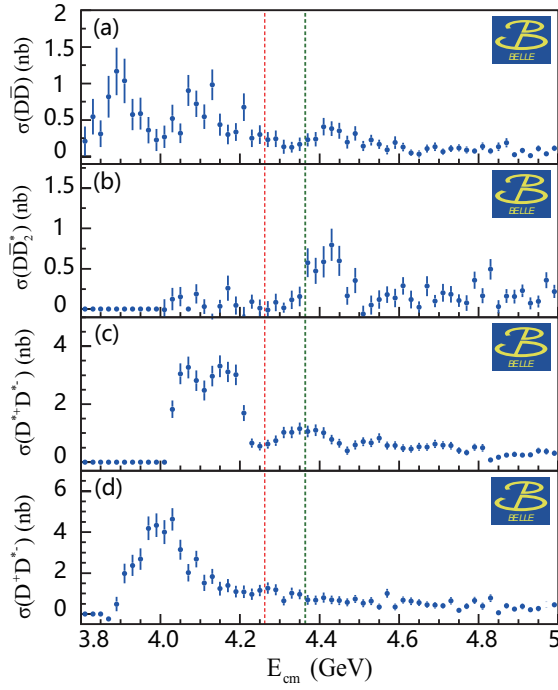


Figure 55: (Color online) The experimental data of the open-charm decay channels from  $e^+e^-$  annihilation. Here, (a)  $e^+e^- \rightarrow D\bar{D}$  [681]; (b)  $e^+e^- \rightarrow D^0D^-\pi^+$  [116]; (c)  $e^+e^- \rightarrow D^{*+}D^{*-}$  [115]; (d)  $e^+e^- \rightarrow D^+D^{*-}$  [115]. The red and green dashed vertical lines correspond to the central values of the masses of  $Y(4260)$  and  $Y(4360)$  [1], respectively.

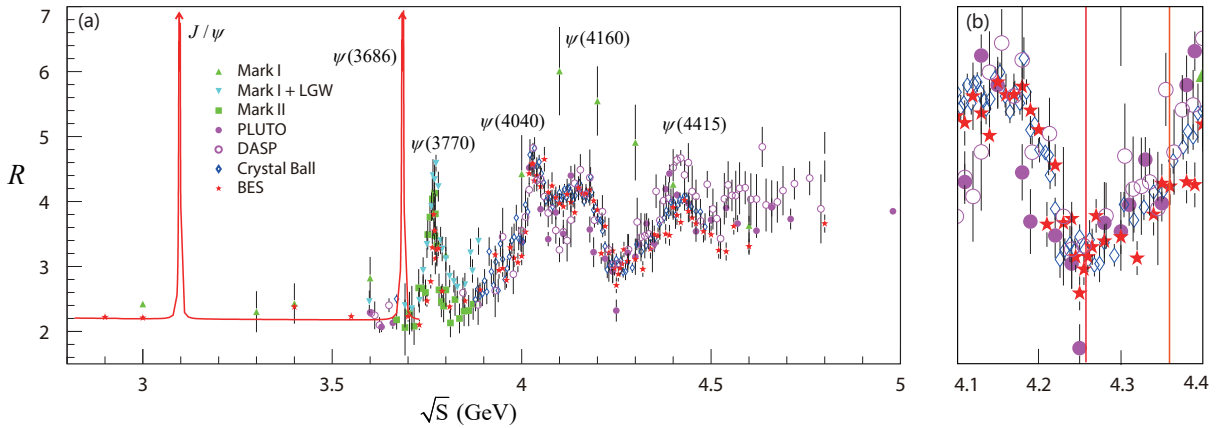


Figure 56: (Color online) (a) The experimental data of  $R$  value from PDG [1]. (b) The detailed data corresponding to the range  $\sqrt{s} = 4.1 \sim 4.4$  GeV from PDG [1]. Here, the vertical lines correspond to the central values of the masses of the  $Y(4260)$  and  $Y(4360)$  [1], respectively. All the data here are taken from <http://pdg.lbl.gov/current/xsect/>.

- The  $Y(4260)$  seems not a hadronic molecule. Its quantum number  $J^{PC} = 1^{--}$  excludes the possibility of the  $\bar{D}_s D_{s0}(2317)$  molecule, which is only 26 MeV above the  $Y(4260)$  meson. The total decay width of the  $Y(4260)$  disfavors the assignments of the  $\bar{D}D_1$ ,  $\bar{D}D'_1$ ,  $\bar{D}_0 D^*$  and  $\bar{D}^* D'_1$  molecules.
- The  $J^{PC} = 1^{--}$  glueball is disfavored by its distinct decay patterns. If it is a glueball, the  $Y(4260)$  meson should mainly decay into multiple light mesons due to the large phase space. However, it was observed in the decay mode  $J/\psi\pi^+\pi^-$ .
- The tetraquark hypothesis is also not favored by the not-so-large total width of the  $Y(4260)$  meson and the absence of the open-charm  $D\bar{D}$  decay mode. The charmonium-like tetraquark states can easily decay into  $D\bar{D}$  final state via the so called “fall-apart” mechanism. The decay width of such modes would be expected to be more than several hundreds MeV due to the big phase space. This is in conflict with total width 80 – 130 MeV of the  $Y(4260)$  meson, as shown in Table 6. To completely exclude the tetraquark possibility, Zhu suggested to search for the isovector partner of  $Y(4260)$ .
- The charmonium hybrid interpretation of the  $Y(4260)$  is strongly favored by the experimental data. As a hybrid meson, its two S-wave meson decay modes are suppressed according to QCD sum rule calculations [683, 684] and flux tube model analysis [685, 686]. Instead the final states with one S-wave meson and one P-wave meson are potentially important. Such a decay pattern is consistent with the experimental data of the  $Y(4260)$  meson, in which the open-charm  $D\bar{D}$  decay mode was not observed. The decay mode  $Y(4260) \rightarrow \omega + \chi_{c0,1,2} \rightarrow 3\pi + \chi_{c0,1,2}$  was suggested to be important in the charmonium hybrid configuration [682].

As a result, the author of Ref. [682] excluded the possibility of the  $Y(4260)$  being a conventional  $c\bar{c}$  state, a molecule, a glueball and a tetraquark state and concluded that the  $Y(4260)$  meson was a good candidate of the charmonium hybrid state.

Kou and Pene supported this charmonium hybrid interpretation with several important dynamical arguments in Ref. [687]. They proposed that the  $Y(4260)$  was a  $1^{--}$  charmonium hybrid state ( $H_B$ ) containing a pseudoscalar colour-octet  $0^{+-} \bar{c}c$  and a magnetic constituent gluon in P-wave. They proved a selection rule that the symmetries of the wave function forbid the decay into two S-wave charmed mesons  $D^{(*)}\bar{D}^{(*)}$  in any potential model. For the decay processes  $H_B \rightarrow D^{(*)}\bar{D}^{(*)}$ , the spatial overlap was described as

$$I = \int \int \frac{d\vec{p}_{c\bar{c}} d\vec{k}}{\sqrt{2\omega}(2\pi)^6} \Psi_{l_{H_B}}^{m_{H_B}}(\vec{p}_{c\bar{c}}, \vec{k}) \Psi_{l_B}^{m_B^*}(\vec{p}_B) \Psi_{l_C}^{m_C^*}(\vec{p}_C) d\Omega_f Y_l^{m^*}(\Omega_f), \quad (145)$$

where  $\Psi_{l_{H_B}}^{m_{H_B}}$ ,  $\Psi_{l_B}^{m_B^*}(\vec{p}_B)$ , and  $\Psi_{l_C}^{m_C^*}(\vec{p}_C)$  were the spacial wave functions for the initial hybrid state and the final  $D^{(*)}$  and  $\bar{D}^{(*)}$  states, respectively. The authors of Ref. [687] proved that this overlap integral vanishes in the case of two S-wave mesons final states. Thus, the decay  $H_B \rightarrow D^{(*)}\bar{D}^{(*)}$  was forbidden in any potential model. Therefore, the hybrid charmonium  $H_B$  had a relatively narrow width, which matches the experimental observation for the  $Y(4260)$ . They also suggested the decay  $Y(4260) \rightarrow D^{**}\bar{D}^{(*)} \rightarrow D^{(*)}\bar{D}^{(*)}\pi'$  ( $D^{**}$  denotes a P-wave charmonium state) to be dominant.

Later, Close and Page also proposed the charmonium hybrid assignment to the  $Y(4260)$  [688]. They assessed the experimental information of the  $Y(4260)$ , including the near  $D_1(2420)\bar{D}$  threshold mass, the dominant  $J/\psi\sigma$ ,  $J/\psi f_0(980)$ ,  $J/\psi a_0(980)$  decay modes and the small partial decay width  $\Gamma(Y(4260) \rightarrow e^+e^-)$ . All these properties were inconsistent with those of conventional  $c\bar{c}$  states. They discussed the previous studies of hybrid meson decays [684, 687] and the mass predictions for charmonium hybrids in the flux-tube model [689, 690], the UKQCD quenched lattice QCD [691, 692, 693] and quenched lattice NRQCD [694, 695]. Accordingly, they proposed the charmonium hybrid interpretation of the  $Y(4260)$  and suggested experimental searches for the  $Y(4260)$  in the  $Y(4260) \rightarrow \{\sigma, \eta\}h_c$  processes [688].

In Ref. [576], Liu *et al.* presented a mass spectrum of the highly excited charmonium mesons and the charmonium hybrid mesons using dynamical lattice QCD simulation. They used the operator of the general form  $\bar{\psi}\Gamma \overleftrightarrow{D}_i \overleftrightarrow{D}_j \cdots \psi$  to evaluate the two-point correlation functions, where the  $\overleftrightarrow{D} = \overrightarrow{D} - \overleftarrow{D}$  is the covariant operator. Using distillation and the variational method with a large basis of operators, they successfully computed the dynamical spectrum of

charmonium hybrids. They identified the lightest hybrid supermultiplet consisting of states with quantum numbers  $J^{PC} = (0, 1, 2)^{-+}, 1^{--}$ , as well as an excited hybrid supermultiplet. The mass of the  $1^{--}$  charmonium hybrid in their mass spectrum was around 4.2 GeV, which allows an interpretation of the  $Y(4260)$  as a vector hybrid meson.

The mass spectra of heavy quarkonium hybrids were also studied in Coulomb gauge QCD with gluon degrees of freedom in the mean field approximation in Ref. [696]. Their predictions of the hybrid masses were systematically higher compared to lattice. For example, they found that the  $1^{++}$  and  $1^{--}$  hybrid states lie at 4.47 GeV. This value was heavier than the mass of the  $Y(4260)$  meson [696]. The mass of the charmonium hybrid meson was also studied in QCD sum rules in Ref. [697, 698, 699, 700, 701, 702, 703].

#### 4.6.3. The vector tetraquark state

In Ref. [704], Maiani, Riquer, Piccinini, and Polosa proposed that the  $Y(4260)$  is the first orbital excitation of a diquark-antidiquark state  $[cs][\bar{c}\bar{s}]$ , and predicted that the  $Y(4260)$  should decay predominantly in  $D_s\bar{D}_s$ , as well as be seen in  $B$  non-leptonic decays in association with one kaon [538]. Later in Ref. [705], Drenska, Faccini, and Polosa studied the  $[cs][\bar{c}\bar{s}]$  diquark-antidiquark particles with different  $J^{PC}$  quantum numbers. They computed their spectrum and decay modes within a constituent diquark-antidiquark model, and predicted  $m_Y = 4330 \pm 70$  MeV for the  $Y(4260)$ .

This idea was updated in their “type-II” diquark-antidiquark model, reviewed in Sec. 4.2.2, by taking into account the orbital angular momentum between diquark and antidiquark. For this case, they used the notation  $|s, \bar{s}; S, L\rangle_J$  to denote the excited tetraquark states with the total spin  $S = s + \bar{s}$  and total angular momentum  $J$ , where  $s = s_{qc}$  and  $\bar{s} = s_{\bar{q}\bar{c}}$  are the diquark and antidiquark spins, respectively. For tetraquark states of  $J^{PC} = 1^{--}$ , there are four states having  $L = 1$  and one state having  $L = 3$ :

$$\begin{aligned} Y_1 &= |0, 0; 0, 1\rangle_1, \\ Y_2 &= \frac{1}{\sqrt{2}}(|1, 0; 1, 1\rangle_1 + |0, 1; 1, 1\rangle_1), \\ Y_3 &= |1, 1; 0, 1\rangle_1, \\ Y_4 &= |1, 1; 2, 1\rangle_1, \\ Y_5 &= |1, 1; 2, 3\rangle_1. \end{aligned} \tag{146}$$

They used a Hamiltonian containing both spin-orbit and spin-spin interactions

$$H = B_c \frac{L^2}{2} - 2a\mathbf{L} \cdot \mathbf{S} + 2\kappa'_{qc} (s_q \cdot s_c + s_{\bar{q}} \cdot s_{\bar{c}}), \tag{147}$$

and discussed possible interpretations of  $Y(4008)$ ,  $Y(4260)$ ,  $Y(4630)$ , etc.

Especially, they fixed the assignment that  $Y(4260) = Y_2 = \frac{1}{\sqrt{2}}(|1, 0; 1, 1\rangle_1 + |0, 1; 1, 1\rangle_1)$ . Hence, in their model the  $Y(4260)$  is just the first orbital excitation of the  $X(3872) = \frac{1}{\sqrt{2}}(|1, 0; 1, 0\rangle_1 + |0, 1; 1, 0\rangle_1)$ . This idea was later used in Ref. [706] by Chen, Maiani, Polosa, and Riquer to calculate the radiative transition  $Y(4260) \rightarrow \gamma X(3872)$ ,  $\Gamma_{\text{rad}} \equiv \Gamma(Y(4260) \rightarrow \gamma X(3872))$ , using a non-relativistic calculation of the electric dipole term of a diquarkonium bound state. Specializing to  $I = 0$  for the  $X(3872)$ , they found  $\Gamma_{\text{rad}} = 496$  keV for the  $Y(4260)$  with  $I = 0$  and  $\Gamma_{\text{rad}} = 179$  keV for  $I = 1$ . They derived upper bounds to  $\mathcal{B}(Y(4260) \rightarrow J/\psi + \pi + \pi)$  and to  $\Gamma(Y(4260) \rightarrow \mu^+ \mu^-)$ , which can be confronted with future data from electron-positron and hadron colliders.

The diquark-antidiquark picture for the  $Y(4260)$  was also studied in Refs. [542, 487] by Ebert, Faustov, and Galkin in the framework of the relativistic quark model. They treated the dynamics of the light quark in a heavy-light diquark completely relativistically, and investigated the internal structure of the diquark by calculating the diquark-gluon form factor in terms of the diquark wave functions. They found that the  $Y(4260)$  cannot be interpreted as the  $1^{--} 1P$  state of the charm-strange diquark-antidiquark tetraquark, i.e.,  $([cs]_{S=0}[\bar{c}\bar{s}]_{S=0})$ . Instead, they found that a more natural tetraquark interpretation for the  $Y(4260)$  is the  $1^{--} 1P$  state of  $([cq]_{S=0}[\bar{c}\bar{q}]_{S=0})_{P\text{-wave}}$ . The other two possibilities are the  $1^{--} 1P$  states of  $\frac{1}{\sqrt{2}}([cq]_{S=0}[\bar{c}\bar{q}]_{S=1})_{P\text{-wave}} - [cq]_{S=1}[\bar{c}\bar{q}]_{S=0})_{P\text{-wave}}$  and  $([cq]_{S=1}[\bar{c}\bar{q}]_{S=1})_{P\text{-wave}}$ .

The authors of Ref. [420] had studied the charmonium-like tetraquark states with  $J^{PC} = 1^{--}$  in QCD sum rules.

They constructed the diquark-antidiquark tetraquark interpolating currents

$$\begin{aligned}
J_{1\mu} &= q_a^T C \gamma_5 Q_b (\bar{q}_a \gamma_\mu \gamma_5 C \bar{Q}_b^T + \bar{q}_b \gamma_\mu \gamma_5 C \bar{Q}_a^T) - q_a^T C \gamma_\mu \gamma_5 Q_b (\bar{q}_a \gamma_5 C \bar{Q}_b^T + \bar{q}_b \gamma_5 C \bar{Q}_a^T), \\
J_{2\mu} &= q_a^T C \gamma^\nu Q_b (\bar{q}_a \sigma_{\mu\nu} C \bar{Q}_b^T - \bar{q}_b \sigma_{\mu\nu} C \bar{Q}_a^T) - q_a^T C \sigma_{\mu\nu} Q_b (\bar{q}_a \gamma^\nu C \bar{Q}_b^T - \bar{q}_b \gamma^\nu C \bar{Q}_a^T), \\
J_{3\mu} &= q_a^T C \gamma_5 Q_b (\bar{q}_a \gamma_\mu \gamma_5 C \bar{Q}_b^T - \bar{q}_b \gamma_\mu \gamma_5 C \bar{Q}_a^T) - q_a^T C \gamma_\mu \gamma_5 Q_b (\bar{q}_a \gamma_5 C \bar{Q}_b^T - \bar{q}_b \gamma_5 C \bar{Q}_a^T), \\
J_{4\mu} &= q_a^T C \gamma^\nu Q_b (\bar{q}_a \sigma_{\mu\nu} C \bar{Q}_b^T + \bar{q}_b \sigma_{\mu\nu} C \bar{Q}_a^T) - q_a^T C \sigma_{\mu\nu} Q_b (\bar{q}_a \gamma^\nu C \bar{Q}_b^T + \bar{q}_b \gamma^\nu C \bar{Q}_a^T), \\
J_{5\mu} &= q_a^T C Q_b (\bar{q}_a \gamma_\mu C \bar{Q}_b^T + \bar{q}_b \gamma_\mu C \bar{Q}_a^T) - q_a^T C \gamma_\mu Q_b (\bar{q}_a C \bar{Q}_b^T + \bar{q}_b C \bar{Q}_a^T), \\
J_{6\mu} &= q_a^T C \gamma^\nu \gamma_5 Q_b (\bar{q}_a \sigma_{\mu\nu} \gamma_5 C \bar{Q}_b^T + \bar{q}_b \sigma_{\mu\nu} \gamma_5 C \bar{Q}_a^T) - q_a^T C \sigma_{\mu\nu} \gamma_5 Q_b (\bar{q}_a \gamma^\nu \gamma_5 C \bar{Q}_b^T + \bar{q}_b \gamma^\nu \gamma_5 C \bar{Q}_a^T), \\
J_{7\mu} &= q_a^T C Q_b (\bar{q}_a \gamma_\mu C \bar{Q}_b^T - \bar{q}_b \gamma_\mu C \bar{Q}_a^T) - q_a^T C \gamma_\mu Q_b (\bar{q}_a C \bar{Q}_b^T - \bar{q}_b C \bar{Q}_a^T), \\
J_{8\mu} &= q_a^T C \gamma^\nu \gamma_5 Q_b (\bar{q}_a \sigma_{\mu\nu} \gamma_5 C \bar{Q}_b^T - \bar{q}_b \sigma_{\mu\nu} \gamma_5 C \bar{Q}_a^T) - q_a^T C \sigma_{\mu\nu} \gamma_5 Q_b (\bar{q}_a \gamma^\nu \gamma_5 C \bar{Q}_b^T - \bar{q}_b \gamma^\nu \gamma_5 C \bar{Q}_a^T),
\end{aligned} \tag{148}$$

where Q is the charm quark for charmonium-like tetraquark systems and bottom quark for bottomonium-like systems. Using these interpolating currents, the two-point correlation functions and spectral densities were calculated up to the dimension eight condensates in the OPE series. The mass spectrum of the  $1^{--}$  charmonium-like tetraquark states was collected in Table 27. The mass of the vector charmonium-like  $qc\bar{q}\bar{c}$  tetraquark state was extracted as 4.5 – 4.8 GeV within the uncertainties. These values were much higher than the mass of the  $Y(4260)$  meson but consistent with that of the  $Y(4660)$ . The numerical results didn't support the tetraquark interpretation of the  $Y(4260)$  state, which was consistent with the discussion in Ref. [682]. The vector hidden-charm and hidden-bottom tetraquark states were also studied in QCD sum rules in Refs. [707, 708].

Table 27: Mass spectrum of the charmonium-like  $qc\bar{q}\bar{c}$  and  $sc\bar{s}\bar{c}$  tetraquark states with  $J^{PC} = 1^{--}$  [420].

	Current	$s_0(\text{GeV}^2)$	Borel window (GeV $^2$ )	$m_X$ (GeV)	PC(%)
$qc\bar{q}\bar{c}$	$J_{1\mu}$	$5.0^2$	2.9 – 3.6	$4.64 \pm 0.09$	44.1
	$J_{4\mu}$	$5.0^2$	2.9 – 3.6	$4.61 \pm 0.10$	46.4
	$J_{7\mu}$	$5.2^2$	2.9 – 4.1	$4.74 \pm 0.10$	47.3
$sc\bar{s}\bar{c}$	$J_{1\mu}$	$5.4^2$	2.8 – 4.5	$4.92 \pm 0.10$	50.3
	$J_{2\mu}$	$5.0^2$	2.8 – 3.5	$4.64 \pm 0.09$	48.6
	$J_{3\mu}$	$4.9^2$	2.8 – 3.4	$4.52 \pm 0.10$	45.6
	$J_{4\mu}$	$5.4^2$	2.8 – 4.5	$4.88 \pm 0.10$	51.7
	$J_{7\mu}$	$5.3^2$	2.8 – 4.3	$4.86 \pm 0.10$	46.0
	$J_{8\mu}$	$4.8^2$	2.8 – 3.1	$4.48 \pm 0.10$	43.2

#### 4.6.4. The molecular state

There are several molecular interpretations for the  $Y(4260)$  state. In Ref. [709], Yuan, Wang, and Mo interpreted the  $Y(4260)$  as an  $\omega\chi_{c1}$  molecular state and discussed both its production and decay properties [709].

Later in Ref. [217], Ding performed a dynamical study of the  $Y(4260)$  and  $Z_2^+(4250)$  simultaneously in the framework of the meson exchange model to see whether they could be the  $D_1\bar{D}$  or  $D_0\bar{D}^*$  hadronic molecule. He employed the heavy meson chiral Lagrangian, which combines the heavy quark symmetry and the chiral symmetry. He found that the off-diagonal interaction induced by the  $\pi$  exchange plays a dominant role. The diagonal interactions contain

the  $\sigma$  exchange and the light vector meson exchange. The contribution of the  $\sigma$  exchange does not favor the formation of the molecular state with  $I^G(J^{PC}) = 0^-(1^{--})$ , but favors the binding of the molecule with  $I^G(J^P) = 1^-(1^-)$ . He suggested that the  $Y(4260)$  could be accommodated as a  $D_1D$  and  $D_0D^*$  molecule. He also studied the bottom analog of the  $Y(4260)$  and proposed to observe it in the  $\pi^+\pi^-\Upsilon$  channel.

In Refs. [202, 203], Close and Downum, and Thomas studied the strong  $S$ -wave pion exchange effects, and suggested that a spectroscopy of quasi-molecular states may arise in the case of charmed mesons  $D$ ,  $D^*$ ,  $D_0$ ,  $D_1$ , which are consistent with enigmatic charmonium states observed above 4 GeV in  $e^+e^-$  annihilations. They discussed the possible interpretations of the  $Y(4260)$  being  $D\bar{D}_1$  and  $D^*\bar{D}_1$  bound states, and proposed to observe the  $D\bar{D}\pi\pi$  channel to compare with the  $D\bar{D}\pi\pi$  channel, which can be used to reveal the mixing between  $D^*\bar{D}_1$  and  $D\bar{D}_1/D^*\bar{D}_0$  molecular systems.

The interaction potentials between one  $S$ -wave and one  $P$ -wave heavy mesons as well as the potentials between two  $P$ -wave heavy mesons were deduced based on a chiral quark model by Li, Wang, Dong, and Zhang in Ref. [483]. They concluded that the  $Y(4260)$  can not be explained as the  $D^*\bar{D}^{*0}$  molecule, but might be explained as a  $0^-(1^{--})D\bar{D}_1$  molecule.

The interpretation of the  $Y(4260)$  as a  $D_1\bar{D}$  molecule was also discussed in Ref. [710] by Cleven *et al.*. They demonstrated that the nontrivial cross section line shapes of  $e^+e^- \rightarrow J/\psi\pi\pi$  and  $h_c\pi\pi$  can be naturally explained by the molecular scenario, and found a significantly smaller mass for the  $Y(4260)$ . They also predicted an unusual line shape of the  $Y(4260)$  in the  $D\bar{D}^*$  channel, which could be a smoking gun for a predominantly molecular nature of the  $Y(4260)$ .

The lattice QCD calculation of  $D$  and  $\bar{D}_1$  interaction can be found in Ref. [711]. In this reference the TWQCD Collaboration used a molecular type operator composed of  $D$  and  $\bar{D}_1$  mesons,  $(\bar{q}\gamma_5\gamma_i c)(\bar{c}\gamma_5 q) - (\bar{c}\gamma_5\gamma_i q)(\bar{q}\gamma_5 c)$ , and detected a  $1^{--}$  signal with a mass around  $4238 \pm 31$  MeV in quenched lattice QCD simulations with exact chiral symmetry, which was identified with the  $Y(4260)$ .

#### 4.6.5. Non-resonant explanations

In Ref. [712], van Beveren and Rupp argued that the puzzling branching ratios of open-charm decays in  $e^+e^-$  annihilations can be reasonably described with a simple form factor, which strongly suppresses open channels far above the threshold. They applied this idea to study the  $e^+e^- \rightarrow J/\psi\pi\pi$  data on the  $Y(4260)$  enhancement, and obtained a good fit with a simple nonresonant cusp structure around the  $D_s^*\bar{D}_s^*$  threshold. Moreover, they found the data shows an oscillatory pattern between a fast (OZI-allowed) and a slow (OZI-forbidden)  $J/\psi f_0(980)$  mode.

In Ref. [713], van Beveren, Rupp, and Segovia reconstructed the shape of the  $Y(4260)$  observed in  $e^+e^- \rightarrow J/\psi\pi^+\pi^-$  by a stepwise study, where they considered the contributions from the open-charm thresholds like  $D\bar{D}$ ,  $D\bar{D}^*$ ,  $D^*\bar{D}^*$ ,  $D_s\bar{D}_s$ ,  $D_s\bar{D}_s^*$ ,  $D_s^*\bar{D}_s^*$ ,  $\Lambda_c\bar{\Lambda}_c$ , and all well-known vector charmonia ( $\psi(4040)$ ,  $\psi(4160)$ , and  $\psi(4415)$ ) with mass above 4 GeV. Additionally, they concluded that the  $\psi(3D)$  charmonium state has been observed in a range of 4.53-4.58 GeV with a width around 40-70 MeV.

Chen, He and Liu also proposed a non-resonant explanation for the  $Y(4260)$  structure observed in the  $e^+e^- \rightarrow J/\psi\pi^+\pi^-$  process [714], where they considered the interference of the production amplitudes of the  $e^+e^- \rightarrow J/\psi\pi^+\pi^-$  process via the direct  $e^+e^-$  annihilation and through intermediate charmonia  $\psi(4160)/\psi(4415)$  (see Fig. 57). The  $Y(4260)$  structure was reproduced well, which is shown in Fig. 58. Since the  $Y(4260)$  is not a genuine resonance within this scheme [714], it naturally answers why there is no evidence of the  $Y(4260)$  in the exclusive open-charm decay channels [681, 116, 115] and  $R$ -value scan [1].

Very recently, Chen, Liu, Li and Ke [715] further pointed out that this nonresonant explanation to the  $Y(4260)$  suggested in Ref. [714] is similar to the Fano interference effect, which extensively exists in atomic physics, condensed matter physics and even nuclear physics, where the asymmetric line shape of the  $Y(4260)$  can be reflected by the Fano-like interference picture [715].

#### 4.6.6. Other theoretical schemes, production and decay patterns

The  $Y(4260)$  was interpreted as a molecular state composed of two colored baryons, i.e., a baryonium state in Refs. [716, 717]. The dynamical generation of the  $Y(4260)$  in the  $J/\psi\pi\pi$  and  $J/\psi K\bar{K}$  systems was studied in Ref. [718]. The  $Y(4260)$  was studied in Ref. [719] within the picture of hadrocharmonium, where a compact charmonium was embedded in a light quark mesonic excitation. The coupled-channel effects and nonresonant explanation

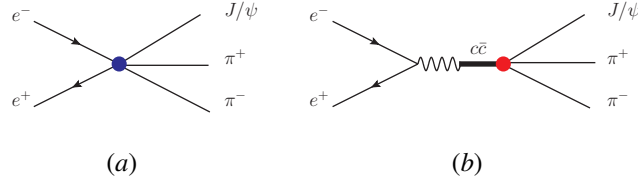


Figure 57: (Color online) The diagrams relevant to  $e^+e^- \rightarrow J/\psi\pi^+\pi^-$ . Here, (a) corresponds to the direct  $e^+e^-$  annihilation into  $J/\psi\pi^+\pi^-$ . (b) is from the contributions of the intermediate charmonia. Taken from Ref. [714].

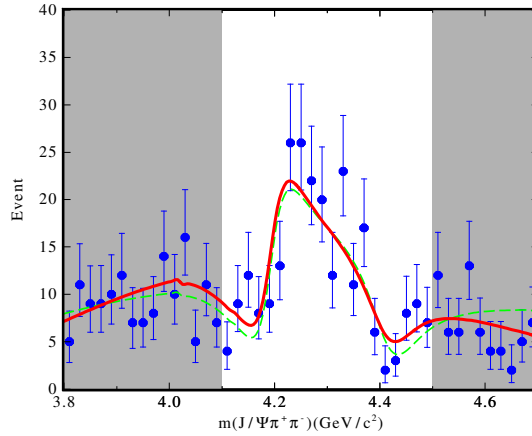


Figure 58: (Color online) The comparison of the obtained fitting result (solid red line) with the experimental data (blue dots with error bar) measured by BaBar [51]. The result is normalized to the experimental data. Taken from Ref. [714].

for the  $Y(4260)$  structure were studied in Refs. [720, 714, 466], while its related threshold effects were studied in Refs. [585, 721]. The bottom counterparts of the  $Y(4260)$ ,  $Y_b$ , were studied in Ref. [616].

Weak productions of the  $Y(4260)$  in semi-leptonic  $B_c$  decays were studied in Ref. [658], where the  $Y(4260)$  was treated as an excited charmonium state. Assuming the  $Y(4260)$  to be a tetraquark state with a hidden  $c\bar{c}$  quark pair, its production at the LHC and Tevatron was studied via the Drell-Yan Mechanism in Ref. [722]. Assuming the  $Y(4260)$  to be a mixture of the charmonium and exotic tetraquark state, its production in  $B$  meson decay was studied using QCD sum rules in Ref. [723].

Assuming the  $Y(4260)$  as a hybrid state, its decays into  $J/\psi\pi\pi$  and open charm mesons were studied in Ref. [687], and its relative decay rates into various  $S$  and  $P$  wave charm meson pairs were calculated using QCD string model in Ref. [724]. Assuming the  $Y(4260)$  to be a  $D_1(2420)\bar{D}$  molecular state, its hidden-charm, charmed pair, and charmless decay channels were studied via the intermediate  $D_1\bar{D}$  meson loops with an effective Lagrangian approach in Refs. [725, 726], while, its strong decay modes  $Z_c(3900)^\pm\pi^\mp$ ,  $J/\psi\pi^+\pi^-$ , and  $\psi(nS)\pi^+\pi^-$ , were studied in Ref. [727]. The authors of Ref. [728] generalized results of lattice QCD to determine the spin-dependent symmetries and factorization properties of the meson production in OZI allowed processes, which were applied to establish the structure of the  $Y(4260)$  from its S-wave decays. The upper limit of the electron width of the  $Y(4260)$ ,  $\Gamma(Y(4260) \rightarrow e^+e^-)$ , was determined to be 580 eV at 90% C.L. in Ref. [729] by Mo, *et al.*

With the spin rearrangement, the authors of Ref. [730] performed a comprehensive investigation of the decay patterns of the  $Y(4260)$  with different inner structures such as the conventional charmonium, the molecule, the P-wave tetraquark and the hybrid charmonium. The  $J/\psi(\pi\pi)_{S\text{-wave}}$  mode is suppressed in the heavy quark symmetry limit if the  $Y(4260)$  is a molecular state and  $(\pi\pi)_{S\text{-wave}}$  arises from either  $\sigma$  or  $f_0(980)$ . Moreover the hybrid charmonium and hidden-charm tetraquark have very similar decay patterns. Both of them decay into the  $J/\psi\pi\pi$  and open charm modes

easily.

#### 4.6.7. A short summary

- There are also some non-resonant explanations for the  $Y(4260)$ , such as the coupled-channel effects, the threshold effects, and the Fano interference effect, etc.
- The  $Y(4260)$  may be the  $\psi(4S)$  or  $\psi(3D)$  charmonium state in some quark models. However, there does not exist an enhancement structure corresponding to the  $Y(4260)$  from the  $R$  value scan. The absence of the open-charm decay channels is also hard to explain.
- Both the  $Y(4260)$  and the  $X(3872)$  were proposed as tetraquark states composed of a pair of diquark and anti-diquark. The  $Y(4260)$  was interpreted as the  $P$ -wave excitation of the  $X(3872)$  state. If the  $Z_c(3885)$  and  $Z_c(4025)$  also turn out to be tetraquark states, the decay process  $e^+e^- \rightarrow Y(4260) \rightarrow \pi^- Z_c(3885)^+ (\rightarrow (D\bar{D}^*)^+)$  and  $e^+e^- \rightarrow Y(4260) \rightarrow \pi^- Z_c(4025)^+ (\rightarrow (D^*\bar{D}^*)^+)$  can be understood naturally. However, some QCD sum rule calculations indicate the vector tetraquark state may lie around 4.6 GeV.
- The  $Y(4260)$  was also suggested as a  $D_1\bar{D}$  molecular state. If the  $Z_c(3885)$  and  $Z_c(4025)$  are also molecular states, the decay process  $e^+e^- \rightarrow Y(4260) \rightarrow \pi^- Z_c(3885)^+ (\rightarrow (D\bar{D}^*)^+)$  and  $e^+e^- \rightarrow Y(4260) \rightarrow \pi^- Z_c(4025)^+ (\rightarrow (D^*\bar{D}^*)^+)$  can also be understood easily. However, the discovery mode  $J/\psi(\pi\pi)_{S\text{-wave}}$  is strongly suppressed in the heavy quark symmetry limit if the  $Y(4260)$  is a molecular state and  $(\pi\pi)_{S\text{-wave}}$  arises from either  $\sigma$  or  $f_0(980)$ .
- The  $Y(4260)$  is a good candidate of the hybrid charmonium state with  $J^{PC} = 1^{--}$ . This interpretation explains the current experimental information, and was supported by the lattice QCD simulations.

#### 4.7. $Y(3940)$ , $Y(4140)$ and $Y(4274)$

The  $Y(3940)$  and  $Y(4140)$ , which were reviewed in Sec. 2.1.1.2 and 2.1.1.3, were observed in the mass spectrum of  $J/\psi + \text{light vector meson}$  in the  $B$  meson decay

$$B \rightarrow K + \begin{cases} Y(3940) & \Rightarrow J/\psi\omega \\ Y(4140) & \Rightarrow J/\psi\phi \end{cases}.$$

Besides the  $Y(4140)$ , the  $Y(4274)$  reviewed in Sec. 2.1.1.3 was also observed in the  $J/\psi\phi$  mass spectrum in the  $B^+ \rightarrow J/\psi\phi K^+$  decay process.

##### 4.7.1. Molecular state scheme

The  $Y(3940)$  and  $Y(4140)$  are close to the thresholds of  $D^*\bar{D}^*$  and  $D_s^*\bar{D}_s^*$ , respectively, and satisfy an almost exact mass relation

$$M_{Y(4140)} - 2M_{D_s^*} \approx M_{Y(3940)} - 2M_{D^*}. \quad (149)$$

Hence, a uniform molecular picture of the  $Y(4140)$  and  $Y(3940)$  was proposed in Refs. [187, 207], where the flavor wave functions of the  $Y(3940)$  and  $Y(4140)$  are:

$$|Y(4140)\rangle = |D_s^{*+} D_s^{*-}\rangle, \quad (150)$$

$$|Y(3940)\rangle = \frac{1}{\sqrt{2}} [ |D^{*0} \bar{D}^{*0}\rangle + |D^{*+} D^{*-}\rangle ]. \quad (151)$$

Moreover, the authors observed a selection rule for the quantum numbers of the  $Y(3940)$  and  $Y(4140)$  under the  $D^*\bar{D}^*$  and  $D_s^*\bar{D}_s^*$  molecular state assignments. They argued that their widths are narrow naturally, because both the hidden-charm and open charm two-body decays occur through the rescattering of the vector components within the molecular states while the three- and four-body open charm decay modes are forbidden kinematically. The possible quantum numbers of the S-wave vector-vector system are  $J^P = 0^+, 1^+, 2^+$ . However, they can only have  $J^P = 0^+$  and  $2^+$ , for

the neutral  $D^*\bar{D}^*$  system with  $C = +$ , due to  $C = (-1)^{L+S}$  and  $J = S$  with  $L = 0$ . This provides an important criterion to test the molecular explanation for the  $Y(3940)$  and  $Y(4140)$ .

The  $Y(4274)$  was interpreted as the  $S$ -wave  $D_s\bar{D}_{s0}(2317)$  molecular state with  $J^P = 0^-$  in Ref. [211]. This interpretation was supported by dynamical study of the system composed of the pseudoscalar and scalar charmed mesons. They also investigated the  $S$ -wave  $D\bar{D}_0(2400)$  molecular charmonium as the molecular partner of the  $Y(4274)$ , which is in accord with the enhancement structure appearing at 4.2 GeV in the  $J/\psi\omega$  invariant mass spectrum from  $B$  decays [85, 86]. There might also exist structures around the thresholds of the  $D_s\bar{D}'_{s1}(2460)$ ,  $D_s^*\bar{D}_{s0}(2317)$ ,  $D_s\bar{D}_{s1}(2536)$ ,  $D_s\bar{D}_{s2}(2573)$ ,  $D_s^*\bar{D}'_{s1}(2460)$  and  $D_s^*\bar{D}_{s1}(2536)$ .

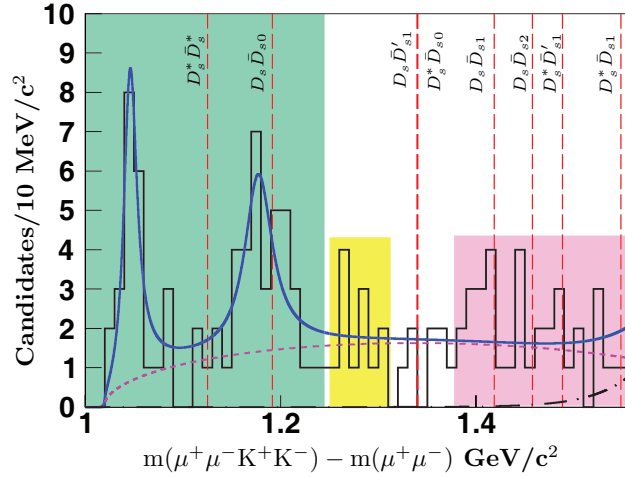


Figure 59: (Color online) The mass difference  $\Delta M = m(\mu^+\mu^-K^+K^-) - m(\mu^+\mu^-)$  distribution (histogram) for events in the  $B^+$  mass window [89]. Besides the  $Y(4140)$ , one explicit enhancement appears around 4274 MeV. Here, the purple dashed line is the background from the three-body phase space. The blue solid line is the fitting result with resonance parameters of the  $Y(4140)$  and  $Y(4270)$  resonances in Ref. [89]. The vertical red dashed lines denote the thresholds of the  $D_s^*D_s^*$ ,  $D_s\bar{D}_{s0}(2317)$ ,  $D_s\bar{D}'_{s1}(2460)$ ,  $D_s^*\bar{D}_{s0}(2317)$ ,  $D_s\bar{D}_{s1}(2536)$ ,  $D_s\bar{D}_{s2}(2573)$ ,  $D_s^*\bar{D}'_{s1}(2460)$  and  $D_s^*\bar{D}_{s1}(2536)$ . Taken from Ref. [211].

The molecular explanation for the  $Y(3940)$  and  $Y(4140)$  was also studied in Refs. [207, 731, 732, 733, 734]. In Ref. [207], the authors performed a dynamical calculation to study whether  $D^*\bar{D}^*$  or  $D_s^*\bar{D}_s^*$  system can be bound. They used the effective Lagrangian approach. The exchanged mesons between the  $D^*$  and  $\bar{D}^*$  ( $D_s^*$  and  $\bar{D}_s^*$ ) include the pseudoscalar, vector and  $\sigma$  mesons. The  $S$ -wave molecular solution was found for the  $Y(4140)$  and  $Y(3940)$  with  $J^P = 0^+, 2^+$ .

In Ref. [731], Mahajan argued that the  $Y(4140)$  is more likely to be a  $D_s^*\bar{D}_s^*$  molecular state or an exotic  $J^{PC} = 1^{-+}$  hybrid charmonium. He also discussed decay modes which would allow unambiguous the identification of the hybrid charmonium option.

In Ref. [732], Branz, Gutsche, and Lyubovitskij suggested that the  $Y(3940)$  and  $Y(4140)$  are heavy hadron molecular states with quantum number  $J^{PC} = 0^{++}$ . They evaluated widths of the strong decays  $Y(3940) \rightarrow J/\psi\omega$ ,  $Y(4140) \rightarrow J/\psi\phi$  and radiative decay  $Y(3940)/Y(4140) \rightarrow \gamma\gamma$  in a phenomenological Lagrangian approach, supporting the molecular interpretation of the  $Y(3940)$  state as a superposition of the  $D^{*+}D^{*-}$  and  $D^{*0}\bar{D}^{*0}$ , and the  $Y(4140)$  as a bound state of the  $D_s^{*+}$  and  $D_s^{*-}$  mesons. They also investigated the alternative assignment of  $J^{PC} = 2^{++}$ , and obtained similar results for the strong decay widths.

In Ref. [733], Ding dynamically studied the interpretation of the  $Y(4140)$  as a  $D_s^*\bar{D}_s^*$  molecule in the one boson exchange approach, where  $\sigma$ ,  $\eta$  and  $\phi$  exchanges were included. He suggested the most favorable quantum number for the  $Y(4140)$  is  $J^{PC} = 0^{++}$ . However,  $0^{++}$  and  $2^{++}$  can not be excluded. He also proposed to search for the  $1^{+-}$  and  $1^{--}$  partners in the  $J/\psi\eta$  and  $J/\psi\eta'$  final states, which is an important test of the molecular hypothesis of the  $Y(4140)$ .

In Ref. [734], Chen and Lu studied the general form of the Bethe-Salpeter wave functions for the bound states composed of two vector fields of arbitrary spin and definite parity, and applied this framework to study the  $Y(3940)$  as a molecule state consisting of the  $D^{*0}$  and  $\bar{D}^{*0}$ . They considered the attractive potential between the  $D^{*0}$  and  $\bar{D}^{*0}$ .

including one light meson ( $\sigma$ ,  $\pi$ ,  $\omega$ , and  $\rho$ ) exchange, and found the obtained mass of the  $Y(3940)$  is consistent with the experimental value.

In QCD sum rules, the  $Y(4140)$  was studied as a scalar  $D_s^* \bar{D}_s^*$  molecular state in Refs. [735, 736, 409]. All these calculations obtained the masses around 4.0 – 4.2 GeV and thus supported the molecular interpretation of the  $Y(4140)$ . However, a negative result was obtained in Refs. [737, 738], in which the mass of the scalar  $D_s^* \bar{D}_s^*$  molecule was extracted at 4.3 – 4.6 GeV. The  $Y(3940)$  was studied as a  $D^* \bar{D}^*$  molecular state in Refs. [736, 409]. These calculations disfavored the molecular interpretation of this state.

A mixed charmonium-molecule scenario was employed to explain the  $Y(3940)$  in Ref. [739], in which the authors used a  $\chi_{c0} - D^* \bar{D}^*$  current with  $J^{PC} = 0^{++}$  to compute the correlation function. For the mixing angle  $\theta = (76.0 \pm 5.0)^\circ$ , the mass was extracted as  $M = (3.95 \pm 0.11)$  GeV and the partial decay width  $\Gamma_{Y \rightarrow J/\psi \omega} = (1.7 \pm 0.6)$  MeV.

In Refs. [740, 741], the  $Y(4274)$  was studied as a  $\bar{D}_s D_{s0}$  hidden-strange charmonium-like molecular state with  $J^{PC} = 0^{-+}$ . The extracted masses were heavier than the mass of the  $Y(4274)$ . The mass of the  $\bar{D} D_0$  was extracted to be  $(4.55 \pm 0.49)$  GeV.

#### 4.7.2. Other theoretical schemes, production and decay patterns

Besides the molecular picture, the  $Y(3940)$ ,  $Y(4140)$  and  $Y(4274)$  were investigated in some other theoretical frameworks [742, 676, 363, 542]. In Ref. [742], Gershtein, Likhoded, and Luchinsky systematically studied heavy quarkonia from Regge trajectories on  $(n, M^2)$  and  $(M^2, J)$  planes, and interpreted the  $Y(3940)$  as the  $\chi_{c0}(2P)$  charmonium state. This was further discussed combining the linearity and parallelism of Regge trajectories with a hyperfine splitting relation in multiplet in Ref. [676].

In the “type-I” diquark-antidiquark model proposed by Maiani, Piccinini, Polosa, and Riquer [363], the  $Y(3940)$  was interpreted as the  $2^{++}$   $S$ -wave state, i.e.,  $Y(3940) = |2^{++}\rangle = |1_{c\bar{q}}, 1_{\bar{c}\bar{q}}; J = 2\rangle$ . In Ref. [542], Ebert, Faustov, and Galkin studied masses of heavy tetraquarks with hidden charm and bottom in the framework of the relativistic quark model, and their results supported the  $Y(3940)$  as a  $2^{++}$  diquark-antidiquark tetraquark, i.e.,  $([c\bar{q}]_{S=1}[\bar{c}\bar{q}]_{S=1})_{J=2}$ .

In Ref. [743], Stancu studied the spectrum of tetraquarks of type  $c\bar{c}s\bar{s}$  within a simple quark model with chromomagnetic interaction, and suggested that the  $Y(4140)$  could possibly be the strange partner of the  $X(3872)$  in a tetraquark interpretation. Later in Ref. [461], Patel, Shah, and Vinodkumar calculated masses of the low-lying four-quark states in the hidden charm sector within the framework of a non-relativistic quark model, and they found that the  $Y(4140)$  can be interpreted as the diquark-antidiquark ( $c\bar{q} - \bar{c}\bar{q}$ ) state, while it can also be interpreted as a  $c\bar{q} - \bar{c}\bar{q}$  molecular-like state only if its parity is positive.

The coupled-channel effects, threshold effects and nonresonant explanation for the  $Y(3940)$ ,  $Y(4140)$  and  $Y(4274)$  were investigated in Refs. [584, 569, 744]. They were also proposed as dynamically generated resonances from the vector-vector interaction within the framework of the hidden gauge formalism in Refs. [745, 746]. Their productions in the  $B$  meson decays were studied using the same approach in Ref. [747]. In Ref. [748], Hidalgo-Duque, Nieves, and Pavon Valderrama proposed an effective field theory incorporating light SU(3)-flavour and heavy quark spin symmetry to describe charmed meson-antimeson bound states. Assuming that the  $X(3915)$  and  $Y(4140)$  are  $D^* \bar{D}^*$  and  $D_s^* \bar{D}_s^*$  molecular states, they determined the full spectrum of molecular states with isospin  $I = 0, 1/2$  and 1.

The weak productions of the  $Y(3940)$ ,  $Y(4140)$ , and  $Y(4274)$  in the semi-leptonic  $B_c$  decays were studied using light-cone QCD sum rules in Ref. [658]. The inclusive production of the  $\chi_{cJ}$  in the  $\eta_b$  decays was studied in Ref. [749], which may help resolve whether some of these states are excited charmonia. In Ref. [750], He and Liu investigated the discovery potential of the  $Y(3940)$  via the photoproduction process  $\gamma p \rightarrow Y(3940)p$ .

Many authors investigated the decay behavior of the  $Y(3940)$ ,  $Y(4140)$ , and  $Y(4274)$ , including their hidden-charm decay, open-charm decay, radiative decay and double-photon decay. The hidden charm decay of the  $Y(3940)$  was investigated in Ref. [653], considering the final state interaction effect. As indicated in Ref. [187], the line shapes of the photon spectrum of  $Y(4140) \rightarrow D_s^{*+} D_s^- \gamma$  and  $Y(3940) \rightarrow D^{*+} D^- \gamma$  are crucial to test the molecule assignment of the  $Y(4140)$  and  $Y(3940)$ . The radiative decay of the  $Y(3940)$  and  $Y(4140)$  was later calculated in Ref. [751].

In Ref. [752], Liu studied the hidden-charm decay of the  $Y(4140)$  assuming it as the second radial excitation of the P-wave charmonium  $\chi_{cJ}''$  ( $J = 0, 1$ ). The upper limit of the branching ratio of the hidden charm decay  $Y(4140) \rightarrow J/\psi \phi$  is of the order of  $10^{-4} \sim 10^{-3}$  for both charmonium assumptions for the  $Y(4140)$ , which disagrees with the large hidden charm decay pattern indicated by the CDF experiment [58]. The assumption of the  $Y(4140)$  as the second radial excitation of the P-wave charmonium  $\chi_{cJ}''$  ( $J = 0, 1$ ) is problematic.

In Ref. [753], He and Liu investigate decay widths and line shapes of the open-charm radiative and pionic decays of the  $Y(4274)$  with the  $D_s\bar{D}_{s0}(2317)$  molecular charmonium assignment. Their calculation indicated that the decay widths of  $Y(4274) \rightarrow D_s^+ D_s^{*-} \gamma$  and  $Y(4274) \rightarrow D_s^+ D_s^- \pi^0$  can reach up to 0.05 keV and 0.75 keV, respectively. The authors suggested future experiments to search for the open-charm radiative and pionic decays of the  $Y(4274)$ .

#### 4.7.3. A short summary

- The  $Y(3940)$ ,  $Y(4140)$ , and  $Y(4274)$  can be interpreted as the  $D^* \bar{D}^*$ ,  $D_s^* \bar{D}_s^*$ , and  $D_s \bar{D}_{s0}(2317)$  molecular states, respectively.
- Some authors interpreted these states as the charmonium states, diquark-antidiquark tetraquark states, etc. There are also non-resonant explanations.

### 4.8. Other charmonium-like states

#### 4.8.1. $Y(4008)$ and $Y(4360)$

There are not so many theoretical studies on the  $Y(4008)$  and  $Y(4360)$ , whose experimental information has been reviewed in Sec. 2.1.2.1 and 2.1.2.2, respectively. In the following, we separately introduce their theoretical research status.

4.8.1.1.  $Y(4008)$ . In Ref. [197], Liu discussed some possible assignments for the  $Y(4008)$ , including both the  $\psi(3S)$  charmonium states and the  $D^* \bar{D}^*$  molecular state. Within both pictures, he found that the branching ratio of  $Y(4008) \rightarrow J/\psi \pi^0 \pi^0$  is comparable with that of  $Y(4008) \rightarrow J/\psi \pi^+ \pi^-$ . He also studied other hidden-charm and open-charm decays, and proposed further experiments to search for missing channels  $D\bar{D}$ ,  $D\bar{D}^*$ ,  $\chi_{cJ} \pi^+ \pi^- \pi^0$ , and  $\eta_c \pi^+ \pi^- \pi^0$ .

These two assignments were also investigated in later studies. In Ref. [570], Li and Chao studied the higher charmonium states in the non-relativistic screened potential model, and interpreted the  $Y(4008)$  as the  $\psi(3S)$  charmonium state. In Ref. [714], Chen, Ye, and Zhang studied strong decays of the radially excited  $\psi(3^3S_1)$  state within the  $^3P_0$  model. They found that the  $Y(4008)$  is hard to be identified with a  $\psi(3^3S_1)$  charmonium if it is confirmed to be below the  $D^* \bar{D}^*$  threshold by experiment. However, it is probably a  $\psi(3^3S_1)$  charmonium once it is above the  $D^* \bar{D}^*$  threshold.

In Ref. [218], Ding studied the  $D^* \bar{D}^*$  system dynamically in the one boson exchange model, and found the interpretation of the  $Y(4008)$  as a  $D^* \bar{D}^*$  molecule is not favored by its huge width, although it is close to the  $D^* \bar{D}^*$  threshold. However, in Ref. [754], Xie, Mo, Wang, and Cotanch studied tetraquark states with hidden charm within an effective Coulomb gauge Hamiltonian approach, and found that the  $Y(4008)$  can be interpreted as the lightest  $1^{--}$  molecule with the  $\eta h_c$  type structure.

The  $Y(4008)$  was studied in Ref. [366] by Maiani, Piccinini, Polosa, and Riquer in their “type-II” diquark-antidiquark model, and interpreted as  $Y(4008) = Y_1 = |0_{c\bar{q}}, 0_{\bar{c}\bar{q}}; 0, 1\rangle_1$ . In Ref. [755], Zhou, Deng, and Ping also interpreted the  $Y(4008)$  as a tetraquark state  $[cq][\bar{c}\bar{q}]$  with  $I J^{PC} = 0 1^{--}$ . They used a color flux-tube model with a four-body confinement potential, and interpreted the  $Y(4008)$  as a tetraquark state  $[cq][\bar{c}\bar{q}]$  with  $n^{2S+1}L_J$  of  $1^1P_1$ .

In Ref. [715], Chen *et al.* proposed that the  $Y(4008)$  is not a genuine resonance, where the broad structure corresponding to the  $Y(4008)$  in  $e^+ e^- \rightarrow J/\psi \pi^+ \pi^-$  can be reproduced when introducing the interference between the continuum and background contributions.

4.8.1.2.  $Y(4360)$ . The  $Y(4360)$  was interpreted as the  $\psi(3D)$  charmonium state in Ref. [570] by Li and Chao using the nonrelativistic screened potential model. In Ref. [756], Ding, Zhu, and Yan also interpreted the  $Y(4360)$  as a  $3^3D_1$   $c\bar{c}$  state, and applied the flux tube model to evaluate its  $e^+ e^-$  leptonic widths, E1 transitions, M1 transitions and the open flavor strong decays. It was interpreted as the  $2S$  bound state in the  $D_1 \bar{D}^*$  system [202, 203], a hadrocharmonium state [719], a tetraquark state [487, 755], a baryonium state [717, 220], and a charmonium hybrid state [724, 697].

The  $Y(4360)$  was interpreted as the  $2S$  bound state in the  $D_1 \bar{D}^*$  system in Refs. [202, 203], while the  $Y(4260)$  was assumed to be the  $1S$  state. In Ref. [719], Li and Voloshin studied the  $Y(4360)$  within the hadrocharmonium picture, where a (relatively) compact charmonium was embedded in a light quark mesonic excitation. They suggested that the  $Y(4260)$  and  $Y(4360)$  are a mixture of two hadrocharmonium states, one containing a spin-triplet  $c\bar{c}$  pair and the other containing a spin-singlet heavy quark pair. Based on this picture, they found a distinctive pattern of interference between the resonances.

In Ref. [366], Maiani, Piccinini, Polosa, and Riquer studied the  $Y(4360)$  in their “type-II” diquark-antidiquark model, and interpreted it as the radial excitation of the  $Y(4008)$ , which has been reviewed in the previous subsection, i.e.  $Y(4008) = Y_1 = |0_{c\bar{q}}, 0_{\bar{c}\bar{q}}; 0, 1\rangle_1$ . In Ref. [487], Ebert, Faustov, and Galkin calculated the masses of the excited heavy tetraquarks with hidden charm within the relativistic diquark-antidiquark picture, and found that the  $Y(4360)$  can be interpreted as the excited  $1^{--} 1P [c\bar{q}][\bar{c}\bar{q}]$  tetraquark state consisting of  $A\bar{A}$ , where  $A$  is an axial vector diquark. In contrast, the  $Y(4360)$  was interpreted as a tetraquark state  $[c\bar{q}][\bar{c}\bar{q}]$  with  $n^{2S+1}L_J$  of  $1^5F_1$  using a color flux-tube model by Zhou, Deng, and Ping in Ref. [755].

In Ref. [717], Qiao proposed that the  $Y(4360)$ , together with the  $Y(4260)$ ,  $Y(4660)$  and  $Z^+(4430)$ , can be systematically embedded into an extended baryonium picture. Later in Ref. [220], Chen and Qiao derived the two-pion exchange interaction potential between heavy baryon and heavy anti-baryon to see whether they can form a bound state. They used the obtained potential to calculate heavy baryonium masses by solving the Schrödinger equation, and found that the  $Y(4360)$  could be interpreted as a  $\Lambda_c\text{-}\bar{\Lambda}_c$  bound state.

In Ref. [724], Kalashnikova and Nefediev employed the QCD string model to calculate the masses and spin splittings of the lowest charmonium hybrid states with a magnetic gluon. The mass of the vector charmonium hybrid state is 4.397 GeV. They argued that strong coupling of the vector hybrid to the  $D\bar{D}_1$  and  $D^*\bar{D}_0$  modes can cause considerable threshold attraction, leading to the formation of the  $Y(4360)$ . Later in Ref. [697], Qiao *et al.* evaluated the masses of the  $1^{--}$  charmonium and bottomonium hybrids in terms of QCD sum rules. They found that the hybrid ground state in charm sector lies in 4.12–4.79 GeV, whose mass resides between the  $Y(4360)$  and  $Y(4660)$ . Hence, they suggested that the  $Y(4360)$ , as well as the  $Y(4660)$ , might be charmonium hybrid candidates.

Moreover, a non-resonant description of the charmonium-like structure  $Y(4360)$  was proposed in Ref. [757]. The authors found that the  $Y(4360)$  structure can be depicted well by the interference effect of the production amplitudes of  $e^+e^- \rightarrow \psi(2S)\pi^+\pi^-$  via the intermediate charmonia  $\psi(4160)/\psi(4415)$  and direct  $e^+e^-$  annihilation into  $\psi(2S)\pi^+\pi^-$  (similar to that in Fig. 57). They argued that the  $Y(4360)$  is not a genuine resonance, which explains why the  $Y(4360)$  was only observed in the hidden-charm decay channel  $\psi(2S)\pi^+\pi^-$  and not observed in the exclusive open-charm decay channel, nor the  $R$ -value scan (see Figures 55 and 56 for more details). In Ref. [715], Chen *et al.* further indicated that the  $Y(4360)$ ,  $Y(4260)$  and  $Y(4008)$  can be due to the Fano-like interference [757].

The Initial Single Pion Emission mechanism was also used to study the hidden-charm dipion decays of the  $Y(4360)$  in Ref. [758]. The authors found that there exist charged charmoniumlike structures near the  $D\bar{D}^*$  and  $D^*\bar{D}^*$  thresholds in the  $J/\psi\pi^+$ ,  $\psi(2S)\pi^+$  and  $h_c(1P)\pi^+$  invariant mass spectra of the hidden-charm dipion decays of the  $Y(4360)$ .

#### 4.8.2. $Y(4660)$ and $Y(4630)$

4.8.2.1.  $Y(4660)$ . The  $Y(4660)$ , which was reviewed in Sec. 2.1.2.2, was observed in the initial-state radiation process  $e^+e^- \rightarrow \gamma_{\text{ISR}}Y(4660)(\rightarrow \pi^+\pi^-\psi(3686))$  [134]. In Ref. [756], Ding, Zhu, and Yan suggested that the  $Y(4660)$  is a good candidate of the  $5^3S_1 c\bar{c}$  state, and evaluated its  $e^+e^-$  leptonic widths, E1 transitions, M1 transitions and the open flavor strong decays in the flux tube model. In contrast, the  $Y(4660)$  was assigned as the  $\psi(6S)$  charmonium state in the screened potential model by Li and Chao in Ref. [570]. However, in Ref. [759], van Beveren and Rupp analyzed the shape of the threshold signals in the production cross sections of the reaction  $e^+e^- \rightarrow D^*\bar{D}^*$  [119], and argued that the  $Y(4660)$  should not be associated with the resonance poles of the  $c\bar{c}$  propagator.

Besides the charmonium state, the  $Y(4660)$  was interpreted as a  $f_0(980)\psi'$  bound state in Refs. [760, 761] and a tetraquark state in Refs. [487, 366], etc. The hadro-charmonium picture was also proposed to explain the  $Y(4660)$  as a compact charmonium resonance bound inside an excited state of light hadronic matter by Dubynskiy and Voloshin in Ref. [762].

In Ref. [760], Guo, Hanhart, and Meissner assumed that the  $Y(4660)$  is a  $f_0(980)\psi'$  bound state, and calculated the invariant mass spectrum of  $\psi'\pi^+\pi^-$  as well as the corresponding  $\pi\pi$  and  $\bar{K}K$  spectra in its mass range. They obtained a good description of both spectra, which suggests that the  $Y(4660)$  may be generated dynamically in the  $f_0(980)\psi'$  channel. They further proposed to measure the  $\psi'\bar{K}K$  channel as a nontrivial test of this hypothesis. Guo, Hanhart, and Meissner also used the heavy quark spin symmetry to study heavy meson hadronic molecules, and predicted an  $f_0(980)\eta'_c$  bound state as the spin-doublet partner of the  $Y(4660)$  [761]. Its mass was evaluated to be  $4616^{+5}_6$  MeV, and was suggested to mainly decay into  $\eta'\pi\pi$  with a width of  $60 \pm 30$  MeV. They also predicted its decays into  $\eta'_c K^+ K^-$ ,  $\eta'_c \gamma\gamma$  and  $\Lambda_c^+ \Lambda_c^-$ , and proposed to search for this state in the  $B^\pm \rightarrow \eta'_c K^\pm \pi^+ \pi^-$  decay.

In Ref. [366], Maiani, Piccinini, Polosa, and Riquer studied the  $Y(4660)$  in their “type-II” diquark-antidiquark

model, and interpreted it as the radial excitation of the  $Y(4260)$ , i.e.,  $Y(4260) = Y_2 = \frac{1}{\sqrt{2}}(|1, 0; 1, 1\rangle_1 + |0, 1; 1, 1\rangle_1)$ , which has been reviewed in Sec. 4.6. In Ref. [487], Ebert, Faustov, and Galkin calculated the masses of the excited heavy tetraquarks with hidden charm within the relativistic diquark-antidiquark picture, and found that the  $Y(4660)$  can be interpreted as the excited  $1^{--} 2P [cq][\bar{c}\bar{q}]$  tetraquark state consisting of  $S\bar{S}$ , where  $S$  is a scalar diquark. The authors had used the  $1^{--} 1P [cq][\bar{c}\bar{q}]$  state to explain the  $Y(4260)$  in their model.

The authors of Ref. [420] studied the charmonium-like tetraquark states with  $J^{PC} = 1^{--}$  in QCD sum rules using the interpolating currents listed in Eq. (148). The obtained masses were collected in Table 27. The masses of the  $qc\bar{q}\bar{c}$  and  $sc\bar{s}\bar{c}$  tetraquark states were extracted around 4.5 – 4.8 GeV and 4.4 – 5.0 GeV, respectively. These masses were consistent with the mass of the  $Y(4660)$ . The  $Y(4660)$  was also proposed as the  $\psi(2S)f_0(980)$  molecular state in Ref. [763]. The authors used a  $\bar{c}c\bar{s}s$  molecular current in QCD sum rules and obtained the mass  $m = (4.67 \pm 0.09)$  GeV.

The initial single chiral particle emission mechanism was proposed to study the hidden-charm di-kaon decays of the  $Y(4660)$  in Ref. [764]. The authors calculated the distributions of differential decay width, and obtained the line shape of the  $J/\psi K^+ K^-$  invariant mass spectrum of  $Y(4660) \rightarrow J/\psi K^+ K^-$ . Their results suggested that there may exist enhancement structures with both hidden-charm and open-strange decays near the  $D\bar{D}_s^*/D^*\bar{D}_s$  and  $D^*\bar{D}_s^*/\bar{D}^*D_s^*$  thresholds. The hidden-charm di-eta decays of the  $Y(4660)$  was studied with the same approach in Ref. [765]. The  $Y(4660)$  was used to search for the missing  $\psi(4S)$  state in Ref. [766].

4.8.2.2.  $Y(4630)$ . The  $Y(4630)$ , reviewed in Sec. 2.1.2.3, was observed in the exclusive  $e^+e^- \rightarrow \Lambda_c\bar{\Lambda}_c$  cross section [136], which might be interpreted as a baryonium state [219]. The authors of Ref. [219] performed a systematic study of the possible loosely bound states composed of two charmed baryons or a charmed baryon and an anti-charmed baryon within the framework of the OBE model, where the exchanged bosons include pseudoscalar mesons  $\pi$  and  $\eta$ , vector mesons  $\rho$ ,  $\omega$ , and  $\phi$ , and the scalar meson  $\sigma$ . They also considered the  $S$ - $D$  mixing effects for the spin-triplets. Especially, their investigation indicated that there does exist strong attraction through the  $\sigma$  and  $\omega$  exchanges in the  $\Lambda_c\bar{\Lambda}_c$  channel, which suggested that the  $Y(4630)$  may be interpreted as a  $\Lambda_c\bar{\Lambda}_c$  bound state.

In Ref. [767], Simonov investigated the nonperturbative baryon-antibaryon production due to the double quark pair  $(q\bar{q})(q\bar{q})$  generation inside a hadron. They applied this mechanism to study the electroproduction of  $\Lambda_c\bar{\Lambda}_c$ , and found an enhancement near 4.61 GeV. This structure was in agreement with experimental data [136], and was used to explain the  $Y(4630)$ .

In Ref. [717], Qiao proposed that the  $Y(4660)$ , together with the  $Y(4260)$ ,  $Y(4360)$  and  $Z^+(4430)$ , can be systematically embedded into an extended baryonium picture. In Ref. [220], Chen and Qiao argued that it is not the  $Y(4660)/Y(4630)$ , but the  $Y(4260)$  and  $Y(4360)$ , which could be interpreted as  $\Lambda_c\bar{\Lambda}_c$  bound states.

In Ref. [768], the authors studied the open-charm decay  $Y(4630) \rightarrow \Lambda_c\bar{\Lambda}_c$  by assuming that the  $Y(4630)$  is a charmonium-like tetraquark made of a diquark and an anti-diquark. Their shows that the  $Y(4630)$  could be a radially excited state of the diquark-antidiquark bound state.

4.8.2.3. *Are  $Y(4630)$  and  $Y(4660)$  the same state?*. The  $Y(4660)$  and  $Y(4630)$  were observed in different processes, i.e.,  $e^+e^- \rightarrow \gamma_{\text{ISR}}\pi^+\pi^-\psi(3686)$  [134] and exclusive  $e^+e^- \rightarrow \Lambda_c\bar{\Lambda}_c$  [136], respectively. However, their masses and widths are consistent with each other within errors [136]. Hence, they can be the same state/structure as pointed out in Refs. [769, 770, 771].

In Ref. [769], Bugg used the  $Y(4660)$  to explain the peak observed in  $\Lambda_c\bar{\Lambda}_c$  channel at 4.63 GeV [136], and suggested that a form factor with a reasonable radius of the interaction can provide an explanation of the shift of mass between the  $Y(4630)$  and  $Y(4660)$ . In Ref. [770], Cotugno, Faccini, Polosa, and Sabelli analyzed the data on the  $Y(4630) \rightarrow \Lambda_c\bar{\Lambda}_c$  [136] and the  $Y(4660) \rightarrow \psi(3686)\pi\pi$  [134]. They suggested that the  $Y(4630)$  and  $Y(4660)$  correspond to a single state, called  $Y_B(4660)$  with  $M_{Y_B} = 4660.7 \pm 8.7$  MeV and  $\Gamma_{Y_B} = 61 \pm 23$  MeV. They further argued that the  $Y_B(4660)$  is an excellent candidate for a  $[cd][\bar{c}\bar{d}]$  diquark-antidiquark bound state.

In Ref. [771], Guo *et al.* considered the  $\Lambda_c\bar{\Lambda}_c$  final state interaction and proposed that the  $Y(4630)$  may be described as the same state as the  $Y(4660)$ , which is assumed as a  $f_0(980)\psi'$  bound state [760]. Moreover, the  $Y(4660)$  was suggested to have a spin partner, which is the  $f_0(980)\eta'_c$  bound state [761]. They discussed this state, and proposed to measure the  $B$  decays to  $K\Lambda_c\bar{\Lambda}_c$  and  $K\eta'_c\pi^+\pi^-$  to test the hypothesis that the  $Y(4630)$  and  $Y(4660)$  are the same molecular state.

### 4.8.3. $X(3915)$ , $X(4350)$ and $Z(3930)$

4.8.3.1.  $Z(3930)$ . Until now, three charmonium-like states have been reported via the  $\gamma\gamma$  fusion process by Belle (see review in Sec. 2.1.4). Among them, the  $Z(3930)$  is a very good candidate of the charmonium  $\chi'_{c2}$  with  $n^{2s+1}J_L = 2^3P_2$  [140, 143]. According to PDG [1], the  $Z(3930)$  is the  $\chi'_{c2}(2P)$  charmonium state and the  $X(3915)$  is the  $\chi_{c0}(2P)$  charmonium state. The hyperfine splitting between the  $Z(3930)$  and  $X(3915)$  is only 6% of that between the  $\chi_{c2}(1P)$  and  $\chi_{c0}(1P)$  [46], which is unexpectedly smaller than the potential model prediction [772]. Such a splitting was also much smaller than the corresponding splitting of  $m_{\chi'_{b2}} - m_{\chi'_{b0}}$  [1]. These puzzles still challenge the P-wave charmonium assignments of the  $Z(3930)$  and  $X(3915)$  [590, 773, 47].

4.8.3.2.  $X(3915)$ . The mass of the  $\chi'_{c0}$  charmonium state was predicted to be around 3916 MeV in the GI model [17, 772], as shown in Fig. 52. In Ref. [774], the charmonium-like state  $X(3915)$  was proposed as the first radial excitation of the  $\chi_{c0}(3415)$ . The authors argued that the  $Z(3930)$ ,  $X(3872)$  and  $X(3915)$  may fill in the spin-triplet  $2P$  charmonium states as shown in Fig. 60 if one considers the strong coupled channel effects in the  $J^{PC} = 1^{++}$  channel which may lower the mass of the  $X(3872)$  [565, 570].

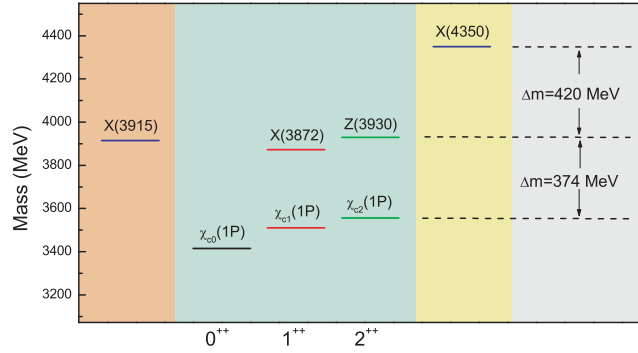


Figure 60: (Color online) The P-wave charmonium states [1] and the candidates for their first radial excitations. Taken from Ref. [774].

Assuming the  $X(3915)$  is the  $\chi_{c0}(2P)$  charmonium state, the authors of Ref. [775] calculated the OZI-allowed open-charm decay  $X(3915) \rightarrow D\bar{D}$  in the  $^3P_0$  model with the Bethe-Salpeter method. They found that the node structure in the  $\chi_{c0}(2P)$  wave function leads to the narrow decay width of the  $X(3915)$ . They suggested a partial decay width ratio  $\Gamma(X(3915) \rightarrow D^+D^-)/\Gamma(X(3915) \rightarrow D^0\bar{D}^0) = 2.3$  to test the  $\chi_{c0}(2P)$  assignment of the  $X(3915)$  [775]. However, Yang, Xia and Ping calculated the strong decay widths of the  $X(3915)$  as the  $\chi_{c0}(2P)$  charmonium state and obtained a much larger strong decay width than the experiment data [776]. A similar conclusion was obtained in Ref. [777].

In Ref. [590], Guo *et al.* doubted the  $\chi'_{c0}$  assignment of the  $X(3915)$ . The OZI-allowed open-charm decay  $X(3915) \rightarrow D\bar{D}$  generally has a larger width than that of the  $X(3915)$ . The mass splitting  $m_{Z(3930)} - m_{X(3915)} = 14 \pm 6$  MeV was too small compared with  $m_{\chi_{c2}} - m_{\chi_{c0}} = 141$  MeV. The mass splitting  $m_{Z(3930)} - m_{X(3915)}$  was even smaller than  $m_{\chi'_{b2}} - m_{\chi'_{b0}} = 36.2 \pm 0.8$  MeV [1]. The authors suggested a signal for the  $\chi_{c0}(2P)$  with a mass around 3840 MeV and width about 200 MeV in the Belle [140] and BaBar [143] data for  $\gamma\gamma \rightarrow D\bar{D}$  in Ref. [778].

The absence of the  $X(3915)$  in  $\gamma\gamma \rightarrow D\bar{D}$  also challenges the  $\chi'_{c0}(2P)$  assignment of the  $X(3915)$  since the  $D\bar{D}$  was argued to be the dominant decay mode of the  $\chi'_{c0}(2P)$  [774]. In Ref. [779], Chen *et al.* pointed out that the  $Z(3930)$  enhancement structure may contain both the  $\chi_{c0}(2P)$  and  $\chi_{c2}(2P)$  signals, according to their analysis of the  $D\bar{D}$  invariant mass spectrum and  $\cos\theta^*$  distribution of  $\gamma\gamma \rightarrow D\bar{D}$  (see Fig. 61).

In Refs. [773, 47], Olsen pointed out that the  $\chi_{c0}(2P)$  assignment of the  $X(3915)$  was in conflict with the experiment data. If the  $X(3915)$  was the  $\chi_{c0}(2P)$ , the branching fraction was estimated to be  $\mathcal{B}(\chi_{c0}(2P) \rightarrow \omega J/\psi) < 7.8\%$ , which was smaller than the 14.3% lower limit derived for the same quantity from the  $B \rightarrow KX(3915)$  decay rate.

The authors of Ref. [780] combined the analysis for the amplitude and the angular distribution of the  $\gamma\gamma \rightarrow D\bar{D}$  and  $\gamma\gamma \rightarrow J/\psi\omega$  data from BaBar [143, 141]. They found that the assignment of  $2^{++}$  to the  $X(3915)$  was more consistent with the data. The authors argues that the  $X(3915)$  and  $Z(3930)$  are the same tensor state.

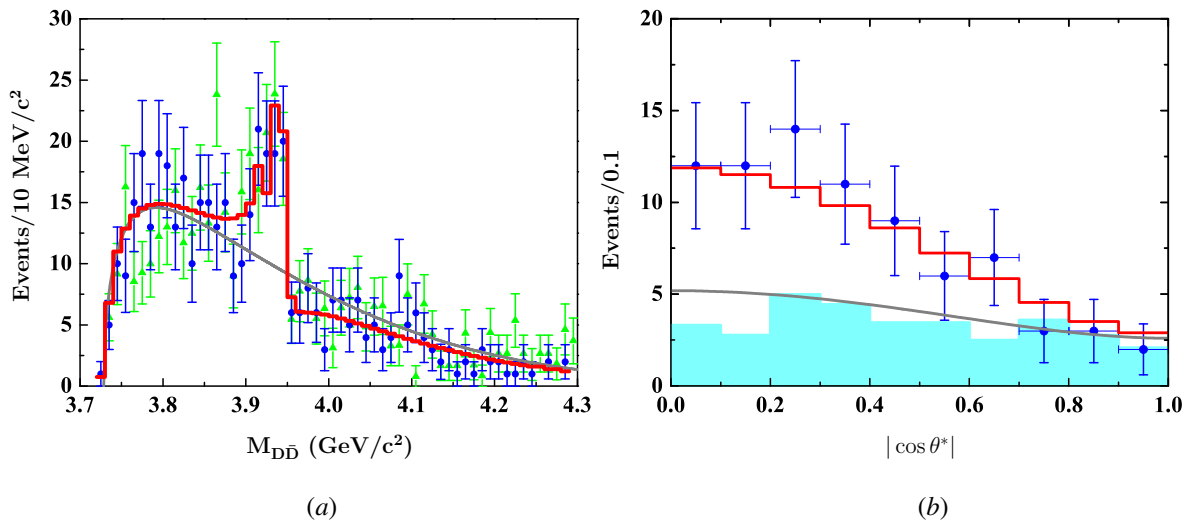


Figure 61: (Color online) (a) The best fit (red histogram) to the experimental data of the  $D\bar{D}$  invariant mass distributions given by Belle [140] (blue dots with error bar) and BaBar [143] (green triangles with error bar). (b) The best fit (red histogram) to the  $\cos \theta^*$  distribution of  $\gamma\gamma \rightarrow D\bar{D}$ . Taken from Ref. [779].

4.8.3.3.  $X(4350)$ . The mass of the  $\chi_{c2}(3P)$  was predicted to be 4337 MeV in the GI model [772]. Hence, the  $X(4350)$  was interpreted as the  $\chi_{c2}(3P)$  charmonium state in Ref. [774]. The authors studied its two-body open-charm decay behaviors within the quark pair creation model. The calculations from QCD sum rules in Refs. [420, 781, 782, 783] disfavored the assignment of the  $X(4350)$  as the exotic charmonium-like tetraquark or molecular state. The  $X(3915)$  and  $X(4350)$  states were also studied with other methods in Refs. [784, 785, 786, 781, 787, 779, 788, 789, 790]

#### 4.8.4. $X(3940)$ and $X(4160)$

The  $X(3940)$  and  $X(4160)$  states were discovered in the double charmonium production process  $e^+e^- \rightarrow J/\psi X$  [87, 88]. They have positive  $C$ -parity. Since the  $X(3940)$  decays into  $D\bar{D}^*$ , its spin-parity quantum numbers can be  $J^P = 1^+, 0^-, 1^-, 2^-$  etc. The  $J^{PC} = 1^{-+}$  combination was disfavored unless it's a hybrid charmonium. As a candidate of the charmonium state, its allowed quantum numbers are  $J^{PC} = 1^{++}, 0^{-+}$  and  $2^{-+}$  etc.

4.8.4.1.  $X(3940)$ . The  $1^{++}$  assignment of the  $X(3940)$  was disfavored by analyzing the recoil mass distribution of the  $J/\psi$  [31]. In Fig. 24, there were four visible enhancements corresponding to the  $\eta_c$  at 2980 MeV, the  $\chi_{c0}$  at 3415 MeV, the  $\eta_c(2S)$  at 3638 MeV and the  $X(3940)$  state. There was no evidence of the  $\chi_{c1}$  in Fig. 24. There was no reason to expect the  $\chi'_{c1}$  to be a stronger signal than the  $\chi_{c1}$  [31].

In Ref. [791], Rosner proposed the  $X(3940)$  as the  $\eta_c(3S)$  charmonium state. The Regge trajectory also indicated that the  $X(3940)$  could be the  $0^{-+}$  charmonium state [742]. In Ref. [792], the authors studied the  $e^+e^- \rightarrow J/\psi X(3940)$  process in the framework of the light cone formalism. They found that the production cross section was in agreement with the experiment if the  $X(3940)$  is the  $\eta_c(3S)$  [792]. In Ref. [793], He *et al.* calculated the two-body open-charm decay widths of the  $X(3940)$  as the  $\eta_c(3S)$  charmonium state. However, a problem of the  $\eta_c(3S)$  interpretation of the  $X(3940)$  is that its mass is a bit lower than theoretical predictions [772, 570].

4.8.4.2.  $X(4160)$ . The  $X(4160)$  was observed only in the  $D^*\bar{D}^*$  final states [137]. In Ref. [794], Chao discussed possible interpretations for the  $X(4160)$  based on NRQCD calculations. The author first proposed the  $X(4160)$  as the D-wave charmonium state  $2^1D_2$  with  $J^{PC} = 2^{-+}$  and calculated its production rate, which was only 5% of that for  $e^+e^- \rightarrow J/\psi + \eta_c(1S)$ , incompatible with the experimental observation of the  $X(4160)$ . Then, Chao considered the  $X(4160)$  as the  $\psi(4160)$ . However, such a possibility was completely ruled out since the production rate was much smaller than that for  $e^+e^- \rightarrow J/\psi + J/\psi$ . Chao found that the production rate of  $e^+e^- \rightarrow J/\psi + \eta_c(4S)$  was not too small in NRQCD, which was consistent with the experiment. Therefore, the  $X(4160)$  was a good candidate of the  $\eta_c(4S)$  charmonium state [794]. If so, the absence of the  $D\bar{D}$  decay channel can be understood easily since such a

decay is forbidden. However, the  $\eta_c(4S)$  was predicted to lie higher than the  $X(4160)$  [772, 570]. He *et al.* indicated that the  $\eta_c(4S)$  may have a very narrow width according to their calculation [793].

The mass of the  $\chi_0(3P)$  was predicted to be 4131 MeV in Ref. [570]. Chao also considered the  $\chi_0(3P)$  interpretation [794]. Such an assignment was particularly interesting if the observed broad peak around 3.8 – 3.9 GeV in the recoil mass of the  $D\bar{D}$  against  $J/\psi$  in  $e^+e^- \rightarrow J/\psi D\bar{D}$  was due to the  $\chi_0(2P)$ .

Molina and Oset proposed the  $X(4160)$  as an isoscalar  $D_s^*\bar{D}_s^*$  molecular state with  $J^{PC} = 2^{++}$  in Ref. [745]. They studied the vector-vector interaction within the framework of the hidden gauge formalism and found there exists strong interaction to bind the  $D_s^*\bar{D}_s^*$  system. A bound state was found around 4157 MeV with  $I^G J^{PC} = 0^+ 2^{++}$ , which was identified as the  $X(4160)$  [745].

#### 4.8.5. Narrow enhancement structures around 4.2 GeV in the hidden-charm channels

In Ref. [793], He *et al.* noticed the similarity between vector charmonium and bottomonium families. The mass gap between the  $\psi(2S)$  and  $J/\psi$  is almost the same as that between the  $\Upsilon(2S)$  and  $\Upsilon(1S)$  and  $M_{\psi(3S)} - M_{\psi(2S)} \approx M_{\Upsilon(3S)} - M_{\Upsilon(2S)}$ , where the  $\psi(3686)$  and  $\psi(4040)$  are treated as the  $\psi(2S)$  and  $\psi(3S)$  charmonium states, respectively. Until now the bottomonia with the radial quantum numbers  $n = 1, 2, 3, 4$  have been established [1]. If this mass gap relation continues to hold for higher states with  $n = 3, 4$  in  $J/\psi$  and  $\Upsilon$  families, the mass of the  $\psi(4S)$  should be located at 4263 MeV [793]. Within this framework, the  $\psi(4415)$  cannot be treated as the  $\psi(4S)$ . Fig. 62 shows the details of the mass gaps for the  $J/\psi$  and  $\Upsilon$  families. This simple estimate of the mass of the  $\psi(4S)$  [793] is consistent with the results obtained with the screened potential in Refs. [795, 570], where the mass of the  $\psi(4S)$  was predicted to be 4247 MeV in Ref. [795] and 4273 MeV in Ref. [570].

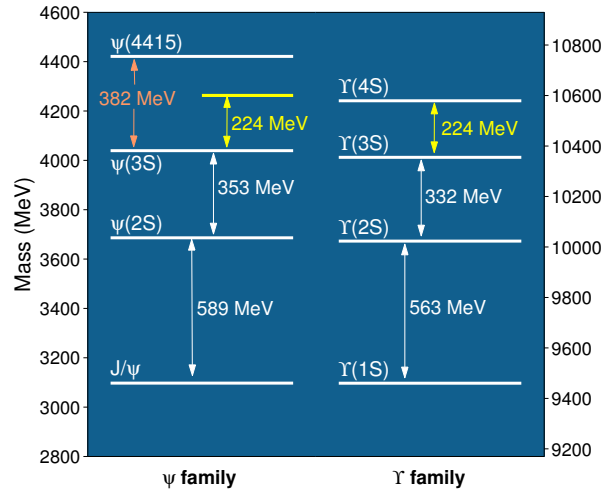


Figure 62: (Color online) A comparison between the  $J/\psi$  and  $\Upsilon$  families. Taken from Ref. [793].

He *et al.* [793] further calculated the partial and total decay widths of the  $\psi(4S)$  through the quark pair creation (QPC) model and found a very interesting result of the decay behavior of the  $\psi(4S)$  (see Fig. 63). The total decay width of the  $\psi(4S)$  is stable over the corresponding  $R$  range adopted, while its partial decay widths strongly depend on the  $R$  value. This phenomenon is due to the node effects. The predicted charmonium  $\psi(4S)$  has a very narrow width around 6 MeV within the QPC model. Thus, the charmonium-like states  $Y(4260)$  and  $Y(4360)$  cannot correspond to this predicted  $\psi(4S)$  state due to their large decay widths [793].

According to the cross sections of  $e^+e^- \rightarrow h_c(1P)\pi^+\pi^-$  at center-of-mass energies 3.90 – 4.42 GeV [149], Yuan fitted the corresponding line shape with two Breit-Wigner functions [797]. He found a narrow structure with mass  $(4216 \pm 18)$  MeV and width  $(39 \pm 22)$  MeV and another broad structure with mass  $(4293 \pm 9)$  MeV and width  $(222 \pm 67)$  MeV [797]. Both structures have  $J^{PC} = 1^{--}$ . The narrow structure was proposed as a good candidate of the  $\psi(4S)$  [793].

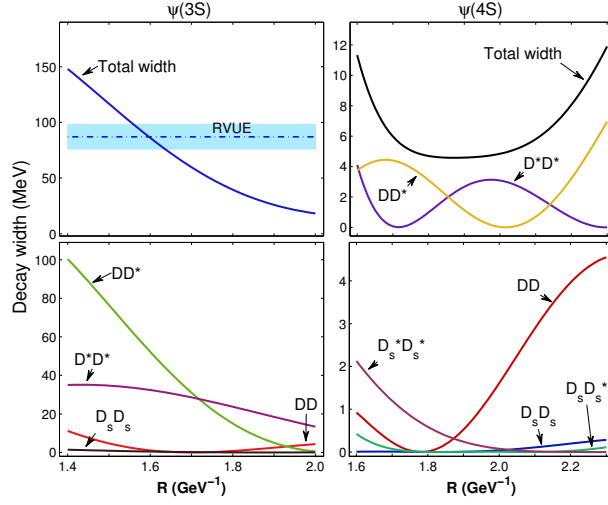


Figure 63: (Color online) The total and partial decay widths of the  $\psi(3S)$  (left) and the  $\psi(4S)$  (right). Here, the dashed line with a band (left) is the experimental data from Ref. [796]. Taken from Ref. [793].

Later, the BESIII Collaboration reported an enhancement structure in  $e^+e^- \rightarrow \omega\chi_{c0}$  [798], which has a mass  $M = (4230 \pm 8)$  MeV and width  $\Gamma = (38 \pm 12)$  MeV. BESIII indicated that this resonance structure is different from the  $Y(4260)$  reported in the analysis of  $e^+e^- \rightarrow J/\psi\pi^+\pi^-$  [51]. Chen, Liu and Matsuki [799] introduced the  $\psi(4S)$  to explain the enhancement in  $e^+e^- \rightarrow \omega\chi_{c0}$ . They calculated the branching ratio of  $\psi(4S) \rightarrow \omega\chi_{c0}$  from the meson loop contribution and estimated the upper limit of the branching ratio of  $\psi(4S) \rightarrow \eta J/\psi$  to be  $1.9 \times 10^{-3}$ , which is consistent with the experimental data [798, 800].

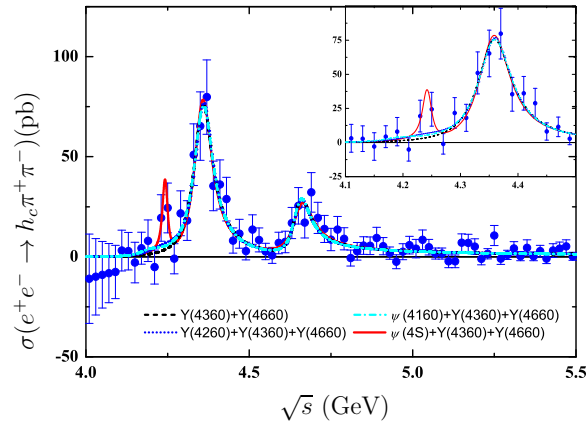


Figure 64: (Color online) A comparison of the fits to the cross section for  $e^+e^- \rightarrow \pi^+\pi^-\psi(2S)$  with different schemes. Taken from Ref. [766].

In Ref. [766], Chen, Liu, and Matsuki further checked the cross section for  $e^+e^- \rightarrow \psi(2S)\pi^+\pi^-$  [134] and found a number of events near 4.2 GeV, other than the structures of the  $Y(4360)$  and  $Y(4660)$  (see Fig. 64). If setting this structure as the  $\psi(4S)$ , the upper limit of the branching ratio of  $\psi(4S) \rightarrow \psi(2S)\pi^+\pi^-$  can be extracted [134], i.e.,  $\mathcal{B}(\psi(4S) \rightarrow \psi(2S)\pi^+\pi^-) < 3 \times 10^{-3}$ , which can be understood by hadronic loop contributions [766].

Since there exist evidences of narrow structures around 4.2 GeV in  $e^+e^- \rightarrow h_c(1P)\pi^+\pi^-$  [149, 797],  $e^+e^- \rightarrow \omega\chi_{c0}$  [798],  $e^+e^- \rightarrow \psi(2S)\pi^+\pi^-$  [134], Chen, Liu, and Matsuki performed a combined fit to these hidden-charm decay channels under two schemes [766]. The mass and width of the  $\psi(4S)$  were extracted to be  $m_{\psi(4S)} = (4234 \pm 5)$  MeV,  $\Gamma_{\psi(4S)} = (29 \pm 14)$  MeV and  $m_{\psi(4S)} = (4220 \pm 8)$  MeV,  $\Gamma_{\psi(4S)} = (43 \pm 9)$  MeV for Scheme I and Scheme II, respectively.

The narrow structure around 4.2 GeV in  $e^+e^- \rightarrow h_c(1P)\pi^+\pi^-$  [149, 797],  $e^+e^- \rightarrow \omega\chi_{c0}$  [798],  $e^+e^- \rightarrow \psi(2S)\pi^+\pi^-$  [134] may be due to the same state  $\psi(4S)$ .

In Ref. [799], Chen, Liu, and Matsuki discussed the possible evidence of a narrow structure around 4.2 GeV in the Belle [681] and BaBar [119] data of  $e^+e^- \rightarrow D\bar{D}$ , which may correspond to the  $\psi(4S)$  (see Fig. 65 for more details).

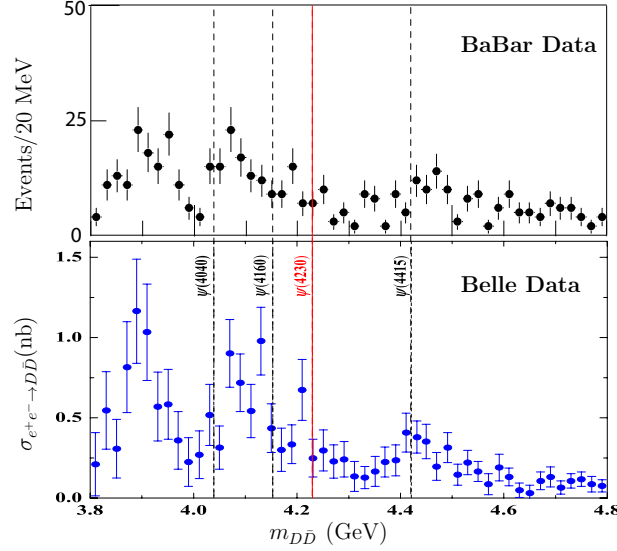


Figure 65: (Color online) The experimental data of  $e^+e^- \rightarrow D\bar{D}$  from the Belle [681] and BaBar [119] collaborations and the comparison with the central masses of  $\psi(4040)$ ,  $\psi(4160)$ ,  $\psi(4415)$  and the predicted  $\psi(4S)$ . Here, the predicted mass is taken from Ref. [51]. Taken from Ref. [799].

#### 4.8.6. $X(3823)$

As indicated in Sec. 2.1.1.7, the  $X(3823)$  agrees with the theoretical predictions for the  $1^3D_2$  state [102, 103, 104, 17, 105, 106]. The  $1^3D_2$  charmonium state with  $J^{PC} = 2^{--}$  is expected to be very narrow. Its open-charm decay mode  $D\bar{D}$  is forbidden by the spin-parity symmetry. The upper limit of  $B(X(3823) \rightarrow \chi_{c2}\gamma)/B(X(3823) \rightarrow \chi_{c1}\gamma)$  was measured to be  $< 0.41$  by Belle [101], and  $< 0.42$  by BESIII [107], consistent with the theoretical calculation for the  $1^3D_2$  state in Refs. [801, 105, 802, 803]. In addition, the partial decay width for  $\psi(1^3D_2) \rightarrow J/\psi\pi^+\pi^-$  obtained in these works was also in agreement with the observation by E705 [100]. Therefore, the  $X(3823)$  is a very good candidate of the  $1^3D_2$  charmonium state.

The charmonium state with  $J^{PC} = 2^{--}$  was investigated in QCD sum rule using the interpolating current [804]

$$J_{\mu\nu} = \bar{c}(x)(\gamma_\mu\gamma_5 \overleftrightarrow{D}_\nu + \gamma_\nu\gamma_5 \overleftrightarrow{D}_\mu - \frac{2}{3}\eta_{\mu\nu}\gamma_5 \overleftrightarrow{D})c(x). \quad (152)$$

The mass of the  $1^3D_2$  charmonium state as  $m = 3.97 \pm 0.25$  GeV.

In Ref. [805], the authors studied the heavy meson properties within a non-relativistic constituent quark model, including the spectroscopy and the electromagnetic, strong and weak decay processes. They obtained the mass of the  $1^3D_2$   $c\bar{c}$  state at 3812 MeV and the ratio  $B(X(3823) \rightarrow \chi_{c2}\gamma)/B(X(3823) \rightarrow \chi_{c1}\gamma) = 0.24$ .

Voloshin discussed the  $e^+e^- \rightarrow \pi\pi X(3823)$  process in the soft pion limit in Ref. [806]. The amplitude of this production process was studied up to the second order in the pion momenta at different energies. The amplitude of  $e^+e^- \rightarrow \pi\pi X(3823)$  rapidly grows with the momenta of the pions.

In Ref. [807], Wang *et al.* studied the  $X(3823) \rightarrow J/\psi\pi^+\pi^-$  process to identify the significance of the coupled-channel effects. They computed the partial decay width distribution with the dipion invariant mass with both the QCD multipole expansion method and the effective Lagrangian approach. Neglecting the coupled-channel effects, they found the disagreement with E705 experiment in Ref. [100]. Including the coupled-channel effect of  $D\bar{D}^*$ , they calculated the same process and found the interference between the direct and the indirect processes [807].

In Ref. [808], the authors studied the electromagnetic transitions of the charmonium states within a constituent quark mode. Considering the  $X(3823)$  as the  $\psi_2(1D)$  state, they calculated the radiative decay widths

$$\begin{aligned}\Gamma[X(3823) \rightarrow \chi_{c0}(1P)\gamma] &\simeq 1.42 \text{ keV}, \\ \Gamma[X(3823) \rightarrow \chi_{c1}(1P)\gamma] &\simeq 227 \text{ keV}, \\ \Gamma[X(3823) \rightarrow \chi_{c2}(1P)\gamma] &\simeq 42 \text{ keV},\end{aligned}\tag{153}$$

in which the  $\chi_{c1}(1P)\gamma$  was a dominant decay mode. The ratio  $\Gamma[X(3823) \rightarrow \chi_{c2}(1P)\gamma]/\Gamma[X(3823) \rightarrow \chi_{c1}(1P)\gamma] \simeq 19\%$  was in agreement with the observations  $< 42\%$  [107].

#### 4.8.7. A short summary

- The  $Y(4008)$  was explained as the  $\psi(3S)$  charmonium state, the  $D^*\bar{D}^*$  or  $\eta h_c$  molecular state, and the diquark-antidiquark tetraquark state. There are also non-resonant explanations.
- The  $Y(4360)$  was explained as the  $\psi(3D)$  charmonium state, the  $2S D_1\bar{D}^*$  molecule, a hadrocharmonium state, a diquark-antidiquark tetraquark state, a baryonium state, and a charmonium hybrid state. Non-resonant explanation was also proposed, such as the Fano-like interference.
- The  $Y(4660)$  was assigned as the  $5^3S_1$  or  $\psi(6S)$  charmonium state, the  $f_0(980)\psi'$  bound state, and a diquark-antidiquark tetraquark state. The  $Y(4630)$  was assigned as the  $\Lambda_c\bar{\Lambda}_c$  baryonium bound state. The  $Y(4660)$  and  $Y(4630)$  may be the same state.
- In PDG [1], the  $X(3915)$  and  $Z(3930)$  were assigned as the  $\chi'_{c0}(2P)$  and  $\chi'_{c2}(2P)$  charmonium states, respectively. This assignment is challenged by the small hyperfine splitting and the absence of the  $X(3915)$  in  $\gamma\gamma \rightarrow D\bar{D}$ .
- The  $X(3940)$  and  $X(4160)$  were suggested as the  $\eta_c(3S)$  and  $\eta_c(4S)$  charmonium state, respectively.
- The  $X(4350)$  was interpreted as the  $\chi_{c2}(3P)$  charmonium state.
- The  $X(3823)$  is the  $1^3D_2$  charmonium state with  $J^{PC} = 2^{--}$ .

## 5. Outlook and summary

Since 2003, many charmonium-like/bottomonium-like  $XYZ$  states have been observed. Recently two hidden-charm pentaquarks  $P_c$  were observed by LHCb. Some of these states do not fit into the quark model spectrum easily. They are good candidates of the hidden-charm tetraquark and pentaquark states and enable us to carry out intensive studies of the exotic hadronic matter, which is one of the most important issues in hadron physics. These states provide us an ideal platform to deepen our understanding of the non-perturbative QCD.

In the past 13 years, the observations of the  $XYZ$  and  $P_c$  states have inspired theorist's extensive interests in revealing their underlying structures. There have accumulated a huge number of theoretical papers on these states, which cover their mass spectroscopy, other static properties, reaction, decay and production behaviors. Various schemes were proposed such as the conventional charmonium states, molecular states, tetraquark states, hybrid charmonium states and so on.

In this report, we have tried our best to summarize the experimental and theoretical progresses on the hidden-charm multi-quark states in order to gain some valuable lessons from the extensive research in the past 13 years.

### 5.1. Current status and future confirmation of the hidden-charm multi-quark states

We collect all the hidden-charm tetraquark and pentaquark states in Tables 28 and 29. We award an overall status \*\*\*\* to those states which have been firmly established by two or more collaborations in two or more decay modes, and \*\*\* to states which have been well established in a single decay mode by two or more collaborations. The states with \*\*\*\* and \*\*\* are listed in Table 28. We award \*\* to those states which have been well established in several decay modes by one collaboration, and \* to those states which was only observed in a single decay mode by one collaboration. The states with \*\* and \* are listed in Table 29.

The  $Y(4660)$  and  $Y(4630)$  may be the same state. The  $Z_c(3900)$  and  $Z_c(3885)$  are probably the same state. The  $Z_c(4020)$  and  $Z_c(4025)$  are probably the same state. We award \* \* \* \* to them. The Belle and LHCb experiments observed the  $Z^+(4430)$ , while the BaBar experiments did not. Moreover, it has only been observed in the  $B \rightarrow KZ^+(4430)(\rightarrow \psi(3686)\pi^+)$  decay process. So we awarded \* \* \* to the  $Z^+(4430)$ .

Future experimental confirmation of those states which were observed in a single decay mode by one collaboration is crucial. Some states were observed in the hidden-charm decay modes. It's also important to search for their open-charm and charm-less decay modes. For example, the  $Y(4260)$  was observed in  $J/\psi\pi\pi$ ,  $\pi Z_c(3900)$  and  $\pi Z_c(4020)$ . Its open-charm modes are still missing.

The two  $P_c$  states were observed in the  $J/\psi p$  mode. If they are molecular states, their open-charm decay modes may be dominant. The compact ‘‘genuine’’ pentaquark states confined within one MIT bag may mainly decay into the  $J/\psi p$  mode. The dynamically generated hidden-charm baryons are generally narrow. The sum of their charm-less partial decay widths is larger than their hidden-charm widths. This feature is characteristic of the dynamically generated resonance and the unitary approach. The observation of significant charm-less decay modes will support the  $P_c$  states as the dynamically generated resonance within the unitary framework.

Table 28: Hidden-charm multi-quark states that have been observed by more than one collaborations.

States	Status	Mass [MeV]	Width [MeV]	$J^G J^{PC} J_1 J_2 P$	Observation	Note
$X(3872)$	****	$3871.69 \pm 0.17$ [1]	$< 1.2$ [1]	$0^+ 1^{++}$	$B \rightarrow KX(3872) \begin{cases} \rightarrow J/\psi\phi^0, J/\psi\pi^+\pi^- \\ \rightarrow J/\psi\omega(\rightarrow \pi^+\pi^-\pi^0) \\ \rightarrow D^0\bar{D}^{*0}, D^0\bar{D}^0\pi^0 \\ \rightarrow \gamma J/\psi, \gamma\psi(3686) \end{cases}$ $p\bar{p} \rightarrow \dots + X(3872)(\rightarrow J/\psi\pi^+\pi^-)$ $pp \rightarrow \dots + X(3872) \begin{cases} \rightarrow J/\psi\pi^+\pi^- \\ \rightarrow \gamma J/\psi, \gamma\psi(3686) \end{cases}$ $e^+e^-[\rightarrow Y(4260)] \rightarrow \gamma X(3872)(\rightarrow J/\psi\pi^+\pi^-)$	Belle [52], BaBar [73] Belle [64], BaBar [79] Belle [65], BaBar [76] Belle [64], BaBar [75] CDF [56], D0 [57] LHCb [80], CMS [62] LHCb [81] BESIII [82]
$Y(4260)$	****	$4251 \pm 9$ [1]	$120 \pm 12$ [1]	$0^- 1^{--}$	$e^+e^- \rightarrow \gamma_{\text{ISR}} Y(4260) \begin{cases} \rightarrow J/\psi\pi^+\pi^- \\ \rightarrow J/\psi f_0(980) \\ \rightarrow J/\psi\pi^0\pi^0 \end{cases}$ $e^+e^- \rightarrow Y(4260) \begin{cases} \rightarrow \pi^- Z_c(3900)^+(\rightarrow J/\psi\pi^+) \\ \rightarrow \pi^- Z_c(3885)^+(\rightarrow (D\bar{D}^*)^+) \\ \rightarrow \pi^- Z_c(4020)^+(\rightarrow h_c\pi^+) \\ \rightarrow \pi^- Z_c(4025)^+(\rightarrow (D^*\bar{D}^*)^+) \end{cases}$ $e^+e^-[\rightarrow Y(4260)] \rightarrow \gamma X(3872)(\rightarrow J/\psi\pi^+\pi^-)$	BaBar [51], CLEO [49], Belle [108] BaBar [112] CLEO [109] BESIII [53], Belle [113] BESIII [148] BESIII [149] BESIII [150] BESIII [82]
$Y(3940)$	***	$3919.1^{+3.8}_{-3.5} \pm 2.0$ [79]	$31^{+10}_{-8} \pm 5$ [79]	$0^+ ?^{2+}$	$B \rightarrow KY(3940)(\rightarrow J/\psi\omega)$	Belle [85], BaBar [86]
$Y(4140)$	***	$4148.0 \pm 2.4 \pm 6.3$ [63]	$28^{+15}_{-11} \pm 19$ [63]	$0^+ ?^{2+}$	$B \rightarrow KY(4140)(\rightarrow J/\psi\phi)$	CDF [58], D0 [91], CMS [63]
$Y(4274)$	***	$4274.4^{+8.4}_{-6.7} \pm 1.9$ [89]	$32.3^{+21.9}_{-15.3} \pm 7.6$ [89]	$0^+ ?^{2+}$	$B \rightarrow KY(4274)(\rightarrow J/\psi\phi)$	CDF [89], CMS [63]
$X(3823)$	****	$3821.7 \pm 1.3 \pm 0.7$ [107]	$< 16$ [107]	$0^- 2^{--}$	$\psi' \rightarrow J/\psi\pi^+\pi^-$ $B \rightarrow KX(3823)(\rightarrow \gamma\chi_{c1})$ $e^+e^- \rightarrow \pi^+\pi^-X(3823)(\rightarrow \gamma\chi_{c1})$	E705 [100], Belle [101], BESIII [107]
$Y(4360)$	***	$4354 \pm 10$ [1]	$78 \pm 16$ [1]	$0^- 1^{--}$	$e^+e^- \rightarrow \gamma_{\text{ISR}} Y(4360)(\rightarrow \psi(3686)\pi^+\pi^-)$	BaBar [133], Belle [134]
$Y(4660)$	****	$4665 \pm 10$ [1]	$53 \pm 16$ [1]	$0^- 1^{--}$	$e^+e^- \rightarrow \gamma_{\text{ISR}} Y(4660)(\rightarrow \psi(3686)\pi^+\pi^-)$	Belle [134], BaBar [135]
$Y(4630)$	****	$4634^{+8+5}_{-7-8}$ [136]	$92^{+40+10}_{-24-21}$ [136]	$0^- 1^{--}$	$e^+e^- \rightarrow \gamma_{\text{ISR}} Y(4630)(\rightarrow \Lambda_c\bar{\Lambda}_c)$	Belle [136]
$X(3915)$	***	$3915 \pm 3 \pm 2$ [141]	$17 \pm 10 \pm 3$ [141]	$0^+ 0^{++}$	$\gamma\gamma \rightarrow X(3915)(\rightarrow J/\psi\omega)$	Belle [141], BaBar [144]
$Z(3930)$	***	$3929 \pm 5 \pm 2$ [140]	$29 \pm 10 \pm 2$ [140]	$0^+ 2^{++}$	$\gamma\gamma \rightarrow Z(3930)(\rightarrow D\bar{D})$	Belle [140], BaBar [143]
$Z^+(4430)$	***	$4478^{+15}_{-18}$ [11]	$181 \pm 31$ [11]	$1^+ 1^{+-}$	$B \rightarrow KZ^+(4430)(\rightarrow \psi(3686)\pi^+)$	Belle [92], LHCb [97]
$Z_c(3900)$	****	$3888.7 \pm 3.4$ [1]	$35 \pm 7$ [1]	$1^+ 1^{+-}$	$e^+e^- \rightarrow Y(4260) \rightarrow \pi^- Z_c(3900)^+(\rightarrow J/\psi\pi^+)$ $e^+e^- \rightarrow \psi(4160) \rightarrow \pi^- Z_c(3900)^+(\rightarrow J/\psi\pi^+)$	BESIII [53], Belle [113], Xiao <i>et al.</i> [50]
$Z_c(3885)$	****	$3883.9 \pm 1.5 \pm 4.2$ [148]	$24.8 \pm 3.3 \pm 11.0$ [148]	$1^+ 1^{+-}$	$e^+e^- \rightarrow Y(4260) \rightarrow \pi^- Z_c(3885)^+(\rightarrow (D\bar{D}^*)^+)$	BESIII [148]
$Z_c(4020)$	****	$4022.9 \pm 0.8 \pm 2.7$ [149]	$7.9 \pm 2.7 \pm 2.6$ [149]	$1^+ 1^{+-}$	$e^+e^- \rightarrow Y(4260) \rightarrow \pi^- Z_c(4020)^+(\rightarrow h_c\pi^+)$	BESIII [149]
$Z_c(4025)$	****	$4026.3 \pm 2.6 \pm 3.7$ [150]	$24.8 \pm 5.6 \pm 7.7$ [150]	$1^+ 1^{+-}$	$e^+e^- \rightarrow Y(4260) \rightarrow \pi^- Z_c(4025)^+(\rightarrow (D^*\bar{D}^*)^+)$	BESIII [150]

Table 29: Hidden-charm multiquark states that have been observed by only one collaboration.

States	Status	Mass [MeV]	Width [MeV]	$J^{PC}/IJ^P$	Observation	Note
$Y(4008)$	*	$4008 \pm 40^{+114}_{-28}$ [108]	$226 \pm 44 \pm 87$ [108]	$0^- 1^{--}$	$e^+ e^- \rightarrow \gamma_{\text{ISR}} Y(4008) (\rightarrow J/\psi \pi^+ \pi^-)$	Belle [108]
$X(3940)$	*	$3942^{+7}_{-6} \pm 6$ [137]	$37^{+26}_{-15} \pm 8$ [137]	$??^2 \gamma^2+$	$e^+ e^- \rightarrow J/\psi X(3940) (\rightarrow \bar{D} D^*)$	Belle [137]
$X(4160)$	*	$4156^{+25}_{-20} \pm 15$ [137]	$139^{+111}_{-61} \pm 21$ [137]	$??^2 \gamma^2+$	$e^+ e^- \rightarrow J/\psi X(4160) (\rightarrow \bar{D}^* D^*)$	Belle [137]
$X(4350)$	*	$4350.6^{+4.6}_{-5.1} \pm 0.7$ [88]	$13^{+18}_{-9} \pm 4$ [88]	$??^2 0^{2+} / 2^{2+}$	$\gamma\gamma \rightarrow X(4350) (\rightarrow J/\psi \phi)$	Belle [88]
$Z^+(4051)$	*	$4051 \pm 14^{+20}_{-41}$ [98]	$82^{+21+47}_{-17-22}$ [98]	$??^2$	$B \rightarrow KZ^+(4051) (\rightarrow X_{c1} \pi^+)$	Belle [98]
$Z^+(4248)$	*	$4248^{+44+180}_{-29-35}$ [98]	$177^{+54+316}_{-39-61}$ [98]	$??^2$	$B \rightarrow KZ^+(4248) (\rightarrow X_{c1} \pi^+)$	Belle [98]
$Z^+(4200)$	*	$4196^{+31+17}_{-29-13}$ [96]	$370^{+70+70}_{-70-132}$ [96]	$1^+ 1^{+-}$	$B \rightarrow KZ^+(4200) (\rightarrow J/\psi \pi^+)$	Belle [96]
$Z^+(4240)$	*	$4239 \pm 18^{+45}_{-10}$ [97]	$220 \pm 47^{+108}_{-74}$ [97]	$??^0 / 21^+$	$B \rightarrow KZ^+(4240) (\rightarrow \psi(3686) \pi^+)$	LHCb [97]
$Z_b(10610)$	**	$10607.2 \pm 2.0$ [161]	$18.4 \pm 2.4$ [161]	$1^+ 1^{+-}$	$\Upsilon(5S) \rightarrow \pi^\mp Z_b^\pm(10610) \begin{cases} \rightarrow \pi^\pm \Upsilon(nS) (n=1, 2, 3) \\ \rightarrow \pi^\pm h_b(mP) (m=1, 2) \end{cases}$ $\Upsilon(10860) \rightarrow \pi^\mp Z_b^\pm(10610) (\rightarrow [B\bar{B}^* + \text{c.c.}]^\pm)$	Belle [161], Belle [166]
$Z_b(10650)$	**	$10652.2 \pm 1.5$ [161]	$11.5 \pm 2.2$ [161]	$1^+ 1^{+-}$	$\Upsilon(5S) \rightarrow \pi^\mp Z_b^\pm(10650) \begin{cases} \rightarrow \pi^\pm \Upsilon(nS) (n=1, 2, 3) \\ \rightarrow \pi^\pm h_b(mP) (m=1, 2) \end{cases}$ $\Upsilon(10860) \rightarrow \pi^\mp Z_b^\pm(10650) (\rightarrow [B^* \bar{B}^*]^\pm)$	Belle [161], Belle [166]
$P_c(4380)^+$	*	$4380 \pm 8 \pm 29$ [2]	$205 \pm 18 \pm 86$ [2]	$\frac{1}{2}^? ?^2$	$\Lambda_b^0 \rightarrow K^- P_c(4380)^+ (\rightarrow J/\psi p)$	LHCb [2]
$P_c(4450)^+$	*	$4449.8 \pm 1.7 \pm 2.5$ [2]	$39 \pm 5 \pm 19$ [2]	$\frac{1}{2}^? ?^2$	$\Lambda_b^0 \rightarrow K^- P_c(4450)^+ (\rightarrow J/\psi p)$	LHCb [2]

## 5.2. Non-resonant schemes

The  $P_c$  and some charmonium-like and bottomonium-like states are very close to the two open-charm/bottom hadron thresholds. Various final state interactions may generate enhancement structures. For example, the cusp effect was proposed to explain the  $Z_c^+(4430)$  [494],  $Z_b(10610)$  and  $Z_b(10650)$  [427, 429]. The initial single pion emission mechanism was applied to interpret the charged  $Z_b$  and  $Z_c$  structures [430, 468]. The triangle singularities were employed to understand the  $Z_b$ ,  $Z_c$  and  $P_c$  structures [428, 378, 380, 382, 379].

There are different versions of the non-resonant schemes and their conclusions are not totally the same. Generally it's not easy to distinguish the exotic state assignment from the non-resonant schemes. With more precise experimental data, the partial wave analysis and the establishment of the phase motion of the signal will be helpful to test different scenarios.

## 5.3. Partner states

The hidden-charm pentaquark states  $P_c(4380)$  and  $P_c(4450)$  shall be accompanied by their hidden-bottom and doubly heavy pentaquark states. The hidden-charm tetraquark states can also have hidden-bottom partner states. For example, the  $X(3872)$  was interpreted as either a diquark-antidiquark state or a  $D\bar{D}^*$  molecular state. Within both schemes its bottom partner  $X_b$  was suggested to exist: the mass of the  $1^{++} [bq][\bar{b}\bar{q}]$  tetraquark was predicted to be 10504 MeV in Ref. [422], and the mass of the  $1^{++} B\bar{B}^*$  molecular state was predicted to be 10580 MeV in Ref. [417]. Hence, the search of the  $X_b$  state is of particular importance to all the hidden-charm and hidden-bottom tetraquark states. Indeed, the observations of these predicted partner states would be the most powerful support of the relevant methods/models.

Within the tetraquark scheme, lots of  $XYZ$  partner states were predicted. Especially, in the ‘‘type-I’’ diquark-antidiquark model [363], six  $[cq][\bar{c}\bar{q}]$  states were constructed, including two states with  $J^{PC} = 0^{++}$ , one state with  $J^P = 1^{++}$ , two states with  $J^P = 1^{+-}$ , and one state with  $J^{PC} = 2^{++}$ . Among them, the  $1^{++}$  state was used to fit the  $X(3872)$ . This idea was developed in Ref. [539] by Maiani, Polosa, and Riquer, where they further proposed four states with  $J^P = 1^+$ :  $X_u = [cu][\bar{c}\bar{u}]$ ,  $X_d = [cd][\bar{c}\bar{d}]$ ,  $X^+ = [cu][\bar{c}\bar{d}]$ , and  $X^- = [cd][\bar{c}\bar{u}]$ . However, the two charged states, as partners of the  $X(3872)$ , were not observed in B meson decays [541]. Now, this ‘‘type-I’’ diquark-antidiquark model has been updated to the ‘‘type-II’’ diquark-antidiquark model, which can explain the quantum numbers of many

$XYZ$  states as well as their decay patterns, but still can not explain why the charged partners of the  $X(3872)$  have not been observed in B meson decays and other experiments [366].

There are also many  $XYZ$  partner states within the molecular scheme. We take the  $Z_b(10610)$  and  $Z_b(10650)$  as an example, which were interpreted as the isovector  $B\bar{B}^*$  and  $B^*\bar{B}$  molecular states of  $I^G J^P = 1^+ 1^+$  [191]. Several other molecular states were predicted as their partners, including isoscalar  $B\bar{B}^*$  molecular states of  $I^G J^{PC} = 0^- 1^{+-}$  and  $0^+ 1^{++}$ , and isoscalar  $B^*\bar{B}$  molecular states of  $0^+ 0^{++}$ ,  $0^- 1^{+-}$ , and  $0^+ 2^{++}$ , etc. Generally speaking, the isoscalar molecular states are bound more tightly than their isovector partners when their other quantum numbers are the same.

#### 5.4. Connections between different $XYZ$ states

The observed  $XYZ$  states are not isolated since there may exist connections between different  $XYZ$  states, which are shown in Fig. 66. We need to emphasize the similarities existing in some of the observed  $XYZ$  states, which may provide us some important clues to their inner structures. For example,

- The similarity between the  $Y(3940)$  and  $Y(4140)$  inspired the explanation of the  $D^*\bar{D}^*$  and  $D_s^*\bar{D}_s^*$  molecular states to the  $Y(3940)$  and  $Y(4140)$ , respectively [187] (see review in Sec. 4.7).
- A unified Fano-like interference picture was proposed to explain the  $Y(4260)$ ,  $Y(4360)$  and  $Y(4008)$  due to their similarity [715] (see review in Sections 4.6 and 4.8.1).

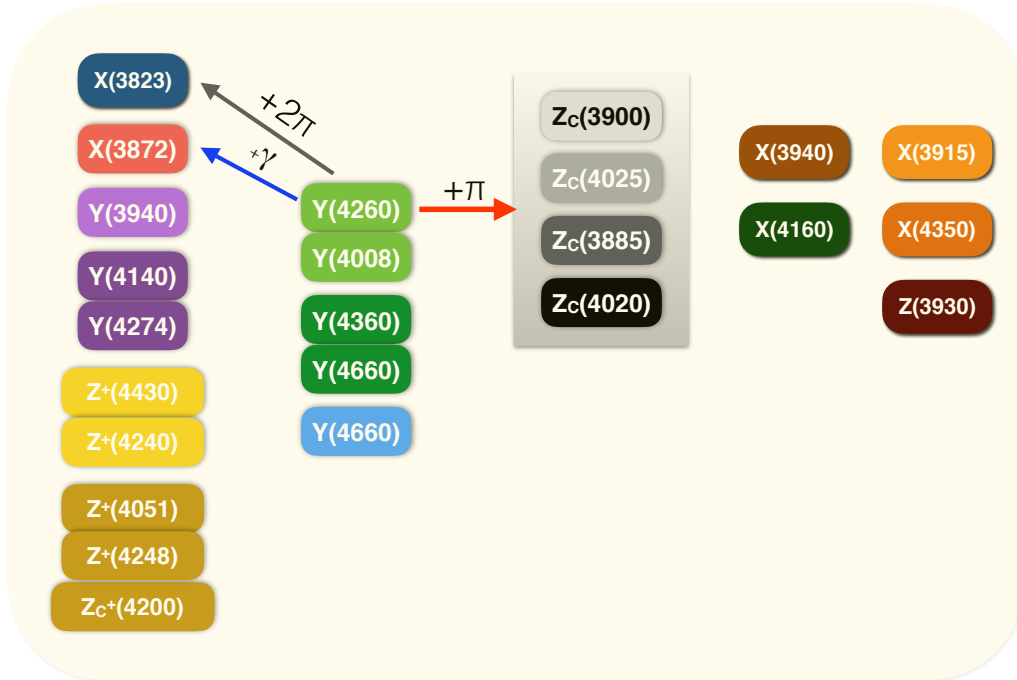


Figure 66: (Color online) The connections between different  $XYZ$  states. Here, the states are marked by the same color background if they have the same production and decay modes, while the states listed in the same column are of similar color background if they have similar decay mode. The red, blue and grey arrows show that there exist pionic, dipion and radiative transitions between  $XYZ$  states, respectively. Additionally, the states listed in the same column have the same production mode (see the categorization shown in Table 2).

The radiative transition  $Y(4260) \rightarrow \gamma X(3872)$  encodes important information on their inner structure. If  $X(3872) = \chi_{c1}(2P)$ , the  $Y(4260)$  may favor the higher charmonium assignment, since  $Y(4260) \rightarrow \gamma X(3872)$  is a typical E1 transition.

We want to emphasize the importance of finding the connections between different  $XYZ$  states. As shown in Fig. 66, the present observed connections between different  $XYZ$  states are not abundant. Future experimental efforts on the transitions between different  $XYZ$  states will shed light on their inner structures.

### 5.5. Open-charm, pionic and radiative decays

The hidden-charm multiquark states have many different inner structures, which lead to very different decay patterns. Especially, the ratio of their open-charm and hidden-charm decay widths is very sensitive to their underlying structures.

In certain cases, either the  $XYZ$  states or the final states belong to the same multiplet which have the same spatial wave function. In the heavy quark symmetry limit, there generally exist model-independent ratios of the decay widths of various decay processes. These ratios are sensitive to different theoretical models and encode important information of their inner structures. Let's take the molecular assignment as an example. For the charmonium-like molecular states, we collect some ratios of their strong and radiative decays derived through the spin rearrangement scheme in the heavy quark symmetry limit [436, 437]:

1. Assuming the  $Y(4260)$  and  $Y(4360)$  to be the isoscalar  $D_1\bar{D}$  and  $D_1\bar{D}^*$  molecular states, respectively, the ratios of their pionic decays were evaluated to be

$$\begin{aligned} \Gamma(Y(4260) \rightarrow \chi_{c0}\pi^+\pi^-\pi^0) : \Gamma(Y(4260) \rightarrow \chi_{c1}\pi^+\pi^-\pi^0) : \Gamma(Y(4260) \rightarrow \chi_{c2}\pi^+\pi^-\pi^0) &= 4 : 3 : 5 (2.11 : 1 : 1.28), \\ \Gamma(Y(4360) \rightarrow \chi_{c0}\pi^+\pi^-\pi^0) : \Gamma(Y(4360) \rightarrow \chi_{c1}\pi^+\pi^-\pi^0) : \Gamma(Y(4360) \rightarrow \chi_{c2}\pi^+\pi^-\pi^0) &= 4 : 3 : 5 (1.94 : 1 : 1.36), \end{aligned}$$

where the ratio in the bracket is the result considering the phase space factors. The ratios of their radiative decays were evaluated to be

$$\begin{aligned} \Gamma(Y(4260) \rightarrow \chi_{c0}\gamma(E1)) : \Gamma(Y(4260) \rightarrow \chi_{c1}\gamma(E1)) : \Gamma(Y(4260) \rightarrow \chi_{c2}\gamma(E1)) &= 4 : 3 : 5 (1.8 : 1 : 1.4), \\ \Gamma(Y(4360) \rightarrow \chi_{c0}\gamma(E1)) : \Gamma(Y(4360) \rightarrow \chi_{c1}\gamma(E1)) : \Gamma(Y(4360) \rightarrow \chi_{c2}\gamma(E1)) &= 4 : 3 : 5 (1.8 : 1 : 1.4). \end{aligned}$$

2. Assuming the  $X(3872)$  to be the isoscalar  $D\bar{D}^*$  molecular state, the ratio of their radiative decays was evaluated to be

$$\Gamma(X(3872) \rightarrow \psi(1^3D_1)\gamma(E1)) : \Gamma(X(3872) \rightarrow \psi(1^3D_2)\gamma(E1)) = 1 : 3 (1 : 2.9).$$

3. Assuming the  $Z_c(3900)$  and  $Z_c(4020)$  to be the charged isovector  $D\bar{D}^*$  and  $D^*\bar{D}^*$  molecular states, respectively, the ratios between their decay widths were evaluated to be

$$\begin{aligned} \frac{\Gamma(Z_c(3900) \rightarrow J/\psi\pi^0)}{\Gamma(Z_c(4020) \rightarrow J/\psi\pi^0)} &= 1 : 1 (1 : 1.07), \\ \frac{\Gamma(Z_c(3900) \rightarrow \eta_c\rho^0)}{\Gamma(Z_c(4020) \rightarrow \eta_c\rho^0)} &= 1 : 1 (1 : 2.47), \\ \frac{\Gamma(Z_c(3900) \rightarrow \eta_c\gamma(E1))}{\Gamma(Z_c(4020) \rightarrow \eta_c\gamma(E1))} &= 1 : 1 (1 : 1.30). \end{aligned}$$

4. Assuming the  $Y(3940)$  and  $Y(4140)$  to be the  $D^*\bar{D}^*$  and  $D_s^*\bar{D}_s^*$  molecular states of  $J^{PC} = 0^{++}$ , respectively, the ratios between their decay widths were evaluated to be

$$\begin{aligned} \frac{\Gamma(Y(3940) \rightarrow J/\psi\gamma(E1))}{\Gamma(Y(4140) \rightarrow J/\psi\gamma(E1))} &= 1 : 1 (1 : 1.6), \\ \frac{\Gamma(Y(3940) \rightarrow h_c\gamma(M1))}{\Gamma(Y(4140) \rightarrow h_c\gamma(M1))} &= 1 : 1 (1 : 2.8), \\ \frac{\Gamma(Y(3940) \rightarrow \psi(1^3D_2)\gamma(E1))}{\Gamma(Y(4140) \rightarrow \psi(1^3D_2)\gamma(E1))} &= 1 : 1. \end{aligned}$$

While, assuming them to be the  $D^*\bar{D}^*$  and  $D_s^*\bar{D}_s^*$  molecular states of  $J^{PC} = 2^{++}$ , respectively, their  $E1$  transition ratios were evaluated to be

$$\begin{aligned} \Gamma(Y(3940) \rightarrow \psi(1^3D_1)\gamma(E1)) : \Gamma(Y(3940) \rightarrow \psi(1^3D_2)\gamma(E1)) : \Gamma(Y(3940) \rightarrow \psi(1^3D_3)\gamma(E1)) &= 1 : 15 : 84, \\ \Gamma(Y(4140) \rightarrow \psi(1^3D_1)\gamma(E1)) : \Gamma(Y(4140) \rightarrow \psi(1^3D_2)\gamma(E1)) : \Gamma(Y(4140) \rightarrow \psi(1^3D_3)\gamma(E1)) &= 1 : 15 : 84. \end{aligned}$$

### 5.6. Hidden-charm baryonium or dibaryons with two charm quarks

The observation of the  $XYZ$  and two  $P_c$  states opened a window to explore the hidden-charm four-quark and five-quark matter. One has good reasons to expect the existence of the hidden-charm baryonium [402, 400], which is the six-quark matter.

The possible S-wave hidden-charm baryonia with configurations  $\Lambda_c \bar{\Lambda}_c$ ,  $\Sigma_c \bar{\Sigma}_c$ , and  $\Lambda_c \bar{\Sigma}_c$  may lie slightly below the thresholds of  $\Lambda_c \bar{\Lambda}_c$ ,  $\Sigma_c \bar{\Sigma}_c$ , and  $\Lambda_c \bar{\Sigma}_c$ , which are 4573 MeV, 4740 MeV, and 4908 MeV, respectively. These states may be searched for through the hidden-charm decay modes such as  $J/\psi$  or  $\eta_c$  plus  $1\pi, \eta, 2\pi, 3\pi$  or other light hadrons in the  $B$  and  $B_s$  decays at LHCb. Their open-charm decays include a pair of charmed and anti-charmed mesons, or a pair of charmed baryon and anti-baryon etc. The hidden-bottom baryonia may also exist.

The existence of the  $XYZ$  and  $P_c$  states also implies the possible existence of the doubly charmed/bottomed molecular systems and doubly charmed/bottomed tetraquark or pentaquark systems. Especially the dimeson, dibaryon and pentaquark molecular systems with two charm/bottom quarks are particularly interesting. These hadrons may be produced either at LHC or through heavy ion collisions or through higher bottomonium decays.

### 5.7. Future facilities

As shown in Tables 28 and 29, many  $XYZ$  states were only observed in one decay channel. Finding more decay modes is important to reveal their structures and distinguish different theoretical models. Although more than 20 charmonium-like  $XYZ$  states and two hidden-charm pentaquark states were observed, we still do not know much about them.

The hadron spectroscopy is a data-driven field. It is inspiring to take a look at the current experiments (BESIII, LHCb, and CMS) and the forthcoming experiments (BelleII and PANDA), all of which have contributed or will contribute to the study of the charmonium-like multi-quark states. Other collaborations such as COMPASS may also have the potential to contribute to this field. See also discussions in Ref. [48].

1. **BESIII**: The whitepaper of BESIII was finished in 2008 [809]. The ‘‘Charmonium Physics’’ was one of its important subjects. With the upgrade of BEPCII’s LINAC in 2012, its center-of-mass energy reaches 4.6 GeV. One year later, the  $Z_c(3900)$  [53] and the  $Z_c(4020)$  were observed [150]. BESIII has collected lots of data samples ranging from 3.8 to 4.6 GeV, which is an ideal platform to study the charmonium-like physics.
2. **LHCb**: The whitepaper of LHCb was also written in 2008 [810]. Its primary goal was to study the CP violation and rare decays of beauty and charm hadrons. The decay mode  $\Lambda_b^0 \rightarrow J/\psi p K^-$  was first observed in 2013 [811]. Two years later, the two hidden-charm pentaquark states  $P_c(4380)$  and  $P_c(4450)$  were discovered [2]. Its current performance can be found in Ref. [812]. LHCb has the world’s largest sample of exclusively reconstructed charm and beauty decays, and is also an ideal platform to study the charmonium-like physics. Moreover, with the update of LHC, LHCb would probably be able to study the charm-bottom and bottomonium-like tetraquarks and pentaquarks.
3. **CMS**: The whitepaper of CMS was again written in 2008 [813], where its primary goal was to study the Higgs mechanism. To meet this goal, its detector is at the energy frontier. CMS may also contribute to the charmonium-like states.
4. **BelleII**: As the update of Belle, BelleII was designed at the rare/precision frontier to observe signatures of new particles or processes [814]. The ‘‘Charmonia and new particles’’ is one of its goals [815]. BelleII is another ideal platform to study the charmonium-like, charm-bottom and bottomonium-like tetraquarks and pentaquarks.
5. **PANDA**: PANDA is another forthcoming experiment to study the hadron spectroscopy up to the region of charm quarks [816]. It is also an ideal platform to study the charmonium-like tetraquark and pentaquark states. Moreover, it is designed to study other exotic hadrons, such as the hybrid charmonium states, glueballs, etc.

### 5.8. Outlook

A large basis of interpolating fields are used to study the  $X(3872)$  in a recent lattice QCD simulation, including  $O^{\bar{c}c}$ ,  $O^{DD^*}$ ,  $O^{J/\psi\omega}$  (for  $I = 0$ ),  $O^{J/\psi\rho}$  (for  $I = 1$ ) and the diquark-antidiquark interpolators [579]. This dynamical lattice QCD simulation was performed with  $N_f = 2$  and  $m_\pi = 266$  MeV. The discrete scattering states were obtained. The contributions of different operators were isolated [579], which helps us understand the structure of the  $X(3872)$  greatly. Hopefully future dynamical simulations on the other important states such as the  $Y(4260)$ ,  $Z_b$  and  $Z_c$  will be

achieved soon. Especially the dynamical simulations with  $m_\pi$  very close to 140 MeV shall play a pivotal role in the confirmation of the molecular scheme.

On the other hand, BESIII has been continuing collecting data. More interesting results on the XYZ states are expected. With the discovery of the two  $P_c$  states, more partner states may be observed at LHCb. One also anticipates more experimental measurements on the XYZ states from CMS. In the near future, BelleII will start collecting data, which is an ideal factory of the hidden-charm multiquark states as emphasized in Sec. 4.1.5.

Since the discovery of the  $J/\psi$ , the past 13 years may be the most important period in the development of hadron spectroscopy. More excitement, puzzles and surprises are waiting for us in the coming golden decade. Let's cherish all the expected and embrace all the unexpected.

## Acknowledgements

We would like to express our gratitude to all the collaborators and colleagues who contributed to the investigations presented here, in particular to Dian-Yong Chen, Rui Chen, Xiao-Lin Chen, Er-Liang Cui, Wei-Zhen Deng, Ning Li, Xiao-Hai Liu, Yan-Rui Liu, Zhi-Gang Luo, Li Ma, T. G. Steele, Zhi-Feng Sun, Takayuki Matsuki, Guan-Juan Wang, Lu Zhao. We also thank Bo Wang for drawing some of the figures in the paper, and thank Dan Zhou for helping prepare some relevant documents. This work was supported in part by the National Natural Science Foundation of China under Grants No. 11205011, No. 11475015, No. 11375024, No. 11222547, No. 11175073, No. 11575008, and No. 11261130311, the Ministry of Education of China (SRFDP under Grant No. 20120211110002 and the Fundamental Research Funds for the Central Universities), the National Youth Top-notch Talent Support Program ("Thousands-of-Talents Scheme"), and the Natural Sciences and Engineering Research Council of Canada (NSERC).

## References

### References

- [1] K. A. Olive, *et al.*, [Particle Data Group Collaboration], Review of Particle Physics, Chin. Phys. C38 (2014) 090001. doi:10.1088/1674-1137/38/9/090001.
- [2] R. Aaij, *et al.*, [LHCb Collaboration], Observation of  $J/\psi p$  Resonances Consistent with Pentaquark States in  $\Lambda_b^0 \rightarrow J/\psi K^- p$  Decays, Phys. Rev. Lett. 115 (2015) 072001. arXiv:1507.03414, doi:10.1103/PhysRevLett.115.072001.
- [3] J. J. Aubert, *et al.*, [E598 Collaboration], Experimental Observation of a Heavy Particle  $J$ , Phys. Rev. Lett. 33 (1974) 1404–1406. doi:10.1103/PhysRevLett.33.1404.
- [4] J. E. Augustin, *et al.*, [SLAC-SP-017 Collaboration], Discovery of a Narrow Resonance in  $e^+e^-$  Annihilation, Phys. Rev. Lett. 33 (1974) 1406–1408, [Adv. Exp. Phys. 5, 141 (1976)]. doi:10.1103/PhysRevLett.33.1406.
- [5] E. Eichten, K. Gottfried, T. Kinoshita, J. B. Kogut, K. D. Lane, T.-M. Yan, The Spectrum of Charmonium, Phys. Rev. Lett. 34 (1975) 369–372, [Erratum: Phys. Rev. Lett. 36, 1276 (1976)]. doi:10.1103/PhysRevLett.34.369.
- [6] T. Appelquist, A. De Rujula, H. D. Politzer, S. L. Glashow, Charmonium Spectroscopy, Phys. Rev. Lett. 34 (1975) 365. doi:10.1103/PhysRevLett.34.365.
- [7] A. De Rujula, H. Georgi, S. L. Glashow, Hadron Masses in a Gauge Theory, Phys. Rev. D12 (1975) 147–162. doi:10.1103/PhysRevD.12.147.
- [8] A. D. Sakharov, Mass Formula for Mesons and Baryons, Sov. Phys. JETP 51 (1980) 1059–1060, [Zh. Eksp. Teor. Fiz. 78, 2112 (1980)].
- [9] P. Federman, H. R. Rubinstein, I. Talmi, DYNAMICAL DERIVATION OF BARYON MASSES IN THE QUARK MODEL, In \*Lichtenberg, D. B. (Ed.), Rosen, S. P. (Ed.): Developments In The Quark Theory Of Hadrons, Vol. 1\*, 289–290.
- [10] D. P. Stanley, D. Robson, Nonperturbative Potential Model for Light and Heavy Quark anti-Quark Systems, Phys. Rev. D21 (1980) 3180–3196. doi:10.1103/PhysRevD.21.3180.
- [11] D. P. Stanley, D. Robson, DO QUARKS INTERACT PAIRWISE AND SATISFY THE COLOR HYPOTHESIS?, Phys. Rev. Lett. 45 (1980) 235–238. doi:10.1103/PhysRevLett.45.235.
- [12] R. Koniuk, N. Isgur, Baryon Decays in a Quark Model with Chromodynamics, Phys. Rev. D21 (1980) 1868, [Erratum: Phys. Rev. D23, 818 (1981)]. doi:10.1103/PhysRevD.21.1868, 10.1103/PhysRevD.23.818.
- [13] J. M. Richard, P. Taxil, Ground State Baryons in the Nonrelativistic Quark Model, Annals Phys. 150 (1983) 267. doi:10.1016/0003-4916(83)90009-X.
- [14] J. M. Richard, P. Taxil, Baryons With Charm and Strangeness in Potential Models, Phys. Lett. B128 (1983) 453. doi:10.1016/0370-2693(83)90938-3.
- [15] S. Ono, F. Schoberl, A Simultaneous and Systematic Study of Meson and Baryon Spectra in the Quark Model, Phys. Lett. B118 (1982) 419. doi:10.1016/0370-2693(82)90216-7.
- [16] J. L. Basdevant, S. Boukraa, Baryon Masses in Relativistic Potential Models, Z. Phys. C30 (1986) 103. doi:10.1007/BF01560683.
- [17] S. Godfrey, N. Isgur, Mesons in a Relativized Quark Model with Chromodynamics, Phys. Rev. D32 (1985) 189–231. doi:10.1103/PhysRevD.32.189.

- [18] M. Gell-Mann, A Schematic Model of Baryons and Mesons, Phys. Lett. 8 (1964) 214–215. doi:10.1016/S0031-9163(64)92001-3.
- [19] G. Zweig, An SU(3) model for strong interaction symmetry and its breaking. Version 1.
- [20] R. L. Jaffe, Multi-Quark Hadrons. 1. Phenomenology of  $Q^2\bar{Q}^2$  Mesons, Phys. Rev. D15 (1977) 267. doi:10.1103/PhysRevD.15.267.
- [21] R. L. Jaffe, Multi-Quark Hadrons. 2. Methods, Phys. Rev. D15 (1977) 281. doi:10.1103/PhysRevD.15.281.
- [22] D. Strottman, Multi-Quark Baryons and the MIT Bag Model, Phys. Rev. D20 (1979) 748–767. doi:10.1103/PhysRevD.20.748.
- [23] H. J. Lipkin, New Possibilities for Exotic Hadrons: Anticharmed Strange Baryons, Phys. Lett. B195 (1987) 484. doi:10.1016/0370-2693(87)90055-4.
- [24] C. Gignoux, B. Silvestre-Brac, J. M. Richard, Possibility of Stable Multi-Quark Baryons, Phys. Lett. B193 (1987) 323. doi:10.1016/0370-2693(87)91244-5.
- [25] T. Nakano, *et al.*, [LEPS Collaboration], Evidence for a narrow  $S = +1$  baryon resonance in photoproduction from the neutron, Phys. Rev. Lett. 91 (2003) 012002. arXiv:hep-ex/0301020, doi:10.1103/PhysRevLett.91.012002.
- [26] K. H. Hicks, On the conundrum of the pentaquark, Eur. Phys. J. H37 (2012) 1–31. doi:10.1140/epjh/e2012-20032-0.
- [27] E. A. Hylleraas, A. Ore, Binding Energy of the Positronium Molecule, Phys. Rev. 71 (1947) 493–496. doi:10.1103/PhysRev.71.493.
- [28] D. B. Cassidy, A. P. Mills, The production of molecular positronium, Nature 449 (2007) 195–197.
- [29] H.-X. Chen, A. Hosaka, S.-L. Zhu, Light Scalar Tetraquark Mesons in the QCD Sum Rule, Phys. Rev. D76 (2007) 094025. arXiv:0707.4586, doi:10.1103/PhysRevD.76.094025.
- [30] R. L. Jaffe, Exotica, Phys. Rept. 409 (2005) 1–45. arXiv:hep-ph/0409065, doi:10.1016/j.physrep.2004.11.005.
- [31] E. S. Swanson, The New heavy mesons: A Status report, Phys. Rept. 429 (2006) 243–305. arXiv:hep-ph/0601110, doi:10.1016/j.physrep.2006.04.003.
- [32] E. Eichten, S. Godfrey, H. Mahlke, J. L. Rosner, Quarkonia and their transitions, Rev. Mod. Phys. 80 (2008) 1161–1193. arXiv:hep-ph/0701208, doi:10.1103/RevModPhys.80.1161.
- [33] S.-L. Zhu, New hadron states, Int. J. Mod. Phys. E17 (2008) 283–322. arXiv:hep-ph/0703225, doi:10.1142/S0218301308009446.
- [34] E. Klempf, A. Zaitsev, Glueballs, Hybrids, Multiquarks. Experimental facts versus QCD inspired concepts, Phys. Rept. 454 (2007) 1–202. arXiv:0708.4016, doi:10.1016/j.physrep.2007.07.006.
- [35] M. B. Voloshin, Charmonium, Prog. Part. Nucl. Phys. 61 (2008) 455–511. arXiv:0711.4556, doi:10.1016/j.ppnp.2008.02.001.
- [36] S. Godfrey, S. L. Olsen, The Exotic XYZ Charmonium-like Mesons, Ann. Rev. Nucl. Part. Sci. 58 (2008) 51–73. arXiv:0801.3867, doi:10.1146/annurev.nucl.58.110707.171145.
- [37] E. Klempf, J.-M. Richard, Baryon spectroscopy, Rev. Mod. Phys. 82 (2010) 1095–1153. arXiv:0901.2055, doi:10.1103/RevModPhys.82.1095.
- [38] M. Nielsen, F. S. Navarra, S. H. Lee, New Charmonium States in QCD Sum Rules: A Concise Review, Phys. Rept. 497 (2010) 41–83. arXiv:0911.1958, doi:10.1016/j.physrep.2010.07.005.
- [39] N. Brambilla, *et al.*, Heavy quarkonium: progress, puzzles, and opportunities, Eur. Phys. J. C71 (2011) 1534. arXiv:1010.5827, doi:10.1140/epjc/s10052-010-1534-9.
- [40] V. P. Druzhinin, S. I. Eidelman, S. I. Serednyakov, E. P. Solodov, Hadron Production via  $e^+e^-$  Collisions with Initial State Radiation, Rev. Mod. Phys. 83 (2011) 1545. arXiv:1105.4975, doi:10.1103/RevModPhys.83.1545.
- [41] N. Li, Z.-F. Sun, J. He, X. Liu, Z.-G. Luo, S.-L. Zhu, Few-Body Systems Composed of Heavy Quarks, Few Body Syst. 54 (2013) 807–812. arXiv:1208.6347, doi:10.1007/s00601-012-0564-2.
- [42] X. Liu, An overview of XYZ new particles, Chin. Sci. Bull. 59 (2014) 3815–3830. arXiv:1312.7408, doi:10.1007/s11434-014-0407-2.
- [43] W. Chen, W.-Z. Deng, J. He, N. Li, X. Liu, Z.-G. Luo, Z.-F. Sun, S.-L. Zhu, XYZ States, PoS Hadron2013 (2013) 005. arXiv:1311.3763.
- [44] W. Chen, T. G. Steele, S.-L. Zhu, Heavy tetraquark states and quarkonium hybrids, The Universe 2 (2014) 13–40. arXiv:1403.7457.
- [45] N. Brambilla, *et al.*, QCD and Strongly Coupled Gauge Theories: Challenges and Perspectives, Eur. Phys. J. C74 (10) (2014) 2981. arXiv:1404.3723, doi:10.1140/epjc/s10052-014-2981-5.
- [46] A. Esposito, A. L. Guerrieri, F. Piccinini, A. Pilloni, A. D. Polosa, Four-Quark Hadrons: an Updated Review, Int. J. Mod. Phys. A30 (04n05) (2014) 1530002. arXiv:1411.5997, doi:10.1142/S0217751X15300021.
- [47] S. L. Olsen, A New Hadron Spectroscopy, Front. Phys. 10 (2015) 101401. arXiv:1411.7738, doi:10.1007/S11467-014-0449-6.
- [48] R. A. Briceno, *et al.*, Issues and Opportunities in Exotic Hadrons, arXiv:1511.06779.
- [49] Q. He, *et al.*, [CLEO Collaboration], Confirmation of the  $Y(4260)$  resonance production in ISR, Phys. Rev. D74 (2006) 091104. arXiv:hep-ex/0611021, doi:10.1103/PhysRevD.74.091104.
- [50] T. Xiao, S. Dobbs, A. Tomaradze, K. K. Seth, Observation of the Charged Hadron  $Z_c^\pm(3900)$  and Evidence for the Neutral  $Z_c^0(3900)$  in  $e^+e^- \rightarrow \pi\pi J/\psi$  at  $\sqrt{s} = 4170$  MeV, Phys. Lett. B727 (2013) 366–370. arXiv:1304.3036, doi:10.1016/j.physletb.2013.10.041.
- [51] B. Aubert, *et al.*, [BaBar Collaboration], Observation of a broad structure in the  $\pi^+\pi^-J/\psi$  mass spectrum around 4.26 GeV/ $c^2$ , Phys. Rev. Lett. 95 (2005) 142001. arXiv:hep-ex/0506081, doi:10.1103/PhysRevLett.95.142001.
- [52] S. K. Choi, *et al.*, [Belle Collaboration], Observation of a narrow charmonium-like state in exclusive  $B^\pm \rightarrow K^\pm\pi^+\pi^-J/\psi$  decays, Phys. Rev. Lett. 91 (2003) 262001. arXiv:hep-ex/0309032, doi:10.1103/PhysRevLett.91.262001.
- [53] M. Ablikim, *et al.*, [BESIII Collaboration], Observation of a Charged Charmoniumlike Structure in  $e^+e^- \rightarrow \pi^+\pi^-J/\psi$  at  $\sqrt{s} = 4.26$  GeV, Phys. Rev. Lett. 110 (2013) 252001. arXiv:1303.5949, doi:10.1103/PhysRevLett.110.252001.
- [54] F. Abe, *et al.*, [CDF Collaboration], Observation of top quark production in  $p\bar{p}$  collisions, Phys. Rev. Lett. 74 (1995) 2626–2631. arXiv:hep-ex/9503002, doi:10.1103/PhysRevLett.74.2626.
- [55] S. Abachi, *et al.*, [D0 Collaboration], Search for high mass top quark production in  $p\bar{p}$  collisions at  $\sqrt{s} = 1.8$  TeV, Phys. Rev. Lett. 74 (1995) 2422–2426. arXiv:hep-ex/9411001, doi:10.1103/PhysRevLett.74.2422.
- [56] D. Acosta, *et al.*, [CDF Collaboration], Observation of the narrow state  $X(3872) \rightarrow J/\psi\pi^+\pi^-$  in  $p\bar{p}$  collisions at  $\sqrt{s} = 1.96$  TeV, Phys. Rev. Lett. 93 (2004) 072001. arXiv:hep-ex/0312021, doi:10.1103/PhysRevLett.93.072001.
- [57] V. M. Abazov, *et al.*, [D0 Collaboration], Observation and properties of the  $X(3872)$  decaying to  $J/\psi\pi^+\pi^-$  in  $p\bar{p}$  collisions at  $\sqrt{s} = 1.96$  TeV, Phys. Rev. Lett. 93 (2004) 162002. arXiv:hep-ex/0405004, doi:10.1103/PhysRevLett.93.162002.

- [58] T. Aaltonen, *et al.*, [CDF Collaboration], Evidence for a Narrow Near-Threshold Structure in the  $J/\psi\phi$  Mass Spectrum in  $B^+ \rightarrow J/\psi\phi K^+$  Decays, Phys. Rev. Lett. 102 (2009) 242002. [arXiv:0903.2229](#), [doi:10.1103/PhysRevLett.102.242002](#).
- [59] R. Aaij, *et al.*, [LHCb Collaboration], Determination of the  $X(3872)$  meson quantum numbers, Phys. Rev. Lett. 110 (2013) 222001. [arXiv:1302.6269](#), [doi:10.1103/PhysRevLett.110.222001](#).
- [60] S. Chatrchyan, *et al.*, [CMS Collaboration], Observation of a new boson at a mass of 125 GeV with the CMS experiment at the LHC, Phys. Lett. B716 (2012) 30–61. [arXiv:1207.7235](#), [doi:10.1016/j.physletb.2012.08.021](#).
- [61] G. Aad, *et al.*, [ATLAS Collaboration], Observation of a new particle in the search for the Standard Model Higgs boson with the ATLAS detector at the LHC, Phys. Lett. B716 (2012) 1–29. [arXiv:1207.7214](#), [doi:10.1016/j.physletb.2012.08.020](#).
- [62] S. Chatrchyan, *et al.*, [CMS Collaboration], Measurement of the  $X(3872)$  production cross section via decays to  $J/\psi\pi\pi$  in pp collisions at  $\sqrt{s} = 7$  TeV, JHEP 04 (2013) 154. [arXiv:1302.3968](#), [doi:10.1007/JHEP04\(2013\)154](#).
- [63] S. Chatrchyan, *et al.*, [CMS Collaboration], Observation of a peaking structure in the  $J/\psi\phi$  mass spectrum from  $B^\pm \rightarrow J/\psi\phi K^\pm$  decays, Phys. Lett. B734 (2014) 261–281. [arXiv:1309.6920](#), [doi:10.1016/j.physletb.2014.05.055](#).
- [64] K. Abe, *et al.*, Evidence for  $X(3872) \rightarrow \gamma J/\psi$  and the sub-threshold decay  $X(3872) \rightarrow \omega J/\psi$ , in: Lepton and photon interactions at high energies. Proceedings, 22nd International Symposium, LP 2005, Uppsala, Sweden, June 30–July 5, 2005, 2005. [arXiv:hep-ex/0505037](#).
- [65] G. Gokhroo, *et al.*, [Belle Collaboration], Observation of a Near-threshold  $D^0\bar{D}^0\pi^0$  Enhancement in  $B \rightarrow D^0\bar{D}^0\pi^0 K$  Decay, Phys. Rev. Lett. 97 (2006) 162002. [arXiv:hep-ex/0606055](#), [doi:10.1103/PhysRevLett.97.162002](#).
- [66] I. Adachi, *et al.*, Study of  $X(3872)$  in  $B$  meson decays, in: Proceedings, 34th International Conference on High Energy Physics (ICHEP 2008), 2008. [arXiv:0809.1224](#).
- [67] T. Aushev, *et al.*, [Belle Collaboration], Study of the  $B \rightarrow X(3872)(\rightarrow D^{*0}\bar{D}^0)K$  decay, Phys. Rev. D81 (2010) 031103. [arXiv:0810.0358](#), [doi:10.1103/PhysRevD.81.031103](#).
- [68] V. Bhardwaj, *et al.*, [Belle Collaboration], Observation of  $X(3872) \rightarrow J/\psi\gamma$  and search for  $X(3872) \rightarrow \psi'\gamma$  in  $B$  decays, Phys. Rev. Lett. 107 (2011) 091803. [arXiv:1105.0177](#), [doi:10.1103/PhysRevLett.107.091803](#).
- [69] S. K. Choi, *et al.*, Bounds on the width, mass difference and other properties of  $X(3872) \rightarrow \pi^+\pi^- J/\psi$  decays, Phys. Rev. D84 (2011) 052004. [arXiv:1107.0163](#), [doi:10.1103/PhysRevD.84.052004](#).
- [70] A. Abulencia, *et al.*, [CDF Collaboration], Measurement of the dipion mass spectrum in  $X(3872) \rightarrow J/\psi\pi^+\pi^-$  decays., Phys. Rev. Lett. 96 (2006) 102002. [arXiv:hep-ex/0512074](#), [doi:10.1103/PhysRevLett.96.102002](#).
- [71] A. Abulencia, *et al.*, [CDF Collaboration], Analysis of the quantum numbers  $J^{PC}$  of the  $X(3872)$ , Phys. Rev. Lett. 98 (2007) 132002. [arXiv:hep-ex/0612053](#), [doi:10.1103/PhysRevLett.98.132002](#).
- [72] T. Aaltonen, *et al.*, [CDF Collaboration], Precision Measurement of the  $X(3872)$  Mass in  $J/\psi\pi^+\pi^-$  Decays, Phys. Rev. Lett. 103 (2009) 152001. [arXiv:0906.5218](#), [doi:10.1103/PhysRevLett.103.152001](#).
- [73] B. Aubert, *et al.*, [BaBar Collaboration], Study of the  $B \rightarrow J/\psi K^-\pi^+\pi^-$  decay and measurement of the  $B \rightarrow X(3872)K^-$  branching fraction, Phys. Rev. D71 (2005) 071103. [arXiv:hep-ex/0406022](#), [doi:10.1103/PhysRevD.71.071103](#).
- [74] B. Aubert, *et al.*, [BaBar Collaboration], Study of  $J/\psi\pi^+\pi^-$  states produced in  $B^0 \rightarrow J/\psi\pi^+\pi^- K^0$  and  $B^- \rightarrow J/\psi\pi^+\pi^- K^-$ , Phys. Rev. D73 (2006) 011101. [arXiv:hep-ex/0507090](#), [doi:10.1103/PhysRevD.73.011101](#).
- [75] B. Aubert, *et al.*, [BaBar Collaboration], Search for  $B^+ \rightarrow X(3872)K^+$ ,  $X(3872) \rightarrow J/\psi\gamma$ , Phys. Rev. D74 (2006) 071101. [arXiv:hep-ex/0607050](#), [doi:10.1103/PhysRevD.74.071101](#).
- [76] B. Aubert, *et al.*, [BaBar Collaboration], Study of Resonances in Exclusive B Decays to  $\bar{D}^{(*)}D^{(*)}K$ , Phys. Rev. D77 (2008) 011102. [arXiv:0708.1565](#), [doi:10.1103/PhysRevD.77.011102](#).
- [77] B. Aubert, *et al.*, [BaBar Collaboration], A Study of  $B \rightarrow X(3872)K$ , with  $X(3872) \rightarrow J/\psi\pi^+\pi^-$ , Phys. Rev. D77 (2008) 111101. [arXiv:0803.2838](#), [doi:10.1103/PhysRevD.77.111101](#).
- [78] B. Aubert, *et al.*, [BaBar Collaboration], Evidence for  $X(3872) \rightarrow \psi(2S)\gamma$  in  $B^\pm \rightarrow X(3872)K^\pm$  decays, and a study of  $B \rightarrow c\bar{c}\gamma K$ , Phys. Rev. Lett. 102 (2009) 132001. [arXiv:0809.0042](#), [doi:10.1103/PhysRevLett.102.132001](#).
- [79] P. del Amo Sanchez, *et al.*, [BaBar Collaboration], Evidence for the decay  $X(3872) \rightarrow J/\psi\omega$ , Phys. Rev. D82 (2010) 011101. [arXiv:1005.5190](#), [doi:10.1103/PhysRevD.82.011101](#).
- [80] R. Aaij, *et al.*, [LHCb Collaboration], Observation of  $X(3872)$  production in  $pp$  collisions at  $\sqrt{s} = 7$  TeV, Eur. Phys. J. C72 (2012) 1972. [arXiv:1112.5310](#), [doi:10.1140/epjc/s10052-012-1972-7](#).
- [81] R. Aaij, *et al.*, [LHCb Collaboration], Evidence for the decay  $X(3872) \rightarrow \psi(2S)\gamma$ , Nucl. Phys. B886 (2014) 665–680. [arXiv:1404.0275](#), [doi:10.1016/j.nuclphysb.2014.06.011](#).
- [82] M. Ablikim, *et al.*, [BESIII Collaboration], Observation of  $e^+e^- \rightarrow \gamma X(3872)$  at BESIII, Phys. Rev. Lett. 112 (9) (2014) 092001. [arXiv:1310.4101](#), [doi:10.1103/PhysRevLett.112.092001](#).
- [83] B. Aubert, *et al.*, [BaBar Collaboration], Observation of the decay  $B \rightarrow J/\psi\eta K$  and search for  $X(3872) \rightarrow J/\psi\eta$ , Phys. Rev. Lett. 93 (2004) 041801. [arXiv:hep-ex/0402025](#), [doi:10.1103/PhysRevLett.93.041801](#).
- [84] B. Aubert, *et al.*, [BaBar Collaboration], Measurements of the absolute branching fractions of  $B^\pm \rightarrow K^\pm X(c\bar{c})$ , Phys. Rev. Lett. 96 (2006) 052002. [arXiv:hep-ex/0510070](#), [doi:10.1103/PhysRevLett.96.052002](#).
- [85] K. Abe, *et al.*, [Belle Collaboration], Observation of a near-threshold omega  $J/\psi$  mass enhancement in exclusive  $B \rightarrow K\omega J/\psi$  decays, Phys. Rev. Lett. 94 (2005) 182002. [arXiv:hep-ex/0408126](#), [doi:10.1103/PhysRevLett.94.182002](#).
- [86] B. Aubert, *et al.*, [BaBar Collaboration], Observation of  $Y(3940) \rightarrow J/\psi\omega$  in  $B \rightarrow J/\psi\omega K$  at BABAR, Phys. Rev. Lett. 101 (2008) 082001. [arXiv:0711.2047](#), [doi:10.1103/PhysRevLett.101.082001](#).
- [87] K. Abe, *et al.*, [Belle Collaboration], Observation of a new charmonium state in double charmonium production in  $e^+e^-$  annihilation at  $\sqrt{s} \approx 10.6$ -GeV, Phys. Rev. Lett. 98 (2007) 082001. [arXiv:hep-ex/0507019](#), [doi:10.1103/PhysRevLett.98.082001](#).
- [88] C. P. Shen, *et al.*, [Belle Collaboration], Evidence for a new resonance and search for the  $Y(4140)$  in the  $\gamma\gamma \rightarrow \phi J/\psi$  process, Phys. Rev. Lett. 104 (2010) 112004. [arXiv:0912.2383](#), [doi:10.1103/PhysRevLett.104.112004](#).
- [89] T. Aaltonen, *et al.*, [CDF Collaboration], Observation of the  $Y(4140)$  structure in the  $J/\psi\phi$  Mass Spectrum in  $B^\pm \rightarrow J/\psi\phi K$  decays, [arXiv:1101.6058](#).
- [90] R. Aaij, *et al.*, [LHCb Collaboration], Search for the  $X(4140)$  state in  $B^\pm \rightarrow J/\psi\phi K^\pm$  decays, Phys. Rev. D85 (2012) 091103. [arXiv:](#)

- 1202.5087, doi:10.1103/PhysRevD.85.091103.
- [91] V. M. Abazov, *et al.*, [D0 Collaboration], Search for the  $X(4140)$  state in  $B^+ \rightarrow J/\psi\phi K^+$  decays with the D0 detector, Phys. Rev. D89 (1) (2014) 012004. [arXiv:1309.6580](#), doi:10.1103/PhysRevD.89.012004.
- [92] S. K. Choi, *et al.*, [Belle Collaboration], Observation of a resonance-like structure in the  $\pi^\pm\psi'$  mass distribution in exclusive  $B \rightarrow K\pi^\pm\psi'$  decays, Phys. Rev. Lett. 100 (2008) 142001. [arXiv:0708.1790](#), doi:10.1103/PhysRevLett.100.142001.
- [93] R. Mizuk, *et al.*, [Belle Collaboration], Dalitz analysis of  $B \rightarrow K\pi^+\psi'$  decays and the  $Z(4430)^+$ , Phys. Rev. D80 (2009) 031104. [arXiv:0905.2869](#), doi:10.1103/PhysRevD.80.031104.
- [94] B. Aubert, *et al.*, [BaBar Collaboration], Search for the  $Z(4430)^-$  at BABAR, Phys. Rev. D79 (2009) 112001. [arXiv:0811.0564](#), doi:10.1103/PhysRevD.79.112001.
- [95] K. Chilikin, *et al.*, [Belle Collaboration], Experimental constraints on the spin and parity of the  $Z(4430)^+$ , Phys. Rev. D88 (7) (2013) 074026. [arXiv:1306.4894](#), doi:10.1103/PhysRevD.88.074026.
- [96] K. Chilikin, *et al.*, [Belle Collaboration], Observation of a new charged charmoniumlike state in  $\bar{B}^0 \rightarrow J/\psi K^- \pi^+$  decays, Phys. Rev. D90 (11) (2014) 112009. [arXiv:1408.6457](#), doi:10.1103/PhysRevD.90.112009.
- [97] R. Aaij, *et al.*, [LHCb Collaboration], Observation of the resonant character of the  $Z(4430)^-$  state, Phys. Rev. Lett. 112 (22) (2014) 222002. [arXiv:1404.1903](#), doi:10.1103/PhysRevLett.112.222002.
- [98] R. Mizuk, *et al.*, [Belle Collaboration], Observation of two resonance-like structures in the  $\pi^+\chi_{c1}$  mass distribution in exclusive  $\bar{B}^0 \rightarrow K^- \pi^+ \chi_{c1}$  decays, Phys. Rev. D78 (2008) 072004. [arXiv:0806.4098](#), doi:10.1103/PhysRevD.78.072004.
- [99] J. P. Lees, *et al.*, [BaBar Collaboration], Search for the  $Z_1(4050)^+$  and  $Z_2(4250)^+$  states in  $\bar{B}^0 \rightarrow \chi_{c1} K^- \pi^+$  and  $B^+ \rightarrow \chi_{c1} K_S^0 \pi^+$ , Phys. Rev. D85 (2012) 052003. [arXiv:1111.5919](#), doi:10.1103/PhysRevD.85.052003.
- [100] L. Antoniazzi, *et al.*, [E705 Collaboration], Search for hidden charm resonance states decaying into  $J/\psi$  or  $\psi'$  plus pions, Phys. Rev. D50 (1994) 4258–4264. doi:10.1103/PhysRevD.50.4258.
- [101] V. Bhardwaj, *et al.*, [Belle Collaboration], Evidence of a new narrow resonance decaying to  $\chi_{c1}\gamma$  in  $B \rightarrow \chi_{c1}\gamma K$ , Phys. Rev. Lett. 111 (3) (2013) 032001. [arXiv:1304.3975](#), doi:10.1103/PhysRevLett.111.032001.
- [102] E. Eichten, K. Gottfried, T. Kinoshita, K. D. Lane, T.-M. Yan, Charmonium: The Model, Phys. Rev. D17 (1978) 3090, [Erratum: Phys. Rev. D21, 313 (1980)]. doi:10.1103/PhysRevD.17.3090, 10.1103/PhysRevD.21.313.
- [103] E. Eichten, K. Gottfried, T. Kinoshita, K. D. Lane, T.-M. Yan, Charmonium: Comparison with Experiment, Phys. Rev. D21 (1980) 203. doi:10.1103/PhysRevD.21.203.
- [104] W. Buchmuller, S. H. H. Tye, Quarkonia and Quantum Chromodynamics, Phys. Rev. D24 (1981) 132. doi:10.1103/PhysRevD.24.132.
- [105] D. Ebert, R. N. Faustov, V. O. Galkin, Properties of heavy quarkonia and  $B_c$  mesons in the relativistic quark model, Phys. Rev. D67 (2003) 014027. [arXiv:hep-ph/0210381](#), doi:10.1103/PhysRevD.67.014027.
- [106] E. J. Eichten, K. Lane, C. Quigg, Charmonium levels near threshold and the narrow state  $X(3872) \rightarrow \pi^+\pi^- J/\psi$ , Phys. Rev. D69 (2004) 094019. [arXiv:hep-ph/0401210](#), doi:10.1103/PhysRevD.69.094019.
- [107] M. Ablikim, *et al.*, [BESIII Collaboration], Observation of the  $\psi(1^3D_2)$  state in  $e^+e^- \rightarrow \pi^+\pi^-\gamma\chi_{c1}$  at BESIII, Phys. Rev. Lett. 115 (1) (2015) 011803. [arXiv:1503.08203](#), doi:10.1103/PhysRevLett.115.011803.
- [108] C. Z. Yuan, *et al.*, [Belle Collaboration], Measurement of  $e^+e^- \rightarrow \pi^+\pi^- J/\psi$  cross-section via initial state radiation at Belle, Phys. Rev. Lett. 99 (2007) 182004. [arXiv:0707.2541](#), doi:10.1103/PhysRevLett.99.182004.
- [109] T. E. Coan, *et al.*, [CLEO Collaboration], Charmonium decays of  $Y(4260)$ ,  $\psi(4160)$  and  $\psi(4040)$ , Phys. Rev. Lett. 96 (2006) 162003. [arXiv:hep-ex/0602034](#), doi:10.1103/PhysRevLett.96.162003.
- [110] C. Z. Yuan, *et al.*, [Belle Collaboration], Observation of  $e^+e^- \rightarrow K^+K^- J/\psi$  via initial state radiation at Belle, Phys. Rev. D77 (2008) 011105. [arXiv:0709.2565](#), doi:10.1103/PhysRevD.77.011105.
- [111] C. P. Shen, *et al.*, [Belle Collaboration], Updated cross section measurement of  $e^+e^- \rightarrow K^+K^- J/\psi$  and  $K_S^0 K_S^0 J/\psi$  via initial state radiation at Belle, Phys. Rev. D89 (7) (2014) 072015. [arXiv:1402.6578](#), doi:10.1103/PhysRevD.89.072015.
- [112] J. P. Lees, *et al.*, [BaBar Collaboration], Study of the reaction  $e^+e^- \rightarrow J/\psi\pi^+\pi^-$  via initial-state radiation at BaBar, Phys. Rev. D86 (2012) 051102. [arXiv:1204.2158](#), doi:10.1103/PhysRevD.86.051102.
- [113] Z. Q. Liu, *et al.*, [Belle Collaboration], Study of  $e^+e^- \rightarrow \pi^+\pi^- J/\psi$  and Observation of a Charged Charmoniumlike State at Belle, Phys. Rev. Lett. 110 (2013) 252002. [arXiv:1304.0121](#), doi:10.1103/PhysRevLett.110.252002.
- [114] B. Aubert, *et al.*, [BaBar Collaboration], Study of the Exclusive Initial-State Radiation Production of the  $D\bar{D}$  System, Phys. Rev. D76 (2007) 111105. [arXiv:hep-ex/0607083](#), doi:10.1103/PhysRevD.76.111105.
- [115] K. Abe, *et al.*, [Belle Collaboration], Measurement of the near-threshold  $e^+e^- \rightarrow D^{(*)\pm} D^{(*)\mp}$  cross section using initial-state radiation, Phys. Rev. Lett. 98 (2007) 092001. [arXiv:hep-ex/0608018](#), doi:10.1103/PhysRevLett.98.092001.
- [116] G. Pakhlova, *et al.*, [Belle Collaboration], Observation of  $\psi(4415) \rightarrow D\bar{D}_s^*(2460)$  decay using initial-state radiation, Phys. Rev. Lett. 100 (2008) 062001. [arXiv:0708.3313](#), doi:10.1103/PhysRevLett.100.062001.
- [117] G. Pakhlova, *et al.*, [Belle Collaboration], Measurement of the  $e^+e^- \rightarrow D^0 D^{*+} \pi^+$  cross section using initial-state radiation, Phys. Rev. D80 (2009) 091101. [arXiv:0908.0231](#), doi:10.1103/PhysRevD.80.091101.
- [118] D. Cronin-Hennessy, *et al.*, [CLEO Collaboration], Measurement of Charm Production Cross Sections in  $e^+e^-$  Annihilation at Energies between 3.97 and 4.26 GeV, Phys. Rev. D80 (2009) 072001. [arXiv:0801.3418](#), doi:10.1103/PhysRevD.80.072001.
- [119] B. Aubert, *et al.*, [BaBar Collaboration], Exclusive Initial-State-Radiation Production of the  $D\bar{D}$ ,  $D^* \bar{D}^*$ , and  $D^* \bar{D}^*$  Systems, Phys. Rev. D79 (2009) 092001. [arXiv:0903.1597](#), doi:10.1103/PhysRevD.79.092001.
- [120] P. del Amo Sanchez, *et al.*, [BaBar Collaboration], Exclusive Production of  $D_s^+ D_s^-$ ,  $D_s^{*+} D_s^-$ , and  $D_s^{*+} D_s^{*-}$  via  $e^+e^-$  Annihilation with Initial-State-Radiation, Phys. Rev. D82 (2010) 052004. [arXiv:1008.0338](#), doi:10.1103/PhysRevD.82.052004.
- [121] Z. Q. Liu, X. S. Qin, C. Z. Yuan, Combined fit to BaBar and Belle data on  $e^+e^- \rightarrow \pi^+\pi^-\psi(2S)$ , Phys. Rev. D78 (2008) 014032. [arXiv:0805.3560](#), doi:10.1103/PhysRevD.78.014032.
- [122] X. L. Wang, Y. L. Han, C. Z. Yuan, C. P. Shen, P. Wang, [Belle Collaboration], Observation of  $\psi(4040)$  and  $\psi(4160)$  decay into  $\eta J/\psi$ , Phys. Rev. D87 (5) (2013) 051101. [arXiv:1210.7550](#), doi:10.1103/PhysRevD.87.051101.
- [123] B. Aubert, *et al.*, [BaBar Collaboration], A Structure at 2175-MeV in  $e^+e^- \rightarrow \phi f_0(980)$  Observed via Initial-State Radiation, Phys. Rev.

- D74 (2006) 091103. [arXiv:hep-ex/0610018](#), [doi:10.1103/PhysRevD.74.091103](#).
- [124] B. Aubert, *et al.*, [BaBar Collaboration], Measurements of  $e^+e^- \rightarrow K^+K^-\eta$ ,  $K^+K^-\pi^0$  and  $K_S^0K^+\pi^+$  cross-sections using initial state radiation events, Phys. Rev. D77 (2008) 092002. [arXiv:0710.4451](#), [doi:10.1103/PhysRevD.77.092002](#).
- [125] B. Aubert, *et al.*, [BaBar Collaboration], A Study of  $e^+e^- \rightarrow p\bar{p}$  using initial state radiation with BABAR, Phys. Rev. D73 (2006) 012005. [arXiv:hep-ex/0512023](#), [doi:10.1103/PhysRevD.73.012005](#).
- [126] J. Burmester, *et al.*, [PLUTO Collaboration], The Total Hadronic Cross-Section for  $e^+e^-$  Annihilation Between 3.1 GeV and 4.8 GeV Center-Of-Mass Energy, Phys. Lett. B66 (1977) 395. [doi:10.1016/0370-2693\(77\)90023-5](#).
- [127] R. Brandelik, *et al.*, [DASP Collaboration], Total Cross-section for Hadron Production by  $e^+e^-$  Annihilation at Center-of-mass Energies Between 3.6 GeV and 5.2 GeV, Phys. Lett. B76 (1978) 361. [doi:10.1016/0370-2693\(78\)90807-9](#).
- [128] J. Siegrist, *et al.*, Hadron Production by  $e^+e^-$  Annihilation at Center-Of-Mass Energies Between 2.6 GeV and 7.8 GeV. Part 1. Total Cross-Section, Multiplicities and Inclusive Momentum Distributions, Phys. Rev. D26 (1982) 969. [doi:10.1103/PhysRevD.26.969](#).
- [129] J. Z. Bai, *et al.*, [BES Collaboration], Measurement of the total cross-section for hadronic production by  $e^+e^-$  annihilation at energies between 2.6 GeV - 5 GeV, Phys. Rev. Lett. 84 (2000) 594–597. [arXiv:hep-ex/9908046](#), [doi:10.1103/PhysRevLett.84.594](#).
- [130] M. Ablikim, *et al.*, [BES Collaboration], R value measurements for  $e^+e^-$  annihilation at 2.60 GeV, 3.07 GeV and 3.65 GeV, Phys. Lett. B677 (2009) 239–245. [arXiv:0903.0900](#), [doi:10.1016/j.physletb.2009.05.055](#).
- [131] K. Abe, *et al.*, Study of the  $Y(4260)$  resonance in  $e^+e^-$  collisions with initial state radiation at Belle, in: Proceedings of the 33rd International Conference on High Energy Physics (ICHEP '06), 2006. [arXiv:hep-ex/0612006](#).
- [132] B. Aubert, *et al.*, Study of the  $\pi^+\pi^-J/\psi$  Mass Spectrum via Initial-State Radiation at BABAR, in: Proceedings, 34th International Conference on High Energy Physics (ICHEP 2008), 2008. [arXiv:0808.1543](#).
- [133] B. Aubert, *et al.*, [BaBar Collaboration], Evidence of a broad structure at an invariant mass of 4.32  $GeV/c^2$  in the reaction  $e^+e^- \rightarrow \pi^+\pi^-\psi(2S)$  measured at BaBar, Phys. Rev. Lett. 98 (2007) 212001. [arXiv:hep-ex/0610057](#), [doi:10.1103/PhysRevLett.98.212001](#).
- [134] X. L. Wang, *et al.*, [Belle Collaboration], Observation of Two Resonant Structures in  $e^+e^- \rightarrow \pi^+\pi^-\psi(2S)$  via Initial State Radiation at Belle, Phys. Rev. Lett. 99 (2007) 142002. [arXiv:0707.3699](#), [doi:10.1103/PhysRevLett.99.142002](#).
- [135] J. P. Lees, *et al.*, [BaBar Collaboration], Study of the reaction  $e^+e^- \rightarrow \psi(2S)\pi^-\pi^+$  via initial-state radiation at BaBar, Phys. Rev. D89 (11) (2014) 111103. [arXiv:1211.6271](#), [doi:10.1103/PhysRevD.89.111103](#).
- [136] G. Pakhlova, *et al.*, [Belle Collaboration], Observation of a near-threshold enhancement in the  $e^+e^- \rightarrow \Lambda_c^+\Lambda_c^-$  cross section using initial-state radiation, Phys. Rev. Lett. 101 (2008) 172001. [arXiv:0807.4458](#), [doi:10.1103/PhysRevLett.101.172001](#).
- [137] P. Pakhlov, *et al.*, [Belle Collaboration], Production of New Charmoniumlike States in  $e^+e^- \rightarrow J/\psi D^{(*)}\bar{D}^{(*)}$  at  $\sqrt{s} \approx 10.6$  GeV, Phys. Rev. Lett. 100 (2008) 202001. [arXiv:0708.3812](#), [doi:10.1103/PhysRevLett.100.202001](#).
- [138] L. D. Landau, On the angular momentum of a system of two photons, Dokl. Akad. Nauk Ser. Fiz. 60 (2) (1948) 207–209. [doi:10.1016/B978-0-08-010586-4.50070-5](#).
- [139] C.-N. Yang, Selection Rules for the Dematerialization of a Particle Into Two Photons, Phys. Rev. 77 (1950) 242–245. [doi:10.1103/PhysRev.77.242](#).
- [140] S. Uehara, *et al.*, [Belle Collaboration], Observation of a  $\chi'_{c2}$  candidate in  $\gamma\gamma \rightarrow D\bar{D}$  production at BELLE, Phys. Rev. Lett. 96 (2006) 082003. [arXiv:hep-ex/0512035](#), [doi:10.1103/PhysRevLett.96.082003](#).
- [141] S. Uehara, *et al.*, [Belle Collaboration], Observation of a charmonium-like enhancement in the  $\gamma\gamma \rightarrow \omega J/\psi$  process, Phys. Rev. Lett. 104 (2010) 092001. [arXiv:0912.4451](#), [doi:10.1103/PhysRevLett.104.092001](#).
- [142] C. R. Munz, Two photon decays of mesons in a relativistic quark model, Nucl. Phys. A609 (1996) 364–376. [arXiv:hep-ph/9601206](#), [doi:10.1016/S0375-9474\(96\)00265-5](#).
- [143] B. Aubert, *et al.*, [BaBar Collaboration], Observation of the  $\chi_{c2}(2p)$  Meson in the Reaction  $\gamma\gamma \rightarrow D\bar{D}$  at BaBar, Phys. Rev. D81 (2010) 092003. [arXiv:1002.0281](#), [doi:10.1103/PhysRevD.81.092003](#).
- [144] J. P. Lees, *et al.*, [BaBar Collaboration], Study of  $X(3915) \rightarrow J/\psi\omega$  in two-photon collisions, Phys. Rev. D86 (2012) 072002. [arXiv:1207.2651](#), [doi:10.1103/PhysRevD.86.072002](#).
- [145] J. Brodzicka, *et al.*, [Belle Collaboration], Observation of a new  $D_{sJ}$  meson in  $B^+ \rightarrow \bar{D}^0 D^0 K^+$  decays, Phys. Rev. Lett. 100 (2008) 092001. [arXiv:0707.3491](#), [doi:10.1103/PhysRevLett.100.092001](#).
- [146] C. P. Shen, *et al.*, [Belle Collaboration], Search for charmonium and charmonium-like states in  $\Upsilon(1S)$  radiative decays, Phys. Rev. D82 (2010) 051504. [arXiv:1008.1774](#), [doi:10.1103/PhysRevD.82.051504](#).
- [147] X. L. Wang, *et al.*, [Belle Collaboration], Search for charmonium and charmonium-like states in  $\Upsilon(2S)$  radiative decays, Phys. Rev. D84 (2011) 071107. [arXiv:1108.4514](#), [doi:10.1103/PhysRevD.84.071107](#).
- [148] M. Ablikim, *et al.*, [BESIII Collaboration], Observation of a charged  $(D\bar{D}^*)^\pm$  mass peak in  $e^+e^- \rightarrow \pi D\bar{D}^*$  at  $\sqrt{s} = 4.26$  GeV, Phys. Rev. Lett. 112 (2) (2014) 022001. [arXiv:1310.1163](#), [doi:10.1103/PhysRevLett.112.022001](#).
- [149] M. Ablikim, *et al.*, [BESIII Collaboration], Observation of a Charged Charmoniumlike Structure  $Z_c(4020)$  and Search for the  $Z_c(3900)$  in  $e^+e^- \rightarrow \pi^+\pi^-h_c$ , Phys. Rev. Lett. 111 (24) (2013) 242001. [arXiv:1309.1896](#), [doi:10.1103/PhysRevLett.111.242001](#).
- [150] M. Ablikim, *et al.*, [BESIII Collaboration], Observation of a charged charmoniumlike structure in  $e^+e^- \rightarrow (D^*\bar{D}^*)^\pm\pi^\mp$  at  $\sqrt{s} = 4.26$  GeV, Phys. Rev. Lett. 112 (13) (2014) 132001. [arXiv:1308.2760](#), [doi:10.1103/PhysRevLett.112.132001](#).
- [151] M. Ablikim, *et al.*, [BESIII Collaboration], Observation of  $e^+e^- \rightarrow \eta J/\psi$  at center-of-mass energy  $\sqrt{s} = 4.009$  GeV, Phys. Rev. D86 (2012) 071101. [arXiv:1208.1857](#), [doi:10.1103/PhysRevD.86.071101](#).
- [152] M. Ablikim, *et al.*, [BESIII Collaboration], Observation of  $Z_c(3900)^0$  in  $e^+e^- \rightarrow \pi^0\pi^0 J/\psi$ , Phys. Rev. Lett. 115 (11) (2015) 112003. [arXiv:1506.06018](#), [doi:10.1103/PhysRevLett.115.112003](#).
- [153] M. Ablikim, *et al.*, [BESIII Collaboration], Observation of a Neutral Structure near the  $D\bar{D}^*$  Mass Threshold in  $e^+e^- \rightarrow (D\bar{D}^*)^0\pi^0$  at  $\sqrt{s} = 4.226$  and 4.257 GeV, Phys. Rev. Lett. 115 (22) (2015) 222002. [arXiv:1509.05620](#), [doi:10.1103/PhysRevLett.115.222002](#).
- [154] C. Adolph, *et al.*, [COMPASS Collaboration], Search for exclusive photoproduction of  $Z_c^\pm(3900)$  at COMPASS, Phys. Lett. B742 (2015) 330–334. [arXiv:1407.6186](#), [doi:10.1016/j.physletb.2015.01.042](#).
- [155] M. Ablikim, *et al.*, [BESIII Collaboration], Search for  $Z_c(3900)^\pm \rightarrow \omega\pi^\pm$ , Phys. Rev. D92 (3) (2015) 032009. [arXiv:1507.02068](#), [doi:10.1103/PhysRevD.92.032009](#).

- [156] M. Ablikim, *et al.*, [BESIII Collaboration], Search for the isospin violating decay  $Y(4260) \rightarrow J/\psi\eta\pi^0$ , Phys. Rev. D92 (1) (2015) 012008. [arXiv:1505.00539](#), [doi:10.1103/PhysRevD.92.012008](#).
- [157] J. He, X. Liu, Z.-F. Sun, S.-L. Zhu,  $Z_c(4025)$  as the hadronic molecule with hidden charm, Eur. Phys. J. C73 (11) (2013) 2635. [arXiv:1308.2999](#), [doi:10.1140/epjc/s10052-013-2635-z](#).
- [158] M. Ablikim, *et al.*, [BESIII Collaboration], Observation of  $e^+e^- \rightarrow \pi^0\pi^0h_c$  and a Neutral Charmoniumlike Structure  $Z_c(4020)^0$ , Phys. Rev. Lett. 113 (21) (2014) 212002. [arXiv:1409.6577](#), [doi:10.1103/PhysRevLett.113.212002](#).
- [159] M. Ablikim, *et al.*, [BESIII Collaboration], Observation of a neutral charmoniumlike state  $Z_c(4025)^0$  in  $e^+e^- \rightarrow (D^*\bar{D}^*)^0\pi^0$ , Phys. Rev. Lett. 115 (18) (2015) 182002. [arXiv:1507.02404](#), [doi:10.1103/PhysRevLett.115.182002](#).
- [160] R. Aaij, *et al.*, [LHCb Collaboration], Study of the production of  $\Lambda_b^0$  and  $\bar{B}^0$  hadrons in  $pp$  collisions and first measurement of the  $\Lambda_b^0 \rightarrow J/\psi p K^-$  branching fraction, [arXiv:1509.00292](#).
- [161] A. Bondar, *et al.*, [Belle Collaboration], Observation of two charged bottomonium-like resonances in  $\Upsilon(5S)$  decays, Phys. Rev. Lett. 108 (2012) 122001. [arXiv:1110.2251](#), [doi:10.1103/PhysRevLett.108.122001](#).
- [162] I. Adachi, Observation of two charged bottomonium-like resonances, in: Flavor physics and CP violation. Proceedings, 9th International Conference, FPCP 2011, Maale HaChamisha, Israel, May 23-27, 2011, 2011. [arXiv:1105.4583](#).
- [163] A. Garmash, *et al.*, [Belle Collaboration], Amplitude analysis of  $e^+e^- \rightarrow \Upsilon(nS)\pi^+\pi^-$  at  $\sqrt{s} = 10.865$  GeV, Phys. Rev. D91 (7) (2015) 072003. [arXiv:1403.0992](#), [doi:10.1103/PhysRevD.91.072003](#).
- [164] I. Adachi, *et al.*, [Belle Collaboration], Evidence for a  $Z_b^0(10610)$  in Dalitz analysis of  $\Upsilon(5S) \rightarrow \Upsilon(nS)\pi^0\pi^0$ , [arXiv:1207.4345](#).
- [165] P. Krokovny, *et al.*, [Belle Collaboration], First observation of the  $Z_b^0(10610)$  in a Dalitz analysis of  $\Upsilon(10860) \rightarrow \Upsilon(nS)\pi^0\pi^0$ , Phys. Rev. D88 (5) (2013) 052016. [arXiv:1308.2646](#), [doi:10.1103/PhysRevD.88.052016](#).
- [166] I. Adachi, *et al.*, Study of Three-Body  $\Upsilon(10860)$  Decays, 2012. [arXiv:1209.6450](#).
- [167] A. Abdesselam, *et al.*, Energy scan of the  $e^+e^- \rightarrow h_b(nP)\pi^+\pi^-$  ( $n = 1, 2$ ) cross sections and evidence for the  $\Upsilon(11020)$  decays into charged bottomonium-like states, in: 27th International Symposium on Lepton Photon Interactions at High Energy (LP15) Ljubljana, Slovenia, August 17-22, 2015, 2015. [arXiv:1508.06562](#).
- [168] X. H. He, *et al.*, [Belle Collaboration], Observation of  $e^+e^- \rightarrow \pi^+\pi^-\pi^0\chi_{bJ}$  and Search for  $X_b \rightarrow \omega\Upsilon(1S)$  at  $\sqrt{s} = 10.867$  GeV, Phys. Rev. Lett. 113 (14) (2014) 142001. [arXiv:1408.0504](#), [doi:10.1103/PhysRevLett.113.142001](#).
- [169] G. Aad, *et al.*, [ATLAS Collaboration], Search for the  $X_b$  and other hidden-beauty states in the  $\pi^+\pi^-\Upsilon(1S)$  channel at ATLAS, Phys. Lett. B740 (2015) 199–217. [arXiv:1410.4409](#), [doi:10.1016/j.physletb.2014.11.055](#).
- [170] G. Zweig, An SU(3) model for strong interaction symmetry and its breaking. Version 2, in: D. Lichtenberg, S. P. Rosen (Eds.), DEVELOPMENTS IN THE QUARK THEORY OF HADRONS. VOL. 1. 1964 - 1978, 1964, pp. 22–101.
- [171] M. B. Voloshin, L. B. Okun, Hadron Molecules and Charmonium Atom, JETP Lett. 23 (1976) 333–336, [Pisma Zh. Eksp. Teor. Fiz. 23, 369 (1976)].
- [172] A. De Rujula, H. Georgi, S. L. Glashow, Molecular Charmonium: A New Spectroscopy?, Phys. Rev. Lett. 38 (1977) 317. [doi:10.1103/PhysRevLett.38.317](#).
- [173] N. A. Tornqvist, On deusons or deuteron-like meson meson bound states, Nuovo Cim. A107 (1994) 2471–2476. [arXiv:hep-ph/9310225](#), [doi:10.1007/BF02734018](#).
- [174] N. A. Tornqvist, From the deuteron to deusons, an analysis of deuteron-like meson meson bound states, Z. Phys. C61 (1994) 525–537. [arXiv:hep-ph/9310247](#), [doi:10.1007/BF01413192](#).
- [175] M. B. Voloshin, Channel coupling in  $e^+e^-$  annihilation into heavy meson pairs at the  $D^*\bar{D}^*$  threshold, [arXiv:hep-ph/0602233](#).
- [176] S. Dubynskiy, M. B. Voloshin, Possible new resonance at the  $D^*\bar{D}^*$  threshold in  $e^+e^-$  annihilation, Mod. Phys. Lett. A21 (2006) 2779–2788. [arXiv:hep-ph/0608179](#), [doi:10.1142/S0217732306022195](#).
- [177] J. D. Weinstein, N. Isgur, Do Multi-Quark Hadrons Exist?, Phys. Rev. Lett. 48 (1982) 659. [doi:10.1103/PhysRevLett.48.659](#).
- [178] J. D. Weinstein, N. Isgur, The  $qq\bar{q}\bar{q}$  System in a Potential Model, Phys. Rev. D27 (1983) 588. [doi:10.1103/PhysRevD.27.588](#).
- [179] J. D. Weinstein, N. Isgur,  $K\bar{K}$  Molecules, Phys. Rev. D41 (1990) 2236. [doi:10.1103/PhysRevD.41.2236](#).
- [180] J. Z. Bai, *et al.*, [BES Collaboration], Observation of a near threshold enhancement in the  $p\bar{p}$  mass spectrum from radiative  $J/\psi \rightarrow \gamma p\bar{p}$  decays, Phys. Rev. Lett. 91 (2003) 022001. [arXiv:hep-ex/0303006](#), [doi:10.1103/PhysRevLett.91.022001](#).
- [181] A. Datta, P. J. O'Donnell, A New state of baryonium, Phys. Lett. B567 (2003) 273–276. [arXiv:hep-ph/0306097](#), [doi:10.1016/j.physletb.2003.06.050](#).
- [182] C.-S. Gao, S.-L. Zhu, Understanding the possible proton anti-proton bound state observed by BES collaboration, Commun. Theor. Phys. 42 (2004) 844. [arXiv:hep-ph/0308205](#).
- [183] X. Liu, X.-Q. Zeng, Y.-B. Ding, X.-Q. Li, H. Shen, P.-N. Shen, Can the observed enhancement in the mass spectrum of  $p\bar{p}$  in  $J/\psi \rightarrow \gamma p\bar{p}$  be interpreted by a possible  $p\bar{p}nd$  bound state, [arXiv:hep-ph/0406118](#).
- [184] E. S. Swanson, Short range structure in the  $X(3872)$ , Phys. Lett. B588 (2004) 189–195. [arXiv:hep-ph/0311229](#), [doi:10.1016/j.physletb.2004.03.033](#).
- [185] B. Aubert, *et al.*, [BaBar Collaboration], Observation of a narrow meson decaying to  $D_s^+\pi^0$  at a mass of 2.32 GeV/c<sup>2</sup>, Phys. Rev. Lett. 90 (2003) 242001. [arXiv:hep-ex/0304021](#), [doi:10.1103/PhysRevLett.90.242001](#).
- [186] T. Barnes, F. E. Close, H. J. Lipkin, Implications of a  $DK$  molecule at 2.32 GeV, Phys. Rev. D68 (2003) 054006. [arXiv:hep-ph/0305025](#), [doi:10.1103/PhysRevD.68.054006](#).
- [187] X. Liu, S.-L. Zhu,  $Y(4143)$  is probably a molecular partner of  $Y(3930)$ , Phys. Rev. D80 (2009) 017502, [Erratum: Phys. Rev. D85, 019902 (2012)]. [arXiv:0903.2529](#), [doi:10.1103/PhysRevD.85.019902](#), [doi:10.1103/PhysRevD.80.017502](#).
- [188] C. Meng, K.-T. Chao,  $Z^+(4430)$  as a resonance in the  $D_1(D_1^*)D^*$  channel, [arXiv:0708.4222](#).
- [189] X. Liu, Y.-R. Liu, W.-Z. Deng, S.-L. Zhu, Is  $Z^+(4430)$  a loosely bound molecular state?, Phys. Rev. D77 (2008) 034003. [arXiv:0711.0494](#), [doi:10.1103/PhysRevD.77.034003](#).
- [190] X. Liu, Y.-R. Liu, W.-Z. Deng, S.-L. Zhu,  $Z^+(4430)$  as a  $D_1^*D^*$  ( $D_D^*$ ) molecular state, Phys. Rev. D77 (2008) 094015. [arXiv:0803.1295](#), [doi:10.1103/PhysRevD.77.094015](#).

- [191] Z.-F. Sun, J. He, X. Liu, Z.-G. Luo, S.-L. Zhu,  $Z_b(10610)^\pm$  and  $Z_b(10650)^\pm$  as the  $B^*\bar{B}$  and  $B^*\bar{B}^*$  molecular states, Phys. Rev. D84 (2011) 054002. [arXiv:1106.2968](#), [doi:10.1103/PhysRevD.84.054002](#).
- [192] Z.-F. Sun, Z.-G. Luo, J. He, X. Liu, S.-L. Zhu, A note on the  $B^*\bar{B}$ ,  $B^*\bar{B}^*$ ,  $D^*\bar{D}$ ,  $D^*\bar{D}^*$  molecular states, Chin. Phys. C36 (2012) 194–204. [doi:10.1088/1674-1137/36/3/002](#).
- [193] D. Besson, *et al.*, [CLEO Collaboration], Observation of a narrow resonance of mass 2.46 GeV/c<sup>2</sup> decaying to  $D_s^*\pi^0$  and confirmation of the  $D_{s1}^*(2317)$  state, Phys. Rev. D68 (2003) 032002, [Erratum: Phys. Rev. D75, 119908 (2007)]. [arXiv:hep-ex/0305100](#), [doi:10.1103/PhysRevD.68.032002](#), [doi:10.1103/PhysRevD.75.119908](#).
- [194] B. Aubert, *et al.*, [BaBar Collaboration], Observation of a charmed baryon decaying to  $D^0 p$  at a mass near 2.94 GeV/c<sup>2</sup>, Phys. Rev. Lett. 98 (2007) 012001. [arXiv:hep-ex/0603052](#), [doi:10.1103/PhysRevLett.98.012001](#).
- [195] R. Mizuk, *et al.*, [Belle Collaboration], Observation of an isotriplet of excited charmed baryons decaying to  $\Lambda b_c^+\pi$ , Phys. Rev. Lett. 94 (2005) 122002. [arXiv:hep-ex/0412069](#), [doi:10.1103/PhysRevLett.94.122002](#).
- [196] X.-G. He, X.-Q. Li, X. Liu, X.-Q. Zeng,  $\Lambda b_c^+(2940)$ : A Possible molecular state?, Eur. Phys. J. C51 (2007) 883–889. [arXiv:hep-ph/0606015](#), [doi:10.1140/epjc/s10052-007-0347-y](#).
- [197] X. Liu, Understanding the newly observed  $Y(4008)$  by Belle, Eur. Phys. J. C54 (2008) 471–474. [arXiv:0708.4167](#), [doi:10.1140/epjc/s10052-008-0551-4](#).
- [198] X. Liu, B. Zhang, What can we learn from the decay of  $N_X(1625)$  in molecule picture?, Eur. Phys. J. C54 (2008) 253–258. [arXiv:0711.3813](#), [doi:10.1140/epjc/s10052-008-0527-4](#).
- [199] N. A. Tornqvist, Comment on the narrow charmonium state of Belle at 3871.8 MeV as a deuson, [arXiv:hep-ph/0308277](#).
- [200] E. S. Swanson, Diagnostic decays of the  $X(3872)$ , Phys. Lett. B598 (2004) 197–202. [arXiv:hep-ph/0406080](#), [doi:10.1016/j.physletb.2004.07.059](#).
- [201] Y.-R. Liu, X. Liu, W.-Z. Deng, S.-L. Zhu, Is  $X(3872)$  Really a Molecular State?, Eur. Phys. J. C56 (2008) 63–73. [arXiv:0801.3540](#), [doi:10.1140/epjc/s10052-008-0640-4](#).
- [202] F. Close, C. Downum, On the possibility of Deeply Bound Hadronic Molecules from single Pion Exchange, Phys. Rev. Lett. 102 (2009) 242003. [arXiv:0905.2687](#), [doi:10.1103/PhysRevLett.102.242003](#).
- [203] F. Close, C. Downum, C. E. Thomas, Novel Charmonium and Bottomonium Spectroscopies due to Deeply Bound Hadronic Molecules from Single Pion Exchange, Phys. Rev. D81 (2010) 074033. [arXiv:1001.2553](#), [doi:10.1103/PhysRevD.81.074033](#).
- [204] I. W. Lee, A. Faessler, T. Gutsche, V. E. Lyubovitskij,  $X(3872)$  as a molecular  $DD^*$  state in a potential model, Phys. Rev. D80 (2009) 094005. [arXiv:0910.1009](#), [doi:10.1103/PhysRevD.80.094005](#).
- [205] Q. Xu, G. Liu, H. Jin, Possible bound state of the double heavy meson-baryon system, Phys. Rev. D86 (2012) 114032. [arXiv:1012.5949](#), [doi:10.1103/PhysRevD.86.114032](#).
- [206] X. Liu, Y.-R. Liu, W.-Z. Deng, Dynamics study of  $Z^+(4430)$  and  $X(3872)$  in molecular picture[AIP Conf. Proc. 1030, 346 (2008)]. [arXiv:0802.3157](#), [doi:10.1063/1.2973525](#).
- [207] X. Liu, Z.-G. Luo, Y.-R. Liu, S.-L. Zhu,  $X(3872)$  and Other Possible Heavy Molecular States, Eur. Phys. J. C61 (2009) 411–428. [arXiv:0808.0073](#), [doi:10.1140/epjc/s10052-009-1020-4](#).
- [208] B. Hu, X.-L. Chen, Z.-G. Luo, P.-Z. Huang, S.-L. Zhu, P.-F. Yu, X. Liu, Possible heavy molecular states composed of a pair of excited charm-strange mesons, Chin. Phys. C35 (2011) 113–125. [arXiv:1004.4032](#), [doi:10.1088/1674-1137/35/2/002](#).
- [209] L.-L. Shen, X.-L. Chen, Z.-G. Luo, P.-Z. Huang, S.-L. Zhu, P.-F. Yu, X. Liu, The Molecular systems composed of the charmed mesons in the  $H\bar{S} + h.c.$  doublet, Eur. Phys. J. C70 (2010) 183–217. [arXiv:1005.0994](#), [doi:10.1140/epjc/s10052-010-1441-0](#).
- [210] J. He, Y.-T. Ye, Z.-F. Sun, X. Liu, The observed charmed hadron  $\Lambda_c(2940)^+$  and the  $D^*N$  interaction, Phys. Rev. D82 (2010) 114029. [arXiv:1008.1500](#), [doi:10.1103/PhysRevD.82.114029](#).
- [211] X. Liu, Z.-G. Luo, S.-L. Zhu, Novel charmonium-like structures in the  $J/\psi\phi$  and  $J/\psi\omega$  invariant mass spectra, Phys. Lett. B699 (2011) 341–344, [Erratum: Phys. Lett. B707, 577 (2012)]. [arXiv:1011.1045](#), [doi:10.1016/j.physletb.2011.12.019](#), [doi:10.1016/j.physletb.2011.04.024](#).
- [212] Y.-R. Liu, Z.-Y. Zhang, The Bound state problem of S-wave heavy quark meson-antimeson systems, Phys. Rev. C80 (2009) 015208. [arXiv:0810.1598](#), [doi:10.1103/PhysRevC.80.015208](#).
- [213] Y.-R. Liu, Z.-Y. Zhang,  $X(3872)$  and the bound state problem of  $D^0\bar{D}^{*0}$  ( $\bar{D}^0D^{*0}$ ) in a chiral quark model, Phys. Rev. C79 (2009) 035206. [arXiv:0805.1616](#), [doi:10.1103/PhysRevC.79.035206](#).
- [214] Y.-R. Liu, Z.-Y. Zhang, A Chiral quark model study of  $Z^+(4430)$  in the molecular picture, [arXiv:0908.1734](#).
- [215] G.-J. Ding, Understanding the Charged Meson  $Z(4430)$ , [arXiv:0711.1485](#).
- [216] G.-J. Ding, W. Huang, J.-F. Liu, M.-L. Yan,  $Z^+(4430)$  and analogous heavy flavor molecules, Phys. Rev. D79 (2009) 034026. [arXiv:0805.3822](#), [doi:10.1103/PhysRevD.79.034026](#).
- [217] G.-J. Ding, Are  $Y(4260)$  and  $Z^+(4248)$  are  $D_1\bar{D}$  or  $D_0\bar{D}^*$  Hadronic Molecules?, Phys. Rev. D79 (2009) 014001. [arXiv:0809.4818](#), [doi:10.1103/PhysRevD.79.014001](#).
- [218] G.-J. Ding, Bound States of the Heavy Flavor Vector Mesons and  $Y(4008)$  and  $Z_1^+(4050)$ , Phys. Rev. D80 (2009) 034005. [arXiv:0905.1188](#), [doi:10.1103/PhysRevD.80.034005](#).
- [219] N. Lee, Z.-G. Luo, X.-L. Chen, S.-L. Zhu, Possible Deuteron-like Molecular States Composed of Heavy Baryons, Phys. Rev. D84 (2011) 014031. [arXiv:1104.4257](#), [doi:10.1103/PhysRevD.84.014031](#).
- [220] Y. D. Chen, C. F. Qiao, Baryonium Study in Heavy Baryon Chiral Perturbation Theory, Phys. Rev. D85 (2012) 034034. [arXiv:1102.3487](#), [doi:10.1103/PhysRevD.85.034034](#).
- [221] N. Li, S.-L. Zhu, Hadronic Molecular States Composed of Heavy Flavor Baryons, Phys. Rev. D86 (2012) 014020. [arXiv:1204.3364](#), [doi:10.1103/PhysRevD.86.014020](#).
- [222] N. Li, S.-L. Zhu, Isospin breaking, Coupled-channel effects and Diagnosis of  $X(3872)$ , Phys. Rev. D86 (2012) 074022. [arXiv:1207.3954](#), [doi:10.1103/PhysRevD.86.074022](#).
- [223] N. Li, Z.-F. Sun, X. Liu, S.-L. Zhu, Coupled-channel analysis of the possible  $D^{(*)}D^{(*)}$ ,  $\bar{B}^{(*)}\bar{B}^{(*)}$  and  $D^{(*)}\bar{B}^{(*)}$  molecular states, Phys. Rev. D88 (11) (2013) 114008. [arXiv:1211.5007](#), [doi:10.1103/PhysRevD.88.114008](#).

- [224] L. Zhao, L. Ma, S.-L. Zhu, Spin-orbit force, recoil corrections, and possible  $B\bar{B}^*$  and  $D\bar{D}^*$  molecular states, Phys. Rev. D89 (9) (2014) 094026. [arXiv:1403.4043](#), [doi:10.1103/PhysRevD.89.094026](#).
- [225] L. Zhao, L. Ma, S.-L. Zhu, The recoil correction and spin-orbit force for the possible  $B^*\bar{B}^*$  and  $D^*\bar{D}^*$  states, Nucl. Phys. A942 (2015) 18–38. [arXiv:1504.04117](#), [doi:10.1016/j.nuclphysa.2015.06.010](#).
- [226] V. B. Berestetsky, E. M. Lifshitz, L. P. Pitaevsky, QUANTUM ELECTRODYNAMICS, 1982.
- [227] R. Machleidt, The High precision, charge dependent Bonn nucleon-nucleon potential (CD-Bonn), Phys. Rev. C63 (2001) 024001. [arXiv:nucl-th/0006014](#), [doi:10.1103/PhysRevC.63.024001](#).
- [228] R. Machleidt, K. Holinde, C. Elster, The Bonn Meson Exchange Model for the Nucleon Nucleon Interaction, Phys. Rept. 149 (1987) 1–89. [doi:10.1016/S0370-1573\(87\)80002-9](#).
- [229] Z.-C. Yang, Z.-F. Sun, J. He, X. Liu, S.-L. Zhu, The possible hidden-charm molecular baryons composed of anti-charmed meson and charmed baryon, Chin. Phys. C36 (2012) 6–13. [arXiv:1105.2901](#), [doi:10.1088/1674-1137/36/1/002](#).
- [230] R. Chen, X. Liu, X.-Q. Li, S.-L. Zhu, Identifying exotic hidden-charm pentaquarks, Phys. Rev. Lett. 115 (13) (2015) 132002. [arXiv:1507.03704](#), [doi:10.1103/PhysRevLett.115.132002](#).
- [231] J. He,  $\bar{D}\Sigma_c^*$  and  $\bar{D}^*\Sigma_c$  interactions and the LHCb hidden-charmed pentaquarks, Phys. Lett. B753 (2016) 547–551. [arXiv:1507.05200](#), [doi:10.1016/j.physletb.2015.12.071](#).
- [232] T.-M. Yan, H.-Y. Cheng, C.-Y. Cheung, G.-L. Lin, Y. C. Lin, H.-L. Yu, Heavy quark symmetry and chiral dynamics, Phys. Rev. D46 (1992) 1148–1164, [Erratum: Phys. Rev. D55, 5851 (1997)]. [doi:10.1103/PhysRevD.46.1148](#), [doi:10.1103/PhysRevD.55.5851](#).
- [233] G. Burdman, J. F. Donoghue, Union of chiral and heavy quark symmetries, Phys. Lett. B280 (1992) 287–291. [doi:10.1016/0370-2693\(92\)90068-F](#).
- [234] M. B. Wise, Chiral perturbation theory for hadrons containing a heavy quark, Phys. Rev. D45 (1992) 2188–2191. [doi:10.1103/PhysRevD.45.R2188](#).
- [235] R. Casalbuoni, A. Deandrea, N. Di Bartolomeo, R. Gatto, F. Feruglio, G. Nardulli, Phenomenology of heavy meson chiral Lagrangians, Phys. Rept. 281 (1997) 145–238. [arXiv:hep-ph/9605342](#), [doi:10.1016/S0370-1573\(96\)00027-0](#).
- [236] A. F. Falk, M. E. Luke, Strong decays of excited heavy mesons in chiral perturbation theory, Phys. Lett. B292 (1992) 119–127. [arXiv:hep-ph/9206241](#), [doi:10.1016/0370-2693\(92\)90618-E](#).
- [237] Y.-R. Liu, M. Oka,  $\Lambda_c N$  bound states revisited, Phys. Rev. D85 (2012) 014015. [arXiv:1103.4624](#), [doi:10.1103/PhysRevD.85.014015](#).
- [238] C. Isola, M. Ladisa, G. Nardulli, P. Santorelli, Charming penguins in  $B \rightarrow K^*\pi$ ,  $K(\rho, \omega, \phi)$  decays, Phys. Rev. D68 (2003) 114001. [arXiv:hep-ph/0307367](#), [doi:10.1103/PhysRevD.68.114001](#).
- [239] G.-J. Wang, L. Ma, X. Liu, S.-L. Zhu, Strong decay patterns of the hidden-charm pentaquark states  $P_c(4380)$  and  $P_c(4450)$ , [arXiv:1511.04845](#).
- [240] J.-J. Wu, R. Molina, E. Oset, B. S. Zou, Prediction of narrow  $N^*$  and  $\Lambda^*$  resonances with hidden charm above 4 GeV, Phys. Rev. Lett. 105 (2010) 232001. [arXiv:1007.0573](#), [doi:10.1103/PhysRevLett.105.232001](#).
- [241] J.-J. Wu, R. Molina, E. Oset, B. S. Zou, Dynamically generated  $N^*$  and  $\Lambda^*$  resonances in the hidden charm sector around 4.3 GeV, Phys. Rev. C84 (2011) 015202. [arXiv:1011.2399](#), [doi:10.1103/PhysRevC.84.015202](#).
- [242] J.-J. Wu, T. S. H. Lee, B. S. Zou, Nucleon Resonances with Hidden Charm in Coupled-Channel Models, Phys. Rev. C85 (2012) 044002. [arXiv:1202.1036](#), [doi:10.1103/PhysRevC.85.044002](#).
- [243] R. Molina, C. W. Xiao, E. Oset,  $J/\psi$  reaction mechanisms and suppression in the nuclear medium, Phys. Rev. C86 (2012) 014604. [arXiv:1203.0979](#), [doi:10.1103/PhysRevC.86.014604](#).
- [244] C. Garcia-Recio, J. Nieves, O. Romanets, L. L. Salcedo, L. Tolos, Hidden charm  $N$  and  $\Delta$  resonances with heavy-quark symmetry, Phys. Rev. D87 (2013) 074034. [arXiv:1302.6938](#), [doi:10.1103/PhysRevD.87.074034](#).
- [245] C. W. Xiao, J. Nieves, E. Oset, Combining heavy quark spin and local hidden gauge symmetries in the dynamical generation of hidden charm baryons, Phys. Rev. D88 (2013) 056012. [arXiv:1304.5368](#), [doi:10.1103/PhysRevD.88.056012](#).
- [246] T. Uchino, W.-H. Liang, E. Oset, Baryon states with hidden charm in the extended local hidden gauge approach, [arXiv:1504.05726](#).
- [247] E. J. Garzon, J.-J. Xie, Effects of a  $N_{cc}^*$  resonance with hidden charm in the  $\pi^- p \rightarrow D^- \Sigma_c^+$  reaction near threshold, Phys. Rev. C92 (3) (2015) 035201. [arXiv:1506.06834](#), [doi:10.1103/PhysRevC.92.035201](#).
- [248] C. W. Xiao, U. G. Meissner,  $J/\psi(\eta_c)N$  and  $\Upsilon(\eta_b)N$  cross sections, Phys. Rev. D92 (11) (2015) 114002. [arXiv:1508.00924](#), [doi:10.1103/PhysRevD.92.114002](#).
- [249] J.-J. Wu, B. S. Zou, Prediction of super-heavy  $N^*$  and  $\Lambda^*$  resonances with hidden beauty, Phys. Lett. B709 (2012) 70–76. [arXiv:1011.5743](#), [doi:10.1016/j.physletb.2012.01.068](#).
- [250] C. W. Xiao, E. Oset, Hidden beauty baryon states in the local hidden gauge approach with heavy quark spin symmetry, Eur. Phys. J. A49 (2013) 139. [arXiv:1305.0786](#), [doi:10.1140/epja/i2013-13139-y](#).
- [251] L. Roca, J. Nieves, E. Oset, LHCb pentaquark as a  $\bar{D}^*\Sigma_c - \bar{D}^*\Sigma_c^*$  molecular state, Phys. Rev. D92 (9) (2015) 094003. [arXiv:1507.04249](#), [doi:10.1103/PhysRevD.92.094003](#).
- [252] A. Feijoo, V. K. Magas, A. Ramos, E. Oset,  $\Lambda_b \rightarrow J/\psi K \Xi$  decay and the higher order chiral terms of the meson baryon interaction, Phys. Rev. D92 (7) (2015) 076015. [arXiv:1507.04640](#), [doi:10.1103/PhysRevD.92.076015](#).
- [253] K. Miyahara, T. Hyodo, E. Oset, Weak decay of  $\Lambda_c^+$  for the study of  $\Lambda(1405)$  and  $\Lambda(1670)$ , Phys. Rev. C92 (5) (2015) 055204. [arXiv:1508.04882](#), [doi:10.1103/PhysRevC.92.055204](#).
- [254] H.-X. Chen, L.-S. Geng, W.-H. Liang, E. Oset, E. Wang, J.-J. Xie, Looking for a hidden-charm pentaquark state with strangeness  $S = -1$  from  $\Xi_b^-$  decay into  $J/\psi K^- \Lambda$ , [arXiv:1510.01803](#).
- [255] C. Garcia-Recio, J. Nieves, O. Romanets, L. L. Salcedo, L. Tolos, Odd parity bottom-flavored baryon resonances, Phys. Rev. D87 (3) (2013) 034032. [arXiv:1210.4755](#), [doi:10.1103/PhysRevD.87.034032](#).
- [256] W. H. Liang, C. W. Xiao, E. Oset, Baryon states with open beauty in the extended local hidden gauge approach, Phys. Rev. D89 (5) (2014) 054023. [arXiv:1401.1441](#), [doi:10.1103/PhysRevD.89.054023](#).
- [257] W. H. Liang, T. Uchino, C. W. Xiao, E. Oset, Baryon states with open charm in the extended local hidden gauge approach, Eur. Phys. J.

- A51 (2) (2015) 16. [arXiv:1402.5293](#), [doi:10.1140/epja/i2015-15016-1](#).
- [258] J.-X. Lu, Y. Zhou, H.-X. Chen, J.-J. Xie, L.-S. Geng, Dynamically generated  $J^P = 1/2^-(3/2^-)$  singly charmed and bottom heavy baryons, *Phys. Rev. D* 92 (1) (2015) 014036. [arXiv:1409.3133](#), [doi:10.1103/PhysRevD.92.014036](#).
- [259] C. Garcia-Recio, C. Hidalgo-Duque, J. Nieves, L. L. Salcedo, L. Tolos, Compositeness of the strange, charm, and beauty odd parity  $\Lambda$  states, *Phys. Rev. D* 92 (3) (2015) 034011. [arXiv:1506.04235](#), [doi:10.1103/PhysRevD.92.034011](#).
- [260] M. Bando, T. Kugo, S. Uehara, K. Yamawaki, T. Yanagida, Is rho Meson a Dynamical Gauge Boson of Hidden Local Symmetry?, *Phys. Rev. Lett.* 54 (1985) 1215. [doi:10.1103/PhysRevLett.54.1215](#).
- [261] M. Bando, T. Kugo, K. Yamawaki, Nonlinear Realization and Hidden Local Symmetries, *Phys. Rept.* 164 (1988) 217–314. [doi:10.1016/0370-1573\(88\)90019-1](#).
- [262] M. Harada, K. Yamawaki, Hidden local symmetry at loop: A new perspective of composite gauge boson and chiral phase transition, *Phys. Rept.* 381 (2003) 1–233. [arXiv:hep-ph/0302103](#), [doi:10.1016/S0370-1573\(03\)00139-X](#).
- [263] H. Nagahiro, L. Roca, A. Hosaka, E. Oset, Hidden gauge formalism for the radiative decays of axial-vector mesons, *Phys. Rev. D* 79 (2009) 014015. [arXiv:0809.0943](#), [doi:10.1103/PhysRevD.79.014015](#).
- [264] E. Oset, A. Ramos, Dynamically generated resonances from the vector octet-baryon octet interaction, *Eur. Phys. J. A* 44 (2010) 445–454. [arXiv:0905.0973](#), [doi:10.1140/epja/i2010-10957-3](#).
- [265] F. Klingl, N. Kaiser, W. Weise, Current correlation functions, QCD sum rules and vector mesons in baryonic matter, *Nucl. Phys. A* 624 (1997) 527–563. [arXiv:hep-ph/9704398](#), [doi:10.1016/S0375-9474\(97\)88960-9](#).
- [266] G. Ecker, Chiral perturbation theory, *Prog. Part. Nucl. Phys.* 35 (1995) 1–80. [arXiv:hep-ph/9501357](#), [doi:10.1016/0146-6410\(95\)00041-G](#).
- [267] V. Bernard, N. Kaiser, U.-G. Meissner, Chiral dynamics in nucleons and nuclei, *Int. J. Mod. Phys. E* 4 (1995) 193–346. [arXiv:hep-ph/9501384](#), [doi:10.1142/S0218301395000092](#).
- [268] E. E. Jenkins, A. V. Manohar, Chiral corrections to the baryon axial currents, *Phys. Lett. B* 259 (1991) 353–358. [doi:10.1016/0370-2693\(91\)90840-M](#).
- [269] J. A. Oller, U. G. Meissner, Chiral dynamics in the presence of bound states: Kaon nucleon interactions revisited, *Phys. Lett. B* 500 (2001) 263–272. [arXiv:hep-ph/0011146](#), [doi:10.1016/S0370-2693\(01\)00078-8](#).
- [270] J. A. Oller, E. Oset,  $N/D$  description of two meson amplitudes and chiral symmetry, *Phys. Rev. D* 60 (1999) 074023. [arXiv:hep-ph/9809337](#), [doi:10.1103/PhysRevD.60.074023](#).
- [271] J. Nieves, E. Ruiz Arriola, Bethe-Salpeter approach for unitarized chiral perturbation theory, *Nucl. Phys. A* 679 (2000) 57–117. [arXiv:hep-ph/9907469](#), [doi:10.1016/S0375-9474\(00\)00321-3](#).
- [272] R. Molina, D. Nicmorus, E. Oset, The  $\rho\rho$  interaction in the hidden gauge formalism and the  $f_0(1370)$  and  $f_2(1270)$  resonances, *Phys. Rev. D* 78 (2008) 114018. [arXiv:0809.2233](#), [doi:10.1103/PhysRevD.78.114018](#).
- [273] L. S. Geng, E. Oset, Vector meson-vector meson interaction in a hidden gauge unitary approach, *Phys. Rev. D* 79 (2009) 074009. [arXiv:0812.1199](#), [doi:10.1103/PhysRevD.79.074009](#).
- [274] T. Hyodo, S. I. Nam, D. Jido, A. Hosaka, Flavor SU(3) breaking effects in the chiral unitary model for meson baryon scatterings, *Phys. Rev. C* 68 (2003) 018201. [arXiv:nucl-th/0212026](#), [doi:10.1103/PhysRevC.68.018201](#).
- [275] T. Sato, T. S. H. Lee, Meson exchange model for  $\pi N$  scattering and  $\gamma N \rightarrow \pi N$  reaction, *Phys. Rev. C* 54 (1996) 2660–2684. [arXiv:nucl-th/9606009](#), [doi:10.1103/PhysRevC.54.2660](#).
- [276] C.-T. Hung, S. N. Yang, T. S. H. Lee, Meson exchange pi N models in three-dimensional Bethe-Salpeter formulation, *Phys. Rev. C* 64 (2001) 034309. [arXiv:nucl-th/0101007](#), [doi:10.1103/PhysRevC.64.034309](#).
- [277] N. Isgur, M. B. Wise, Weak Decays of Heavy Mesons in the Static Quark Approximation, *Phys. Lett. B* 232 (1989) 113–117. [doi:10.1016/0370-2693\(89\)90566-2](#).
- [278] M. Neubert, Heavy quark symmetry, *Phys. Rept.* 245 (1994) 259–396. [arXiv:hep-ph/9306320](#), [doi:10.1016/0370-1573\(94\)90091-4](#).
- [279] A. V. Manohar, M. B. Wise, Heavy quark physics, *Camb. Monogr. Part. Phys. Nucl. Phys. Cosmol.* 10 (2000) 1–191.
- [280] M. A. Shifman, A. I. Vainshtein, V. I. Zakharov, QCD and Resonance Physics. Theoretical Foundations, *Nucl. Phys. B* 147 (1979) 385–447. [doi:10.1016/0550-3213\(79\)90022-1](#).
- [281] L. J. Reinders, H. Rubinstein, S. Yazaki, Hadron Properties from QCD Sum Rules, *Phys. Rept.* 127 (1985) 1. [doi:10.1016/0370-1573\(85\)90065-1](#).
- [282] S. Narison, QCD as a theory of hadrons from partons to confinement, [arXiv:hep-ph/0205006](#).
- [283] P. Colangelo, A. Khodjamirian, QCD sum rules, a modern perspective, [arXiv:hep-ph/0010175](#).
- [284] B. Grinstein, The Static Quark Effective Theory, *Nucl. Phys. B* 339 (1990) 253–268. [doi:10.1016/0550-3213\(90\)90349-I](#).
- [285] E. Eichten, B. R. Hill, An Effective Field Theory for the Calculation of Matrix Elements Involving Heavy Quarks, *Phys. Lett. B* 234 (1990) 511. [doi:10.1016/0370-2693\(90\)92049-0](#).
- [286] A. F. Falk, H. Georgi, B. Grinstein, M. B. Wise, Heavy Meson Form-factors From QCD, *Nucl. Phys. B* 343 (1990) 1–13. [doi:10.1016/0550-3213\(90\)90591-Z](#).
- [287] E. Bagan, P. Ball, V. M. Braun, H. G. Dosch, QCD sum rules in the effective heavy quark theory, *Phys. Lett. B* 278 (1992) 457–464. [doi:10.1016/0370-2693\(92\)90585-R](#).
- [288] M. Neubert, Heavy meson form-factors from QCD sum rules, *Phys. Rev. D* 45 (1992) 2451–2466. [doi:10.1103/PhysRevD.45.2451](#).
- [289] D. J. Broadhurst, A. G. Grozin, Operator product expansion in static quark effective field theory: Large perturbative correction, *Phys. Lett. B* 274 (1992) 421–427. [arXiv:hep-ph/9908363](#), [doi:10.1016/0370-2693\(92\)92009-6](#).
- [290] P. Ball, V. M. Braun, Next-to-leading order corrections to meson masses in the heavy quark effective theory, *Phys. Rev. D* 49 (1994) 2472–2489. [arXiv:hep-ph/9307291](#), [doi:10.1103/PhysRevD.49.2472](#).
- [291] T. Huang, C.-W. Luo, Light quark dependence of the Isgur-Wise function from QCD sum rules, *Phys. Rev. D* 50 (1994) 5775–5780. [arXiv:hep-ph/9408303](#), [doi:10.1103/PhysRevD.50.5775](#).
- [292] Y.-B. Dai, C.-S. Huang, M.-Q. Huang, C. Liu, QCD sum rules for masses of excited heavy mesons, *Phys. Lett. B* 390 (1997) 350–358.

- [arXiv:hep-ph/9609436](#), [doi:10.1016/S0370-2693\(96\)01412-8](#).
- [293] Y.-B. Dai, C.-S. Huang, H.-Y. Jin, Bethe-Salpeter wave functions and transition amplitudes for heavy mesons, *Z. Phys. C60* (1993) 527–534. [doi:10.1007/BF01560051](#).
- [294] Y.-B. Dai, C.-S. Huang, M.-Q. Huang,  $O(1/m_Q)$  order corrections to masses of excited heavy mesons from QCD sum rules, *Phys. Rev. D55* (1997) 5719–5726. [arXiv:hep-ph/9702384](#), [doi:10.1103/PhysRevD.55.5719](#).
- [295] P. Colangelo, F. De Fazio, N. Paver, Universal  $\tau_{1/2}(y)$  Isgur-Wise function at the next-to-leading order in QCD sum rules, *Phys. Rev. D58* (1998) 116005. [arXiv:hep-ph/9804377](#), [doi:10.1103/PhysRevD.58.116005](#).
- [296] Y.-B. Dai, C.-S. Huang, C. Liu, S.-L. Zhu, Understanding the  $D_{sJ}^+(2317)$  and  $D_{sJ}^+(2460)$  with sum rules in HQET, *Phys. Rev. D68* (2003) 114011. [arXiv:hep-ph/0306274](#), [doi:10.1103/PhysRevD.68.114011](#).
- [297] D. Zhou, E.-L. Cui, H.-X. Chen, L.-S. Geng, X. Liu, S.-L. Zhu, D-wave heavy-light mesons from QCD sum rules, *Phys. Rev. D90* (11) (2014) 114035. [arXiv:1410.1727](#), [doi:10.1103/PhysRevD.90.114035](#).
- [298] D. Zhou, H.-X. Chen, L.-S. Geng, X. Liu, S.-L. Zhu, F-wave heavy-light meson spectroscopy in QCD sum rules and heavy quark effective theory, *Phys. Rev. D92* (11) (2015) 114015. [arXiv:1506.00766](#), [doi:10.1103/PhysRevD.92.114015](#).
- [299] E. V. Shuryak, Hadrons Containing a Heavy Quark and QCD Sum Rules, *Nucl. Phys. B198* (1982) 83. [doi:10.1016/0550-3213\(82\)90546-6](#).
- [300] A. G. Grozin, O. I. Yakovlev, Baryonic currents and their correlators in the heavy quark effective theory, *Phys. Lett. B285* (1992) 254–262. [arXiv:hep-ph/9908364](#), [doi:10.1016/0370-2693\(92\)91462-I](#).
- [301] Y.-B. Dai, C.-S. Huang, C. Liu, C.-D. Lu,  $1/m$  corrections to heavy baryon masses in the heavy quark effective theory sum rules, *Phys. Lett. B371* (1996) 99–104. [arXiv:hep-ph/9602242](#), [doi:10.1016/0370-2693\(96\)01602-3](#).
- [302] Y.-B. Dai, C.-S. Huang, M.-Q. Huang, C. Liu, QCD sum rule analysis for the  $\Lambda_b \rightarrow \Lambda_c$  semileptonic decay, *Phys. Lett. B387* (1996) 379–385. [arXiv:hep-ph/9608277](#), [doi:10.1016/0370-2693\(96\)01029-5](#).
- [303] S. Groote, J. G. Korner, O. I. Yakovlev, QCD sum rules for heavy baryons at next-to-leading order in  $\alpha_s$ , *Phys. Rev. D55* (1997) 3016–3026. [arXiv:hep-ph/9609469](#), [doi:10.1103/PhysRevD.55.3016](#).
- [304] S.-L. Zhu, Strong and electromagnetic decays of p wave heavy baryons  $\Lambda_{c1}$ ,  $\Lambda_{c1}^*$ , *Phys. Rev. D61* (2000) 114019. [arXiv:hep-ph/0002023](#), [doi:10.1103/PhysRevD.61.114019](#).
- [305] J.-P. Lee, C. Liu, H. S. Song, QCD sum rule analysis of excited  $\Lambda_c$  mass parameter, *Phys. Lett. B476* (2000) 303–308. [arXiv:hep-ph/0002034](#), [doi:10.1016/S0370-2693\(00\)00144-1](#).
- [306] C.-S. Huang, A.-I. Zhang, S.-L. Zhu, Excited heavy baryon masses in HQET QCD sum rules, *Phys. Lett. B492* (2000) 288–296. [arXiv:hep-ph/0007330](#), [doi:10.1016/S0370-2693\(00\)01088-1](#).
- [307] D.-W. Wang, M.-Q. Huang, Excited heavy baryon masses to order  $\Lambda_{QCD}/m_Q$  from QCD sum rules, *Phys. Rev. D68* (2003) 034019. [arXiv:hep-ph/0306207](#), [doi:10.1103/PhysRevD.68.034019](#).
- [308] X. Liu, H.-X. Chen, Y.-R. Liu, A. Hosaka, S.-L. Zhu, Bottom baryons, *Phys. Rev. D77* (2008) 014031. [arXiv:0710.0123](#), [doi:10.1103/PhysRevD.77.014031](#).
- [309] H.-X. Chen, W. Chen, Q. Mao, A. Hosaka, X. Liu, S.-L. Zhu, P-wave charmed baryons from QCD sum rules, *Phys. Rev. D91* (5) (2015) 054034. [arXiv:1502.01103](#), [doi:10.1103/PhysRevD.91.054034](#).
- [310] Q. Mao, H.-X. Chen, W. Chen, A. Hosaka, X. Liu, S.-L. Zhu, QCD sum rule calculation for P-wave bottom baryons, *Phys. Rev. D92* (2015) 114007. [arXiv:1510.05267](#), [doi:10.1103/PhysRevD.92.114007](#).
- [311] H.-X. Chen, W. Chen, X. Liu, T. G. Steele, S.-L. Zhu, Towards exotic hidden-charm pentaquarks in QCD, *Phys. Rev. Lett. 115* (17) (2015) 172001. [arXiv:1507.03717](#), [doi:10.1103/PhysRevLett.115.172001](#).
- [312] H.-X. Chen, E.-L. Cui, W. Chen, X. Liu, T. G. Steele, S.-L. Zhu, QCD sum rule study of hidden-charm pentaquarks, in preparation.
- [313] H.-X. Chen, V. Dmitrasinovic, A. Hosaka, K. Nagata, S.-L. Zhu, Chiral Properties of Baryon Fields with Flavor SU(3) Symmetry, *Phys. Rev. D78* (2008) 054021. [arXiv:0806.1997](#), [doi:10.1103/PhysRevD.78.054021](#).
- [314] H.-X. Chen, V. Dmitrasinovic, A. Hosaka, Baryon fields with  $U_L(3) \times U_R(3)$  chiral symmetry II: Axial currents of nucleons and hyperons, *Phys. Rev. D81* (2010) 054002. [arXiv:0912.4338](#), [doi:10.1103/PhysRevD.81.054002](#).
- [315] H.-X. Chen, V. Dmitrasinovic, A. Hosaka, Baryon Fields with  $U_L(3) \times U_R(3)$  Chiral Symmetry III: Interactions with Chiral  $(3, \bar{3}) + (\bar{3}, 3)$  Spinless Mesons, *Phys. Rev. D83* (2011) 014015. [arXiv:1009.2422](#), [doi:10.1103/PhysRevD.83.014015](#).
- [316] H.-X. Chen, V. Dmitrasinovic, A. Hosaka, Baryons with  $U_L(3) \times U_R(3)$  Chiral Symmetry IV: Interactions with Chiral  $(8, 1) + (1, 8)$  Vector and Axial-vector Mesons and Anomalous Magnetic Moments, *Phys. Rev. C85* (2012) 055205. [arXiv:1109.3130](#), [doi:10.1103/PhysRevC.85.055205](#).
- [317] V. Dmitrasinovic, H.-X. Chen, Bi-local baryon interpolating fields with two flavours, *Eur. Phys. J. C71* (2011) 1543. [arXiv:1101.5906](#), [doi:10.1140/epjc/s10052-011-1543-3](#).
- [318] H.-X. Chen, V. Dmitrasinovic, Bilocal baryon interpolating fields with three flavors, *Phys. Rev. D88* (3) (2013) 036013. [arXiv:1309.0387](#), [doi:10.1103/PhysRevD.88.036013](#).
- [319] H.-X. Chen, Baryon Tri-local Interpolating Fields, *Eur. Phys. J. C72* (2012) 2129. [arXiv:1205.5328](#), [doi:10.1140/epjc/s10052-012-2129-4](#).
- [320] H.-X. Chen, Chiral Baryon Fields in the QCD Sum Rule, *Eur. Phys. J. C72* (2012) 2180. [arXiv:1203.3260](#), [doi:10.1140/epjc/s10052-012-2180-1](#).
- [321] H.-X. Chen, A. Hosaka, S.-L. Zhu, Exotic Tetraquark  $ud\bar{s}\bar{s}$  of  $J^P = 0^+$  in the QCD Sum Rule, *Phys. Rev. D74* (2006) 054001. [arXiv:hep-ph/0604049](#), [doi:10.1103/PhysRevD.74.054001](#).
- [322] H.-X. Chen, A. Hosaka, S.-L. Zhu, QCD sum rule study of the masses of light tetraquark scalar mesons, *Phys. Lett. B650* (2007) 369–372. [arXiv:hep-ph/0609163](#), [doi:10.1016/j.physletb.2007.05.031](#).
- [323] H.-X. Chen, The “Closed” Chiral Symmetry and Its Application to Tetraquark, *Eur. Phys. J. C72* (2012) 2204. [arXiv:1210.3399](#), [doi:10.1140/epjc/s10052-012-2204-x](#).
- [324] H.-X. Chen, Chiral Structure of Scalar and Pseudoscalar Mesons, *Adv. High Energy Phys.* 2013 (2013) 750591. [arXiv:1311.4434](#), [doi:10.1155/2013/750591](#).

- [325] H.-X. Chen, Chiral Structure of Vector and Axial-Vector Tetraquark Currents, Eur. Phys. J. C73 (2013) 2628. [arXiv:1311.4992](#), [doi:10.1140/epjc/s10052-013-2628-y](#).
- [326] H.-X. Chen, E.-L. Cui, W. Chen, T. G. Steele, S.-L. Zhu, QCD sum rule study of the  $d^*(2380)$ , Phys. Rev. C91 (2) (2015) 025204. [arXiv:1410.0394](#), [doi:10.1103/PhysRevC.91.025204](#).
- [327] Z.-G. Wang, Analysis of the  $P_c(4380)$  and  $P_c(4450)$  as pentaquark states in the diquark model with QCD sum rules, [arXiv:1508.01468](#).
- [328] Z.-G. Wang, T. Huang, Analysis of the  $\frac{1}{2}^\pm$  pentaquark states in the diquark model with QCD sum rules, [arXiv:1508.04189](#).
- [329] Y. Chung, H. G. Dosch, M. Kremer, D. Schall, Baryon Sum Rules and Chiral Symmetry Breaking, Nucl. Phys. B197 (1982) 55. [doi:10.1016/0550-3213\(82\)90154-7](#).
- [330] D. Jido, N. Kodama, M. Oka, Negative parity nucleon resonance in the QCD sum rule, Phys. Rev. D54 (1996) 4532–4536. [arXiv:hep-ph/9604280](#), [doi:10.1103/PhysRevD.54.4532](#).
- [331] Y. Kondo, O. Morimatsu, T. Nishikawa, Coupled QCD sum rules for positive and negative-parity nucleons, Nucl. Phys. A764 (2006) 303–312. [arXiv:hep-ph/0503150](#), [doi:10.1016/j.nuclphysa.2005.09.003](#).
- [332] K. Ohtani, P. Gubler, M. Oka, Parity projection of QCD sum rules for the nucleon, Phys. Rev. D87 (3) (2013) 034027. [arXiv:1209.1463](#), [doi:10.1103/PhysRevD.87.034027](#).
- [333] M. Gell-Mann, M. Levy, The axial vector current in beta decay, Nuovo Cim. 16 (1960) 705. [doi:10.1007/BF02859738](#).
- [334] F. Fernandez, A. Valcarce, U. Straub, A. Faessler, The Nucleon-nucleon interaction in terms of quark degrees of freedom, J. Phys. G19 (1993) 2013–2026. [doi:10.1088/0954-3899/19/12/007](#).
- [335] Z.-Y. Zhang, A. Faessler, U. Straub, L. Ya. Glozman, The Baryon baryon interaction in a modified quark model, Nucl. Phys. A578 (1994) 573–585. [doi:10.1016/0375-9474\(94\)90761-7](#).
- [336] Z. Y. Zhang, Y. W. Yu, P. N. Shen, L. R. Dai, A. Faessler, U. Straub, Hyperon nucleon interactions in a chiral SU(3) quark model, Nucl. Phys. A625 (1997) 59–70. [doi:10.1016/S0375-9474\(97\)00033-X](#).
- [337] Z.-Y. Zhang, Y.-W. Yu, P. Wang, L.-R. Dai, An extended chiral SU(3) quark model, Commun. Theor. Phys. 39 (2003) 569–572.
- [338] X. Q. Yuan, Z. Y. Zhang, Y. W. Yu, P. N. Shen, Deltaron dibaryon structure in chiral SU(3) quark model, Phys. Rev. C60 (1999) 045203. [arXiv:nucl-th/9901069](#), [doi:10.1103/PhysRevC.60.045203](#).
- [339] L.-R. Dai, Z.-Y. Zhang, Y.-W. Yu, Structure of Di- $\Omega$  dibaryon, Chin. Phys. Lett. 23 (2006) 3215–3218. [doi:10.1088/0256-307X/23/12/026](#).
- [340] D. Zhang, F. Huang, L. R. Dai, Y. W. Yu, Z. Y. Zhang, Study on  $N\bar{\Omega}$  systems in a chiral quark model, Phys. Rev. C75 (2007) 024001. [arXiv:nucl-th/0609008](#), [doi:10.1103/PhysRevC.75.024001](#).
- [341] F. Huang, Z. Y. Zhang, A Study of  $NK$  and  $\Delta K$  states in the chiral SU(3) quark model, Phys. Rev. C70 (2004) 064004. [arXiv:nucl-th/0409029](#), [doi:10.1103/PhysRevC.70.064004](#).
- [342] F. Huang, Z. Y. Zhang,  $\Delta K$ ,  $\Lambda K$  and  $\Sigma K$  states in the extended chiral SU(3) quark model, Phys. Rev. C72 (2005) 068201. [arXiv:nucl-th/0511057](#), [doi:10.1103/PhysRevC.72.068201](#).
- [343] F. Huang, Z. Y. Zhang, Y. W. Yu,  $N\phi$  state in chiral quark model, Phys. Rev. C73 (2006) 025207. [arXiv:nucl-th/0512079](#), [doi:10.1103/PhysRevC.73.025207](#).
- [344] F. Huang, D. Zhang, Z. Y. Zhang, Y. W. Yu, Coupled-channel study of  $\Lambda K$  and  $\Sigma K$  states in the chiral SU(3) quark model, Phys. Rev. C71 (2005) 064001. [arXiv:hep-ph/0501102](#), [doi:10.1103/PhysRevC.71.064001](#).
- [345] W. L. Wang, F. Huang, Z. Y. Zhang, Y. W. Yu, F. Liu, A Possible  $\Omega\pi$  molecular state, Eur. Phys. J. A32 (2007) 293–297. [arXiv:nucl-th/0612007](#), [doi:10.1140/epja/i2007-10376-7](#).
- [346] W.-L. Wang, F. Huang, Z.-Y. Zhang, Y.-W. Yu, F. Liu,  $\Omega\omega$  states in a chiral quark model, Commun. Theor. Phys. 48 (2007) 695–698. [doi:10.1088/0253-6102/48/4/025](#).
- [347] W. L. Wang, F. Huang, Z. Y. Zhang, B. S. Zou,  $\Sigma_c\bar{D}$  and  $\Lambda_c\bar{D}$  states in a chiral quark model, Phys. Rev. C84 (2011) 015203. [arXiv:1101.0453](#), [doi:10.1103/PhysRevC.84.015203](#).
- [348] M. Oka, K. Yazaki, Short Range Part of Baryon Baryon Interaction in a Quark Model. I. Formulation, Prog. Theor. Phys. 66 (1981) 556–571. [doi:10.1143/PTP.66.556](#).
- [349] H. Huang, C. Deng, J. Ping, F. Wang, Possible pentaquarks with heavy quarks, [arXiv:1510.04648](#).
- [350] F. Wang, G.-h. Wu, L.-j. Teng, J. T. Goldman, Quark delocalization, color screening, and nuclear intermediate range attraction, Phys. Rev. Lett. 69 (1992) 2901–2904. [arXiv:nucl-th/9210002](#), [doi:10.1103/PhysRevLett.69.2901](#).
- [351] G.-H. Wu, L.-J. Teng, J. L. Ping, F. Wang, J. T. Goldman, Quark delocalization, color screening, and  $NN$  intermediate range attraction: P waves, Phys. Rev. C53 (1996) 1161–1166. [doi:10.1103/PhysRevC.53.1161](#).
- [352] J.-L. Ping, F. Wang, J. T. Goldman, Effective baryon baryon potentials in the quark delocalization and color screening model, Nucl. Phys. A657 (1999) 95–109. [arXiv:nucl-th/9812068](#), [doi:10.1016/S0375-9474\(99\)00321-8](#).
- [353] G.-h. Wu, J.-L. Ping, L.-j. Teng, F. Wang, J. T. Goldman, Quark delocalization, color screening model and nucleon baryon scattering, Nucl. Phys. A673 (2000) 279–297. [arXiv:nucl-th/9812079](#), [doi:10.1016/S0375-9474\(00\)00141-X](#).
- [354] J.-l. Ping, F. Wang, J. T. Goldman, Dynamical calculation of  $d^*$  mass and  $NN$  decay width in the quark delocalization, color screening model, Nucl. Phys. A688 (2001) 871–881. [arXiv:nucl-th/0007040](#), [doi:10.1016/S0375-9474\(00\)00593-5](#).
- [355] H. R. Pang, J. L. Ping, F. Wang, J. T. Goldman, Phenomenological study of hadron interaction models, Phys. Rev. C65 (2002) 014003. [arXiv:nucl-th/0106056](#), [doi:10.1103/PhysRevC.65.014003](#).
- [356] H. Huang, P. Xu, J. Ping, F. Wang, The effect of hidden color channels on nucleon-nucleon interaction, Phys. Rev. C84 (2011) 064001. [arXiv:1109.5607](#), [doi:10.1103/PhysRevC.84.064001](#).
- [357] L. Chen, H. Pang, H. Huang, J. Ping, F. Wang, An Alternative approach to the  $\sigma$ -meson-exchange in nucleon-nucleon interaction, Phys. Rev. C76 (2007) 014001. [arXiv:nucl-th/0703103](#), [doi:10.1103/PhysRevC.76.014001](#).
- [358] J. L. Ping, H. X. Huang, H. R. Pang, F. Wang, C. W. Wong, Quark models of dibaryon resonances in nucleon-nucleon scattering, Phys. Rev. C79 (2009) 024001. [arXiv:0806.0458](#), [doi:10.1103/PhysRevC.79.024001](#).
- [359] J.-L. Ping, F. Wang, J. T. Goldman, The  $d^*$  dibaryon in the extended quark delocalization, color screening model, Phys. Rev. C65 (2002) 044003. [arXiv:nucl-th/0012011](#), [doi:10.1103/PhysRevC.65.044003](#).

- [360] M. Chen, H. Huang, J. Ping, F. Wang, Quark model study of strange dibaryon resonances, Phys. Rev. C83 (2011) 015202. [doi:10.1103/PhysRevC.83.015202](#).
- [361] G. Yang, J. Ping, The structure of pentaquarks  $P_c^+$  in the chiral quark model, [arXiv:1511.09053](#).
- [362] L. Maiani, A. D. Polosa, V. Riquer, The New Pentaquarks in the Diquark Model, Phys. Lett. B749 (2015) 289–291. [arXiv:1507.04980](#), [doi:10.1016/j.physletb.2015.08.008](#).
- [363] L. Maiani, F. Piccinini, A. D. Polosa, V. Riquer, Diquark-antidiquarks with hidden or open charm and the nature of  $X(3872)$ , Phys. Rev. D71 (2005) 014028. [arXiv:hep-ph/0412098](#), [doi:10.1103/PhysRevD.71.014028](#).
- [364] F. E. Close, N. A. Tornqvist, Scalar mesons above and below 1 GeV, J. Phys. G28 (2002) R249–R267. [arXiv:hep-ph/0204205](#), [doi:10.1088/0954-3899/28/10/201](#).
- [365] R. L. Jaffe, F. Wilczek, Diquarks and exotic spectroscopy, Phys. Rev. Lett. 91 (2003) 232003. [arXiv:hep-ph/0307341](#), [doi:10.1103/PhysRevLett.91.232003](#).
- [366] L. Maiani, F. Piccinini, A. D. Polosa, V. Riquer, The  $Z(4430)$  and a New Paradigm for Spin Interactions in Tetraquarks, Phys. Rev. D89 (2014) 114010. [arXiv:1405.1551](#), [doi:10.1103/PhysRevD.89.114010](#).
- [367] A. De Rujula, H. Georgi, S. L. Glashow, Hadron Masses in a Gauge Theory, Phys. Rev. D12 (1975) 147–162. [doi:10.1103/PhysRevD.12.147](#).
- [368] L. Maiani, A. D. Polosa, V. Riquer, From pentaquarks to dibaryons in  $\Lambda_b(5620)$  decays, Phys. Lett. B750 (2015) 37–38. [arXiv:1508.04459](#), [doi:10.1016/j.physletb.2015.08.049](#).
- [369] V. V. Anisovich, M. A. Matveev, J. Nyiri, A. V. Sarantsev, A. N. Semenova, Pentaquarks and resonances in the  $pJ/\psi$  spectrum, [arXiv:1507.07652](#).
- [370] V. V. Anisovich, M. A. Matveev, J. Nyiri, A. V. Sarantsev, A. N. Semenova, Non-strange and strange pentaquarks with hidden charm, Int. J. Mod. Phys. A30 (2015) 1550190. [arXiv:1509.04898](#), [doi:10.1142/S0217751X15501900](#).
- [371] G.-N. Li, M. He, X.-G. He, Some Predictions of Diquark Model for Hidden Charm Pentaquark Discovered at the LHCb, [arXiv:1507.08252](#).
- [372] R. Ghosh, A. Bhattacharya, B. Chakrabarti, The masses of  $P_c^*(4380)$  and  $P_c^*(4450)$  in the quasi particle diquark model, [arXiv:1508.00356](#).
- [373] V. V. Anisovich, M. A. Matveev, A. V. Sarantsev, A. N. Semenova, Exotic mesons with hidden charm as diquark-antidiquark states, Int. J. Mod. Phys. A30 (2015) 1550186. [arXiv:1507.07232](#), [doi:10.1142/S0217751X15501869](#).
- [374] R. F. Lebed, The Pentaquark Candidates in the Dynamical Diquark Picture, Phys. Lett. B749 (2015) 454–457. [arXiv:1507.05867](#), [doi:10.1016/j.physletb.2015.08.032](#).
- [375] S. J. Brodsky, D. S. Hwang, R. F. Lebed, Dynamical Picture for the Formation and Decay of the Exotic XYZ Mesons, Phys. Rev. Lett. 113 (11) (2014) 112001. [arXiv:1406.7281](#), [doi:10.1103/PhysRevLett.113.112001](#).
- [376] R. F. Lebed, Do the  $P_c^+$  Pentaquarks Have Strange Siblings?, Phys. Rev. D92 (11) (2015) 114030. [arXiv:1510.06648](#), [doi:10.1103/PhysRevD.92.114030](#).
- [377] R. Zhu, C.-F. Qiao, Novel Pentaquarks from Diquark-Triquark Model, [arXiv:1510.08693](#).
- [378] F.-K. Guo, U.-G. Meissner, W. Wang, Z. Yang, How to reveal the exotic nature of the  $P_c(4450)$ , Phys. Rev. D92 (7) (2015) 071502. [arXiv:1507.04950](#), [doi:10.1103/PhysRevD.92.071502](#).
- [379] M. Mikhasenko, A triangle singularity and the LHCb pentaquarks, [arXiv:1507.06552](#).
- [380] X.-H. Liu, Q. Wang, Q. Zhao, Understanding the newly observed heavy pentaquark candidates, [arXiv:1507.05359](#).
- [381] F.-K. Guo, C. Hanhart, Q. Wang, Q. Zhao, Could the near-threshold XYZ states be simply kinematic effects?, Phys. Rev. D91 (5) (2015) 051504. [arXiv:1411.5584](#), [doi:10.1103/PhysRevD.91.051504](#).
- [382] X.-H. Liu, M. Oka, Q. Zhao, Searching for observable effects induced by anomalous triangle singularities, Phys. Lett. B753 (2016) 297–302. [arXiv:1507.01674](#), [doi:10.1016/j.physletb.2015.12.027](#).
- [383] N. N. Scoccola, D. O. Riska, M. Rho, Pentaquark candidates  $P_c^+(4380)$  and  $P_c^+(4450)$  within the soliton picture of baryons, Phys. Rev. D92 (5) (2015) 051501. [arXiv:1508.01172](#), [doi:10.1103/PhysRevD.92.051501](#).
- [384] U.-G. Meissner, J. A. Oller, Testing the  $\chi_{c1} p$  composite nature of the  $P_c(4450)$ , Phys. Lett. B751 (2015) 59–62. [arXiv:1507.07478](#), [doi:10.1016/j.physletb.2015.10.015](#).
- [385] A. Mironov, A. Morozov, Is the pentaquark doublet a hadronic molecule?, JETP Lett. 102 (5) (2015) 271–273. [arXiv:1507.04694](#), [doi:10.7868/S0370274X15170038](#), [doi:10.1134/S0021364015170099](#).
- [386] Y.-s. Oh, B.-Y. Park, D.-P. Min, Pentaquark exotic baryons in the Skyrme model, Phys. Lett. B331 (1994) 362–370. [arXiv:hep-ph/9405297](#), [doi:10.1016/0370-2693\(94\)91065-0](#).
- [387] Y.-s. Oh, B.-Y. Park, Energy levels of the soliton - heavy meson bound states, Phys. Rev. D51 (1995) 5016–5029. [arXiv:hep-ph/9501356](#), [doi:10.1103/PhysRevD.51.5016](#).
- [388] T. J. Burns, Phenomenology of  $P_c(4380)^+$ ,  $P_c(4450)^+$  and related states, Eur. Phys. J. A51 (11) (2015) 152. [arXiv:1509.02460](#), [doi:10.1140/epja/i2015-15152-6](#).
- [389] M. I. Eides, V. Yu. Petrov, M. V. Polyakov, Narrow Nucleon- $\psi(2S)$  Bound State and LHCb Pentaquarks, [arXiv:1512.00426](#).
- [390] D. E. Kahana, S. H. Kahana, LHCb  $P_c^+$  Resonances as Molecular States, [arXiv:1512.01902](#).
- [391] E. Wang, H.-X. Chen, L.-S. Geng, D.-M. Li, E. Oset, A hidden-charm pentaquark state in  $\Lambda_b^0 \rightarrow J/\psi p \pi^-$  decay, [arXiv:1512.01959](#).
- [392] J.-X. Lu, E. Wang, J.-J. Xie, L.-S. Geng, E. Oset, The  $\Lambda_b \rightarrow J/\psi K^0 \Lambda$  reaction and a hidden-charm pentaquark state with strangeness, [arXiv:1601.00075](#).
- [393] H.-Y. Cheng, C.-K. Chua, Bottom Baryon Decays to Pseudoscalar Meson and Pentaquark, Phys. Rev. D92 (9) (2015) 096009. [arXiv:1509.03708](#), [doi:10.1103/PhysRevD.92.096009](#).
- [394] Y. K. Hsiao, C. Q. Geng, Pentaquarks from intrinsic charms in  $\Lambda_b$  decays, Phys. Lett. B751 (2015) 752–755. [arXiv:1508.03910](#), [doi:10.1016/j.physletb.2015.11.016](#).
- [395] Q. Wang, X.-H. Liu, Q. Zhao, Photoproduction of hidden charm pentaquark states  $P_c^+(4380)$  and  $P_c^+(4450)$ , Phys. Rev. D92 (2015) 034022. [arXiv:1508.00339](#), [doi:10.1103/PhysRevD.92.034022](#).
- [396] M. Karliner, J. L. Rosner, Photoproduction of Exotic Baryon Resonances, Phys. Lett. B752 (2016) 329–332. [arXiv:1508.01496](#), [doi:10.1016/j.physletb.2015.11.016](#).

- 10.1016/j.physletb.2015.11.068.
- [397] V. Kubarovsky, M. B. Voloshin, Formation of hidden-charm pentaquarks in photon-nucleon collisions, Phys. Rev. D92 (3) (2015) 031502. [arXiv:1508.00888](#), [doi:10.1103/PhysRevD.92.031502](#).
- [398] Q.-F. Lu, X.-Y. Wang, J.-J. Xie, X.-R. Chen, Y.-B. Dong, Neutral hidden charm pentaquark states  $P_c^0(4380)$  and  $P_c^0(4450)$  in  $\pi^- p \rightarrow J/\psi n$  reaction, [arXiv:1510.06271](#).
- [399] Z. Ouyang, L.-P. Zou, Role of the hidden charm  $N_{cc}^*(4261)$  resonance in the  $\pi^- p \rightarrow J/\psi n$  reaction, [arXiv:1512.02130](#).
- [400] M. Karliner, J. L. Rosner, New Exotic Meson and Baryon Resonances from Doubly-Heavy Hadronic Molecules, Phys. Rev. Lett. 115 (12) (2015) 122001. [arXiv:1506.06386](#), [doi:10.1103/PhysRevLett.115.122001](#).
- [401] M. Karliner, J. L. Rosner, Exotic resonances due to  $\eta$  exchange, [arXiv:1601.00565](#).
- [402] X.-Q. Li, X. Liu, A possible global group structure for exotic states, Eur. Phys. J. C74 (12) (2014) 3198. [arXiv:1409.3332](#), [doi:10.1140/epjc/s10052-014-3198-3](#).
- [403] Y. Yang, J. Ping, C. Deng, H.-S. Zong, Possible interpretation of the  $Z_b(10610)$  and  $Z_b(10650)$  in a chiral quark model, J. Phys. G39 (2012) 105001. [arXiv:1105.5935](#), [doi:10.1088/0954-3899/39/10/105001](#).
- [404] A. Ozpineci, C. W. Xiao, E. Oset, Hidden beauty molecules within the local hidden gauge approach and heavy quark spin symmetry, Phys. Rev. D88 (2013) 034018. [arXiv:1306.3154](#), [doi:10.1103/PhysRevD.88.034018](#).
- [405] J. M. Dias, F. Aceti, E. Oset, Study of  $B\bar{B}^*$  and  $B^*\bar{B}^*$  interactions in  $I = 1$  and relationship to the  $Z_b(10610)$ ,  $Z_b(10650)$  states, Phys. Rev. D91 (7) (2015) 076001. [arXiv:1410.1785](#), [doi:10.1103/PhysRevD.91.076001](#).
- [406] J.-R. Zhang, M. Zhong, M.-Q. Huang, Could  $Z_b(10610)$  be a  $B^*\bar{B}$  molecular state?, Phys. Lett. B704 (2011) 312–315. [arXiv:1105.5472](#), [doi:10.1016/j.physletb.2011.09.039](#).
- [407] C.-Y. Cui, Y.-L. Liu, M.-Q. Huang, Investigating different structures of the  $Z_b(10610)$  and  $Z_b(10650)$ , Phys. Rev. D85 (2012) 074014. [arXiv:1107.1343](#), [doi:10.1103/PhysRevD.85.074014](#).
- [408] Z.-G. Wang, T. Huang, Possible assignments of the  $X(3872)$ ,  $Z_c(3900)$  and  $Z_b(10610)$  as axial-vector molecular states, Eur. Phys. J. C74 (5) (2014) 2891. [arXiv:1312.7489](#), [doi:10.1140/epjc/s10052-014-2891-6](#).
- [409] Z.-G. Wang, Reanalysis of the  $Y(3940)$ ,  $Y(4140)$ ,  $Z_c(4020)$ ,  $Z_c(4025)$  and  $Z_b(10650)$  as molecular states with QCD sum rules, Eur. Phys. J. C74 (7) (2014) 2963. [arXiv:1403.0810](#), [doi:10.1140/epjc/s10052-014-2963-7](#).
- [410] W. Chen, T. G. Steele, H.-X. Chen, S.-L. Zhu, Mass spectra of  $Z_c$  and  $Z_b$  exotic states as hadron molecules, Phys. Rev. D92 (5) (2015) 054002. [arXiv:1505.05619](#), [doi:10.1103/PhysRevD.92.054002](#).
- [411] W. Chen, T. G. Steele, M.-L. Du, S.-L. Zhu,  $D^*\bar{D}^*$  molecule interpretation of  $Z_c(4025)$ , Eur. Phys. J. C74 (2) (2014) 2773. [arXiv:1308.5060](#), [doi:10.1140/epjc/s10052-014-2773-y](#).
- [412] Z.-G. Wang, Mass spectrum of the axial-vector hidden charmed and hidden bottom tetraquark states, Eur. Phys. J. C70 (2010) 139–154. [arXiv:1003.5354](#), [doi:10.1140/epjc/s10052-010-1447-7](#).
- [413] Z.-G. Wang, T. Huang, The  $Z_b(10610)$  and  $Z_b(10650)$  as axial-vector tetraquark states in the QCD sum rules, Nucl. Phys. A930 (2014) 63–85. [arXiv:1312.2652](#), [doi:10.1016/j.nuclphysa.2014.08.084](#).
- [414] A. E. Bondar, A. Garmash, A. I. Milstein, R. Mizuk, M. B. Voloshin, Heavy quark spin structure in  $Z_b$  resonances, Phys. Rev. D84 (2011) 054010. [arXiv:1105.4473](#), [doi:10.1103/PhysRevD.84.054010](#).
- [415] M. B. Voloshin, Charged-to-neutral heavy meson yield ratio at the  $Z_b^0$  resonances as a probe of the  $I^G(J^P) = 0^-(1^+)$  channel, Phys. Rev. D86 (2012) 034013. [arXiv:1204.1945](#), [doi:10.1103/PhysRevD.86.034013](#).
- [416] J. Nieves, M. P. Valderrama, Deriving the existence of  $B\bar{B}^*$  bound states from the  $X(3872)$  and Heavy Quark Symmetry, Phys. Rev. D84 (2011) 056015. [arXiv:1106.0600](#), [doi:10.1103/PhysRevD.84.056015](#).
- [417] F.-K. Guo, C. Hidalgo-Duque, J. Nieves, M. P. Valderrama, Consequences of Heavy Quark Symmetries for Hadronic Molecules, Phys. Rev. D88 (2013) 054007. [arXiv:1303.6608](#), [doi:10.1103/PhysRevD.88.054007](#).
- [418] M. Cleven, F.-K. Guo, C. Hanhart, U.-G. Meissner, Bound state nature of the exotic  $Z_b$  states, Eur. Phys. J. A47 (2011) 120. [arXiv:1107.0254](#), [doi:10.1140/epja/i2011-11120-6](#).
- [419] M. P. Valderrama, Power Counting and Perturbative One Pion Exchange in Heavy Meson Molecules, Phys. Rev. D85 (2012) 114037. [arXiv:1204.2400](#), [doi:10.1103/PhysRevD.85.114037](#).
- [420] W. Chen, S.-L. Zhu, The Vector and Axial-Vector Charmonium-like States, Phys. Rev. D83 (2011) 034010. [arXiv:1010.3397](#), [doi:10.1103/PhysRevD.83.034010](#).
- [421] K. F. Chen, *et al.*, [Belle Collaboration], Observation of anomalous  $\Upsilon(1S)\pi^+\pi^-$  and  $\Upsilon(2S)\pi^+\pi^-$  production near the  $\Upsilon(5S)$  resonance, Phys. Rev. Lett. 100 (2008) 112001. [arXiv:0710.2577](#), [doi:10.1103/PhysRevLett.100.112001](#).
- [422] A. Ali, C. Hambrook, I. Ahmed, M. J. Aslam, A case for hidden  $b\bar{b}$  tetraquarks based on  $e^+e^- \rightarrow b\bar{b}$  cross section between  $\sqrt{s} = 10.54$  and  $11.20$  GeV, Phys. Lett. B684 (2010) 28–39. [arXiv:0911.2787](#), [doi:10.1016/j.physletb.2009.12.053](#).
- [423] A. Ali, C. Hambrook, M. J. Aslam, A Tetraquark interpretation of the BELLE data on the anomalous  $\Upsilon(1S)\pi^+\pi^-$  and  $\Upsilon(2S)\pi^+\pi^-$  production near the  $\Upsilon(5S)$  resonance, Phys. Rev. Lett. 104 (2010) 162001, [Erratum: Phys. Rev. Lett. 107, 049903 (2011)]. [arXiv:0912.5016](#), [doi:10.1103/PhysRevLett.104.162001](#), [doi:10.1103/PhysRevLett.107.049903](#).
- [424] A. Ali, C. Hambrook, W. Wang, Tetraquark Interpretation of the Charged Bottomonium-like states  $Z_b^+(10610)$  and  $Z_b^+(10650)$  and Implications, Phys. Rev. D85 (2012) 054011. [arXiv:1110.1333](#), [doi:10.1103/PhysRevD.85.054011](#).
- [425] A. Ali, C. Hambrook, W. Wang, Hadroproduction of  $\Upsilon(nS)$  above  $B\bar{B}$  Thresholds and Implications for  $Y_b(10890)$ , Phys. Rev. D88 (5) (2013) 054026. [arXiv:1306.4470](#), [doi:10.1103/PhysRevD.88.054026](#).
- [426] A. Ali, L. Maiani, A. D. Polosa, V. Riquer, Hidden-Beauty Charged Tetraquarks and Heavy Quark Spin Conservation, Phys. Rev. D91 (1) (2015) 017502. [arXiv:1412.2049](#), [doi:10.1103/PhysRevD.91.017502](#).
- [427] D. V. Bugg, An Explanation of Belle states  $Z_b(10610)$  and  $Z_b(10650)$ , Europhys. Lett. 96 (2011) 11002. [arXiv:1105.5492](#), [doi:10.1209/0295-5075/96/11002](#).
- [428] A. P. Szczepaniak, Triangle Singularities and XYZ Quarkonium Peaks, Phys. Lett. B747 (2015) 410–416. [arXiv:1501.01691](#), [doi:10.1016/j.physletb.2015.06.029](#).
- [429] E. Swanson,  $Z_b$  and  $Z_c$  Exotic States as Coupled Channel Cusps, Phys. Rev. D91 (3) (2015) 034009. [arXiv:1409.3291](#), [doi:10.1103/](#)

- PhysRevD.91.034009.
- [430] D.-Y. Chen, X. Liu,  $Z_b(10610)$  and  $Z_b(10650)$  structures produced by the initial single pion emission in the  $\Upsilon(5S)$  decays, Phys. Rev. D84 (2011) 094003. [arXiv:1106.3798](#), [doi:10.1103/PhysRevD.84.094003](#).
- [431] M. B. Voloshin, Radiative transitions from  $\Upsilon(5S)$  to molecular bottomonium, Phys. Rev. D84 (2011) 031502. [arXiv:1105.5829](#), [doi:10.1103/PhysRevD.84.031502](#).
- [432] Y. Dong, A. Faessler, T. Gutsche, V. E. Lyubovitskij, Decays of  $Z_b^+$  and  $Z_b'^+$  as Hadronic Molecules, J. Phys. G40 (2013) 015002. [arXiv:1203.1894](#), [doi:10.1088/0954-3899/40/1/015002](#).
- [433] X. Li, M. B. Voloshin,  $Z_b(10610)$  and  $Z_b(10650)$  decays to bottomonium plus pion, Phys. Rev. D86 (2012) 077502. [arXiv:1207.2425](#), [doi:10.1103/PhysRevD.86.077502](#).
- [434] G. Li, F.-I. Shao, C.-W. Zhao, Q. Zhao,  $Z_b/Z_b' \rightarrow \Upsilon\pi$  and  $h_b\pi$  decays in intermediate meson loops model, Phys. Rev. D87 (3) (2013) 034020. [arXiv:1212.3784](#), [doi:10.1103/PhysRevD.87.034020](#).
- [435] S. Ohkoda, S. Yasui, A. Hosaka, Decays of  $Z_b \rightarrow \Upsilon\pi$  via triangle diagrams in heavy meson molecules, Phys. Rev. D89 (7) (2014) 074029. [arXiv:1310.3029](#), [doi:10.1103/PhysRevD.89.074029](#).
- [436] L. Ma, Z.-F. Sun, X.-H. Liu, W.-Z. Deng, X. Liu, S.-L. Zhu, Probing the XYZ states through radiative decays, Phys. Rev. D90 (3) (2014) 034020. [arXiv:1403.7907](#), [doi:10.1103/PhysRevD.90.034020](#).
- [437] L. Ma, X.-H. Liu, X. Liu, S.-L. Zhu, Strong decays of the XYZ states, Phys. Rev. D91 (3) (2015) 034032. [arXiv:1406.6879](#), [doi:10.1103/PhysRevD.91.034032](#).
- [438] T. Mehen, J. W. Powell, Heavy Quark Symmetry Predictions for Weakly Bound  $B$  Meson Molecules, Phys. Rev. D84 (2011) 114013. [arXiv:1109.3479](#), [doi:10.1103/PhysRevD.84.114013](#).
- [439] M. B. Voloshin, Enhanced mixing of partial waves near threshold for heavy meson pairs and properties of  $Z_b(10610)$  and  $Z_b(10650)$  resonances, Phys. Rev. D87 (7) (2013) 074011. [arXiv:1301.5068](#), [doi:10.1103/PhysRevD.87.074011](#).
- [440] S. Ohkoda, Y. Yamaguchi, S. Yasui, A. Hosaka, Decays and productions via bottomonium for  $Z_b$  resonances and other  $B\bar{B}$  molecules, Phys. Rev. D86 (2012) 117502. [arXiv:1210.3170](#), [doi:10.1103/PhysRevD.86.117502](#).
- [441] X. Li, M. B. Voloshin, Contribution of  $Z_b$  resonances to  $\Upsilon(5S) \rightarrow \pi\pi\pi\chi_b$ , Phys. Rev. D90 (1) (2014) 014036. [arXiv:1406.0082](#), [doi:10.1103/PhysRevD.90.014036](#).
- [442] M. Cleven, Q. Wang, F.-K. Guo, C. Hanhart, U.-G. Meissner, Q. Zhao, Confirming the molecular nature of the  $Z_b(10610)$  and the  $Z_b(10650)$ , Phys. Rev. D87 (7) (2013) 074006. [arXiv:1301.6461](#), [doi:10.1103/PhysRevD.87.074006](#).
- [443] Y.-H. Chen, J. T. Daub, F.-K. Guo, B. Kubis, U.-G. Meissner, B.-S. Zou, The effect of  $Z_b$  states on  $\Upsilon(3S) \rightarrow \Upsilon(1S)\pi\pi$  decays, [arXiv:1512.03583](#).
- [444] J. He, Study of the  $B\bar{B}^*/D\bar{D}^*$  bound states in a Bethe-Salpeter approach, Phys. Rev. D90 (7) (2014) 076008. [arXiv:1409.8506](#), [doi:10.1103/PhysRevD.90.076008](#).
- [445] S. Prelovsek, L. Leskovec, Search for  $Z_c^+(3900)$  in the  $1^{+-}$  Channel on the Lattice, Phys. Lett. B727 (2013) 172–176. [arXiv:1308.2097](#), [doi:10.1016/j.physletb.2013.10.009](#).
- [446] S. Prelovsek, C. B. Lang, L. Leskovec, D. Mohler, Study of the  $Z_c^+$  channel using lattice QCD, Phys. Rev. D91 (1) (2015) 014504. [arXiv:1405.7623](#), [doi:10.1103/PhysRevD.91.014504](#).
- [447] Y. Chen, *et al.*, Low-energy scattering of the  $(D\bar{D}^*)^\pm$  system and the resonance-like structure  $Z_c(3900)$ , Phys. Rev. D89 (9) (2014) 094506. [arXiv:1403.1318](#), [doi:10.1103/PhysRevD.89.094506](#).
- [448] Y. Chen, *et al.*, [CLQCD Collaboration], Low-energy Scattering of  $(D^*\bar{D}^*)^\pm$  System and the Resonance-like Structure  $Z_c(4025)$ , Phys. Rev. D92 (5) (2015) 054507. [arXiv:1503.02371](#), [doi:10.1103/PhysRevD.92.054507](#).
- [449] F. Aceti, M. Bayar, E. Oset, A. Martinez Torres, K. P. Khemchandani, J. M. Dias, F. S. Navarra, M. Nielsen, Prediction of an  $I = 1$   $D\bar{D}^*$  state and relationship to the claimed  $Z_c(3900)$ ,  $Z_c(3885)$ , Phys. Rev. D90 (1) (2014) 016003. [arXiv:1401.8216](#), [doi:10.1103/PhysRevD.90.016003](#).
- [450] F. Aceti, M. Bayar, J. M. Dias, E. Oset, Prediction of a  $Z_c(4000)$   $D^*\bar{D}^*$  state and relationship to the claimed  $Z_c(4025)$ , Eur. Phys. J. A50 (2014) 103. [arXiv:1401.2076](#), [doi:10.1140/epja/i2014-14103-1](#).
- [451] J. He, The  $Z_c(3900)$  as a resonance from the  $D\bar{D}^*$  interaction, Phys. Rev. D92 (3) (2015) 034004. [arXiv:1505.05379](#), [doi:10.1103/PhysRevD.92.034004](#).
- [452] J.-R. Zhang, Improved QCD sum rule study of  $Z_c(3900)$  as a  $\bar{D}D^*$  molecular state, Phys. Rev. D87 (11) (2013) 116004. [arXiv:1304.5748](#), [doi:10.1103/PhysRevD.87.116004](#).
- [453] C.-Y. Cui, Y.-L. Liu, W.-B. Chen, M.-Q. Huang, Could  $Z_c(3900)$  be a  $I^G J^P = 1^+ 1^+ D^*\bar{D}$  molecular state?, J. Phys. G41 (2014) 075003. [arXiv:1304.1850](#), [doi:10.1088/0954-3899/41/7/075003](#).
- [454] C.-Y. Cui, Y.-L. Liu, M.-Q. Huang, Could  $Z_c(4025)$  be a  $J^P = 1^+ D^*\bar{D}^*$  molecular state? [arXiv:1308.3625](#).
- [455] K. P. Khemchandani, A. Martinez Torres, M. Nielsen, F. S. Navarra, Relating  $D^*\bar{D}^*$  currents with  $J^\pi = 0^+, 1^+$  and  $2^+$  to  $Z_c$  states, Phys. Rev. D89 (1) (2014) 014029. [arXiv:1310.0862](#), [doi:10.1103/PhysRevD.89.014029](#).
- [456] Z.-G. Wang, Reanalysis of the  $Z_c(4020)$ ,  $Z_c(4025)$ ,  $Z(4050)$  and  $Z(4250)$  as tetraquark states with QCD sum rules, Commun. Theor. Phys. 63 (4) (2015) 466–480. [arXiv:1312.1537](#), [doi:10.1088/0253-6102/63/4/466](#).
- [457] C.-F. Qiao, L. Tang, Interpretation of  $Z_c(4025)$  as the hidden charm tetraquark states via QCD Sum Rules, Eur. Phys. J. C74 (2014) 2810. [arXiv:1308.3439](#), [doi:10.1140/epjc/s10052-014-2810-x](#).
- [458] Z.-G. Wang, Analysis of the  $Z_c(4200)$  as axial-vector molecule-like state, Int. J. Mod. Phys. A30 (30) (2015) 1550168. [arXiv:1502.01459](#), [doi:10.1142/S0217751X15501687](#).
- [459] L. Maiani, A. D. Polosa, V. Riquer, The Charged  $Z(4433)$ : Towards a new spectroscopy, [arXiv:0708.3997](#).
- [460] L. Maiani, V. Riquer, R. Faccini, F. Piccinini, A. Pilloni, A. D. Polosa, A  $J^{PG} = 1^{++}$  Charged Resonance in the  $Y(4260) \rightarrow \pi^+\pi^-J/\psi$  Decay?, Phys. Rev. D87 (11) (2013) 111102. [arXiv:1303.6857](#), [doi:10.1103/PhysRevD.87.111102](#).
- [461] S. Patel, M. Shah, P. C. Vinodkumar, Mass spectra of four-quark states in the hidden charm sector, Eur. Phys. J. A50 (2014) 131. [arXiv:1402.3974](#), [doi:10.1140/epja/i2014-14131-9](#).
- [462] C. Deng, J. Ping, H. Huang, F. Wang, Systematic study of  $Z_c^+$  family from a multi-quark color flux-tube model, Phys. Rev. D92 (3) (2015)

034027. [arXiv:1507.06408](https://arxiv.org/abs/1507.06408), [doi:10.1103/PhysRevD.92.034027](https://doi.org/10.1103/PhysRevD.92.034027).
- [463] C. Deng, J. Ping, F. Wang, Interpreting  $Z_c(3900)$  and  $Z_c(4025)/Z_c(4020)$  as charged tetraquark states, Phys. Rev. D90 (5) (2014) 054009. [arXiv:1402.0777](https://arxiv.org/abs/1402.0777), [doi:10.1103/PhysRevD.90.054009](https://doi.org/10.1103/PhysRevD.90.054009).
- [464] L. Zhao, W.-Z. Deng, S.-L. Zhu, Hidden-Charm Tetraquarks and Charged  $Z_c$  States, Phys. Rev. D90 (9) (2014) 094031. [arXiv:1408.3924](https://arxiv.org/abs/1408.3924), [doi:10.1103/PhysRevD.90.094031](https://doi.org/10.1103/PhysRevD.90.094031).
- [465] M. B. Voloshin,  $Z_c(3900)$  - what is inside?, Phys. Rev. D87 (9) (2013) 091501. [arXiv:1304.0380](https://arxiv.org/abs/1304.0380), [doi:10.1103/PhysRevD.87.091501](https://doi.org/10.1103/PhysRevD.87.091501).
- [466] D.-Y. Chen, X. Liu, Predicted charged charmonium-like structures in the hidden-charm dipion decay of higher charmonia, Phys. Rev. D84 (2011) 034032. [arXiv:1106.5290](https://arxiv.org/abs/1106.5290), [doi:10.1103/PhysRevD.84.034032](https://doi.org/10.1103/PhysRevD.84.034032).
- [467] T. K. Pedlar, *et al.*, [CLEO Collaboration], Observation of the  $h_c(1P)$  using  $e^+e^-$  collisions above  $D\bar{D}$  threshold, Phys. Rev. Lett. 107 (2011) 041803. [arXiv:1104.2025](https://arxiv.org/abs/1104.2025), [doi:10.1103/PhysRevLett.107.041803](https://doi.org/10.1103/PhysRevLett.107.041803).
- [468] D.-Y. Chen, X. Liu, T. Matsuki, Reproducing the  $Z_c(3900)$  structure through the initial-single-pion-emission mechanism, Phys. Rev. D88 (3) (2013) 036008. [arXiv:1304.5845](https://arxiv.org/abs/1304.5845), [doi:10.1103/PhysRevD.88.036008](https://doi.org/10.1103/PhysRevD.88.036008).
- [469] E. S. Swanson, Cusps and Exotic Charmonia, [arXiv:1504.07952](https://arxiv.org/abs/1504.07952).
- [470] M. Albaladejo, F.-K. Guo, C. Hidalgo-Duque, J. Nieves,  $Z_c(3900)$ : what has been really seen? [arXiv:1512.03638](https://arxiv.org/abs/1512.03638).
- [471] E. Wilbring, H. W. Hammer, U. G. Meissner, Electromagnetic Structure of the  $Z_c(3900)$ , Phys. Lett. B726 (2013) 326–329. [arXiv:1304.2882](https://arxiv.org/abs/1304.2882), [doi:10.1016/j.physletb.2013.08.059](https://doi.org/10.1016/j.physletb.2013.08.059).
- [472] G. Li, Hidden-charmonium decays of  $Z_c(3900)$  and  $Z_c(4025)$  in intermediate meson loops model, Eur. Phys. J. C73 (11) (2013) 2621. [arXiv:1304.4458](https://arxiv.org/abs/1304.4458), [doi:10.1140/epjc/s10052-013-2621-5](https://doi.org/10.1140/epjc/s10052-013-2621-5).
- [473] Y. Dong, A. Faessler, T. Gutsche, V. E. Lyubovitskij, Strong decays of molecular states  $Z_c^+$  and  $Z_c'^+$ , Phys. Rev. D88 (1) (2013) 014030. [arXiv:1306.0824](https://arxiv.org/abs/1306.0824), [doi:10.1103/PhysRevD.88.014030](https://doi.org/10.1103/PhysRevD.88.014030).
- [474] H.-W. Ke, Z.-T. Wei, X.-Q. Li, Is  $Z_c(3900)$  a molecular state, Eur. Phys. J. C73 (10) (2013) 2561. [arXiv:1307.2414](https://arxiv.org/abs/1307.2414), [doi:10.1140/epjc/s10052-013-2561-0](https://doi.org/10.1140/epjc/s10052-013-2561-0).
- [475] A. Esposito, A. L. Guerrieri, A. Pilloni, Probing the nature of  $Z_c^{(\prime)}$  states via the  $\eta_c\rho$  decay, Phys. Lett. B746 (2015) 194–201. [arXiv:1409.3551](https://arxiv.org/abs/1409.3551), [doi:10.1016/j.physletb.2015.04.057](https://doi.org/10.1016/j.physletb.2015.04.057).
- [476] T. Gutsche, M. Kesenheimer, V. E. Lyubovitskij, Radiative and dilepton decays of the hadronic molecule  $Z_c^+(3900)$ , Phys. Rev. D90 (9) (2014) 094013. [arXiv:1410.0259](https://arxiv.org/abs/1410.0259), [doi:10.1103/PhysRevD.90.094013](https://doi.org/10.1103/PhysRevD.90.094013).
- [477] D.-Y. Chen, Y.-B. Dong, Radiative decays of the neutral  $Z_c(3900)$ , [arXiv:1510.00829](https://arxiv.org/abs/1510.00829).
- [478] Q.-Y. Lin, X. Liu, H.-S. Xu, Charged charmoniumlike state  $Z_c(3900)^\pm$  via meson photoproduction, Phys. Rev. D88 (2013) 114009. [arXiv:1308.6345](https://arxiv.org/abs/1308.6345), [doi:10.1103/PhysRevD.88.114009](https://doi.org/10.1103/PhysRevD.88.114009).
- [479] A. Martinez Torres, K. P. Khemchandani, F. S. Navarra, M. Nielsen, E. Oset, Reanalysis of the  $e^+e^- \rightarrow (D^*\bar{D}^*)^\pm\pi^\mp$  reaction and the claim for the  $Z_c(4025)$  resonance, Phys. Rev. D89 (1) (2014) 014025. [arXiv:1310.1119](https://arxiv.org/abs/1310.1119), [doi:10.1103/PhysRevD.89.014025](https://doi.org/10.1103/PhysRevD.89.014025).
- [480] J. L. Rosner, Threshold effect and  $\pi^\pm\psi(2S)$  peak, Phys. Rev. D76 (2007) 114002. [arXiv:0708.3496](https://arxiv.org/abs/0708.3496), [doi:10.1103/PhysRevD.76.114002](https://doi.org/10.1103/PhysRevD.76.114002).
- [481] S. H. Lee, A. Mihara, F. S. Navarra, M. Nielsen, QCD sum rules study of the meson  $Z^+(4430)$ , Phys. Lett. B661 (2008) 28–32. [arXiv:0710.1029](https://arxiv.org/abs/0710.1029), [doi:10.1016/j.physletb.2008.01.062](https://doi.org/10.1016/j.physletb.2008.01.062).
- [482] J.-R. Zhang, M.-Q. Huang, Q anti-quanti-Q-(prime)q molecular states, Phys. Rev. D80 (2009) 056004. [arXiv:0906.0090](https://arxiv.org/abs/0906.0090), [doi:10.1103/PhysRevD.80.056004](https://doi.org/10.1103/PhysRevD.80.056004).
- [483] M.-T. Li, W.-L. Wang, Y.-B. Dong, Z.-Y. Zhang, A Study of P-wave Heavy Meson Interactions in A Chiral Quark Model, [arXiv:1303.4140](https://arxiv.org/abs/1303.4140).
- [484] G.-Z. Meng, *et al.*, [CLQCD Collaboration], Low-energy  $D^{*+}D_0^+$  Scattering and the Resonance-like Structure  $Z^+(4430)$ , Phys. Rev. D80 (2009) 034503. [arXiv:0905.0752](https://arxiv.org/abs/0905.0752), [doi:10.1103/PhysRevD.80.034503](https://doi.org/10.1103/PhysRevD.80.034503).
- [485] T. Barnes, F. E. Close, E. S. Swanson, Molecular Interpretation of the Supercharmonium State  $Z(4475)$ , Phys. Rev. D91 (1) (2015) 014004. [arXiv:1409.6651](https://arxiv.org/abs/1409.6651), [doi:10.1103/PhysRevD.91.014004](https://doi.org/10.1103/PhysRevD.91.014004).
- [486] L. Ma, X.-H. Liu, X. Liu, S.-L. Zhu, Exotic Four Quark Matter:  $Z_1(4475)$ , Phys. Rev. D90 (3) (2014) 037502. [arXiv:1404.3450](https://arxiv.org/abs/1404.3450), [doi:10.1103/PhysRevD.90.037502](https://doi.org/10.1103/PhysRevD.90.037502).
- [487] D. Ebert, R. N. Faustov, V. O. Galkin, Excited heavy tetraquarks with hidden charm, Eur. Phys. J. C58 (2008) 399–405. [arXiv:0808.3912](https://arxiv.org/abs/0808.3912), [doi:10.1140/epjc/s10052-008-0754-8](https://doi.org/10.1140/epjc/s10052-008-0754-8).
- [488] M. R. Hadizadeh, A. Khaledi-Nasab, Heavy tetraquarks in the diquarkCantidiquark picture, Phys. Lett. B753 (2016) 8–12. [arXiv:1511.08542](https://arxiv.org/abs/1511.08542), [doi:10.1016/j.physletb.2015.11.072](https://doi.org/10.1016/j.physletb.2015.11.072).
- [489] G. B. Mohanty, Recent results on hot topics from Belle, Nucl. Part. Phys. Proc. 263-264 (2015) 10–14. [arXiv:1410.8232](https://arxiv.org/abs/1410.8232), [doi:10.1016/j.nuclphysbps.2015.04.003](https://doi.org/10.1016/j.nuclphysbps.2015.04.003).
- [490] X.-H. Liu, L. Ma, L.-P. Sun, X. Liu, S.-L. Zhu, Resolving the puzzling decay patterns of charged  $Z_c$  and  $Z_b$  states, Phys. Rev. D90 (7) (2014) 074020. [arXiv:1407.3684](https://arxiv.org/abs/1407.3684), [doi:10.1103/PhysRevD.90.074020](https://doi.org/10.1103/PhysRevD.90.074020).
- [491] K.-m. Cheung, W.-Y. Keung, T.-C. Yuan, Bottomed analog of  $Z^+(4433)$ , Phys. Rev. D76 (2007) 117501. [arXiv:0709.1312](https://arxiv.org/abs/0709.1312), [doi:10.1103/PhysRevD.76.117501](https://doi.org/10.1103/PhysRevD.76.117501).
- [492] S. J. Brodsky, R. F. Lebed, QCD dynamics of tetraquark production, Phys. Rev. D91 (2015) 114025. [arXiv:1505.00803](https://arxiv.org/abs/1505.00803), [doi:10.1103/PhysRevD.91.114025](https://doi.org/10.1103/PhysRevD.91.114025).
- [493] R. F. Lebed, A New Dynamical Picture for the Production and Decay of the XYZ Mesons, 2015. [arXiv:1508.03320](https://arxiv.org/abs/1508.03320).
- [494] D. V. Bugg, How Resonances can synchronise with Thresholds, J. Phys. G35 (2008) 075005. [arXiv:0802.0934](https://arxiv.org/abs/0802.0934), [doi:10.1088/0954-3899/35/7/075005](https://doi.org/10.1088/0954-3899/35/7/075005).
- [495] N. A. Tornqvist, Understanding the scalar meson  $q\bar{q}$  nonet, Z. Phys. C68 (1995) 647–660. [arXiv:hep-ph/9504372](https://arxiv.org/abs/hep-ph/9504372), [doi:10.1007/BF01565264](https://doi.org/10.1007/BF01565264).
- [496] Y. Li, C.-D. Lu, W. Wang, Partners of  $Z(4430)$  and productions in B decays, Phys. Rev. D77 (2008) 054001. [arXiv:0711.0497](https://arxiv.org/abs/0711.0497), [doi:10.1103/PhysRevD.77.054001](https://doi.org/10.1103/PhysRevD.77.054001).
- [497] B. Grinstein, R. Jora, A. D. Polosa, A Note on large N scalar QCD<sub>2</sub>, Phys. Lett. B671 (2009) 440–444. [arXiv:0812.0637](https://arxiv.org/abs/0812.0637), [doi:10.1016/j.physletb.2009.09.044](https://doi.org/10.1016/j.physletb.2009.09.044).

- 1016/j.physletb.2008.12.046.
- [498] T. Matsuki, T. Morii, K. Sudoh, Is the  $Z_{4430}^+$  a radially excited state of  $D_s^+$ ?, Phys. Lett. B669 (2008) 156–159. [arXiv:0805.2442](#), [doi:10.1016/j.physletb.2008.09.050](#).
- [499] I. V. Danilkin, P. Yu. Kulikov, The possibility of  $Z(4430)$  resonance structure description in  $\pi\psi'$  reaction, JETP Lett. 89 (2009) 390–392. [arXiv:0902.2010](#), [doi:10.1134/S0021364009080037](#).
- [500] X.-H. Liu, Q. Zhao, F. E. Close, Search for tetraquark candidate  $Z(4430)$  in meson photoproduction, Phys. Rev. D77 (2008) 094005. [arXiv:0802.2648](#), [doi:10.1103/PhysRevD.77.094005](#).
- [501] G. Galata, Photoproduction of  $Z(4430)$  through mesonic Regge trajectories exchange, Phys. Rev. C83 (2011) 065203. [arXiv:1102.2070](#), [doi:10.1103/PhysRevC.83.065203](#).
- [502] H.-W. Ke, X. Liu, The Signal of  $Z^\pm(4430)$  in nucleon-antinucleon scattering, Eur. Phys. J. C58 (2008) 217–221. [arXiv:0806.0998](#), [doi:10.1140/epjc/s10052-008-0744-x](#).
- [503] X.-Y. Wang, J.-J. Xie, X.-R. Chen, Production of the neutral  $Z^0(4430)$  in  $\bar{p}p \rightarrow \psi'\pi^0$  reaction, Phys. Rev. D91 (1) (2015) 014032. [doi:10.1103/PhysRevD.91.014032](#).
- [504] P. Pakhlov, Charged charmonium-like states as rescattering effects in  $B \rightarrow D_{sJ}D^{(*)}$  decays, Phys. Lett. B702 (2011) 139–142. [arXiv:1105.2945](#), [doi:10.1016/j.physletb.2011.06.079](#).
- [505] P. Pakhlov, T. Uglov, Charged charmonium-like  $Z^+(4430)$  from rescattering in conventional  $B$  decays, Phys. Lett. B748 (2015) 183–186. [arXiv:1408.5295](#), [doi:10.1016/j.physletb.2015.06.074](#).
- [506] S. S. Gershtein, A. K. Likhoded, G. P. Pronko, Possible nature of  $Z^+(4430)$ , [arXiv:0709.2058](#).
- [507] T. Branz, T. Gutsche, V. E. Lyubovitskij, Hidden-charm and radiative decays of the  $Z(4430)$  as a hadronic  $D_1\bar{D}^*$  bound state, Phys. Rev. D82 (2010) 054025. [arXiv:1005.3168](#), [doi:10.1103/PhysRevD.82.054025](#).
- [508] X. Liu, B. Zhang, S.-L. Zhu, The Two-body open charm decays of  $Z^+(4430)$ , Phys. Rev. D77 (2008) 114021. [arXiv:0803.4270](#), [doi:10.1103/PhysRevD.77.114021](#).
- [509] E. Braaten, M. Lu, Line Shapes of the  $Z(4430)$ , Phys. Rev. D79 (2009) 051503. [arXiv:0712.3885](#), [doi:10.1103/PhysRevD.79.051503](#).
- [510] I. Bediaga, J. M. de Miranda, F. Rodrigues, M. Nielsen, Phase motion in the  $Z^-(4430)$  amplitude in  $B^0 \rightarrow \psi'\pi^-K^+$  decay, Phys. Lett. B748 (2015) 187–190. [arXiv:1504.04313](#), [doi:10.1016/j.physletb.2015.06.079](#).
- [511] S. H. Lee, K. Morita, M. Nielsen, Can the  $\pi^+\chi_{c1}$  resonance structures be  $D^*\bar{D}^*$  and  $D_1\bar{D}$  molecules?, Nucl. Phys. A815 (2009) 29–39. [arXiv:0808.0690](#), [doi:10.1016/j.nuclphysa.2008.10.012](#).
- [512] W. Chen, T. G. Steele, H.-X. Chen, S.-L. Zhu,  $Z_c(4200)^+$  decay width as a charmonium-like tetraquark state, Eur. Phys. J. C75 (8) (2015) 358. [arXiv:1501.03863](#), [doi:10.1140/epjc/s10052-015-3578-3](#).
- [513] X.-Y. Wang, X.-R. Chen, A. Guskov, Photoproduction of the charged charmoniumlike  $Z_c^+(4200)$ , Phys. Rev. D92 (9) (2015) 094017. [arXiv:1503.02125](#), [doi:10.1103/PhysRevD.92.094017](#).
- [514] X.-Y. Wang, X.-R. Chen, Discovery Potential for the Neutral Charmonium-Like by Annihilation, Adv. High Energy Phys. 2015 (2015) 918231. [arXiv:1509.08553](#), [doi:10.1155/2015/918231](#).
- [515] Y.-R. Liu, M. Oka, M. Takizawa, X. Liu, W.-Z. Deng, S.-L. Zhu,  $D\bar{D}$  production and their interactions, Phys. Rev. D82 (2010) 014011. [arXiv:1005.2262](#), [doi:10.1103/PhysRevD.82.014011](#).
- [516] N. A. Tornqvist, Isospin breaking of the narrow charmonium state of Belle at 3872 MeV as a deuson, Phys. Lett. B590 (2004) 209–215. [arXiv:hep-ph/0402237](#), [doi:10.1016/j.physletb.2004.03.077](#).
- [517] C.-Y. Wong, Molecular states of heavy quark mesons, Phys. Rev. C69 (2004) 055202. [arXiv:hep-ph/0311088](#), [doi:10.1103/PhysRevC.69.055202](#).
- [518] M. T. AlFiky, F. Gabbiani, A. A. Petrov,  $X(3872)$ : Hadronic molecules in effective field theory, Phys. Lett. B640 (2006) 238–245. [arXiv:hep-ph/0506141](#), [doi:10.1016/j.physletb.2006.07.069](#).
- [519] S. Weinberg, Effective chiral Lagrangians for nucleon - pion interactions and nuclear forces, Nucl. Phys. B363 (1991) 3–18. [doi:10.1016/0550-3213\(91\)90231-L](#).
- [520] S. Weinberg, Nuclear forces from chiral Lagrangians, Phys. Lett. B251 (1990) 288–292. [doi:10.1016/0370-2693\(90\)90938-3](#).
- [521] S. Fleming, M. Kusunoki, T. Mehen, U. van Kolck, Pion interactions in the  $X(3872)$ , Phys. Rev. D76 (2007) 034006. [arXiv:hep-ph/0703168](#), [doi:10.1103/PhysRevD.76.034006](#).
- [522] M. Suzuki, The  $X(3872)$  boson: Molecule or charmonium, Phys. Rev. D72 (2005) 114013. [arXiv:hep-ph/0508258](#), [doi:10.1103/PhysRevD.72.114013](#).
- [523] C. E. Thomas, F. E. Close, Is  $X(3872)$  a molecule?, Phys. Rev. D78 (2008) 034007. [arXiv:0805.3653](#), [doi:10.1103/PhysRevD.78.034007](#).
- [524] P. Wang, X. G. Wang, Study on  $X(3872)$  from effective field theory with pion exchange interaction, Phys. Rev. Lett. 111 (4) (2013) 042002. [arXiv:1304.0846](#), [doi:10.1103/PhysRevLett.111.042002](#).
- [525] V. Baru, E. Epelbaum, A. A. Filin, F.-K. Guo, H. W. Hammer, C. Hanhart, U.-G. Meissner, A. V. Nefediev, Remarks on study of  $X(3872)$  from effective field theory with pion-exchange interaction, Phys. Rev. D91 (3) (2015) 034002. [arXiv:1501.02924](#), [doi:10.1103/PhysRevD.91.034002](#).
- [526] S. Prelovsek, L. Leskovec, Evidence for  $X(3872)$  from  $DD^*$  scattering on the lattice, Phys. Rev. Lett. 111 (2013) 192001. [arXiv:1307.5172](#), [doi:10.1103/PhysRevLett.111.192001](#).
- [527] S. H. Lee, M. Nielsen, U. Wiedner,  $D(s)D^*$  molecule as an axial meson, J. Korean Phys. Soc. 55 (2009) 424. [arXiv:0803.1168](#), [doi:10.3938/jkps.55.424](#).
- [528] S. H. Lee, K. Morita, M. Nielsen, Width of exotics from QCD sum rules: Tetraquarks or molecules?, Phys. Rev. D78 (2008) 076001. [arXiv:0808.3168](#), [doi:10.1103/PhysRevD.78.076001](#).
- [529] F. S. Navarra, M. Nielsen,  $X(3872) \rightarrow J/\psi\pi^+\pi^-$  and  $X(3872) \rightarrow J/\psi\pi^+\pi^-\pi^0$  decay widths from QCD sum rules, Phys. Lett. B639 (2006) 272–277. [arXiv:hep-ph/0605038](#), [doi:10.1016/j.physletb.2006.06.054](#).
- [530] R. D. Matheus, F. S. Navarra, M. Nielsen, C. M. Zanetti, QCD Sum Rules for the  $X(3872)$  as a mixed molecule-charmonium state, Phys.

- Rev. D80 (2009) 056002. [arXiv:0907.2683](#), [doi:10.1103/PhysRevD.80.056002](#).
- [531] M. Nielsen, C. M. Zanetti, Radiative decay of the  $X(3872)$  as a mixed molecule-charmonium state in QCD Sum Rules, Phys. Rev. D82 (2010) 116002. [arXiv:1006.0467](#), [doi:10.1103/PhysRevD.82.116002](#).
- [532] B.-K. Wang, W.-Z. Deng, X.-L. Chen, Dynamical study of the possible molecular state  $X(3872)$  with the s-channel one gluon exchange interaction, Chin. Phys. C34 (2010) 1052. [arXiv:0910.4787](#), [doi:10.1088/1674-1137/34/8/003](#).
- [533] P. G. Ortega, D. R. Entem, F. Fernandez, Molecular Structures in Charmonium Spectrum: The XYZ Puzzle, J. Phys. G40 (2013) 065107. [arXiv:1205.1699](#), [doi:10.1088/0954-3899/40/6/065107](#).
- [534] F.-K. Guo, C. Hidalgo-Duque, J. Nieves, A. Ozpineci, M. P. Valderrama, Detecting the long-distance structure of the  $X(3872)$ , Eur. Phys. J. C74 (5) (2014) 2885. [arXiv:1404.1776](#), [doi:10.1140/epjc/s10052-014-2885-4](#).
- [535] A. Tomaradze, S. Dobbs, T. Xiao, K. K. Seth, Precision Measurement of the Mass of the  $D^{*0}$  Meson and the Binding Energy of the  $X(3872)$  Meson as a  $D^0\bar{D}^{*0}$  Molecule, Phys. Rev. D91 (1) (2015) 011102. [arXiv:1501.01658](#), [doi:10.1103/PhysRevD.91.011102](#).
- [536] V. Baru, E. Epelbaum, A. A. Filin, J. Gegelia, A. V. Nefediev, Binding energy of the  $X(3872)$  at unphysical pion masses, Phys. Rev. D92 (11) (2015) 114016. [arXiv:1509.01789](#), [doi:10.1103/PhysRevD.92.114016](#).
- [537] L. Maiani, F. Piccinini, A. D. Polosa, V. Riquer, A New look at scalar mesons, Phys. Rev. Lett. 93 (2004) 212002. [arXiv:hep-ph/0407017](#), [doi:10.1103/PhysRevLett.93.212002](#).
- [538] I. Bigi, L. Maiani, F. Piccinini, A. D. Polosa, V. Riquer, Four-quark mesons in non-leptonic B decays: Could they resolve some old puzzles?, Phys. Rev. D72 (2005) 114016. [arXiv:hep-ph/0510307](#), [doi:10.1103/PhysRevD.72.114016](#).
- [539] L. Maiani, A. D. Polosa, V. Riquer, Indications of a Four-Quark Structure for the  $X(3872)$  and  $X(3876)$  Particles from Recent Belle and BABAR Data, Phys. Rev. Lett. 99 (2007) 182003. [arXiv:0707.3354](#), [doi:10.1103/PhysRevLett.99.182003](#).
- [540] T. J. Burns, F. Piccinini, A. D. Polosa, C. Sabelli, The  $2^{++}$  assignment for the  $X(3872)$ , Phys. Rev. D82 (2010) 074003. [arXiv:1008.0018](#), [doi:10.1103/PhysRevD.82.074003](#).
- [541] B. Aubert, *et al.*, [BaBar Collaboration], Search for a charged partner of the  $X(3872)$  in the  $B$  meson decay  $B \rightarrow X^- K$ ,  $X^- \rightarrow J/\psi\pi^-\pi^0$ , Phys. Rev. D71 (2005) 031501. [arXiv:hep-ex/0412051](#), [doi:10.1103/PhysRevD.71.031501](#).
- [542] D. Ebert, R. N. Faustov, V. O. Galkin, Masses of heavy tetraquarks in the relativistic quark model, Phys. Lett. B634 (2006) 214–219. [arXiv:hep-ph/0512230](#), [doi:10.1016/j.physletb.2006.01.026](#).
- [543] K. Terasaki, A New tetra-quark interpretation of  $X(3872)$ , Prog. Theor. Phys. 118 (2007) 821–826. [arXiv:0706.3944](#), [doi:10.1143/PTP.118.821](#).
- [544] R. D. Matheus, S. Narison, M. Nielsen, J. M. Richard, Can the  $X(3872)$  be a  $1^{++}$  four-quark state?, Phys. Rev. D75 (2007) 014005. [arXiv:hep-ph/0608297](#), [doi:10.1103/PhysRevD.75.014005](#).
- [545] Z.-G. Wang, T. Huang, Analysis of the  $X(3872)$ ,  $Z_c(3900)$  and  $Z_c(3885)$  as axial-vector tetraquark states with QCD sum rules, Phys. Rev. D89 (5) (2014) 054019. [arXiv:1310.2422](#), [doi:10.1103/PhysRevD.89.054019](#).
- [546] H. Hogaasen, J. M. Richard, P. Sorba, A Chromomagnetic mechanism for the  $X(3872)$  resonance, Phys. Rev. D73 (2006) 054013. [arXiv:hep-ph/0511039](#), [doi:10.1103/PhysRevD.73.054013](#).
- [547] Y. Cui, X.-L. Chen, W.-Z. Deng, S.-L. Zhu, The Possible Heavy Tetraquarks  $qQ\bar{q}\bar{Q}$ ,  $qq\bar{Q}\bar{Q}$  and  $qQ\bar{Q}\bar{Q}$ , HEPNP 31 (2007) 7–13. [arXiv:hep-ph/0607226](#).
- [548] F. Buccella, H. Hogaasen, J.-M. Richard, P. Sorba, Chromomagnetism, flavour symmetry breaking and S-wave tetraquarks, Eur. Phys. J. C49 (2007) 743–754. [arXiv:hep-ph/0608001](#), [doi:10.1140/epjc/s10052-006-0142-1](#).
- [549] J. Vijande, E. Weissman, N. Barnea, A. Valcarce, Do  $c\bar{c}n\bar{n}$  bound states exist?, Phys. Rev. D76 (2007) 094022. [arXiv:0708.3285](#), [doi:10.1103/PhysRevD.76.094022](#).
- [550] F. E. Close, P. R. Page, The  $D^{*0}\bar{D}^0$  threshold resonance, Phys. Lett. B578 (2004) 119–123. [arXiv:hep-ph/0309253](#), [doi:10.1016/j.physletb.2003.10.032](#).
- [551] T. Barnes, S. Godfrey, Charmonium options for the  $X(3872)$ , Phys. Rev. D69 (2004) 054008. [arXiv:hep-ph/0311162](#), [doi:10.1103/PhysRevD.69.054008](#).
- [552] Y.-M. Kong, A. Zhang, Charmonium possibility of  $X(3872)$ , Phys. Lett. B657 (2007) 192–197. [arXiv:hep-ph/0610245](#), [doi:10.1016/j.physletb.2007.09.062](#).
- [553] P. G. Ortega, J. Segovia, D. R. Entem, F. Fernandez, Coupled channel approach to the structure of the  $X(3872)$ , Phys. Rev. D81 (2010) 054023. [arXiv:1001.3948](#), [doi:10.1103/PhysRevD.81.054023](#).
- [554] Yu. S. Kalashnikova, A. V. Nefediev,  $X(3872)$  as a  $^1D_2$  charmonium state, Phys. Rev. D82 (2010) 097502. [arXiv:1008.2895](#), [doi:10.1103/PhysRevD.82.097502](#).
- [555] C. Yang, B.-F. Li, X.-L. Chen, W.-Z. Deng, Fine Splitting in Charmonium Spectrum with Channel Coupling Effect, Chin. Phys. C35 (2011) 797–803. [arXiv:1011.6124](#), [doi:10.1088/1674-1137/35/9/001](#).
- [556] M. Takizawa, S. Takeuchi,  $X(3872)$  as a hybrid state of charmonium and the hadronic molecule, PTEP 2013 (2013) 0903D01. [arXiv:1206.4877](#), [doi:10.1093/ptep/ptt063](#).
- [557] J. Ferretti, G. Galata, E. Santopinto, Interpretation of the  $X(3872)$  as a charmonium state plus an extra component due to the coupling to the meson-meson continuum, Phys. Rev. C88 (1) (2013) 015207. [arXiv:1302.6857](#), [doi:10.1103/PhysRevC.88.015207](#).
- [558] M. Butenschoen, Z.-G. He, B. A. Kniehl, NLO NRQCD disfavors the interpretation of  $X(3872)$  as  $\chi_{c1}(2P)$ , Phys. Rev. D88 (2013) 011501. [arXiv:1303.6524](#), [doi:10.1103/PhysRevD.88.011501](#).
- [559] J. Ferretti, G. Galata, E. Santopinto, Quark structure of the  $X(3872)$  and  $\chi_{b1}(3P)$  resonances, Phys. Rev. D90 (5) (2014) 054010. [arXiv:1401.4431](#), [doi:10.1103/PhysRevD.90.054010](#).
- [560] S. Takeuchi, K. Shimizu, M. Takizawa, On the origin of the narrow peak and the isospin symmetry breaking of the  $X(3872)$ , PTEP 2014 (2014) 123D01. [arXiv:1408.0973](#), [doi:10.1093/ptep/ptu160](#).
- [561] T. M. Aliev, M. Savci, Determination of the mixing angle between new charmonium states, Eur. Phys. J. C75 (4) (2015) 169. [arXiv:1409.5248](#), [doi:10.1140/epjc/s10052-015-3388-7](#).
- [562] T. M. Aliev, H. Ozsahin, M. Savci, More about the mass of the new charmonium states, Adv. High Energy Phys. 2015 (2015) 728098. [arXiv:1410.2012](#), [doi:10.1155/2015/728098](#).

- [563] C. Meng, J. J. Sanz-Cillero, M. Shi, D.-L. Yao, H.-Q. Zheng, Refined analysis on the  $X(3872)$  resonance, Phys. Rev. D92 (3) (2015) 034020. [arXiv:1411.3106](#), [doi:10.1103/PhysRevD.92.034020](#).
- [564] J. H. Yang, S. K. Lee, E.-J. Kim, J. B. Choi, Analysis of  $X$  Particle Spectra in Quarkonium Model, [arXiv:1506.04481](#).
- [565] Yu. S. Kalashnikova, Coupled-channel model for charmonium levels and an option for  $X(3872)$ , Phys. Rev. D72 (2005) 034010. [arXiv:hep-ph/0506270](#), [doi:10.1103/PhysRevD.72.034010](#).
- [566] O. Zhang, C. Meng, H. Q. Zheng, Ambiversion of  $X(3872)$ , Phys. Lett. B680 (2009) 453–458. [arXiv:0901.1553](#), [doi:10.1016/j.physletb.2009.09.033](#).
- [567] Yu. S. Kalashnikova, A. V. Nefediev, Nature of  $X(3872)$  from data, Phys. Rev. D80 (2009) 074004. [arXiv:0907.4901](#), [doi:10.1103/PhysRevD.80.074004](#).
- [568] I. V. Danilkin, Yu. A. Simonov, Dynamical origin and the pole structure of  $X(3872)$ , Phys. Rev. Lett. 105 (2010) 102002. [arXiv:1006.0211](#), [doi:10.1103/PhysRevLett.105.102002](#).
- [569] I. V. Danilkin, Yu. A. Simonov, Channel coupling in heavy quarkonia: Energy levels, mixing, widths and new states, Phys. Rev. D81 (2010) 074027. [arXiv:0907.1088](#), [doi:10.1103/PhysRevD.81.074027](#).
- [570] B.-Q. Li, K.-T. Chao, Higher Charmonia and  $X, Y, Z$  states with Screened Potential, Phys. Rev. D79 (2009) 094004. [arXiv:0903.5506](#), [doi:10.1103/PhysRevD.79.094004](#).
- [571] B.-Q. Li, C. Meng, K.-T. Chao, Coupled-Channel and Screening Effects in Charmonium Spectrum, Phys. Rev. D80 (2009) 014012. [arXiv:0904.4068](#), [doi:10.1103/PhysRevD.80.014012](#).
- [572] S. Coito, G. Rupp, E. van Beveren, Delicate interplay between the  $D^0D^{*0}$ ,  $\rho^0J/\psi$ , and  $\omega J/\psi$  channels in the  $X(3872)$  resonance, Eur. Phys. J. C71 (2011) 1762. [arXiv:1008.5100](#), [doi:10.1140/epjc/s10052-011-1762-7](#).
- [573] S. Coito, G. Rupp, E. van Beveren,  $X(3872)$  is not a true molecule, Eur. Phys. J. C73 (3) (2013) 2351. [arXiv:1212.0648](#), [doi:10.1140/epjc/s10052-013-2351-8](#).
- [574] T.-W. Chiu, T.-H. Hsieh, [TWQCD Collaboration],  $X(3872)$  in lattice QCD with exact chiral symmetry, Phys. Lett. B646 (2007) 95–99. [arXiv:hep-ph/0603207](#), [doi:10.1016/j.physletb.2007.01.019](#).
- [575] T.-W. Chiu, T.-H. Hsieh, [TWQCD Collaboration], Pseudovector meson with strangeness and closed-charm, Phys. Rev. D73 (2006) 111503, [Erratum: Phys. Rev. D75, 019902 (2007)]. [arXiv:hep-lat/0604008](#), [doi:10.1103/PhysRevD.73.111503](#), [doi:10.1103/PhysRevD.75.019902](#).
- [576] L. Liu, G. Moir, M. Peardon, S. M. Ryan, C. E. Thomas, P. Vilaseca, J. J. Dudek, R. G. Edwards, B. Joo, D. G. Richards, [Hadron Spectrum Collaboration], Excited and exotic charmonium spectroscopy from lattice QCD, JHEP 07 (2012) 126. [arXiv:1204.5425](#), [doi:10.1007/JHEP07\(2012\)126](#).
- [577] Y.-B. Yang, Y. Chen, L.-C. Gui, C. Liu, Y.-B. Liu, Z. Liu, J.-P. Ma, J.-B. Zhang, [CLQCD Collaboration], Lattice study on  $\eta_{c2}$  and  $X(3872)$ , Phys. Rev. D87 (1) (2013) 014501. [arXiv:1206.2086](#), [doi:10.1103/PhysRevD.87.014501](#).
- [578] C. Meng, Y.-J. Gao, K.-T. Chao,  $B \rightarrow \chi_{c1}(1P, 2P)K$  decays in QCD factorization and  $X(3872)$ , Phys. Rev. D87 (7) (2013) 074035. [arXiv:hep-ph/0506222](#), [doi:10.1103/PhysRevD.87.074035](#).
- [579] M. Padmanath, C. B. Lang, S. Prelovsek,  $X(3872)$  and  $Y(4140)$  using diquark-antidiquark operators with lattice QCD, Phys. Rev. D92 (3) (2015) 034501. [arXiv:1503.03257](#), [doi:10.1103/PhysRevD.92.034501](#).
- [580] B. A. Li, Is  $X(3872)$  a possible candidate of hybrid meson, Phys. Lett. B605 (2005) 306–310. [arXiv:hep-ph/0410264](#), [doi:10.1016/j.physletb.2004.11.062](#).
- [581] K. K. Seth, An Alternative Interpretation of  $X(3872)$ , Phys. Lett. B612 (2005) 1–4. [arXiv:hep-ph/0411122](#), [doi:10.1016/j.physletb.2005.02.057](#).
- [582] P. G. Ortega, J. Segovia, D. R. Entem, F. Fernandez, Coupled channel approach to the  $X(3872)$  structure, Phys. Rev. D81 (2010) 0054023. [arXiv:0907.3997](#), [doi:10.1103/PhysRevD.81.0054023](#).
- [583] D. V. Bugg, Reinterpreting several narrow ‘resonances’ as threshold cusps, Phys. Lett. B598 (2004) 8–14. [arXiv:hep-ph/0406293](#), [doi:10.1016/j.physletb.2004.07.047](#).
- [584] D. V. Bugg, The  $X(3872)$  and the 3941 MeV peak in  $\omega J/\psi$ , Phys. Rev. D71 (2005) 016006. [arXiv:hep-ph/0410168](#), [doi:10.1103/PhysRevD.71.016006](#).
- [585] J. L. Rosner, Effects of S-wave thresholds, Phys. Rev. D74 (2006) 076006. [arXiv:hep-ph/0608102](#), [doi:10.1103/PhysRevD.74.076006](#).
- [586] S. H. Blitz, R. F. Lebed, Tetraquark Cusp Effects from Diquark Pair Production, Phys. Rev. D91 (9) (2015) 094025. [arXiv:1503.04802](#), [doi:10.1103/PhysRevD.91.094025](#).
- [587] M. B. Voloshin, Isospin properties of the  $X$  state near the  $D\bar{D}^*$  threshold, Phys. Rev. D76 (2007) 014007. [arXiv:0704.3029](#), [doi:10.1103/PhysRevD.76.014007](#).
- [588] W. Dunwoodie, V. Ziegler, A Simple explanation for the  $X(3872)$  mass shift observed for decay to  $D^{*0}\bar{D}^0$ , Phys. Rev. Lett. 100 (2008) 062006. [arXiv:0710.5191](#), [doi:10.1103/PhysRevLett.100.062006](#).
- [589] D. L. Canham, H. W. Hammer, R. P. Springer, On the scattering of  $D$  and  $D^*$  mesons off the  $X(3872)$ , Phys. Rev. D80 (2009) 014009. [arXiv:0906.1263](#), [doi:10.1103/PhysRevD.80.014009](#).
- [590] F.-K. Guo, C. Hanhart, G. Li, U.-G. Meissner, Q. Zhao, Effect of charmed meson loops on charmonium transitions, Phys. Rev. D83 (2011) 034013. [arXiv:1008.3632](#), [doi:10.1103/PhysRevD.83.034013](#).
- [591] Z.-Y. Zhou, Z. Xiao, Comprehending heavy charmonia and their decays by hadron loop effects, Eur. Phys. J. A50 (10) (2014) 165. [arXiv:1309.1949](#), [doi:10.1140/epja/i2014-14165-y](#).
- [592] D. Gamermann, E. Oset, Axial resonances in the open and hidden charm sectors, Eur. Phys. J. A33 (2007) 119–131. [arXiv:0704.2314](#), [doi:10.1140/epja/i2007-10435-1](#).
- [593] D. Gamermann, E. Oset, Hidden charm dynamically generated resonances and the  $e^+e^- \rightarrow J/\psi D\bar{D}, J/\psi D\bar{D}^*$  reactions, Eur. Phys. J. A36 (2008) 189–194. [arXiv:0712.1758](#), [doi:10.1140/epja/i2007-10580-5](#).
- [594] D. Gamermann, E. Oset, Isospin breaking effects in the  $X(3872)$  resonance, Phys. Rev. D80 (2009) 014003. [arXiv:0905.0402](#), [doi:10.1103/PhysRevD.80.014003](#).

- [595] D. Gamermann, J. Nieves, E. Oset, E. Ruiz Arriola, Couplings in coupled channels versus wave functions: application to the  $X(3872)$  resonance, Phys. Rev. D81 (2010) 014029. [arXiv:0911.4407](#), [doi:10.1103/PhysRevD.81.014029](#).
- [596] D. Gamermann, C. E. Jimenez-Tejero, A. Ramos, Radiative decays of dynamically generated charmed baryons, Phys. Rev. D83 (2011) 074018. [arXiv:1011.5381](#), [doi:10.1103/PhysRevD.83.074018](#).
- [597] M. V. Carlucci, F. Giannuzzi, G. Nardulli, M. Pellicoro, S. Stramaglia, AdS-QCD quark-antiquark potential, meson spectrum and tetraquarks, Eur. Phys. J. C57 (2008) 569–578. [arXiv:0711.2014](#), [doi:10.1140/epjc/s10052-008-0687-2](#).
- [598] E. Braaten, H. W. Hammer, T. Mehen, Scattering of an Ultrasoft Pion and the  $X(3872)$ , Phys. Rev. D82 (2010) 034018. [arXiv:1005.1688](#), [doi:10.1103/PhysRevD.82.034018](#).
- [599] S. Fleming, T. Mehen, The decay of the  $X(3872)$  into  $\chi_{cJ}$  and the Operator Product Expansion in XEFT, Phys. Rev. D85 (2012) 014016. [arXiv:1110.0265](#), [doi:10.1103/PhysRevD.85.014016](#).
- [600] M. Jansen, H. W. Hammer, Y. Jia, Light quark mass dependence of the  $X(3872)$  in an effective field theory, Phys. Rev. D89 (1) (2014) 014033. [arXiv:1310.6937](#), [doi:10.1103/PhysRevD.89.014033](#).
- [601] E. Braaten, Galilean-invariant effective field theory for the  $X(3872)$ , Phys. Rev. D91 (11) (2015) 114007. [arXiv:1503.04791](#), [doi:10.1103/PhysRevD.91.114007](#).
- [602] M. Jansen, H. W. Hammer, Y. Jia, Finite volume corrections to the binding energy of the  $X(3872)$ , Phys. Rev. D92 (11) (2015) 114031. [arXiv:1505.04099](#), [doi:10.1103/PhysRevD.92.114031](#).
- [603] E. Braaten, M. Lu, J. Lee, Weakly-bound Hadronic Molecule near a 3-body Threshold, Phys. Rev. D76 (2007) 054010. [arXiv:hep-ph/0702128](#), [doi:10.1103/PhysRevD.76.054010](#).
- [604] V. Baru, A. A. Filin, C. Hanhart, Yu. S. Kalashnikova, A. E. Kudryavtsev, A. V. Nefediev, Three-body  $D\bar{D}\pi$  dynamics for the  $X(3872)$ , Phys. Rev. D84 (2011) 074029. [arXiv:1108.5644](#), [doi:10.1103/PhysRevD.84.074029](#).
- [605] M. B. Voloshin, Heavy quark spin selection rule and the properties of the  $X(3872)$ , Phys. Lett. B604 (2004) 69–73. [arXiv:hep-ph/0408321](#), [doi:10.1016/j.physletb.2004.11.003](#).
- [606] M. H. Alhakami, M. C. Birse, Power counting for three-body decays of a near-threshold state, Phys. Rev. D91 (5) (2015) 054019. [arXiv:1501.06750](#), [doi:10.1103/PhysRevD.91.054019](#).
- [607] E. Braaten, M. Kusunoki, Factorization in the production and decay of the  $X(3872)$ , Phys. Rev. D72 (2005) 014012. [arXiv:hep-ph/0506087](#), [doi:10.1103/PhysRevD.72.014012](#).
- [608] E. Braaten, M. Lu, Line shapes of the  $X(3872)$ , Phys. Rev. D76 (2007) 094028. [arXiv:0709.2697](#), [doi:10.1103/PhysRevD.76.094028](#).
- [609] E. Braaten, M. Lu, The Effects of charged charm mesons on the line shapes of the  $X(3872)$ , Phys. Rev. D77 (2008) 014029. [arXiv:0710.5482](#), [doi:10.1103/PhysRevD.77.014029](#).
- [610] P. Artoisenet, E. Braaten, D. Kang, Using Line Shapes to Discriminate between Binding Mechanisms for the  $X(3872)$ , Phys. Rev. D82 (2010) 014013. [arXiv:1005.2167](#), [doi:10.1103/PhysRevD.82.014013](#).
- [611] G.-Y. Chen, W.-S. Huo, Q. Zhao, Identifying the structure of near-threshold states from the line shape, Chin. Phys. C39 (9) (2015) 093101. [arXiv:1309.2859](#), [doi:10.1088/1674-1137/39/9/093101](#).
- [612] M. Albaladejo, C. Hidalgo-Duque, J. Nieves, E. Oset, Hidden charm molecules in finite volume, Phys. Rev. D88 (2013) 014510. [arXiv:1304.1439](#), [doi:10.1103/PhysRevD.88.014510](#).
- [613] V. Baru, E. Epelbaum, A. A. Filin, C. Hanhart, U. G. Meissner, A. V. Nefediev, Quark mass dependence of the  $X(3872)$  binding energy, Phys. Lett. B726 (2013) 537–543. [arXiv:1306.4108](#), [doi:10.1016/j.physletb.2013.08.073](#).
- [614] E. J. Garzon, R. Molina, A. Hosaka, E. Oset, Strategies for an accurate determination of the  $X(3872)$  energy from QCD lattice simulations, Phys. Rev. D89 (2014) 014504. [arXiv:1310.0972](#), [doi:10.1103/PhysRevD.89.014504](#).
- [615] M. Kalinowski, M. Wagner, Masses of  $D$  mesons,  $D_s$  mesons and charmonium states from twisted mass lattice QCD, Phys. Rev. D92 (9) (2015) 094508. [arXiv:1509.02396](#), [doi:10.1103/PhysRevD.92.094508](#).
- [616] W.-S. Hou, Searching for the bottom counterparts of  $X(3872)$  and  $Y(4260)$  via  $\pi^+\pi^-\nu$ , Phys. Rev. D74 (2006) 017504. [arXiv:hep-ph/0606016](#), [doi:10.1103/PhysRevD.74.017504](#).
- [617] S. M. Gerasyuta, V. I. Kochkin, S-wave bottom tetraquarks, Int. J. Mod. Phys. E19 (2010) 2181–2188. [arXiv:0905.4914](#), [doi:10.1142/S0218301310016582](#).
- [618] J. Nieves, M. P. Valderrama, The Heavy Quark Spin Symmetry Partners of the  $X(3872)$ , Phys. Rev. D86 (2012) 056004. [arXiv:1204.2790](#), [doi:10.1103/PhysRevD.86.056004](#).
- [619] C. Hidalgo-Duque, J. Nieves, A. Ozpineci, V. Zamiralov,  $X(3872)$  and its Partners in the Heavy Quark Limit of QCD, Phys. Lett. B727 (2013) 432–437. [arXiv:1305.4487](#), [doi:10.1016/j.physletb.2013.10.056](#).
- [620] F.-K. Guo, U.-G. Meissner, W. Wang, Z. Yang, Production of the bottom analogs and the spin partner of the  $X(3872)$  at hadron colliders, Eur. Phys. J. C74 (9) (2014) 3063. [arXiv:1402.6236](#), [doi:10.1140/epjc/s10052-014-3063-4](#).
- [621] G. Li, W. Wang, Hunting for the  $X_b$  via Radiative Decays, Phys. Lett. B733 (2014) 100–104. [arXiv:1402.6463](#), [doi:10.1016/j.physletb.2014.04.029](#).
- [622] F.-K. Guo, U.-G. Meissner, Z. Yang, Production of the spin partner of the  $X(3872)$  in  $e^+e^-$  collisions, Phys. Lett. B740 (2015) 42–45. [arXiv:1410.4674](#), [doi:10.1016/j.physletb.2014.11.030](#).
- [623] M. Karliner, J. L. Rosner,  $X(3872)$ ,  $X_b$ , and the  $\chi_{b1}(3P)$  state, Phys. Rev. D91 (1) (2015) 014014. [arXiv:1410.7729](#), [doi:10.1103/PhysRevD.91.014014](#).
- [624] G. Li, Z. Zhou, Hunting for the  $X_b$  via hidden bottomonium decays, Phys. Rev. D91 (3) (2015) 034020. [arXiv:1502.02936](#), [doi:10.1103/PhysRevD.91.034020](#).
- [625] M. Albaladejo, F. K. Guo, C. Hidalgo-Duque, J. Nieves, M. P. Valderrama, Decay widths of the spin-2 partners of the  $X(3872)$ , Eur. Phys. J. C75 (11) (2015) 547. [arXiv:1504.00861](#), [doi:10.1140/epjc/s10052-015-3753-6](#).
- [626] M. B. Voloshin, Interference and binding effects in decays of possible molecular component of  $X(3872)$ , Phys. Lett. B579 (2004) 316–320. [arXiv:hep-ph/0309307](#), [doi:10.1016/j.physletb.2003.11.014](#).
- [627] S. Dubynskiy, M. B. Voloshin, Pionic transitions from  $X(3872)$  to  $\chi_{cJ}$ , Phys. Rev. D77 (2008) 014013. [arXiv:0709.4474](#), [doi:10.1103/](#)

- PhysRevD.77.014013.
- [628] S. Fleming, T. Mehen, Hadronic Decays of the  $X(3872) \rightarrow \chi_{cJ}$  in Effective Field Theory, Phys. Rev. D78 (2008) 094019. [arXiv:0807.2674](#), [doi:10.1103/PhysRevD.78.094019](#).
- [629] T. Mehen, Hadronic loops versus factorization in effective field theory calculations of  $X(3872) \rightarrow \chi_{cJ}\pi^0$ , Phys. Rev. D92 (3) (2015) 034019. [arXiv:1503.02719](#), [doi:10.1103/PhysRevD.92.034019](#).
- [630] E. Braaten, D. Kang,  $J/\psi \omega$  Decay Channel of the  $X(3872)$  Charm Meson Molecule, Phys. Rev. D88 (1) (2013) 014028. [arXiv:1305.5564](#), [doi:10.1103/PhysRevD.88.014028](#).
- [631] A. Abd El-Hady, Superradiance and subradiance in the electromagnetic radiative decay of  $X(3872)$ , Phys. Rev. D73 (2006) 073010. [arXiv:hep-ph/0603109](#), [doi:10.1103/PhysRevD.73.073010](#).
- [632] P. Colangelo, F. De Fazio, S. Nicotri,  $X(3872) \rightarrow D\bar{D}\gamma$  decays and the structure of  $X_{3872}$ , Phys. Lett. B650 (2007) 166–171. [arXiv:hep-ph/0701052](#), [doi:10.1016/j.physletb.2007.05.012](#).
- [633] Y.-b. Dong, A. Faessler, T. Gutsche, V. E. Lyubovitskij, Estimate for the  $X(3872) \rightarrow \gamma J/\psi$  decay width, Phys. Rev. D77 (2008) 094013. [arXiv:0802.3610](#), [doi:10.1103/PhysRevD.77.094013](#).
- [634] F. De Fazio, Radiative transitions of heavy quarkonium states, Phys. Rev. D79 (2009) 054015, [Erratum: Phys. Rev. D83, 099901 (2011)]. [arXiv:0812.0716](#), [doi:10.1103/PhysRevD.83.099901](#), [doi:10.1103/PhysRevD.79.054015](#).
- [635] T.-H. Wang, G.-L. Wang, Radiative E1 decays of  $X(3872)$ , Phys. Lett. B697 (2011) 233–237. [arXiv:1006.3363](#), [doi:10.1016/j.physletb.2011.02.014](#).
- [636] Y. Jia, W.-L. Sang, J. Xu, Is the  $J^P = 2^-$  assignment for the  $X(3872)$  compatible with the radiative transition data? [arXiv:1007.4541](#).
- [637] M. Harada, Y.-L. Ma, Strong and radiative decays of  $X(3872)$  as a hadronic molecule with a negative parity, Prog. Theor. Phys. 126 (2011) 91–113. [arXiv:1010.3607](#), [doi:10.1143/PTP.126.91](#).
- [638] T. Mehen, R. Springer, Radiative Decays  $X(3872) \rightarrow \psi(2S)\gamma$  and  $\psi(4040)^- \rightarrow X(3872)\gamma$  in Effective Field Theory, Phys. Rev. D83 (2011) 094009. [arXiv:1101.5175](#), [doi:10.1103/PhysRevD.83.094009](#).
- [639] S. Dubnicka, A. Z. Dubnickova, M. A. Ivanov, J. G. Koerner, P. Santorelli, G. G. Saidullaeva, One-photon decay of the tetraquark state  $X(3872) \rightarrow \gamma + J/\psi$  in a relativistic constituent quark model with infrared confinement, Phys. Rev. D84 (2011) 014006. [arXiv:1104.3974](#), [doi:10.1103/PhysRevD.84.014006](#).
- [640] S. Pakvasa, M. Suzuki, On the hidden charm state at 3872 MeV, Phys. Lett. B579 (2004) 67–73. [arXiv:hep-ph/0309294](#), [doi:10.1016/j.physletb.2003.11.005](#).
- [641] T. Kim, P. Ko, Dipion invariant mass spectrum in  $X(3872) \rightarrow J/\psi\pi\pi$ , Phys. Rev. D71 (2005) 034025, [Erratum: Phys. Rev. D71, 099902 (2005)]. [arXiv:hep-ph/0405265](#), [doi:10.1103/PhysRevD.71.099902](#), [doi:10.1103/PhysRevD.71.034025](#).
- [642] J. L. Rosner, Angular distributions in  $J/\psi(\rho^0, \omega)$  states near threshold, Phys. Rev. D70 (2004) 094023. [arXiv:hep-ph/0408334](#), [doi:10.1103/PhysRevD.70.094023](#).
- [643] E. Braaten, M. Kusunoki, Decays of the  $X(3872)$  into  $J/\psi$  and light hadrons, Phys. Rev. D72 (2005) 054022. [arXiv:hep-ph/0507163](#), [doi:10.1103/PhysRevD.72.054022](#).
- [644] D. Melikhov, B. Stech, Fall-apart decays of poliquark hadrons, Phys. Rev. D74 (2006) 034022. [arXiv:hep-ph/0606203](#), [doi:10.1103/PhysRevD.74.034022](#).
- [645] K. Terasaki,  $\omega - \rho^0$  mixing as a possible origin of the hypothetical isospin non-conservation in the  $X(3872) \rightarrow \pi^+\pi^- J/\psi$  decay, Prog. Theor. Phys. 122 (2010) 1285–1290. [arXiv:0904.3368](#), [doi:10.1143/PTP.122.1285](#).
- [646] C. Hanhart, Yu. S. Kalashnikova, A. E. Kudryavtsev, A. V. Nefediev, Remarks on the quantum numbers of  $X(3872)$  from the invariant mass distributions of the  $\rho J/\psi$  and  $\omega J/\psi$  final states, Phys. Rev. D85 (2012) 011501. [arXiv:1111.6241](#), [doi:10.1103/PhysRevD.85.011501](#).
- [647] C. Hanhart, Yu. S. Kalashnikova, A. E. Kudryavtsev, A. V. Nefediev, Reconciling the  $X(3872)$  with the near-threshold enhancement in the  $D^0\bar{D}^{*0}$  final state, Phys. Rev. D76 (2007) 034007. [arXiv:0704.0605](#), [doi:10.1103/PhysRevD.76.034007](#).
- [648] E. Braaten, J. Stapleton, Analysis of  $J/\psi\pi^+\pi^-$  and  $D^0\bar{D}^0\pi^0$  Decays of the  $X(3872)$ , Phys. Rev. D81 (2010) 014019. [arXiv:0907.3167](#), [doi:10.1103/PhysRevD.81.014019](#).
- [649] S. Dubnicka, A. Z. Dubnickova, M. A. Ivanov, J. G. Korner, Quark model description of the tetraquark state  $X(3872)$  in a relativistic constituent quark model with infrared confinement, Phys. Rev. D81 (2010) 114007. [arXiv:1004.1291](#), [doi:10.1103/PhysRevD.81.114007](#).
- [650] Y. Dong, A. Faessler, T. Gutsche, V. E. Lyubovitskij,  $J/\psi\gamma$  and  $\psi(2S)\gamma$  decay modes of the  $X(3872)$ , J. Phys. G38 (2011) 015001. [arXiv:0909.0380](#), [doi:10.1088/0954-3899/38/1/015001](#).
- [651] F.-K. Guo, C. Hanhart, Yu. S. Kalashnikova, U.-G. Meissner, A. V. Nefediev, What can radiative decays of the  $X(3872)$  teach us about its nature?, Phys. Lett. B742 (2015) 394–398. [arXiv:1410.6712](#), [doi:10.1016/j.physletb.2015.02.013](#).
- [652] Y. Dong, A. Faessler, T. Gutsche, S. Kovalenko, V. E. Lyubovitskij,  $X(3872)$  as a hadronic molecule and its decays to charmonium states and pions, Phys. Rev. D79 (2009) 094013. [arXiv:0903.5416](#), [doi:10.1103/PhysRevD.79.094013](#).
- [653] X. Liu, B. Zhang, S.-L. Zhu, The Hidden Charm Decay of  $X(3872)$ ,  $Y(3940)$  and Final State Interaction Effects, Phys. Lett. B645 (2007) 185–188. [arXiv:hep-ph/0610278](#), [doi:10.1016/j.physletb.2006.12.031](#).
- [654] C. Meng, K.-T. Chao, Decays of the  $X(3872)$  and  $\chi_{c1}(2P)$  charmonium, Phys. Rev. D75 (2007) 114002. [arXiv:hep-ph/0703205](#), [doi:10.1103/PhysRevD.75.114002](#).
- [655] E. Braaten, Inclusive production of the  $X(3872)$ , Phys. Rev. D73 (2006) 011501. [arXiv:hep-ph/0408230](#), [doi:10.1103/PhysRevD.73.011501](#).
- [656] E. Braaten, M. Kusunoki, Production of the  $X(3870)$  at the  $\Upsilon(4S)$  by the coalescence of charm mesons from B decays, Phys. Rev. D69 (2004) 114012. [arXiv:hep-ph/0402177](#), [doi:10.1103/PhysRevD.69.114012](#).
- [657] E. Braaten, M. Kusunoki, S. Nussinov, Production of the  $X(3870)$  in B meson decay by the coalescence of charm mesons, Phys. Rev. Lett. 93 (2004) 162001. [arXiv:hep-ph/0404161](#), [doi:10.1103/PhysRevLett.93.162001](#).
- [658] Y.-M. Wang, C.-D. Lu, Weak productions of new charmonium in semi-leptonic decays of  $B_c$ , Phys. Rev. D77 (2008) 054003. [arXiv:0707.4439](#), [doi:10.1103/PhysRevD.77.054003](#).

- [659] W. Wang, Y.-L. Shen, C.-D. Lu, The Study of  $B_c^- \rightarrow X(3872)\pi^-(K^-)$  decays in the covariant light-front approach, Eur. Phys. J. C51 (2007) 841–847. [arXiv:0704.2493](#), [doi:10.1140/epjc/s10052-007-0334-3](#).
- [660] F.-K. Guo, C. Hanhart, U.-G. Meissner, Q. Wang, Q. Zhao, Production of the  $X(3872)$  in charmonia radiative decays, Phys. Lett. B725 (2013) 127–133. [arXiv:1306.3096](#), [doi:10.1016/j.physletb.2013.06.053](#).
- [661] S. Dubynskiy, M. B. Voloshin,  $e^+e^- \rightarrow \gamma X(3872)$  near the  $D^*\bar{D}^*$  threshold, Phys. Rev. D74 (2006) 094017. [arXiv:hep-ph/0609302](#), [doi:10.1103/PhysRevD.74.094017](#).
- [662] Y.-J. Li, G.-Z. Xu, K.-Y. Liu, Y.-J. Zhang, Search for  $C = +$  charmonium and XYZ states in  $e^+e^- \rightarrow \gamma + H$  at BESIII, JHEP01 (2014) 022. [arXiv:1310.0374](#), [doi:10.1007/JHEP01\(2014\)022](#).
- [663] A. Denig, F.-K. Guo, C. Hanhart, A. V. Nefediev, Direct  $X(3872)$  production in  $e+e-$  collisions, Phys. Lett. B736 (2014) 221–225. [arXiv:1405.3404](#), [doi:10.1016/j.physletb.2014.07.027](#).
- [664] A. M. Torres, K. P. Khemchandani, F. S. Navarra, M. Nielsen, L. M. Abreu, On  $X(3872)$  production in high energy heavy ion collisions, Phys. Rev. D90 (11) (2014) 114023. [arXiv:1405.7583](#), [doi:10.1103/PhysRevD.90.114023](#).
- [665] S. Cho, S. H. Lee, Hadronic effects on the  $X(3872)$  meson abundance in heavy ion collisions, Phys. Rev. C88 (2013) 054901. [arXiv:1302.6381](#), [doi:10.1103/PhysRevC.88.054901](#).
- [666] G. Y. Chen, J. P. Ma, Production of  $X(3872)$  at PANDA, Phys. Rev. D77 (2008) 097501. [arXiv:0802.2982](#), [doi:10.1103/PhysRevD.77.097501](#).
- [667] A. B. Larionov, M. Strikman, M. Bleicher, Determination of the structure of the  $X(3872)$  in  $\bar{p}A$  collisions, Phys. Lett. B749 (2015) 35–43. [arXiv:1502.03311](#), [doi:10.1016/j.physletb.2015.07.045](#).
- [668] P. Artoisenet, E. Braaten, Production of the  $X(3872)$  at the Tevatron and the LHC, Phys. Rev. D81 (2010) 114018. [arXiv:0911.2016](#), [doi:10.1103/PhysRevD.81.114018](#).
- [669] C. Bignamini, B. Grinstein, F. Piccinini, A. D. Polosa, C. Sabelli, Is the  $X(3872)$  Production Cross Section at Tevatron Compatible with a Hadron Molecule Interpretation?, Phys. Rev. Lett. 103 (2009) 162001. [arXiv:0906.0882](#), [doi:10.1103/PhysRevLett.103.162001](#).
- [670] C. Bignamini, B. Grinstein, F. Piccinini, A. D. Polosa, V. Riquer, C. Sabelli, More loosely bound hadron molecules at CDF?, Phys. Lett. B684 (2010) 228–230. [arXiv:0912.5064](#), [doi:10.1016/j.physletb.2010.01.037](#).
- [671] E. Braaten, M. Kusunoki, Exclusive production of the  $X(3872)$  in  $B$  meson decay, Phys. Rev. D71 (2005) 074005. [arXiv:hep-ph/0412268](#), [doi:10.1103/PhysRevD.71.074005](#).
- [672] G. Bauer, [CDF Collaboration], The  $X(3872)$  at CDF II, Int. J. Mod. Phys. A20 (2005) 3765–3767. [arXiv:hep-ex/0409052](#), [doi:10.1142/S0217751X05027552](#).
- [673] C. Meng, H. Han, K.-T. Chao,  $X(3872)$  and its production at hadron colliders, [arXiv:1304.6710](#).
- [674] Y.-Q. Ma, K. Wang, K.-T. Chao, QCD radiative corrections to  $\chi_{cJ}$  production at hadron colliders, Phys. Rev. D83 (2011) 111503. [arXiv:1002.3987](#), [doi:10.1103/PhysRevD.83.111503](#).
- [675] F. J. Llanes-Estrada,  $Y(4260)$  and possible charmonium assignment, Phys. Rev. D72 (2005) 031503. [arXiv:hep-ph/0507035](#), [doi:10.1103/PhysRevD.72.031503](#).
- [676] A. Zhang, Charmonium spectrum and new observed states, Phys. Lett. B647 (2007) 140–144. [arXiv:hep-ph/0603093](#), [doi:10.1016/j.physletb.2007.01.062](#).
- [677] M. Shah, A. Parmar, P. C. Vinodkumar, Leptonic and Digamma decay Properties of S-wave quarkonia states, Phys. Rev. D86 (2012) 034015. [arXiv:1203.6184](#), [doi:10.1103/PhysRevD.86.034015](#).
- [678] E. J. Eichten, K. Lane, C. Quigg, New states above charm threshold, Phys. Rev. D73 (2006) 014014, [Erratum: Phys. Rev. D73, 079903 (2006)]. [arXiv:hep-ph/0511179](#), [doi:10.1103/PhysRevD.73.014014](#), [doi:10.1103/PhysRevD.73.079903](#).
- [679] J. Segovia, A. M. Yasser, D. R. Entem, F. Fernandez,  $J^{PC} = 1^{--}$  hidden charm resonances, Phys. Rev. D78 (2008) 114033. [doi:10.1103/PhysRevD.78.114033](#).
- [680] L. Y. Dai, M. Shi, G.-Y. Tang, H. Q. Zheng, Nature of  $X(4260)$ , Phys. Rev. D92 (1) (2015) 014020. [arXiv:1206.6911](#), [doi:10.1103/PhysRevD.92.014020](#).
- [681] G. Pakhlova, *et al.*, [Belle Collaboration], Measurement of the near-threshold  $e^+e^- \rightarrow D\bar{D}$  cross section using initial-state radiation, Phys. Rev. D77 (2008) 011103. [arXiv:0708.0082](#), [doi:10.1103/PhysRevD.77.011103](#).
- [682] S.-L. Zhu, The Possible interpretations of  $Y(4260)$ , Phys. Lett. B625 (2005) 212. [arXiv:hep-ph/0507025](#), [doi:10.1016/j.physletb.2005.08.068](#).
- [683] S.-L. Zhu, Masses and decay widths of heavy hybrid mesons, Phys. Rev. D60 (1999) 014008. [arXiv:hep-ph/9812405](#), [doi:10.1103/PhysRevD.60.014008](#).
- [684] S.-L. Zhu, Some decay modes of the  $1^{--}$  hybrid meson in QCD sum rules revisited, Phys. Rev. D60 (1999) 097502. [arXiv:hep-ph/9903537](#), [doi:10.1103/PhysRevD.60.097502](#).
- [685] F. E. Close, P. R. Page, The Production and decay of hybrid mesons by flux tube breaking, Nucl. Phys. B443 (1995) 233–254. [arXiv:hep-ph/9411301](#), [doi:10.1016/0550-3213\(95\)00085-7](#).
- [686] F. E. Close, S. Godfrey, Charmonium hybrid production in exclusive B meson decays, Phys. Lett. B574 (2003) 210–216. [arXiv:hep-ph/0305285](#), [doi:10.1016/j.physletb.2003.09.011](#).
- [687] E. Kou, O. Pene, Suppressed decay into open charm for the  $Y(4260)$  being an hybrid, Phys. Lett. B631 (2005) 164–169. [arXiv:hep-ph/0507119](#), [doi:10.1016/j.physletb.2005.09.013](#).
- [688] F. E. Close, P. R. Page, Gluonic charmonium resonances at BaBar and BELLE?, Phys. Lett. B628 (2005) 215–222. [arXiv:hep-ph/0507199](#), [doi:10.1016/j.physletb.2005.09.016](#).
- [689] T. Barnes, F. E. Close, E. S. Swanson, Hybrid and conventional mesons in the flux tube model: Numerical studies and their phenomenological implications, Phys. Rev. D52 (1995) 5242–5256. [arXiv:hep-ph/9501405](#), [doi:10.1103/PhysRevD.52.5242](#).
- [690] J. Merlin, J. E. Paton, Spin Interactions in the Flux Tube Model and Hybrid Meson Masses, Phys. Rev. D35 (1987) 1668. [doi:10.1103/PhysRevD.35.1668](#).
- [691] P. Lacock, C. Michael, P. Boyle, P. Rowland, [UKQCD Collaboration], Hybrid mesons from quenched QCD, Phys. Lett. B401 (1997) 308–312. [arXiv:hep-lat/9611011](#), [doi:10.1016/S0370-2693\(97\)00384-5](#).

- [692] T. Manke, I. T. Drummond, R. R. Horgan, H. P. Shanahan, [UKQCD Collaboration], Heavy hybrids from NRQCD, Phys. Rev. D57 (1998) 3829–3832. [arXiv:hep-lat/9710083](#), [doi:10.1103/PhysRevD.57.3829](#).
- [693] K. J. Juge, J. Kuti, C. J. Morningstar, The Heavy hybrid spectrum from NRQCD and the Born-Oppenheimer approximation, Nucl. Phys. Proc. Suppl. 83 (2000) 304–306. [arXiv:hep-lat/9909165](#), [doi:10.1016/S0920-5632\(00\)91655-4](#).
- [694] I. T. Drummond, N. A. Goodman, R. R. Horgan, H. P. Shanahan, L. C. Stononi, Spin effects in heavy hybrid mesons on an anisotropic lattice, Phys. Lett. B478 (2000) 151–160. [arXiv:hep-lat/9912041](#), [doi:10.1016/S0370-2693\(00\)00225-2](#).
- [695] T. Manke, [CP-PACS Collaboration], Exotic quarkonia from anisotropic lattices, Nucl. Phys. Proc. Suppl. 86 (2000) 397–400. [arXiv:hep-lat/9909038](#), [doi:10.1016/S0920-5632\(00\)00593-4](#).
- [696] P. Guo, A. P. Szczepaniak, G. Galata, A. Vassallo, E. Santopinto, Heavy quarkonium hybrids from Coulomb gauge QCD, Phys. Rev. D78 (2008) 056003. [arXiv:0807.2721](#), [doi:10.1103/PhysRevD.78.056003](#).
- [697] C.-F. Qiao, L. Tang, G. Hao, X.-Q. Li, Determining  $1^{--}$  Heavy Hybrid Masses via QCD Sum Rules, J. Phys. G39 (2012) 015005. [arXiv:1012.2614](#), [doi:10.1088/0954-3899/39/1/015005](#).
- [698] W. Chen, R. T. Kleiv, T. G. Steele, B. Bulthuis, D. Harnett, J. Ho, T. Richards, S.-L. Zhu, Mass Spectrum of Heavy Quarkonium Hybrids, JHEP 09 (2013) 019. [arXiv:1304.4522](#), [doi:10.1007/JHEP09\(2013\)019](#).
- [699] J. Govaerts, L. J. Reinders, P. Francken, X. Gonze, J. Weyers, Coupled QCD Sum Rules for Hybrid Mesons, Nucl. Phys. B284 (1987) 674. [doi:10.1016/0550-3213\(87\)90056-3](#).
- [700] J. Govaerts, L. J. Reinders, H. R. Rubinstein, J. Weyers, Hybrid Quarkonia From QCD Sum Rules, Nucl. Phys. B258 (1985) 215. [doi:10.1016/0550-3213\(85\)90609-1](#).
- [701] J. Govaerts, F. de Viron, D. Gusbin, J. Weyers, QCD Sum Rules and Hybrid Mesons, Nucl. Phys. B248 (1984) 1. [doi:10.1016/0550-3213\(84\)90583-2](#).
- [702] D. Harnett, R. T. Kleiv, T. G. Steele, H.-y. Jin, Axial Vector  $J^{PC} = 1^{++}$  Charmonium and Bottomonium Hybrid Mass Predictions with QCD Sum-Rules, J. Phys. G39 (2012) 125003. [arXiv:1206.6776](#), [doi:10.1088/0954-3899/39/12/125003](#).
- [703] R. Berg, D. Harnett, R. T. Kleiv, T. G. Steele, Mass Predictions for Pseudoscalar  $J^{PC} = 0^{++}$  Charmonium and Bottomonium Hybrids in QCD Sum-Rules, Phys. Rev. D86 (2012) 034002. [arXiv:1204.0049](#), [doi:10.1103/PhysRevD.86.034002](#).
- [704] L. Maiani, V. Riquer, F. Piccinini, A. D. Polosa, Four quark interpretation of  $Y(4260)$ , Phys. Rev. D72 (2005) 031502. [arXiv:hep-ph/0507062](#), [doi:10.1103/PhysRevD.72.031502](#).
- [705] N. V. Drenska, R. Faccini, A. D. Polosa, Exotic Hadrons with Hidden Charm and Strangeness, Phys. Rev. D79 (2009) 077502. [arXiv:0902.2803](#), [doi:10.1103/PhysRevD.79.077502](#).
- [706] H. X. Chen, L. Maiani, A. D. Polosa, V. Riquer,  $Y(4260) \rightarrow \gamma + X(3872)$  in the diquarkonium picture, Eur. Phys. J. C75 (11) (2015) 550. [arXiv:1510.03626](#), [doi:10.1140/epjc/s10052-015-3781-2](#).
- [707] Z.-G. Wang, Mass spectrum of the vector hidden charmed and bottomed tetraquark states, J. Phys. G36 (2009) 085002. [arXiv:0903.0754](#), [doi:10.1088/0954-3899/36/8/085002](#).
- [708] J.-R. Zhang, M.-Q. Huang, The  $P$ -wave  $[c\bar{s}][\bar{c}\bar{s}]$  tetraquark state:  $Y(4260)$  or  $Y(4660)$ ?, Phys. Rev. D83 (2011) 036005. [arXiv:1011.2818](#), [doi:10.1103/PhysRevD.83.036005](#).
- [709] C. Z. Yuan, P. Wang, X. H. Mo, The  $Y(4260)$  as an  $\omega\chi_{c1}$  molecular state, Phys. Lett. B634 (2006) 399–402. [arXiv:hep-ph/0511107](#), [doi:10.1016/j.physletb.2006.01.031](#).
- [710] M. Cleven, Q. Wang, F.-K. Guo, C. Hanhart, U.-G. Meissner, Q. Zhao,  $Y(4260)$  as the first  $S$ -wave open charm vector molecular state?, Phys. Rev. D90 (7) (2014) 074039. [arXiv:1310.2190](#), [doi:10.1103/PhysRevD.90.074039](#).
- [711] T.-W. Chiu, T.-H. Hsieh, [TWQCD Collaboration],  $Y(4260)$  on the lattice, Phys. Rev. D73 (2006) 094510. [arXiv:hep-lat/0512029](#), [doi:10.1103/PhysRevD.73.094510](#).
- [712] E. van Beveren, G. Rupp, Interference effects in the  $X(4260)$  signal, Phys. Rev. D79 (2009) 111501. [arXiv:0905.1595](#), [doi:10.1103/PhysRevD.79.111501](#).
- [713] E. van Beveren, G. Rupp, J. Segovia, A Very broad  $X(4260)$  and the resonance parameters of the  $\psi(3D)$  vector charmonium state, Phys. Rev. Lett. 105 (2010) 102001. [arXiv:1005.1010](#), [doi:10.1103/PhysRevLett.105.102001](#).
- [714] D.-Y. Chen, J. He, X. Liu, Nonresonant explanation for the  $Y(4260)$  structure observed in the  $e^+e^- \rightarrow J/\psi\pi^+\pi^-$  process, Phys. Rev. D83 (2011) 054021. [arXiv:1012.5362](#), [doi:10.1103/PhysRevD.83.054021](#).
- [715] D.-Y. Chen, X. Liu, X.-Q. Li, H.-W. Ke, A unified Fano-like interference picture for charmonium-like states  $Y(4008)$ ,  $Y(4260)$  and  $Y(4360)$  [arXiv:1512.04157](#).
- [716] C.-F. Qiao, One explanation for the exotic state  $Y(4260)$ , Phys. Lett. B639 (2006) 263–265. [arXiv:hep-ph/0510228](#), [doi:10.1016/j.physletb.2006.06.038](#).
- [717] C.-F. Qiao, A Uniform description of the states recently observed at  $B$  factories, J. Phys. G35 (2008) 075008. [arXiv:0709.4066](#), [doi:10.1088/0954-3899/35/7/075008](#).
- [718] A. Martinez Torres, K. P. Khemchandani, D. Gamermann, E. Oset, The  $Y(4260)$  as a  $J/\psi K\bar{K}$  system, Phys. Rev. D80 (2009) 094012. [arXiv:0906.5333](#), [doi:10.1103/PhysRevD.80.094012](#).
- [719] X. Li, M. B. Voloshin,  $Y(4260)$  and  $Y(4360)$  as mixed hadrocharmonium, Mod. Phys. Lett. A29 (12) (2014) 1450060. [arXiv:1309.1681](#), [doi:10.1142/S0217732314500606](#).
- [720] E. van Beveren, G. Rupp, Is the  $Y(4260)$  just a coupled-channel signal? [arXiv:hep-ph/0605317](#).
- [721] X.-H. Liu, G. Li, Exploring the threshold behavior and implications on the nature of  $Y(4260)$  and  $Z_c(3900)$ , Phys. Rev. D88 (2013) 014013. [arXiv:1306.1384](#), [doi:10.1103/PhysRevD.88.014013](#).
- [722] A. Ali, W. Wang, Production of the Exotic  $1^{--}$  Hadrons  $\phi(2170)$ ,  $X(4260)$  and  $Y_b(10890)$  at the LHC and Tevatron via the Drell-Yan Mechanism, Phys. Rev. Lett. 106 (2011) 192001. [arXiv:1103.4587](#), [doi:10.1103/PhysRevLett.106.192001](#).
- [723] R. M. Albuquerque, M. Nielsen, C. M. Zanetti, Production of the  $Y(4260)$  State in  $B$  Meson Decay, Phys. Lett. B747 (2015) 83–87. [arXiv:1502.00119](#), [doi:10.1016/j.physletb.2015.05.022](#).
- [724] Yu. S. Kalashnikova, A. V. Nefediev, Spectra and decays of hybrid charmonia, Phys. Rev. D77 (2008) 054025. [arXiv:0801.2036](#), [doi:10.1103/PhysRevD.77.054025](#).

- [725] G. Li, X.-H. Liu, Investigating possible decay modes of  $Y(4260)$  under  $D_1(2420)\bar{D} + c.c.$  molecular state ansatz, Phys. Rev. D88 (9) (2013) 094008. [arXiv:1307.2622](#), [doi:10.1103/PhysRevD.88.094008](#).
- [726] G. Li, C.-S. An, P.-Y. Li, D. Liu, X. Zhang, Z. Zhou, Investigations on the charmless decays of  $Y(4260)$ , Chin. Phys. C39 (6) (2015) 063102. [arXiv:1412.3221](#), [doi:10.1088/1674-1137/39/6/063102](#).
- [727] Y. Dong, A. Faessler, T. Gutsche, V. E. Lyubovitskij, Selected strong decay modes of  $Y(4260)$ , Phys. Rev. D89 (3) (2014) 034018. [arXiv:1310.4373](#), [doi:10.1103/PhysRevD.89.034018](#).
- [728] T. J. Burns, F. E. Close, C. E. Thomas, Dynamics of hadron strong production and decay, Phys. Rev. D77 (2008) 034008. [arXiv:0709.1816](#), [doi:10.1103/PhysRevD.77.034008](#).
- [729] X. H. Mo, G. Li, C. Z. Yuan, K. L. He, H. M. Hu, J. H. Hu, P. Wang, Z. Y. Wang, Determining the upper limit of  $\Gamma_{ee}$  for the  $Y(4260)$ , Phys. Lett. B640 (2006) 182–187. [arXiv:hep-ex/0603024](#), [doi:10.1016/j.physletb.2006.07.060](#).
- [730] L. Ma, W.-Z. Deng, X.-L. Chen, S.-L. Zhu, Strong decay patterns of the hidden-charm tetraquarks, [arXiv:1512.01938](#).
- [731] N. Mahajan,  $Y(4140)$ : Possible options, Phys. Lett. B679 (2009) 228–230. [arXiv:0903.3107](#), [doi:10.1016/j.physletb.2009.07.043](#).
- [732] T. Branz, T. Gutsche, V. E. Lyubovitskij, Hadronic molecule structure of the  $Y(3940)$  and  $Y(4140)$ , Phys. Rev. D80 (2009) 054019. [arXiv:0903.5424](#), [doi:10.1103/PhysRevD.80.054019](#).
- [733] G.-J. Ding, Possible Molecular States of  $D_s^* \bar{D}_s^*$  System and  $Y(4140)$ , Eur. Phys. J. C64 (2009) 297–308. [arXiv:0904.1782](#), [doi:10.1140/epjc/s10052-009-1146-4](#).
- [734] X. Chen, X. Lu, Mass of  $Y(3940)$  in Bethe-Salpeter equation for quarks, Eur. Phys. J. C75 (3) (2015) 98. [arXiv:1411.3424](#), [doi:10.1140/epjc/s10052-015-3315-y](#).
- [735] J.-R. Zhang, M.-Q. Huang,  $(Q \text{ anti-}s)(\bar{s})(\text{anti-}Qs)$  molecular states from QCD sum rules: A view on  $Y(4140)$ , J. Phys. G37 (2010) 025005. [arXiv:0905.4178](#), [doi:10.1088/0954-3899/37/2/025005](#).
- [736] R. M. Albuquerque, M. E. Bracco, M. Nielsen, A QCD sum rule calculation for the  $Y(4140)$  narrow structure, Phys. Lett. B678 (2009) 186–190. [arXiv:0903.5540](#), [doi:10.1016/j.physletb.2009.06.022](#).
- [737] Z.-G. Wang, Analysis of the  $Y(4140)$  with QCD sum rules, Eur. Phys. J. C63 (2009) 115–122. [arXiv:0903.5200](#), [doi:10.1140/epjc/s10052-009-1097-9](#).
- [738] Z.-G. Wang, Z.-C. Liu, X.-H. Zhang, Analysis of the  $Y(4140)$  and related molecular states with QCD sum rules, Eur. Phys. J. C64 (2009) 373–386. [arXiv:0907.1467](#), [doi:10.1140/epjc/s10052-009-1156-2](#).
- [739] R. M. Albuquerque, J. M. Dias, M. Nielsen, C. M. Zanetti,  $Y(3940)$  as a Mixed Charmonium-Molecule State, Phys. Rev. D89 (7) (2014) 076007. [arXiv:1311.6411](#), [doi:10.1103/PhysRevD.89.076007](#).
- [740] S. I. Finazzo, M. Nielsen, X. Liu, QCD sum rule calculation for the charmonium-like structures in the  $J/\psi\phi$  and  $J/\psi\omega$  invariant mass spectra, Phys. Lett. B701 (2011) 101–106. [arXiv:1102.2347](#), [doi:10.1016/j.physletb.2011.05.042](#).
- [741] Z.-G. Wang, Analysis of the  $Y(4274)$  with QCD sum rules, Int. J. Mod. Phys. A26 (2011) 4929–4943. [arXiv:1102.5483](#), [doi:10.1142/S0217751X1105484X](#).
- [742] S. S. Gershtein, A. K. Likhoded, A. V. Luchinsky, Systematics of heavy quarkonia from Regge trajectories on  $(n, M^2)$  and  $(M^2, J)$  planes, Phys. Rev. D74 (2006) 016002. [arXiv:hep-ph/0602048](#), [doi:10.1103/PhysRevD.74.016002](#).
- [743] F. Stancu, Can  $Y(4140)$  be a  $c \text{ anti-}c s \text{ anti-}s$  tetraquark?, J. Phys. G37 (2010) 075017. [arXiv:0906.2485](#), [doi:10.1088/0954-3899/37/7/075017](#).
- [744] E. van Beveren, G. Rupp, The  $Y(4140)$ ,  $X(4260)$ ,  $\psi(2D)$ ,  $\psi(4S)$  and tentative  $\psi(3D)$ , [arXiv:0906.2278](#).
- [745] R. Molina, E. Oset, The  $Y(3940)$ ,  $Z(3930)$  and the  $X(4160)$  as dynamically generated resonances from the vector-vector interaction, Phys. Rev. D80 (2009) 114013. [arXiv:0907.3043](#), [doi:10.1103/PhysRevD.80.114013](#).
- [746] T. Branz, R. Molina, E. Oset, Radiative decays of the  $Y(3940)$ ,  $Z(3930)$  and the  $X(4160)$  as dynamically generated resonances, Phys. Rev. D83 (2011) 114015. [arXiv:1010.0587](#), [doi:10.1103/PhysRevD.83.114015](#).
- [747] W.-H. Liang, J.-J. Xie, E. Oset, R. Molina, M. Doring, Predictions for the  $\bar{B}^0 \rightarrow \bar{K}^{*0}X(YZ)$  and  $\bar{B}_s^0 \rightarrow \phi X(YZ)$  with  $X(4160)$ ,  $Y(3940)$ ,  $Z(3930)$ , Eur. Phys. J. A51 (5) (2015) 58. [arXiv:1502.02932](#), [doi:10.1140/epja/i2015-15058-3](#).
- [748] C. Hidalgo-Duque, J. Nieves, M. P. Valderrama, Light flavor and heavy quark spin symmetry in heavy meson molecules, Phys. Rev. D87 (7) (2013) 076006. [arXiv:1210.5431](#), [doi:10.1103/PhysRevD.87.076006](#).
- [749] Z.-G. He, B.-Q. Li, Inclusive decays of  $\eta_b$  into S- and P-wave charmonium states, Phys. Lett. B693 (2010) 36–43. [arXiv:0910.0220](#), [doi:10.1016/j.physletb.2010.08.013](#).
- [750] J. He, X. Liu, Discovery potential for charmonium-like state  $Y(3940)$  by the meson photoproduction, Phys. Rev. D80 (2009) 114007. [arXiv:0910.5867](#), [doi:10.1103/PhysRevD.80.114007](#).
- [751] X. Liu, H.-W. Ke, The Line shape of the radiative open-charm decay of  $Y(4140)$  and  $Y(3930)$ , Phys. Rev. D80 (2009) 034009. [arXiv:0907.1349](#), [doi:10.1103/PhysRevD.80.034009](#).
- [752] X. Liu, The Hidden charm decay of  $Y(4140)$  by the rescattering mechanism, Phys. Lett. B680 (2009) 137–140. [arXiv:0904.0136](#), [doi:10.1016/j.physletb.2009.08.049](#).
- [753] J. He, X. Liu, The open-charm radiative and pionic decays of molecular charmonium  $Y(4274)$ , Eur. Phys. J. C72 (2012) 1986. [arXiv:1102.1127](#), [doi:10.1140/epjc/s10052-012-1986-1](#).
- [754] W. Xie, L. Q. Mo, P. Wang, S. R. Cotanch, Coulomb gauge model for hidden charm tetraquarks, Phys. Lett. B725 (2013) 148–152. [arXiv:1302.5737](#), [doi:10.1016/j.physletb.2013.07.003](#).
- [755] P. Zhou, C.-R. Deng, J.-L. Ping, Identification of  $Y(4008)$ ,  $Y(4140)$ ,  $Y(4260)$ , and  $Y(4360)$  as Tetraquark States, Chin. Phys. Lett. 32 (10) (2015) 101201. [doi:10.1088/0256-307X/32/10/101201](#).
- [756] G.-J. Ding, J.-J. Zhu, M.-L. Yan, Canonical Charmonium Interpretation for  $Y(4360)$  and  $Y(4660)$ , Phys. Rev. D77 (2008) 014033. [arXiv:0708.3712](#), [doi:10.1103/PhysRevD.77.014033](#).
- [757] D.-Y. Chen, J. He, X. Liu, A Novel explanation of charmonium-like structure in  $e^+e^- \rightarrow \psi(2S)\pi^+\pi^-$ , Phys. Rev. D83 (2011) 074012. [arXiv:1101.2474](#), [doi:10.1103/PhysRevD.83.074012](#).
- [758] D.-Y. Chen, X. Liu, T. Matsuki, Novel charged charmoniumlike structures in the hidden-charm dipion decays of  $Y(4360)$ , Phys. Rev. D88 (1)

- (2013) 014034. [arXiv:1306.2080](#), [doi:10.1103/PhysRevD.88.014034](#).
- [759] E. van Beveren, G. Rupp, Evidence for further charmonium vector resonances, *Chin. Phys.* C35 (2011) 319–324. [arXiv:1004.4368](#), [doi:10.1088/1674-1137/35/4/001](#).
- [760] F.-K. Guo, C. Hanhart, U.-G. Meissner, Evidence that the  $Y(4660)$  is a  $f_0(980)\psi'$  bound state, *Phys. Lett.* B665 (2008) 26–29. [arXiv:0803.1392](#), [doi:10.1016/j.physletb.2008.05.057](#).
- [761] F.-K. Guo, C. Hanhart, U.-G. Meissner, Implications of heavy quark spin symmetry on heavy meson hadronic molecules, *Phys. Rev. Lett.* 102 (2009) 242004. [arXiv:0904.3338](#), [doi:10.1103/PhysRevLett.102.242004](#).
- [762] S. Dubynskiy, M. B. Voloshin, Hadro-Charmonium, *Phys. Lett.* B666 (2008) 344–346. [arXiv:0803.2224](#), [doi:10.1016/j.physletb.2008.07.086](#).
- [763] R. M. Albuquerque, M. Nielsen, R. R. da Silva, Exotic  $1^{--}$  States in QCD Sum Rules, *Phys. Rev.* D84 (2011) 116004. [arXiv:1110.2113](#), [doi:10.1103/PhysRevD.84.116004](#).
- [764] D.-Y. Chen, X. Liu, T. Matsuki, Predictions of Charged Charmoniumlike Structures with Hidden-Charm and Open-Strange Channels, *Phys. Rev. Lett.* 110 (23) (2013) 232001. [arXiv:1303.6842](#), [doi:10.1103/PhysRevLett.110.232001](#).
- [765] D.-Y. Chen, X. Liu, T. Matsuki, Prediction of isoscalar charmoniumlike structures in the hidden-charm di-eta decays of higher charmonia, *J. Phys.* G42 (1) (2015) 015002. [arXiv:1309.4528](#), [doi:10.1088/0954-3899/42/1/015002](#).
- [766] D.-Y. Chen, X. Liu, T. Matsuki, Search for missing  $\psi(4S)$  in the  $e^+e^- \rightarrow \pi^+\pi^-\psi(2S)$  process, [arXiv:1509.00736](#).
- [767] Yu. A. Simonov, Theory of hadron decay into baryon-antibaryon final state, *Phys. Rev.* D85 (2012) 105025. [arXiv:1109.5545](#), [doi:10.1103/PhysRevD.85.105025](#).
- [768] X. Liu, H.-W. Ke, X. Liu, X.-Q. Li, Exploring open-charm decay mode  $\Lambda_c\bar{\Lambda}_c$  of charmonium-like state  $Y(4630)$ , [arXiv:1601.00762](#).
- [769] D. V. Bugg, An Alternative fit to Belle mass spectra for  $D\bar{D}$ ,  $D^*\bar{D}^*$  and  $\Lambda_c\bar{\Lambda}_{c\lambda}$ , *J. Phys.* G36 (2009) 075002. [arXiv:0811.2559](#), [doi:10.1088/0954-3899/36/7/075002](#).
- [770] G. Cotugno, R. Faccini, A. D. Polosa, C. Sabelli, Charmed Baryonium, *Phys. Rev. Lett.* 104 (2010) 132005. [arXiv:0911.2178](#), [doi:10.1103/PhysRevLett.104.132005](#).
- [771] F.-K. Guo, J. Haidenbauer, C. Hanhart, U.-G. Meissner, Reconciling the  $X(4630)$  with the  $Y(4660)$ , *Phys. Rev.* D82 (2010) 094008. [arXiv:1005.2055](#), [doi:10.1103/PhysRevD.82.094008](#).
- [772] T. Barnes, S. Godfrey, E. S. Swanson, Higher charmonia, *Phys. Rev.* D72 (2005) 054026. [arXiv:hep-ph/0505002](#), [doi:10.1103/PhysRevD.72.054026](#).
- [773] S. L. Olsen, Is the  $X(3915)$  the  $\chi_{c0}(2P)$ ?, *Phys. Rev.* D91 (5) (2015) 057501. [arXiv:1410.6534](#), [doi:10.1103/PhysRevD.91.057501](#).
- [774] X. Liu, Z.-G. Luo, Z.-F. Sun,  $X(3915)$  and  $X(4350)$  as new members in P-wave charmonium family, *Phys. Rev. Lett.* 104 (2010) 122001. [arXiv:0911.3694](#), [doi:10.1103/PhysRevLett.104.122001](#).
- [775] Y. Jiang, G.-L. Wang, T. Wang, W.-L. Ju, Why  $X(3915)$  is so narrow as a  $\chi_{c0}(2P)$  state?, *Int. J. Mod. Phys.* A28 (2013) 1350145. [arXiv:1310.2317](#), [doi:10.1142/S0217751X13501455](#).
- [776] Y.-c. Yang, Z. Xia, J. Ping, Are the  $X(4160)$  and  $X(3915)$  charmonium states?, *Phys. Rev.* D81 (2010) 094003. [arXiv:0912.5061](#), [doi:10.1103/PhysRevD.81.094003](#).
- [777] Z.-J. Zhao, D.-M. Pan, Estimating strong decays of  $X(3915)$  and  $X(4350)$ , [arXiv:1104.1838](#).
- [778] F.-K. Guo, U.-G. Meissner, Where is the  $\chi_{c0}(2P)$ ?, *Phys. Rev.* D86 (2012) 091501. [arXiv:1208.1134](#), [doi:10.1103/PhysRevD.86.091501](#).
- [779] D.-Y. Chen, J. He, X. Liu, T. Matsuki, X. Liu, T. Matsuki, Does the enhancement observed in  $\gamma\gamma \rightarrow D\bar{D}$  contain two P-wave higher charmonia?, *Eur. Phys. J.* C72 (2012) 2226. [arXiv:1207.3561](#), [doi:10.1140/epjc/s10052-012-2226-4](#).
- [780] Z.-Y. Zhou, Z. Xiao, H.-Q. Zhou, Could the  $X(3915)$  and the  $X(3930)$  Be the Same Tensor State?, *Phys. Rev. Lett.* 115 (2) (2015) 022001. [arXiv:1501.00879](#), [doi:10.1103/PhysRevLett.115.022001](#).
- [781] R. M. Albuquerque, J. M. Dias, M. Nielsen, Can the  $X(4350)$  narrow structure be a  $1^{++}$  exotic state?, *Phys. Lett.* B690 (2010) 141–144. [arXiv:1001.3092](#), [doi:10.1016/j.physletb.2010.05.024](#).
- [782] Z. Mo, C.-Y. Cui, Y.-L. Liu, M.-Q. Huang, QCD sum rules study of  $X(4350)$ , *Commun. Theor. Phys.* 61 (4) (2014) 501–505. [arXiv:1403.6906](#), [doi:10.1088/0253-6102/61/4/16](#).
- [783] Z.-g. Wang, Y.-f. Tian, Tetraquark state candidates:  $Y(4140)$ ,  $Y(4274)$  and  $X(4350)$ , *Int. J. Mod. Phys.* A30 (2015) 1550004. [arXiv:1502.04619](#), [doi:10.1142/S0217751X15500049](#).
- [784] Z.-G. Wang, Analysis of the  $X(4350)$  as a scalar  $\bar{c}c$  and  $D_s^*\bar{D}_s^*$  mixing state with QCD sum rules, *Phys. Lett.* B690 (2010) 403–406. [arXiv:0912.4626](#), [doi:10.1016/j.physletb.2010.05.068](#).
- [785] Y. Yang, J. Ping, Dynamical study of the  $X(3915)$  as a molecular  $D^*\bar{D}^*$  state in a quark model, *Phys. Rev.* D81 (2010) 114025. [arXiv:1004.2444](#), [doi:10.1103/PhysRevD.81.114025](#).
- [786] M. Abud, F. Buccella, F. Tramontano, Hints for the existence of hexaquark states in the baryon-antibaryon sector, *Phys. Rev.* D81 (2010) 074018. [arXiv:0912.4299](#), [doi:10.1103/PhysRevD.81.074018](#).
- [787] Y.-L. Ma, Estimates for  $X(4350)$  Decays from the Effective Lagrangian Approach, *Phys. Rev.* D82 (2010) 015013. [arXiv:1006.1276](#), [doi:10.1103/PhysRevD.82.015013](#).
- [788] X. Li, M. B. Voloshin,  $X(3915)$  as a  $D_s\bar{D}_s$  bound state, *Phys. Rev.* D91 (11) (2015) 114014. [arXiv:1503.04431](#), [doi:10.1103/PhysRevD.91.114014](#).
- [789] Q.-Y. Lin, X. Liu, H.-S. Xu, Probing charmoniumlike state  $X(3915)$  through meson photoproduction, *Phys. Rev.* D89 (3) (2014) 034016. [arXiv:1312.7073](#), [doi:10.1103/PhysRevD.89.034016](#).
- [790] D.-Y. Chen, X. Liu, T. Matsuki, Hidden-charm decays of  $X(3915)$  and  $Z(3930)$  as the P-wave charmonia, *PTEP* 2015 (4) (2015) 043B05. [arXiv:1311.6274](#), [doi:10.1093/ptep/ptv038](#).
- [791] J. L. Rosner, Hadron spectroscopy: A 2005 snapshot, *AIP Conf. Proc.* 815 (2006) 218–232, [,218(2005)]. [arXiv:hep-ph/0508155](#), [doi:10.1063/1.2173591](#).
- [792] V. V. Braguta, A. K. Likhoded, A. V. Luchinsky, The Process  $e^+e^- \rightarrow J/\psi X(3940)$  at  $\sqrt{s} = 10.6$  GeV in the framework of light cone formalism, *Phys. Rev.* D74 (2006) 094004. [arXiv:hep-ph/0602232](#), [doi:10.1103/PhysRevD.74.094004](#).

- [793] L.-P. He, D.-Y. Chen, X. Liu, T. Matsuki, Prediction of a missing higher charmonium around 4.26 GeV in  $J/\psi$  family, *Eur. Phys. J. C* 74 (12) (2014) 3208. [arXiv:1405.3831](#), [doi:10.1140/epjc/s10052-014-3208-5](#).
- [794] K.-T. Chao, Interpretations for the  $X(4160)$  observed in the double charm production at B factories, *Phys. Lett. B* 661 (2008) 348–353. [arXiv:0707.3982](#), [doi:10.1016/j.physletb.2008.02.039](#).
- [795] Y.-B. Dong, Y.-W. Yu, Z.-Y. Zhang, P.-N. Shen, Leptonic decay of charmonium, *Phys. Rev. D* 49 (1994) 1642–1644. [doi:10.1103/PhysRevD.49.1642](#).
- [796] X. H. Mo, C. Z. Yuan, P. Wang, On the leptonic partial widths of the excited  $\psi$  states, *Phys. Rev. D* 82 (2010) 077501. [arXiv:1007.0084](#), [doi:10.1103/PhysRevD.82.077501](#).
- [797] C.-Z. Yuan, Evidence for resonant structures in  $e^+e^- \rightarrow \pi^+\pi^-h_c$ , *Chin. Phys. C* 38 (2014) 043001. [arXiv:1312.6399](#), [doi:10.1088/1674-1137/38/4/043001](#).
- [798] M. Ablikim, *et al.*, [BESIII Collaboration], Study of  $e^+e^- \rightarrow \omega\chi_{cJ}$  at center-of-mass energies from 4.21 to 4.42 GeV, *Phys. Rev. Lett.* 114 (9) (2015) 092003. [arXiv:1410.6538](#), [doi:10.1103/PhysRevLett.114.092003](#).
- [799] D.-Y. Chen, X. Liu, T. Matsuki, Observation of  $e^+e^- \rightarrow \chi_{c0}\omega$  and missing higher charmonium  $\psi(4S)$ , *Phys. Rev. D* 91 (9) (2015) 094023. [arXiv:1411.5136](#), [doi:10.1103/PhysRevD.91.094023](#).
- [800] G. Xu-yang, W. Xiao-long, S. Cheng-ping, Search for  $\psi(4S) \rightarrow \eta J/\psi$  in  $B^\pm \rightarrow \eta J/\psi K^\pm$  and  $e^+e^- \rightarrow \eta J/\psi$  processes, *Chin. Phys. C* 40 (2016) 013001. [arXiv:1506.04960](#), [doi:10.1088/1674-1137/40/1/013001](#).
- [801] E. J. Eichten, K. Lane, C. Quigg,  $B$  meson gateways to missing charmonium levels, *Phys. Rev. Lett.* 89 (2002) 162002. [arXiv:hep-ph/0206018](#), [doi:10.1103/PhysRevLett.89.162002](#).
- [802] P.-w. Ko, J. Lee, H. S. Song, Color octet mechanism in the inclusive D wave charmonium productions in  $B$  decays, *Phys. Lett. B* 395 (1997) 107–112. [arXiv:hep-ph/9701235](#), [doi:10.1016/S0370-2693\(97\)00041-5](#).
- [803] C.-f. Qiao, F. Yuan, K.-T. Chao, A Crucial test for color octet production mechanism in  $Z^0$  decays, *Phys. Rev. D* 55 (1997) 4001–4004. [arXiv:hep-ph/9609284](#), [doi:10.1103/PhysRevD.55.4001](#).
- [804] W. Chen, Z.-X. Cai, S.-L. Zhu, Masses of the tensor mesons with  $J^P = 2^-$ , *Nucl. Phys. B* 887 (2014) 201–215. [arXiv:1107.4949](#), [doi:10.1016/j.nuclphysb.2014.08.006](#).
- [805] J. Segovia, D. R. Entem, F. Fernandez, E. Hernandez, Constituent quark model description of charmonium phenomenology, *Int. J. Mod. Phys. E* 22 (2013) 1330026. [arXiv:1309.6926](#), [doi:10.1142/S0218301313300269](#).
- [806] M. B. Voloshin, Process  $e^+e^- \rightarrow \pi\pi X(3823)$  in the soft pion limit, *Phys. Rev. D* 91 (11) (2015) 114029. [arXiv:1504.02973](#), [doi:10.1103/PhysRevD.91.114029](#).
- [807] B. Wang, H. Xu, X. Liu, D.-Y. Chen, S. Coito, E. Eichten, Using  $X(3823) \rightarrow J/\psi\pi^+\pi^-$  to Identify Coupled-Channel Effects, [arXiv:1507.07985](#).
- [808] W.-J. Deng, L.-Y. Xiao, L.-C. Gui, X.-H. Zhong, Radiative transitions of charmonium states, [arXiv:1510.08269](#).
- [809] D. M. Asner, *et al.*, Physics at BES-III, *Int. J. Mod. Phys. A* 24 (2009) S1–794. [arXiv:0809.1869](#).
- [810] A. A. Alves, Jr., *et al.*, [LHCb Collaboration], The LHCb Detector at the LHC, *JINST* 3 (2008) S08005. [doi:10.1088/1748-0221/3/08/S08005](#).
- [811] R. Aaij, *et al.*, [LHCb Collaboration], Precision measurement of the  $\Lambda_b^0$  baryon lifetime, *Phys. Rev. Lett.* 111 (2013) 102003. [arXiv:1307.2476](#), [doi:10.1103/PhysRevLett.111.102003](#).
- [812] R. Aaij, *et al.*, [LHCb Collaboration], LHCb Detector Performance, *Int. J. Mod. Phys. A* 30 (07) (2015) 1530022. [arXiv:1412.6352](#), [doi:10.1142/S0217751X15300227](#).
- [813] S. Chatrchyan, *et al.*, [CMS Collaboration], The CMS experiment at the CERN LHC, *JINST* 3 (2008) S08004. [doi:10.1088/1748-0221/3/08/S08004](#).
- [814] T. Abe, *et al.*, [Belle-II Collaboration], Belle II Technical Design Report, [arXiv:1011.0352](#).
- [815] T. Aushev, *et al.*, Physics at Super B Factory, [arXiv:1002.5012](#).
- [816] M. F. M. Lutz, *et al.*, [PANDA Collaboration], Physics Performance Report for PANDA: Strong Interaction Studies with Antiprotons, [arXiv:0903.3905](#).